UNDERSTANDING AND MODULATING BONE AND CARTILAGE CELL FATE FOR REGENERATIVE MEDICINE

EDITED BY: Roberto Narcisi and Eric Farrell

PUBLISHED IN: Frontiers in Bioengineering and Biotechnology

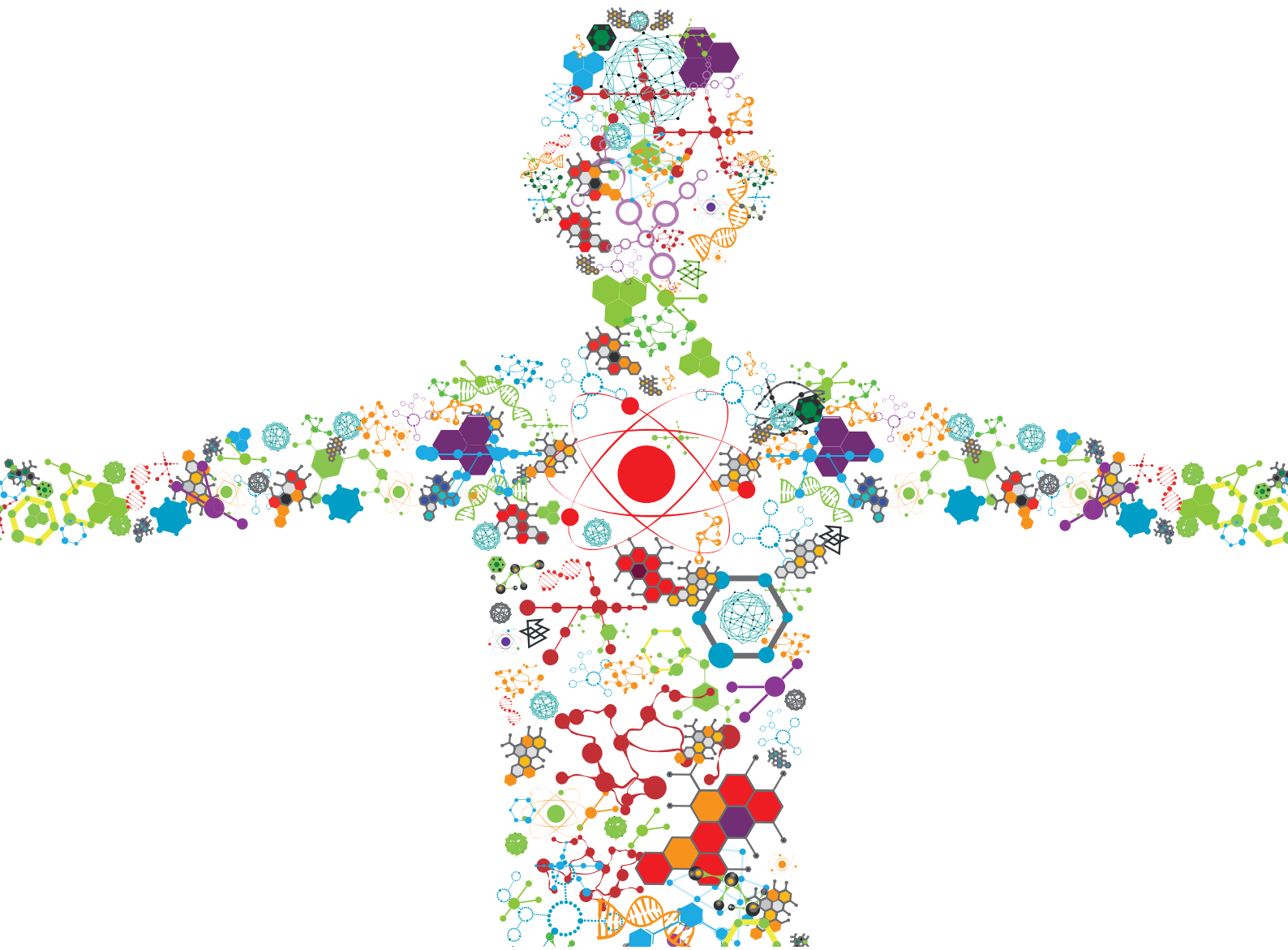

frontiers Research Topics

frontiers

ISSN 1664-8714
ISBN 978-2-88945-790-8
DOI 10.3389/978-2-88945-790-8

About Frontiers

Frontiers is more than just an open-access publisher of scholarly articles: it is a pioneering approach to the world of academia, radically improving the way scholarly research is managed. The grand vision of Frontiers is a world where all people have an equal opportunity to seek, share and generate knowledge. Frontiers provides immediate and permanent online open access to all its publications, but this alone is not enough to realize our grand goals.

Frontiers Journal Series

The Frontiers Journal Series is a multi-tier and interdisciplinary set of open-access, online journals, promising a paradigm shift from the current review, selection and dissemination processes in academic publishing. All Frontiers journals are driven by researchers for researchers; therefore, they constitute a service to the scholarly community. At the same time, the Frontiers Journal Series operates on a revolutionary invention, the tiered publishing system, initially addressing specific communities of scholars, and gradually climbing up to broader public understanding, thus serving the interests of the lay society, too.

Dedication to Quality

Each Frontiers article is a landmark of the highest quality, thanks to genuinely collaborative interactions between authors and review editors, who include some of the world's best academicians. Research must be certified by peers before entering a stream of knowledge that may eventually reach the public - and shape society; therefore, Frontiers only applies the most rigorous and unbiased reviews.
Frontiers revolutionizes research publishing by freely delivering the most outstanding research, evaluated with no bias from both the academic and social point of view. By applying the most advanced information technologies, Frontiers is catapulting scholarly publishing into a new generation.

What are Frontiers Research Topics?

Frontiers Research Topics are very popular trademarks of the Frontiers Journals Series: they are collections of at least ten articles, all centered on a particular subject. With their unique mix of varied contributions from Original Research to Review Articles, Frontiers Research Topics unify the most influential researchers, the latest key findings and historical advances in a hot research area! Find out more on how to host your own Frontiers Research Topic or contribute to one as an author by contacting the Frontiers Editorial Office: researchtopics@frontiersin.org

UNDERSTANDING AND MODULATING BONE AND CARTILAGE CELL FATE FOR REGENERATIVE MEDICINE

Topic Editors:
Roberto Narcisi, Erasmus MC, University Medical Center Rotterdam, Netherlands
Eric Farrell, Erasmus MC, University Medical Center Rotterdam, Netherlands

Citation: Narcisi, R., Farrell, E., eds. (2019). Understanding and Modulating Bone and Cartilage Cell Fate for Regenerative Medicine. Lausanne: Frontiers Media.
doi: 10.3389/978-2-88945-790-8

Table of Contents

frontiers in Bioengineering and Biotechnology

EDITORIAL
published: 28 January 2019
doi: 10.3389/fbioe.2019.00008

Editorial: Understanding and Modulating Bone and Cartilage Cell Fate for Regenerative Medicine

Roberto Narcisi[1]* *and Eric Farrell*[2]

[1] Department of Orthopedics, Erasmus MC, University Medical Center, Rotterdam, Netherlands, [2] Department of Oral and Maxillofacial Surgery, Special Dental Care and Orthodontics, Erasmus MC, University Medical Center, Rotterdam, Netherlands

Keywords: endochondral ossification, cartilage, bone, cell fate, mechanical loading, osteoarthritis

Editorial on the Research Topic

Understanding and Modulating Bone and Cartilage Cell Fate for Regenerative Medicine

With this research topic we provide an overview of the main tools regenerative medicine and stem cells research have to better understand and modulate bone and cartilage cell fate, both during natural healing processes and during the development of joint pathologies. Moreover, the contribution to the research topic with original research articles allow a further exploration toward the most advanced research in the field.

What is the role of mechanical loading to determine cell fate during bone development? How can we modulate biomaterial proprieties to drive cellular differentiation of stem cells toward cartilage and bone? What we can learn about bone and cartilage cell fate by following natural healing processes and osteoarthritis development? This Research Topic explores these and other crucial questions in the field of bone and cartilage regeneration, with the intention to trigger the development of new research lines and further increase of knowledge.

Scaffold manufacturing and specific types and regimes of mechanical stimulation are known to be essential for supporting and promoting cellular differentiation. Specifically, Hendrikson et al. show how different scaffold architectures have significant influence on stress and strain distribution, but also on the effective pore size and shape, which subsequently influence the fluid shear stress distribution. Angelozzi et al. discuss how the use of microfibrous alginate scaffolds containing gelatin or the more innovative urinary bladder matrix (UBM) are able to stimulate dedifferentiated chondrocyte to re-acquire their natural phenotype. Mesenchymal stem/progenitor cells (MSC) are often use to recapitulate the endochondral ossification process. For this reason Carroll et al. used MSC as a model to explore the role of cyclic tensile strain during their differentiation showing that this specific mechanical stimuli can play a role in promoting both intramembranous and endochondral ossification of MSC in a context-dependent manner. Dynamic mechanical compression is also one of the most used strategies to regulate cellular phenotype. However, as highlighted by Anderson and Johnstone, the lack of standardized methods and analysis to study chondrogenic differentiation and maintenance under this mechanical regimes make the comparison between the current literature difficult.

Understanding the role and the mechanism of action of endogenous bone and cartilage repair by progenitor cells is pivotal to increase the knowledge around endogenous progenitor cell function and therefore improve the development of tissue repair strategies. Lo Sicco and Tasso provide an

OPEN ACCESS

Edited by:
Ranieri Cancedda, Biorigen Srl., Italy

Reviewed by:
Mauro Alini, AO Foundation, Switzerland

***Correspondence:**
Roberto Narcisi
r.narcisi@erasmusmc.nl

Specialty section:
This article was submitted to Tissue Engineering and Regenerative Medicine, a section of the journal Frontiers in Bioengineering and Biotechnology

Received: *19 December 2018*
Accepted: *08 January 2019*
Published: *28 January 2019*

Citation:
Narcisi R and Farrell E (2019) Editorial: Understanding and Modulating Bone and Cartilage Cell Fate for Regenerative Medicine. Front. Bioeng. Biotechnol. 7:8. doi: 10.3389/fbioe.2019.00008

overview on the novel findings that impact bone fracture healing, with a particular focus on the role of inflammation, progenitor cell recruitment and their differentiation. Lozito TP's group, on the other hand, used the lizard tail regeneration model to determine the cellular origin of regenerated cartilage and muscle following tail loss, interestingly showing how cartilage cells can contribute to the regeneration of both muscle and cartilage tissue (Londono et al.).

In order to have a whole overview on endochondral fracture healing, Wong et al. reviewed the molecular pathways that (may) play a role in modulating cellular fate during endochondral fracture healing, Lesage et al. discussed the current methodologies to analyze cell differentiation during endochondral ossification using computational modeling and Javaheri et al. reviewed the interesting recent findings supporting the idea that hypertrophic chondrocytes have pluripotent capacity and may transdifferentiate into osteoblastic cells. To complete the overview on fracture healing, the group of Correa D proposed a comprehensive summary on tissue engineering strategies for fractures and bone defects, discussing not only the role of the cells but also the impact of the use of different biomaterials and grow factors to stimulate the healing process (Perez et al.).

Sometimes a pathological situation can be very useful to study physiological processes. Osteoarthritis (OA), a pathology of the diarthoroidal joints, is a diseased state where all the joint tissues are involved, leading to cartilage and bone changes. Raman et al. addressed the key inflammatory factors and the main epigenetic changes that occur in chondrocytes during OA and how we may be able to reverse them. In parallel, the group of Welting TJM discussed the current knowledge regarding the cartilage endochondral changes occurring during OA (Ripmeester et al.), overall covering most of the literature available in the field up to date. It is also interesting to observe how knowledge on the endochondral ossification process can also derive by the observation of physiological processes apparently non related to it. One great example are vascular diseases, such as atherosclerosis, where vascular calcification is observed, with many aspects of the process of endochondral ossification apparent. Leszczynska and Murphy reviewed this scenario focusing on the (circulating) cellular players contributing to form ectopic bone and cartilage during atherosclerosis.

The issues discussed in this Research Topic address several important biological aspects that determine the fate of cells in the cartilage and bone leading to the repair of damaged tissues or the onset of disease. Improving our understanding of these processes will allow us to further refine regenerative medicine based approaches to the treatment of many bone and cartilage related pathologies.

AUTHOR CONTRIBUTIONS

All authors listed have made a substantial, direct and intellectual contribution to the work, and approved it for publication.

FUNDING

RN is financially supported by a TTW Perspectief Grant: William Hunter Revisited from NWO (#P15-23). EF is financially supported by a European Union's Horizon 2020 research and innovation programme under the Marie Sklodowska-Curie grant agreement (#721432).

ACKNOWLEDGMENTS

The editors would like to thank all the authors that contributed to the research topic.

Conflict of Interest Statement: The authors declare that the research was conducted in the absence of any commercial or financial relationships that could be construed as a potential conflict of interest.

frontiers in Bioengineering and Biotechnology

ORIGINAL RESEARCH
published: 10 February 2017
doi: 10.3389/fbioe.2017.00006

Influence of Additive Manufactured Scaffold Architecture on the Distribution of Surface Strains and Fluid Flow Shear Stresses and Expected Osteochondral Cell Differentiation

*Wim J. Hendrikson[1], Anthony J. Deegan[2], Ying Yang[2], Clemens A. van Blitterswijk[1,3], Nico Verdonschot[4,5], Lorenzo Moroni[1,3] and Jeroen Rouwkema[4]**

[1] Department of Tissue Regeneration, MIRA Institute for Biomedical Technology and Technical Medicine, University of Twente, Enschede, Netherlands, [2] Institute for Science and Technology in Medicine, School of Medicine, Keele University, Stoke on Trent, UK, [3] Complex Tissue Regeneration Department, MERLN Institute for Technology Inspired Regenerative Medicine, University of Maastricht, Maastricht, Netherlands, [4] Department of Biomechanical Engineering, MIRA Institute for Biomedical Technology and Technical Medicine, University of Twente, Enschede, Netherlands, [5] Orthopaedic Research Laboratory, Radboud Nijmegen Medical Centre, Nijmegen, Netherlands

OPEN ACCESS

Edited by:
Eric Farrell,
Erasmus University Rotterdam, Netherlands

Reviewed by:
Dimitrios I. Zeugolis,
National University of Ireland Galway, Ireland
Antonella Motta,
University of Trento, Italy

***Correspondence:**
Jeroen Rouwkema
j.rouwkema@utwente.nl

Specialty section:
This article was submitted to Tissue Engineering and Regenerative Medicine, a section of the journal Frontiers in Bioengineering and Biotechnology

Received: 18 November 2016
Accepted: 23 January 2017
Published: 10 February 2017

Citation:
Hendrikson WJ, Deegan AJ, Yang Y, van Blitterswijk CA, Verdonschot N, Moroni L and Rouwkema J (2017) Influence of Additive Manufactured Scaffold Architecture on the Distribution of Surface Strains and Fluid Flow Shear Stresses and Expected Osteochondral Cell Differentiation. Front. Bioeng. Biotechnol. 5:6. doi: 10.3389/fbioe.2017.00006

Scaffolds for regenerative medicine applications should instruct cells with the appropriate signals, including biophysical stimuli such as stress and strain, to form the desired tissue. Apart from that, scaffolds, especially for load-bearing applications, should be capable of providing mechanical stability. Since both scaffold strength and stress–strain distributions throughout the scaffold depend on the scaffold's internal architecture, it is important to understand how changes in architecture influence these parameters. In this study, four scaffold designs with different architectures were produced using additive manufacturing. The designs varied in fiber orientation, while fiber diameter, spacing, and layer height remained constant. Based on micro-CT (μCT) scans, finite element models (FEMs) were derived for finite element analysis (FEA) and computational fluid dynamics (CFD). FEA of scaffold compression was validated using μCT scan data of compressed scaffolds. Results of the FEA and CFD showed a significant impact of scaffold architecture on fluid shear stress and mechanical strain distribution. The average fluid shear stress ranged from 3.6 mPa for a 0/90 architecture to 6.8 mPa for a 0/90 offset architecture, and the surface shear strain from 0.0096 for a 0/90 offset architecture to 0.0214 for a 0/90 architecture. This subsequently resulted in variations of the predicted cell differentiation stimulus values on the scaffold surface. Fluid shear stress was mainly influenced by pore shape and size, while mechanical strain distribution depended mainly on the presence or absence of supportive columns in the scaffold architecture. Together, these results corroborate that scaffold architecture can be exploited to design scaffolds with regions that guide specific tissue development under compression and perfusion. In conjunction with optimization of stimulation regimes during bioreactor cultures, scaffold architecture optimization can be used to improve scaffold design for tissue engineering purposes.

Keywords: FEA, CFD, additive manufacturing, scaffold architecture, tissue engineering, cell differentiation

INTRODUCTION

In the field of tissue engineering, a scaffold can be used to provide a temporary or permanent support structure for cells to form a tissue. In the specific case of musculoskeletal regeneration, a general tenet is the need for a scaffold design capable of withstanding load-bearing forces. From literature, it is known that scaffold architecture influences the apparent stiffness of the scaffold (Moroni et al., 2006a,b). The scaffold design can, for instance, be tailored to match the mechanical properties of native tissues (Moroni et al., 2006a). However, since changing scaffold architecture will change stress and strain distributions within the scaffolds during bioreactor cultures under compression and perfusion conditions, it is important to understand the relationship between scaffold design and biophysical signals (Guilak et al., 2014).

It is becoming clear that cells are sensitive to deformations within their environment and adjust their behavior accordingly (Brown and Discher, 2009; Wang et al., 2009; Buxboim et al., 2010). A number of mechano-regulation theories exist that relate the biophysical stimuli to specific tissue formation (Pauwels, 1960; Carter et al., 1988; Prendergast et al., 1997; Claes and Heigele, 1999). By predicting the stress and strain distribution in a scaffold using finite element analysis (FEA), and coupling this with cell differentiation and tissue formation (Byrne et al., 2007; Checa and Prendergast, 2010; Milan et al., 2010; Sandino and Lacroix, 2011), these theories can be used to optimize scaffold design parameters, such as the type of biomaterial, porosity, and architecture. Most mechano-regulation theories reported in literature are based on a model proposed by Prendergast (Lacroix and Prendergast, 2002). With the aid of FEA, this mechano-regulation theory has been used extensively to predict bone healing in multiple settings (Isaksson et al., 2006; Checa et al., 2011) and also to investigate the effect of scaffold properties on tissue formation in hypothetical (Byrne et al., 2007) and computer aided design (CAD)-based models of additive manufactured scaffolds (Olivares et al., 2009) in a tissue engineering setting.

Byrne et al. (2007) used the mechano-regulation theory of Prendergast to investigate the effect of scaffold design on tissue formation. They showed that the Young's modulus, porosity, and dissolution rate of the scaffold were influential on cell differentiation and tissue formation in the scaffold. Olivares et al. (2009) investigated the effects of porosity, and pore shape and size on cell differentiation stimulus values using two variations of regular scaffold architectures. This study also showed a strong relationship between pore size and porosity, and cell differentiation stimulus, but acknowledged the pore shape to be as important.

Even though it has been shown that pore shape within a scaffold has a large effect on stress and strain distribution, a CAD-based finite element model (FEM) is generally not able to capture the stress and strain distribution in actual scaffolds due to variations in scaffold architecture inherent to most fabrication processes (Hendrikson et al., 2014). This means that FEMs should be based on micro-CT (μCT) scans of actual scaffolds to obtain accurate representations of the pore shapes to investigate the effect of scaffold architecture on cell differentiation stimulus.

Previous studies on the prediction of tissue formation based on μCT scans have been performed for salt-leached scaffolds (Checa and Prendergast, 2010; Milan et al., 2010; Sandino and Lacroix, 2011). It proved to be valuable in showing the influence of pore shape on stress and strain distributions. Yet, the salt leaching fabrication process makes it difficult to control pore size, shape, and porosity and obtain reproducible scaffolds, thereby rendering it a suboptimal method to investigate the influence of scaffold architecture on cell behavior.

Additionally, mechano-regulation models reported in literature are based on volumetric strains. However, at the initial stage of cell differentiation, the cell is attached to the scaffold surface. Since cells can only sense deformations up to a small distance (Sen et al., 2009; Buxboim et al., 2010), a model using surface strains instead of volumetric strains will provide a better representation of the initial signals that cells seeded on a scaffold will experience. We have shown previously for a single scaffold architecture that the predicted strain for the scaffold material volume is considerably higher than the predicted strain for the scaffold surface on which cells are attached (Hendrikson et al., 2014), indicating that most current models overestimate the mechanobiological signals that cells experience.

In this study, additive manufacturing (AM) was used to produce scaffolds with four different scaffold designs. AM ensures a high controllability and reproducibility of the scaffold architecture, so that fiber diameter, fiber spacing, and layer thickness were constant across the different designs. By changing the angle of layer deposition and shifting layers laterally, different architectures were obtained. Most notably, designs where the layers were not shifted laterally contained crossing fibers at the same position in each layer. This created vertical supporting columns for the load. In designs where layers were shifted laterally, the locations of crossing fibers in successive layers varied, resulting in the absence of supporting columns. In order to investigate the effect of scaffold architecture on stress and strain distribution and subsequently cell differentiation stimulus prediction, μCT-based models of the scaffolds were prepared, and stress and strain distributions within the scaffolds were predicted using computational fluid dynamics (CFD) and FEA.

The goal of this study was to investigate the influence of additive manufactured scaffold architecture on the distribution of surface strains and fluid flow shear stresses within the scaffold, and subsequently the expected cell differentiation. The results show a distinct effect of the scaffold architecture on surface strains and fluid flow shear stresses under mechanical compression and imposed fluid flow. As reported before, the octahedral shear strain magnitudes exceed the surface shear strain magnitudes, which are reflected in the cell differentiation stimulus values on the scaffold surface. The results of the study show that regions of the scaffold could be designed favoring specific cell differentiation stimuli. Coupling with biophysical loading regimes *a priori in silico* could accelerate the design of scaffolds and optimize the loading regimes for tissue engineering purposes.

MATERIALS AND METHODS

Scaffold Fabrication

Scaffolds were fabricated by a bioscaffolder (SYSeng, Germany), as previously described (Hendrikson et al., 2014). Briefly, granules of the block copolymer 300PEOT55PBT45 (PolyVation B.V.) were heated to 190–200°C. An applied nitrogen pressure of 5 bar and an auger screw rotating at 200 RPM extruded the molten polymer through a 250 μm inner diameter needle (DL technology) on a stationary platform. Scaffolds were fabricated through layer-by-layer deposition, in which the angle between layers, fiber spacing, and layer thickness can be set. A scaffold block of 30 mm × 30 mm × 2.1 mm was created for four different architectures (Figure S1 in Supplementary Material). All architectures had a fiber spacing of 1,000 μm and a layer thickness of 150 μm. The 0/90 architecture had a 90° angle between successive layers, while the 0/45 had a 45° angle between layers. The 0/90 offset and 0/45 offset had the same parameters as the 0/90 and 0/45 architectures, respectively, but the layers with the same fiber direction were shifted 500 μm in the lateral direction of subsequent layers creating a staggered architecture. Cylindrical scaffolds of 8 mm in diameter were obtained by using a biopsy puncher (Miltex). The actual fiber diameter, spacing, and layer height were measured from μCT images in the freeware program MicroView 2.1.2. Five measurements were taken at different random locations for each scaffold, and the average and SD were calculated. The porosity was determined for the whole scaffold and the selection of the scaffold used to make the model. The porosity was calculated as the ratio of the material volume to the total volume, as determined by MicroView.

μCT Scanning

Scaffolds were scanned with a Scanco μCT 40 (Scanco Medical, Sweden) in a custom designed holder with which a fixed compression can be applied, as previously described (Baas and Kuiper, 2008). Briefly, a scaffold was placed in a cylinder and compressed by a piston that was fixated in position by two screws. The compression was displacement controlled by using a Bose Electroforce 3200. Scaffolds were scanned with or without a 10% compression applied. The energy used was 55 kV, with an intensity of 145 μA, an integration time of 1.5 s, and 1,000 projections per 180°. Voxel sizes were 10 μm × 10 μm × 10 μm for all scans performed. Scans were exported as DICOM for further processing to FEA and CFD meshes.

Meshes for FEA and CFD

In order to limit the number of finite elements and therefore to be able to compare the simulated deformation with the compression-scanned deformation, all scans of the uncompressed scaffolds were downsampled to a voxel size of 20 μm × 20 μm × 10 μm. The result was segmented for the material part to obtain a surface mesh of the whole scaffold. Remeshing was applied to improve the quality of the mesh and reduce the number of finite elements in order to simulate the whole scaffold with FEA.

In order to investigate the influence of scaffold architecture on tissue stimulus predictions on the scaffold surface, a region-of-interest was selected from the center of the scaffold consisting of at least two pores in the lateral directions and nine layers in the vertical direction. Fluid flow inlets were added on top and below the scaffold by expanding the selection in the vertical direction with a 100 μm void on both sides. The results were exported as DICOM to Mimics (Materialise) and segmented with the material as scaffold and the void as fluid volume. Remeshing was applied to improve the quality of the meshes.

FEA and CFD Setup

Linear elastic and isotropic material properties of 300PEOT55PBT45 were taken from literature, for which a bulk Young's modulus of 88 MPa (Sakkers et al., 1998) and a Poisson's ratio of 0.48 (Moroni et al., 2006a) were considered. An unconfined compression was simulated in Marc Mentat 2014 (MSC software). The FEM was placed between two dies from which the top die applied the 10% compression. The bottom nodes of the model were fixed in the loading direction. Additionally, two corner nodes at the bottom were fixed in either the *X*-direction or the *Y*-direction along the *Y*-axis or *X*-axis, respectively, to prevent rotation of the FEM while allowing for lateral expansion.

The boundary conditions for CFD, fluid inlet, zero pressure outlet, and no slip at the boundary wall were assigned to the fluid volume mesh in Mimics simulating a close fit of the scaffold in a bioreactor. CFD simulations were performed in Fluent 13.0 (ANSYS) with a fluid velocity of 100 μm/s. The fluid was modeled as an incompressible Newtonian fluid based on culture medium properties, with a density of 1,000 kg/m^3 and a viscosity of 1.45×10^{-3} Pa s (Bacabac et al., 2005).

Simulations

Validations

For the validation between the scanned and simulated compression of the scaffold, the deformed mesh of the FEM from the complete scaffold was exported. In Mimics, the meshes were superimposed for their fit and visually assessed for their similarities.

Differentiation Stimulus

A custom-made MATLAB script identified the shared surface faces of the CFD and FEA models. A Fortran subroutine with user code was written and executed during an FEA simulation by Marc Mentat to calculate the surface strains; the strains of the element face lying on the surface of the material FEM (Hendrikson et al., 2014). The octahedral shear strains were also calculated for the same elements. The surface and octahedral shear strain were defined as

$$\gamma_{surf} = \frac{\varepsilon_1 - \varepsilon_2}{2} \tag{1}$$

with ϵ_1 and ϵ_2 the principal strains of the element face on the surface (Figure S2A in Supplementary Material).

$$\gamma_{oct} = \frac{2}{3}\sqrt{\left(\varepsilon_I - \varepsilon_{II}\right)^2 + \left(\varepsilon_{II} - \varepsilon_{III}\right)^2 + \left(\varepsilon_{III} - \varepsilon_I\right)^2} \tag{2}$$

with ϵ_I, ϵ_{II}, and ϵ_{III} the principal strains at the integration point of the same element (Sandino and Lacroix, 2011) (Figure S2B in Supplementary Material).

Identification of the shared element faces enabled the visualization of the CFD simulation results on the material model in Marc Mentat. CFD simulation results were used to link the biophysical stimuli with cell differentiation throughout the FEA simulation through an adapted version of the mechano-regulation theory of Prendergast (Lacroix and Prendergast, 2002).

$$S = \frac{\gamma}{a} + \frac{\tau}{b}. \quad (3)$$

The fluid flow was substituted with the fluid wall shear stress τ (Sandino and Lacroix, 2011) as calculated by Fluent, with γ either the surface shear strain or the octahedral shear strain. Constants a and b were chosen as 0.0375 and 0.010 Pa, respectively, as reported in literature (Olivares et al., 2009; Sandino and Lacroix, 2011). The cell stimulus value (S) thresholds used for cell differentiation were $0 \leq S < 0.001$ for resorption, $0.001 \leq S < 1$ for bone, $1 \leq S < 3$ for cartilage, $3 \leq S < 6$ for fibrous tissue (FBT), and $S \geq 6$ for necrosis (Olivares et al., 2009; Sandino and Lacroix, 2011).

RESULTS

Scaffold Characterization

The experimentally determined fiber spacing and layer thickness was similar for scaffolds of all prepared geometries (**Table 1**). The measured fiber diameter was slightly smaller for the 0/45 offset geometry, which could be due to the larger unsupported gaps these fibers have to span in this conformation, leading to local variations in the fiber thickness. A slight variation in the porosity of the printed scaffolds was observed, ranging from 64% for the 0/45 offset geometry to 74% for the 0/45 geometry. The porosity of the FEMs correlated well with the printed scaffolds.

Model Validation

To validate the FEA simulation, a FEM was made for both the compressed and non-compressed μCT-scanned scaffold using the same methodology. The compression-simulated FEM was exported and superimposed on the compression scanned FEM in Mimics. Ideally, the compression-simulated FEM would overlap perfectly with the FEM prepared based on the compressed μCT-scanned scaffold. A visual fit of the simulated and compressed model for the different architectures is shown in **Figure 1** for the 0/90, 0/90 offset, and 0/45 offset architectures. There is a high degree of overlap between the simulated and compressed models for the different architectures, showing that the FEA simulation replicates the compression of the scaffolds well. Small differences were mainly seen in the compression direction.

TABLE 1 | Scaffold measurements based on μCT scans.

Architecture	Fiber diameter (μm)	Fiber spacing (μm)	Layer thickness (μm)	Porosity scaffold % (porosity model %)
0/45	194 ± 11	992 ± 21	151 ± 3	74.4 (72.6)
0/45 offset	214 ± 5	982 ± 21	151 ± 4	64.1 (63.6)
0/90	212 ± 13	990 ± 20	150 ± 13	66.3 (62.4)
0/90 offset	222 ± 13	982 ± 13	151 ± 3	68.5 (67.0)

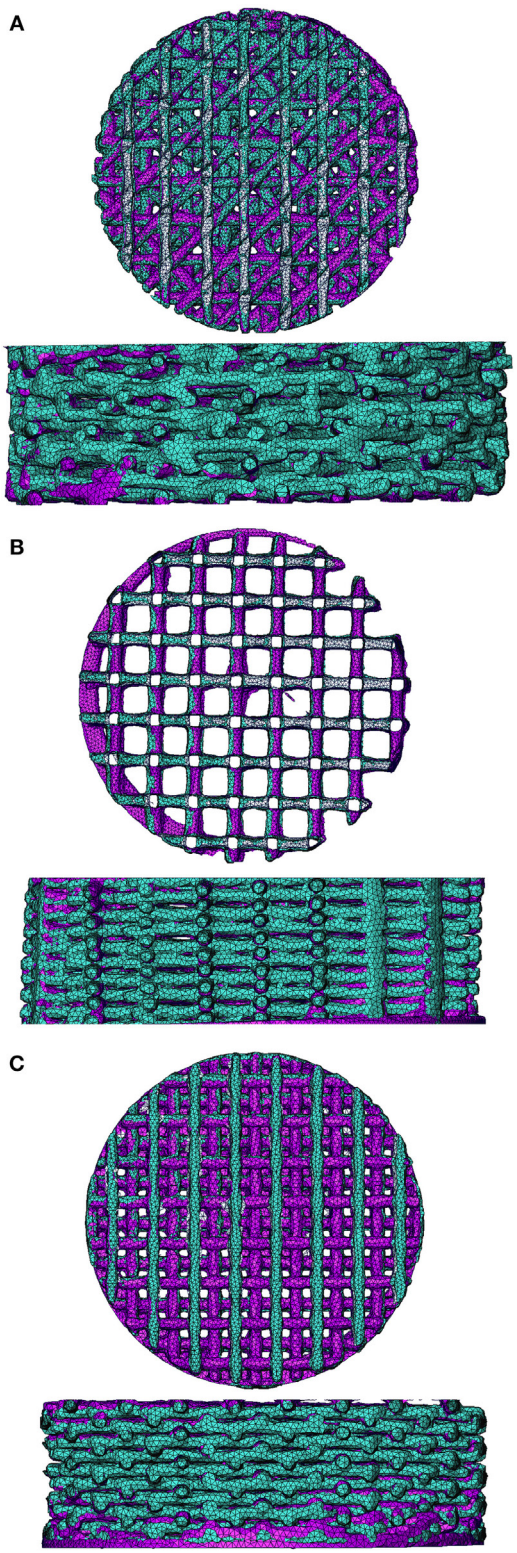

FIGURE 1 | Superimposed image of compression-scanned (pink) and compression-simulated (green) scaffolds for 0/45 offset (A), 0/90 (B), and 0/90 offset (C) architectures shows good overlap. The 0/45 architecture is omitted due to lack of pre- and post-compression scans of the same scaffold.

FEA Simulation

Using FEA simulation, FEMs of the different architectures were subjected to a compressive strain of 10%. For the 0/90 and 0/45 scaffolds, the strain was confined to the area where the fibers cross and minimally extends along the fiber. In the 0/90 offset and 0/45 offset, the strain also developed at the crossing of the fibers but extended further (**Figure 2**; Figure S3 in Supplementary Material). The fraction of the surface area affected by the mechanical compression was, therefore, higher for the offset architectures. For the 0/90 architecture, the strain magnitudes were higher compared to its offset architecture counterpart while the strain magnitudes for 0/45 offset were higher than the 0/45 architecture (**Table 2**; **Figure 2I**). For all architectures, the average strain magnitudes were higher for the octahedral shear strain than for the surface strain (0.076 and 0.021, respectively, for 0/90, 0.028, and 0.0096, respectively, for 0/90 offset, 0.035 and 0.011, respectively, for 0/45, and 0.053 and 0.017, respectively, for 0/45 offset).

CFD Simulation

The fluid wall shear stress magnitude was highest on the lateral sides of the fibers in all architectures (**Figure 3**). The mean magnitude of shear stress was highest for the architectures with the offset (**Table 2**), while it was the lowest for the 0/90 scaffold. The shear stress histogram (**Figure 3E**) showed a higher frequency of higher shear stress magnitudes for the 0/45 offset (yellow) and 0/90 offset (blue), while it showed a higher frequency of the lower shear stress magnitudes for the 0/90 (green) and 0/45 (red) scaffold. In the 0/90 scaffold, the top fibers shielded the lower fibers from shear stress along the top side of the fiber. For the 0/90 offset scaffold, the shielding effect was reduced. The shielding could be seen to a lesser extent in the 0/45 and 0/45 offset scaffolds. Additional models using different fluid flow velocities showed that the magnitudes of the shear stress depended on fluid flow velocity, but that the shear stress distributions were independent on inlet fluid velocities (data not shown).

Cell Differentiation Stimulus Prediction on the Surface

For the prediction of cell differentiation stimuli, a current mechano-regulation theory was applied relating the shear strain and fluid flow shear stress with cell differentiation. As expected given the methodology, prediction of the cell differentiation stimulus

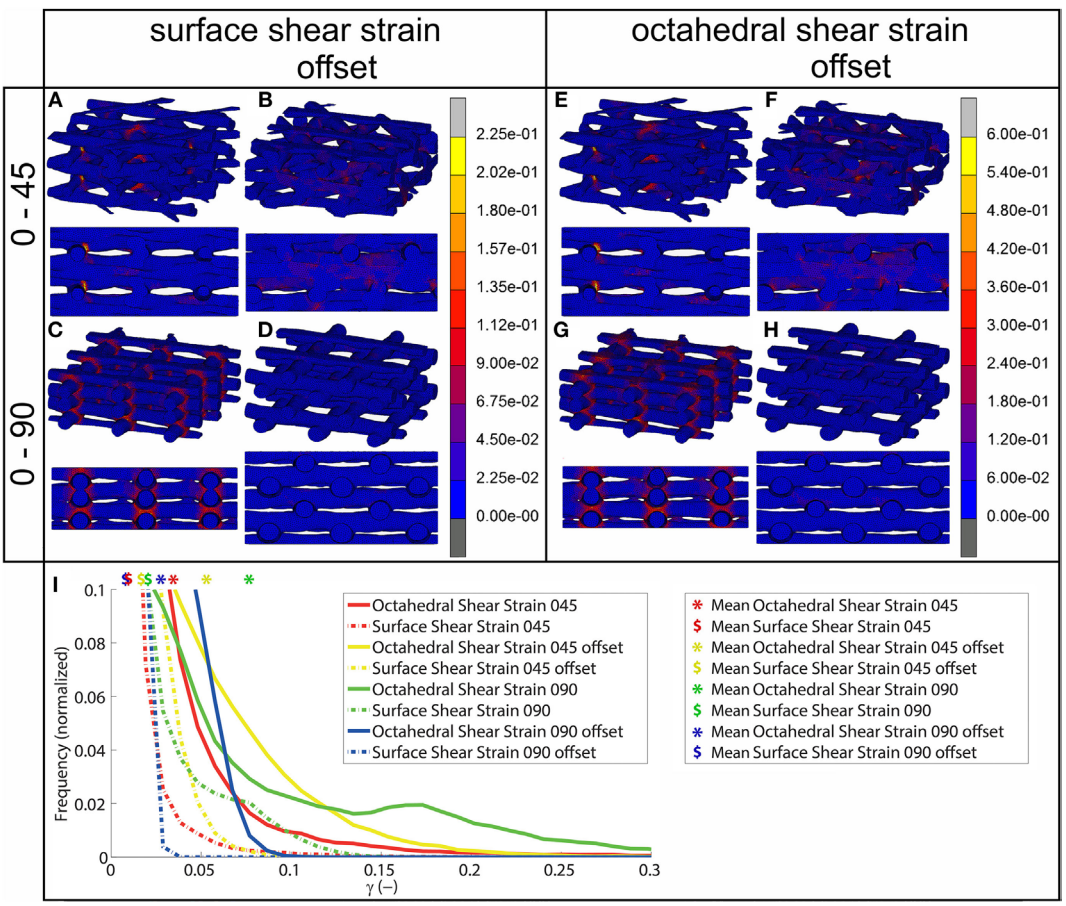

FIGURE 2 | Shear strain distribution of 0/45 (A,E), 0/45 offset (B,F), 0/90 (C,G), and 0/90 offset (D,H) architectures for surface shear strain (A–D) and octahedral shear strain (E–H) and histogram of the shear strains developed (I) after 10% compression applied. Both trimetric and side views are shown. For a better appreciation of the strain profile in the 0/90 offset geometry, the reader is referred to Figure S3 in Supplementary Material, which shows the strain distributions using a different color scale.

TABLE 2 | Average mechanical shear strains and fluid flow shear stresses.

Architecture	Surface shear strain (–)	Octahedral shear strain (–)	Fluid wall shear stress (mPa)
0/45	0.0110	0.0350	4.4
0/45 offset	0.0166	0.0531	5.6
0/90	0.0214	0.0756	3.6
0/90 offset	0.0096	0.0276	6.8

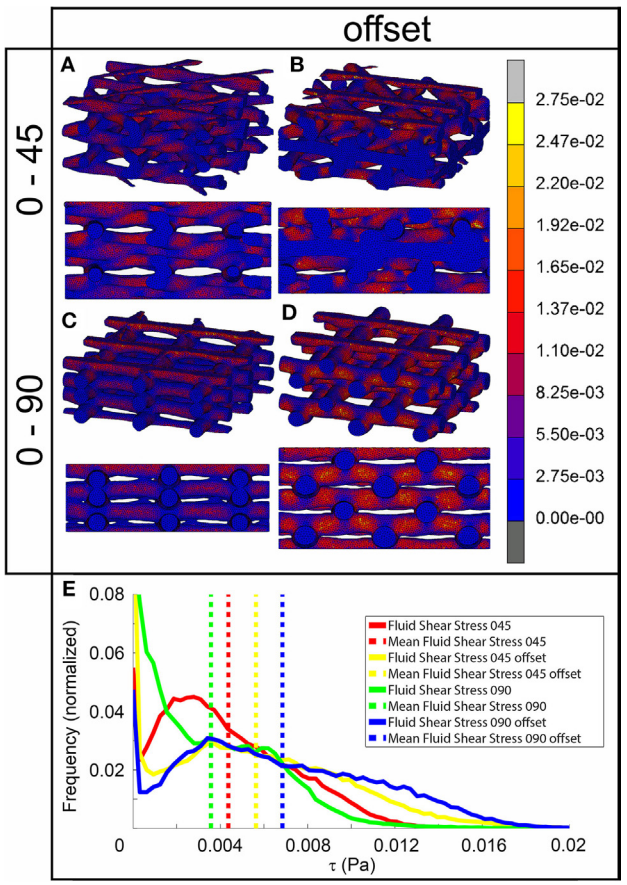

FIGURE 3 | Fluid shear stress distribution of 0/45 (A), 0/45 offset (B), 0/90 (C), and 0/90 offset (D) architectures and histogram of the fluid shear stresses developed (E) with a 100 μm/s inlet fluid velocity. Both trimetric and side views are shown.

based on the surface shear strain with mechanical compression alone showed a profile similar to the strain distribution (**Figures 2**, **4** and **5**). At the crossings of fibers, higher stimulus values were found resulting in cartilage for all but the 0/90 offset architecture, while in the 0/45 and 0/90 scaffolds patches of FBT were predicted (**Figure 6**). The 0/90 offset predicted bone formation and even some resorption for the 10% applied compression. However, the cell differentiation prediction based on the octahedral shear strain showed 63% cartilage in the 0/90 offset. For the 0/45 and 0/90 architectures, all stimulus values were increased and even showed considerable amounts of necrotic stimulus values.

The cell differentiation prediction stimulus based on fluid wall shear stress shows high similarities with the shear stress distribution (**Figures 3**–**5**). In the 0/45 and 0/90 scaffolds, bone and small amounts of cartilage for a fluid velocity up to 100 μm/s were predicted. However, for the 0/45 offset and especially for the 0/90 offset, cartilage was predicted already at 75 μm/s (data not shown) and showed a considerable amount of this tissue at 100 μm/s; 15 and 25%, respectively (**Figure 6**).

When the cell differentiation prediction was based on a combination of surface shear strain and fluid shear stress, the effects of 10% mechanical compression and 100 μm/s fluid velocity were additive. Within the 0/45 scaffold, the amount of cartilage increased from 4 to 21%, and small patches of FBT were predicted (4%). However, with the octahedral shear strain, besides more cartilage (51%), also necrotic tissue was predicted (2%) (**Figure 6**). The 0/45 offset showed a higher prediction for the amount of cartilage with the octahedral shear strain (46 vs 59%), while more fibrous (14%) and necrotic (3%) cell stimuli values were also predicted. For the 0/90 scaffold, more cartilage and FBT were predicted with the octahedral shear strain compared to the surface strain (33 and 1% vs 45 and 13%, respectively). With the octahedral shear strain, significant amounts of necrotic tissue (15%) were also predicted. In the 0/90 offset, the amount of cartilage predicted increased with both shear strains (from 25% without strain to 43% and 63% with surface strain or octahedral strain, respectively) while with octahedral shear strain, some FBT was also predicted (3%).

DISCUSSION

In tissue engineering, scaffolds designed for load-bearing applications should provide an environment that is capable of withstanding the forces that arise during the daily activities of a patient. In addition, the scaffold should provide differentiation stimuli to cells to ensure optimal tissue development. An important stimulus in this aspect is the dynamic mechanical environment that a scaffold can offer to the cells residing on the scaffold (Martin et al., 2004; Janssen et al., 2006; Koch et al., 2010; Sinha et al., 2015). By adapting the scaffold architecture, different stress and strain distributions can be achieved resulting in different cell differentiation stimuli for different architectures. In this paper, four scaffold designs were used, which only differed in the pore shape by using the same fiber diameter, spacing, porosity, and layer thickness. By changing the layer orientation, the effect of scaffold architecture on the stress and strain distribution, and subsequently the cell differentiation stimulus, was investigated. Measurements of fiber diameter, spacing, and layer thickness from the μCT scans showed similar values across all the architectures. As for the measured porosity, the values were slightly higher for the 0/45 architecture and slightly lower for the 0/45 offset architecture. Even though this will have an effect on the absolute strain values, strain distribution profiles are less likely to be directly affected by small differences in porosity values. The derived FEM from the respective scaffold showed the same porosities, indicating that a representative FEM was obtained for each architecture. Taken together, these results showed that the orientation angle

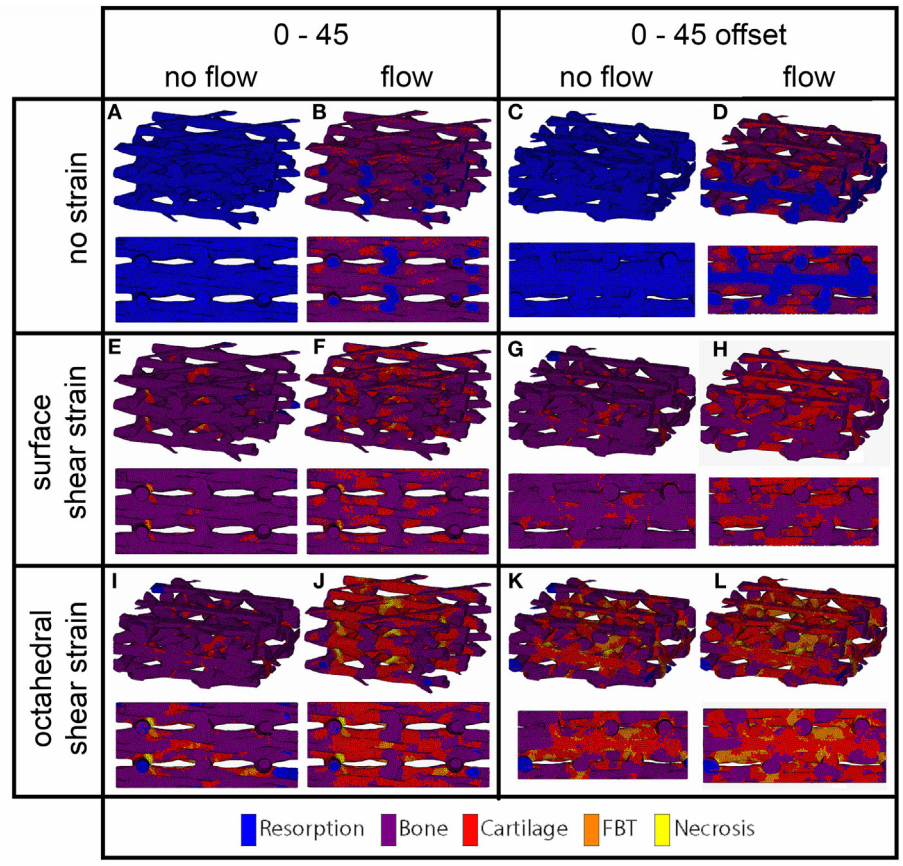

FIGURE 4 | Cell differentiation stimulus distribution for 0/45 (A,B,E,F,I,J) and 0/45 offset (C,D,G,H,K,L) architectures based on fluid flow alone (B,D), surface shear strain alone (E,G), octahedral shear strain alone (I,K), fluid flow and surface shear strain (F,H), fluid flow and octahedral shear strain (J,L) for an imposed fluid flow of 100 μm/s and 10% compression. Both trimetric and side views are shown.

between layers was the main variable across the four different scaffolds.

Using a device previously reported by Baas and Kuiper (2008), scaffolds were fixed at a compression of 10% and subsequently scanned. FEMs of the same complete scaffold were simulated to the same 10% compression. The simulated FEM was subsequently superimposed on the compressed scaffold scan in order to validate the simulation results (**Figure 1**). Small differences were visible mainly in the compression direction, which could be due to the scaffold not being positioned perfectly flat on the supporting surface during compression. Unfortunately, applying the same mesh mapping on both the compressed scaffold and FEM was not possible, and, therefore, no value for the correctness of the fit could be determined (Narra et al., 2015). However, comparison of the μCT scans with the FEA results showed a high degree of correlation, thus indicating that the results of the FEA are valid.

Upon mechanical compression of the scaffolds, strains mainly developed at the crossing of fibers. Both the magnitude of the strain and the surface area affected by the mechanical compression were influenced by the scaffold architecture (**Figure 2**). In the 0/90 and 0/45 scaffolds, the crossings of the fibers were located at the same position in each layer creating a vertical supporting column for the load. When looking at a 2 × 2 pore section of the scaffolds, the 0/90 architecture has nine of these vertical supporting columns, while the 0/45 architecture has six. Therefore, the 0/45 offers less support for the load which resulted in higher strain magnitudes in this architecture. Additionally, because of the columns, the surface area that was affected by the mechanical compression was confined to a small area around the crossing of the fibers. In the 0/45 offset and 0/90 offset architectures, vertical supporting columns were absent, resulting in a larger surface area affected by the mechanical compression. This was accompanied by strain magnitudes, which were lower in the case of the 0/90 offset architecture but higher in the case of the 0/45 offset architecture. Even though the higher values for the 0/45 offset architecture may be partially explained by the slightly lower porosity of this architecture in comparison with 0/45, this shows that the strain distribution is highly dependent on the scaffold architecture and that average strain values are inversely related to the fraction of the scaffold that actively carries the load. The dependence of strain profiles on the scaffold pore architecture is in line with previous literature (Sandino et al., 2008; Olivares et al., 2009; Milan et al., 2010). However, by investigating the

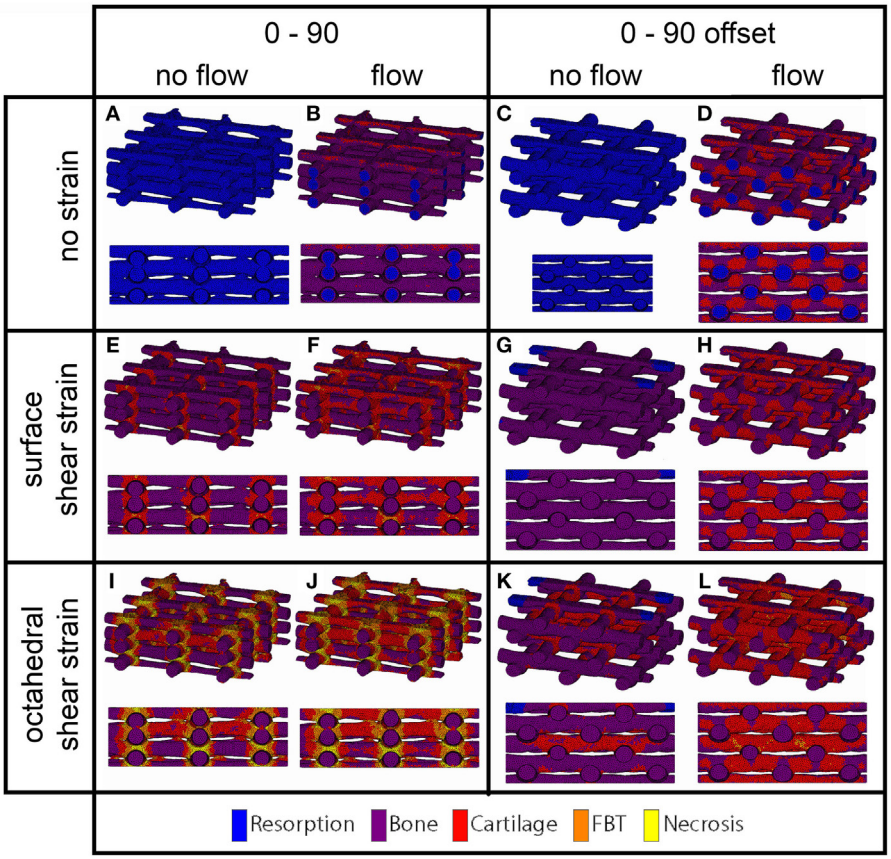

FIGURE 5 | **Cell differentiation stimulus distribution for 0/90 (A,B,E,F,I,J) and 0/90 offset (C,D,G,H,K,L) architectures based on fluid flow alone (B,D), surface shear strain alone (E,G), octahedral shear strain alone (I,K), fluid flow and surface shear strain (F,H), fluid flow and octahedral shear strain (J,L) for an imposed fluid flow of 100 μm/s and 10% compression**. Both trimetric and side views are shown.

strains that were developed on the scaffold surface, this study provides a better understanding of the exact mechanical signals that the cells attached to the scaffold surface experience.

In addition to strain values, the results of fluid flow analysis also depended on the pore shape (**Figure 3**). In all architectures, the fluid flow acted mainly at the sides of the fibers. Fibers located closest to the fluid inlet shielded the fibers in the lower layers from fluid flow and thus fluid shear stress. This was especially apparent in the 0/90 architecture. This means that the average shear stress values reported depend on the number of fiber layers included in the CFD model. For all architectures, the effective pore shape and size dictated the shear stress magnitude. The 0/90 architecture had effectively the largest pore size and, therefore, the lowest fluid shear stresses. On the other hand, the 0/90 offset had effectively the smallest pore size resulting in the highest shear stresses throughout the scaffold. For the 0/45 and 0/45 offset architectures, the offset of the fibers effectively reduced the pore size and shape, which increased the fluid shear stresses. Both scaffolds had shear stress magnitudes, which were in between the values for the 0/90 and 0/90 offset architectures. Comparing our results with literature, similar shear stress magnitudes with a 100 μm/s fluid velocity can be inferred (Milan et al., 2009). Also, Olivares et al. (2009) showed that the shear stress distribution and the magnitude of the stresses depended on the pore shape architecture, which corroborates our findings.

In order to determine the effect of different stress and strain distributions on the potential cell differentiation in the initial stage of cell attachment and differentiation on the surface of a tissue engineering scaffold, an adaptation of the mechano-regulation theory of Prendergast was used. The original theory combines octahedral shear strains with fluid flow shear stresses to predict cell differentiation (Lacroix et al., 2002). However, since the octahedral shear strain is a strain that acts in the volume of a material, the original model is not able to correctly predict the behavior of cells that are seeded on the surface of a material. This study shows that for all scaffold architectures, the octahedral shear strain is higher than the surface shear strain, which means that current models available in literature overestimate the mechanical signals that cells experience when seeded on a scaffold surface, resulting in an incorrect prediction of the cellular response.

The higher shear strain values seen from the mechanical compression at the crossing of the fibers resulted in the prediction of more cartilage formation and in some cases FBT at these

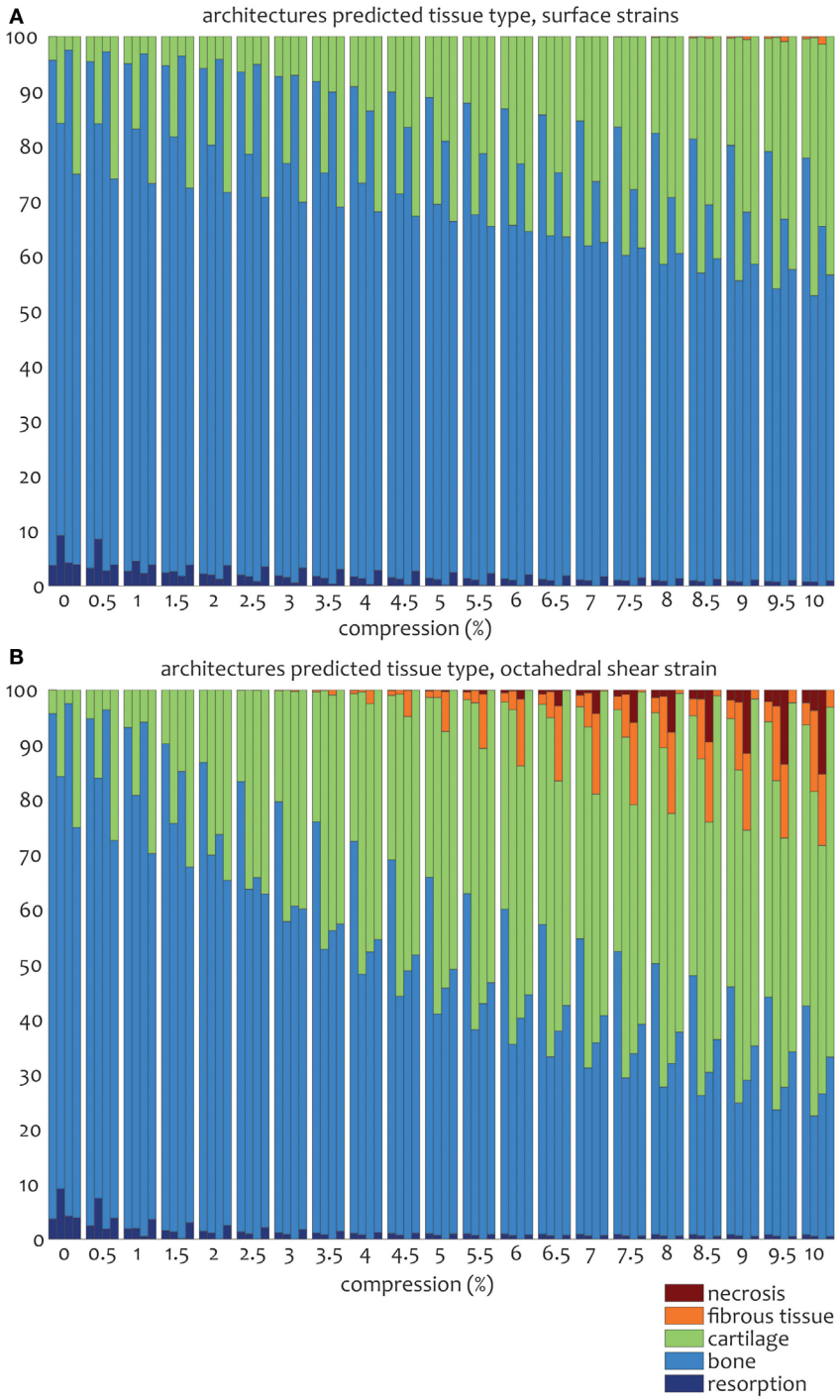

FIGURE 6 | Percentages of cell differentiation stimulus values on the surface of the scaffold for the 0/45 (left column), 0/45 offset (second to left column), 0/90 (third to left column), and 0/90 offset (fourth to left column) architectures based on the surface shear strain (A) and octahedral shear strain (B) for an imposed fluid flow of 100 μm/s and 10% compression.

locations. Large differences could be seen between the different scaffold architectures, depending on the strain magnitudes that were developed in the scaffolds. The influence of fluid flow on cell differentiation prediction correlated with fluid shear stress distributions. For the 0/90 offset architecture, the higher fluid shear stresses resulted in a larger amount of cartilage prediction, while predicted cartilage formation was lowest for the 0/90 architecture. The results from this study correlate well with a

study by Olivares et al. (2009). At an inlet velocity of 100 μm/s, they reported predicted percentages for cartilage differentiation ranging from 18 to 45% depending on the scaffold architecture. The higher amount of cartilage predicted by Olivares compared to our study can be linked to the lower porosity of some of the architectures studied by Olivares, which ranged from 55 to 70% compared to the approximate 70% porosity for the architectures used in our study.

The combination of fluid flow and mechanical compression on cell differentiation stimulus prediction showed that the scaffold architecture had an effect on the relative contribution of both mechanical stimuli on cell differentiation stimulus values. Even though **Figure 6** shows that stimulus values increase with an increasing applied compression for all geometries, this effect is relatively strong for the 0/90 geometry and relatively weak for the 0/90 offset geometry. This implies that in a geometry where compressive loads are distributed well over the scaffold volume, such as the 0/90 offset geometry, the relative effect of fluid perfusion on cell differentiation is increased. In a geometry where compressive loads are concentrated at specific locations due to supporting columns, high local stimulus values will arise as a result of compression, which means that the relative effect of compression on cell differentiation is high.

In this study, different software packages were used for the CFD and FEA simulations. Therefore, the effect of compression-induced fluid flow, as well as possible scaffold deformation due to fluid flow, cannot be taken into account. Although the fluid flow is low and can probably be neglected as a factor for scaffold deformation, the compression-induced fluid flow is likely to have a significant effect on cell differentiation predictions. When a total compression of 10% is applied, it is not unrealistic to assume that a significant fluid flow will occur due to this compression. Ideally, a coupled fluid-structure interaction model should be developed in order to address this aspect. However, these models are computationally very demanding, and it may be difficult to devise such a model for the complex geometries used in this study.

Finally, it should be noted that the scaffold architecture, and specifically the orientation of subsequent layers in scaffolds that are acquired using 3D fiber deposition, can have an effect on MSC cell differentiation even without external compression or fluid perfusion. A recent study by Di Luca et al. (2016) shows that in a gradient scaffold where the deposition pattern ranges from 0–90 to 0–15, squared pores support enhanced chondrogenic differentiation, whereas cells residing in the rhomboidal pores display enhanced osteogenic differentiation. This means that a model focusing solely on surface strains and fluid flow shear stresses is unlikely to provide a perfect prediction of cell differentiation and tissue development. Apart from that, the actual mechanical signals perceived by cells at the cellular level may be different from the values reported in this study. Zhao et al. (2015) used a multiscale model of an idealized CAD model and showed that the cellular placement on either the surface wall or bridging the scaffold pore has an effect on the signals experienced by the cell. Although the amount of cells placed were low and their morphology was not representative, the idea of using multiscale models to better estimate the local shear strain and stress perceived by cells is a valid one.

CONCLUSION

The results of this study show that the scaffold architecture has a significant influence on stress and strain distributions. In particular, removing the possibility of load bearing with solid structures spanning from the top to the bottom of the scaffold, or even reducing the amount of these structures in a scaffold, has a great effect on the strain distribution. Additionally, the different architectures result in differences in the effective pore size and shape, which subsequently influence the fluid shear stress distribution. Therefore, by only changing the angle of orientation, varying stress and strain distributions can be exploited to design scaffolds for specific applications. Although in this study the material properties are based on the polymer PEOT/PBT, this methodology can be used for different biomaterials with different mechanical properties. The possibilities to design a scaffold with desired stress and strain distribution are therefore vast. Coupling these models with bioreactor studies to experimentally determine cellular differentiation within scaffolds subjected to specific fluid perfusion and compression regimes can provide valuable insights in the design of scaffolds and culture conditions for osteochondral, bone and cartilage replacements.

AUTHOR CONTRIBUTIONS

WH, YY, LM, and JR designed the experiments. WH and AD conducted the experiments. WH, LM, and JR analyzed data and wrote the manuscript. All the authors discussed the results and revised the manuscript.

FUNDING

This study was funded by the Netherlands Institute of Regenerative Medicine (grant number FES0908) and by The Royal Society, International Exchange Scheme (grant number IE110288).

SUPPLEMENTARY MATERIAL

The Supplementary Material for this article can be found online at http://journal.frontiersin.org/article/10.3389/fbioe.2017.00006/full#supplementary-material.

FIGURE S1 | **The four architectures of the scaffolds with 0/45 (A), 0/45 offset (B), 0/90 (C), and 0/90 offset (D) layers**.

FIGURE S2 | **Circles of Mohr depicting the principal shear strain ϵ_1, ϵ_2 for the strains developed on the element face, which are used in Eq. 1 in this paper (A) and the principal strains ϵ_I, ϵ_{II}, and ϵ_{III} for the strains developed in the entire element which are used in Eq. 2 in this paper (B) lying on the surface of the model**.

FIGURE S3 | **Shear strain distribution of the 0/90 offset architecture for surface shear strain (A) and octahedral shear strain (B)**. Both trimetric and side views are shown.

REFERENCES

Baas, E., and Kuiper, J. (2008). A numerical model of heterogeneous surface strains in polymer scaffolds. *J. Biomech.* 41, 1374–1378. doi:10.1016/j.jbiomech.2008.01.018

Bacabac, R. G., Smit, T. H., Cowin, S. C., Van Loon, J. J., Nieuwstadt, F. T., Heethaar, R., et al. (2005). Dynamic shear stress in parallel-plate flow chambers. *J. Biomech.* 38, 159–167. doi:10.1016/j.jbiomech.2004.03.020

Brown, A. E. X., and Discher, D. E. (2009). Conformational changes and signaling in cell and matrix physics. *Curr. Biol.* 19, R781–R789. doi:10.1016/j.cub.2009.06.054

Buxboim, A., Ivanovska, I. L., and Discher, D. E. (2010). Matrix elasticity, cytoskeletal forces and physics of the nucleus: how deeply do cells 'feel' outside and in? *J. Cell. Sci.* 123, 297–308. doi:10.1242/jcs.041186

Byrne, D. P., Lacroix, D., Planell, J. A., Kelly, D. J., and Prendergast, P. J. (2007). Simulation of tissue differentiation in a scaffold as a function of porosity, Young's modulus and dissolution rate: application of mechanobiological models in tissue engineering. *Biomaterials* 28, 5544–5554. doi:10.1016/j.biomaterials.2007.09.003

Carter, D. R., Blenman, P. R., and Beaupré, G. S. (1988). Correlations between mechanical stress history and tissue differentiation in initial fracture healing. *J. Orthop. Res.* 6, 736–748. doi:10.1002/jor.1100060517

Checa, S., and Prendergast, P. J. (2010). Effect of cell seeding and mechanical loading on vascularization and tissue formation inside a scaffold: a mechano-biological model using a lattice approach to simulate cell activity. *J. Biomech.* 43, 961–968. doi:10.1016/j.jbiomech.2009.10.044

Checa, S., Prendergast, P. J., and Duda, G. N. (2011). Inter-species investigation of the mechano-regulation of bone healing: comparison of secondary bone healing in sheep and rat. *J. Biomech.* 44, 1237–1245. doi:10.1016/j.jbiomech.2011.02.074

Claes, L. E., and Heigele, C. A. (1999). Magnitudes of local stress and strain along bony surfaces predict the course and type of fracture healing. *J. Biomech.* 32, 255–266. doi:10.1016/S0021-9290(98)00153-5

Di Luca, A., Lorenzo-Moldero, I., Mota, C., Lepedda, A., Auhl, D., Van Blitterswijk, C., et al. (2016). Tuning cell differentiation into a 3D scaffold presenting a pore shape gradient for osteochondral regeneration. *Adv. Healthc. Mater.* 5, 1753–1763. doi:10.1002/adhm.201600083

Guilak, F., Butler, D. L., Goldstein, S. A., and Baaijens, F. P. (2014). Biomechanics and mechanobiology in functional tissue engineering. *J. Biomech.* 47, 1933–1940. doi:10.1016/j.jbiomech.2014.04.019

Hendrikson, W. J., van Blitterswijk, C. A., Verdonschot, N., Moroni, L., and Rouwkema, J. (2014). Modeling mechanical signals on the surface of microCT and CAD based rapid prototype scaffold models to predict (early stage) tissue development. *Biotechnol. Bioeng.* 111, 1864–1875. doi:10.1002/bit.25231

Isaksson, H., Wilson, W., van Donkelaar, CC, Huiskes, R., and Ito, K. (2006). Comparison of biophysical stimuli for mechano-regulation of tissue differentiation during fracture healing. *J. Biomech.* 39, 1507–1516. doi:10.1016/j.jbiomech.2005.01.037

Janssen, F. W., Oostra, J., Oorschot, Av, and van Blitterswijk, C. A. (2006). A perfusion bioreactor system capable of producing clinically relevant volumes of tissue-engineered bone: in vivo bone formation showing proof of concept. *Biomaterials* 27, 315–323. doi:10.1016/j.biomaterials.2005.07.044

Koch, M. A., Vrij, E. J., Engel, E., Planell, J. A., and Lacroix, D. (2010). Perfusion cell seeding on large porous PLA/calcium phosphate composite scaffolds in a perfusion bioreactor system under varying perfusion parameters. *J. Biomed. Mater. Res. A* 95, 1011–1018. doi:10.1002/jbm.a.32927

Lacroix, D., and Prendergast, P. J. (2002). A mechano-regulation model for tissue differentiation during fracture healing: analysis of gap size and loading. *J. Biomech.* 35, 1163–1171. doi:10.1016/S0021-9290(02)00086-6

Lacroix, D., Prendergast, P. J., Li, G., and Marsh, D. (2002). Biomechanical model to simulate tissue differentiation and bone regeneration: application to fracture healing. *Med. Biol. Eng. Comput.* 40, 14–21. doi:10.1007/BF02347690

Martin, I., Wendt, D., and Heberer, M. (2004). The role of bioreactors in tissue engineering. *Trends Biotechnol.* 22, 80–86. doi:10.1016/j.tibtech.2003.12.001

Milan, J.-L., Planell, J. A., and Lacroix, D. (2009). Computational modelling of the mechanical environment of osteogenesis within a polylactic acid–calcium phosphate glass scaffold. *Biomaterials* 30, 4219–4226. doi:10.1016/j.biomaterials.2009.04.026

Milan, J. L., Planell, J. A., and Lacroix, D. (2010). Simulation of bone tissue formation within a porous scaffold under dynamic compression. *Biomech. Model. Mechanobiol.* 9, 583–596. doi:10.1007/s10237-010-0199-5

Moroni, L., de Wijn, J. R., and van Blitterswijk, C. A. (2006a). 3D fiber-deposited scaffolds for tissue engineering: influence of pores geometry and architecture on dynamic mechanical properties. *Biomaterials* 27, 974–985. doi:10.1016/j.biomaterials.2005.07.023

Moroni, L., Poort, G., Van Keulen, F., de Wijn, J. R., and van Blitterswijk, C. A. (2006b). Dynamic mechanical properties of 3D fiber-deposited PEOT/PBT scaffolds: an experimental and numerical analysis. *J. Biomed. Mater. Res. A.* 78, 605–614. doi:10.1002/jbm.a.30716

Narra, N., Blanquer, S. B., Haimi, S. P., Grijpma, D. W., and Hyttinen, J. (2015). μCT based assessment of mechanical deformation of designed PTMC scaffolds. *Clin. Hemorheol. Microcirc.* 60, 99–108. doi:10.3233/CH-151931

Olivares, A. L., Marsal, E., Planell, J. A., and Lacroix, D. (2009). Finite element study of scaffold architecture design and culture conditions for tissue engineering. *Biomaterials* 30, 6142–6149. doi:10.1016/j.biomaterials.2009.07.041

Pauwels, F. (1960). Eine neue Theorie über den Einfluß mechanischer Reize auf die Differenzierung der Stützgewebe. *Anat. Embryol.* 121, 478–515.

Prendergast, P. J., Huiskes, R., and Søballe, K. (1997). Biophysical stimuli on cells during tissue differentiation at implant interfaces. *J. Biomech.* 30, 539–548. doi:10.1016/S0021-9290(96)00140-6

Sakkers, R. J., de Wijn, J. R., Dalmeyer, R. A., van Blitterswijk, C. A., and Brand, R. (1998). Evaluation of copolymers of polyethylene oxide and polybutylene terephthalate (polyactive): mechanical behaviour. *J. Mater. Sci. Mater. Med.* 9, 375–379. doi:10.1023/A:1013227428530

Sandino, C., and Lacroix, D. (2011). A dynamical study of the mechanical stimuli and tissue differentiation within a CaP scaffold based on micro-CT finite element models. *Biomech. Model. Mechanobiol.* 10, 565–576. doi:10.1007/s10237-010-0256-0

Sandino, C., Planell, J. A., and Lacroix, D. (2008). A finite element study of mechanical stimuli in scaffolds for bone tissue engineering. *J. Biomech.* 41, 1005–1014. doi:10.1016/j.jbiomech.2007.12.011

Sen, S., Engler, A. J., and Discher, D. E. (2009). Matrix strains induced by cells: computing how far cells can feel. *Cell. Mol. Bioeng.* 2, 39–48. doi:10.1007/s12195-009-0052-z

Sinha, R., Le Gac, S., Verdonschot, N., van den Berg, A., Koopman, B., and Rouwkema, J. (2015). A medium throughput device to study the effects of combinations of surface strains and fluid-flow shear stresses on cells. *Lab. Chip* 15, 429–439. doi:10.1039/C4LC01259C

Wang, N., Tytell, J. D., and Ingber, D. E. (2009). Mechanotransduction at a distance: mechanically coupling the extracellular matrix with the nucleus. *Nat. Rev. Mol. Cell Biol.* 10, 75–82. doi:10.1038/nrm2594

Zhao, F., Vaughan, T. J., and McNamara, L. M. (2015). Multiscale fluid–structure interaction modelling to determine the mechanical stimulation of bone cells in a tissue engineered scaffold. *Biomech. Model. Mechanobiol.* 14, 231–243. doi:10.1007/s10237-014-0599-z

Conflict of Interest Statement: The authors declare that the research was conducted in the absence of any commercial or financial relationships that could be construed as a potential conflict of interest.

frontiers in Bioengineering and Biotechnology

ORIGINAL RESEARCH
published: 13 June 2017
doi: 10.3389/fbioe.2017.00035

Dedifferentiated Chondrocytes in Composite Microfibers As Tool for Cartilage Repair

Marco Angelozzi [1], Letizia Penolazzi [1], Stefania Mazzitelli [2], Elisabetta Lambertini [1], Andrea Lolli [3], Roberta Piva [1] and Claudio Nastruzzi [2]**

[1] Department of Biomedical and Specialty Surgical Sciences, University of Ferrara, Ferrara, Italy, [2] Department of Life Sciences and Biotechnology, University of Ferrara, Ferrara, Italy, [3] Department of Orthopaedics, Erasmus MC, University Medical Center, Rotterdam, Netherlands

Tissue engineering (TE) approaches using biomaterials have gain important roles in the regeneration of cartilage. This paper describes the production by microfluidics of alginate-based microfibers containing both extracellular matrix (ECM)-derived biomaterials and chondrocytes. As ECM components gelatin or decellularized urinary bladder matrix (UBM) were investigated. The effectiveness of the composite microfibers has been tested to modulate the behavior and redifferentiation of dedifferentiated chondrocytes. The complete redifferentiation, at the single-cell level, of the chondrocytes, without cell aggregate formation, was observed after 14 days of cell culture. Specific chondrogenic markers and high cellular secretory activity was observed in embedded cells. Notably, no sign of collagen type 10 deposition was determined. The obtained data suggest that dedifferentiated chondrocytes regain a functional chondrocyte phenotype when embedded in appropriate 3D scaffold based on alginate plus gelatin or UBM. The proposed scaffolds are indeed valuable to form a cellular microenvironment mimicking the *in vivo* ECM, opening the way to their use in cartilage TE.

Keywords: microfibers, extracellular matrix-derived biomaterials, chondrocytes, cartilage tissue engineering, gene expression

OPEN ACCESS

Edited by:
Ivan Martin,
University of Basel, Switzerland

Reviewed by:
Wael Kafienah,
University of Bristol, United Kingdom
Andrea Barbero,
University-Hospital Basel, Switzerland

***Correspondence:**
Roberta Piva
piv@unife.it;
Claudio Nastruzzi
nas@unife.it

Specialty section:
This article was submitted to Tissue Engineering and Regenerative Medicine, a section of the journal Frontiers in Bioengineering and Biotechnology

Received: *01 March 2017*
Accepted: *19 May 2017*
Published: *13 June 2017*

Citation:
Angelozzi M, Penolazzi L, Mazzitelli S, Lambertini E, Lolli A, Piva R and Nastruzzi C (2017) Dedifferentiated Chondrocytes in Composite Microfibers As Tool for Cartilage Repair. Front. Bioeng. Biotechnol. 5:35. doi: 10.3389/fbioe.2017.00035

INTRODUCTION

The main component of the articular cartilage is an extracellular matrix (ECM) containing a relative small number of cells. The ECM is mainly composed of collagen type II and proteoglycans, determining the typical mechanical characteristics of cartilage (i.e., tensile strength, flexibility, and resistance to compressive loads) (Muir, 1995). Self-healing of damaged cartilage is unfortunately very limited, being chondrocytes unable to grow in the dense ECM. Nowadays, the cartilage reparative strategies, aiming to generate a functional tissue, are mainly based on the combined use of cells, scaffolds, and biomolecules (Poole et al., 2001; Chang et al., 2005; Moutos and Guilak, 2008; Liao et al., 2014).

Tissue engineering (TE) approaches for cartilage require some key factors: they include (a) an ideal cell source, (b) a precise control of cell differentiation (e.g., using soluble chemical factors and mechanical stimulation), and (c) an adequate scaffold based on specific biomaterials (Chang et al., 2005; Brown and Badylak, 2014).

With respect to the cells, chondrocytes being the cellular component of the mature cartilage are the most obvious choice for cartilage TE (Dell'Accio et al., 2001; Melero-Martin and Al-Rubeai, 2007). However, the use of chondrocytes is limited by rareness of the donor tissues, the instability

in *in vitro* culture, and the loss of differentiated phenotype due to cell expansion. The maintenance of the chondrocytic phenotype is currently performed by 3D environments supplemented with chondrogenic inducers (i.e., TGFβ) (Khaghani et al., 2012). The approaches are mainly consisting of natural or synthetic scaffold offering a favorable milieu for chondrogenesis (Yang et al., 2008; Youngstrom et al., 2015).

Hydrogels, particularly those based on alginate, resulted successful in chondrocyte redifferentiation (Guo et al., 1989; Häuselmann et al., 1996; Caron et al., 2012). Alginates form indeed biocompatible, biodegradable, and shape-adaptable structures that are largely employed for cell embedding. Notably, alginate gels were proposed for different *in vivo* applications; they allow bidirectional exchange of nutrient, oxygen, and cell waste products, protecting at the same time the cells from the host immune system (Calafiore, 2003; Penolazzi et al., 2010; Mazzitelli et al., 2013; Bidarra et al., 2014). Alginate is particularly appealing for chondrocytes immobilization since it supports the phenotype maintenance as proved by the typical rounded morphology displayed by chondrocyte in alginate, sustaining the cartilage ECM production (Guo et al., 1989; Bonaventure et al., 1994; Häuselmann et al., 1996).

Despite many positive properties, alginate scaffolds are far from representing an environment strictly mimicking the biological ECM where chondrocytes reside, reach of various biochemical signals. Their lack affects the interaction between the entrapped/seeded cells and the biomaterial and compromises the onset of molecular signaling that guides the effective integration of the implanted construct with the surrounding host tissue (Lee and Mooney, 2001).

For possibly solving the limitations of alginate-based scaffolds, in this study, an improvement has been proposed, developing microfibrous alginate scaffold containing ECM components such as gelatin (a soluble, partially hydrolyzed, and collagen derivative) or the urinary bladder matrix (UBM) (a natural decellularized matrix, derived from porcine bladder).

These natural materials confer to the scaffold elements resembling the original ECM collagenous network and supporting cell adhesion, migration, and differentiation by the presence of glycosaminoglycans (GAGs) (Badylak et al., 2009; Gómez-Guillén et al., 2011; Santoro et al., 2014). Notably, UBM is one of the most representative decellularized materials that have received regulatory approval for use in human patients (Gilbert et al., 2006). It has been demonstrated that the presence and integrity of basement membrane complex in UBM promotes inductive tissue remodeling (Brown and Badylak, 2014), but little is known about the supporting activity of UBM toward chondrocyte function. UBM was recently used for articular cartilage regeneration in canine and murine models demonstrating its efficacy in treating dogs or mice with chronic osteoarthritis of the hip or knee joint, respectively (Rose et al., 2009; Tottey et al., 2011; Jacobs et al., 2017).

Particularly, composite microfibers (i.e., 3D scaffolds), potentially suitable for a fiber-based tissue such as cartilage, have been designed and produced by a specific microfluidic approach (Angelozzi et al., 2015).

Lab-on-a-chip (LOC) devices based on microfluidic chips have been recently proposed as miniaturized bioanalytical systems for chemical/biological applications being able to perform multiple tasks associated with many laboratory procedures. LOC devices offer indeed many advantages over standard (i.e., macroscopic) systems, including reduced sample and reagent consumption, faster analysis, and higher levels of throughput and automation. Despite these advantages, the production of biomaterial based scaffold by microfluidics has still limited example in the current literature.

As cellular component, human advanced dedifferentiated nasal chondrocytes from monolayer passage P6 were employed. Chondrocytes derived from the nasal septum are highly promising cell source for the repair of articular cartilage defects since a great capacity to generate hyaline-like cartilage tissues, with the plasticity to adapt to a joint environment has been demonstrated (Kafienah et al., 2002; Wolf et al., 2008; Mumme et al., 2016).

This paper describes the potential of composite microfibers with respect to their ability to control chondrocyte differentiation for proper cartilage matrix reconstruction.

The effect of microenvironment around individual mature chondrocytes in microfibers was also considered; it is well known indeed that chondrocytes in their natural environment are present as single cells with a spherical shape, surrounded by ECM not allowing for cell-to-cell contacts. The properties of the produced composite microfibers were investigated *in vitro* conditions excluding the presence of exogenously added chondrogenic inducers.

In addition, in view of a possible use of the composite microfibers as scaffold for cryopreservation, experiments were undertaken to evaluate their potential as banking for chondrocytes.

In this respect, the properties of the embedded chondrocytes after a freeze and thaw procedure have been investigated. The obtained results suggest that the microfibrous embedded chondrocytes could be employed to deliver the freshly thawed constructs at the operating theater.

MATERIALS AND METHODS

Chondrocyte Cultures

Cartilage fragments from nasal septum were obtained from 15 donors between 25 and 60 years old, which underwent septoplasty surgery procedures, after informed consent and approval of the Ethics Committee of the University of Ferrara and S. Anna Hospital. Briefly, cartilage fragments were minced into small pieces and rapidly incubated with type VIII Collagenase (Sigma-Aldrich Chemical Co., St. Louis, MO, USA) at 37°C for 16 h (do Amaral et al., 2012). Cells were harvested by centrifugation and plated (p0) at a density of 20,000 cells/cm^2 in tissue culture flasks (25 cm^2) or 8-well culture slides in standard medium (50% DMEM high-glucose/50% DMEM F-12/10% fetal calf serum) (Euroclone S.p.A., Milan, Italy) supplemented with antibiotics (penicillin 100 mg/mL and streptomycin 10 mg/mL), at 37°C in a humidified atmosphere of 5% CO_2. After 7 days, the culture medium was removed and then changed twice a week. At 70–80% confluence, cells were scraped off by 0.05% TRYPSIN EDTA (Gibco, Grand Island, NE, USA), washed, plated, and allowed to proliferate in standard conditions (50% DMEM

high-glucose/50% DMEM F-12/10% fetal calf serum) to induce chondrocyte dedifferentiation (until p6). Dedifferentiated chondrocytes at different culture passages were scraped off counted by hemocytometric analysis, assayed for viability, and thereafter used for molecular analysis or for encapsulation procedures. During the *in vitro* expansion, dedifferentiated chondrocytes underwent a total of 19–21 population doublings.

UBM Isolation and Purification

Porcine urinary bladders were harvested from pigs, immediately following euthanasia. The connective tissue excess and the residual urine were removed. By mechanical treatment, the tunica serosa, tunica muscularis externa, tunica submucosa, and majority of the tunica muscularis mucosa were removed; thereafter, urothelial cells of the tunica mucosa were detached from the luminal surface by incubating the tissue in saline solution. The resulting tissue, which was composed of the basement membrane of the urothelial cells plus lamina propria, is termed "urinary bladder matrix," shortly UBM. The obtained UBM sheets were then treated by a solution containing 0.1% (v/v) peracetic acid (Sigma), 4.0% (v/v) ethanol (Sigma), and 95.9% (v/v) sterile water for 2 h. Peracetic acid residues were then removed with washes with phosphate-buffered saline (PBS, pH 7.4) and sterile water. The decellularized UBM was then lyophilized and milled to obtain a particulate form using a Wiley Mini Mill (Thomas Scientific, Swedesboro, NJ, USA).

Microfiber Production and Encapsulation Procedure

Fluidic reagents were introduced into the microfluidic network from glass gastight syringes (Hamilton, Reno, NV, USA) by syringe pumps (model KD100, KD scientific Inc., Holliston, MA, USA).

"Empty" and "multifunctional" (containing cells, ECM components or both) barium alginate microfibers were produced with a snake micromixing microfluidic device (**Figure 1A**). A sodium alginate dispersion in water (1.5–2.5%, w/v), used as main constituent of the microfibers was introduced into one inlet of the microchip at appropriate flow rates (0.50–1.50 mL/min). Plain sodium alginate dispersion or sodium alginate suspensions were delivered *via* the second inlet. The suspensions contained different amounts (1.125–4.500% for gelatin or 0.1–1.0% for UBM) of either ECM components (i.e., gelatin or UBM) or cells (i.e., dedifferentiated chondrocytes at 2×10^6 cells/mL). Notably, gelatin forms a homogeneous dispersion in the aqueous sodium alginate, whereas UBM, being unsoluble in water, forms a suspension. The output from the outlet of the chip was transferred *via* a Teflon tube, into a $BaCl_2$ solution (6.0 mM in water) where the Na-alginate flow stream was gelled to produce the final Ba-alginate consolidated microfibers. The plain alginate, the alginate/gelatin, or alginate/UBM microfibers are named *Af*, *AGf*, and *AUBMf*, respectively. Cells-containing microfibers were washed three times with saline before culturing in standard chondrocyte medium at 37°C in a humidified atmosphere of 5% CO_2.

Geometrical and Morphological Analysis of Microfibers

The dimension and morphology of microfibers were evaluated by optical stereomicroscopy. Quantitative analyses were performed using the photomicrograph analysis software EclipseNet. The mean diameter of the microfibers (±SD) was obtained by taking nine measurements along the (10 mm) length of the samples at equal intervals, in triplicate. Additionally, the distribution of different amount of gelatin (1.125, 2.25, and 4.5% w/v) and UBM (0.1, 0.5, and 1% w/v) in composite microfibers was evaluated by Coomassie Brilliant Blue staining. For the staining, the microfibers were incubated in 0.1% Coomassie Brilliant Blue R-250, 50% methanol, and 10% glacial acetic acid at room temperature for 1 h and then washed overnight at room temperature in the destaining solution (40% methanol and 10% glacial acetic acid). Gelatin and UBM distribution was determined by optical stereomicroscopy.

Micromass Culture System

Dedifferentiated chondrocytes from monolayer culture were harvested and resuspended in standard medium at 2×10^7 cells/mL density. Droplets (10 μL) were carefully placed in a 12-well plate. Cells were allowed to adhere for 3 h, followed by the addition of 1 mL of standard medium supplemented with 10% FCS. After 24 h, the cell droplets coalesced and became spherical. Medium was changed every 3 days, and micromasses were harvested on days 7 and 14.

Viability Analysis of Encapsulated Cells

Viability of encapsulated cells was assessed immediately after encapsulation procedure and at days 7 and 14 of culture. Cell viability was evaluated by Calcein-AM/propidium iodide (PI) staining (Cellstain double staining kit, Sigma-Aldrich).

Before staining, the medium was removed from the wells, and 500 μL of the staining solution was added to each well. The samples were incubated in the dark at room temperature for 15 min, thereafter the wells were rinsed with PBS and immediately imaged using epifluorescent microscopy. Viability was measured *via* cell counting and automated analysis using ImageJ. Samples were visualized under a fluorescence microscope (Nikon, Optiphot-2; Nikon Corporation, Tokyo, Japan) dead cells stained red, while viable ones appeared green (Penolazzi et al., 2012).

Microfiber Dissolution and Cell Recovery

The cells embedded in microfibrous scaffolds were retrieved, after gel dissolution at days 7 and 14 of *in vitro* culture. Microfibers were dissolved by incubation at 37°C in a 100 mM EDTA solution (pH 7.0) for 10 min. Cell suspension after microfiber dissolution was filtered with a Falcon™ 70 μM Nylon Cell strainer (BD Biosciences, Franklin Lakes, NJ, USA) and employed for successive analyses.

GAG and DNA Quantification

Dedifferentiated chondrocytes before encapsulation procedure or recovered chondrocytes from microfibers or micromasses were

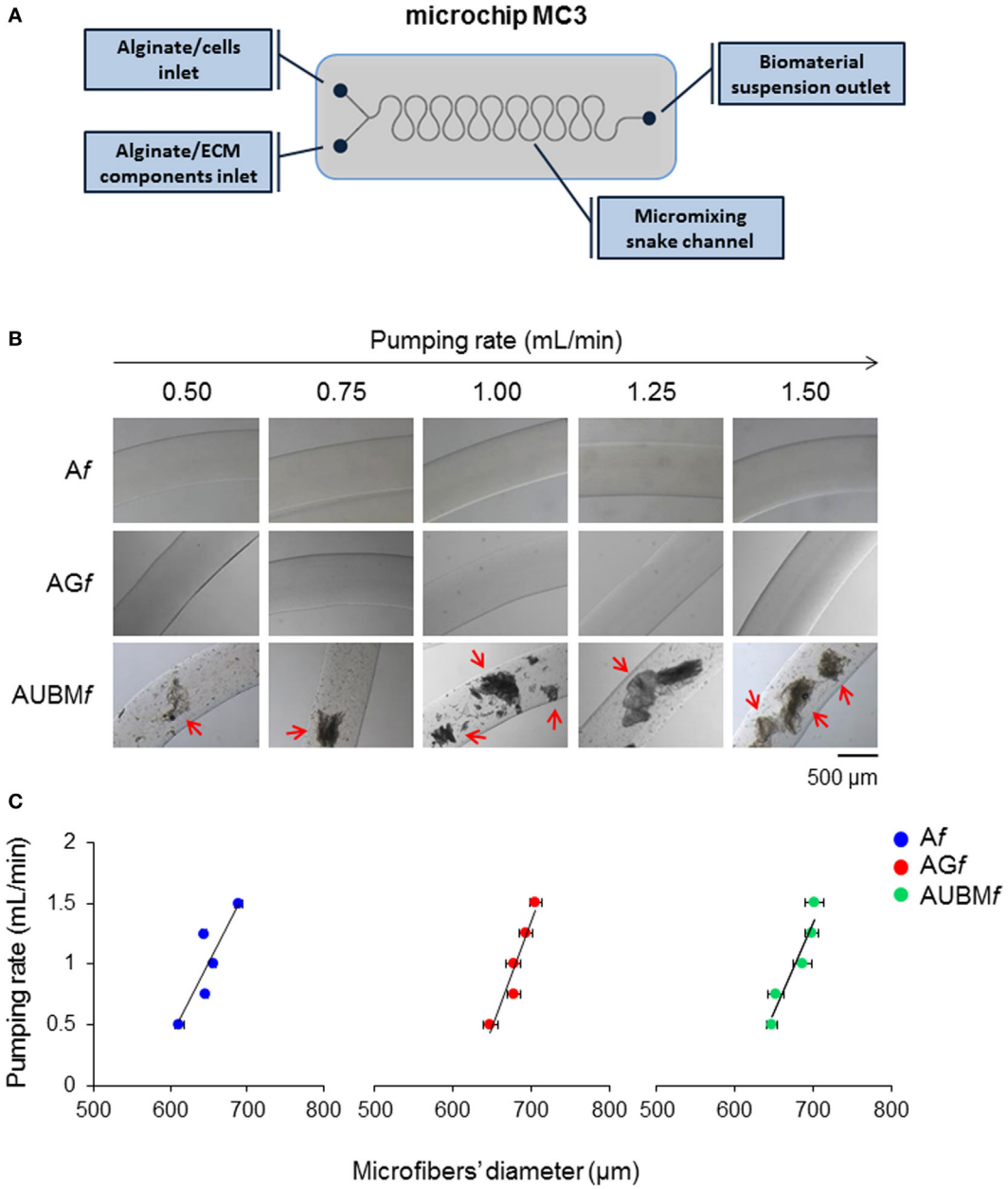

FIGURE 1 | Production and characterization of composite microfibers. **(A)** Schematic representation of the snake micromixing microfluidic device employed for the production of composite microfibers. The device presents two inlets where the alginate suspension containing cells or gelatin or UBM were delivered through the micromixing snake geometry channel and a 700-µm outlet tube (#T3) into a $BaCl_2$ solution in order to obtain alginate (A*f*), alginate plus gelatin (AG*f*), or alginate plus UBM (AUBM*f*) microfibers. **(B)** Photomicrographs of A*f*, AG*f*, and AUBM*f* obtained at different pumping rates (from 0.5 to 1.5 mL/min). Arrows indicate the presence in AUBM*f* of UBM particles, in form of flat flakes. Bar corresponds to 500 µm. **(C)** Effect of the pumping rate on the dimension of the produced microfibers.

lysed with 50 µL of RIPA buffer. Total sulfated GAG content was determined in RIPA samples from days 7 and 14 cultures by using 1,9-dimethylmethylene blue (DMMB), as previously described (Caron et al., 2012). A standard curve of chondroitin sulfate in PBS-EDTA was included to determine the GAG concentration in the samples. About 100 µL of diluted RIPA sample (5 µL RIPA sample and 95 µL PBS-EDTA) or standard (95 µL standard and 5 µL RIPA) was added to 200 µL of DMMB solution, and the extinctions were determined spectrophotometrically at 595 nm. GAG content was determined using the generated standard curve corrected for DNA content and expressed as µg GAG/ng DNA. DNA content in the same RIPA samples was determined using SYBR® Green I Nucleic Acid stain (Invitrogen). A serially diluted standard curve of genomic control DNA (DNA Ladder G571A, Promega) in TE buffer was included to quantify DNA concentration in the samples. Before measurement, RIPA

samples were diluted in TE buffer (1 µL RIPA sample and 99 µL TE buffer) and standard were prepared (99 µL standard in TE and 1 µL RIPA buffer). SYBR® Green was diluted 10,000 times in TE buffer, and 100 µL of this solution was added to 100 µL of the above prepared samples or standards. Fluorescence was determined in standard 96-well plates in a SpectraFluor Plus reader (Tecan): excitation 485 nm and emission 535 nm. DNA concentration was determined using the standard curve.

Gene Expression Analysis

Total RNA was extracted from dedifferentiated chondrocytes before encapsulation procedure, encapsulated chondrocytes cultured in alginate-based scaffolds, or the same cells maintained in micromass by using the RNeasy Mini Kit (Qiagen, Hilden, Germany), according to the manufacturer's instruction. Total RNA was used for reverse transcription and stored at −80°C. Briefly, cDNA was synthesized from total RNA (500 ng) in a 20-µL reaction volume using the TaqMan High-Capacity cDNA Reverse Transcription kit (Applied Biosystems), as previously described (Lolli et al., 2014).

Gene expression analyses by RT-qPCR were performed for Col1A1, Col2A1, Aggrecan, and Col10A1 mRNA levels. The following Taqman probes were used: Col1A1 5′FAM-AAGACGAAGACATCCCACCAATCAC-NFQ3′, Col2A1 5′FAM-CCTGGTCTTGGTGGAAACTTTGCTG-NFQ3′, Aggrecan 5′FAM-CGCTGCCAGGGATCCTTCCTACTTG-NFQ3′, Col10A1 5′FAM-ATAAAGAGTAAAGGTATAGCAGTAA-NFQ3′ (Life Technologies, Carlsbad, CA, USA).

The CFX96™ PCR detection system (Bio-Rad, Hercules, CA, USA) was used, and results were calculated using the $2^{-\Delta\Delta Ct}$ method using glyceraldehyde 3-phosphate dehydrogenase as reference gene for normalization.

Alcian Blue Staining

Glycosaminoglycan content was assessed by Alcian Blue staining in monolayered cells. Cells were rinsed with PBS and fixed in 10% formaldehyde in PBS for 10 min. Cultures were then stained with Alcian Blue pH 2 (1% in 3% acetic acid) (Sigma-Aldrich Chemical Co., St. Louis, MO, USA) 30 min at 37°C. Subsequently, cells were washed with water and observed using a Leitz microscope. The presence of GAG deposits appeared as blue staining areas.

Immunocytochemistry

Immunocytochemistry analysis was performed on freshly, dedifferentiated, and recovered chondrocytes employing the ImmPRESS (Vectorlabs, Burlingame, CA, USA) or 4plus AP universal (Biocare Medical, Concord, CA, USA) detection kits. Cells grown in chamber slides were fixed in cold 100% methanol and permeabilized with 0.2% (v/v) Triton X-100 (Sigma-Aldrich Chemical Co., St. Louis, MO, USA) in TBS (Tris-buffered saline). Cells were treated with 3% H_2O_2 in TBS and incubated in 2% normal horse serum (Vectorlabs, Burlingame, CA, USA) for 15 min at room temperature. After the incubation in blocking serum, the different primary antibodies were added and incubated at 4°C overnight: polyclonal antibodies for Col1A1 (rabbit anti-human, 1:200 dilution, Santa Cruz Biotechnology, CA, USA), Col2A1 (mouse anti-human, 1:200 dilution, Abcam, Cambridge, UK), Aggrecan (mouse anti-human, 1:200 dilution, Santa Cruz Biotechnology, CA, USA), and Sox9 (rabbit anti-human, Santa Cruz Biotechnology, CA, USA). Cells were then incubated in Vecstain ABC (Vectorlabs, Burlingame, CA, USA) or Universal AP detection (Biocare Medical, Concord, CA, USA) reagents for 30 min and stained, respectively, with DAB solution (Vectorlabs, Burlingame, CA, USA) or Vulcan Fast Red chromogen kit (Biocare Medical, Concord, CA, USA). After washing, cells were mounted in glycerol/TBS 9:1 and observed using a Leitz microscope. Quantitative image analysis of immunostained cells was obtained by a computerized video-camera-based image-analysis system (with NIH, USA ImageJ software, public domain available at: http://rsb.info.nih.gov/nih-image/) under brightfield microscopy. Briefly, images were grabbed with single stain, without carrying out nuclear counterstaining with hematoxylin, and unaltered TIFF images were digitized and converted to black and white picture to evaluate the distribution of relative gray values (i.e., number of pixels in the image as a function of gray value 0–256), which reflected chromogen stain intensity. Images were then segmented using a consistent arbitrary threshold 50% to avoid a floor or ceiling effect and binarized (black versus white); total black pixels per field were counted, and average values were calculated for each sample. Three replicate samples and at least four fields per replicate were subjected to densitometric analysis. We performed the quantification of pixels per 100 cells and not per area in order to take into account the different cell morphology and confluence.

Transmission Electronic Microscope (TEM) Analysis and Toluidine Staining

Cell-containing microfibers were fixed in glutaraldehyde 2.5% buffered solution and osmium tetroxide 2% buffered solution and dehydrated through an ethanol gradient; samples were araldite embedded (ACM Fluka Sigma-Aldrich Co., St. Louis, MO, USA) and the ultra-thin sections of a selected area were contrasted with uranyl acetate lead citrate and observed at transmission electron microscopy (TEM; ZEISS EM 910 electron microscope; Zeiss, Oberkochen, Germany). For toluidine staining, 5 µm sections from the same specimens were obtained with a glass blade. Sections were stained with toluidine blue, mounted in glycerol, and observed using a Leitz microscope.

Microfibers Cryopreservation

Cryopreservation of A*f*, AG*f*, and AUBM*f* embedded chondrocytes was performed by adapting a previously published protocol (Pravdyuk et al., 2013). Microfibers embedded cells were directly freezed in standard culture medium with 10% FCS and supplemented with 10% of DMSO. The samples were cryopreserved at −20°C for 30 min, maintained at −80°C for 24 h, and then immersed in liquid nitrogen, where they were kept until the thawing day. Cryovials within microfibers were thawed in a warm water bath (37°C) and, when ice was totally melted, microfibers were washed twice with culture medium and subsequently cultured in standard conditions prior to performing morphological, viability, and immunocytochemical analysis.

Statistical Analysis

All cell-related experiments were repeated with chondrocytes derived from five different donors and performed in triplicate for each donor. Data are presented as means ± SEM. The normal distribution of data was verified using the Kolmogorov–Smirnov test. In case of single comparison, statistical significance was determined by paired Student's *t*-test for normally distributed data and Wilcoxon matched-pairs signed-ranks test for non-normally distributed data. In case of multiple comparisons, statistical significance was analyzed by one-way analysis of variance (ANOVA) and Bonferroni *post hoc* test if the values followed a normal distribution, or by Kruskal–Wallis analysis (non-parametric one-way ANOVA) and Dunn's *post hoc* test if the values were not normally distributed. For all statistical analyses, differences were considered statistically significant for p-values ≤ 0.05.

RESULTS

Production and Characterization of Composite Microfibers

Alginate (A*f*), alginate-gelatin (AG*f*), and alginate-UBM (AUBM*f*) microfibers were produced by a microfluidic procedure by a snake micromixing chip, consisting in two inlets, a mixing element, and an outlet tube with an internal diameter of 700 μm (**Figure 1A**). The dimensional analysis of photomicrographs of microfibers produced at different flow rates (from 0.5 to 1.5 mL/min) demonstrates that the microfluidic procedure allows a good control on microfibers' morphology and dimensions (**Figures 1B,C**). Microfibers present a smooth surface and a uniform morphology, with constant dimensions (in diameter); particularly, the pumping rate has an important effect of the microfiber dimensions. High pumping rates resulted in an increase in microfiber diameters; this behavior is indeed attributed to the well-known Barus effect (Malkin et al., 1976). Moreover, the analysis of the photomicrographs reported in **Figures 1B,C** demonstrates that the addition of gelatin or UBM does not affect the general microfiber morphology (i.e., in term of dimension and surface smoothness). Both gelatin and UBM caused only a moderate enlargement of the microfiber diameter. The produced microfiber presents good structural and morphological properties as proved by the Coomassie Blue Brilliant staining (**Figure 2**). Particularly, AG*f* are characterized by uniform staining, since gelatin is homogeneously present within the entire microfiber structure (i.e., being gelatin soluble in the aqueous sodium alginate); on the contrary, AUBM*f* display the presence of UBM particles evenly distributed within the microfiber matrix arrowed in **Figure 2** (i.e., being UBM particles unsoluble in water). Therefore, the images reported in **Figure 2** indicate that the snake micromixing chip allowed a homogeneous distribution of gelatin and ECM along the whole microfiber.

With respect to the concentrations of biomaterial used for the preparation of microfibers (sodium alginate, gelatin, and UBM), the selected amounts were chosen on the basis of a large number of previously published observations (Penolazzi et al., 2010, 2012; Mazzitelli et al., 2013; Angelozzi et al., 2015; Vecchiatini et al., 2015). For instance, alginate is typically used in the concentration range comprised between 0.5 and 2.5% (w/v) depending on the stiffness required by the specific application of the gel.

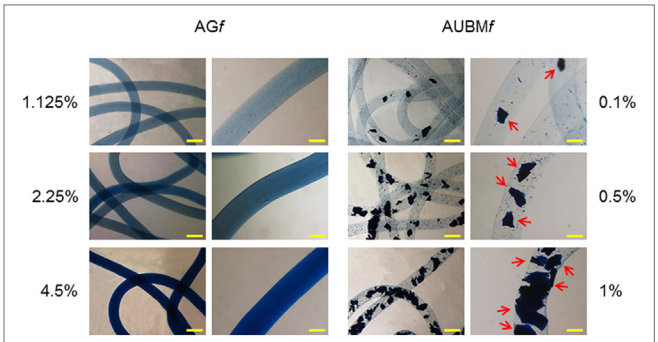

FIGURE 2 | Distribution of gelatin and UBM in composite microfibers. Different amounts of gelatin (1.125, 2.25, and 4.5% w/v) or UBM (0.1, 0.5, and 1% w/v) were added to the alginate solution, respectively. Microfibers containing different amount gelatin/UBM were stained with Coomassie Blue Brilliant. The presence and distribution of UBM particles are indicated by arrows. Bar corresponds to 1 mm in lower magnification photomicrographs and to 400 μm in higher magnification images.

Chondrocytes Expansion and Dedifferentiation Process

To obtain dedifferentiated cells, P0 chondrocytes from five different donors were expanded up to six passages (**Figure 3**). As expected (Caron et al., 2012), the cartilaginous phenotype was progressively lost over several passages in culture. In fact, compared to P0 freshly isolated chondrocytes, P6 expanded chondrocytes exhibited a substantial change in cell morphology, from rounded to flattened fibroblast-like shape as it is evident from hematoxylin staining. Immunohistochemical analysis showed that expansion dramatically decreased the expression of typical chondrogenic markers including collagen type II (Col2A1), aggrecan, Sox9, and, in contrast, increased the positivity for collagen type I (Col1A1). Dedifferentiation status was confirmed by a dramatic decrease of sulfate GAG content in ECM composition (as demonstrated by Alcian Blue staining).

P6 chondrocytes expanded as dedifferentiated chondrocytes were then embedded in composite microfibers, which were subjected to specific analyses at days 7 and 14, as described below.

Embedding of Dedifferentiated Chondrocytes in Composite Microfibers

Dedifferentiated chondrocytes were suspended, at 2×10^6 cells/mL in (i) alginate 2%, (ii) alginate 2% plus gelatin 2.25%, or (iii) alginate 2% plus UBM 0.5%. The different cells/biomaterial suspensions were used to produce microfibers (A*f*, AG*f*, and AUBM*f*) by letting flow the cell suspension in a $BaCl_2$ gelling bath at a pumping rate of 1.5 mL/min, resulting in microfibers with diameters comprised between 650 and 750 μm. The obtained alginate-based microfibers were maintained in culture medium without chondrogenic inducers up to 14 days, and the embedded cells were analyzed for viability at different time of culture. As shown in the lower part of **Figure 3**, after embedding in microfibres, cell

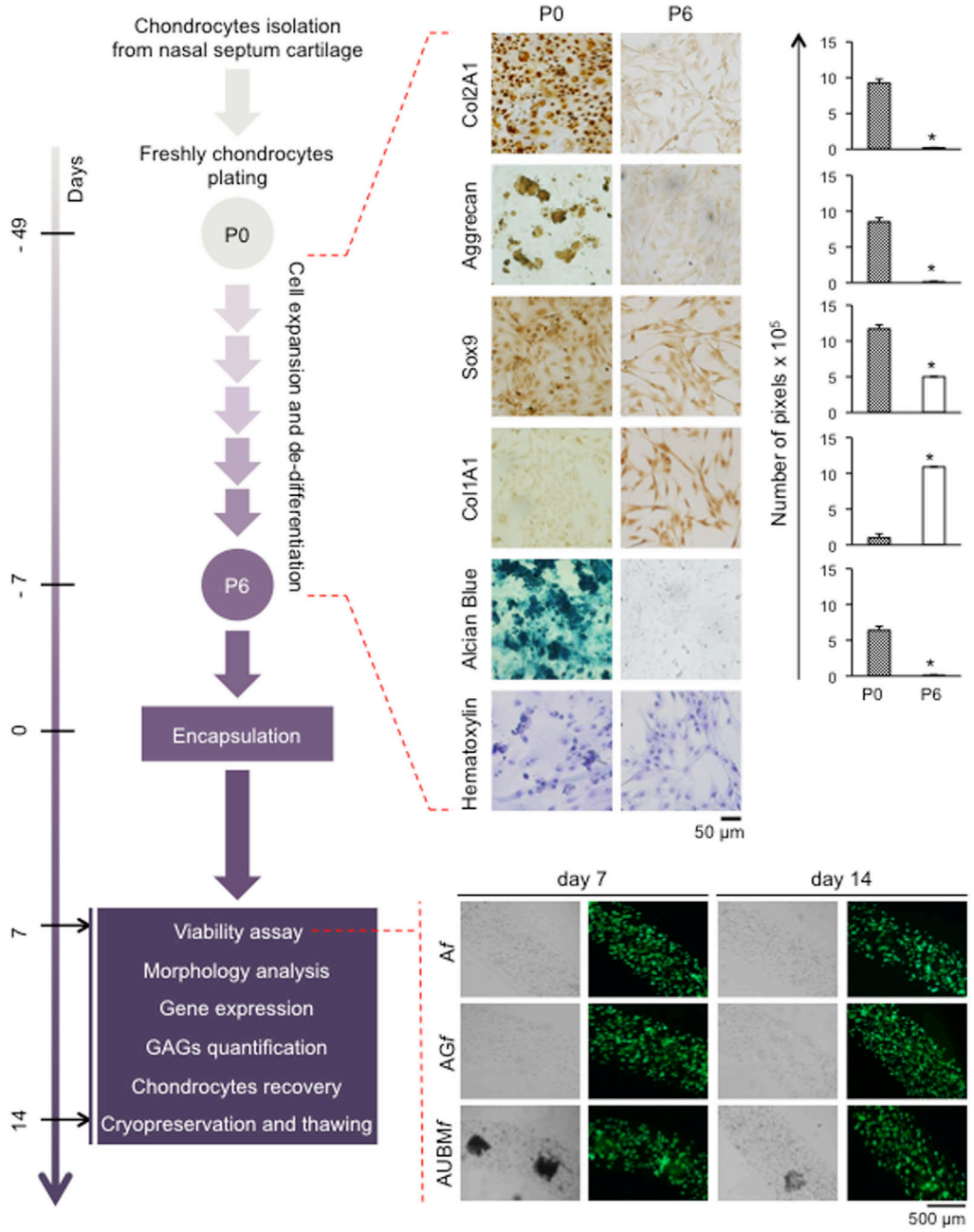

FIGURE 3 | Schematic representation of the experimental approach. Human chondrocytes were isolated from nasal septum biopsy, expanded, and dedifferentiated up to the sixth culture passage (P6). Cells were then embedded in A*f*, AG*f*, and AUBM*f* and subjected to the indicated analysis at days 7 and 14. Dedifferentiation process from passage 0 (P0) to passage 6 (P6) has been monitored: protein expression of cartilage-related genes (Col2A1, Aggrecan, and Sox9), and Col1A1 was investigated by immunocytochemical analysis. Alcian Blue staining for sulfate glycosaminoglycans (GAGs) detection is also reported. Cell morphology was evaluated by hematoxylin staining. Representative optical photomicrographs are reported. Pictures of at least four random fields of three replicates were captured for densitometric analysis using ImageJ software. Data are presented as means of pixels per 100 cells ±SEM (*$p \leq 0.05$). Cell viability of embedded cells has also been investigated, and optical and fluorescence photomicrographs after double staining with Calcein-AM/propidium iodide at days 7 and 14 of culture in basal medium are reported. The green fluorescence indicates the presence of calcein-labeled live cells, while propidium iodide-labeled dead cells are revealed by red fluorescence. Merged photomicrographs are reported.

viability was not compromised as confirmed by double staining with Calcein-AM/PI.

The properties of the embedded cells were further investigated in term of cell morphology, and proteoglycan deposition, by toluidine blue metachromasia of matrix. As shown in **Figure 4**, the embedded cells revert to a spherical shape in just 7 days. Interestingly, during the entire period of culture, up to 14 days, the embedded cells are mainly present as single cells, well dispersed

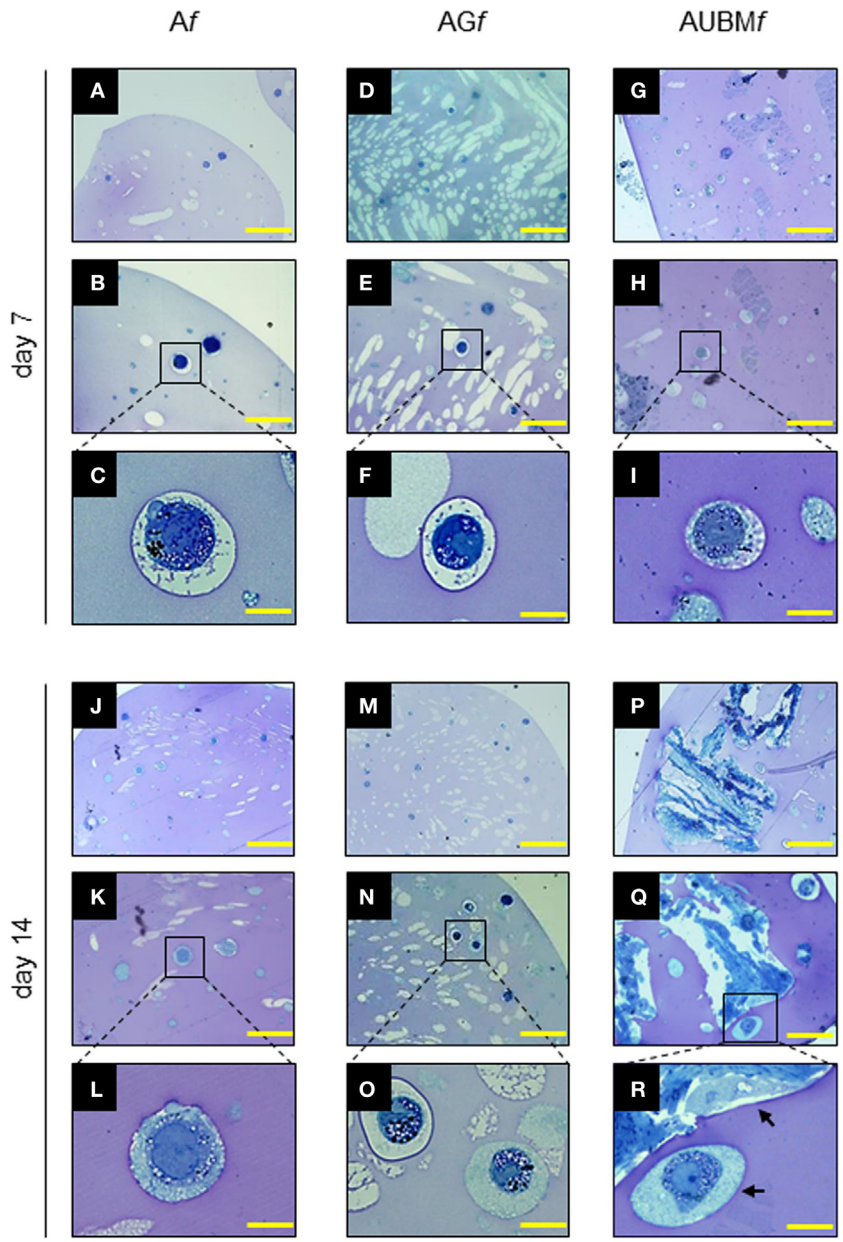

FIGURE 4 | Properties of the embedded cells: presence of secretory vesicles and metachromatic areas in the extracellular matrix (ECM). A*f*, AG*f*, and AUBM*f* embedded cells at days 7 and 14 of culture were stained with toluidine blue. Representative photomicrographs showed the presence of ECM deposition in the pericellular space of the single cells (as clearly evidenced in the higher magnification images) and the presence of metachromatic area (pink). Black arrows: single or UBM-attached cell. Bar corresponds to 50 μm for photomicrographs **(A,D,G,J,M,P)**, to 25 μm for photomicrographs **(B,E,H,K,N,Q)**, and to 10 μm for photomicrographs **(C,F,I,L,O,R)**.

in the alginate, showing an aspect resembling the environment of mature chondrocytes in cartilage. In addition, the presence of metachromatic areas with secretory vesicles in a well-defined pericellular space at days 7 and 14 was clearly detectable, indicating the effective release and deposition of cartilage-like ECM. The A*f*, AG*f*, and AUBM*f* composite microfibers represent therefore a microenvironment supporting the maturation of chondrocyte phenotype also in the absence of chondrogenic inducers.

Chondrogenic Properties of Embedded Cells

Transmission electronic microscope ultrastructural analysis of embedded cells at day 14 revealed a high cellular secretory activity. As shown in **Figure 5**, the presence of secretory vesicles containing ECM dense materials, and collagen fibers with their typical banding pattern is clearly appreciable. The released materials accumulated and assembled in a sparse matrix in the

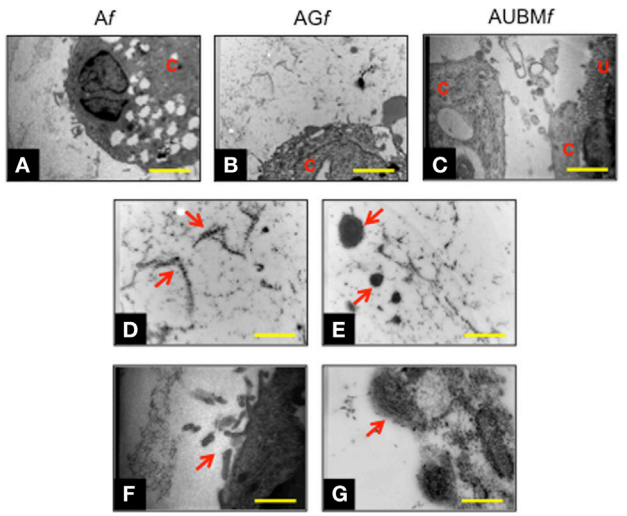

FIGURE 5 | Chondrogenic properties of A*f*, AG*f*, and AUBM*f* embedded cells: transmission electronic microscope ultrastructural analysis at day 14 of culture. Lower magnification photomicrographs showed the ultrastructure of an embedded redifferentiated chondrocyte in A*f* **(A)**, AG*f* **(B)**, and AUBM*f* **(C)**. In the images at higher magnification, red arrows indicated the presence of ECM dense material and collagen fibers with their typical banding pattern in the pericellular space **(D,E)** and evidenced the ECM-containing vesicles release from embedded cells **(F,G)**. Bar corresponds to 2.6 μm in a-c, 1 μm in **(D–F)** and 0.4 μm in grams. C, cell; U, UBM.

surrounding lacuna, resembling the biological microenvironment of chondrocytes. These preliminary evidences confirmed the deposition of a cartilage-like ECM in this area, as hypothesized after the toluidine blue staining (see **Figure 4**). Interestingly, AUBM*f* showed the presence of cells able to interact with each other and with UBM flakes (characterized by typical collagen fibers) located in the closed areas.

The chondrogenic properties of the embedded cells were then investigated with two different approaches (**Figures 6** and **7**). In a first step, embedded cells were harvested from microfibers at days 7 and 14 of culture and subjected to evaluation of chondrogenic markers. RT-qPCR revealed that the main cartilage-specific ECM component, Col2A1, and the major proteoglycan in cartilage, aggrecan, were highly expressed in cells embedded in A*f*, AG*f*, and AUBM*f* compared to chondrocytes cultured in standard micromass (MM) and P6 dedifferentiated chondrocytes (**Figure 6A**). Micromass culture system has been chosen instead of pellet culture since it may be maintained in culture medium also without adding TGFβ supplementation. The remarkable increase of Col2A1 expression and decrease of Col1A1 was particularly appreciable calculating the ratio between Col2A1 and Col1A1 (differential index) which significantly increased from 20 to 120 times in all embedded cells compared to MM cultured cells (**Figure 6B**). Moreover, gene expression analysis showed also the absence of expression of Col10A1, which encodes the collagen type 10 alpha 1 chain traditionally associated with chondrocyte hypertrophy, both at 7 and 14 days (**Figure 6B**). This suggested that microfiber environment is suitable to prevent undesired hypertrophic maturation that can widely affect the successful outcome of the graft transplantation.

The reacquistiton of chondrogenic properties by the embedded cells was confirmed by GAG quantification performed as total GAG content normalized to DNA content (**Figure 6B**), and comparable GAG content was found in A*f*, AG*f*, and AUBM*f* embedded cells.

It is important to underline that with these experiments we also demonstrated that the small amount of TGFβ in the FCS containing medium is not sufficient to support chondrogenesis in standard conditions of MM that requires exogenous chondrogenic inducers. Conversely, microenvironments created by microfibers support redifferentiation capacity of expanded chondrocytes without the need of adding chondrogenic inducers.

In a second step, embedded cells were recovered at day 14 from the microfibers, reseeded, and grown up to 7 days as monolayered culture in standard medium without adding chondrogenic inducers. These experiments were aimed both at validating the previous RT-qPCR data by immunocytochemical analysis and at further demonstrating the intrinsic potency of microfibers in maintaining chondrogenic activity of the cells once released from the confined 3D microenvironment of the scaffolds.

Interestingly, even if plated in unfavorable conditions, the cells maintained a round morphology, a low adhesion ability, and generated microaggregates, demonstrating a behavior comparable to freshly isolated chondrocytes. As shown in **Figure 7**, the cells were intensively stained by Alcian blue for sulfated GAGs and immunostained for Col2A1. The presence of UBM was particularly effective in promoting the maintenance of chondrogenic phenotype as evidenced by a larger number of Col2A1 positive spontaneous microaggregates that persisted over 7 days.

Cryopreservation of *Af*, *AGf*, and *AUBMf* Embedded Cells

To explore the possibility to set up a bank of "microfibrous scaffolds embedded chondrocytes" for further *in vitro* and *in vivo* manipulations, we performed a preliminary assessment of the properties of thawed A*f*, AG*f*, and AUBM*f* embedded cells after freezing procedure. The redifferentiated chondrocytes were frozen directly within microfibers in complete culture medium supplemented with 10% DMSO, stored at −196°C in liquid nitrogen, thawed, and then assessed for cellular viability and chondrogenic properties. Similar to the freshly A*f*, AG*f*, and AUBM*f* embedded cells, thawed samples maintained highly viable cells with a round shaped morphology (**Figure 8**). When recovered from microfibers and grown in monolayer in standard medium without chondrogenic inducers for 24 h (the conditions are the same described in **Figure 7**), thawed samples preserved GAG production and Col2A1 expression as shown by Alcian Blue staining and immunocytochemistry (**Figure 8**).

Therefore, the alginate-based microfibers appear resistant to freezing and allow us to recover highly viable and functional cells also after thawing.

DISCUSSION

This paper describes the production of microfiber constructs containing redifferentiated chondrocytes into alginate hydrogels for the treatment of cartilage defects.

Cells have been embedded in hydrogels combined with ECM-derived components (i.e., gelatin or decellularized UBM) without any chondrogenic growth factors supplementation (i.e., TGFβ). Alginate was chosen as main constituent of the construct since its beneficial on improving chondrocyte properties and supporting chondrogenesis have been previously

A

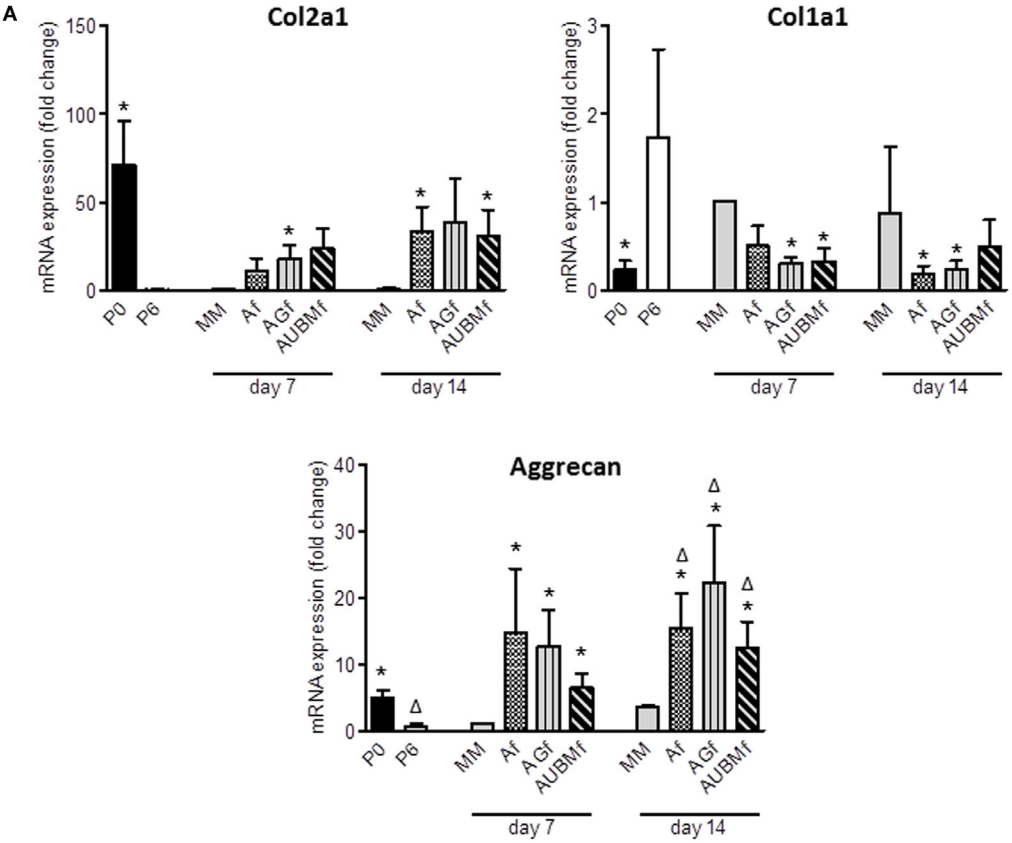

B

	Condition	Col2A1/Col1A1 ratio	Col10A1	GAG content *(μg GAG/ng DNA)*
	P6	0.01 ± 0.01	ND	ND
day 7	MM	0.17 ± 0.12	ND	1.15 ± 0.51
	A*f*	20.97 ± 13.31	ND	8.53 ± 4.80
	AG*f*	17.64 ± 11.71	ND	11.73 ± 9.41
	AUBM*f*	15.58 ± 10.02	ND	5.26 ± 0.62*
day 14	MM	0.52 ± 0.49	ND	0.09 ± 0.06
	A*f*	31.99 ± 18.14*	ND	18.11 ± 8.95
	AG*f*	20.69 ± 11.03*	ND	11.28 ± 7.67
	AUBM*f*	11.51 ± 5.37*	ND	9.47 ± 5.45

ND = not detectable

FIGURE 6 | Continued

FIGURE 6 | Continued
Chondrogenic properties of A*f*, AG*f*, and AUBM*f* embedded cells: analysis of cartilage-specific markers. A*f*, AG*f*, and AUBM*f* embedded redifferentiated chondrocytes or chondrocyte micromasses (MM) cultured for 7 or 14 days were compared for chondrogenic capacity by analyzing the expression of cartilage markers. **(A)** The expression of Col2A1, Col1A1, and aggrecan was evaluated by RT-qPCR. Values obtained from freshly isolated (P0) and dedifferentiated chondrocytes (P6) are also included. Results were calculated using $2^{-\Delta\Delta Ct}$ method, and data are presented as fold change means respect to MM day 7. **(B)** Quantification of Col2a1/Col1a1 ratio, Col10A1 expression, and GAG content for each experimental condition are reported. Col10a1 expression was assessed by RT-qPCR and resulted not detectable (ND) in all tested conditions. GAG content was quantified by DMMB staining on cellular lysates, and values are reported as μg GAG/ng DNA. All data are presented as means ± SEM of three independent experiments performed on chondrocytes from four different donors ($n = 4$). Statistical analysis was performed all conditions versus MM day 7 ($^{*}p < 0.05$) or versus MM day 14 ($^{\Delta}p < 0.05$).

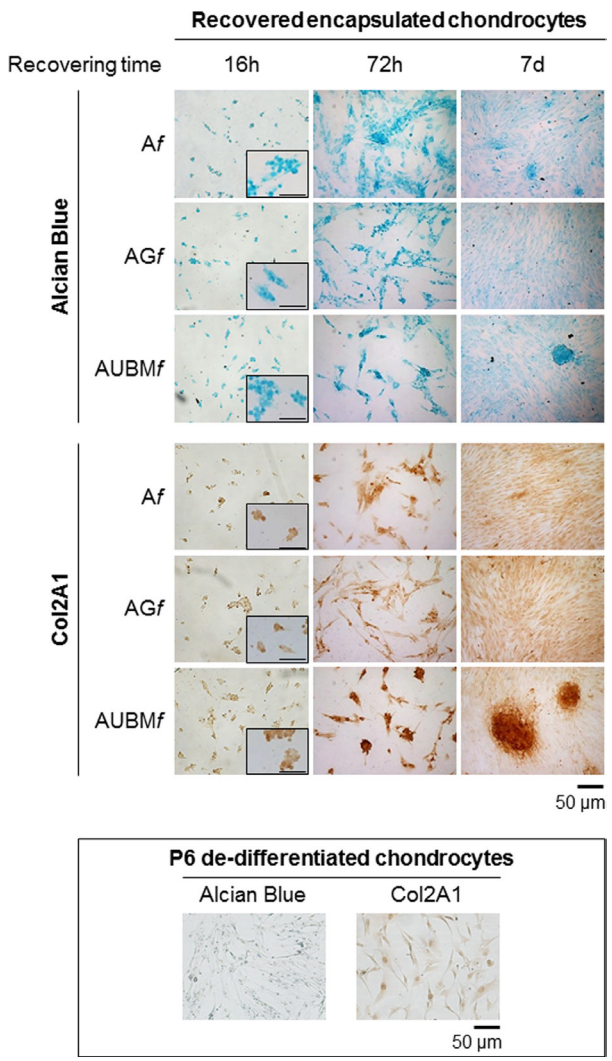

FIGURE 7 | Behavior of the embedded cells after they are recovered from the microfibers. Redifferentiated chondrocytes were recovered from microfibers after 14 days of culture, reseeded, grown up to 7 days as monolayered culture in standard medium without adding chondrogenic inducers, and compared with P6 dedifferentiated chondrocytes. The cells were stained by Alcian blue for sulfated GAGs and immunostained for Col2A1 after growing in monolayer for 16 h, 72 h, or 7 days. Optical photomicrographs indicate the maintenance of acquired chondrogenic properties. Bar corresponds to 50 and 100 μm for the insets.

described (Moutos and Guilak, 2008). In addition, it has been demonstrated that the concomitant presence of ECM-derived materials can ameliorate the performances of the scaffold for cartilage TE, accelerating the tissue regeneration (Zhang et al., 2016).

The novelty of our experimental approach lies indeed not only in the microfluidic approach developed for microfibers production but primarily on the combined presence of alginate and gelatin/UBM in a multifunctional scaffold containing nasal chondrocytes. Moreover, the behavior of embedded cells has been investigated with various techniques, allowing to finely assess how the biomaterial constructs were mimicking cartilage physiological microenvironment.

It is important to underline that many researchers involved in cell-based regenerative medicine are promoting the employment of cells by ethical and non-invasive procedures such as those isolated from tissues representing surgical wastes. In this regard, nasal septum, easily harvested from surgical procedures with minimal morbidity, represents an ideal source for cartilage cells.

In this respect, the presented data, strengthen the interest toward chondrocytes from the nasal septum, which show superior and more reproducible chondrogenic capacity, compared with chondrocytes from articular cartilage (Kafienah et al., 2002; Rotter et al., 2002; Wolf et al., 2008; Mumme et al., 2016). The comparison with articular chondrocytes demonstrated that nasal chondrocytes were able to support the production of a cartilage matrix with adequate functional and biomechanical characteristics both *in vitro* and *in vivo* (do Amaral et al., 2012; Pleumeekers et al., 2014). Therefore, it is reasonable to suppose that good mechanical integrity and structural stability of surgical specimens from nasal septum may remain in the memory of chondrocytes if cultured in a favorable environment. This might explain the highly chondrogenic properties exhibited by our redifferentiated chondrocytes recovered from microfibers after long-term culture.

Importantly, the high passage (P6) cells were highly capable to redifferentiate when properly embedded in alginate-based microfibrous scaffolds. This finding is of particular relevance since P6 dedifferentiated chondrocytes are widely described as irreversibly dedifferentiated chondrocytes.

They are usually not recommended for transplantation since become apoptotic, inhibit key signaling proteins in the MAP kinase pathway, produce matrix-degrading enzymes, losing, as a whole, their chondrogenic potential definitively (Dell'Accio et al., 2001; Schulze-Tanzil et al., 2004). On the contrary, the alginate-based composite scaffolds allowed to support chondrogenic process of advanced dedifferentiated chondrocytes from monolayer passage P6. This evidence appear particularly notable since the use of cells at higher culture passages allows to expand the cell populations to a much higher level for further clinical applications, overcoming the issue of relative small and insufficient donor samples (Melero-Martin and Al-Rubeai, 2007).

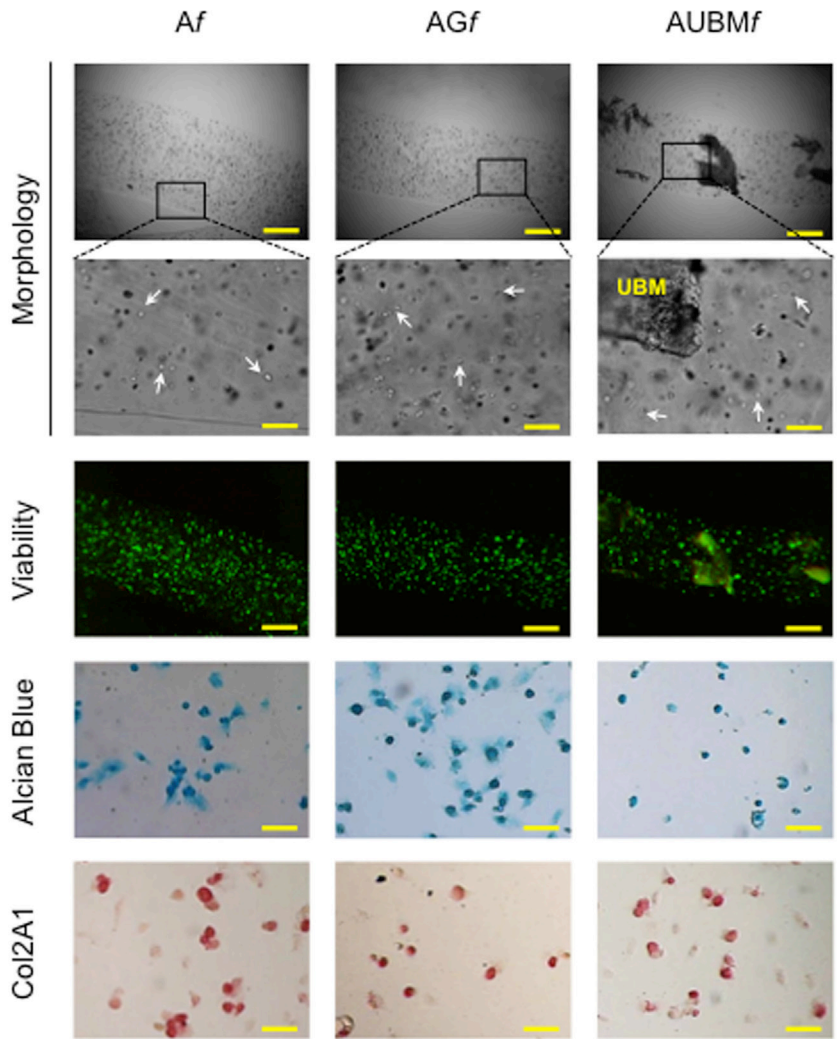

FIGURE 8 | Cryopreservation of *Af, AGf*, and *AUBMf* embedded cells. A*f*, AG*f*, and AUBM*f* embedded redifferentiated chondrocytes were frozen, stored in liquid nitrogen, thawed, and assessed for cell morphology, viability, and chondrogenic properties. Optical images of microfibers show the rounded shape retention by the thawed embedded cells (particularly evident at higher magnification: see white arrows). Fluorescence merged images of the Calcein-AM (green)/propidium iodide (red) double staining demonstrated the high cell viability. The presence of GAGs and Col2A1 was detected by Alcian Blue staining and immunocytochemical analysis on the thawed embedded cells recovered from microfibers and grown in monolayer for 24 h. Bar corresponds to: 300 μm in lower magnification images of morphology and viability, 60 μm in higher magnification, and 50 μm in Alcian Blue staining and Col2A1 immunocytochemical analysis.

Interestingly, the effects of 3D microenvironments based on alginate plus gelatin or UBM on the embedded cells occurred without the addition of the typical chondrogenic inducers such as TGFβ. This evidence represents an important added value considering the recently reported controversial action of TGFβ. Despite many well-described advantages, the use of differentiating agents is indeed questioned for the undesired off target effects and controversial outcomes. For instance, it has been reported that TGFβ may be detrimental for the redifferentiation process of chondrocytes and may promote the rapid and undesirable differentiation into fibroblast-like cells (Mueller et al., 2010; Narcisi et al., 2012). The negative effect of TGFβ in wound repair of cartilage has been also observed in several experimental models supporting the hypothesis that the inhibition of TGFβ may induce cartilage repair (Blaney Davidson et al., 2007; Khaghani et al., 2012) without the onset of undesired hypertrophy. Hypertrophy represents, in fact, one of the major drawbacks in autologous chondrocytes implantation and in MSC-based strategies (Melero-Martin and Al-Rubeai, 2007; Niethammer et al., 2014).

Notably, the here described composite microfibers represent a favorable microenvironment for the embedded cells supporting their viability and maturation. The alginate 3D matrix in combination with UBM prevents cell-to-cell contacts, mimicking the physiological microenvironment typical of mature cartilage. The embedded cells were indeed mainly present as single cells, well dispersed in the alginate, showing a morphology resembling that of mature chondrocytes in cartilage. This evidence is essential in view of the *in vivo* use of microfibers, showing for

the first time that the presence of UBM is not detrimental for chondrocytes activity, rather it seems particularly effective in maintaining chondrogenic activity of the cells and their ability to form aggregates once released from the confined 3D microenvironment of the scaffolds (**Figure 7**). This point is intriguing and allow us to hypothesize that UBM may act as a guide for a proper cell arrangement when implanted within a complex mixture of structural and bioactive molecules such as cartilage tissue, without risk of rejection since decellularization removes or masks antigenic epitopes (Turner and Badylak, 2015). Moreover, considering that the use of decellularized allografts and xenografts in the repair of damaged cartilage is just beginning, our data may give useful information for generating biomimetic engineered cartilage constructs.

A further advantage of alginate microfibers relies on the cryoconservation of the cells for further therapeutic uses. Alginate microfibers appear resistant to freezing and allow to maintain highly viable and functional cells after thawing. Consequently, the presented scaffolds may be proposed as tool for *in vitro* redifferentiation process and recovering of an effective and functional chondrocyte population potentially able to produce a neocartilage tissue *in vivo*. This evidence is also important in view of a future chondrocyte bank that would be of great help as a permanent source of cartilage cells.

In conclusion, to the best of our knowledge, few reports focused on the effect of ECM-derived biomaterials in cartilage regeneration (Jin et al., 2007; Yang et al., 2008; Baugé et al., 2014; Grogan et al., 2014; Lee et al., 2014; Youngstrom et al., 2015) and in any case the combination with alginate properties has not been described. This interaction is an essential feature for the success of a TE strategy, allowing to maintain the low friction and the load-bearing characteristics of the native cartilage (Moutos and Guilak, 2008; Grogan et al., 2014). Therefore, the hypothesis to guide cartilage neoformation *in vivo* by such cell-based microfibrous constructs is worth further consideration, especially given that fibrous versus non-fibrous scaffolds offer interesting advantages for cell delivery in biomedical application since guided growth, alignment, and migration of cells are favored (Blaney Davidson et al., 2007; Yang et al., 2008; Grogan et al., 2014; Youngstrom et al., 2015). In conclusion, our results provide a proof of concept for developing a next experimental design based on the implantation of microfibers or recovered redifferentiated chondrocytes on animal models with critical size defect affecting the whole joint.

ETHICS STATEMENT

Cartilage fragments from nasal septum were obtained from 15 donors between 25 and 60 years old, which underwent septoplasty surgery procedures, after informed consent and approval of the Ethics Committee of the University of Ferrara and S. Anna Hospital.

AUTHOR CONTRIBUTIONS

MA conception and design, collection and assembly of data, data analysis and interpretation, manuscript writing, and final approval of manuscript. LP, SM, EL, and AL conception and design, data analysis and interpretation, and final approval of manuscript. RP and CN conception and design, provision of study material, data analysis and interpretation, manuscript writing, and final approval of manuscript.

ACKNOWLEDGMENTS

This work was funded by the "FIRB FUTURO IN RICERCA 2010 (grant number RBFR10XKHS_002)" from the Ministry of the University and Research of Italy. We are grateful to Prof. Stephen F. Badylak, McGowan Institute for Regenerative Medicine, University of Pittsburgh, USA, for providing UBM, Dr. Eleonora Gallerani, Department of Life Sciences and Biotechnology, Dr. Agnese Pellati, Department of Morphology, Surgery and Experimental Medicine, Dr. Paola Boldrini and Dr. Maria Rita Bovolenta, Centro di Microscopia Elettronica, University of Ferrara, for technical assistance.

SUPPLEMENTARY MATERIAL

The Supplementary Material for this article can be found online at http://journal.frontiersin.org/article/10.3389/fbioe.2017.00035/full#supplementary-material.

REFERENCES

Angelozzi, M., Miotto, M., Penolazzi, L., Mazzitelli, S., Keane, T., Badylak, S. F., et al. (2015). Composite ECM-alginate microfibers produced by microfluidics as scaffolds with biomineralization potential. *Mater. Sci. Eng. C Mater. Biol. Appl.* 56, 141–153. doi:10.1016/j.msec.2015.06.004

Badylak, S. F., Freytes, D. O., and Gilbert, T. W. (2009). Extracellular matrix as a biological scaffold material: structure and function. *Acta Biomater.* 5, 1–13. doi:10.1016/j.actbio.2008.09.013

Baugé, C., Girard, N., Lhuissier, E., Bazille, C., and Boumediene, K. (2014). Regulation and role of TGFβ signaling pathway in aging and osteoarthritis joints. *Aging Dis.* 5, 394–405. doi:10.14336/AD.2014.0500394

Bidarra, S. J., Barrias, C. C., and Granja, P. L. (2014). Injectable alginate hydrogels for cell delivery in tissue engineering. *Acta Biomater.* 10, 1646–1662. doi:10.1016/j.actbio.2013.12.006

Blaney Davidson, E. N., van der Kraan, P. M., and van den Berg, W. B. (2007). TGF-beta and osteoarthritis. *Osteoarthr. Cartil.* 15, 597–604. doi:10.1016/j.joca.2007.02.005

Bonaventure, J., Kadhom, N., Cohen-Solal, L., Ng, K. H., Bourguignon, J., Lasselin, C., et al. (1994). Reexpression of cartilage-specific genes by dedifferentiated human articular chondrocytes cultured in alginate beads. *Exp. Cell. Res.* 212, 97–104. doi:10.1006/excr.1994.1123

Brown, B. N., and Badylak, S. F. (2014). Extracellular matrix as an inductive scaffold for functional tissue reconstruction. *Transl. Res.* 163, 268–285. doi:10.1016/j.trsl.2013.11.003

Calafiore, R. (2003). Alginate microcapsules for pancreatic islet cell graft immunoprotection: struggle and progress towards the final cure for type 1 diabetes mellitus. *Expert Opin. Biol. Ther.* 3, 201–205. doi:10.1517/14712598.3.2.201

Caron, M. M. J., Emans, P. J., Coolsen, M. M. E., Voss, L., Surtel, D. A. M., Cremers, A., et al. (2012). Redifferentiation of dedifferentiated human articular chondrocytes: comparison of 2D and 3D cultures. *Osteoarthr. Cartil.* 20, 1170–1178. doi:10.1016/j.joca.2012.06.016

Chang, C. H., Lin, F. H., Kuo, T. F., and Liu, H. C. (2005). Cartilage tissue engineering. *Biomed. Eng. Appl. Basis Comm.* 17, 1–11. doi:10.4015/S101623720500010X

Dell'Accio, F., De Bari, C., and Luyten, F. P. (2001). Molecular markers predictive of the capacity of expanded human articular chondrocytes to form stable

cartilage in vivo. *Arthritis Rheum.* 44, 1608–1619. doi:10.1002/1529-0131(200107)44:7<1608::AID-ART284>3.0.CO;2-T

do Amaral, R. J., Pedrosa Cda, S., Kochem, M. C., Silva, K. R., Aniceto, M., Claudio- da-Silva, C., et al. (2012). Isolation of human nasoseptal chondrogenic cells: a promise for cartilage engineering. *Stem Cell Res.* 8, 292–299. doi:10.1016/j.scr.2011.09.006

Gilbert, T. W., Sellaro, T. L., and Badylak, S. F. (2006). Decellularization of tissues and organs. *Biomaterials* 27, 3675–3683. doi:10.1016/j.biomaterials.2006.02.014

Gómez-Guillén, M. C., Giménez, B., López-Caballero, M. E., and Montero, M. P. (2011). Functional and bioactive properties of collagen and gelatin from alternative sources: a review. *Food Hydrocolloids* 25, 1813–1827. doi:10.1016/j.foodhyd.2011.02.007

Grogan, S. P., Chen, X., Sovani, S., Taniguchi, N. Jr., Colwell, C. W., Lotz, M. K., et al. (2014). Influence of cartilage extracellular matrix molecules on cell phenotype and neocartilage formation. *Tissue Eng. Part A* 20, 264–274. doi:10.1089/ten.TEA.2012.0618

Guo, J. F., Jourdian, G. W., and MacCallum, D. K. (1989). Culture and growth characteristics of chondrocytes encapsulated in alginate beads. *Connect. Tissue Res.* 19, 277–297. doi:10.3109/03008208909043901

Häuselmann, H., Masuda, K., Hunziker, E. B., Neidhart, M., Mok, S. S., Michel, B. A., et al. (1996). Adult human chondrocytes cultured in alginate form a matrix similar to native human articular cartilage. *Am. J. Physiol.* 271, C742–C752.

Jacobs, H. N., Rathod, S., Wolf, M. T., and Elisseeff, J. H. (2017). Intra-articular injection of urinary bladder matrix reduces osteoarthritis development. *AAPS J.* 19, 141–149. doi:10.1208/s12248-016-9999-6

Jin, C. Z., Park, S. R., Choi, B. H., Park, K., and Min, B. H. (2007). In vivo cartilage tissue engineering using a cell-derived extracellular matrix scaffold. *Artif. Organs* 31, 183–192. doi:10.1111/j.1525-1594.2007.00363.x

Kafienah, W., Jakob, M., Demarteau, O., Frazer, A., Barker, M. D., Martin, I., et al. (2002). Three-dimensional tissue engineering of hyaline cartilage: comparison of adult nasal and articular chondrocytes. *Tissue Eng.* 8, 817–826. doi:10.1089/10763270260424178

Khaghani, S. A., Denyer, M. C. T., and Youseffi, M. (2012). Effect of transforming growth factor-β1 in biological regulation of primary chondrocyte. *Am. J. Biomed. Eng.* 2, 1–8. doi:10.5923/j.ajbe.20120201.01

Lee, K. Y., and Mooney, D. J. (2001). Hydrogels for tissue engineering. *Chem. Rev.* 101, 1869–1880. doi:10.1021/cr000108x

Lee, P., Tran, K., Chang, W., Shelke, N. B., Kumbar, S. G., and Yu, X. (2014). Influence of chondroitin sulfate and hyaluronic acid presence in nanofibers and its alignment on the bone marrow stromal cells: cartilage re generation. *J. Biomed. Nanotechnol.* 10, 1469–1479. doi:10.1166/jbn.2014.1831

Liao, J., Shi, K., Ding, Q., Qu, Y., Luo, F., and Qian, Z. (2014). Recent developments in scaffold-guided cartilage tissue regeneration. *J. Biomed. Nanotechnol.* 10, 3085–3104. doi:10.1166/jbn.2014.1934

Lolli, A., Lambertini, E., Penolazzi, L., Angelozzi, M., Morganti, C., Franceschetti, T., et al. (2014). Pro-chondrogenic effect of miR-221 and Slug depletion in human MSCs. *Stem Cell. Rev.* 10, 841–855. doi:10.1007/s12015-014-9532-1

Malkin, A. Y. A., Goncharenko, V. V., and Malinovskii, V. V. (1976). Barus effect in polymer flows through cylindrical and flat dies. *Mekhanika Polimerov* 3, 487–492.

Mazzitelli, S., Capretto, L., Quinci, F., Piva, R., and Nastruzzi, C. (2013). Preparation of cell-encapsulation devices in confined microenvironment. *Adv. Drug Deliv. Rev.* 65, 1533–1555. doi:10.1016/j.addr.2013.07.021

Melero-Martin, J. M., and Al-Rubeai, M. (2007). "In vitro expansion of chondrocytes," in *Topics in Tissue Engineering*, Vol. 3, Chap. 2, eds N. Ashammakhi, R. Reis, and E. Chiellini.

Moutos, F. T., and Guilak, F. (2008). Composite scaffolds for cartilage tissue engineering. *Biorheology* 45, 501–512. doi:10.3233/BIR-2008-0491

Mueller, M. B., Fischer, M., Zellner, J., Berner, A., Dienstknecht, T., Prantl, L., et al. (2010). Hypertrophy in mesenchymal stem cell chondrogenesis: effect of TGF-beta isoforms and chondrogenic conditioning. *Cells Tissues Organs* 192, 158–166. doi:10.1159/000313399

Muir, H. (1995). The chondrocyte, architect of cartilage. Biomechanics, structure, function and molecular biology of cartilage matrix macromolecules. *Bioessays* 17, 1039–1048. doi:10.1002/bies.950171208

Mumme, M., Barbero, A., Miot, S., Wixmerten, A., Feliciano, S., Wolf, F., et al. (2016). Nasal chondrocyte-based engineered autologous cartilage tissue for repair of articular cartilage defects: an observational first-in-human trial. *Lancet* 388, 1985–1994. doi:10.1016/S0140-6736(16)31658-0

Narcisi, R., Signorile, L., Verhaar, J. A., Giannoni, P., and van Osch, G. J. (2012). TGFβ inhibition during expansion phase increases the chondrogenic redifferentiation capacity of human articular chondrocytes. *Osteoarthr. Cartil.* 20, 1152–1160. doi:10.1016/j.joca.2012.06.010

Niethammer, T. R., Pietschmann, M. F., Horng, A., Roßbach, B. P., Ficklscherer, A., Jansson, V., et al. (2014). Graft hypertrophy of matrix-based autologous chondrocyte implantation: a two-year follow-up study of NOVOCART 3D implantation in the knee. *Knee Surg. Sports Traumatol. Arthrosc.* 22, 1329–1336. doi:10.1007/s00167-013-2454-7

Penolazzi, L., Mazzitelli, S., Vecchiatini, R., Torreggiani, E., Lambertini, E., Johnson, S., et al. (2012). Human mesenchymal stem cells seeded on extracellular matrix-scaffold: viability and osteogenic potential. *J. Cell. Physiol.* 227, 857–866. doi:10.1002/jcp.22983

Penolazzi, L., Tavanti, E., Vecchiatini, R., Lambertini, E., Vesce, F., Gambari, R., et al. (2010). Encapsulation of mesenchymal stem cells from Wharton's jelly in alginate microbeads. *Tissue Eng. Part C Methods* 16, 141–155. doi:10.1089/ten.TEC.2008.0582

Pleumeekers, M. M., Nimeskern, L., Koevoet, W. L., Kops, N., Poublon, R. M., Stok, K. S., et al. (2014). The in vitro and in vivo capacity of culture-expanded human cells from several sources encapsulated in alginate to form cartilage. *Eur. Cell. Mater.* 27, 264–280. doi:10.22203/eCM.v027a19

Poole, A. R., Kojima, T., Yasuda, T., Mwale, F., Kobayashi, M., and Laverty, S. (2001). Composition and structure of articular cartilage: a template for tissue repair. *Clin. Orthop. Relat. Res.* 391, S26–S33. doi:10.1097/00003086-200110001-00004

Pravdyuk, A. I., Petrenko, Y. A., Fuller, B. J., and Petrenko, A. Y. (2013). Cryopreservation of alginate encapsulated mesenchymal stromal cells. *Cryobiology* 66, 215–222. doi:10.1016/j.cryobiol.2013.02.002

Rose, W., Wood, J. D., Simmons-Byrd, A., and Spievack, A. R. (2009). Effect of a xenogeneic urinary bladder injectable bioscaffold on lameness in dogs with osteoarthritis of the coxofemoral joint (hip): a randomized, double blinded controlled trial. *Int. J. Appl. Res. Vet. Med.* 7, 13–22.

Rotter, N., Bonassar, L. J., Tobias, G., Lebl, M., Roy, A. K., and Vacanti, C. A. (2002). Age dependence of biochemical and biomechanical properties of tissue-engineered human septal cartilage. *Biomaterials* 23, 3087–3094. doi:10.1016/S0142-9612(02)00031-5

Santoro, M., Tatara, A. M., and Mikos, A. G. (2014). Gelatin carriers for drug and cell delivery in tissue engineering. *J. Control Release* 190, 210–218. doi:10.1016/j.jconrel.2014.04.014

Schulze-Tanzil, G., Mobasheri, A., de Souza, P., John, T., and Shakibaei, M. (2004). Loss of chondrogenic potential in dedifferentiated chondrocytes correlates with deficient Shc-Erk interaction and apoptosis. *Osteoarthr. Cartil.* 12, 448–458. doi:10.1016/j.joca.2004.02.007

Tottey, S., Corselli, M., Jeffries, E. M., Londono, R., Peault, B., and Badylak, S. F. (2011). Extracellular matrix degradation products and low-oxygen conditions enhance the regenerative potential of perivascular stem cells. *Tissue Eng. Part A* 17, 37–44. doi:10.1089/ten.TEA.2010.0188

Turner, N. J., and Badylak, S. F. (2015). The use of biologic scaffolds in the treatment of chronic nonhealing wounds. *Adv. Wound Care* 4, 490–500. doi:10.1089/wound.2014.0604

Vecchiatini, R., Penolazzi, L., Lambertini, E., Angelozzi, M., Morganti, C., Mazzitelli, S., et al. (2015). Effect of dynamic three-dimensional culture on osteogenic potential of human periodontal ligament-derived mesenchymal stem cells entrapped in alginate microbeads. *J. Periodont. Res.* 50, 544–553. doi:10.1111/jre.12225

Wolf, F., Haug, M., Farhadi, J., Candrian, C., Martin, I., and Barbero, A. (2008). A low percentage of autologous serum can replace bovine serum to engineer human nasal cartilage. *Eur. Cell. Mater.* 5, 1–10. doi:10.22203/eCM.v015a01

Yang, Q., Peng, J., Guo, Q., Huang, J., Zhang, L., Yao, J., et al. (2008). A cartilage ECM-derived 3-D porous acellular matrix scaffold for in vivo cartilage tissue engineering with PKH26-labeled chondrogenic bone marrow-derived mesenchymal stem cells. *Biomaterials* 29, 2378–2387. doi:10.1016/j.biomaterials.2008.01.037

Youngstrom, D. W., Cakstina, I., and Jakobsons, E. (2015). Cartilage-derived extracellular matrix extract promotes chondrocytic phenotype in three-dimensional tissue culture. *Artif. Cells Nanomed. Biotechnol.* 24, 1–8. doi:10.3109/21691401.2015.1014091

Zhang, W., Zhu, Y., Li, J., Guo, Q., Peng, J., Liu, S., et al. (2016). Cell-derived extracellular matrix: basic characteristics and current applications in orthopedic tissue engineering. *Tissue Eng. Part B Rev.* 22, 193–207. doi:10.1089/ten.TEB.2015.0290

Conflict of Interest Statement: The authors declare that the research was conducted in the absence of any commercial or financial relationships that could be construed as a potential conflict of interest.

The reviewer, AB, and handling editor declared their shared affiliation, and the handling editor states that the process nevertheless met the standards of a fair and objective review.

frontiers in Bioengineering and Biotechnology

ORIGINAL RESEARCH
published: 27 November 2017
doi: 10.3389/fbioe.2017.00073

Cyclic Tensile Strain Can Play a Role in Directing both Intramembranous and Endochondral Ossification of Mesenchymal Stem Cells

*Simon F. Carroll [1,2], Conor T. Buckley[1,2,4] and Daniel J. Kelly [1,2,3,4]**

[1] Trinity Centre for Bioengineering, Trinity Biomedical Sciences Institute, Trinity College Dublin, Dublin, Ireland, [2] Department of Mechanical and Manufacturing Engineering, School of Engineering, Trinity College Dublin, Dublin, Ireland, [3] Department of Anatomy, Royal College of Surgeons in Ireland, Dublin, Ireland, [4] Advanced Materials and Bioengineering Research Centre (AMBER), Royal College of Surgeons in Ireland and Trinity College Dublin, Dublin, Ireland

Successfully regenerating damaged or diseased bone and other joint tissues will require a detailed understanding of how joint specific environmental cues regulate the fate of progenitor cells that are recruited or delivered to the site of injury. The goal of this study was to explore the role of cyclic tensile strain (CTS) in regulating the initiation of mesenchymal stem cell/multipotent stromal cell (MSC) differentiation, and specifically their progression along the endochondral pathway. To this end, we first explored the influence of CTS on the differentiation of MSCs in the absence of any specific growth factor, and secondly, we examined the influence of the long-term application of this mechanical stimulus on markers of endochondral ossification in MSCs maintained in chondrogenic culture conditions. A custom bioreactor was developed to apply uniaxial tensile deformation to bone marrow-derived MSCs encapsulated within physiological relevant 3D fibrin hydrogels. Mechanical loading, applied in the absence of soluble differentiation factors, was found to enhance the expression of both tenogenic (COL1A1) and osteogenic markers (BMP2, RUNX2, and ALPL), while suppressing markers of adipogenesis. No evidence of chondrogenesis was observed, suggesting that CTS can play a role in initiating direct intramembranous ossification. During long-term culture in the presence of a chondrogenic growth factor, CTS was shown to induce MSC re-organization and alignment, increase proteoglycan and collagen production, and to enhance the expression of markers associated with endochondral ossification (BMP2, RUNX2, ALPL, OPN, and COL10A1) in a strain magnitude-dependent manner. Taken together, these findings indicate that tensile loading may play a key role in promoting both intramembranous and endochondral ossification of MSCs in a context-dependent manner. In both cases, this loading-induced promotion of osteogenesis was correlated with an increase in the expression of the osteogenic growth factor BMP2. The results of this study demonstrate the potent role that extrinsic mechanical loading plays in guiding stem cell fate, which must be carefully considered when designing cell and tissue-engineering therapies if they are to realize their clinical potential.

Keywords: mesenchymal stem cells, endochondral ossification, intramembranous ossification, tensile strain, mechanical stimulation, osteogenesis, chondrogenesis

OPEN ACCESS

Edited by:
Roberto Narcisi,
Erasmus Medical Center, Netherlands

Reviewed by:
Silvia Lopa,
IRCCS Galeazzi Orthopedic Institute, Italy
Anna Lange-Consiglio,
University of Milan, Italy

***Correspondence:**
Daniel J. Kelly
kellyd9@tcd.ie

Specialty section:
This article was submitted to Tissue Engineering and Regenerative Medicine, a section of the journal Frontiers in Bioengineering and Biotechnology

Received: *23 August 2017*
Accepted: *02 November 2017*
Published: *27 November 2017*

Citation:
Carroll SF, Buckley CT and Kelly DJ (2017) Cyclic Tensile Strain Can Play a Role in Directing both Intramembranous and Endochondral Ossification of Mesenchymal Stem Cells. Front. Bioeng. Biotechnol. 5:73. doi: 10.3389/fbioe.2017.00073

INTRODUCTION

Understanding the etiology of diseases such as osteoarthritis requires an in-depth understanding of the role that joint specific environmental factors play in the maintenance of cartilage and its conversion into bone. Furthermore, successfully regenerating damaged or diseased bone and other joint tissues also requires an understanding of how such environmental factors regulate the fate of cells that are recruited or delivered to the site of injury. Multipotent stromal cells (MSCs) isolated from bone marrow can be induced to differentiate toward multiple lineages, making them an attractive cell type for cartilage and bone tissue engineering (Caplan, 1991; Yoo et al., 1998; Steinert et al., 2012; Vinardell et al., 2012; Grayson et al., 2015). Bone development occurs *via* two distinct mechanisms—intramembranous or endochondral ossification. Intramembranous ossification involves the direct differentiation of MSCs into osteoblasts, whereas endochondral ossification first involves differentiation of precursor cells into chondrocytes, the formation of a cartilage template and its subsequent replacement by bone (Frohlich et al., 2008). The latter is the process by which all long bones are formed. It has long been suggested that endochondral ossification during limb development is mechanoregulated, with early studies linking femoral ossification to the regions of maximal tensile strains (Carey, 1922). More recent work has confirmed this relationship between the mechanical environment and bone development (Nowlan et al., 2010). It has also been reported that, during bone healing, callus distraction can produce a systemic increase in concentrations of several bone growth factors (Sato et al., 1999; Weiss et al., 2002). While clearly mechanical cues are integral to directing bone growth, development, and healing, the underlying mechanisms remain poorly understood. A more complete understanding of these processes will benefit not only the fields of cartilage and bone tissue engineering but will also be integral to the development of novel therapeutic strategies to treat complex diseases such as osteoarthritis.

There has been increased interest in the use of *in vitro* bioreactor systems to examine how different mechanical stimuli regulate both osteogenesis and chondrogenesis of stem cells (Kelly and Jacobs, 2010). It has been demonstrated that the application of uniaxial cyclic tensile strain (CTS) to MSCs cultured on 2D substrates can induce osteogenic and fibrogenic gene expression (Simmons et al., 2003; Friedl et al., 2007; Qi et al., 2008, Diederichs et al., 2009). The magnitude of tensile loading has also been shown to be important, with low strains inducing osteogenesis and higher strains promoting the expression of fibrous or myogenic markers (Chen et al., 2008, Jang et al., 2011). These 2D culture systems are generally not considered truly representative of the physiological environment of cells *in vivo*, and MSCs have been shown to respond differentially to tensile loading when seeded on 2D substrates compared with when they are encapsulated within 3D matrices (Rathbone et al., 2012). Of the studies that have explored the influence of tensile strain on directing the differentiation of MSCs in 3D matrices, many have concluded that the application of uniaxial CTS promotes a more ligamentous or fibro-chondrogenic phenotype in MSCs (Altman et al., 2002; Juncosa-Melvin et al., 2007; Farng et al., 2008; Kuo and Tuan, 2008; Connelly et al., 2010; Doroski et al., 2010; Baker et al., 2011; Kreja et al., 2012; Yang et al., 2012). However, it has also been demonstrated that the application of CTS to MSCs in 3D collagen gels in the absence of osteogenic supplements can lead to the upregulation of *BMP2* (Sumanasinghe et al., 2006), suggesting that this mechanical stimulus may also be osteoinductive. Furthermore, it has been reported that tensile strain and dynamic compression differentially regulate MSC differentiation (Haudenschild et al., 2009), with CTS upregulating osteogenic markers *BMP1*, *ALP*, and *NELL1*, whereas compression was found to promote chondrogenesis of MSCs encapsulated in 3D alginate matrices. This latter finding agrees with a number of separate studies demonstrating that compressive loading can enhance chondrogenesis of MSCs (Huang et al., 2004; Campbell et al., 2006; Thorpe et al., 2012; Steward et al., 2014; Luo et al., 2015). Additionally, it has been demonstrated that high magnitudes of cyclic hydrostatic pressure and dynamic compression can suppress hypertrophy and endochondral ossification of MSCs (Bian et al., 2012; Thorpe et al., 2013; Carroll et al., 2014; Luo et al., 2015, Zhang et al., 2015). Collectively, these studies point to the integral role that mechanical cues play in directing both the initial phenotype of MSCs and in determining their ultimate fate.

Despite the fact that long bones form and regenerate through the process of endochondral ossification, relatively little is known about the role mechanical cues can play in directing this process. Motivated by previous work pointing to a role for tensile strain in directing bone development and healing, the objective of this study was to explore the role of CTS in directing osteogenesis of MSCs within physiologically relevant 3D hydrogels using a custom developed bioreactor system. Recognizing that bone can form and heal through either an intramembranous or an endochondral pathway, we first sought to explore the influence of CTS on the differentiation of MSCs in the absence of specific growth factors to determine if loading alone could initiate osteogenesis. We then examined the influence of the long-term application of this mechanical stimulus on markers of endochondral ossification in MSCs maintained in chondrogenic culture conditions. Our hypothesis was that CTS would enhance endochondral ossification in chondrogenically primed MSCs. The dependency of this process on the magnitude and frequency of the applied strain was also examined.

MATERIALS AND METHODS

CTS Bioreactor

A novel bioreactor system was developed for the aseptic application of uniaxial CTS to soft 3D hydrogels. The entire system was housed within a cell culture incubator for the duration of each study. Custom rubber strips (**Figure 1A**) were molded using a commercially available silicone elastomer kit (Sylgard 184, Dow Corning) by mixing the base with the curing agent at a ratio of 20:1, pouring into a PTFE mold, de-gassing by vacuum and cross-linking for 1 h at 100°C. Each strip had a dog-bone shaped recess (1.5 mm deep) to accommodate hydrogel samples. Gelation of hydrogel samples occurred within these recesses. The strips were soaked and washed in ethanol and water to ensure removal of residual curing agent, then autoclaved before use.

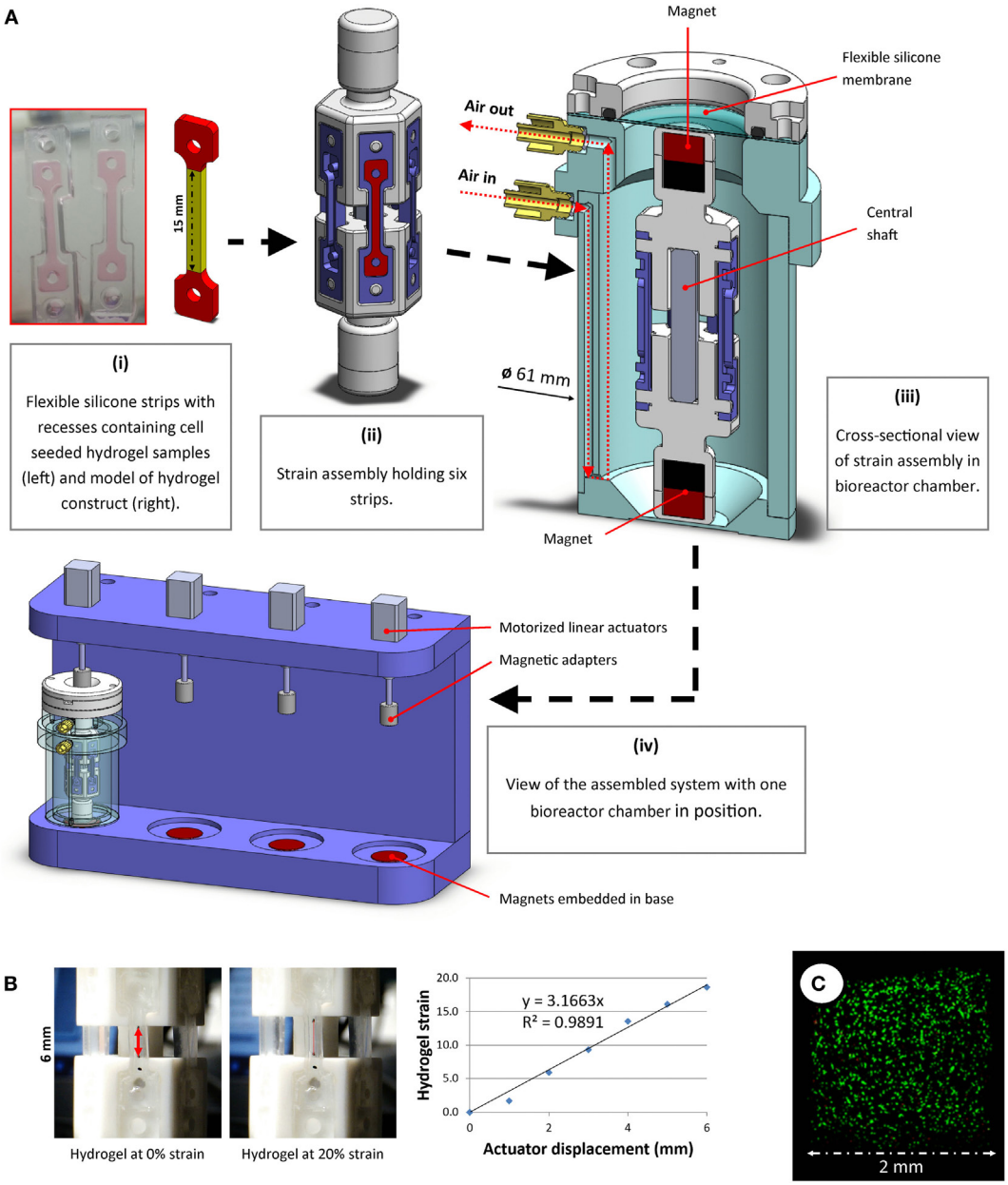

FIGURE 1 | **(A)** A novel bioreactor system for application of uniaxial cyclic tensile strain to soft 3D hydrogels was developed. Dog-bone-shaped cell-seeded hydrogel constructs were molded in recesses within flexible silicone strips. The dimensions of the hydrogel "strain section" (highlighted in yellow) were 15 mm × 2 mm × 1.5 mm (i). These strips were mounted on strain assemblies (ii), which were then sealed into the bioreactor chamber (iii) under sterile conditions. The displacement of external actuators (iv) was aseptically transferred to accurately stretch the strips in the bioreactor using magnets, both outside of and within the chamber, connected around a flexible membrane separator. **(B)** Tensile testing image analyses were performed to correlate actuator displacement with hydrogel strain. Representative images and data from hydrogel strain validation image analyses are shown. **(C)** Multipotent stromal cells encapsulated in hydrogels and cultured in the bioreactor remained viable over 7 days.

Polymer hexagonal strain mounts were fabricated and assembled. Each strain assembly was designed to allow fixation of six rubber strips, positioned vertically (**Figure 1A**, ii). Strain assembly parts were free to move along a square shaft, which allowed uniaxial translation whilst constraining rotational movement about the shaft axis. Magnets were embedded at each end of the strain assembly. A cylindrical bioreactor chamber (**Figure 1A**, iii) was developed to house the strain assembly and maintain samples under sterile conditions. Luer adapters were fitted to air inlet/outlet ports and syringe pumps were used to supply filtered air recycled from within the incubator at a rate of 3 mL/min. When used in conjunction with an oxygen tension controllable incubator, the pumps allowed for gentle agitation and re-oxygenation of the culture medium, thus maintaining uniform dissolved oxygen

and nutrient levels at the surface of the samples. A flexible silicone membrane allowed the magnetic adapters outside the chamber to connect to and displace the magnets inside the chamber without compromising the sterility of the chamber. These adapters were fixed to motorized linear actuators (NA08A30, Zaber Technologies Inc., microstep size <0.1 μm). The actuators were mounted on a rig (**Figure 1A**, iv), into which the bioreactor chambers could be placed. Strong magnets (>20 kg pull force) embedded in the base of this rig below each bioreactor held the lower magnets inside the chamber fixed in position, whereas the magnets attached to the actuators above the bioreactor allowed vertical displacement of the upper magnets within the chamber. Bioreactor components were sterilized using ethylene oxide gas treatment before use.

A custom Matlab (version R2015b, Mathworks Inc.) script was developed that allowed precise control of applied strain, frequency and loading duration. The system was calibrated by mounting hydrogels marked with ink at the extremities and displacing the actuators in 1 mm increments. Image analyses of hydrogels being strained were performed to correlate hydrogel deformation with actuator displacement (**Figure 1B**). Oxygen levels in the media were monitored near the chamber base using non-invasive oxygen sensors (Fibox 3, PreSens GmbH, data not shown), and MSC viability was monitored and confirmed over the duration of a 7-day pilot study (**Figure 1C**).

Cell Isolation and Expansion

Animals were bred and raised for food and not research purposes and were not subject to any scientific procedures before their sacrifice, hence no specific ethical approval was required for this study. Bone marrow-derived MSCs were isolated aseptically from the femoral diaphysis of a single porcine donor for use in multiple studies and expanded *in vitro*, as described previously (Thorpe et al., 2013; Carroll et al., 2014). Briefly, isolated MSCs were plated and cultured in a standard expansion media formulation consisting of high glucose Dulbecco's Modified Eagle Medium (DMEM, GlutaMAX™) containing 10% fetal bovine serum and 1% penicillin (100 U/mL)–streptomycin (100 mg/mL) (all from GIBCO, Biosciences, Dublin, Ireland) and supplemented with fibroblast growth factor-2 (5 ng/mL; ProSpec-Tany TechnoGene Ltd., Israel) and amphotericin B (0.25 mg/mL; Sigma-Aldrich, Arklow, Ireland). Following colony formation, the cells were trypsinized, counted and plated at a seeding density of 5×10^3 cells/cm^2 at each passage. Complete media exchanges were performed twice weekly.

Fibrin Hydrogel Fabrication and Culture

Multipotent stromal cells were suspended in 10,000 KIU/mL aprotinin solution (Nordic Pharma) containing 19 mg/mL sodium chloride and 100 mg/mL bovine fibrinogen type I-S (60–85% protein, 10% sodium citrate, and 15% sodium chloride; Sigma-Aldrich), which was combined 1:1 with 5 U/mL thrombin in 40 mM $CaCl_2$ (pH 7) and transferred by syringe to recesses in custom designed flexible silicone strips. These strips were then incubated at 37°C for 45 min to allow cross-linking to complete, producing dog-boned shaped constructs with final concentrations of 50 mg/mL fibrinogen, 2.5 U/mL thrombin, 5,000 KIU/mL aprotinin, 17 mg/mL sodium chloride, 20 mM $CaCl_2$, and 10×10^6 cells/mL. The constructs were then loaded into bioreactors containing differentiation medium (DM), consisting of DMEM supplemented with 100 U/mL penicillin/streptomycin (both from Gibco), 100 mg/mL sodium pyruvate, 40 mg/mL L-proline, 50 mg/mL L-ascorbic acid-2-phosphate, 1.5 mg/mL bovine serum albumin, 1× insulin–transferrin–selenium, and 100 nM dexamethasone (all Sigma-Aldrich). For studies requiring chondro-inductive stimuli, constructs were culture in chondrogenic medium [DM supplemented with 10 ng/mL of transforming growth factor-β3 (TGF-β3, ProSpec-Tany TechnoGene, Ltd., Israel)]. Media changes were performed twice weekly.

Mechanical Stimulation of Hydrogel Encapsulated MSCs

Uniaxial CTS was applied to MSC seeded hydrogels in the bioreactor system described earlier. All bioreactors were housed in incubators set at 5% oxygen, 37°C, and a reciprocating syringe air pump system was employed to pass air bubbles through the culture medium, thereby gently agitating the system and maintaining a uniform dissolved oxygen content of 5%. In the initial study undertaken using differentiation media, hydrogels were deformed at a strain magnitude of 10% and frequency of 0.5 Hz for 4 h each day for 7 days. In the second, long-term study exploring the role of mechanical cues on endochondral ossification, the influence of strain magnitude and frequency was also investigated. Therefore, this study involved four experimental groups (non-loaded control, 5% strain at 0.5 Hz, 10% strain at 0.5 Hz, and 10% strain at 1 Hz) cultured in chondrogenic medium (+TGF-β3) for 21 days.

Biochemical Analysis

The central (strained) sections of dog-bone constructs ($n \geq 3$) were used for quantitative analysis of DNA, sulfated glycosaminoglycan (sGAG) and collagen content. The wet weight of each section was measured, then the samples were digested with papain (125 μg/mL) in 0.1 M sodium acetate, 5 mM L-cysteine–HCl, and 0.05 M EDTA (pH 6.0, all Sigma-Aldrich) at 60°C under constant rotation for 18 h. DNA content was quantified using the Hoechst Bisbenzimide 33258 dye assay as described previously (Kim et al., 1988), with a calf thymus DNA standard. Sulfated glycosaminoglycan (GAG) content was quantified using the dimethylmethylene blue dye-binding assay (DMMB; Blyscan, Biocolor Ltd., Northern Ireland) with a chondroitin sulfate standard. Collagen content was determined by measuring the hydroxyproline content. Samples were hydrolyzed at 110°C for 18 h in 38% HCl and assayed using a chloramine-T assay with a hydroxyproline: collagen ratio of 1:7.69 (Kafienah and Sims, 2004; Ignat'eva et al., 2007). Total sGAG and collagen values and values normalized to DNA content are reported.

RNA Isolation and Real-time Reverse Transcriptase Polymerase Chain Reaction

Quantitative real-time reverse transcription-polymerase chain reaction (qRT-PCR) was used to determine the relative gene expression changes in RNA isolated from MSCs cultured in

tensile strain bioreactors. The central sections of dog-bone shape samples were mechanically disrupted in buffer RLT (Qiagen) supplemented with β-mercaptoethanol (10 μL/mL), frozen in liquid nitrogen, and stored at −80°C before analysis. Thawed samples were then transferred to spin columns for homogenization (QIAShredder, Qiagen), followed by RNA isolation (RNeasy Micro Kit, Qiagen) according to the manufacturer's instructions, and subsequently resuspended in RNase-free water.

RNA concentrations were quantified using a NanoDropTM (ND-1000) spectrophotometer, and RNA was reverse transcribed into cDNA using the High Capacity cDNA Reverse Transcription Kit (Applied Biosystems, Paisley, UK). Real-time PCR reactions were performed in 20 μL volumes containing 10 μL SYBR Green Master Mix (Applied Biosystems), 0.4 μM forward primer and 0.4 μM reverse primer (KiCqStart SYBR Green, Sigma-Aldrich), RNase-free water, and sufficient sample for 50 ng of cDNA. Primers used and gene abbreviations are listed in **Table 1**. Reactions were carried out in duplicate on an ABI 7500 real-time PCR system (Applied Biosystems) with an amplification profile of 50°C for 2 min, 95°C for 10 min, followed by 40–45 cycles of denaturation at 95°C for 15 s and annealing/amplification at 60°C for 1 min. Quantitative expression of target genes relative to the endogenous control reference gene (*GAPDH*) and the selected calibrator was carried out using the $2^{-\Delta\Delta CT}$ method as previously described (Livak and Schmittgen, 2001).

Fluorescent Staining and Quantification of Cellular Anisotropy of MSC Filamentous Actin

Fluorescent images were taken from the central (strained) section only. F-actin cytoskeletal filaments were visualized using rhodamine 110 conjugated phalloidin (VWR). Dog-boned shaped MSC seeded constructs were sectioned for imaging through the depth of the sample and fixed in 4% paraformaldehyde solution. Cells were permeabilized in 0.5% Triton-X100 (Sigma-Aldrich), then incubated overnight in phosphate-buffered saline (PBS) with 1.5% BSA and rhodamine 110 conjugated phalloidin (1:40; 200 U/mL; VWR). Construct slices were washed in PBS and imaged with an Olympus FluoView FV1000 Confocal Microscope. Anisotropy of actin filaments was quantified by performing analysis of confocal images ($n = 4$) using the ImageJ FibrilTool plugin (Boudaoud et al., 2014).

Statistical Analysis

All statistical analyses were performed using GraphPad Prism (Version 6.01) software. Data were checked for normal distribution (using D'Agostino–Pearson omnibus K^2 method) before performing parametric tests. Study groups consisted of constructs created using MSCs derived from a single porcine donor, and n indicates the number of experimental replicates within each group. Student's t-tests were used where appropriate and one-way analyses of variance with Tukey's post-test were used to compare multiple conditions. Numerical and graphical results are reported in the form of mean ± SE from the mean. Significance was accepted at a level of $p \leq 0.05$, and multiplicity adjusted p-values thresholds are indicated for individual comparisons. Gene expression data are present as fold differences normalized to the mean of the free-swelling (non-loaded) control group and fold increase or fold decrease, where relevant, are indicated in the text below by ↑ or ↓, respectively.

RESULTS

CTS in the Absence of Soluble Differentiation Factors Promotes the Expression of Tenogenic (TNC) and Osteogenic Markers while Inhibiting Adipogenesis

Multipotent stromal cells encapsulated in fibrin hydrogels were cultured in bioreactors in the absence of specific growth factors for 7 days. The application of 10% CTS at 0.5 Hz was

TABLE 1 | KiCqStart SYBR green primers used for real-time reverse transcription polymerase chain reactions.

Symbol	Gene	Forward primer	Reverse primer
ACAN	Aggrecan	GACCACTTTACTCTTGGTG	TCAGGCTCAGAAACTTCTAC
ACTA2	Smooth muscle aortic alpha-actin	CAAAAGAGGAATCCTGACC	CATTGTAGAAAGAGTGGTGC
ALPL	Alkaline phosphatase	TTTCACTCTTCTTAGTGCTG	CGTTACGGAATGAGGAAAC
BMP2	Bone morphogenic protein-2	ATGTGGAGGCTCTTTCAATG	CATGGTCGACCTTTAGGAG
CNN1	Calponin 1, basic, smooth muscle	AGATGGCATCATTCTTTGC	ATGAAGTTGCCAATGTTCTC
COL10A1	Collagen type 10, alpha-1	GTAGGTGTTTGGTATTGCTC	GAGCAATACCAAACACCTAC
COL1A1	Collagen type 1, alpha-1	TAGACATGTTCAGCTTTGTG	GTGGGATGTCTTCTTCTTG
COL2A1	Collagen type 2, alpha-1	CGACGACATAATCTGTGAAG	TCCTTTGGGTCCTACAATATC
COL3A1	Collagen type 3, alpha-1	TCATCCCACTGTTATTTTGG	CTCTATCCGCATAGGACTG
FABP4	Fatty acid binding protein-4	CTGAAGAGAGTCATTGCAC	CATTTTGTGAGCACTCTAGG
GAPDH	Glyceraldehyde 3-phosphate dehydrogenase	TTTAACTCTGGCAAAGTGG	GAACATGTAGACCATGTAGTG
LECT1	Leukocyte cell derived chemotaxin-1	ACCTTTAAAATGGGAAACGG	GCTTTGATGTAGCACTTCTC
LPL	Lipoprotein lipase	ACCTAACTTCGAGTATGCAG	GGTGAATGTGTGTAAGACG
MYH1	Myosin, heavy chain 1	GAGTCACTTTCCAGCTAAAG	CATTTCAATGAGCTCTGGC
OPN	Secreted phosphoprotein 1 (osteopontin)	CTGCAGACCAAGGAAAATC	AGCATCTGTGTATTTGTTGG
RUNX2	Runt-related transcription factor-2	CCAACAGAGGCATTTAAGG	CCAAAAGAAGTTTTGCTGAC
SOX9	SRY (sex determining region Y)-Box-9	CAGACCTTGAGGAGACTTAG	GTTCGAGTTGCCTTTAGTG
TNC	Tenascin-C	ATCTAGTCTTTCTCAACTCCG	GAGTAGAATCCAAACCAGTTG

found to upregulate the TNC markers *TNC* and *COL1A1* (↑ 54.56 ± 10.83 and ↑ 3.11 ± 0.34, respectively; $p < 0.003$) and to suppress the expression of the adipogenic marker *LPL* (↓ 6.84 ± 0.62, $p = 0.0001$). Mechanical stimulation had no effect on the expression of the myogenic markers *ACTA2*, *CNN1*, and *MYH1* (**Figure 2**). CTS was also found to enhance the expression of a number of markers of osteogenesis, including *ALPL* and *BMP2* (↑ 7.09 ± 1.46 and ↑ 4.61 ± 0.74; $p < 0.003$). Furthermore, *COL10A1* was found to be expressed in all loaded samples but was not detected in samples in the non-loaded control group (data not shown). Since no expression of chondrogenic markers *COL2A1* or *SOX9* was detected, while the osteogenic markers *ALPL* and *BMP2* were upregulated following mechanical loading, it would appear that CTS may have a positive role in promoting (intramembranous) osteogenesis of MSCs in the absence of exogenously supplied growth factors. However, since long bones are known to develop and heal *via* the process of endochondral ossification, we therefore next sought to explore the role of CTS

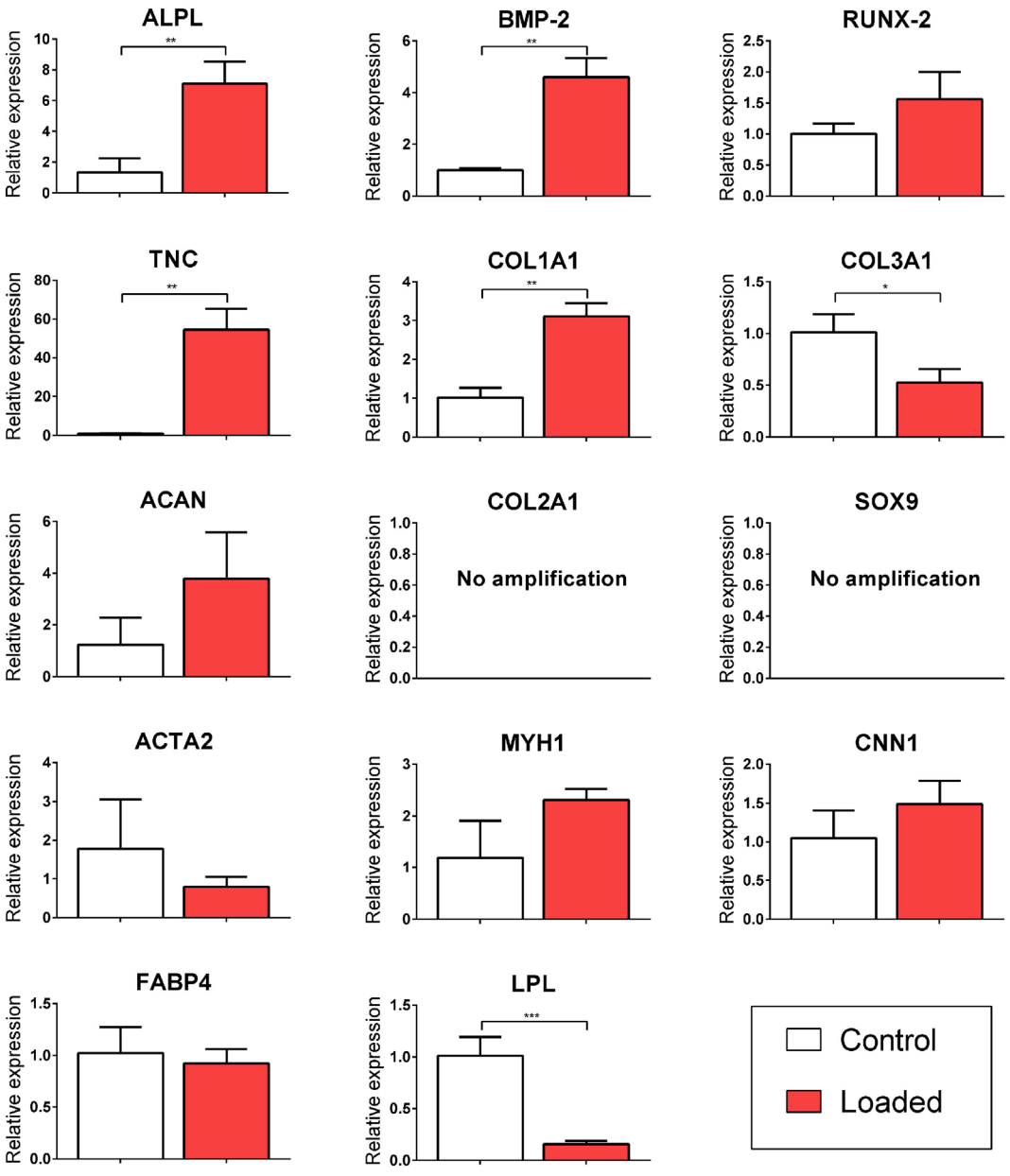

FIGURE 2 | Relative gene expression of multipotent stromal cells (MSCs) encapsulated in fibrin hydrogels and cultured in tensile strain bioreactor in the absence of growth factors for 7 days. The application of 10% cyclic tensile strain at 0.5 Hz was found to promote intramembranous ossification and inhibit adipogenic differentiation of MSCs. Data are presented as fold changes, relative to the non-loaded (control) group. Significant differences are indicated where present (*$p < 0.05$; **$p < 0.01$; ***$p < 0.001$; $n = 5$). See **Table 1** for details of gene symbols.

on MSCs maintained in chondro-inductive medium for a long-term culture duration.

CTS Promotes Endochondral Ossification of Chondrogenically Primed MSCs in a Magnitude-Dependent Manner

Multipotent stromal cells encapsulated within fibrin hydrogels and maintained in media supplemented with the chondrogenic growth factor TGF-β3 for 21 days were found to synthesize cartilage extracellular matrix components (**Figure 3**) and express genes associated with a chondrogenic phenotype (**Figure 4**). The application of 10% strain at 0.5 Hz was found to promote cellular proliferation, which led to increased overall GAG and collagen synthesis (**Figure 3**). However, when normalized to DNA content, there was no difference in ECM synthesis rates on a per cell basis.

10% CTS at 1 Hz was also found to significantly enhance several markers of chondrogenesis (*ACAN* and *SOX9*) but inhibit *COL2A1* expression in MSCs cultured in chondrogenic media for 3 weeks (**Figure 4**). Furthermore, CTS was found to enhance the expression of markers associated with an osteogenic phenotype in a magnitude- and frequency-dependent manner (**Figure 4**). Application of smaller strains appeared to be insufficient to invoke a response in many of the osteogenic markers investigated, with only *ALPL* upregulated following the application of 5% CTS ($\uparrow 2.24 \pm 0.18$, $p < 0.0001$). Of the loading regimens investigated, a tensile stimulus of 10% strain at 1 Hz was observed to invoke the largest increase in osteogenic gene expression and resulted in a significant upregulation of *BMP2*, *RUNX2*, *COL3A1*, and *OPN* ($\uparrow 7.02 \pm 0.92$, $\uparrow 39.41 \pm 0.4.34$, $\uparrow 2.05 \pm 0.25$, and $\uparrow 2.24 \pm 0.31$; $p < 0.015$) when compared with the non-loaded control group. Furthermore, the ratio of *RUNX2* expression to *SOX9* expression was dramatically increased in the 10% CTS groups. The magnitude of strain appeared to effect gene expression to a greater degree than frequency, with the only apparent difference due to strain frequency being a smaller increase in *BMP2* expression in samples strained at 0.5 Hz compared with 1 Hz. However, *BMP2* levels in this 10% CTS group still remained greater than those in hydrogels strained by both 0 and 5%. In contrast to the 5% CTS group, the application of 10% strain lead to a significant downregulation in *ALPL* expression after 21 days compared with non-loaded controls.

CTS Promotes Cellular Alignment of MSCs in 3D Fibrin Hydrogels

Filamentous-actin staining and confocal imaging of MSC laden 3D hydrogels showed spindle-shaped, spread cells with well-developed actin networks in all groups (**Figure 5A**). Image analysis and quantification of cellular organization revealed that the application of CTS resulted in increased cellular anisotropy/alignment in all groups subjected to mechanical strain (**Figure 5B**).

DISCUSSION

Our long bones develop and heal through the process of endochondral ossification. The objective of this study was to explore the role of mechanical cues in regulating the initiation and progression of endochondral ossification. Our hypothesis was that uniaxial CTS would promote an endochondral phenotype in MSCs encapsulated within physiologically relevant 3D fibrin hydrogels. While it has previously been reported that CTS promotes a fibro-chondrogenic phenotype in MSCs seeded in 3D hydrogels (Connelly et al., 2010), the role of this mechanical stimulus in regulating the conversion of cartilage into bone remains poorly understood. The findings of this study suggest

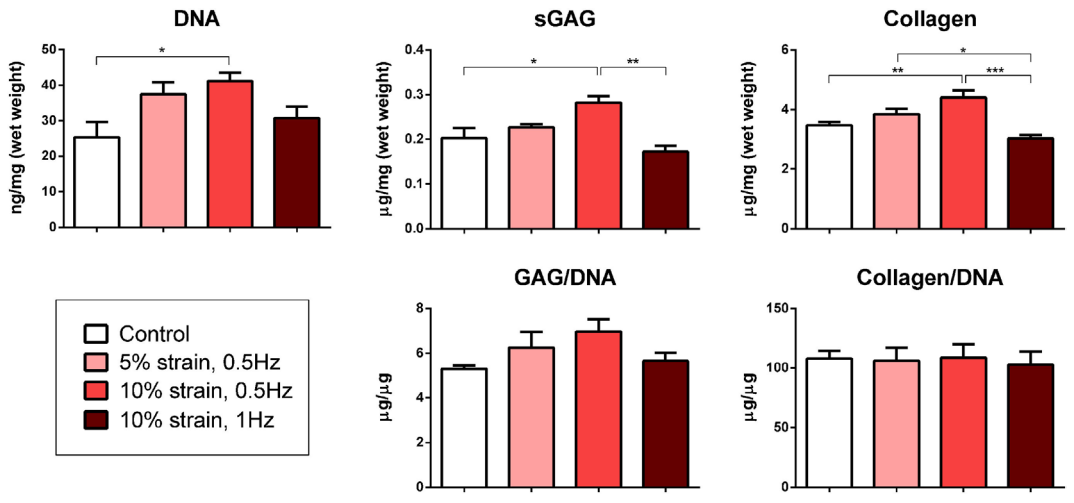

FIGURE 3 | Biochemical analysis of multipotent stromal cell encapsulated fibrin hydrogels cultured in tensile strain bioreactors in media supplemented with chondrogenic growth factor transforming growth factor-β3 for 21 days. The application of 10% cyclic tensile strain at 0.5 Hz was found to promote cellular proliferation, which led to an increase in total cartilage matrix deposition. Significant differences are indicated where present (*$p < 0.05$; **$p < 0.01$; ***$p < 0.001$; $n = 5$).

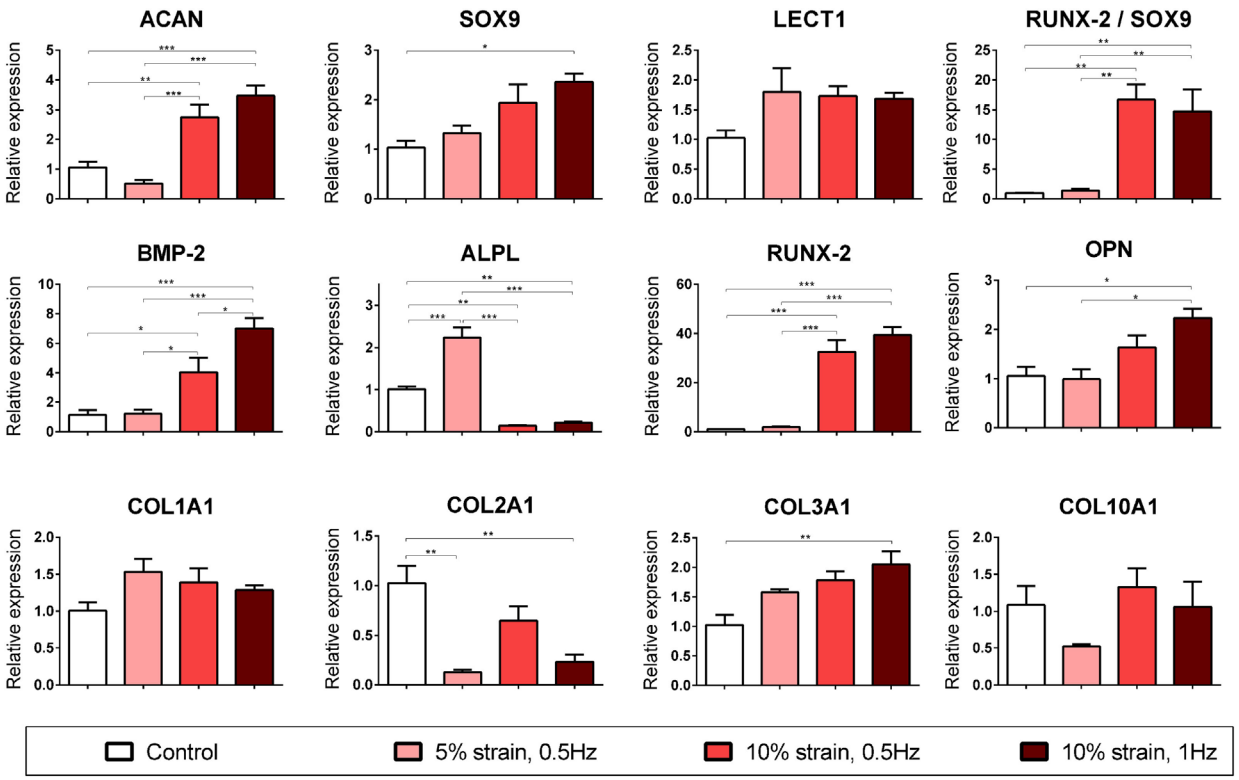

FIGURE 4 | Chondrogenic and osteogenic gene expression of multipotent stromal cells (MSCs) encapsulated in fibrin hydrogels and cultured in media supplemented with chondrogenic growth factor transforming growth factor-β3 for 21 days. Cyclic tensile strain was found to promote endochondral ossification of chondrogenically primed MSCs in a magnitude- and frequency-dependent manner. Data are presented as fold changes, relative to the non-loaded (control) group. *RUNX2/SOX9* ratio is presented as fold change/fold change. Significant differences are indicated where present (*$p < 0.05$; **$p < 0.01$; ***$p < 0.001$; $n = 5$). See **Table 1** for explanation of gene symbols.

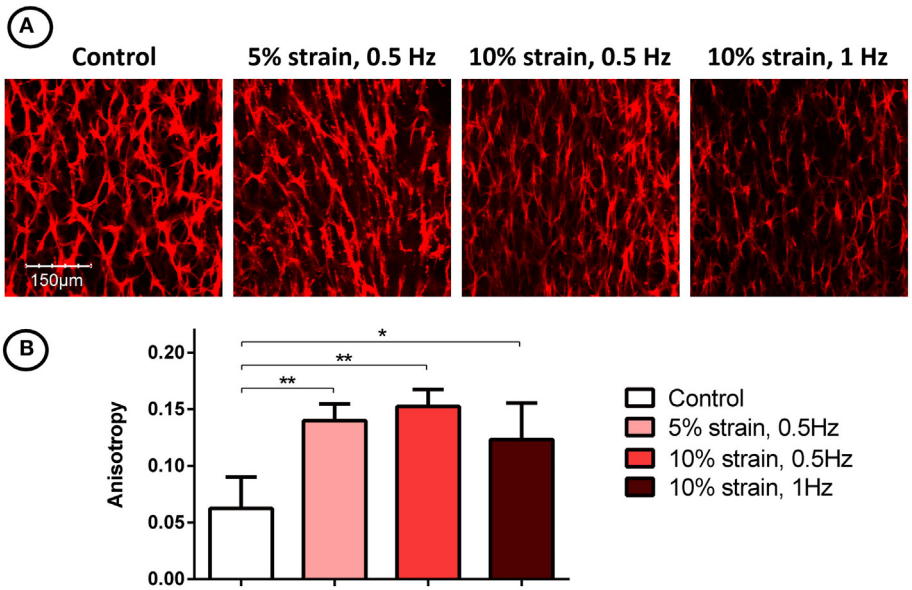

FIGURE 5 | F-actin staining **(A)** and quantification of filament anisotropy **(B)** of multipotent stromal cells encapsulated in fibrin hydrogels and cultured in tensile strain bioreactors in media supplemented with chondrogenic growth factor transforming growth factor-β3 for 21 days. The application of cyclic tensile strain was found to increase cellular organization. Significant differences are indicated where present (*$p < 0.05$; **$p < 0.01$; $n = 5$).

that CTS can promote osteogenesis of MSCs, either directly or indirectly through a cartilage intermediate, and hence plays a key role in both intramembranous and endochondral ossification of MSCs.

The application of CTS to MSCs cultured in the absence of soluble differentiation factors was found to increase the expression of osteogenic and TNC markers. Furthermore, in agreement with recently reported findings in 2D culture systems (Li et al., 2015), it was found that tensile loading suppressed adipogenesis of MSCs. This suggests that CTS is a positive stimulus for intramembranous ossification of MSCs, although not uniquely promoting differentiation down this pathway. Enhanced osteogenesis and a suppression of adipogenesis have also been observed in response to other mechanical cues such as increases in substrate stiffness (Huebsch et al., 2010; Dupont et al., 2011). Increased osteogenesis on stiff substrates has been linked to cytoskeletal tension and RhoA and Rho-associated protein kinase (ROCK) signaling, a pathway that is known to regulate remodeling of the actin cytoskeleton and play a key role as a dynamic mechanosensor (Peyton et al., 2007; Guilak et al., 2009; Khatiwala et al., 2009; Holle and Engler, 2011). Mechanical cues such as cyclic stretch and fluid flow have previously been shown to promote cell stiffening and enhance cytoskeletal tension in a RhoA/ROCK-dependent manner, suggesting that common molecular mechanisms translate diverse mechanical cues into increases in osteogenesis (Chiquet et al., 2004; Lee et al., 2006; Matthews et al., 2006; Arnsdorf et al., 2009). These findings add to the growing body of work pointing to the role of different mechanical cues, from substrate stiffness (Huebsch et al., 2010; Park et al., 2011) to CTS, in directing either an osteogenic or adipogenic phenotype in MSCs.

Given that long bones form and generally regenerate *via* endochondral ossification, we examined the influence of long-term CTS on chondrogenically primed MSC laden 3D hydrogels to explore how this mechanical cue regulates the process of endochondral ossification. While CTS did not appear to initiate chondrogenesis in the absence of soluble differentiation factors, in the presence of exogenously supplied TGF-β3 this mechanical cue was found to influence the expression of both chondrogenic and osteogenic genes in a strain magnitude- and frequency-dependent manner. 10% tensile strain at 1 Hz was found to promote both chondrogenic (*ACAN* and *SOX9*) and osteogenic (*BMP2*, *RUNX2*, *OPN*, and *COL3A1*) gene expression, whereas 5% strain was determined to be insufficient to induce upregulation of many of these markers. Interestingly, mechanical stimulation was observed to lead to an inhibition of *COL2A1* expression. *COL2A1* expression has previously been shown to follow a temporal profile during endochondral ossification, with peak expression observed at day 7 after *BMP2* induced bone formation (Clancy et al., 2003). MSCs in hydrogels strained at 10% also exhibited a downregulation in *ALPL* expression after 21 days, whereas those strained at 5% showed enhanced *ALPL* expression (**Figure 4**). *ALPL* is considered to be an early marker of osteogenesis in MSCs and is upregulated during the differentiation phase and then downregulated before mineralization (Kulterer et al., 2007). Therefore, the downregulation in *ALPL* expression observed in MSCs subjected to higher magnitude strains may further suggest that CTS is accelerating the process of endochondral ossification. Furthermore, the ratio of *RUNX2* to *SOX9* was dramatically increased (>14-fold increase) following application of 10% CTS. *SOX9* has been shown to be highly expressed in pre-hypertrophic chondrocytes, but not in hypertrophic chondrocytes (Zhao et al., 1997; Hattori et al., 2010). It exerts an inhibitory effect on *RUNX2* function (Zhou et al., 2006) and therefore has been reported to be a negative regulator of bone marrow formation and endochondral ossification (Hattori et al., 2010). There is also evidence to suggest that increased expression of *RUNX2* combined with *SOX9* downregulation in hypertrophic chondrocytes is a prerequisite to initiation of the cartilage–bone transition in the growth plate (Hattori et al., 2010). Furthermore, the *RUNX2*:*SOX9* ratio has been reported to be a positive indicator of osteogenic potential in MSCs (Loebel et al., 2014).

The application of uniaxial CTS was also found to promote re-organization of actin filaments and increase overall anisotropy in the actin network, consistent with previously reported studies of MSCs cultured on both 2D substrates (Hamilton et al., 2004; Chen et al., 2008) and in 3D environments (Altman et al., 2002). Anisotropic cellular and matrix organization is a characteristic of many developing biological tissues. For example, it has been shown that collagen orientation in the perichondrium of long bones align with the direction of growth, and it has been suggested that this is due to the combination of mechanical tissue strain and the synthesis of new tissue matrix (Foolen et al., 2008). Growth plate tissue is also highly anisotropic, with distinct cellular organization; chondrocytes are arranged into vertical columns, which act as functional units of longitudinal bone growth (Hunziker, 1994). Since chondrocyte alignment is a hallmark of hypertrophy and endochondral ossification in developing limbs, it is likely that novel cell culture systems that direct cellular anisotropy and guide structural alignment will be required when engineering grafts to repair structurally complex tissues.

In either the presence or absence of exogenously supplied TGF-β3, increases in the expression of osteogenic markers in response to mechanical loading correlated with increases in *BMP2* expression. CTS induced increases in osteogenic growth factor expression is a likely mechanism that warrants further investigation. Other loading modalities such as dynamic compression and shear loading have also been shown to lead to increased expression of other members of the TGF-β superfamily in MSCs (Huang et al., 2004; Li et al., 2009, 2010). The molecular mechanisms by which mechanical loading leads to increases in growth factor expression, and whether different loading modalities such as cyclic tension and compression lead to distinct growth factor expression profiles, are important questions that warrant further study.

The novel bioreactor system developed as part of this study has a number of potential applications, both as a tool for fundamental mechanobiology experiments and in the field of tissue engineering. The majority of studies reported in the literature that explore the role of CTS in regulating cellular behavior involve the application of stretch to 2D substrates (Simmons et al., 2003; Friedl et al., 2007; Qi et al., 2008; Diederichs et al., 2009), whereas the system described in this study involves encapsulating cells in more physiologically relevant 3D hydrogels. The bioreactor system should be compatible with any hydrogel used for cell encapsulation, thereby enabling studies exploring how CTS and factors such

as matrix stiffness (Huebsch et al., 2010) or ligand presentation (Bian et al., 2013) might interact to regulate stem cell fate. In this study, we selected fibrin hydrogels as our substrate as they mimic the clot that forms within a fracture callus and hence represent a useful model when exploring the role of environmental cues in regulating bone healing. When used in conjunction with an oxygen tension controllable incubator, the fact that the bioreactor supplies filtered air recycled from within the incubator enables studies exploring the interaction between CTS and altered levels of oxygen availability, another key regulator of intramembranous and endochondral ossification (Meyer et al., 2010; Sheehy et al., 2012). For all of these reasons, the bioreactor should find broad utility in musculoskeletal tissue engineering; not only for producing grafts for endochondral bone tissue engineering (Scotti et al., 2010; Farrell et al., 2011; Thompson et al., 2015, 2016; Cunniffe et al., 2017) but also for generating other biological tissues that are subjected to large tensile loads, such as ligament and tendon.

CONCLUSION

While it is clear that the application of extrinsic mechanical loading can guide stem cell fate, a more complete understanding of how MSCs respond to specific mechanical signals is needed for successful cell based strategies in musculoskeletal medicine. The data presented here demonstrates that, depending on the context in which the stimulus is applied, cyclic tensile strain can be a positive stimulus for the promotion of both intramembranous and endochondral ossification of MSC. These new insights can inform the development of novel tissue-engineering strategies for cartilage and bone regeneration.

AUTHOR CONTRIBUTIONS

SC—developed bioreactor, performed experiments and data analysis, author. CB—co-supervisor, coauthor. DK—co-supervisor, coauthor, principal investigator, and corresponding author.

FUNDING

This study was funding provided by Science Foundation Ireland (President of Ireland Young Researcher Award: 08/YI5/B1336) and the European Research Council (StemRepair—Project number 258463).

REFERENCES

Altman, G. H., Horan, R. L., Martin, I., Farhadi, J., Stark, P. R., Volloch, V., et al. (2002). Cell differentiation by mechanical stress. *FASEB J.* 16, 270–272. doi:10.1096/fj.01-0656fje

Arnsdorf, E. J., Tummala, P., Kwon, R. Y., and Jacobs, C. R. (2009). Mechanically induced osteogenic differentiation – the role of RhoA, ROCKII and cytoskeletal dynamics. *J. Cell. Sci.* 122(Pt 4), 546–553. doi:10.1242/jcs.036293

Baker, B. M., Shah, R. P., Huang, A. H., and Mauck, R. L. (2011). Dynamic tensile loading improves the functional properties of mesenchymal stem cell-laden nanofiber-based fibrocartilage. *Tissue Eng. Part A* 17, 1445–1455. doi:10.1089/ten.TEA.2010.0535

Bian, L., Guvendiren, M., Mauck, R. L., and Burdick, J. A. (2013). Hydrogels that mimic developmentally relevant matrix and N-cadherin interactions enhance MSC chondrogenesis. *Proc. Natl. Acad. Sci. U.S.A* 110, 10117–10122. doi:10.1073/pnas.1214100110

Bian, L., Zhai, D. Y., Zhang, E. C., Mauck, R. L., and Burdick, J. A. (2012). Dynamic compressive loading enhances cartilage matrix synthesis and distribution and suppresses hypertrophy in hMSC-laden hyaluronic acid hydrogels. *Tissue Eng. Part A* 18, 715–724. doi:10.1089/ten.TEA.2011.0455

Boudaoud, A., Burian, A., Borowska-Wykręt, D., Uyttewaal, M., Wrzalik, R., Kwiatkowska, D., et al. (2014). FibrilTool, an ImageJ plug-in to quantify fibrillar structures in raw microscopy images. *Nat. Protoc.* 9, 457–463. doi:10.1038/nprot.2014.024

Campbell, J. J., Lee, D. A., and Bader, D. L. (2006). Dynamic compressive strain influences chondrogenic gene expression in human mesenchymal stem cells. *Biorheology* 43, 455–470.

Caplan, A. I. (1991). Mesenchymal stem cells. *J. Orthop. Res.* 9, 641–650. doi:10.1002/jor.1100090504

Carey, E. J. (1922). Direct observations on the transformation of the mesenchyme in the thigh of the pig embryo (*Sus scrofa*), with especial reference to the genesis of the thigh muscles, of the knee-and hip-joints, and of the primary bone of the femur. *J. Morphol.* 37, 1–77. doi:10.1002/jmor.1050370102

Carroll, S. F., Buckley, C. T., and Kelly, D. J. (2014). Cyclic hydrostatic pressure promotes a stable cartilage phenotype and enhances the functional development of cartilaginous grafts engineered using multipotent stromal cells isolated from bone marrow and infrapatellar fat pad. *J. Biomech.* 47, 2115–2121. doi:10.1016/j.jbiomech.2013.12.006

Chen, Y. J., Huang, C. H. I, Lee, C., Lee, Y. T., Chen, M. H., and Young, T. H. (2008). Effects of cyclic mechanical stretching on the mRNA expression of tendon/ligament-related and osteoblast-specific genes in human mesenchymal stem cells. *Connect. Tissue Res.* 49, 7–14. doi:10.1080/03008200701818561

Chiquet, M., Sarasa-Renedo, A., and Tunc-Civelek, V. (2004). Induction of tenascin-C by cyclic tensile strain versus growth factors: distinct contributions by Rho/ROCK and MAPK signaling pathways. *Biochim. Biophys. Acta* 1693, 193–204. doi:10.1016/j.bbamcr.2004.08.001

Clancy, B. M., Johnson, J. D., Lambert, A.-J., Rezvankhah, S., Wong, A., Resmini, C., et al. (2003). A gene expression profile for endochondral bone formation: oligonucleotide microarrays establish novel connections between known genes and BMP-2-induced bone formation in mouse quadriceps. *Bone* 33, 46–63. doi:10.1016/S8756-3282(03)00116-9

Connelly, J. T., Vanderploeg, E. J., Mouw, J. K., Wilson, C. G., and Levenston, M. E. (2010). Tensile loading modulates bone marrow stromal cell differentiation and the development of engineered fibrocartilage constructs. *Tissue Eng. Part A* 16, 1913–1923. doi:10.1089/ten.TEA.2009.0561

Cunniffe, G., Díaz-Payno, P., Ramey, J., Mahon, O., Dunne, A., Thompson, E. M., et al. (2017). Growth plate extracellular matrix-derived scaffolds for large bone defect healing. *Eur. Cell Mater.* 33, 130–142. doi:10.22203/eCM.v033a10

Diederichs, S., Freiberger, F., and van Griensven, M. (2009). Effects of repetitive and short time strain in human bone marrow stromal cells. *J. Biomed. Mater. Res. A.* 88, 907–915. doi:10.1002/jbm.a.31944

Doroski, D. M., Levenston, M. E., and Temenoff, J. S. (2010). Cyclic tensile culture promotes fibroblastic differentiation of marrow stromal cells encapsulated in poly(ethylene glycol)-based hydrogels. *Tissue Eng. Part A* 16, 3457–3466. doi:10.1089/ten.tea.2010.0233

Dupont, S., Morsut, L., Aragona, M., Enzo, E., Giulitti, S., Cordenonsi, M., et al. (2011). Role of YAP/TAZ in mechanotransduction. *Nature* 474, 179. doi:10.1038/nature10137

Farng, E., Urdaneta, A. R., Barba, D., Esmende, S., and McAllister, D. R. (2008). The effects of GDF-5 and uniaxial strain on mesenchymal stem cells in 3-D culture. *Clin. Orthop. Relat. Res.* 466, 1930–1937. doi:10.1007/s11999-008-0300-x

Farrell, E., Both, S. K., Odörfer, K. I., Koevoet, W., Kops, N., O'Brien, F. J., et al. (2011). In-vivo generation of bone via endochondral ossification by in-vitro chondrogenic priming of adult human and rat mesenchymal stem cells. *BMC Musculoskelet. Disord.* 12:31. doi:10.1186/1471-2474-12-31

Foolen, J., van Donkelaar, C., Nowlan, N., Murphy, P., Huiskes, R., and Ito, K. (2008). Collagen orientation in periosteum and perichondrium is aligned with preferential directions of tissue growth. *J. Orthop. Res.* 26, 1263–1268. doi:10.1002/jor.20586

Friedl, G., Schmidt, H., Rehak, I., Kostner, G., Schauenstein, K., and Windhager, R. (2007). Undifferentiated human mesenchymal stem cells (hMSCs) are highly sensitive to mechanical strain: transcriptionally controlled early osteo-chondrogenic response in vitro. *Osteoarthr. Cartil.* 15, 1293–1300. doi:10.1016/j.joca.2007.04.002

Frohlich, M., Grayson, W. L., Wan, L. Q., Marolt, D., Drobnic, M., and Vunjak-Novakovic, G. (2008). Tissue engineered bone grafts: biological requirements, tissue culture and clinical relevance. *Curr. Stem Cell Res. Ther.* 3, 254–264. doi:10.2174/157488808786733962

Grayson, W. L., Bunnell, B. A., Martin, E., Frazier, T., Hung, B. P., and Gimble, J. M. (2015). Stromal cells and stem cells in clinical bone regeneration. *Nat. Rev. Endocrinol.* 11, 140–150. doi:10.1038/nrendo.2014.234

Guilak, F., Cohen, D. M., Estes, B. T., Gimble, J. M., Liedtke, W., and Chen, C. S. (2009). Control of stem cell fate by physical interactions with the extracellular matrix. *Cell Stem Cell* 5, 17–26. doi:10.1016/j.stem.2009.06.016

Hamilton, D. W., Maul, T. M., and Vorp, D. A. (2004). Characterization of the response of bone marrow-derived progenitor cells to cyclic strain: implications for vascular tissue-engineering applications. *Tissue Eng.* 10, 361–369. doi:10.1089/107632704323061726

Hattori, T., Müller, C., Gebhard, S., Bauer, E., Pausch, F., Schlund, B., et al. (2010). SOX9 is a major negative regulator of cartilage vascularization, bone marrow formation and endochondral ossification. *Development* 137, 901–911. doi:10.1242/dev.045203

Haudenschild, A. K., Hsieh, A. H., Kapila, S., and Lotz, J. C. (2009). Pressure and distortion regulate human mesenchymal stem cell gene expression. *Ann. Biomed. Eng.* 37, 492–502. doi:10.1007/s10439-008-9629-2

Holle, A. W., and Engler, A. J. (2011). More than a feeling: discovering, understanding, and influencing mechanosensing pathways. *Curr. Opin. Biotechnol.* 22, 648–654. doi:10.1016/j.copbio.2011.04.007

Huang, C. Y., Hagar, K. L., Frost, L. E., Sun, Y., and Cheung, H. S. (2004). Effects of cyclic compressive loading on chondrogenesis of rabbit bone-marrow derived mesenchymal stem cells. *Stem Cells* 22, 313–323. doi:10.1634/stemcells.22-3-313

Huebsch, N., Arany, P. R., Mao, A. S., Shvartsman, D., Ali, O. A., Bencherif, S. A., et al. (2010). Harnessing traction-mediated manipulation of the cell/matrix interface to control stem-cell fate. *Nat. Mater.* 9, 518–526. doi:10.1038/nmat2732

Hunziker, E. B. (1994). Mechanism of longitudinal bone growth and its regulation by growth plate chondrocytes. *Microsc. Res. Tech.* 28, 505–519. doi:10.1002/jemt.1070280606

Ignat'eva, N. Y., Danilov, N., Averkiev, S., Obrezkova, M., and Lunin, V. (2007). Determination of hydroxyproline in tissues and the evaluation of the collagen content of the tissues. *J. Anal. Chem.* 62, 51–57. doi:10.1134/s106193480701011x

Jang, J. Y., Lee, S. W., Park, S. H., Shin, J. W., Mun, C., Kim, S. H., et al. (2011). Combined effects of surface morphology and mechanical straining magnitudes on the differentiation of mesenchymal stem cells without using biochemical reagents. *J. Biomed. Biotechnol.* 2011, 860652. doi:10.1155/2011/860652

Juncosa-Melvin, N., Matlin, K. S., Holdcraft, R. W., Nirmalanandhan, V. S., and Butler, D. L. (2007). Mechanical stimulation increases collagen type I and collagen type III gene expression of stem cell-collagen sponge constructs for patellar tendon repair. *Tissue Eng.* 13, 1219–1226. doi:10.1089/ten.2006.0339

Kafienah, W., and Sims, T. J. (2004). Biochemical methods for the analysis of tissue-engineered cartilage. *Biopolym. Methods Tissue Eng*, 217–229. doi:10.1385/1-59259-428-X:217

Kelly, D. J., and Jacobs, C. R. (2010). The role of mechanical signals in regulating chondrogenesis and osteogenesis of mesenchymal stem cells. *Birth Defects Res. C Embryo Today* 90, 75–85. doi:10.1002/bdrc.20173

Kim, Y.-J., Sah, R. L., Doong, J.-Y. H., and Grodzinsky, A. J. (1988). Fluorometric assay of DNA in cartilage explants using Hoechst 33258. *Anal. Biochem.* 174, 168–176. doi:10.1016/0003-2697(88)90532-5

Khatiwala, C. B., Kim, P. D., Peyton, S. R., and Putnam, A. J. (2009). ECM compliance regulates osteogenesis by influencing MAPK signaling downstream of RhoA and ROCK. *J. Bone Miner. Res.* 24, 886–898. doi:10.1359/jbmr.081240

Kreja, L., Liedert, A., Schlenker, H., Brenner, R. E., Fiedler, J., Friemert, B., et al. (2012). Effects of mechanical strain on human mesenchymal stem cells and ligament fibroblasts in a textured poly(L-lactide) scaffold for ligament tissue engineering. *J. Mater. Sci. Mater. Med.* 23, 2575–2582. doi:10.1007/s10856-012-4710-7

Kulterer, B., Friedl, G., Jandrositz, A., Sanchez-Cabo, F., Prokesch, A., Paar, C., et al. (2007). Gene expression profiling of human mesenchymal stem cells derived from bone marrow during expansion and osteoblast differentiation. *BMC Genomics* 8:70. doi:10.1186/1471-2164-8-70

Kuo, C. K., and Tuan, R. S. (2008). Mechanoactive tenogenic differentiation of human mesenchymal stem cells. *Tissue Eng. Part A* 14, 1615–1627. doi:10.1089/ten.tea.2006.0415

Lee, J. S., Panorchan, P., Hale, C. M., Khatau, S. B., Kole, T. P., Tseng, Y., et al. (2006). Ballistic intracellular nanorheology reveals ROCK-hard cytoplasmic stiffening response to fluid flow. *J. Cell. Sci.* 119(Pt 9), 1760–1768. doi:10.1242/jcs.02899

Li, R., Liang, L., Dou, Y., Huang, Z., Mo, H., Wang, Y., et al. (2015). Mechanical stretch inhibits mesenchymal stem cell adipogenic differentiation through TGFβ1/Smad2 signaling. *J. Biomech.* 48, 3656–3662. doi:10.1016/j.jbiomech.2015.08.013

Li, Z., Kupcsik, L., Yao, S. J., Alini, M., and Stoddart, M. J. (2010). Mechanical load modulates chondrogenesis of human mesenchymal stem cells through the TGF-β pathway. *J. Cell. Mol. Med.* 14, 1338–1346. doi:10.1111/j.1582-4934.2009.00780.x

Li, Z., Yao, S.-J., Alini, M., and Stoddart, M. J. (2009). Chondrogenesis of human bone marrow mesenchymal stem cells in fibrin–polyurethane composites is modulated by frequency and amplitude of dynamic compression and shear stress. *Tissue Eng. Part A* 16, 575–584. doi:10.1089/ten.tea.2009.0262

Livak, K. J., and Schmittgen, T. D. (2001). Analysis of relative gene expression data using real-time quantitative PCR and the 2−ΔΔCT method. *Methods* 25, 402–408. doi:10.1006/meth.2001.1262

Loebel, C., Czekanska, E. M., Bruderer, M., Salzmann, G., Alini, M., and Stoddart, M. J. (2014). In vitro osteogenic potential of human mesenchymal stem cells is predicted by runx2/sox9 ratio. *Tissue Eng. Part A* 21, 115–123. doi:10.1089/ten.tea.2014.0096

Luo, L., Thorpe, S. D., Buckley, C. T., and Kelly, D. J. (2015). The effects of dynamic compression on the development of cartilage grafts engineered using bone marrow and infrapatellar fat pad derived stem cells. *Biomed. Mater.* 10, 055011. doi:10.1088/1748-6041/10/5/055011

Matthews, B. D., Overby, D. R., Mannix, R., and Ingber, D. E. (2006). Cellular adaptation to mechanical stress: role of integrins, Rho, cytoskeletal tension and mechanosensitive ion channels. *J. Cell. Sci.* 119(Pt 3), 508–518. doi:10.1242/jcs.02760

Meyer, E. G., Buckley, C. T., Thorpe, S. D., and Kelly, D. J. (2010). Low oxygen tension is a more potent promoter of chondrogenic differentiation than dynamic compression. *J. Biomech.* 43, 2516–2523. doi:10.1016/j.jbiomech.2010.05.020

Nowlan, N. C., Sharpe, J., Roddy, K. A., Prendergast, P. J., and Murphy, P. (2010). Mechanobiology of embryonic skeletal development: insights from animal models. *Birth Defects Res. C Embryo Today* 90, 203–213. doi:10.1002/bdrc.20184

Park, J. S., Chu, J. S., Tsou, A. D., Diop, R., Tang, Z., Wang, A., et al. (2011). The effect of matrix stiffness on the differentiation of mesenchymal stem cells in response to TGF-beta. *Biomaterials* 32, 3921–3930. doi:10.1016/j.biomaterials.2011.02.019

Peyton, S. R., Ghajar, C. M., Khatiwala, C. B., and Putnam, A. J. (2007). The emergence of ECM mechanics and cytoskeletal tension as important regulators of cell function. *Cell Biochem. Biophys.* 47, 300–320. doi:10.1007/s12013-007-0004-y

Qi, M. C., Hu, J., Zou, S. J., Chen, H. Q., Zhou, H. X., and Han, L. C. (2008). Mechanical strain induces osteogenic differentiation: Cbfa1 and Ets-1 expression in stretched rat mesenchymal stem cells. *Int. J. Oral Maxillofac. Surg.* 37, 453–458. doi:10.1016/j.ijom.2007.12.008

Rathbone, S. R., Glossop, J. R., Gough, J. E., and Cartmell, S. H. (2012). Cyclic tensile strain upon human mesenchymal stem cells in 2D and 3D culture differentially influences CCNL2, WDR61 and BAHCC1 gene expression levels. *J. Mech. Behav. Biomed. Mater.* 11, 82–91. doi:10.1016/j.jmbbm.2012.01.019

Sato, M., Ochi, T., Nakase, T., Hirota, S., Kitamura, Y., Nomura, S., et al. (1999). Mechanical tension-stress induces expression of bone morphogenetic protein (BMP)-2 and BMP-4, but Not BMP-6, BMP-7, and GDF-5 mRNA, during distraction osteogenesis. *J. Bone Miner. Res.* 14, 1084–1095. doi:10.1359/jbmr.1999.14.7.1084

Scotti, C., Tonnarelli, B., Papadimitropoulos, A., Scherberich, A., Schaeren, S., Schauerte, A., et al. (2010). Recapitulation of endochondral bone formation using human adult mesenchymal stem cells as a paradigm for developmental engineering. *Proc. Natl. Acad. Sci. U.S.A.* 107, 7251–7256. doi:10.1073/pnas.1000302107

Sheehy, E. J., Buckley, C. T., and Kelly, D. J. (2012). Oxygen tension regulates the osteogenic, chondrogenic and endochondral phenotype of bone marrow

derived mesenchymal stem cells. *Biochem. Biophys. Res. Commun.* 417, 305–310. doi:10.1016/j.bbrc.2011.11.105

Simmons, C. A., Matlis, S., Thornton, A. J., Chen, S., Wang, C. Y., and Mooney, D. J. (2003). Cyclic strain enhances matrix mineralization by adult human mesenchymal stem cells via the extracellular signal-regulated kinase (ERK1/2) signaling pathway. *J. Biomech.* 36, 1087–1096. doi:10.1016/S0021-9290(03)00110-6

Steinert, A. F., Rackwitz, L., Gilbert, F., Noth, U., and Tuan, R. S. (2012). Concise review: the clinical application of mesenchymal stem cells for musculoskeletal regeneration: current status and perspectives. *Stem Cells Transl. Med.* 1, 237–247. doi:10.5966/sctm.2011-0036

Steward, A. J., Wagner, D. R., and Kelly, D. J. (2014). Exploring the roles of integrin binding and cytoskeletal reorganization during mesenchymal stem cell mechanotransduction in soft and stiff hydrogels subjected to dynamic compression. *J. Mech. Behav. Biomed. Mater.* 38, 174–182. doi:10.1016/j.jmbbm.2013.07.020

Sumanasinghe, R. D., Bernacki, S. H., and Loboa, E. G. (2006). Osteogenic differentiation of human mesenchymal stem cells in collagen matrices: effect of uniaxial cyclic tensile strain on bone morphogenetic protein (BMP-2) mRNA expression. *Tissue Eng.* 12, 3459–3465. doi:10.1089/ten.2006.12.3459

Thompson, E. M., Matsiko, A., Farrell, E., Kelly, D. J., and O'Brien, F. J. (2015). Recapitulating endochondral ossification: a promising route to in vivo bone regeneration. *J. Tissue Eng. Regen. Med.* 9, 889–902. doi:10.1002/term.1918

Thompson, E. M., Matsiko, A., Kelly, D. J., Gleeson, J. P., and O'Brien, F. J. (2016). An endochondral ossification-based approach to bone repair: chondrogenically primed mesenchymal stem cell-laden scaffolds support greater repair of critical-sized cranial defects than osteogenically stimulated constructs in vivo. *Tissue Eng. Part A* 22, 556–567. doi:10.1089/ten.TEA.2015.0457

Thorpe, S. D., Buckley, C. T., Steward, A. J., and Kelly, D. J. (2012). European Society of Biomechanics S.M. Perren Award 2012: the external mechanical environment can override the influence of local substrate in determining stem cell fate. *J. Biomech.* 45, 2483–2492. doi:10.1016/j.jbiomech.2012.07.024

Thorpe, S. D., Nagel, T., Carroll, S. F., and Kelly, D. J. (2013). Modulating gradients in regulatory signals within mesenchymal stem cell seeded hydrogels: a novel strategy to engineer zonal articular cartilage. *PLoS ONE* 8:e60764. doi:10.1371/journal.pone.0060764

Vinardell, T., Sheehy, E. J., Buckley, C. T., and Kelly, D. J. (2012). A comparison of the functionality and in vivo phenotypic stability of cartilaginous tissues engineered from different stem cell sources. *Tissue Eng. Part A* 18, 1161–1170. doi:10.1089/ten.TEA.2011.0544

Weiss, S., Baumgart, R., Jochum, M., Strasburger, C. J., and Bidlingmaier, M. (2002). Systemic regulation of distraction osteogenesis: a cascade of biochemical factors. *J. Bone Miner. Res.* 17, 1280–1289. doi:10.1359/jbmr.2002.17.7.1280

Yang, P. J., Levenston, M. E., and Temenoff, J. S. (2012). Modulation of mesenchymal stem cell shape in enzyme-sensitive hydrogels is decoupled from upregulation of fibroblast markers under cyclic tension. *Tissue Eng. Part A* 18, 2365–2375. doi:10.1089/ten.TEA.2011.0727

Yoo, J. U., Barthel, T. S., Nishimura, K., Solchaga, L., Caplan, A. I., Goldberg, V. M., et al. (1998). The chondrogenic potential of human bone-marrow-derived mesenchymal progenitor cells. *J. Bone Joint Surg. Am.* 80, 1745–1757. doi:10.2106/00004623-199812000-00004

Zhang, T., Wen, F., Wu, Y., Goh, G. S., Ge, Z., Tan, L. P., et al. (2015). Cross-talk between TGF-beta/SMAD and integrin signaling pathways in regulating hypertrophy of mesenchymal stem cell chondrogenesis under deferral dynamic compression. *Biomaterials* 38, 72–85. doi:10.1016/j.biomaterials.2014.10.010

Zhao, Q., Eberspaecher, H., Lefebvre, V., and De Crombrugghe, B. (1997). Parallel expression of Sox9 and Col2a1 in cells undergoing chondrogenesis. *Dev. Dyn.* 209, 377–386. doi:10.1002/(SICI)1097-0177(199708)209:4<377::AID-AJA5>3.0.CO;2-F

Zhou, G., Zheng, Q., Engin, F., Munivez, E., Chen, Y., Sebald, E., et al. (2006). Dominance of SOX9 function over RUNX2 during skeletogenesis. *Proc. Natl. Acad. Sci. U.S.A* 103, 19004–19009. doi:10.1073/pnas.0605170103

Conflict of Interest Statement: The authors declare that the research was conducted in the absence of any commercial or financial relationships that could be construed as a potential conflict of interest.

frontiers in Bioengineering and Biotechnology

REVIEW
published: 11 December 2017
doi: 10.3389/fbioe.2017.00076

Dynamic Mechanical Compression of Chondrocytes for Tissue Engineering: A Critical Review

*Devon E. Anderson and Brian Johnstone**

Department of Orthopaedics and Rehabilitation, Oregon Health & Science University, Portland, OR, United States

Articular cartilage functions to transmit and translate loads. In a classical structure–function relationship, the tissue resides in a dynamic mechanical environment that drives the formation of a highly organized tissue architecture suited to its biomechanical role. The dynamic mechanical environment includes multiaxial compressive and shear strains as well as hydrostatic and osmotic pressures. As the mechanical environment is known to modulate cell fate and influence tissue development toward a defined architecture *in situ*, dynamic mechanical loading has been hypothesized to induce the structure–function relationship during attempts at *in vitro* regeneration of articular cartilage. Researchers have designed increasingly sophisticated bioreactors with dynamic mechanical regimes, but the response of chondrocytes to dynamic compression and shear loading remains poorly characterized due to wide variation in study design, system variables, and outcome measurements. We assessed the literature pertaining to the use of dynamic compressive bioreactors for *in vitro* generation of cartilaginous tissue from primary and expanded chondrocytes. We used specific search terms to identify relevant publications from the PubMed database and manually sorted the data. It was very challenging to find consensus between studies because of species, age, cell source, and culture differences, coupled with the many loading regimes and the types of analyses used. Early studies that evaluated the response of primary bovine chondrocytes within hydrogels, and that employed dynamic single-axis compression with physiologic loading parameters, reported consistently favorable responses at the tissue level, with upregulation of biochemical synthesis and biomechanical properties. However, they rarely assessed the cellular response with gene expression or mechanotransduction pathway analyses. Later studies that employed increasingly sophisticated biomaterial-based systems, cells derived from different species, and complex loading regimes, did not necessarily corroborate prior positive results. These studies report positive results with respect to very specific conditions for cellular responses to dynamic load but fail to consistently achieve significant positive changes in relevant tissue engineering parameters, particularly collagen content and stiffness. There is a need for standardized methods and analyses of dynamic mechanical loading systems to guide the field of tissue engineering toward building cartilaginous implants that meet the goal of regenerating articular cartilage.

Keywords: chondrocyte, chondrogenesis, dynamic compression, dynamic loading, bioreactor, tissue engineering

OPEN ACCESS

Edited by:
Roberto Narcisi,
Erasmus Medical Center, Netherlands

Reviewed by:
Henrique de Amorim Almeida,
Polytechnic Institute of Leiria, Portugal
Dimitrios I. Zeugolis,
National University of Ireland Galway, Ireland
Daniel John Kelly,
Trinity College, Dublin, Ireland

***Correspondence:**
Brian Johnstone
johnstob@ohsu.edu

Specialty section:
This article was submitted to Tissue Engineering and Regenerative Medicine, a section of the journal Frontiers in Bioengineering and Biotechnology

Received: *10 August 2017*
Accepted: *23 November 2017*
Published: *11 December 2017*

Citation:
Anderson DE and Johnstone B (2017) Dynamic Mechanical Compression of Chondrocytes for Tissue Engineering: A Critical Review. Front. Bioeng. Biotechnol. 5:76. doi: 10.3389/fbioe.2017.00076

INTRODUCTION

Articular cartilage resides in a complex and dynamic mechanical environment *in vivo*, characterized by compressive and shear stresses along multiple axes and hydrostatic and osmotic pressures throughout (Mansour, 2003; Mow and Huiskes, 2005). The biomechanical environment, in part, governs the development and maturation of the native structural architecture through a classical structure–function relationship (Williams et al., 2008). The heterogeneous and anisotropic extracellular matrix of mature tissue exhibits complex biomechanical properties, including biphasic viscoelasticity and strain stiffening behavior, and the tissue is avascular to accommodate dynamic loading (Mow and Huiskes, 2005). Without a blood supply, articular cartilage lacks the ability for intrinsic repair following disruption of tissue structure and alterations in the mechanical environment during injury. Cartilage injuries range from acute focal tears to chronic degeneration and are a significant cause of disability worldwide (Woolf and Pfleger, 2003; McCormick et al., 2014). To date, tissue-engineered cartilage intended for repair does not exhibit the structural or biomechanical properties of native tissue, and biomaterial-based tissues are governed in part by the mechanical properties inherent to the exogenous scaffold. A mismatch in mechanical properties between a repair tissue and the surrounding native tissue following surgical intervention will necessarily contribute to a continued disruption in joint biomechanics and therapeutic failure. Thus, a successful tissue-engineered construct needs not only to repair the tissue defect but also to integrate into the native tissue to restore joint mechanics to a preinjury state. Bioreactors that recreate one or more components of the mechanical environment of native cartilage have emerged as a primary laboratory tool in tissue engineering; directing tissue development through mechanical stimulation, with the goal of providing the construct with native tissue properties.

In the previous century, many groups developed dynamic single-axis compression or multiaxis compression and shear bioreactors to monitor the metabolic and biochemical responses of chondrocytes within native tissue explants to various loading regimes. A major finding was that static compression inhibits but dynamic compression promotes biochemical anabolism (Grodzinsky et al., 2000). Thereafter, investigators sought to characterize the response of biomaterial-seeded chondrocytes to similar loading regimes. Testing the hypotheses that the mechanical environment drives cell differentiation and tissue development *in vitro,* the field of cartilage tissue engineering experienced a rapid expansion of bioreactor-based methods. As research groups independently developed systems to investigate the response of chondrocytes to mechanical stimulation, there was little opportunity for standardization. As a result, the field contains a large body of literature that is varied with respect to both input parameters and outcomes (**Figure 1**). Input variables, for instance, include those for cells (source, number, state and differentiation), biomaterials (type, fabrication, and preloading culture conditions), bioreactor (type and axes), and loading regime (frequency, amplitude and duration). Furthermore, there is a wide variation in the outcomes measured following bioreactor stimulation that make comparisons more challenging.

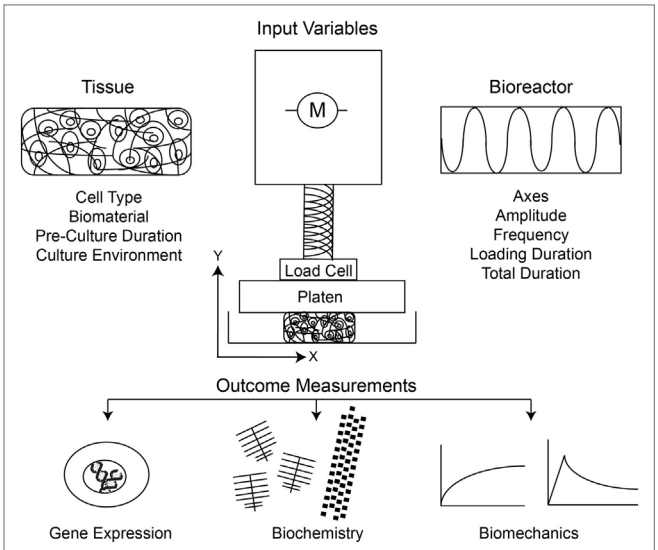

FIGURE 1 | Schematic of the input variables and outcome measurements under consideration in study design, and interpretation thereof, for dynamic compression of chondrocytes.

The most consistently measured outcome parameters are gene expression of various matrix proteins, with protein expression of proteoglycans [actually generally inferred from measuring glycosaminoglycan (GAG) sugar content] and/or collagens often, but not always, included and the bulk mechanical properties frequently, but again not always, included. A limited number of groups have further investigated mechanistic pathways involved in mechanotransduction of loaded chondrocytes. Without standardized loading protocols, the results from these complex and multistep tissue-engineering methods widely differ among individual groups, and the true effect of mechanical loading on chondrocyte-based tissue development remains unclear.

In this review, we sought to summarize the literature regarding dynamic loading of chondrocytes for tissue engineering applications to identify trends based on both input variables and resultant outcomes. Compilation of the literature provides a basis to critically evaluate a wide range of experimental systems relative to one another, as each has been previously reported in isolation. We sought to identify system variables across studies that generate positive or negative results with respect to cartilage tissue engineering, from chondrogenesis measured by gene expression to tissue development measured by biochemical and biomechanical analyses. This thorough review of the expansive literature regarding dynamic compression of chondrocytes illuminates trends that can inform future experimental design for the ultimate goal of engineering tissue with the articular cartilage phenotype.

METHODS

We performed a literature search of the MEDLINE PubMed database for all English language peer-reviewed articles published between January 1, 1995 and December 31, 2016 and that were indexed according to the following search terms in title and/

or abstract: (chondrocyte OR chondroprogenitor OR chondrogenesis) AND (dynamic compression OR dynamic loading OR bioreactor OR compression bioreactor OR dynamic compression bioreactor). These searches yielded a total of 1,799 results; however, many individual publications were repetitive with alternative search terms. We then manually assessed the manuscripts to find those in which articular chondrocytes or articular cartilage-derived progenitor cells were used in experiments and dynamic compression was included as at least one element of the loading regime. This resulted in a final list of 63 manuscripts, which we then critically evaluated for their major findings and compared them to each other, noting the many differences in input and output variables used. The results are comprehensively detailed in the tables that accompany this review.

Dynamic loading parameters including frequency, amplitude, duration, and timing clearly influence biochemical and biomechanical outcomes in these studies; however, comparisons between studies should be performed cautiously as each study employs a unique cell source and culture conditions. It is also worth noting that less than half of the compiled studies report sample sizes. In compiling the review, we specifically noted the lack of discussion of species differences by authors when comparing their results with the work of others. Thus, we used this parameter as part of the structural separation of the types of studies we found to emphasize its importance as a variable in the results obtained.

RESULTS

Non-Human Large Mammal Chondrocytes in Hydrogel Substrates

Effect of Loading Duration

The earliest studies to define the role of dynamic mechanical stimulation of chondrocytes within a tissue engineering system, as opposed to explant culture, used primary bovine chondrocytes seeded into hydrogel-based substrates and investigated the cellular biochemical response, using assays to quantify changes in proteoglycan, collagen, and total protein content. These studies showed that chondrocytes significantly increased proteoglycan synthesis but variably regulated collagen synthesis in response to short-duration dynamic loading at various frequencies, with a majority of positive results at 1 Hz (Buschmann et al., 1995; Lee and Bader, 1997). Using primary bovine chondrocytes seeded at low cell density within agarose hydrogels, Mauck et al. began to define the roles of tissue engineering system parameters, including hydrogel substrate, cell seeding density, growth factor co-stimulation, and serum concentration, finding significant increases in proteoglycan and collagen production, and tissue stiffness with dynamic loading in comparison with free-swelling controls (Mauck et al., 2000, 2003a,b). Importantly, positive results from these studies only arose with greater than 45 total loading hours and appeared to be duration dependent. A time-dependent increase in proteoglycan production, but not overall protein synthesis, was also reported with substantially fewer total loading hours by Chowdhury et al. (2003), with maximal proteoglycan production following an intermittent loading regime of two times 12 h on, 12 h off. Kisiday et al. (2004) similarly reported superior results for an intermittent loading regime, such that alternating days of intermittent dynamic stimulation with days of free-swelling culture drove significant increases in GAG production and accumulation as well as increases in equilibrium and dynamic moduli when compared with free-swelling controls. Another study found that 3 or 6 h of continuous daily loading was superior to a 1 h on/1 h off for three cycles per day protocol in terms of resultant mechanical properties at day 28 (Ng et al., 2009). It can be hypothesized that intermittent loading is superior because the rest period allows the cells to respond to the stimulus with both the production of extracellular matrix molecules and the integration of these molecules into the existing matrix whereas continuous loading drives the newly synthesized molecules out of the tissue through mass transport.

Effect of Preload Culture and Timing of Load Initiation

While increased total loading duration has a positive effect on proteoglycan synthesis and accumulation in hydrogel-based systems, the timing of initiation of load application relative to total duration in culture appears to correlate with the resultant hydrogel compressive mechanical properties. Lima et al. showed that application of load immediately following cell seeding caused a significant decrease in GAGs, collagen, Young's compressive modulus, and dynamic modulus after 32 and 56 days of intermittent loading when compared with free-swelling controls. When application of initial load was delayed by 14 days, there was no difference in GAG or collagen content but there was a significant increase in both moduli in comparison with free-swelling controls (Lima et al., 2007). These results, however, were only partially corroborated by a follow-up study from the same group such that minimal differences existed when the delayed and immediate loading regimes were directly compared (Bian et al., 2010). At the gene level, Nicodemus et al. reported that intermittent loading regimes significantly upregulated both anabolic (*COL2A1* and *ACAN*) and catabolic (*MMP1*, *MMP3*, and *MMP13*) genes with increased loading duration relative to both preload gene expression and to continuously loaded hydrogels. For the same intermittent regime, investigation of delayed versus immediate loading was performed in a cross-over study with 7 days in free-swelling or dynamic loading with a subsequent switch, and both anabolic and catabolic genes increased under dynamic loading regardless of timing without significant differences in the total GAG content (Nicodemus and Bryant, 2010). Delayed loading likely provides the cells with time to build a preliminary pericellular matrix under chemical stimuli before dynamic loading. The matrix elaborated during a period of delayed stimulation may be necessary for effective mechanotransduction and resultant tissue stiffening in the dynamic mechanical environment.

Effect of Cell Source

Bovine and other non-human large mammal-derived chondrocytes are a readily available cell source for laboratory-based tissue engineering protocol development; however, results from experiments utilizing these easily harvested cells appear highly

dependent on co-variables of donor age, *in situ* location, and *in vitro* expansion. In comparison with adult-derived chondrocytes, juvenile and neonatal-derived bovine cells have a higher capacity to produce cartilaginous extracellular matrix components at both the gene and protein level (Liu et al., 2013). This effect was noted in a study defining the differences in metabolic response of chondrocytes to dynamic loading based on donor age and location within the joint. Only primary chondrocytes derived from low load-bearing areas of 5-month-old donors significantly increased proteoglycan and protein production with dynamic load in comparison with static load; whereas, cells derived from high load-bearing areas, and neonatal- and adult-derived chondrocytes were unresponsive to the same dynamic loading regime (Wiseman et al., 2003). Farnsworth et al. (2013) similarly showed that while adult chondrocytes that were dynamically loaded at 1 Hz and 5% compression significantly increased total GAGs by 88% at day 14, juvenile chondrocytes loaded at 0.3 Hz and 5% compression significantly increases total GAGs by 220% at day 7 and 280% at day 14, both relative to respective free-swelling controls. Shelton et al. (2003) investigated the differences between deep and superficial chondrocytes, and found that while superficial zone chondrocytes upregulated total protein production under dynamic load at all tested frequencies (0.3, 1, and 3 Hz), only deep zone chondrocytes significantly increased proteoglycan synthesis and likely account for the majority of the response of full-depth chondrocytes to dynamic loading at 1 Hz. These few studies demonstrate a simple principle that not all bovine chondrocytes are equivalent.

Effect of Cell Expansion

Primary chondrocytes from large mammals are readily available in quantities sufficient for scalable tissue engineering experiments. Monolayer expansion of any chondrocyte, however, induces modulation of the articular chondrocyte phenotype in a process known as dedifferentiation, which is characterized by a shift from expression of type II to type I collagen at both the gene and protein level (Goessler et al., 2004), loss of gene expression for aggrecan and lubricin (Darling and Athanasiou, 2005), changes to the integrin profile on the cell surface (Goessler et al., 2006a), and differential expression of metabolic mediators and growth factors that regulate extracellular matrix homeostasis (Goessler et al., 2005, 2006b). Though the mechanism for phenotypic modulation is not entirely known, the presence of serum in cell propagation and a two-dimensional growth environment facilitate these changes (Malpeli et al., 2004). A single study investigated the effect of monolayer expansion on the response of bovine chondrocytes to dynamic loading in agarose hydrogels and found that cells passaged once exhibited significantly greater sulfate and thymidine incorporation into matrix components than unstrained controls, however, primary chondrocytes actually significantly decreased sulfate incorporation when loaded compared with free-swelling controls. Chondrocytes expanded beyond two passages significantly decreased both sulfate and thymidine incorporation under dynamic load in comparison with unstrained controls. Cells derived from the same batches but cultured in alginate beads demonstrated the phenotypic modulation from type II to type I collagen with increased passage (Wiseman et al., 2004). Significant differences for results generated with primary versus expanded cells may inhibit translation of the majority of results generated with primary bovine chondrocytes to a human model that will likely necessitate *in vitro* expansion for autologous tissue restoration.

Effect of Hydrogel Substrate

Similar to cell factors, hydrogel substrate alone mediates cell response to dynamic loading. When cultured in a fibrin-based hydrogel, bovine chondrocytes responded to dynamic compression in a manner opposite to the previously described agarose-based systems with a significant decrease in GAGs, total collagen, and dynamic stiffness in comparison with free-swelling or statically compressed controls (Hunter et al., 2004). The dramatic differences in chondrocyte response to dynamic load between hydrogel substrates highlights the importance of the cell-matrix interaction, primarily mediated by integrins; however, only agarose and alginate hydrogels have been directly compared in a single study (Mauck et al., 2000). Not all hydrogels are equivalent, and results of these studies must be carefully interpreted to account for differences in substrate.

Effect of Soluble Factors

Hydrogel systems have been used to evaluate the influence of co-variables to the dynamic loading culture system, including serum, soluble growth factors, vitamins, and small molecule inhibitors to guide chondrogenic tissue development and evaluate mechanotransduction mechanisms in the dynamic mechanical environment. Mauck et al. (2003a) showed addition of either TGF-β1 and IGF-1 to 10% FBS-supplemented basal media significantly enhanced the response of chondrocytes to dynamic loading with respect to aggregate equilibrium modulus, GAG content, and collagen content, especially with longer duration culture. A study that evaluated the temporal effect of TGF-β supplementation found that a preculture period in TGF-β3 for 14 days before the onset of loading followed by dynamic loading without TGF-β3 primed the constructs for superior mechanical and biochemical properties at 42 days compared with free-swelling controls or with immediate loading and TGF-β3 removal at day 14 (Lima et al., 2007). When cells were seeded at high density of 60×10^6 and loaded in dynamic compression, increasing the FBS concentration from 10 to 20% increased both the Young's compressive and dynamic moduli but had no effect on collagen or GAG content. This effect was not seen for lower cell seeding density at 10×10^6, which highlights the importance of nutrient demands of cells and transport of those nutrients through tissues in the dynamic environment (Mauck et al., 2003b). Another study using high cell density hydrogels at 60×10^6 showed that addition of ITS and increasing concentration of FBS from 0 to 20% significantly enhanced the biochemical and biomechanical properties of free-swelling constructs in the absence of dynamic load, with the greatest benefit at 2% FBS with ITS supplementation (Kelly et al., 2008). When these constructs were cultured in a dynamic loading environment, the addition of supplements for the entire loading duration was actually detrimental to resultant mechanical properties at days 28 and 42 when compared with free-swelling controls. Priming the constructs in 20% FBS for

the first week before transfer to respective FBS concentration plus ITS, rescued the mechanical properties for a significant improvement compared with free-swelling controls (Kelly et al., 2008). These four studies from a single laboratory highlight the importance of media formulation on the tissue level responses to dynamic loading, specifically mechanical properties. Tissues generated in chemically defined media with TGF-β benefit from delayed loading while those cultured in the presence of serum benefit from immediate loading following cell seeding. These differences in biomechanical outcomes may be a result of differences in the biochemical makeup of the extracellular matrix, which was characterized by total proteoglycan and collagen content without a differential analysis into specific types of collagen or other matrix molecules. Increases in tissue stiffness without detectable differences in the bulk collagen or proteoglycan content in some of these studies may represent unmeasured differences in extracellular matrix organization such as collagen type, cross-linking, or organization, which are known to independently modulate overall tissue biomechanical properties in native tissue (Gannon et al., 2015). In consideration of collagen synthesis, Omata et al. (2012) found that increasing the concentration of ascorbic acid in culture media significantly increased the tangent modulus and the pericellular matrix formation compared with free-swelling controls, revealing the importance of ascorbic acid concentration for adequate collagen synthesis.

Adding nutrients to media does not necessarily mean that the cells will have access to them since delivery of nutrients into a thick hydrogel filled with dense extracellular matrix may be limited by diffusion and a consequential nutrient gradient. Dynamic loading inherently increases bulk flow and perfusion through neocartilage tissues, but the addition of nutrient channels to hydrogels has not been shown to further enhance the GAG or collagen profile of tissues beyond that of dynamic loading of solid hydrogels (Mesallati et al., 2013). While bulk flow mediates nutrient delivery in the dynamic system, the tissue is also under the influence of osmotic loading through fixed charge density of the extracellular matrix, and Kelly et al. (2013) showed that dynamic loading in hypotonic salt solution likely removed salts that shield the fixed charges within the tissue and significantly increased the measured mechanical properties, potentially giving a more accurate and promising readout for tissue stiffness. Nutrient availability is relatively easily modeled in a hydrogel system; however, as tissue engineering systems become more complex in both scaffold-based and scaffold-free extracellular matrix tissues, these principles may not hold.

Overall, agarose hydrogels have proven a relatively universal substrate with which to investigate the response of chondrocytes to dynamic compressive loading. This system has allowed the field to systematically investigate: variables of dynamic loading regimes including frequency, strain, duration and timing; differences among cells from varied sources and culture conditions; and additive effects of soluble factors and delivery thereof. These results, which are summarized in **Table 1**, provide us with very specific parameters by which chondrocytes seeded in hydrogels

TABLE 1 | Compilation of studies that investigated the response of non-human, large mammal-derived chondrocytes seeded into hydrogels and subjected to uniaxial dynamic compressive loading.

Reference	Study design/ investigation	Cell source (*n*), hydrogel, and preculture duration	Loading parameters	Results [PG = proteoglycans, Eeq = equilibrium, Edyn = dynamic, Ey = Young's, and H(A) = aggregate]
Buschmann et al. (1995)	Cellular metabolic response to single dynamic loading period	Neonatal primary bovine chondrocytes in 2 or 3% agarose precultured 3, 13, or 24 days	Frequency: 0.001, 0.01, 0.1, and 1 Hz Amplitude: 1% Duration: 10 h continuous Max duration: 10 h	RNA: not assessed PG: ↑ all frequencies at days 5 and 23 Collagen: ↑ all frequencies at days 5 and 23 Biomechanics: not assessed
Lee and Bader (1997)	Effect of loading frequency	18-month-old primary bovine chondrocytes in 3% agarose precultured for 16 h	Frequency: 0.1, 1, and 3 Hz Amplitude: 15% Duration: 48 h continuous Max duration: 48 h	RNA: not assessed PG: ↑ 1 Hz, ↓ 0.3 Hz, and ↔ 3 Hz Collagen: ↓ all conditions Biomechanics: not assessed
Mauck et al. (2000)	Agarose versus alginate hydrogels and subsequent dynamic loading of agarose hydrogels	3- to 5-month-old primary bovine chondrocytes in 1–5% alginate without preculture	Frequency: 1 Hz Amplitude: 10% Duration: 3× 1 h on/1 h off, 5 days/week for 28 days Max duration: 60 h	RNA: not assessed PG: ↑ on day 21 Collagen: ↑ on day 21 Biomechanics: ↑ Eeq and peak stress on days 21–28
Mauck et al. (2003a)	Effect of TGF-β, IGF 1, and load	2- to 12-day-old primary bovine chondrocytes ($n = 3$) in 2% agarose precultured for 0 or 22 days	Frequency: 1 Hz Amplitude: 10% Duration: 3× 1 h on/1 h off, 5 days/week for 35 days Max duration: 75 h	RNA: not assessed PG: ↑ on day 28–35 Collagen: ↑ on day 35 Biomechanics: ↑ H(A) on day 35, increase with TGF-β
Mauck et al. (2003b)	Cell seeding density in agarose and effect of increased FBS concentration	4- to 6-month-old primary bovine ($n = 5$) in 2% agarose without preculture	Frequency: 1 Hz Amplitude: 10% Duration: 3× 1 h on/1 h off, 5 days/week for 56 days Max duration: 105 h	RNA: not assessed PG: ↑ low cell density on day 42 Collagen: ↑ low cell density on days 28–56 Biomechanics: ↑ Eeq and Edyn, α cell seeding density, and % FBS

(*Continued*)

TABLE 1 | Continued

Reference	Study design/ investigation	Cell source (*n*), hydrogel, and preculture duration	Loading parameters	Results [PG = proteoglycans, Eeq = equilibrium, Edyn = dynamic, Ey = Young's, and H(A) = aggregate]
Shelton et al. (2003)	Effect of dynamic loading frequency on constructs with full-depth, superficial, or deep chondrocytes	18-month-old primary bovine chondrocytes in 3% agarose without preculture	Frequency: 0.1, 1, and 3 Hz Amplitude: 15% Duration: 48 h continuous Max duration: 48 h	RNA: not assessed PG: full thickness or deep cells: ↓ 0.3 Hz, ↑ 1 Hz, and ↔ 3 Hz; superficial cells: ↓ 0.3 Hz, ↔ 1 Hz, and ↓ 3 Hz Collagen: not assessed Biomechanics: not assessed
Wiseman et al. (2003)	Effect of cell maturity (donor age) on response to dynamic loading and the production of NO as a readout for degenerative processes	Fetal through adult primary equine chondrocytes in 4% agarose without preculture	Frequency: 1 Hz Amplitude: 15% Duration: 24 h continuous Max duration: 24 h	RNA: not assessed PG: ↑ 5-month-old chondrocytes from low-load region, ↔ any other condition Collagen: not assessed Biomechanics: not assessed
Chowdhury et al. (2003)	Effect of continuous versus intermittent dynamic loading on cell metabolism	18-month-old primary bovine chondrocytes in 2% agarose precultured for 1 day	Frequency: 1 Hz Amplitude: 15% Duration: 24 h on/24 h off or 1.5, 3, 6, and 12 h continuous Max duration: 24 h	RNA: not assessed PG: ↑ all conditions Collagen: not assessed Biomechanics: not assessed
Wiseman et al. (2004)	Effect of cell passage on response to loading	Adult primary or expanded bovine chondrocytes in 4% agarose without preculture	Frequency: 1 Hz Amplitude: 15% Duration: 24 h continuous Max duration: 24 h	RNA: not assessed PG: ↓ p0 cells, ↑ p1 and p2 cells, ↔ p3 and p4 (p = passage #) Collagen: not assessed Biomechanics: not assessed
Kisiday et al. (2004)	Effect of varied intermittent loading regimes	Neonatal primary bovine chondrocytes in 0.2 or 0.4% agarose with self-assembling peptides precultured for 0 or 22 days	Frequency: 1 Hz Amplitude: 2.5% Duration: 30 min on/30 min off, 1 h on/1 h off, or 3, 5, 7 h/day for 3, 5, 11, or 39 days Max duration: 150 h	RNA: not assessed PG: ↑ intermittent loading Collagen: not assessed Biomechanics: ↑ Eeq and Edyn for intermittent loading
Hung et al. (2004)	Summary of data regarding loading regimes, growth factors, and cell seeding density	4- to 6-month-old primary bovine chondrocytes (*n* = 3–5) in 2% agarose without preculture	Frequency: 1 Hz Amplitude: 10% Duration: 3× 1 h on/1 h off, 5 days/week for 3, 28, or 56 days Max duration: 105 h	RNA: ↑ ACAN at 3 days only PG: not assessed Collagen: not assessed Biomechanics: ↑ H(A) on days 21–28, ↑ Ey on days 28–56, ↑ Edyn on day 56
Hunter et al. (2004)	Static versus dynamic compression in fibrin-based gel biomaterial	2- to 3-week-old previously frozen primary bovine chondrocytes in fibrin gel precultured for 3 days	Frequency: 0.1, 1 Hz Amplitude: 4% Duration: 10 or 20 days continuous Max duration: 480 h	RNA: not assessed PG: ↓ for 0.1 and 1 Hz at days 10 and 20 Collagen: ↓ for 0.1 and 1 Hz at days 10 and 20 Biomechanics: ↓ Edyn for 0.1 and 1 Hz at days 10 and 20
Mouw et al. (2007)	Role of voltage-gated K+ and Ca2+ channels, stretch-dependent ion channels, and ATP-dependent Ca2+ channels in response to loading	2- to 3-week-old primary bovine chondrocytes in 2% agarose precultured for 1 day	Frequency: 1 Hz Amplitude: 3% Duration: 20 h continuous Max duration: 20 h	RNA: not assessed PG: ↑ dynamic load, decreased with blockage voltage-gated Ca++ channels Collagen: not assessed Biomechanics: not assessed
Mauck et al. (2007)	Effect of loading frequency and duration with gene transcription reporter promoter constructs	3- to 6-month-old primary bovine chondrocytes in 2% agarose precultured for 3 days	Frequency: 0.33, 1, and 3 Hz Amplitude: 10% Duration: 1 or 3 h continuous Max duration: 3 h	RNA: ↑ ACAN and ↓ COL2A1 promotor activity PG: not assessed Collagen: not assessed Biomechanics: not assessed
Lima et al. (2007)	Temporal effect of TGF-β and dynamic loading	4- to 6-month-old primary bovine chondrocytes (*n* = 3–5) in 2% agarose precultured for 0 or 14 days	Frequency: 1 Hz Amplitude: 10% Duration: 3 h/day, 5 days/week for 42 or 56 days Max duration: 105 h	RNA: not assessed PG: ↔ preculture, ↓ loaded from day 0 Collagen: ↔ preculture, ↓ loaded from day 0 Biomechanics: ↑ Ey and Edyn with preculture, ↓ Ey and Edyn when loaded from day 0

(*Continued*)

TABLE 1 | Continued

Reference	Study design/ investigation	Cell source (*n*), hydrogel, and preculture duration	Loading parameters	Results [PG = proteoglycans, Eeq = equilibrium, Edyn = dynamic, Ey = Young's, and H(A) = aggregate]
Kelly et al. (2008)	Effect of FBS and ITS in mechanical environment	3- to 4-month-old primary bovine chondrocytes (n = 4–8 pooled) in 2% agarose without preculture	Frequency: 1 Hz Amplitude: 10% Duration: 3 h/day for 28 or 42 days Max duration: 126 h	RNA: not assessed PG: ↔ 0% FBS/ITS, ↑ 0.2% FBS/ITS, and 20% FBS groups, Collagen: ↔ any group Biomechanics: ↔ Ey for 0% FBS/ITS or 20% FBS, ↑ Ey for 0.2% FBS/ITS and 2% FBS/ITS groups
Ng et al. (2009)	Effect of removal of TGF-β from system	3- to 4-month-old primary bovine chondrocytes (n = 5) in 2% agarose without preculture	Frequency: 1 Hz Amplitude: 10% Duration: 3× 1 h on/1 h off or 3 or 6 h continuous for 28 days Max duration: 168 h	RNA: not assessed PG: ↔ any group Collagen:↑ type II and type IX collagen on quant IHC Biomechanics: ↑ Eeq for all loading regimes, ↑ Edyn only 3 or 6 h continuous
Villanueva et al. (2009)	Effect of increasing concentrations of RGD in PEG hydrogel	1- to 2-year-old primary bovine chondrocytes (n = 6) in 10% PEG ± RGD precultured for 1 day	Frequency: 0.3 Hz Amplitude: 15% Duration: 48 h continuous Max duration: 48 h	RNA: not assessed relative to control PG: not assessed relative to control Collagen: not assessed relative to control Biomechanics: ↔ with 48 h loading
Nicodemus and Bryant (2010)	Continuous versus intermittent and immediate versus delayed loading regimes	1- to 3–week-old primary bovine chondrocytes (n = 2) in PEG precultured for 1 or 7 days	Frequency: 0.3 Hz Amplitude: 15% Duration: 1 h on/1 h off or continuous for 7 or 15 days Max duration: 180 h	RNA: ↑ ACAN continuous load at day 7, ↔ ACAN and ↑ COL2, MMP1, MMP3, and MMP13 intermittent load at day 7, ↔ COL2, ACAN and ↑ MMP1, MMP3 preculture + intermittent load PG: ↑ continuous load over 7 days, ↔ for intermittent load or preculture followed by continuous or intermittent load Collagen: not assessed Biomechanics: not assessed
Stojkovska et al. (2010)	Validate bioreactor and alginate system, not necessarily tissue engineering	6-month-old expanded bovine chondrocytes in 1.5% alginate microbeads without preculture	Frequency: 0.42 Hz Amplitude: 10% Duration: 1 h on/1 h off for 14 days Max duration: 168 h	RNA: not assessed PG: not assessed Collagen: not assessed Biomechanics: ↔ any group
Bian et al. (2010)	Immediate versus delayed loading and addition of shear	2- to 4-year-old expanded canine chondrocytes in 2% agarose precultured for 0, 14, or 28 days	Frequency: 1 Hz Amplitude: 5% Duration: 3 h/day, 5 days/week for 28 days Max duration: 60 h	RNA: not assessed PG: ↔ any group Collagen: ↔ any group Biomechanics: ↑ Ey continuous load at days 28–56, delayed load at day 56 only. ↑ Edyn for all loading regimes at day 56
Kaupp et al. (2012)	Effect of duration of dynamic loading	Adult primary bovine chondrocytes (n = 10–15) in 2% agarose without preculture	Frequency: 1 Hz Amplitude: 10% Duration: 20, 30, or 60 min continuous Max duration: 1 h	RNA: not assessed PG: ↑ 20 or 30 min load Collagen: ↔ any group Biomechanics: not assessed
Omata et al. (2012)	Cumulative effects of vitamin C and mechanical load	Adult primary bovine chondrocytes in 1% agarose precultured for 1 day	Frequency: 1 Hz Amplitude: 15% Duration: 6 h/day for 22 days Max duration: 132 h	RNA: not assessed PG: not assessed Collagen: ↔ any group Biomechanics: ↑ Etan with increasing AA2P
Kelly et al. (2013)	Role of osmotic loading in conditioning tissues for response to dynamic load	Adult primary canine chondrocytes (n = 3–5 pooled) in 2% agarose precultured for 14 days	Frequency: 1 Hz Amplitude: 10% Duration: 3 h/day, 5 days/week for 42 or 56 days Max duration: 105 h	RNA: not assessed PG: ↔ any group Collagen: ↑ collagen/DNA Biomechanics: ↑ Ey(steady state) and Ey(max incremental) with dynamic compression only with osmotic load
Farnsworth et al. (2013)	Effect of cell maturity (donor age) on the response to dynamic loading	2- to 3-year-old primary bovine or 1–3 week old primary bovine chondrocytes (n = 2–3) in PEG without preculture	Frequency: 0.3 and 1 Hz Amplitude: 5 or 10% Duration: 30 min on/90 min off for 16 h/day for 14 days Max duration: 56 h	RNA: not assessed PG: ↑ adult chondrocytes at 1 Hz/5% at day 14; ↑ juvenile chondrocytes at 0.3 Hz/5% at days 7 and 14 Collagen: adult chondrocytes ↑ type II collagen and pericellular type VI with quant IHC; juvenile chondrocytes ↓ type II and VI Biomechanics: not assessed

(*Continued*)

TABLE 1 | Continued

Reference	Study design/ investigation	Cell source (*n*), hydrogel, and preculture duration	Loading parameters	Results [PG = proteoglycans, Eeq = equilibrium, Edyn = dynamic, Ey = Young's, and H(A) = aggregate]
Mesallati et al. (2013)	Nutrient flow through microchannels versus solid hydrogels	4-month-old expanded porcine chondrocytes ($n = 1$) in 2% agarose without preculture	Frequency: Hz Amplitude: 10% Duration: 2 h/day, 5 days/week for 21 days Max duration: 30 h	RNA: not assessed PG: ↑ for solid gels but not channeled gels Collagen: ↑ for solid and channeled gels Biomechanics: not assessed

respond to dynamic compression. We must realize, however, that positive results published in these studies highlight nuances discovered within narrow investigations. For instance, many positive results did not show up until extended culture duration with intermittent loading. Negative data or lack of changes seen in other studies may have simply been the result of too short of study duration to identify positive changes. As seen in the following sections, direct comparison of studies becomes ever more difficult with increasing complexity of tissue engineering and bioreactor systems.

Non-Human Large Mammal Chondrocytes in Non-Hydrogel Substrates

In the age of regenerative medicine, we are tasked with interpreting results from increasingly complex tissue engineering systems. Over the past two decades, a primary focus of regenerative medicine has been on biomaterial science for the production of scaffolds and substrates upon which to build increasingly sophisticated tissues. Two general categories of biomaterials used for soft tissue engineering include synthetic polymers produced through chemical reactions and natural polymers, either protein- or carbohydrate-based, produced by living organisms.

Synthetic Polymer Scaffolds

Synthetic polymers including poly-lactic acid, poly-glycolic acid (PGA), and poly-caprolactone can be manufactured to meet specifications including porosity, bioresorption rate, and mechanical stiffness. These properties, in turn, highly influence cell phenotype and modulate the cellular responses to the mechanical environment, specifically through load distribution and mechanotransduction. Unlike the prototypical agarose hydrogel system described earlier, the large variety of scaffold-based substrates make it harder to gain an understanding of the response to chondrocytes to a dynamic loading regime when using them. Nonetheless, it is worth reviewing the results from these studies in isolation. When neonatal primary bovine chondrocytes were seeded into PGA scaffolds, precultured for 21 days, and continuously loaded at either 0.001 or 0.1 Hz and 10 or 50% compression for 24 h, they significantly increased both total protein and GAG production in comparison with free-swelling and 10% statically loaded controls, with greatest effect seen at 0.1 Hz and 50% compression (Davisson et al., 2002). When Seidel et al. (2004) dynamically and intermittently loaded primary bovine chondrocytes in a PGA scaffold for long durations, they noted a significant decrease in total collagen content and no difference in total GAG or mechanical properties when compared with free-swelling controls; however, the distribution of GAGs and collagen varied between resultant tissues based on proposed differences in bulk interstitial flow between experimental groups. At the cellular level, Xie et al. (2006) showed that lapine chondrocytes seeded in poly(L-lactide-co-ε-caprolactone) significantly upregulated *COL2A1* mRNA when subjected to dynamic load compared with static load, that gene expression is directly correlated to loading duration, and that the proximal region of the *COL2A1* gene promotor mediates transcriptional activity under dynamic compression. When the same group investigated extracellular matrix production under dynamic load in the same system, they found that dynamic compression increased both GAG and collagen production when normalized to cell count; however, they did not compare the groups statistically (Xie et al., 2007). Contrary to their first study, they found no difference for *COL2A1*, *ACAN*, or *COL1A1* expression after one day of dynamic loading or free-swelling culture, and continuous loading completely abrogated *COL2A1* and *ACAN* expression after 6 days. An intermittent loading regime that introduced resting periods between dynamic loading cycles rescued *COL2A1* and *ACAN* expression (Xie et al., 2007). Another investigation utilizing lapine chondrocytes seeded in polyurethane scaffolds showed that both 20% and 30% strain at 0.1 Hz increases *ACAN* expression up to 12 h (Wang et al., 2008). Encapsulation of chondrocytes in a collagen gel derived from bovine skin before seeding into the scaffold increased *COL1A1* expression and decreased *COL2A1* expression as would likely be expected with a type I collagen gel (Wang et al., 2008). None of these experiments compared the dynamically stimulated groups with an unloaded or statically loaded control. While the biomaterial itself influences cellular response to loading, El-Ayoubi et al. (2011) showed that biomaterial morphology and pore size independently mediate the canine chondrocyte viability under static and dynamic loading regimes but did not investigate gene or matrix level changes.

Natural Polymer Scaffolds

The manufacturability and tunable properties of synthetic scaffolds make them attractive substrates for tissue engineering, but scaffolds derived from natural polymers are generally more biocompatible and non-toxic to cells. Under static compression in type II collagen scaffolds, adult expanded canine chondrocytes exhibited a time- and dose-dependent decrease in protein and proteoglycan production consistent with static compression of native tissue explants. In comparison with both static compression and free-swelling controls, dynamic compression

upregulated both total protein and proteoglycan production, but the majority of newly synthesized proteins were lost from the scaffold to the media with dynamic stimulation (Lee et al., 2003). Lapine chondrocytes seeded into a chitosan and gelatin scaffold significantly upregulated *COL2A1* and *ACAN* expression after 3 h of dynamic loading in comparison with unloaded controls, but *COL2A1* was then significantly downregulated after 9 h of compression. After 3 weeks of dynamic loading for 6 h per day, chondrocytes had significantly proliferated and produced more GAGs than the unloaded controls, but this study did not investigate collagen protein to correlate to gene expression data (Wang et al., 2009). When this same group added collagen gel and varied concentrations of genipin to induce collagen cross-linking to the chitosan scaffold base, they found that dynamic loading and increasing genipin concentration increased cell proliferation but decreased normalized GAG production (Wang and Tsai, 2013). While natural polymers provide a framework for cells in the mechanical environment, the scaffold is substantially different from the extracellular matrix of native tissue. In order the build a tissue more representative of the native structure, a handful of groups have relied on the cells to build an extracellular matrix *in vitro* through scaffold-free tissue engineering approaches before dynamic mechanical stimulation.

Non-Human Large Mammal Chondrocytes in Scaffold-Free Systems

In contrast to seeding chondrocytes within synthetic or natural polymers, scaffold-free methods utilize a preculture period in which the cells elaborate their own extracellular matrix as the substrate for later loading studies. It should be noted that even in scaffold-free tissue engineering, biomaterial substrates are often used to guide and/or constrain the tissue during its development period. The Kandel group developed an early method of scaffold-free tissue engineering by seeding juvenile bovine primary chondrocytes at high density onto a calcium phosphate surface and culturing the cells for 4 weeks such that the they produce substantial extracellular matrix before dynamic compressive and/or shear loading (Waldman et al., 2003). Once stimulated with uniaxial dynamic compressive load at 5% strain and 1 Hz for 4,000 cycles every 48 h for 4 weeks, the resultant tissues accumulated significantly more proteoglycans and collagen and exhibited a threefold increase in tissue stiffness than controls in static culture (Waldman et al., 2004). The same group later evaluated the cell level response to short-duration dynamic loading. They reported *MMP3* and *MMP13*—genes coding for matrix metalloproteinases 3 and 13 that degrade type II collagen—were maximally and significantly upregulated 2 h after dynamic compression in comparison with static culture. These genes subsequently declined, and *COL2A1* and *ACAN* were maximally and significantly upregulated 12 h after stimulation. At the protein level, MMP13 was most active 6 h after stimulation as measured by both enzyme activity and fold-change of collagen and proteoglycans released into the media, presumably as a result of MMP cleavage. Despite this, stimulated tissues had significantly greater total synthesis and retention of collagen and proteoglycans 24 h after loading than unloaded controls. These results collectively highlight that tissue remodeling, through both catabolic and anabolic mechanisms, is an important response to dynamic compression (De Croos et al., 2006). Another method to create *de novo* cartilage of cell-derived ECM is to preculture chondrocytes in an alginate hydrogel to provide the cells time to produce matrix molecules. The alginate is then dissolved to leave a suspension of cells with pericellular matrix that can be subsequently seeded to form cartilaginous tissues free of exogenous scaffolding. Hoenig et al. (2011) seeded alginate-released porcine chondrocytes onto a hydroxyapatite mold before dynamic stimulation and reported no differences in quantitative measures of GAGs, type I collagen, or type II collagen regardless of loading amplitude when compared with unloaded controls. Dynamic compression at 5 and 10% strain, however, significantly increased the resultant tissue stiffness, and 20% strain significantly increased Young's modulus, again all in comparison with unloaded controls. In a similar model, Stoddart et al. (2006) cultured alginate-released bovine chondrocytes in a silicon mold for 14 days before application of dynamic load to create *de novo* tissues from cartilaginous ECM, and found that type II collagen and aggrecan mRNA was significantly upregulated within 1 h of loading relative to unloaded controls, remained upregulated with loading through 3 h, but subsequently declined with 4 h of continuous load. Over 4 days of dynamic stimulation and consistent with aggrecan gene expression, total GAG production was significantly reduced with continuous 24-h loading, significantly increased with intermittent loading regimes equivalent to 2–4 h loading per day, and not changed for a loading regime of 2× 30 min per day. Regardless of intermittent loading regime and relative to unloaded controls, chondrocytes continued to produce significantly more GAGs for an additional 7 days after 4 days of loading, and continuously loaded tissues recovered GAG production from an initial detriment. These results are consistent with those from bovine chondrocytes loaded in agarose hydrogels, such that intermittent regimes are favorable to continuous loading in terms of ECM production. Finally, Tran et al. (2011) investigated the response of neonatal porcine chondrocytes in a self-assembly model of scaffold-free tissue engineering by which cells were seeded into non-adherent agarose wells and again provided time for matrix elaboration before further studies. When these tissues were subjected to concurrent perfusion and dynamic load, total GAG content and equilibrium compressive modulus, but not collagen content, are significantly increased in comparison with tissues maintained in static culture (Tran et al., 2011). These results, however, appear attributable to perfusion alone since they persist in the absence of dynamic loading.

Overall, the response of non-human, large mammal chondrocytes seeded into scaffolds and subjected to dynamic compression modestly favors dynamic compression over static compression and free-swelling controls. These results are summarized in **Table 2**. The complexity of scaffold-based systems, however, means that the conclusions drawn from more controlled hydrogel-based systems are not fully supported. It is thus fascinating that despite being conducted with mostly young chondrocytes without monolayer preculture (and thus phenotypic modulation), these studies taken together do not definitively show that dynamic compression drives ECM production and biomechanical stiffening, a phenomenon

TABLE 2 | Compilation of studies that investigated the response of non-human, large mammal-derived chondrocytes seeded into biomaterial scaffolds and subjected to uniaxial dynamic compressive loading.

Reference	Study design/ investigation	Cell source (*n*), scaffold, and preculture duration	Loading parameters	Results [PG = proteoglycans, Eeq = equilibrium, Edyn = dynamic, Ey = Young's, H(A) = aggregate]
Davisson et al. (2002)	Static versus dynamic compression	Neonatal primary bovine chondrocytes ($n = 2$) in poly-glycolic acid (PGA) scaffold precultured for 21 days	Frequency: 0.001 and 0.1 Hz Amplitude: 5% Duration: 24 h continuous Max duration: 24 h	RNA: not assessed PG: ↑ dependent on static preload and frequency Collagen: ↑ dependent on static preload and frequency Biomechanics: not assessed
Lee et al. (2003)	Static versus dynamic loading regimes in comparison with explants	Adult expanded canine chondrocytes in type II collagen scaffold precultured for 2, 7, 14, or 30 days	Frequency: 0.1 Hz Amplitude: 3% Duration: 24 h continuous Max duration: 24 h	RNA: not assessed PG: ↑ total protein, ↔ proteoglycan Collagen: not assessed Biomechanics: not assessed
Seidel et al. (2004)	Static versus dynamic compression combined with perfusion	Calf primary bovine chondrocytes in PGA scaffold precultured for 30 days	Frequency: 0.3 Hz Amplitude: 5% Duration: 1 h/day Max duration: 37 h	RNA: not assessed PG: ↔ static and dynamic load Collagen: ↓ static and dynamic load Biomechanics: ↔ Eeq static and dynamic load
Waldman et al. (2004)	Study short-term loading regimes to optimize conditions for longer duration loading	6- to 9-month-old primary bovine chondrocytes on calcium phosphate surface precultured for 28 days	Frequency: 1 Hz Amplitude: 5, 10, or 20% Duration: either 400 or 2,000 cycles every 48 h for 7, 14, or 28 days Max duration: 2.8 h	RNA: not assessed PG: ↑ glycosaminoglycan/DNA at day 28 Collagen: ↑ collagen/DNA at day 28 Biomechanics: ↑ Eeq at day 28
De Croos et al. (2006)	Catabolic activity and mitogen-activated protein kinase mechanotransduction in dynamically stimulated tissues	6- to 9-month-old primary bovine chondrocytes ($n = 2$–3) on calcium phosphate surface precultured for 3 days	Frequency: not reported Amplitude: 1.4% Duration: 30 min continuous Max duration: 30 min	RNA: ↑ COL2, ACAN only at 12 h; ↑ MMP3, MMP13 only at 2 h PG: ↑ all conditions Collagen: ↑ all conditions Biomechanics: not assessed
Stoddart et al. (2006)	Loading duration and intermittent loading regimes	10-month-old primary bovine chondrocytes in alginate-released matrix precultured for 14 days	Frequency: 0.276 Hz Amplitude: 0.5 N Duration: varied 30 min to 8 h for 4 days Max duration: 32 h	RNA: ↑ COL2, ACAN only from 1 to 3 h load, ↔ 4 h of continuous load PG: ↑ 2× 30 min or 2× 2 h loading, ↓ continuous loading Collagen: not assessed Biomechanics: not assessed
Xie et al. (2006)	Mechanism of COL2A1 upregulation with dynamic compression	6-week-old expanded lapine chondrocytes in poly(L-lactide-co-ε-caprolactone) (PLCL) sponge precultured for 2 days	Frequency: 0.1 Hz Amplitude: 10% Duration: 24 h continuous Max duration: 24 h	RNA: ↑ COL2 with activity at proximal promoter PG: not assessed Collagen: not assessed Biomechanics: not assessed
Xie et al. (2007)	Role of loading duration and frequency on gene expression	6-week-old expanded lapine chondrocytes in PLCL sponge precultured for 3 days	Frequency: 0.01, 0.05, 0.1, or 0.5 Hz Amplitude: 10% Duration: continuous or intermittent (6 h on/6 h off or 12 h on/12 h off) for 1, 3, or 6 days Max duration: 72 h	RNA: ↔ COL1, COL2, and ACAN for any loading regime. No comparison to control PG: ↑ at days, 3, and 6 of continuous load, no comparison to control Collagen: ↑ at days 1 and 3 of continuous load, no comparison to control Biomechanics: not assessed
Wang et al. (2008)	Role of dynamic compression on chondrogenic gene expression, not comparison to unloaded or static controls	Neonatal expanded lapine chondrocytes in mixed polyurethane and collagen matrix precultured for 1 day	Frequency: 0.1 Hz Amplitude: 20 or 30% Duration: 4, 8, 12, or 24 h continuous Max duration: 24 h	RNA: ↑ ACAN at 30% compression, no comparison to unloaded control PG: not assessed Collagen: not assessed Biomechanics: not assessed
Wang et al. (2009)	Single loading regime outcomes	Neonatal expanded lapine chondrocytes in a 2% chitosan + 2% gelatin matrix precultured for 3 days	Frequency: 0.1 Hz Amplitude: 40% Duration: 6 h/day for 7 or 21 days Max duration: 126 h	RNA: ↑ COL2, ACAN with 3 h load, ↓ COL2 with 9 h load, ↔ COL1 PG: ↑ 3 weeks loading only Collagen: not assessed Biomechanics: not assessed

(*Continued*)

TABLE 2 | Continued

Reference	Study design/ investigation	Cell source (*n*), scaffold, and preculture duration	Loading parameters	Results [PG = proteoglycans, Eeq = equilibrium, Edyn = dynamic, Ey = Young's, H(A) = aggregate]
El-Ayoubi et al. (2011)	Effect of varied biomaterial combinations, not functional tissue	Adult expanded canine chondrocytes in bioprinted PLLA scaffold precultured for 1 day	Frequency: 1 Hz Amplitude: 10% Duration: 1 h on/7 h off continuous cycling for 14 days Max duration: 56 h	RNA: not assessed PG: not assessed Collagen: not assessed Biomechanics: not assessed
Hoenig et al. (2011)	Response of scaffold-free tissues to variable compressive strain amplitudes	4- to 6-month-old expanded porcine chondrocytes ($n = 5$) in alginate-released matrix and on hydroxyapatite mold without preculture	Frequency: 1 Hz Amplitude: 5, 10, or 20% Duration: 5 min on/30 min off for total 6 h/day for 14 days Max duration: 84 h	RNA: not assessed PG: ↔ quantitative histology Collagen: ↔ quantitative IHC Biomechanics: ↑ stiffness at 5 and 10% load strain ↑ Ey at 20% load strain
Tran et al. (2011)	Response of scaffold-free tissues to dynamic stimulation and perfusion	Neonatal primary porcine chondrocytes ($n = 5$) in self-assembled matrix precultured for 17 days	Frequency: 1 Hz Amplitude: 0.5 N first week, 10 N second week, and 20 N third week Duration: 4 h/day, 5 days/week for 21 days Max duration: 60 h	RNA: not assessed PG: ↑ perfusion and dynamic load Collagen: ↔ any group Biomechanics: ↑ Eeq and Edyn at final time point
Wang et al. (2013)	Varied concentrations of genipin for collagen cross-linking	Primary lapine chondrocytes in a chitosan/collagen cross-linked matrix precultured for 3 days	Frequency: 0.1 Hz Amplitude: 40% Duration: 30 min/day for 14 days Max duration: 7 h	RNA: not assessed PG: ↓ at final time Collagen: not assessed Biomechanics: not assessed

that is accepted as fact in cartilage science. The following sections, summarizing results with chondrocytes and chondroprogenitors of other species, indicate just how different the conclusions are without standardization of input and output parameters.

Rodent Chondrocytes in Hydrogels and Scaffolds

There are a number of studies that have investigated the response of rodent chondrocytes to dynamic mechanical compression in agarose hydrogels or collagen scaffolds. In addition to isolating articular chondrocytes, several groups have investigated the response of costal-derived chondrocytes, presumably due to the difficulty of isolating sufficient cell numbers from articular cartilage. Over a long-duration intermittent dynamic loading regime, murine costal chondrocytes cultured in 2% agarose gels significantly upregulated type II collagen gene and protein expression with a concomitant increase in the aggregate modulus when compared with unloaded controls (Chokalingam et al., 2009). Consistent with results from bovine chondrocyte studies described earlier, tissue-level responses were only evident with increased total duration in dynamic culture. These similarities between species and chondrocyte source offer some model validity to the agarose hydrogel system. Another study that dynamically compressed expanded rat chondrocytes embedded in agarose hydrogels showed that an increase in total GAG content is a delayed response following continuous loading for 24 h, and GAG production persists with continued free-swelling culture (Tsuang et al., 2008).

As large-scale tissue engineering studies are limited by cell number, the majority of studies utilizing rodent chondrocytes focused primarily on cellular level responses to dynamic mechanical stimulation, specifically gene expression and mechanotransduction pathway analysis, instead of tissue level responses of biochemical and biomechanical properties. Bougalt et al. demonstrated that chondrocytes seeded in agarose gels had phosphorylated ERK1/2 and p38 within 15 min following dynamic compressive stimulation, and these proteins were subsequently dephosphorylated within 60 min. Chondrocytes additionally significantly downregulated *COL2A1* promotor activity with compressive load in comparison with unloaded controls (Bougault et al., 2008). These results are consistent with earlier studies that demonstrated ERK1/2 phosphorylation is mediated by the release of FGF2 from the pericellular matrix on short-duration cyclic loading of porcine cartilage explants and chondrocytes seeded in alginate gels (Vincent et al., 2004, 2007). FGF2 is known to upregulate catabolic enzymes including matrix metalloproteinases 1 and 3 (MMP1, MMP3) and anti-catabolic factors including tissue inhibitor of metalloproteinases 1 (TIMP1) in response to cartilage injury through induction of the mitogen-activated protein kinase pathway (Vincent et al., 2002; Chong et al., 2013). Bougault et al. (2012) later demonstrated with microarray analysis that murine chondrocytes subjected to dynamic loading downregulated 85% of the identified mechanosensitive genes with short-duration stimulation, but downstream TGF-β signaling of smad2 was activated under loading conditions. TGF-β signaling is well known to regulate cell proliferation and chondrogenic differentiation through Sox9 transcriptional control of genes coding for extracellular matrix molecules, primarily type II collagen and aggrecan of articular cartilage. Consistent with this mechanism, primary rat chondrocytes in a collagen I gel were compressed for 60 min per day for 7 days and significantly

upregulated *COL2A1* and *ACAN* expression with concomitant decrease in *COL1A1* compared with unloaded controls and longer or shorter daily loading durations (Ando et al., 2009). Addition of exogenous FGF2 or BMP2 independently increased *COL2A1* and *ACAN* mRNA expression; however, each growth factor diminished chondrogenic matrix production when combined with dynamic stimulation, which suggests that proliferation driven by exogenous growth factors can override differentiation induced by mechanical stimulation. Temporally restricted gene expression alone, however, does not necessarily predict tissue-level protein responses to either growth factor or dynamic mechanical stimulation. A combinatorial analysis of the addition of serum to growth media, dynamic compression, or both serum and compression showed that higher concentrations of serum suppress matrix catabolism during tissue formation while dynamic compression increases catabolic activity to potentially rearrange molecules in the resultant tissue (Wu et al., 2013). Unfortunately, experiments testing the overall effect of serum on cell metabolism are unable to distinguish individual contributions of the myriad soluble factors within serum to correlate these results with those testing individual growth factors. Taken together, this set of studies that evaluated the responses of rodent-derived chondrocytes to dynamic stimulation (summarized in **Table 3**) highlight the importance of tissue remodeling during tissue development and growth in the mechanical environment, but the details of this metabolic regulation under dynamic loading remain vague in our current literature.

Healthy and Osteoarthritic Human Chondrocytes in Hydrogels, Scaffolds, and Scaffold-Free Systems

Ultimately, the field of articular cartilage tissue engineering seeks to develop translatable therapies to repair focal traumatic defects in adult human populations, yet few groups have investigated the response of adult human chondrocytes to dynamic compressive loading. Of those studies that utilized human chondrocytes, the majority used expanded cell populations from osteoarthritic tissue, which is readily available as discarded tissue from total joint arthroplasty. In contrast to cells isolated from bovine tissue, primary human chondrocyte yields are relatively poor, whether utilizing autologous or allogeneic chondrocytes, and studies that employ human chondrocytes almost always expand cells *in vitro* to achieve sufficient cell numbers for experimentation. A

TABLE 3 | Compilation of studies that investigated the response of rodent-derived chondrocytes subjected to uniaxial dynamic compressive loading.

Reference	Study design/investigation	Cell source (*n*), scaffold, and preculture duration	Loading parameters	Results [PG = proteoglycans, Eeq = equilibrium, Edyn = dynamic, Ey = Young's, H(A) = aggregate]
Bougault et al. (2008)	Mechanotransduction through ERK and p38 pathways	Embryonic primary murine costal chondrocytes in 2% agarose hydrogel precultured for 7 days	Frequency: 2 s on/1 s off Amplitude: 20 kPa Duration: 30 min continuous Max duration: 30 min	RNA: not assessed PG: not assessed Collagen: not assessed Biomechanics: not assessed
Tsuang et al. (2008)	Effect of dynamic compression on chondrocyte metabolism	Expanded rat chondrocytes in 3% agarose hydrogel without preculture	Frequency: 0.5, 1, 2, or 3 Hz Amplitude: 5, 10, or 15% Duration: 24 h continuous Max duration: 24 h	RNA: not assessed PG: ↑ 10–15% strain and 1 Hz Collagen: not assessed Biomechanics: not assessed
Chokalingam et al. (2009)	Effect of dynamic compression on construct stiffness and collagen expression in col2 reporter mice	Neonatal expanded murine costal chondrocytes ($n = 6$) in 2% agarose hydrogel precultured for 2 days	Frequency: 1 Hz Amplitude: 10% Duration: 3× 1 h on/1 h off, 5 days/week for 7, 14, 21, or 28 days Max duration: 60 h	RNA: ↑ COL2 for all time points with max at day 14 PG: not assessed Collagen: ↑ type II collagen content at days 21 and 28 Biomechanics: ↑ H(A) at day 28 only
Ando et al. (2009)	Effect of mechanical loading and growth factors	5-week-old primary rat chondrocytes in type I collagen scaffold without preculture	Frequency: 0.33 Hz Amplitude: 5% Duration: 10, 60, or 120 min/day for 7 days Max duration: 14 h	RNA: ↑ ACAN, COL2 only 60 min/day loading, ↓ COL1 all groups PG: not assessed Collagen: not assessed Biomechanics: not assessed
Bougault et al. (2012)	Early molecular events triggered by dynamic loading including mitogen-activated protein kinase (MAPK) and TGF-β signaling pathways	Embroyonic primary murine costal chondrocytes in 2% agarose hydrogel precultured for 6 days	Frequency: 0.5 Hz Amplitude: 20–40 kPa Duration: continuous for 5, 15, or 30 days Max duration: 720 h	RNA: not assessed for chondro genes: investigated the MAPK, SMAD signaling pathways PG: not assessed Collagen: not assessed Biomechanics: not assessed
Wu et al. (2013)	Effect of serum and dynamic load on spatiotemporal pericellular matrix distribution	Neonatal primary murine costal chondrocytes ($n = 50$ pooled) in 2% agarose hydrogel without preculture	Frequency: 1 Hz Amplitude: 10% Duration: 5 h/day, 7 days/week for 1, 7, 9, 15, or 21 days Max duration: 105 h	RNA: ↑ COL2A1 with load in no serum, ↓ ACAN with load regardless serum, ↔ COL6A1, ↑ COMP with load in serum-free and 10% FBS, ↑ MMP3 with load, ↓ MMP13 with load and no serum or 10% FBS. PG: ↓ all load Collagen: ↓ type II collagen width of distribution from cell with loading Biomechanics: not assessed

single study to utilize expanded chondrocytes derived exclusively from healthy human donors found high intra-donor variability with regard to GAG production in dynamic compression, such that the cells that showed the greatest response to loading were those that produced abundant GAGs before application of load (Démarteau et al., 2003). This study found no difference in gene expression with application of load. The remainder of studies utilized chondrocytes derived from osteoarthritic tissue. When gene expression analysis was investigated temporally by collecting RNA at defined time points following the completion of a loading regime, Jeon et al. (2012) reported a significant increase in *ACAN*, *COL2A1*, *COL1A1*, *COL10A1*, and *PRG4* only 2 h after a single 1 h loading period of osteoarthritic chondrocytes seeded in alginate hydrogels, and the response was greater for superficial zone-derived cells than for those derived from the middle zone of diseased tissue. This study also showed that *ACAN* and *PRG4* expression was significantly increased in both superficial and middle zone chondrocytes at 50% strain relative to 5 and 15% strain and after 3 h of loading relative to 1 or 12 h of loading at 15% strain. Relative to unloaded controls, superficial zone-derived chondrocytes, but not middle zone-derived cells, significantly increased GAG content, equilibrium modulus, storage/loss moduli, and type II collagen and aggrecan protein expression when dynamically compressed under the optimized loading regime of 3 h/day at 50% strain and 1 Hz for 2 weeks (Jeon et al., 2012). A follow-up study by the same group showed that both superficial and middle zone-derived chondrocytes that were precultured in hydrogels for 2 weeks before the onset of dynamic loading responded more sensitively to loading than those without preculture and had increased gene expression (*COL2A1*, *COL1A1*, *ACAN*, *FN1*, *IL1B*, *IL4*, and *MMP2*) and matrix accumulation (type II and VI collagens, fibronectin, and laminin) when compared with unloaded controls (Jeon et al., 2013). Another study that employed the same commercial bioreactor as that used by Jeon et al. but with an added perfusion system showed modest effects of culturing human chondrocytes under perfusion with non-significant increases in *COL2A1*, *COL1A1*, *COL6A*, and *PRG4* gene expression and a decrease in GAG/DNA relative to free-swelling controls (Grogan et al., 2012). Adding a dynamic compression regime of 20% strain, 0.5 Hz, and 1 h/day to perfusion had no further effect on gene expression or ECM production. These results are similar to those presented above for porcine chondrocytes cultured under perfusion and dynamic compression in the bioreactor system, such that increases in GAG content and equilibrium modulus were attributable to perfusion in the absence of compressive loading (Tran et al., 2011). Both of these studies, however, did not investigate alternative loading regimes or optimize the time frame after loading in which to investigate gene expression.

In accordance with other mammalian studies, increased total dynamic compression duration of human osteoarthritic chondrocytes in type I collagen hydrogels significantly increased ECM production (type II collagen via quantitative IHC), gene expression (*COL2A1*, *ACAN*, *MMP13*, and *COL1A1*), and stiffness when compared with unloaded controls after 28 days in culture (Nebelung et al., 2012a); these results from 28 days dynamic stimulation were not significant after just 14 days in culture (Nebelung et al., 2012b). Similarly, dynamic compression of human osteoarthritic chondrocytes in a type I collagen gel for 7 days resulted in no significant differences in *SOX9*, *COL2A1*, *ACAN*, or various integrin genes, nor a change in GAG/DNA, relative to free-swelling controls, but they did find increased intracellular Sox9 transcription factor and decreased collagen degradation products with loading potentially favoring early activation of anabolism for eventual matrix production (Diao et al., 2017). A more thorough investigation of the metabolome of human osteoarthritic chondrocytes seeded in agarose gels identified hundreds of target metabolites that were responsive to dynamic compression (Zignego et al., 2015). Each metabolome was patient- and age-specific, but consistently showed an increase in metabolites involved in central energy production, such as glycolysis and TCA cycle, and chondroitin sulfate degradation mechanisms. To date relatively few studies have investigated the response of human chondrocytes to dynamic compression (summarized in **Table 4**), and these studies have almost exclusively utilized chondrocytes derived from diseased tissue. To work toward production of tissue-engineered human articular cartilage for repair of focal defects in otherwise healthy tissue,

TABLE 4 | Compilation of studies that investigated the response of human-derived chondrocytes subjected to uniaxial dynamic compressive loading.

Reference	Study design/ investigation	Cell source (*n*), scaffold, and preculture duration	Loading parameters	Results [PG = proteoglycans, Eeq = equilibrium, Edyn = dynamic, Ey = Young's, and H(A) = aggregate]
Démarteau et al. (2003)	Effect of culture duration and donor variability	22- to 47-year-old expanded human chondrocytes from healthy donors (n = 4) in PEGT/PBT (55:45) scaffold precultured for 3 or 14 days	Frequency: 0.1 Hz Amplitude: 5% Duration: 2 h on/10 h off for 6 total cycles Max duration: 12 h	RNA: ↔ COL2, COL1, ACAN, VCAN, and SOX9 PG: highly variable b/n donors, trended ↓ Collagen: not assessed Biomechanics: not assessed
Nebelung et al. (2012a)	Effect of dynamic compression on gene expression and mechanical stiffness	67-year-old (mean) primary human chondrocytes from osteoarthritic donors (n = 12) in type I collagen hydrogel precultured for 0.5 days	Frequency: 0.3 Hz Amplitude: 10% Duration: 14 days continuous Max duration: 336 h	RNA: ↑ ratio COL2:COL1, ↔ COL2, COL1, ACAN, and MMP13 PG: ↔ Collagen: ↔ Biomechanics: ↓ Eeq relative to baseline, no diff with loading

(*Continued*)

TABLE 4 | Continued

Reference	Study design/ investigation	Cell source (*n*), scaffold, and preculture duration	Loading parameters	Results [PG = proteoglycans, Eeq = equilibrium, Edyn = dynamic, Ey = Young's, and H(A) = aggregate]
Nebelung et al. (2012b)	Effect of long-term continuous dynamic compression	67-year-old (mean) primary human chondrocytes from osteoarthritic donors ($n = 8$) in type I collagen hydrogel precultured for 0.5 days	Frequency: 0.3 Hz Amplitude: 10% Duration: 28 days continuous Max duration: 672 h	RNA: ↑ COL2, MMP13, and COL1 after 28 days. ↔ for ACAN PG: not quantified Collagen: ↑ type II on IHC Biomechanics: not significant ↑ Eeq
Grogan et al. (2012)	Combinatorial effect of perfusion and dynamic compression	14- to 55-year-old expanded human chondrocytes from healthy or osteoarthritic donors ($n = 9$) in 2% alginate hydrogel precultured for 1 or 2 days	Frequency: 0.5 Hz Amplitude: 20% Duration: 1 h/day for 7 or 14 days Max duration: 14 h	RNA: ↔ COL2, COL6, COL10, ACAN, PRG4, COL1, MMP3, iNOS, and CCL20 for perfusion or perfusion + load PG: ↓ in glycosaminoglycan (GAG)/DNA for perfusion and load Collagen: not quantified Biomechanics: ↔ stiffness
Jeon et al. (2012)	Zonal chondrocyte differences in response to loading, characterized timeline of gene changes	49- to 78-year-old expanded human chondrocytes from osteoarthritic donors ($n = 4$) in 2% alginate precultured for 14 days	Frequency: 1 Hz Amplitude: varied Duration: 3 h/day for 14 days Max duration: 42 h	RNA: ↑ ACAN, COL2, COL1, COL10, and PRG4 for superficial chondrocytes 2 h post-compression. ↑ ACAN, PRG4, and COL1 at 3 h PG: ↑ retained and total Collagen: ↑ type II *via* quant IHC Biomechanics: ↑ Eeq, E(storage), E(loss)
Jeon et al. (2013)	Differences between zonal chondrocytes in response to loading and preculture duration	Primary or expanded human chondrocytes from osteoarthritic donors in 2% alginate hydrogel precultured for 1 or 14 days	Frequency: 1 Hz Amplitude: 50% Duration: 3 h/day for 14 days Max duration: 42 h	RNA: ↑ COL2, COL1, ACAN, FN1, and HSP2 after 14 days of preculture and 14 days loading. Investigated suite of inflammatory genes PG: not assessed Collagen: ↑ in type II and VI via quantitative IHC Biomechanics: not assessed
Zignego et al. (2015)	Changes in chondrocyte metabolomic profile with loading	50- to 84-year-old expanded human chondrocytes from osteoarthritic donors ($n = 5$) in 4.5% agarose hydrogel without preculture	Frequency: 1.1 Hz Amplitude: 5% Duration: 15 or 30 min continuous Max duration: 30 min	RNA: metabalome analysis only: glycolysis and central energy metabolism ↑ with load PG: metabalome analysis only: chondroitin sulfate degradation pathway ↑ with load Collagen: not assessed Biomechanics: not assessed
Diao et al. (2017)	Regulation of catabolic genes with loading	60- to 80-year-old expanded human chondrocytes from osteoarthritic donors ($n = 8$) in type I collagen microcapsules precultured for 4 days	Frequency: 1 Hz Amplitude: 10% Duration: 3 h/day for 1 or 7 days Max duration: 21 h	RNA: ↔ SOX9, COL2, ACAN, integrins, MMP14, ↓ MMP1, 2, and 13 PG: ↔ GAG/DNA Collagen: not assessed Biomechanics: not assessed

standardization of cell source and compression protocols will be crucial to derive meaningful results for translation of laboratory studies to clinical application.

The Next Dimension: Addition of Shear to Dynamic Loading Regimes

The overall goal of stimulating chondrocytes *in vitro* for tissue regeneration is to provide the cells with mechanical cues representative of those in the native joint environment, and dynamic shear loading is a well-defined component of the native loading regime during articulation. Due to complexity of bioreactor design needed to integrate dynamic compression and shear loading, few groups have investigated the additive effect of dynamic shear to a compressive loading regime. An initial study by Waldman et al. (2003) showed that relative to scaffold-free tissues in static culture, dynamic 5% compressive strain of bovine chondrocytes cultured on a ceramic surface slightly increased proteoglycan and collagen content and equilibrium modulus, and the addition of 2% shear strain to the compressive regime significantly enhanced these tissue-level outcomes. A follow-up study in the same tissue and bioreactor systems reported that tissues subjected to a loading regime of 5% compressive and 5% shear strains for one week produced greater amounts of collagen and proteoglycans relative to both unloaded controls and loading regimes of 2 and 2%, 2 and 5%, and 5 and 2% compressive and shear strains, respectively (Waldman et al., 2007). When subjected to 4 weeks of dynamic stimulation at 5% compressive and 5% shear strains, tissues accumulated 46% more collagen and 54% more proteoglycans compared with unstimulated controls. The increase in ECM accumulation was complemented by a 3-fold increase in compressive modulus and 1.75-fold increase in shear modulus of the stimulated tissues compared with those cultured in the absence of multiaxial loading. While this group previously reported results for tissues subjected to a uniaxial compressive regime, they did not include direct comparison to this group in the multiaxial studies, which limits the ability to directly compare outcomes.

Another group that pioneered use of a multiaxial bioreactor initially compared dynamic compression, dynamic shear, and

combinations of compression and uniaxial or multiaxial shear loading regimes for bovine chondrocytes seeded in polyurethane scaffolds (Grad et al., 2006). Compared with free-swelling controls, dynamic compression or uniaxial oscillating rotation of the scaffold (shear) had no effect on the mRNA expression levels of *PRG4*, *ACAN*, *COMP*, *COL1A1*, *COL2A1*, *MMP3*, *MMP13*, *TIMP1*, or *TIMP3*. The combination of dynamic compression with either unidirectional or multidirectional shear-inducing oscillation, however, resulted in a significant upregulation of several genes, including *PRG4*, *ACAN*, *COMP*, *COL2A1*, *TIMP3*, and a downregulation of *MMP13*, which again favors anabolism. At the protein level, combined compression and shear led to significantly increased levels of lubricin, COMP, and hyaluronic acid released into the culture media relative to unloaded controls, isolated compression, or isolated shear. These phenotypic changes at the gene and protein level correlate with upregulation of the articular chondrocyte phenotype. Over long-duration loading in the same system, lower oxygen levels further improved the phenotype with increased GAG/DNA content though not to the significance achieved from the effect of lowered oxygen on unloaded controls (Wernike et al., 2007). At the gene level, loading in low oxygen conditions significantly reduced *COL1A1* gene expression to further favor the articular chondrocyte phenotype. Consistent with results from bovine cells cultured in agarose hydrogels under uniaxial compression, longer duration and delayed application of combined dynamic compressive and shear loading of bovine cells in polyurethane scaffolds produced tissues of significantly greater GAG content and favored upregulation of articular chondrocyte genes *COL2*, *ACAN*, *COMP*, and *PRG4* (Wang et al., 2013). These cells, however, still highly expressed type I collagen at the gene and protein levels in a polyurethane scaffold regardless of loading regime, and primary chondrocytes responded more favorably than expanded chondrocytes to dynamic loading with respect to GAG production and chondrogenic gene expression. Toward the goal of further modeling the *in situ* cartilage environment for cartilage regeneration *in vitro*, Hilz et al. (2013) added an electromagnetic field as a variable to the dynamic compression and shear loading of bovine chondrocytes in polyurethane scaffolds to mimic a fixed charge density gradient in native tissue. They found that stimulation with load and a 3 mT electromagnetic field produced significantly greater GAG/DNA compared with static control, mechanical stimulus only, and 3 mT field only (Hilz et al., 2013). Continued experimentation utilizing the bioreactor, tissue engineering scaffold system, and cells initially described by Grad et al. has allowed this group to define increasingly specific parameters that favor dynamic loading regimes of combined compressive and shear loading. When a foundational variable was changed by utilizing human-derived cloned articular cartilage progenitor cells instead of primary bovine chondrocytes, this group found a consistent increase in GAG content for loaded tissues relative to unloaded controls, although they did not find significant differences in gene expression (Neumann et al., 2015).

Few other groups have integrated shear into a multiaxial dynamic compressive loading regime. Bian et al. (2010) reported that the addition of shear loading to dynamic compression for tissues derived from expanded canine chondrocytes seeded in agarose hydrogels not only significantly decreased the coefficient of friction but also significantly increased the Young's compressive modulus relative to unloaded controls and all other dynamic compression regimes. These results, however, only became significant at 56 days in culture. Another study with substantially shorter preculture and loading durations, found no difference in the amount of GAGs produced by tissues under various dynamic shear, compression, and perfusion regimes (Pourmohammadali et al., 2013). Finally, a study that utilized human fetal epiphyseal chondrocytes cultured at varied cell density in either PGA scaffolds or PGA-alginate scaffold-hydrogels sought to characterize differences between preculture in a shaking flask or a perfusion bioreactor before subsequent loading in a dynamic shear and compressive bioreactor (Shahin and Doran, 2011). They found that preculture in a perfusion bioreactor followed by short-duration dynamic stimulation produced the greatest quantity of GAGs and total collagen; however, they did not analyze the individual effects of compression or shear, and they tested many confounding variables in each experiment.

Taken together, studies that added shear to a dynamic compressive loading regime suggest that shear has a significant effect on chondrocyte gene expression, tissue extracellular matrix metabolism, and tissue mechanical properties (**Table 5**). This conclusion is convincingly shown in studies that introduced shear as a single variable for comparison with dynamic compressive loading regimes.

TABLE 5 | Compilation of studies that investigated the response of chondrocytes subjected to multiaxial dynamic compressive loading regimes, including shear.

Reference	Study design/ investigation	Cell source (*n*), scaffold, and preculture duration	Loading parameters	Results [PG = proteoglycans, Eeq = equilibrium, Edyn = dynamic, Ey = Young's, and H(A) = aggregate]
Waldman et al. (2003)	Uniaxial compression versus shear	Adult bovine carpal-metacarpal chondrocytes on calcium phosphate ceramic surface precultured for 28 days	Frequency: 1 Hz Amplitude: 5% compress or 2% shear Duration: 400 cycles (6 min)/48 h for 28 days Max duration: 1.4 h	RNA: not assessed PG: ↑ only shear load Collagen: trended ↑ for only shear load Biomechanics: ↑ Eeq for both compressive and shear load

(*Continued*)

TABLE 5 | Continued

Reference	Study design/ investigation	Cell source (*n*), scaffold, and preculture duration	Loading parameters	Results [PG = proteoglycans, Eeq = equilibrium, Edyn = dynamic, Ey = Young's, and H(A) = aggregate]
Grad et al. (2006)	Effect of unidirectional and multidirectional loading	3- to 4-month-old primary bovine chondrocytes in polyurethane scaffold precultured for 5 days	Frequency: 1 Hz Amplitude: 10% compress ±25° oscillation Duration: 2× 1 h/day for 5 days Max duration: 10 h	RNA: ↔ for dynamic compression only, ↑ in PRG4, ACAN, COMP, COL2, and TIMP3 shear/multiaxial relative to dynamic compression PG: ELISAs: ↔ COMP, PRG4, or HA for compression, ↑ COMP, PRG4, HA for multiaxial relative to dynamic compression Collagen: not assessed Biomechanics: not assessed
Waldman et al. (2007)	Effect of multiaxial loading	6- to 9-month-old primary bovine chondrocytes (*n* = 2–3 pooled) on calcium phosphate ceramic surface precultured for 28 days	Frequency: 0.5 Hz Amplitude: 2 or 5% compress and shear Duration: 400 cycles (6 min)/48 h for 6 days Max duration: 18 min	RNA: not assessed PG: ↑ only for 5% compression + 5% shear Collagen: ↑ only for 5% compression + 5% shear Biomechanics: ↑ in Eeq and G(shear), strain stiffening for compression + shear load
Wernike et al. (2007)	Additive effect of low oxygen environment to multiaxial loading	4- to 8-month-old primary bovine chondrocytes in polyurethane scaffold precultured for 6 days	Frequency: 0.5 Hz Amplitude: 10% compress ±25° oscillation Duration: 1 h/day, 6 days/ week for 28 days Max duration: 28 h	RNA: ↓ COL1 in load and low oxygen at days 8 and 34, ↔ COL2, ACAN PG: ↓ with loading, but not compared with control Collagen: not quantified Biomechanics: not assessed
Bian et al. (2010)	Investigated immediate versus delayed loading and addition of shear	2- to 4-year-old expanded canine chondrocytes in 2% agarose hydrogel precultured for 0, 14, or 28 days	Frequency: 1 Hz Amplitude: 10% compress ±180° oscillation Duration: 3 h/day, 5 days/ week for 42 days Max duration: 90 h	RNA: not assessed PG: ↔ any loading regime at any time point Collagen: ↔ any loading regime at any time Biomechanics: ↑ Ey continuous load at days 28 and 56, delayed load at day 56. ↑ Edyn all loading regimes at days 56, reduced μ (friction coefficient) for shear load
Shahin and Doran (2011)	Effect of dynamic loading after preculture in perfusion or shaking flasks with varied cell concentration and scaffold	16- to 20-week-old expanded human fetal epiphyseal chondrocytes (*n* = 3 pooled) in poly-glycolic acid (PGA) or PGA + 1.2% alginate scaffold precultured for 3 or 14 days	Frequency: 0.05 Hz Amplitude: 8.7% compress + 3 rpm revolution strain Duration: 10 min/day for 17 days Max duration: 2.8 h	RNA: not assessed PG: ↑ for all scaffold and cell density variations with loading and shaking flask preculture. Highest content with long preculture in perfusion Collagen: ↑ for all scaffold and cell density variations with loading. Highest content with long preculture in perfusion Biomechanics: not assessed
Wang et al. (2013)	Effect of cell expansion and passage on response to loading	3- to 4-month-old primary or expanded bovine chondrocytes (*n* = 3) in polyurethane scaffold precultured for 1 or 14 days	Frequency: 1 Hz Amplitude: 10% compress ±25° oscillation Duration: 10 min/day for 17 days Max duration: 2.8 h	RNA: ↑ COL2, COMP, ACAN, and PRG4 for continuous and delayed load and p0 and p3 chondrocytes PG: ↑ continuous and delayed loading Collagen: ↑ type II, ↔ type I on IHC Biomechanics: not assessed
Pourmohammadali et al. (2013)	Effect of perfusion and multiaxial loading	Primary bovine chondrocytes in 3% agarose hydrogel precultured for 7 days	Frequency: 8–14 mm/s Amplitude: 18% + shear flow Duration: 30 min/day for 21 days Max duration: 10.5 h	RNA: not assessed PG: ↔ perfusion ± compression and shear Collagen: not assessed Biomechanics: not assessed
Hilz et al. (2013)	Effect of low-frequency, low-energy electromagnetic fields combined with multiaxial loading	2- to 3-month-old primary bovine chondrocytes in polyurethane scaffold precultured for 7 days	Frequency: 1 Hz Amplitude: 10% compress ±25° oscillation Duration: 2× 1 h/day every other day for 21 days Max duration: 16 h	RNA: ↑ COL2/COL1 ratio, PRG4, ↔ MMP3, MMP13, COMP, and SOX9 PG: ↑ with load Collagen: ↑ type II, ↓ type I on Remmele score Biomechanics: not assessed
Neumann et al. (2015)	Response of chondroprogenitors to dynamic loading and/or BMP2	30- to 75-year-old expanded clonal human articular cartilage progenitor cells (*n* = 4) in polyurethane scaffold precultured for 3 days	Frequency: 1 Hz Amplitude: 10% compress ±25° oscillation Duration: 1 h/day, 6 days/ week for 7 or 28 days Max duration: 24 h	RNA: ↑ COL1 (day 7), ACAN (days 7 and 28),↑ COLX (day 28 with BMP2); COL2 undetectable PG: ↑ with load, ↓ with addition of BMP2 Collagen: not assessed Biomechanics: not assessed

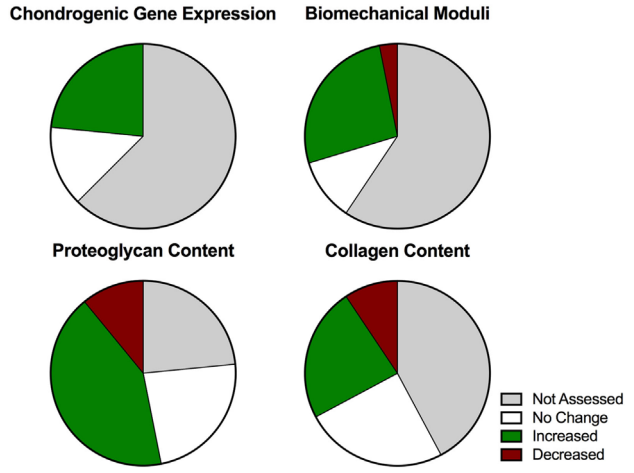

FIGURE 2 | Graphic representation of compiled results ($n = 63$) from studies investigating dynamic compressive stimulation of chondrocytes to summarize the overall effect with respect to standard outcome measures.

CONCLUSION

Before starting this review, the authors were convinced that dynamic compressive loading of chondrocytes is an important factor to include when creating articular cartilage-like tissue *in vitro*. After reviewing the literature, it has become clear that there exists little standardization in the work done in this area to date, such that the variability of results obtained weakens the basis for our conviction. When plotted by percentages of positive, negative, or no effect data from this collective set of studies, we can clearly see that dynamic loading had a positive effect on the expression of chondrogenic genes in a majority of studies in which they were examined (**Figure 2**). This is also true for biomechanical moduli and proteoglycan content; although some negative effects were noted for these parameters in some studies, a greater proportion of studies reported positive effects than the sum of "decreased" plus "no change" results. However, this was not true for effects of dynamic compression on collagen content. This is a very important distinction that may be highly relevant for the creation of functional articular cartilage implants with the extracellular matrix and stiffness necessary to fulfill its biomechanical role in the joint. Finding loading parameters that increase collagen production would seem to be a priority going forward. To date, agarose represents the most standardized substrate in which to seed cartilaginous cells for loading studies. Upon review, we noted that the following loading conditions favor the development of an articular cartilage-like tissue phenotype in this type of hydrogel: dynamic compressive loading at physiologic frequency (1 Hz); delayed loading after a preculture period to allow initial extracellular matrix elaboration; intermittent loading regimes with substantial daily rest periods; and total loading duration greater than 50 h.

Further, adequate characterization of cells with respect to phenotype based on donor age, primary versus expanded populations, and site of derivation (superficial versus deep, load bearing versus non-load bearing) is necessary to fully appreciate the response of cells to a complex loading regime. Primary cells retain their chondrocytic phenotype. However, if expansion of cells is needed, techniques that effectively limit the dedifferentiation seen in monolayer will need to be further developed. Expansion at physioxia, or with certain growth factors have been shown to influence phenotypic drift, but no such techniques were used in the studies we analyzed (Jakob et al., 2001; Mandl et al., 2004; Schrobback et al., 2012). While focus on substrate, cells, and loading environment is necessary to define tissue engineering within a dynamic loading environment, many studies failed to appreciate or report the added effects of soluble factors, which may independently influence cellular metabolism and tissue development. All of these considerations highlight the complexity of tissue engineering within a bioreactor, and all elements must be given adequate consideration to draw meaningful conclusions.

Those conclusions notwithstanding, it is clear from our analysis that it is time for standardized protocols and analyses to be introduced. At the gene level, Jeon et al. (2012, 2013) showed that gene expression is dependent on the time of RNA extraction relative to loading; thus, studies that report gene expression without standardization or consideration of RNA extraction timing, potentially report results out of context. As with every story told regarding tissues with extensive extracellular matrices, it is vital that protein-level analysis accompany gene analysis, something not always considered appropriately in chondrocyte dynamic loading studies. Gene expression does not necessarily correlate to structural proteins being secreted and incorporated into the extracellular matrix of developing tissues. Just as gene expression helps to define cellular phenotype, so too is collagen protein quantification and differential characterization of collagen type by quantitative methods such as ELISA necessary to define the tissue phenotype of cartilaginous tissues. Furthermore, paying close attention to the differences in bioreactor design, loading regime, biomaterial, cell source, and culture conditions between studies is vital when drawing conclusions about their relative significance. While this review exclusively includes dynamic loading effects on chondrocytes, the conclusions drawn apply equally to studies with other cell types, namely stem/progenitor cells, also used for cartilage tissue engineering. At the very least, the field would greatly benefit from transparency in reporting sample size, including biological versus technical replicates, which were neglected in greater than half of studies evaluated. The galvanizing effects of adding shear to dynamic compression protocols provides a very important lesson regarding the "deconstruction of complexity" that is present in *in vitro* loading systems: care must be taken when drawing conclusions from the results obtained in such simplified conditions in the laboratory.

This review focused exclusively on *in vitro* methods to generate articular cartilage utilizing chondrocytes cultured in a dynamic mechanical environment. These various methods have been developed with the goal to generate articular cartilage for

the repair of focal tissue defects following traumatic injury. For successful translation of these methods to clinical application consideration must also be given to scalability, reproducibility, and cost. Presently, there are no FDA approved biologic implants grown in a dynamic compressive bioreactor; the first therapeutic would require substantial investment for comparison with either microfracture or autologous chondrocyte implantation for repair of focal articular cartilage defects. Furthermore, the few studies utilizing human-derived cells in dynamic compressive bioreactors did not reach significance for most outcome parameters measured, highlighting wide variation between donors. It must also be noted that these studies primarily utilized chondrocytes derived from osteoarthritic tissue, which is not representative of either the target tissue or the intended population for focal cartilage repair. Moving forward, we must learn from these studies not only to work toward standardization of bioreactors but also to pay attention to translation for clinical application with use of human cells from non-diseased tissue.

ETHICS STATEMENT

No human or animal subjects were used in this study.

AUTHOR CONTRIBUTIONS

DA and BJ conceived of the review topic and participated in manuscript writing, editing, and preparation for publication. DA reviewed the primary literature and cataloged the results.

ACKNOWLEDGMENTS

The authors would like to thank Dr. Brandon Markway (OHSU, Portland, OR, USA) for his critical review of the manuscript.

FUNDING

This work was supported by funding from NIH/NIAMS (1R21AR064431) and the OHSU Foundation.

REFERENCES

Ando, K., Imai, S., Isoya, E., Kubo, M., Mimura, T., Shioji, S., et al. (2009). Effect of dynamic compressive loading and its combination with a growth factor on the chondrocytic phenotype of 3-dimensional scaffold-embedded chondrocytes. *Acta Orthop.* 80, 724–733. doi:10.3109/17453670903413111

Bian, L., Fong, J. V., Lima, E. G., Stoker, A. M., Ateshian, G. A., Cook, J. L., et al. (2010). Dynamic mechanical loading enhances functional properties of tissue-engineered cartilage using mature canine chondrocytes. *Tissue Eng. Part A* 16, 1781–1790. doi:10.1089/ten.tea.2009.0482

Bougault, C., Aubert-Foucher, E., Paumier, A., Perrier-Groult, E., Huot, L., Hot, D., et al. (2012). Dynamic compression of chondrocyte-agarose constructs reveals new candidate mechanosensitive genes. *PLoS ONE* 7:e36964. doi:10.1371/journal.pone.0036964

Bougault, C., Paumier, A., Aubert-Foucher, E., and Mallein-Gerin, F. (2008). Molecular analysis of chondrocytes cultured in agarose in response to dynamic compression. *BMC Biotechnol.* 8:71. doi:10.1186/1472-6750-8-71

Buschmann, M. D., Gluzband, Y. A., Grodzinsky, A. J., and Hunziker, E. B. (1995). Mechanical compression modulates matrix biosynthesis in chondrocyte/agarose culture. *J. Cell. Sci.* 108, 1497–1508.

Chokalingam, K., Hunter, S., Gooch, C., Frede, C., Florer, J., Wenstrup, R., et al. (2009). Three-dimensional in vitro effects of compression and time in culture on aggregate modulus and on gene expression and protein content of collagen type II in murine chondrocytes. *Tissue Eng. Part A* 15, 2807–2816. doi:10.1089/ten.TEA.2008.0560

Chong, K.-W., Chanalaris, A., Burleigh, A., Jin, H., Watt, F. E., Saklatvala, J., et al. (2013). Fibroblast growth factor 2 drives changes in gene expression following injury to murine cartilage in vitro and in vivo. *Arthritis Rheum.* 65, 2346–2355. doi:10.1002/art.38039

Chowdhury, T. T., Bader, D. L., Shelton, J. C., and Lee, D. A. (2003). Temporal regulation of chondrocyte metabolism in agarose constructs subjected to dynamic compression. *Arch. Biochem. Biophys.* 417, 105–111. doi:10.1016/S0003-9861(03)00340-0

Darling, E. M., and Athanasiou, K. A. (2005). Rapid phenotypic changes in passaged articular chondrocyte subpopulations. *J. Orthop. Res.* 23, 425–432. doi:10.1016/j.orthres.2004.08.008

Davisson, T., Kunig, S., Chen, A., Sah, R., and Ratcliffe, A. (2002). Static and dynamic compression modulate matrix metabolism in tissue engineered cartilage. *J. Orthop. Res.* 20, 842–848. doi:10.1016/S0736-0266(01)00160-7

De Croos, J. N. A., Dhaliwal, S. S., Grynpas, M. D., Pilliar, R. M., and Kandel, R. A. (2006). Cyclic compressive mechanical stimulation induces sequential catabolic and anabolic gene changes in chondrocytes resulting in increased extracellular matrix accumulation. *Matrix Biol.* 25, 323–331. doi:10.1016/j.matbio.2006.03.005

Démarteau, O., Wendt, D., Braccini, A., Jakob, M., Schäfer, D., Heberer, M., et al. (2003). Dynamic compression of cartilage constructs engineered from expanded human articular chondrocytes. *Biochem. Biophys. Res. Commun.* 310, 580–588. doi:10.1016/j.bbrc.2003.09.099

Diao, H. J., Fung, H. S., Yeung, P., Lam, K. L., Yan, C. H., and Chan, B. P. (2017). Dynamic cyclic compression modulates the chondrogenic phenotype in human chondrocytes from late stage osteoarthritis. *Biochem. Biophys. Res. Commun.* 486, 14–21. doi:10.1016/j.bbrc.2017.02.073

El-Ayoubi, R., DeGrandpre, C., DiRaddo, R., Yousefi, A. M., and Lavigne, P. (2011). Design and dynamic culture of 3D-scaffolds for cartilage tissue engineering. *J. Biomater. Appl.* 25, 429–444. doi:10.1177/0885328209355332

Farnsworth, N. L., Antunez, L. R., and Bryant, S. J. (2013). Dynamic compressive loading differentially regulates chondrocyte anabolic and catabolic activity with age. *Biotechnol. Bioeng.* 110, 2046–2057. doi:10.1002/bit.24860

Gannon, A. R., Nagel, T., Bell, A. P., Avery, N. C., and Kelly, D. J. (2015). Postnatal changes to the mechanical properties of articular cartilage are driven by the evolution of its collagen network. *Eur. Cell Mater.* 29, 105–123. doi:10.22203/eCM.v029a09

Goessler, U. R., Bieback, K., Bugert, P., Heller, T., Sadick, H., Hörmann, K., et al. (2006a). In vitro analysis of integrin expression during chondrogenic differentiation of mesenchymal stem cells and chondrocytes upon dedifferentiation in cell culture. *Int. J. Mol. Med.* 17, 301–307. doi:10.3892/ijmm.17.2.301

Goessler, U. R., Bugert, P., Bieback, K., Sadick, H., Baisch, A., Hörmann, K., et al. (2006b). In vitro analysis of differential expression of collagens, integrins, and growth factors in cultured human chondrocytes. *Otolaryngol. Head Neck Surg.* 134, 510–515. doi:10.1016/j.otohns.2005.10.026

Goessler, U. R., Bieback, K., Bugert, P., Naim, R., Schafer, C., Sadick, H., et al. (2005). Human chondrocytes differentially express matrix modulators during in vitro expansion for tissue engineering. *Int. J. Mol. Med.* 16, 509–515. doi:10.3892/ijmm.16.4.509

Goessler, U. R., Bugert, P., Bieback, K., Baisch, A., Sadick, H., Verse, T., et al. (2004). Expression of collagen and fiber-associated proteins in human septal cartilage during in vitro dedifferentiation. *Int. J. Mol. Med.* 14, 1015–1022. doi:10.3892/ijmm.14.6.1015

Grad, S., Gogolewski, S., Alini, M., and Wimmer, M. A. (2006). Effects of simple and complex motion patterns on gene expression of chondrocytes seeded in 3D scaffolds. *Tissue Eng. Part A* 12, 3171–3179. doi:10.1089/ten.2006.12.3171

Grodzinsky, A. J., Levenston, M. E., Jin, M., and Frank, E. H. (2000). Cartilage tissue remodeling in response to mechanical forces. *Annu. Rev. Biomed. Eng.* 2, 691–713. doi:10.1146/annurev.bioeng.2.1.691

Grogan, S. P., Sovani, S., Pauli, C., Chen, J., Hartmann, A., Colwell, C. W. Jr., et al. (2012). Effects of perfusion and dynamic loading on human neocartilage formation in alginate hydrogels. *Tissue Eng. Part A* 18, 1784–1792. doi:10.1089/ten.tea.2011.0506

Hilz, F. M., Ahrens, P., Grad, S., Stoddart, M. J., Dahmani, C., Wilken, F. L., et al. (2013). Influence of extremely low frequency, low energy electromagnetic fields and combined mechanical stimulation on chondrocytes in 3-D constructs for cartilage tissue engineering. *Bioelectromagnetics* 35, 116–128. doi:10.1002/bem.21822

Hoenig, E., Winkler, T., Mielke, G., Paetzold, H., Schuettler, D., Goepfert, C., et al. (2011). High amplitude direct compressive strain enhances mechanical properties of scaffold-free tissue-engineered cartilage. *Tissue Eng. Part A* 17, 1401–1411. doi:10.1089/ten.tea.2010.0395

Hung, C. T., Mauck, R. L., Wang, C. B., Lima, E. G., and Ateshian, G. A. (2004). A paradigm for functional tissue engineering of articular cartilage via applied physiologic deformational loading. *Ann. Biomed. Eng.* 32, 35–49. doi:10.1023/B:ABME.0000007789.99565.42

Hunter, C. J., Mouw, J. K., and Levenston, M. E. (2004). Dynamic compression of chondrocyte-seeded fibrin gels: effects on matrix accumulation and mechanical stiffness. *Osteoarthr. Cartil.* 12, 117–130. doi:10.1016/j.joca.2003.08.009

Jakob, M., Démarteau, O., Schäfer, D., Hinterman, B., Dick, W., Heberer, M., et al. (2001). Specific growth factors during the expansion and redifferentiation of adult human articular chondrocytes enhance chondrogenesis and cartilaginous tissue formation in vitro. *J. Cell. Biochem.* 81, 369–377. doi:10.1002/1097-4644(20010501)81:2<368::AID-JCB1051>3.0.CO;2-J

Jeon, J. E., Schrobback, K., Hutmacher, D. W., and Klein, T. J. (2012). Dynamic compression improves biosynthesis of human zonal chondrocytes from osteoarthritis patients. *Osteoarthr. Cartil.* 20, 906–915. doi:10.1016/j.joca.2012.04.019

Jeon, J. E., Schrobback, K., Meinert, C., Sramek, V., Hutmacher, D. W., and Klein, T. J. (2013). Effect of preculture and loading on expression of matrix molecules, matrix metalloproteinases, and cytokines by expanded osteoarthritic chondrocytes. *Arthritis Rheum.* 65, 2356–2367. doi:10.1002/art.38049

Kaupp, J. A., Weber, J. F., and Waldman, S. D. (2012). Mechanical Stimulation of Chondrocyte-agarose Hydrogels. *J. Vis. Exp.* 68, e4229. doi:10.3791/4229

Kelly, T.-A. N., Fisher, M. B., Oswald, E. S., Tai, T., Mauck, R. L., Ateshian, G. A., et al. (2008). Low-serum media and dynamic deformational loading in tissue engineering of articular cartilage. *Ann. Biomed. Eng.* 36, 769–779. doi:10.1007/s10439-008-9476-1

Kelly, T.-A. N., Roach, B. L., Weidner, Z. D., Mackenzie-Smith, C. R., O'Connell, G. D., Lima, E. G., et al. (2013). Tissue-engineered articular cartilage exhibits tension – compression nonlinearity reminiscent of the native cartilage. *J. Biomech.* 46, 1784–1791. doi:10.1016/j.jbiomech.2013.05.017

Kisiday, J. D., Jin, M., DiMicco, M. A., Kurz, B., and Grodzinsky, A. J. (2004). Effects of dynamic compressive loading on chondrocyte biosynthesis in self-assembling peptide scaffolds. *J. Biomech.* 37, 595–604. doi:10.1016/j.jbiomech.2003.10.005

Lee, C. R., Grodzinsky, A. J., and Spector, M. (2003). Biosynthetic response of passaged chondrocytes in a type II collagen scaffold to mechanical compression. *J. Biomed. Mater. Res. A.* 64, 560–569. doi:10.1002/jbm.a.10443

Lee, D. A., and Bader, D. L. (1997). Compressive strains at physiological frequencies influence the metabolism of chondrocytes seeded in agarose. *J. Orthop. Res.* 15, 181–188. doi:10.1002/jor.1100150205

Lima, E. G., Bian, L., Ng, K. W., Mauck, R. L., Byers, B. A., Tuan, R. S., et al. (2007). The beneficial effect of delayed compressive loading on tissue-engineered cartilage constructs cultured with TGF-β3. *Osteoarthr. Cartil.* 15, 1025–1033. doi:10.1016/j.joca.2007.03.008

Liu, H., Zhao, Z., Clarke, R. B., Gao, J., Garrett, I. R., and Margerrison, E. E. C. (2013). Enhanced tissue regeneration potential of juvenile articular cartilage. *Am. J. Sports Med.* 41, 2658–2667. doi:10.1177/0363546513502945

Malpeli, M., Randazzo, N., Cancedda, R., and Dozin, B. (2004). Serum-free growth medium sustains commitment of human articular chondrocyte through maintenance of Sox9 expression. *Tissue Eng.* 10, 145–155. doi:10.1089/107632704322791790

Mandl, E. W., Jahr, H., Koevoet, J. L. M., van Leeuwen, J. P. T. M., Weinans, H., Verhaar, J. A. N., et al. (2004). Fibroblast growth factor-2 in serum-free medium is a potent mitogen and reduces dedifferentiation of human ear chondrocytes in monolayer culture. *Matrix Biol.* 23, 231–241. doi:10.1016/j.matbio.2004.06.004

Mansour, J. M. (2003). "Biomechanics of cartilage," in *Kinesiology: The Mechanics and Pathomechanics of Human Movement*, ed. C. A. Oatis (Philadelphia: Lippincott Williams & Wilkens), 66–79.

Mauck, R. L., Byers, B. A., Yuan, X., and Tuan, R. S. (2007). Regulation of cartilaginous ECM gene transcription by chondrocytes and MSCs in 3D culture in response to dynamic loading. *Biomech. Model. Mechanobiol.* 6, 113–125. doi:10.1007/s10237-006-0042-1

Mauck, R. L., Nicoll, S. B., Seyhan, S. L., Ateshian, G. A., and Hung, C. T. (2003a). Synergistic action of growth factors and dynamic loading for articular cartilage tissue engineering. *Tissue Eng.* 9, 597–611. doi:10.1089/107632703768247304

Mauck, R. L., Wang, C., Oswald, E. S., and Ateshian, G. A. (2003b). The role of cell seeding density and nutrient supply for articular cartilage tissue engineering with deformational loading. *Osteoarthr. Cartil.* 11, 879–890. doi:10.1016/j.joca.2003.08.006

Mauck, R. L., Soltz, M. A., Wang, C. C. B., Wong, D. D., Chao, P.-H. G., Valhmu, W. B., et al. (2000). Functional tissue engineering of articular cartilage through dynamic loading of chondrocyte-seeded agarose gels. *J. Biomech. Eng.* 122, 252–260. doi:10.1115/1.429656

McCormick, F., Harris, J. D., Abrams, G. D., Frank, R., Gupta, A., Hussey, K., et al. (2014). Trends in the surgical treatment of articular cartilage lesions in the United States: an analysis of a large private-payer database over a period of 8 years. *Arthroscopy* 30, 222–226. doi:10.1016/j.arthro.2013.11.001

Mesallati, T., Buckley, C. T., Nagel, T., and Kelly, D. J. (2013). Scaffold architecture determines chondrocyte response to externally applied dynamic compression. *Biomech. Model. Mechanobiol.* 12, 889–899. doi:10.1007/s10237-012-0451-2

Mouw, J. K., Imler, S. M., and Levenston, M. E. (2007). Ion-channel regulation of chondrocyte matrix synthesis in 3D culture under static and dynamic compression. *Biomech. Model. Mechanobiol.* 6, 33–41. doi:10.1007/s10237-006-0034-1

Mow, V. C., and Huiskes, R. (eds) (2005). *Basic Orthopaedic Biomechanics & Mechano-Biology*, 3rd Edn. Philadelphia: Lippincott Williams & Wilkins.

Nebelung, S., Gavenis, K., Lüring, C., Zhou, B., Mueller-Rath, R., Stoffel, M., et al. (2012a). Simultaneous anabolic and catabolic responses of human chondrocytes seeded in collagen hydrogels to long-term continuous dynamic compression. *Ann. Anat.* 194, 351–358. doi:10.1016/j.aanat.2011.12.008

Nebelung, S., Gavenis, K., Rath, B., Tingart, M., Ladenburger, A., Stoffel, M., et al. (2012b). Continuous cyclic compressive loading modulates biological and mechanical properties of collagen hydrogels seeded with human chondrocytes. *Biorheology* 48, 247–261. doi:10.3233/BIR-2012-0597

Neumann, A. J., Gardner, O. F. W., Williams, R., Alini, M., Archer, C. W., and Stoddart, M. J. (2015). Human articular cartilage progenitor cells are responsive to mechanical stimulation and adenoviral-mediated overexpression of bone-morphogenetic protein 2. *PLoS ONE* 10:e0136229. doi:10.1371/journal.pone.0136229.t003

Ng, K. W., Mauck, R. L., Wang, C. C. B., Kelly, T.-A. N., Ho, M. M. Y., Chen, F. H., et al. (2009). Duty cycle of deformational loading influences the growth of engineered articular cartilage. *Cell Mol. Bioeng.* 2, 386–394. doi:10.1007/s12195-009-0070-x

Nicodemus, G. D., and Bryant, S. J. (2010). Mechanical loading regimes affect the anabolic and catabolic activities by chondrocytes encapsulated in PEG hydrogels. *Osteoarthr. Cartil.* 18, 126–137. doi:10.1016/j.joca.2009.08.005

Omata, S., Sonokawa, S., Sawae, Y., and Murakami, T. (2012). Effects of both vitamin C and mechanical stimulation on improving the mechanical characteristics of regenerated cartilage. *Biochem. Biophys. Res. Commun.* 424, 724–729. doi:10.1016/j.bbrc.2012.07.019

Pourmohammadali, H., Chandrashekar, N., and Medley, J. B. (2013). Hydromechanical stimulator for chondrocyte-seeded constructs in articular cartilage tissue engineering applications. *Proc. Inst. Mech. Eng. H.* 227, 310–316. doi:10.1177/0954411912468638

Schrobback, K., Malda, J., Crawford, R. W., Upton, Z., Leavesley, D. I., and Klein, T. J. (2012). Effects of oxygen on zonal marker expression in human articular chondrocytes. *Tissue Eng. Part A* 18, 920–933. doi:10.1089/ten.tea.2011.0088

Seidel, J. O., Pei, M., Gray, M. L., Langer, R., Freed, L. E., and Vunjak-Novakovic, G. (2004). Long-term culture of tissue engineered cartilage in a perfused chamber with mechanical stimulation. *Biorheology* 41, 445–458.

Shahin, K., and Doran, P. M. (2011). Tissue engineering of cartilage using a mechanobioreactor exerting simultaneous mechanical shear and compression to simulate the rolling action of articular joints. *Biotechnol. Bioeng.* 109, 1060–1073. doi:10.1002/bit.24372

Shelton, J. C., Bader, D. L., and Lee, D. A. (2003). Mechanical conditioning influences the metabolic response of cell-seeded constructs. *Cells Tissues Organs* 175, 140–150. doi:10.1159/000074630

Stoddart, M. J., Ettinger, L., and Häuselmann, H. J. (2006). Enhanced matrix synthesis in de novo, scaffold free cartilage-like tissue subjected to compression and shear. *Biotechnol. Bioeng.* 95, 1043–1051. doi:10.1002/bit.21052

Stojkovska, J., Bugarski, B., and Obradovic, B. (2010). Evaluation of alginate hydrogels under in vivo–like bioreactor conditions for cartilage tissue engineering. *J. Mater. Sci. Mater. Med.* 21, 2869–2879. doi:10.1007/s10856-010-4135-0

Tran, S. C., Cooley, A. J., and Elder, S. H. (2011). Effect of a mechanical stimulation bioreactor on tissue engineered, scaffold-free cartilage. *Biotechnol. Bioeng.* 108, 1421–1429. doi:10.1002/bit.23061

Tsuang, Y.-H., Lin, Y.-S., Chen, L.-T., Cheng, C.-K., and Sun, J.-S. (2008). Effect of dynamic compression on in vitro chondrocyte metabolism. *Int. J. Artif. Organs* 31, 439–449.

Villanueva, I., Weigel, C. A., and Bryant, S. J. (2009). Cell–matrix interactions and dynamic mechanical loading influence chondrocyte gene expression and bioactivity in PEG-RGD hydrogels. *Acta. Biomater.* 5, 2832–2846. doi:10.1016/j.actbio.2009.05.039

Vincent, T., Hermansson, M., Bolton, M., Wait, R., and Saklatvala, J. (2002). Basic FGF mediates an immediate response of articular cartilage to mechanical injury. *Proc. Natl. Acad. Sci. U.S.A.* 99, 8259–8264. doi:10.1073/pnas.122033199

Vincent, T. L., Hermansson, M. A., Hansen, U. N., Amis, A. A., and Saklatvala, J. (2004). Basic fibroblast growth factor mediates transduction of mechanical signals when articular cartilage is loaded. *Arthritis Rheum.* 50, 526–533. doi:10.1002/art.20047

Vincent, T. L., McLean, C. J., Full, L. E., Peston, D., and Saklatvala, J. (2007). FGF-2 is bound to perlecan in the pericellular matrix of articular cartilage, where it acts as a chondrocyte mechanotransducer. *Osteoarthr. Cartil.* 15, 752–763. doi:10.1016/j.joca.2007.01.021

Waldman, S. D., Couto, D. C., Grynpas, M. D., Pilliar, R. M., and Kandel, R. A. (2007). Multi-axial mechanical stimulation of tissue engineered cartilage: review. *Eur. Cell Mater.* 13, 66–74. doi:10.22203/eCM.v013a07

Waldman, S. D., Spiteri, C. G., Grynpas, M. D., Pilliar, R. M., Hong, J., and Kandel, R. M. (2003). Effect of biomechanical conditioning on cartilaginous tissue formation in vitro. *J. Bone Joint Surg.* 85-A, 1–5. doi:10.2106/00004623-200300002-00013

Waldman, S. D., Spiteri, C. G., Grynpas, M. D., Pilliar, R. M., and Kandel, R. A. (2004). Long-term intermittent compressive stimulation improves the composition and mechanical properties of tissue-engineered cartilage. *Tissue Eng.* 10, 1323–1331. doi:10.1089/ten.2004.10.1323

Wang, N., Grad, S., Stoddart, M. J., Niemeyer, P., Sudkamp, N. P., Pestka, J., et al. (2013). Bioreactor-induced chondrocyte maturation is dependent on cell passage and onset of loading. *Cartilage* 4, 165–176. doi:10.1177/1947603512471345

Wang, P.-Y., Chow, H.-H., Lai, J.-Y., Liu, H.-L., and Tsai, W.-B. (2009). Dynamic compression modulates chondrocyte proliferation and matrix biosynthesis in chitosan/gelatin scaffolds. *J. Biomed. Mater. Res.* 91, 143–152. doi:10.1002/jbm.b.31384

Wang, P. Y., Chow, H. H., Tsai, W. B., and Fang, H. W. (2008). Modulation of gene expression of rabbit chondrocytes by dynamic compression in polyurethane scaffolds with collagen gel encapsulation. *J. Biomater. Appl.* 23, 347–366. doi:10.1177/0885328208093684

Wang, P.-Y., and Tsai, W.-B. (2013). Modulation of the proliferation and matrix synthesis of chondrocytes by dynamic compression on genipin-crosslinked chitosan/collagen scaffolds. *J. Biomater. Sci. Polym. Ed.* 24, 507–519. doi:10.1080/09205063.2012.696310

Wernike, E., Li, Z., Alini, M., and Grad, S. (2007). Effect of reduced oxygen tension and long-term mechanical stimulation on chondrocyte-polymer constructs. *Cell Tissue Res.* 331, 473–483. doi:10.1007/s00441-007-0500-9

Williams, G. M., Klisch, S. M., and Sah, R. L. (2008). Bioengineering cartilage growth, maturation, and form. *Pediatr. Res.* 63, 527–534. doi:10.1203/PDR.0b013e31816b4fe5

Wiseman, M., Bader, D. L., Reisler, T., and Lee, D. A. (2004). Passage in monolayer influences the response of chondrocytes to dynamic compression. *Biorheology* 41, 283–298.

Wiseman, M., Henson, F., Lee, D. A., and Bader, D. L. (2003). Dynamic compressive strain inhibits nitric oxide synthesis by equine chondrocytes isolated from different areas of the cartilage surface. *Equine Vet. J.* 35, 451–456. doi:10.2746/042516403775600532

Woolf, A. D., and Pfleger, B. (2003). Burden of major musculoskeletal conditions. *Bull. World Health Organ.* 81, 1–11.

Wu, P., DeLassus, E., Patra, D., Liao, W., and Sandell, L. J. (2013). Effects of serum and compressive loading on the cartilage matrix synthesis and spatiotemporal deposition around chondrocytes in 3D culture. *Tissue Eng. Part A* 19, 1199–1208. doi:10.1089/ten.tea.2012.0559

Xie, J., Han, Z., Kim, S. H., Kim, Y. H., and Matsuda, T. (2007). Mechanical loading-dependence of mRNA expressions of extracellular matrices of chondrocytes inoculated into elastomeric microporous poly(L-lactide-co-ε-caprolactone) scaffold. *Tissue Eng.* 13, 29–40. doi:10.1089/ten.2006.0060

Xie, J., Han, Z. Y., and Matsuda, T. (2006). Mechanical compressive loading stimulates the activity of proximal region of human COL2A1 gene promoter in transfected chondrocytes. *Biochem. Biophys. Res. Commun.* 344, 1192–1199. doi:10.1016/j.bbrc.2006.03.243

Zignego, D. L., Hilmer, J. K., and June, R. K. (2015). Mechanotransduction in primary human osteoarthritic chondrocytes is mediated by metabolism of energy, lipids, and amino acids. *J. Biomech.* 48, 4253–4261. doi:10.1016/j.jbiomech.2015.10.038

Conflict of Interest Statement: The authors declare that the research was conducted in the absence of any commercial or financial relationships that could be construed as a potential conflict of interest.

frontiers in Bioengineering and Biotechnology

MINI REVIEW
published: 04 September 2017
doi: 10.3389/fbioe.2017.00052

Harnessing Endogenous Cellular Mechanisms for Bone Repair

*Claudia Lo Sicco[1] and Roberta Tasso[2]**

[1]Department of Experimental Medicine, University of Genoa, Genoa, Italy, [2]Ospedale Policlinico San Martino, Istituto di Ricovero e Cura a Carattere Scientifico per l'Oncologia, Genoa, Italy

Although autologous tissue transplantation represents a valid approach for bone repair, it has encountered crucial barriers in therapeutic translation, not least the invasive process necessary for stem cell isolation. In recent years, the scientific community has made significant strides for identifying new treatment options, and great emphasis has been placed on the tight interaction between skeletal and immune system in modulating the outcome of bone repair. Within the context of specific injury environmental cues, the cross talk among inflammatory cells and tissue resident and/or circulating progenitor cells is crucial to finely coordinate repair and remodeling processes. The appropriate modulation of the inflammatory response can now be considered a new trend in the field of regenerative medicine, as it raises the attracting possibility to enhance endogenous progenitor cell functions, finally leading to tissue repair. Therefore, new treatment options have been developed considering the wide spectrum of bone–inflammation interplay, considering in particular the cell intrinsic cues responsible for the modulation of the injured environment. In this review, we will provide a panoramic overview focusing on novel findings developed to uphold endogenous bone repair.

Keywords: inflammation, injury microenvironment, bone repair, endogenous progenitor cells, circulating progenitor cells, skeletal progenitor cells, regenerative medicine

OPEN ACCESS

Edited by:
Eric Farrell, Erasmus University Rotterdam, Netherlands

Reviewed by:
Mikaël M. Martino, Monash University, Australia
Marie-Noëlle Giraud, University of Fribourg, Switzerland

****Correspondence:***
Roberta Tasso
robertatasso@gmail.com

Specialty section:
This article was submitted to Tissue Engineering and Regenerative Medicine, a section of the journal Frontiers in Bioengineering and Biotechnology

Received: *09 June 2017*
Accepted: *08 August 2017*
Published: *04 September 2017*

Citation:
Lo Sicco C and Tasso R (2017) Harnessing Endogenous Cellular Mechanisms for Bone Repair. Front. Bioeng. Biotechnol. 5:52. doi: 10.3389/fbioe.2017.00052

INTRODUCTION

Bone regeneration represents a series of biological events orchestrated by a large number of mediators and cellular elements leading to cell recruitment, proliferation, and differentiation (Einhorn and Gerstenfeld, 2014). Most skeletal fractures heal in the first 8 weeks without major clinical concerns (Marsell and Einhorn, 2011). However, in the case of impaired bone healing, fractures can be associated with a range of complications (Kostenuik and Mirza, 2017). Conventionally, if no healing is detectable after 4 months, the fracture can be considered a delayed union. If the failure of the fracture to consolidate persists for more than 6 months, it can be considered a non-union (Marsh, 1998). The dynamic process underlying bone healing involves the interactions of cells, cytokines and matrix and requires concerted events, consisting of early inflammatory response, hard callus formation, and bone union followed by remodeling (Giannoudis et al., 2007; Gómez-Barrena et al., 2015). Bone autograft is the harmless and most efficient grafting procedure. However, due to limitations related to quantity and harvesting, "it represents an additional surgical intervention, with frequent consequences of pain and complications" (Roberts and Rosenbaum, 2012; Gómez-Barrena et al., 2015). Having said that, the scientific community moved on to allograft, primarily hailing from tissue banks. Nevertheless, also this strategy could be impaired by virus-inactivation treatments and freezing procedures (Gómez-Barrena et al., 2015). Thus, it has been long searched for biocompatible materials, in combination or not with osteogenic factors, resembling the properties of the autografts (Giannoudis et al., 2005), but none of them has reached the same osteogenic potential. In view

of these limitations, cell therapy can be considered an effective alternative to bone grafting (Rosset et al., 2014). Until now, different osteoprogenitors have been used in combination with suitable scaffolds. However, the application of these approaches led to a limited clinical success due to several reasons, such as the high commercialization costs, the regulatory issues, as well as the hitches of clinical translation (Bruder and Fox, 1999; Amini et al., 2012).

Among the most important biological interactions involved in the bone healing process, the cross talk between skeletal and immune system has received great attention, enough to establish an interdisciplinary field named osteoimmunology (Greenblatt and Shim, 2013). The appropriate modulation of the inflammatory response that occurs following tissue injury can be considered an important regulator of the bone repair cascade, leading to activation, mobilization, and recruitment of osteoprogenitors to the injured sites (Mountziaris and Mikos, 2008). In light of such considerations, the search is now on identifying the finest strategies to enhance and potentiate endogenous regenerative events for future therapy.

In this review, we will discuss the latest and most relevant findings on multiple features that impact fracture healing, with particular emphasis on the role of inflammation and progenitor cell recruitment.

INFLAMMATORY RESPONSES INDUCED BY FRACTURE HEALING

Platelet activation and concurrent inflammatory reaction are the first tissue responses to damage. The sum of biological effects generated during these early phases will direct the entire healing process (Tasso et al., 2013). It is known that "a brief and highly regulated secretion of pro-inflammatory cytokines at the time of the acute injury is crucial for the healing process" (Marsell and Einhorn, 2011). Bone fracture leads to blood vessel disruption not only inside bone, but also in the adjacent soft tissues, and to a generalized damage of cells and tissues that, as a whole, induce a strong inflammatory reaction (Claes et al., 2012). The acutely inflamed surrounding tissues are characterized by vasodilatation and fast arrival of innate immune cells. Within the fracture gap, fibrinogen is converted in fibrin and the hematoma takes shape (Claes et al., 2012). The resulting environment is highly hypoxic and marked by low pH and strong infiltration of inflammatory cells and cytokines (Einhorn and Gerstenfeld, 2014). In this context, literature data indicate that interleukin-6 (IL-6) and tumor necrosis factor-alpha (TNF-α) play key roles in the regulation of osteoclast activity by stimulating hematopoietic progenitor cells to differentiate along an osteoclastic lineage or enhancing the resorptive capacity of existing osteoclasts (Sarahrudi et al., 2009; Yokota et al., 2014). The idea that a certain degree of inflammation is required is reinforced by literature data indicating that treatment with anti-inflammatory drugs such as cyclooxygenase 2 (COX-2) inhibitors impairs the fracture healing process (Claes et al., 2012). Indeed, COX-2 promotes both angiogenesis and differentiation of mesenchymal stem cells (MSCs) into osteoblasts during fracture healing (Boursinos et al., 2017). To back this up, in 2011 Liu and colleagues have demonstrated that the *in situ* administration of the non-steroidal anti-inflammatory drug aspirin significantly promoted MSC-mediated bone repair in a mouse model of calvarial defect (Liu et al., 2011b). Moreover, the inhibition of NF-kB, a transcription factor involved in inflammation, or pathways leading to its activation improved "MSC-mediated craniofacial bone regeneration and repair *in vivo*" contrasting β-catenin degradation (Chang et al., 2013). The involvement of the β-catenin pathway in bone repair was further demonstrated in a recent paper indicating that signaling associated with the danger molecule interleukin-1 receptor, type 1 (IL-1R1) impaired MSC activation and differentiation by inhibiting β-catenin pathway (Martino et al., 2016).

The reason why the initial cell interactions are essential to obtain a correct repair is that innate immune cells guide revascularization and reparative events at injury sites, promoting progenitor cell migration (**Figure 1**). In 2012, a study was conducted to evaluate how biomaterials designed to incorporate inflammatory signals affected the behavior of natural killer (NK) cells, one of the first population arriving at the injury site, and the NK/MSC interactions. "It was found that NK cells are capable of stimulating a three-fold increase in human bone marrow MSC invasion, suggesting the importance of designing novel biomaterials leading to rational modulation of the inflammatory response as an alternative to current bone regeneration strategies" (Almeida et al., 2012).

During the early inflammatory phase, polymorphonuclear leukocytes followed by blood monocytes/macrophages entrapped in the fibrin cloth release molecules that favor the chemoattraction of different cell types. Due to their plasticity, macrophages represent one of the most studied innate immune cell populations (Mantovani et al., 2013). Classically activated, or M1, macrophages, whose prototypical activating stimulus is interferon-gamma (IFN-γ) and TNF-α (Varga et al., 2016) exhibit potent antimicrobial properties, high capacity to present antigen, and high interleukin-12 (IL-12) and IL-23 production (Verreck et al., 2004). In response to IL-4 and IL-13 signaling pathways, macrophages undergo an alternative activation, or M2, program that takes part in polarized Th2 responses, dampening of inflammation, promotion of tissue remodeling (Wynn, 2004), and angiogenesis (Chambers et al., 2013). Recently, it has been suggested a more appropriate nomenclature for macrophages based on "a set of standards encompassing three principles—the source of macrophages, definition of the activators, and a consensus collection of markers to describe macrophage activation—with the goal of unifying experimental standards for diverse experimental scenarios" (Murray et al., 2014). Different studies indicate that the interaction with *bona fide* stem/progenitor cells is an important task of macrophages, and this is particularly true when these cells are in a M2 activation state (Lolmede et al., 2009; Tasso et al., 2013). It has been reported that "depletion of macrophages led to early skeletal growth retardation and progressive osteoporosis" (Vi et al., 2015). Resident- and circulating macrophages recruited to the injury site exert pivotal functions for intramembranous and endochondral ossification, respectively (Claes et al., 2012). *In vivo* depletion of resident macrophages, named osteomacs, indicated that these cells were required for deposition of matrix expressing type I collagen and bone mineralization (Alexander et al., 2011). Conversely, when the fracture healing process was examined in

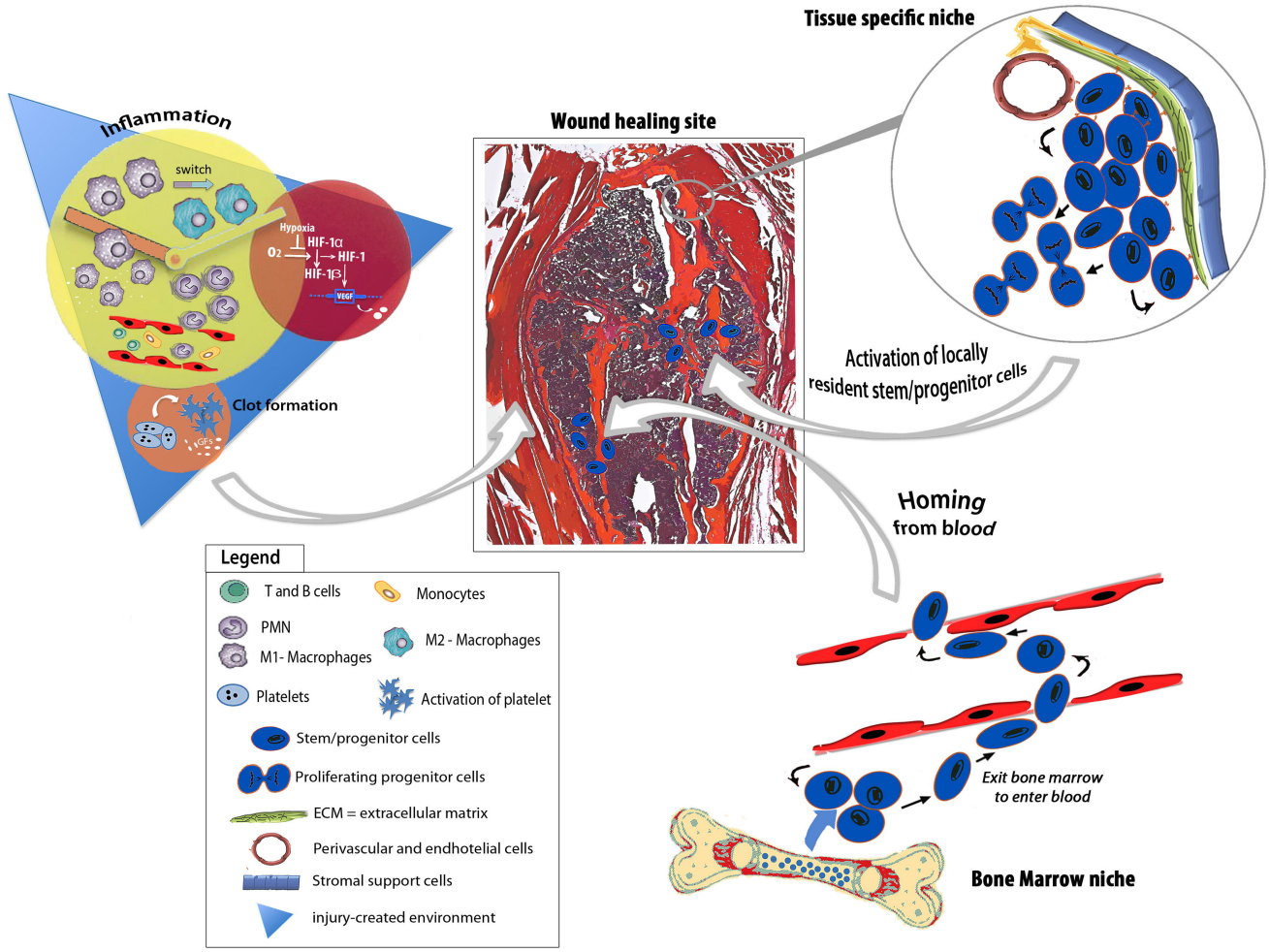

FIGURE 1 | Schematic depicting endogenous regenerative responses underpinning bone tissue repair. The injury-generated environment is enriched of growth factors, chemokines, pro- and anti-inflammatory cytokines as well as hypoxic stimuli that evoke feedbacks to the niches, deploying programs for endogenous progenitor activation, mobilization, and recruitment to the healing site. The healing process involves either circulating progenitor cells or tissue-specific progenitors.

CCR2−/− mice that underwent a non-stabilized tibial fracture that heals through robust endochondral ossification, an impaired vascularization and decreased callus formation associated with a lower number of circulating macrophages were observed (Xing et al., 2010). The functional effect of macrophages on fracture healing has been recently confirmed using a preclinical model of osteotomy induced in rats subjected to splenectomy (Xiao et al., 2017). Moreover, studies conducted with human fracture tissues indicate that the presence of macrophages persists in the injured sites in association with areas of bone formation, even if their numbers are higher in early fracture samples (Andrew et al., 1994; Alexander et al., 2017). Overall, these data suggest that macrophage contribution to bone repair goes far beyond the early inflammatory events. Noteworthy, some recently published papers stressed the closed relationship between the adaptive immune system and the healing outcome. Mice totally lacking the adaptive immune system, as well as mice depleted of CD8+ T lymphocytes are characterized by an enhanced endogenous fracture regeneration (Toben et al., 2011; Reinke et al., 2013).

The milieu induced by the initial inflammatory response together with the angiogenic factors released as an effect of the hypoxic condition generated within the fracture gap (Mirhadi et al., 2013), guide revascularization of the injured site, a central event not only for the re-establishment of a normoxic environment, but also because the newly formed blood vessels allow the direct interaction with host cells and provide the access to host osteoprogenitor cells, enhancing matrix deposition.

ENDOGENOUS PROGENITOR CELLS IN BONE REPAIR: LOCALLY RESIDENT VERSUS CIRCULATING PROGENITORS

It has been described that signals associated with the environment generated by an injured bone stimulate the mobilization and proliferation of both resident and circulating progenitor cells needed for tissue repair (Hadjiargyrou and O'Keefe, 2014) (**Figure 1**). As early as 1965, a paper published on Science by Urist (1965)

indicated that the process leading to new bone tissue formation was strictly related to the interactions with endogenous host cells and that differentiation of osteoprogenitors was elicited by local environment signals.

Just like different types of bone damages lead to different inflammatory cascades and, consequently, to different ossification processes (Colnot et al., 2012), also the involvement of progenitor cells is affected. When a fracture occurs in the absence of stabilization, a strong periosteal reaction takes place and the repair process brings about the formation of a large callus formed through an endochondral ossification process (Le et al., 2001; Chang and Knothe Tate, 2012). On the contrary, when fractures are firmly stabilized, the periosteal reaction is not efficient, and a minimal callus formation is driven by an intramembranous ossification process (van Gastel et al., 2014). In line with these concepts, holding over stabilization during the early phases of fracture healing does not affect either the volume or the mechanical properties of the callus, but it induces the formation of more cartilage, thus altering the involvement of endogenous progenitors and the modality of bone repair (Miclau et al., 2007). In this context, literature data indicate that different types of fractures cause changes in the expression of inflammatory genes, including matrix metalloproteinase 9 (*MMP9*), and in the subsequent activation and differentiation of resident periosteal progenitors (Wang et al., 2013). Periosteum-derived mesenchymal progenitors are vital for both endochondral and intramembranous cortical bone formation (Hutmacher and Sittinger, 2003). The contribution of periosteal progenitors to callus formation was examined using a mouse model of Rosa26 segmental bone graft transplantation (Zhang et al., 2008; Colnot et al., 2012). The study demonstrates that periosteal progenitors contribute to the initial phases of new bone formation, suggesting that this resident cell population act as an essential trigger for bone repair processes. Indeed, periosteal progenitors can act directly, differentiating to cartilage/bone tissue or indirectly, releasing osteoinductive factors that recruit and activate other host-osteoprogenitors (Zhang et al., 2005), although the relative contribution of these two mechanisms is still not clear. In 2009, it has been clearly demonstrated that periosteum and endosteum, the main sources of resident progenitors, differently participated to bone repair processes. To back this up, periosteal progenitors show a dose-dependent migratory effect under chemokine receptor ligands stimulation, such as CXCR4 and CXCR5 (Ferretti and Mattioli-Belmonte, 2014). Recently, using a combination of markers including AlphaV integrin, Chan et al. (2015) have defined a skeletal stem cell population present in the proximity of the growth plate of long bones and capable of differentiating bone, cartilage, and stroma *in vivo*. Meanwhile, another study highlighted the existence of Gremlin-1 osteochondroreticular (Grem1-OCR) stem cells concentrated within the metaphysis of long bones contributing to bone healing and possessing the ability to self-renew after serial transplantations (Worthley et al., 2015).

The severity of fracture healing is directly proportional to a reduced soft tissue envelope and "increasing severity of the surrounding muscle is associated with the development of nonunions" (Friedrich et al., 2011; Papakostidis et al., 2011; Shah et al., 2013). In light of these observations, muscle has been considered a "potential source of cells and signals for bone healing" (Shah et al., 2013). A recent study conducted in mice using an elegant cell lineage tracing approach has demonstrated that muscle precursor cells participate in callus formation only in the case of open fractures with periosteal stripping and muscle injury (Liu et al., 2011a). Related evidence further indicate that muscle-derived cells present within the fracture callus shift their gene expression from the muscle marker Paired Box Gene 3 (Pax3) to the chondrogenic markers SRY-Box 9 (Sox9) and Homeobox protein Nkx3 (Nkx3) (Cairns et al., 2012).

In addition to locally resident osteoprogenitors, other skeletal progenitors have been proposed to participate in bone repair processes (Pignolo and Kassem, 2011), including circulating bone marrow-derived progenitors (**Table 1**). However, to date, a precise comprehension on the signals released from the injured tissues responsible for the mobilization of bone marrow-derived progenitor cells and the accurate molecular mechanisms governing their fate, homing, and engraftment are very limited. Moreover, "it's likely that individual circulating progenitors detected by different experimental strategies are overlapping but indicated with different names, such as circulating osteoprogenitors (COPs), alkaline phosphatase-positive (ALP+) circulating progenitors, circulating CD34-positive (CD34+) precursors, contributing to increase the confusion regarding their exact identification" (Lo Sicco et al., 2015).

So far, a population of adherent fibroblast-like cells with osteogenic potential has been isolated from the blood of different species, indicating that "cells with multiple differentiation potential analogous to that of post-natal marrow stromal cells can negotiate the circulation" (Kuznetsov et al., 2001). A first proof-of-principle set of experiments elucidating the differentiation potential of circulating CD34-positive (CD34+) cells into not only endothelial cells but also osteoblasts goes back to 2008 (Matsumoto et al., 2008). These cells were described to create a milieu favorable to a functional recovery from fracture. In the same year, taking advantage of parabiosis experiments, it was demonstrated that the injury-associated signals triggered by bone fracture induced a stimulus for recruitment of circulating alkaline phosphatase-positive (ALP+) cells, although the exact origin of recruited cells remains uncertain (Kumagai et al., 2008). More recently, a similar parabiotic approach was adopted to reveal that the exposure to a youthful circulation affected bone repair through the modulation of β-catenin (Baht et al., 2015), raising the possibility that agents that modulate this pathway could improve the extent and quality of fracture repair in the aging population. In 2015, the existence of a rare and undifferentiated cell population—circulating healing (CH) cells—involved in bone tissue healing and present in the peripheral blood of immunocompetent mice has been described (Lo Sicco et al., 2015). It has been shown how the injury signals were sufficient to specifically direct CH cell recruitment toward the fractured bone and how the peculiar local environment guided CH cell differentiation and appropriate integration into the specific tissue.

These different preclinical animal models have shown that small numbers of progenitor cells derived from the systemic circulation participate in the bone healing process (Hadjiargyrou and O'Keefe, 2014). Less amount of work has been performed to study the involvement of progenitor cells in humans, and the results

TABLE 1 | Resident and circulating progenitors involved in adult bone repair.

	Name	Markers	Localization	Activation stimuli	Reference
Resident progenitors	Periosteal stem/progenitors	Sca-I+ CD105+ SSEA-4+ CD29+ CD140+	Periosteum	Hedgehog (Hh) signaling pathway	Wang et al. (2013)
	Bone, cartilage, stromal progenitor	CD45– Ter119– Tie2– AlphaV+ CD105+ CD200+	Growth plate	Hh. BMP. FGF, and Notch signaling pathways	Chang et al., (2013), Chan et al. (2015)
	Osteochondroreticular stem cells	CD45– Ter119– CD31– Grem1+	Growth plate and trabecular bone	BMP signaling pathway	Worthley et al. (2015)
Circulating progenitors	Connective tissue progenitors	ALP+	Peripheral blood	Injury-associated signals	Kumagai et al. (2008)
	Circulating osteogenic precursors	CXCR4+ CD44+ CD45–	Peripheral blood	BMP-2 signaling pathway	Otsuru et al. (2007)
	Myeloid CD34+	CD34+ OC+	Peripheral blood	SDF-1 signaling pathway	Matsumoto et al. (2008)
	Human osteoblast lineages cells	OC+ BAP+	Peripheral blood	BMP signaling pathway	Eghbali-Fatourechi et al. (2005)
	Circulating healing cells	Lineage– CD45–	Peripheral blood	Injury-associated signals	Lo Sicco et al. (2015)

obtained were controversial. Although some papers indicate that no circulating mesenchymal osteoprogenitors were detectable neither in healthy subjects nor in patients with end-stage renal or liver disease or in heart transplant patients (Hoogduijn et al., 2014), COPs were identified in the blood of a single patient with multiple fractures (Hoogduijn et al., 2014). The authors suggested that disruption of bone marrow, as a result of skeletal injury, could have allowed egress of mesenchymal progenitors into the circulation (Hadjiargyrou and O'Keefe, 2014). However, several cell types, other than classical mesenchymal progenitors, have been described to undergo osteogenic differentiation and migrate toward an injured bone under the action of appropriate stimuli (Szulc, 2016). A population of circulating cells with a myeloid origin expressing osteocalcin and bone alkaline phosphatase (OC+BAP+) has been demonstrated to possess an osteogenic activity *in vitro* and *in vivo*. Interestingly, the percentage of myeloid OC+BAP+ cells was higher in peripheral blood and bone marrow of type 2 diabetic patients, and in diabetic carotid endarterectomy specimens, a higher degree of calcification and amounts of OC and BAP-expressing cells were detected in the α-smooth muscle actin-negative areas surrounding calcified nodules, where CD68+ macrophages colocalized (Fadini et al., 2011). The increased percentage of COPs in pathological conditions was evidenced also in other clinical studies and it is supposed to be "linked to the presence of vascular damage, such as arterial stiffness and aortic calcification" (Pal et al., 2010; Pirro et al., 2011; Rattazzi et al., 2016). However, in 2005, Eghbali-Fatourechi et al. (2005) showed that the presence of a population of osteoblast-lineage cells circulating in physiological condition endowed with expression of markers of bone formation and markedly increasing during pubertal growth, thus representing a previously unknown component of bone formation process (**Table 1**).

CONCLUSION

In recent years, significant advances have been accomplished in the comprehension of endogenous mechanisms promoting bone repair. Despite these advances, a huge confusion in endogenous COP identification still exists. This misperception could be due to various causes, such as the low understanding of the molecular mechanisms leading to the mobilization of progenitor cells from the niche in which they physiologically reside, the rate of their differentiation, and last but not least their prospective heterogeneity. In any case, altogether, the studies herein reviewed show the great potential of the endogenous repair mechanisms, envisaging new ways of thinking and new ways of moving forward in regenerative medicine.

AUTHOR CONTRIBUTIONS

CS and RT conceived the idea of this mini review and wrote the Abstract, Introduction, and Conclusion. RT revised and finalized the mini review.

FUNDING

This work was supported by the Italian Ministry of Health ("Young Investigator Grant"—GR-2013-02357519) to RT.

REFERENCES

Alexander, K. A., Chang, M. K., Maylin, E. R., Kohler, T., Müller, R., Wu, A. C., et al. (2011). Osteal macrophages promote in vivo intramembranous bone healing in a mouse tibial injury model. *J. Bone Miner. Res.* 26, 1517–1532. doi:10.1002/jbmr.354

Alexander, K. A., Raggatt, L.-J., Millard, S., Batoon, L., Chiu-Ku Wu, A., Chang, M. K., et al. (2017). Resting and injury-induced inflamed periosteum contain multiple macrophage subsets that are located at sites of bone growth and regeneration. *Immunol. Cell Biol.* 95, 7–16. doi:10.1038/icb.2016.74

Almeida, C. R., Vasconcelos, D. P., Goncalves, R. M., and Barbosa, M. A. (2012). Enhanced mesenchymal stromal cell recruitment via natural killer cells by incorporation of inflammatory signals in biomaterials. *J. R. Soc. Interface* 9, 261–271. doi:10.1098/rsif.2011.0357

Amini, A. R., Laurencin, C. T., and Nukavarapu, S. P. (2012). Bone tissue engineering: recent advances and challenges. *Crit. Rev. Biomed. Eng.* 40, 363–408. doi:10.1615/CritRevBiomedEng.v40.i5.10

Andrew, J. G., Andrew, S. M., Freemont, A. J., and Marsh, D. R. (1994). Inflammatory cells in normal human fracture healing. *Acta Orthop. Scand.* 65, 462–466. doi:10.3109/17453679408995493

Baht, G. S., Silkstone, D., Vi, L., Nadesan, P., Amani, Y., Whetstone, H., et al. (2015). Exposure to a youthful circulaton rejuvenates bone repair through modulation of β-catenin. *Nat. Commun.* 6, 7131. doi:10.1038/ncomms8131

Boursinos, L. A., Karachalios, T., Poultsides, L., and Malizos, K. N. (2017). Do steroids, conventional non-steroidal anti-inflammatory drugs and selective Cox-2 inhibitors adversely affect fracture healing? *J. Musculoskelet. Neuronal. Interact.* 9, 44–52.

Bruder, S. P., and Fox, B. S. (1999). Tissue engineering of bone. Cell based strategies. *Clin. Orthop. Relat. Res.* S68–S83. Available at: http://www.ncbi.nlm.nih.gov/pubmed/10546637

Cairns, D. M., Liu, R., Sen, M., Canner, J. P., Schindeler, A., Little, D. G., et al. (2012). Interplay of Nkx3.2, Sox9 and Pax3 regulates chondrogenic differentiation of muscle progenitor cells. *PLoS ONE* 7:e39642. doi:10.1371/journal.pone.0039642

Chambers, S. E. J., O'Neill, C. L., O'Doherty, T. M., Medina, R. J., and Stitt, A. W. (2013). The role of immune-related myeloid cells in angiogenesis. *Immunobiology* 218, 1370–1375. doi:10.1016/j.imbio.2013.06.010

Chan, C. K. F., Seo, E. Y., Chen, J. Y., Lo, D., McArdle, A., Sinha, R., et al. (2015). Identification and specification of the mouse skeletal stem cell. *Cell* 160, 285–298. doi:10.1016/j.cell.2014.12.002

Chang, H., and Knothe Tate, M. L. (2012). Concise review: the periosteum: tapping into a reservoir of clinically useful progenitor cells. *Stem Cells Transl. Med.* 1, 480–491. doi:10.5966/sctm.2011-0056

Chang, J., Liu, F., Lee, M., Wu, B., Ting, K., Zara, J. N., et al. (2013). NF-κB inhibits osteogenic differentiation of mesenchymal stem cells by promoting β-catenin degradation. *Proc. Natl. Acad. Sci. U.S.A* 110, 9469–9474. doi:10.1073/pnas.1300532110

Claes, L., Recknagel, S., and Ignatius, A. (2012). Fracture healing under healthy and inflammatory conditions. *Nat. Rev. Rheumatol.* 8, 133–143. doi:10.1038/nrrheum.2012.1

Colnot, C., Zhang, X., and Knothe Tate, M. L. (2012). Current insights on the regenerative potential of the periosteum: molecular, cellular, and endogenous engineering approaches. *J. Orthop. Res.* 30, 1869–1878. doi:10.1002/jor.22181

Eghbali-Fatourechi, G. Z., Lamsam, J., Fraser, D., Nagel, D., Riggs, B. L., and Khosla, S. (2005). Circulating osteoblast-lineage cells in humans. *N. Engl. J. Med.* 352, 1959–1966. doi:10.1056/NEJMoa044264

Einhorn, T. A., and Gerstenfeld, L. C. (2014). Fracture healing: mechanisms and interventions. *Nat. Rev. Rheumatol.* 11, 45–54. doi:10.1038/nrrheum.2014.164

Fadini, G. P., Albiero, M., Menegazzo, L., Boscaro, E., Vigili de Kreutzenberg, S., Agostini, C., et al. (2011). Widespread increase in myeloid calcifying cells contributes to ectopic vascular calcification in type 2 diabetes. *Circ. Res.* 108, 1112–1121. doi:10.1161/CIRCRESAHA.110.234088

Ferretti, C., and Mattioli-Belmonte, M. (2014). Periosteum derived stem cells for regenerative medicine proposals: boosting current knowledge. *World J Stem Cells* 6, 266–277. doi:10.4252/wjsc.v6.i3.266

Friedrich, J. B., Katolik, L. I., and Hanel, D. P. (2011). Reconstruction of soft-tissue injury associated with lower extremity fracture. *J. Am. Acad. Orthop. Surg.* 19, 81–90. doi:10.5435/00124635-201102000-00003

Giannoudis, P. V., Dinopoulos, H., and Tsiridis, E. (2005). Bone substitutes: an update. *Injury* 36, S20–S27. doi:10.1016/j.injury.2005.07.029

Giannoudis, P. V., Einhorn, T. A., and Marsh, D. (2007). Fracture healing: the diamond concept. *Injury* 38(Suppl. 4), S3–S6. doi:10.1016/S0020-1383(08)70003-2

Gómez-Barrena, E., Rosset, P., Lozano, D., Stanovici, J., Ermthaller, C., and Gerbhard, F. (2015). Bone fracture healing: cell therapy in delayed unions and nonunions. *Bone* 70, 93–101. doi:10.1016/j.bone.2014.07.033

Greenblatt, M. B., and Shim, J.-H. (2013). Osteoimmunology: a brief introduction. *Immune Netw.* 13, 111–115. doi:10.4110/in.2013.13.4.111

Hadjiargyrou, M., and O'Keefe, R. J. (2014). The convergence of fracture repair and stem cells: interplay of genes, aging, environmental factors and disease. *J. Bone Miner. Res.* 29, 2307–2322. doi:10.1002/jbmr.2373

Hoogduijn, M. J., Verstegen, M. M. A., Engela, A. U., Korevaar, S. S., Roemeling-van Rhijn, M., Merino, A., et al. (2014). No evidence for circulating mesenchymal stem cells in patients with organ injury. *Stem Cells Dev.* 23, 2328–2335. doi:10.1089/scd.2014.0269

Hutmacher, D. W., and Sittinger, M. (2003). Periosteal cells in bone tissue engineering. *Tissue Eng.* 9, 45–64. doi:10.1089/10763270360696978

Kostenuik, P., and Mirza, F. M. (2017). Fracture healing physiology and the quest for therapies for delayed healing and nonunion. *J. Orthop. Res.* 35, 213–223. doi:10.1002/jor.23460

Kumagai, K., Vasanji, A., Drazba, J. A., Butler, R. S., and Muschler, G. F. (2008). Circulating cells with osteogenic potential are physiologically mobilized into the fracture healing site in the parabiotic mice model. *J. Orthop. Res.* 26, 165–175. doi:10.1002/jor.20477

Kuznetsov, S. A., Mankani, M. H., Gronthos, S., Satomura, K., Bianco, P., and Robey, P. G. (2001). Circulating skeletal stem cells. *J. Cell Biol.* 153, 1133–1140. doi:10.1083/jcb.153.5.1133

Le, A. X., Miclau, T., Hu, D., and Helms, J. A. (2001). Molecular aspects of healing in stabilized and non-stabilized fractures. *J. Orthop. Res.* 19, 78–84. doi:10.1016/S0736-0266(00)00006-1

Liu, R., Birke, O., Morse, A., Peacock, L., Mikulec, K., Little, D. G., et al. (2011a). Myogenic progenitors contribute to open but not closed fracture repair. *BMC Musculoskelet. Disord.* 12:288. doi:10.1186/1471-2474-12-288

Liu, Y., Wang, L., Kikuiri, T., Akiyama, K., Chen, C., Xu, X., et al. (2011b). Mesenchymal stem cell–based tissue regeneration is governed by recipient T lymphocytes via IFN-γ and TNF-α. *Nat. Med.* 17, 1594–1601. doi:10.1038/nm.2542

Lo Sicco, C., Tasso, R., Reverberi, D., Cilli, M., Pfeffer, U., and Cancedda, R. (2015). Identification of a new cell population constitutively circulating in healthy conditions and endowed with a homing ability toward injured sites. *Sci. Rep.* 5, 16574. doi:10.1038/srep16574

Lolmede, K., Campana, L., Vezzoli, M., Bosurgi, L., Tonlorenzi, R., Clementi, E., et al. (2009). Inflammatory and alternatively activated human macrophages attract vessel-associated stem cells, relying on separate HMGB1- and MMP-9-dependent pathways. *J. Leukoc. Biol.* 85, 779–787. doi:10.1189/jlb.0908579

Mantovani, A., Biswas, S. K., Galdiero, M. R., Sica, A., and Locati, M. (2013). Macrophage plasticity and polarization in tissue repair and remodelling. *J. Pathol.* 229, 176–185. doi:10.1002/path.4133

Marsell, R., and Einhorn, T. A. (2011). The biology of fracture healing. *Injury* 42, 551–555. doi:10.1016/j.injury.2011.03.031

Marsh, D. (1998). Concepts of fracture union, delayed union, and nonunion. *Clin. Orthop. Relat. Res.* S22–S30. Available at: http://www.ncbi.nlm.nih.gov/pubmed/9917623

Martino, M. M., Maruyama, K., Kuhn, G. A., Satoh, T., Takeuchi, O., Müller, R., et al. (2016). Inhibition of IL-1R1/MyD88 signalling promotes mesenchymal stem cell-driven tissue regeneration. *Nat. Commun.* 7, 11051. doi:10.1038/ncomms11051

Matsumoto, T., Kuroda, R., Mifune, Y., Kawamoto, A., Shoji, T., Miwa, M., et al. (2008). Circulating endothelial/skeletal progenitor cells for bone regeneration and healing. *Bone* 43, 434–439. doi:10.1016/j.bone.2008.05.001

Miclau, T., Lu, C., Thompson, Z., Choi, P., Puttlitz, C., Marcucio, R., et al. (2007). Effects of delayed stabilization on fracture healing. *J. Orthop. Res.* 25, 1552–1558. doi:10.1002/jor.20435

Mirhadi, S., Ashwood, N., and Karagkevrekis, B. (2013). Factors influencing fracture healing. *Trauma* 15, 140–155. doi:10.1177/1460408613486571

Mountziaris, P. M., and Mikos, A. G. (2008). Modulation of the inflammatory response for enhanced bone tissue regeneration. *Tissue Eng. Part B Rev.* 14, 179–186. doi:10.1089/ten.teb.2008.0038

Murray, P. J., Allen, J. E., Biswas, S. K., Fisher, E. A., Gilroy, D. W., Goerdt, S., et al. (2014). Macrophage activation and polarization: nomenclature and experimental guidelines. *Immunity* 41, 14–20. doi:10.1016/j.immuni.2014.06.008

Otsuru, S., Tamai, K., Yamazaki, T., Yoshikawa, H., and Yasufumin, K. (2007). Circulating bone marrow-derived osteoblast progenitor cells are recruited to the bone-forming site by the CXCR4/stromal cell-derived factor-1 pathway. *Stem Cells* 26, 223–234. doi:10.1634/stemcells.2007-0515

Pal, S. N., Rush, C., Parr, A., Van Campenhout, A., and Golledge, J. (2010). Osteocalcin positive mononuclear cells are associated with the severity of aortic calcification. *Atherosclerosis* 210, 88–93. doi:10.1016/j.atherosclerosis.2009.11.001

Papakostidis, C., Kanakaris, N. K., Pretel, J., Faour, O., Morell, D. J., and Giannoudis, P. V. (2011). Prevalence of complications of open tibial shaft fractures stratified as per the Gustilo–Anderson classification. *Injury* 42, 1408–1415. doi:10.1016/j.injury.2011.10.015

Pignolo, R. J., and Kassem, M. (2011). Circulating osteogenic cells: implications for injury, repair, and regeneration. *J. Bone Miner. Res.* 26, 1685–1693. doi:10.1002/jbmr.370

Pirro, M., Schillaci, G., Mannarino, M. R., Scarponi, A. M., Manfredelli, M. R., Callarelli, L., et al. (2011). Circulating immature osteoprogenitor cells and arterial stiffening in postmenopausal osteoporosis. *Nutr. Metab. Cardiovasc. Dis.* 21, 636–642. doi:10.1016/j.numecd.2010.01.015

Rattazzi, M., Faggin, E., Buso, R., Di Virgilio, R., Puato, M., Plebani, M., et al. (2016). Atorvastatin reduces circulating osteoprogenitor cells and T-cell RANKL expression in osteoporotic women: implications for the bone-vascular axis. *Cardiovasc. Ther.* 34, 13–20. doi:10.1111/1755-5922.12163

Reinke, S., Geissler, S., Taylor, W. R., Schmidt-Bleek, K., Juelke, K., Schwachmeyer, V., et al. (2013). Terminally differentiated $CD8^+$ T cells negatively affect bone regeneration in humans. *Sci. Transl. Med.* 5, 177ra36. doi:10.1126/scitranslmed.3004754

Roberts, T. T., and Rosenbaum, A. J. (2012). Bone grafts, bone substitutes and orthobiologics: the bridge between basic science and clinical advancements in fracture healing. *Organogenesis* 8, 114–124. doi:10.4161/org.23306

Rosset, P., Deschaseaux, F., and Layrolle, P. (2014). Cell therapy for bone repair. *Orthop. Traumatol. Surg. Res.* 100, S107–S112. doi:10.1016/j.otsr.2013.11.010

Sarahrudi, K., Mousavi, M., Grossschmidt, K., Sela, N., König, F., Vécsei, V., et al. (2009). The impact of colony-stimulating factor-1 on fracture healing: an experimental study. *J. Orthop. Res.* 27, 36–41. doi:10.1002/jor.20680

Shah, K., Majeed, Z., Jonason, J., and O'Keefe, R. J. (2013). The role of muscle in bone repair: the cells, signals, and tissue responses to injury. *Curr. Osteoporos. Rep.* 11, 130–135. doi:10.1007/s11914-013-0146-3

Szulc, P. (2016). Abdominal aortic calcification: a reappraisal of epidemiological and pathophysiological data. *Bone* 84, 25–37. doi:10.1016/j.bone.2015.12.004

Tasso, R., Ulivi, V., Reverberi, D., Lo Sicco, C., Descalzi, F., and Cancedda, R. (2013). In vivo implanted bone marrow-derived mesenchymal stem cells trigger a cascade of cellular events leading to the formation of an ectopic bone regenerative niche. *Stem Cells Dev.* 22, 3178–3191. doi:10.1089/scd.2013.0313

Toben, D., Schroeder, I., El Khassawna, T., Mehta, M., Hoffmann, J.-E., Frisch, J.-T., et al. (2011). Fracture healing is accelerated in the absence of the adaptive immune system. *J. Bone Miner. Res.* 26, 113–124. doi:10.1002/jbmr.185

Urist, M. R. (1965). Bone: formation by autoinduction. *Science* 150, 893–899. doi:10.1126/science.150.3698.893

van Gastel, N., Stegen, S., Stockmans, I., Moermans, K., Schrooten, J., Graf, D., et al. (2014). Expansion of murine periosteal progenitor cells with fibroblast growth factor 2 reveals an intrinsic endochondral ossification program mediated by bone morphogenetic protein 2. *Stem Cells* 32, 2407–2418. doi:10.1002/stem.1783

Varga, T., Mounier, R., Horvath, A., Cuvellier, S., Dumont, F., Poliska, S., et al. (2016). Highly dynamic transcriptional signature of distinct macrophage subsets during sterile inflammation, resolution, and tissue repair. *J. Immunol.* 196, 4771–4782. doi:10.4049/jimmunol.1502490

Verreck, F. A. W., de Boer, T., Langenberg, D. M. L., Hoeve, M. A., Kramer, M., Vaisberg, E., et al. (2004). Human IL-23-producing type 1 macrophages promote but IL-10-producing type 2 macrophages subvert immunity to (myco)bacteria. *Proc. Natl. Acad. Sci. U.S.A* 101, 4560–4565. doi:10.1073/pnas.0400983101

Vi, L., Baht, G. S., Whetstone, H., Ng, A., Wei, Q., Poon, R., et al. (2015). Macrophages promote osteoblastic differentiation in vivo: implications in fracture repair and bone homeostasis. *J. Bone Miner. Res.* 30, 1090–1102. doi:10.1002/jbmr.2422

Wang, X., Yu, Y. Y., Lieu, S., Yang, F., Lang, J., Lu, C., et al. (2013). MMP9 regulates the cellular response to inflammation after skeletal injury. *Bone* 52, 111–119. doi:10.1016/j.bone.2012.09.018

Worthley, D. L., Churchill, M., Compton, J. T., Tailor, Y., Rao, M., Si, Y., et al. (2015). Gremlin 1 identifies a skeletal stem cell with bone, cartilage, and reticular stromal potential. *Cell* 160, 269–284. doi:10.1016/j.cell.2014.11.042

Wynn, T. A. (2004). Fibrotic disease and the T(H)1/T(H)2 paradigm. *Nat. Rev. Immunol.* 4, 583–594. doi:10.1038/nri1412

Xiao, W., Hu, Z., Li, T., and Li, J. (2017). Bone fracture healing is delayed in splenectomic rats. *Life Sci.* 173, 55–61. doi:10.1016/j.lfs.2016.12.005

Xing, Z., Lu, C., Hu, D., Yu, Y., Wang, X., Colnot, C., et al. (2010). Multiple roles for CCR2 during fracture healing. *Dis. Model Mech.* 3, 451–458. doi:10.1242/dmm.003186

Yokota, K., Sato, K., Miyazaki, T., Kitaura, H., Kayama, H., Miyoshi, F., et al. (2014). Combination of tumor necrosis factor α and interleukin-6 induces mouse osteoclast-like cells with bone resorption activity both in vitro and in vivo. *Arthritis Rheumatol.* 66, 121–129. doi:10.1002/art.38218

Zhang, X., Awad, H. A., O'Keefe, R. J., Guldberg, R. E., and Schwarz, E. M. (2008). A perspective: engineering periosteum for structural bone graft healing. *Clin. Orthop. Relat. Res.* 466, 1777–1787. doi:10.1007/s11999-008-0312-6

Zhang, X., Xie, C., Lin, A. S. P., Ito, H., Awad, H., Lieberman, J. R., et al. (2005). Periosteal progenitor cell fate in segmental cortical bone graft transplantations: implications for functional tissue engineering. *J. Bone Miner. Res.* 20, 2124–2137. doi:10.1359/JBMR.050806

Conflict of Interest Statement: The authors declare that all financial, commercial or other relationships that might be perceived by the academic community as representing a potential conflict of interest are disclosed.

frontiers in Bioengineering and Biotechnology

ORIGINAL RESEARCH
published: 02 November 2017
doi: 10.3389/fbioe.2017.00070

Cartilage and Muscle Cell Fate and Origins during Lizard Tail Regeneration

*Ricardo Londono[1], Wei Wenzhong[2], Bing Wang[2], Rocky S. Tuan[1] and Thomas P. Lozito[1]**

[1] Department of Orthopaedic Surgery, Center for Cellular and Molecular Engineering, University of Pittsburgh School of Medicine, Pittsburgh, PA, United States, [2] Molecular Therapy Laboratory, University of Pittsburgh School of Medicine, Pittsburgh, PA, United States

Introduction: Human cartilage is an avascular tissue with limited capacity for repair. By contrast, certain lizards are capable of musculoskeletal tissue regeneration following tail loss throughout all stages of their lives. This extraordinary ability is the result of a complex process in which a blastema forms and gives rise to the tissues of the regenerate. Blastemal cells have been shown to originate either from dedifferentiated tissues or from existing progenitor cells in various species, but their origin has not been determined in lizards. As reptiles, lizards are the closest relatives to mammals with enhanced regenerative potential, and the origin of blastemal cells has important implications for the regenerative process. Hence, the aim of this study is to determine the cellular origin of regenerated cartilage and muscle tissues in reptiles using the mourning gecko lizard as the regenerative model.

Methods: To trace the fate and differentiation potential of cartilage during tail regeneration, cartilage cells pre-labeled with the fluorescent tracer DiI were injected into lizard tails, and the contribution of cartilage cells to regenerated tail tissues was assessed by histologic examination at 7, 14, and 21 days post-tail amputation. The contribution of muscle cells to regenerated tail tissues was evaluated using muscle creatine kinase promoter-driven Cre recombinase in conjunction with the Cre-responsive green-to-red fluorescence shift construct CreStoplight. 21 days after amputation, tail tissues were analyzed by histology for red fluorescent protein (RFP)-positive cells.

Results: At 7 days post-amputation, DiI-labeled cartilage cells localized to the subapical space contributing to the blastema. At 14 and 21 days post-amputation, DiI-labeled cells remained in the subapical space and colocalized with Collagen type II (Col2) staining in the cartilage tube and myosin heavy chain (MHC) staining in regenerated muscle. Lineage tracing of myocytes showed colocalization of RFP with Col2 and MHC in differentiated tissues at 21 days post-amputation.

Conclusion: This study demonstrates that differentiated cartilage cells contribute to both regenerated muscle and cartilage tissues following tail loss, and in turn, differentiated muscle cells contribute to both tissue types as well. These findings suggest that dedifferentiation and/or transdifferentiation are at least partially responsible for the regenerative outcome in the mourning gecko.

Keywords: lizard, cartilage, muscle, tail, regeneration, blastema, dedifferentiation, epimorphosis

OPEN ACCESS

Edited by:
Roberto Narcisi, Erasmus Medical Center, Netherlands

Reviewed by:
Andrea Barbero, University-Hospital Basel, Switzerland
Roberta Tasso, Ospedale San Martino (IRCCS), Italy

****Correspondence:***
Thomas P. Lozito
tpl9@pitt.edu

Specialty section:
This article was submitted to Tissue Engineering and Regenerative Medicine, a section of the journal Frontiers in Bioengineering and Biotechnology

Received: *01 August 2017*
Accepted: *19 October 2017*
Published: *02 November 2017*

Citation:
Londono R, Wenzhong W, Wang B, Tuan RS and Lozito TP (2017) Cartilage and Muscle Cell Fate and Origins during Lizard Tail Regeneration. Front. Bioeng. Biotechnol. 5:70. doi: 10.3389/fbioe.2017.00070

INTRODUCTION

Cartilage damage usually occurs as a result of physical trauma or degenerative disease (Aurich et al., 2014; Naraghi and White, 2016; Saxby and Lloyd, 2017) oftentimes resulting in substantial pain, loss of function, and significant health-care costs (Bhatia et al., 2013; Losina et al., 2015; Brittberg et al., 2016). Unfortunately, cartilage is an avascular tissue with very limited capacity for spontaneous repair (Hunter, 1995), and although treatment strategies are available—including microfracture, mosaicplasty, and osteochondral allografts, these options have limited effectiveness and significant failure rates (Lewis et al., 2006; Farr and Yao, 2011; Tetteh et al., 2012).

In contrast to humans, certain lizard species including scincids, gekkotans, lacertids, and anoles are capable of regenerating cartilage and other musculoskeletal tissues at all stages of life (Moffat and Bellairs, 1964; Bellairs and Bryant, 1985; Alibardi, 2010; Fisher et al., 2012). When faced with a predatorial threat, these species have the ability to undergo tail autotomy—a defense mechanism through which the lizard can shed or discard its tail to distract the predator and escape the attack (Woodland, 1920; Moffat and Bellairs, 1964), and to then regenerate the missing appendage during the weeks following the event. Although some anatomical differences exist between the original tail and its regenerated counterpart—including a different scale pattern and a modified arrangement of skeletal muscle (Kamrin and Singer, 1955; Simpson, 1964; Gilbert et al., 2015), some of these differences such as the replacement of the original vertebrae with a cartilage tube that resists ossification are particularly interesting because they indicate that cartilage regeneration is, at least in some species, mechanistically possible (Lozito and Tuan, 2015).

The extraordinary regenerative response observed in lizards—known as epimorphic regeneration (Morgan, 1901)—is the result of a complex process that begins with hemostasis and re-epithelialization of the open wound immediately after tail loss. As these processes take place, soft tissues retract into the tail stump and a thickened specialized signaling epithelium known as the apical epithelial cap (AEC) begins to form (McLean and Vickaryous, 2011). The diameter of the wound starts to decrease (Cox, 1969) and cells localized distally to the original spinal cord begin to aggregate underneath the AEC resulting in the formation of the blastema (Woodland, 1920; Werner, 1967; Bellairs and Bryant, 1985; Delorme et al., 2012). The blastema is a pool of progenitor cells that becomes apparent as early as 1 week after tail loss (McLean and Vickaryous, 2011) and has the remarkable capability to give rise to the differentiated tissues of the regenerated tail, including skeletal muscle and cartilage tissue in the distal portion of the cartilage tube (French et al., 1976; Bryant et al., 1981).

Not surprisingly, the origin of cells that contribute to the blastema and eventually become the regenerated tissues has been a topic of great interest and debate not only in lizards, but in other regenerative species as well (Slack, 2006). Originally thought to be composed of a homogenous cell population, blastemal cells are now known to represent a heterogeneous population of what appear to be lineage-restricted progenitor cells (Kragl et al., 2009). The origin of blastemal cells has been investigated in "super-healing" anamniote organisms including newts and salamanders (Kragl et al., 2009; Sandoval-Guzmán et al., 2014), but the specific source of reptilian blastemal cells remains largely unknown. Since its identification in lizards, blastemal cells have been proposed to originate either from dedifferentiated tissues that acquire the ability to differentiate into other lineages as they course through the blastemal state (Needham, 1965; Burgess, 1967; Bellairs and Bryant, 1985), or from adult progenitor cells that reside in pre-existing niches and become activated when the need arises (e.g., following autotomy) (Kahn and Simpson, 1974; Zhou et al., 2013; Alibardi, 2014).

This study aims to determine the cellular origin of the differentiated cartilage and muscular tissues in the regenerated lizard tail using the mourning gecko lizards (*Lepidodactylus lugubris*) as regenerative model. The mourning gecko is a particularly versatile organism for two reasons. First, as a parthenogenic species with chromosomal polymorphism (Volobouev and Pasteur, 1988; Trifonov et al., 2015), it allows for transplantation of cells and tissues among members of the same colony without rejection, and second, as reptiles, lizards are the only amniotes with extraordinary musculoskeletal healing abilities and therefore are the closest relatives to mammals with enhanced natural regenerative potential. The mourning gecko is one of the only species that is diploid, parthenogenetic, and capable of tail regeneration. Taken together, these features make the mourning gecko an attractive model for the study of tissue regeneration and repair (Alibardi, 2010).

MATERIALS AND METHODS

All procedures were approved by and performed according to the guidelines of the Institutional Animal Care and Use Committee at the University of Pittsburgh (Protocol Number 15114947).

Cartilage Cell Isolation and Culture

Cartilage cells were isolated from cartilage tubes in mourning geckos and cultured *in vitro* for 2 weeks prior to transplantation ($n = 4$). Briefly, cartilage tubes were isolated using sterile technique as previously described (Lozito and Tuan, 2015) and washed three times in Leibovitz's L-15 medium (Gibco). Cells were isolated by placing the cartilage tubes in digestion solution and incubated for 1 h at 37°C: 40 mg trypsin (Gibco), 50 mg of collagenase II (Sigma), and 40 ml of HBSS (Gibco) containing penicillin/streptomycin (Gibco). Digestion was stopped by adding 10 ml of fetal bovine serum (FBS) (Gibco). The suspension containing dissociated cells was then filtered through a 40-μm cell strainer and the cells were centrifuged at 1,500 rpm and resuspended in cartilage cell growth media: 440 ml DMEM/F12, 50 ml FBS, 5 ml 1:1:1 penicillin/streptomycin/fungizone, 5 ml Glutamax, 5% chicken embryo extract (Gemini Bioproducts), and 20 ng/ml FGF-2 (Peprotech). Cells were plated on T-75 uncoated flasks ($n = 4$) for culture at a density of approximately five tail yield/flask. Cells were cultured to confluence (2 weeks) with media changes every 3–4 days.

Cartilage Cell Dil Labeling and Transplantation

Dil labeling of cartilage cells was performed using CellTracker™ CM-Dil (Molecular Probes, Invitrogen) following the manufacturer's instructions. Briefly, after culturing for 2-week cells were trypsinized and incubated in suspension with 1 μM Dilute Vybrant® CM-Dil labeling solution for 5 min at 37°C followed by an additional 15-min incubation at 4°C. Cells were then washed with phosphate-buffered saline (PBS) and resuspended at a density of 5,000 cells/μl. The Dil-labeled cartilage cell suspension (2.5 million cells/animal) was then injected intramuscularly in the dorsal region of the lizard tail using a BD insulin syringe and a microinjector system (Sutter Instrument). Following injection, Dil-labeled cartilage cells were allowed to engraft for 24 h and tails were amputated at injection sites. Regenerated tails were then collected at 7 days, 14 days, and 21 days post-initial amputation ($n = 4$ animals per time point).

Myocyte Lineage Tracing

Muscle creatine kinase (MCK)-Cre plasmids were constructed by replacing CAG promoters in pCAG-Cre expression plasmids (Addgene Plasmid #13775) with tMCK promoters (Wang et al., 2008). CreStoplight constructs were acquired from Addgene (Plasmid #37402). Plasmids were purified *via* CsCl gradients and resuspended in 10 mM Tris–HCl (pH 8.5) at 1.0 μg/μl. MCK-Cre and CreStoplight plasmid solutions were mixed 1:1 (1.0 μg/μl total DNA concentration) and injected (5 μl) into lizard tail blastemas (10 days postamputation) using a microinjection system (Sutter Instrument). An ECM 830 square wave electroporation system (BTX) and a pair of paddle electrodes (BTX) were used for electroporation. Five 50-V pulses with a length of 50 m and an interval of 1 s were applied to each blastema after injection. Treated tails regenerated for 2 weeks and were re-amputated. A fluoresce dissecting microscope (Leica) were used to visualize transfected muscle bundles during tail amputations. Re-amputated tails regenerated for an additional 3 weeks before sample collection ($n = 4$ animals per time point).

Tail Amputation and Sample Collection

Mourning geckos have the natural ability to autotomize their tails and exhibit several adaptations that limit pain, hemorrhage, and tissue damage including fracture planes, decreased innervation, and arterial sphincters (Woodland, 1920; Moffat and Bellairs, 1964).

Regenerated tails were harvested at predetermined time points (7, 14, and 21 days). Prior to amputation, the tails were wiped three times with alcohol wipes to remove oils in the surface that may interfere with the fixation process. Regenerated tails were removed with a sterile #10 scalpel blade by cutting 3 mm proximally to the original amputation site with the intention to include tail stump tissues in the histology sample to allow for visualization of the boundary between original and regenerated tissues. The animals were then returned to their cages and allowed to recover. Tissue samples were then fixed overnight in 4% paraformaldehyde (Electron Microscopy Sciences).

Immunohistochemistry

Following fixation, the samples were washed with PBS (Life Technologies), decalcified for 4 days in Versenate EDTA solution (American Master Tech). Processed samples were then taken through a sucrose gradient (10, 20, 30%), embedded in OCT compound (Tissue-Tek), sectioned (16 μm thick) on a cryotome (Leica), and mounted on glass slides ($n = 4$ section per sample). Antigen retrieval was performed with 1 mg/ml chondroitinase (Sigma-Aldrich) and 5 mg/ml hyaluronidase (Sigma-Aldrich) for 30 min at 37°C. Nonspecific binding was suppressed with 1% horse serum (Vector Labs) in PBS for 45 min. Slides were then washed with 0.1% Triton X-100/TBS, blocked in 1% BSA, incubated with primary antibodies against collagen type II (Col2) (Abcam), myosin heavy chain (MHC) (Developmental Studies Hybridoma Bank), and/or proliferating cell nuclear antigen (PCNA) (Abcam) overnight at 4°C, and incubated with fluorescently labeled secondary antibodies (Invitrogen) for 1 h at room temperature. Samples were counterstained with DAPI (Invitrogen) and imaged with an Olympus CKX41 microscope outfitted with a Leica DFC 3200 camera.

RESULTS

Cartilage Cells Contribute to Blastema Formation

To analyze the contribution of cartilage cells to the blastema and regenerated tissues, cartilage cells were pre-labeled *in vitro* with the fluorescent tracer Dil and injected into original tails. Two important requirements for this procedure were the verification that cartilage cell cultures were free of muscle cells prior to Dil labeling and retention of Col2 marker while *in vitro* culture to verify the differentiated state of chondrocytes throughout the duration of this process (Figure S1 in Supplementary Material). Following cell engraftment, tails were amputated at injection sites. Histologic examination of tail stumps 7 days post-amputation allowed for visualization of Dil-labeled cartilage cell distribution during the early stages of the regenerative process as blastema formation has been reported to occur as early as 1 week post-amputation (McLean and Vickaryous, 2011) (**Figure 1A**). Identification of original vertebral and skeletal muscle tissues within the tail stump was achieved by immunolabeling of Col2+ (red) and MHC+ (purple) cells, respectively. At 7 days post-amputation, Dil-labeled cartilage cells (green) were visualized at three different locations with the majority of cells remaining at the original injection site and smaller fractions of cells migrating to the subapical space in between the regenerated spinal cord and the AEC (**Figure 1B**), and adjacently to degenerating muscle (**Figures 1C–E**) (see Figure S2 in Supplementary Material for immunolabeling and vehicle control samples). Blastemal cells typically aggregate in the subapical space, therefore suggesting that cartilage cells contribute to the blastema.

Cartilage Cells Contribute to Cartilage and Muscle Formation during Regeneration

To analyze whether cartilage cells produce differentiated cartilage and/or muscle tissues during the regenerative process, Dil-labeled

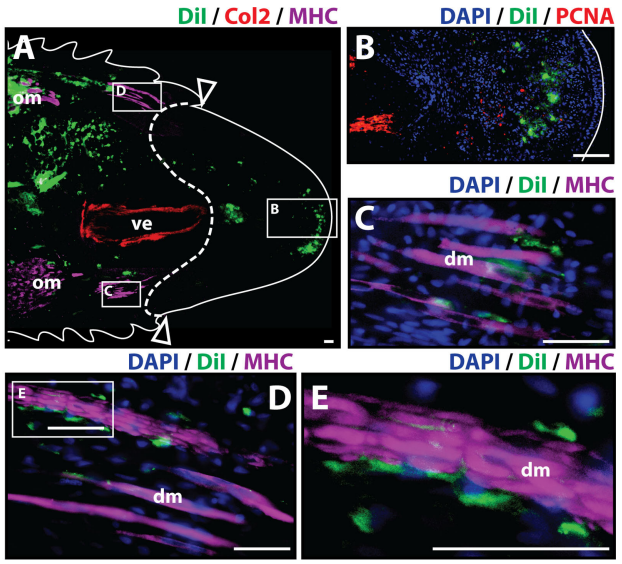

FIGURE 1 | Cartilage cells contribute to the blastema. Dil-labeled (green) cartilage cells were injected into original tails and visualized histologically 7 days post-amputation. **(A)** Longitudinal tissue sections of tail stump. Tissue section containing original tissues (left of dotted line) and regenerated tissues (right of dotted line) were immunolabeled with antibodies against Collagen type II (Col2—cartilage—red) and myosin heavy chain (MHC—muscle—purple). Dil-labeled cells (green) are visualized at the original injection site in the tail stump (left of dotted line) and contributing to the blastema in the subapical space at the distal end (inset). **(B)** Higher magnification of inset in panel (A) showing the presence of Dil-labeled cartilage cells at the site of blastema formation. **(C,D)** Higher magnification of insets in panel (A) showing association of Dil-labeled cells and degenerating muscle. **(E)** Higher magnification of inset in panel **(D)**. Nuclei are stained with DAPI (blue). b, blastema; dm, degenerated muscle; om, original muscle; ve, vertebra. Bar = 75 μm.

cartilage cells were injected into original tails, and the regenerated tissues were evaluated histologically at 14 and 21 days after amputation. At 14 days post-amputation the regenerated tail was about 0.5 cm long. The regenerated tail contained both a small segment of the early cartilage tube at its proximal end and islands of mature skeletal muscle scattered throughout its length as shown by Col2+ and MHC+ staining, respectively (**Figure 2A**). Dil-labeled cartilage cells (green) were identified in multiple locations throughout the stump and regenerated tail with the majority of cells still localizing at the original injection site in the tail stump. A more prominent contribution of Dil-labeled cells to the subapical space population was observed at 14 days in comparison to samples obtained at the 7-day time point (**Figures 2A,B**). Dil-labeled cells were also observed to colocalize with Col2+ cells (**Figures 2A,C**) and with MHC+ skeletal muscle in different segments and at various intervals throughout the regenerated tail (**Figures 2A,D–K**), suggesting that cartilage cells have the ability to mobilize beyond the blastema during the regenerative process and in fact, contribute to the regeneration of both cartilage and skeletal muscle tissues (see Figure S3 in Supplementary Material for immunolabeling and vehicle control samples).

At 21 days post-amputation (**Figure 3**), the regenerated tail measures around 1.3 cm and a mature hollow cartilage tube can be observed along its entire length of the tail accompanied by well-organized skeletal muscle in the periphery (**Figure 3A**). The most prominent presence of Dil-labeled cells at 21 days post-amputation remains at the injection site. A smaller fraction of Dil-labeled cells was visible in the subapical space (**Figures 3A,D**), and individual cells were observed to colocalize with Col2+ staining in the cartilage tube (**Figures 3C,F**) and MHC+ staining in regenerated muscle (**Figures 3B,E**) (see Figure S4 in Supplementary Material for immunolabeling and vehicle control samples). Taken together, these observations suggest that at 21 days post-amputation, cartilage cells contribute to regenerated cartilage and skeletal muscle tissues while remaining at the subapical space as a possible reservoir for these tissues as the regenerated tail grows.

Muscle Cells Contribute to Cartilage and Muscle Formation

To study whether muscle cells contribute to differentiated cartilage and/or muscle tail tissues during the regenerative process, it was necessary to selectively label myocytes during regeneration. Myocyte lineage tracing was achieved through the use of MCK promoter-driven Cre recombinase in conjunction with a Cre-responsive green-to-red fluorescence shift construct (CreStoplight) (**Figure 4A**). Following injection of plasmids into tail blastemas and electroporation, tails were allowed to regenerate for 2 weeks and red fluorescent protein (RFP) expression was confirmed to be confined to the myocyte lineage by colocalization with MHC+ immunolabeling prior to re-amputation (**Figure 4B**). After re-amputation, lizard tails were allowed to regenerate for an additional 21 days before sample collection and immunolabeling. Histologic examination demonstrated colocalization of RFP and MHC+ cells (**Figures 4C,D**) as well as colocalization of RFP and Col2+ cells (**Figures 4C,E**) (see Figure S5 in Supplementary Material for higher magnification lineage tracing images). These findings suggest that differentiated muscle cells contribute to both regenerated cartilage and skeletal muscle tissues.

DISCUSSION

The present study confirms that during the process of tail regeneration, differentiated cartilage cells contribute to muscle regeneration and reciprocally, differentiated muscle cells contribute to cartilage regeneration in the mourning gecko. These findings suggest that dedifferentiation and/or transdifferentiation may be at least partially responsible for the regenerative outcome observed in this species.

The cellular origin of blastemal cells in organisms capable of epimorphic regeneration has been a topic of great interest and debate for decades (Slack, 2006). In various protostome and deuterostome organisms, both stem cells and dedifferentiated cell populations have been shown to contribute to blastemal formation. For example, in platyhelminthes and acoels, blastemas seem to form exclusively from stem cells (Bely and Nyberg, 2010), whereas in amphibian species, both mechanisms seem to contribute to this process. In a recent study, Kragl et al. (2009) used an integrated GFP transgene to track the major limb tissues during

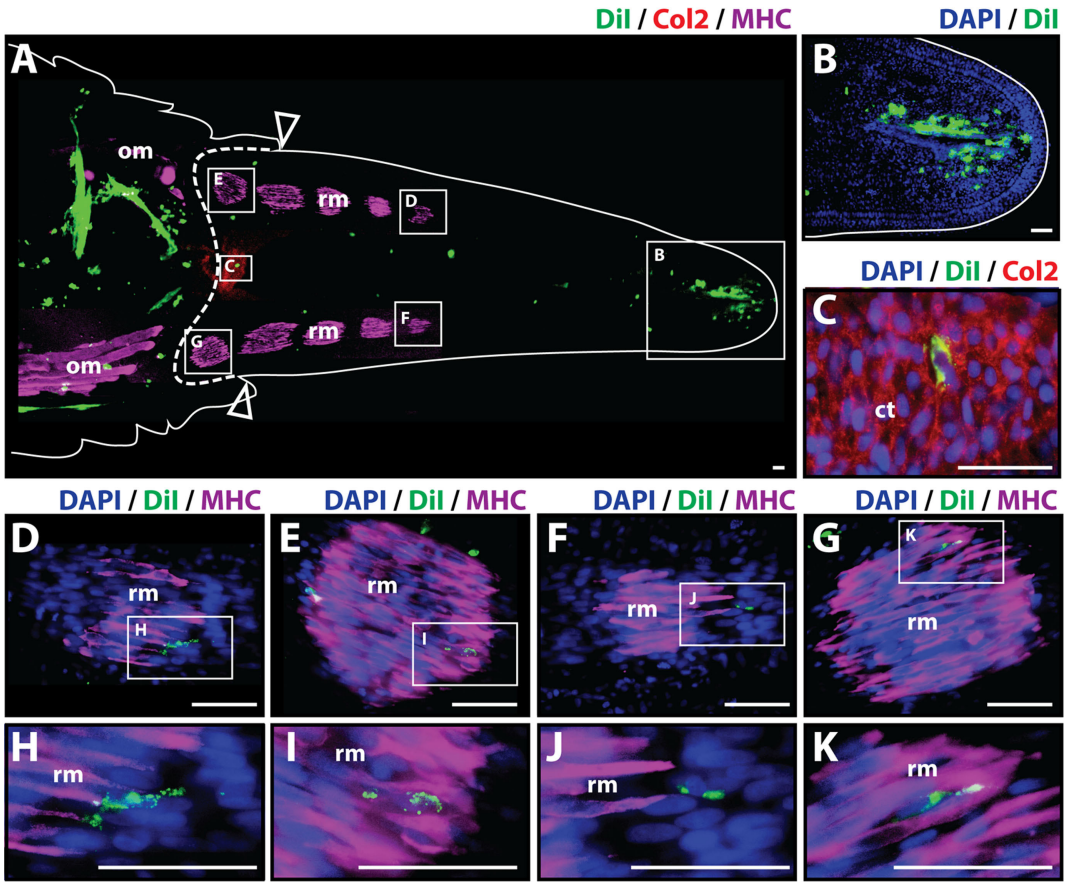

FIGURE 2 | Cartilage cells contribute to cartilage and muscle formation. DiI-labeled (green) cartilage cells were injected into original tails and visualized histologically 14 days post-amputation. **(A)** Longitudinal tissue section of regenerated tail. Tissue section includes original tissues (left of dotted line) and regenerated tissues (right of dotted line). Sections were immunolabeled with antibodies against Collagen type II (Col2—cartilage—red) and myosin heavy chain (MHC—muscle—purple). DiI-labeled cells (green) are visualized at the original injection site in the tail stump (left of dotted line) and subapical space at the distal end (inset B). **(B)** Higher magnification of inset in panel (A) showing the presence of DiI-labeled cartilage cells in the subapical space. **(C)** Higher magnification of inset in panel (A) showing the colocalization of DiI-labeled cells and Col2+ staining (cartilage). **(D–G)** Higher magnification of insets in panel (A) showing colocalization of MHC+ staining (muscle) and DiI-labeled cartilage cells. **(H–K)** Higher magnification of insets of panel **(D)** through panel **(G)**. Nuclei are stained with DAPI (blue). b, blastema; om, original muscle; ct, cartilage tube; rm, regenerated muscle. Bar = 75 μm.

limb regeneration in the axolotl. This study showed that each major tissue produces progenitor cells with restricted potential within their embryonic layer: Dermis was able to produce cartilage and tendons, but not muscle or Schwann cells; muscle cells were able to regenerate muscle but not cartilage; cartilage was able to produce tendons and dermis, but not muscle; and in turn, Schwann cells were found to be restricted to nerve tracts. This study concluded that limb blastema cells do not switch between embryonic germ layers, although they do maintain some fate flexibility, and therefore, differentiated tissues do not necessarily have to completely dedifferentiate into a pluripotent state during limb regeneration.

The differentiation ranges during tail regeneration appear to be somewhat more promiscuous. For example, both muscle cells and GFAP+ ependymal cells contribute to cartilage cells during salamander tail regeneration (Echeverri et al., 2001; Echeverri and Tanaka, 2002). Findings in this study in the regenerated tail of the mourning gecko partially corroborate these observations. This study shows that muscle cells contribute to regenerated cartilage and that cartilage cells can form muscle during lizard tail regrowth. Thus, findings concerning regenerating tails are in direct contrast to the hard lineage restrictions reported during limb regeneration and suggest that different rules apply to limb versus tail regeneration in terms of cell differentiation potential. These differences may reflect the embryonic differences in the cell sources that make up limb vs. tail buds. For example, unlike limb buds, tail bud mesenchyme give rise to skeletal, muscular, and ectodermal lineages (Griffith et al., 1992). Future work will study the limits of lineage flexibility during tail regeneration by investigating the degree of crossing between mesodermal and ectodermal lineages.

The concept of cellular dedifferentiation is not new. Contribution from dedifferentiated cells to the regenerative process was first described by Elizabeth D. Hay based on electron microscopy studies (Hay, 1959). The concept was further confirmed *via* lineage tracing experiments using triploid axolotl donor

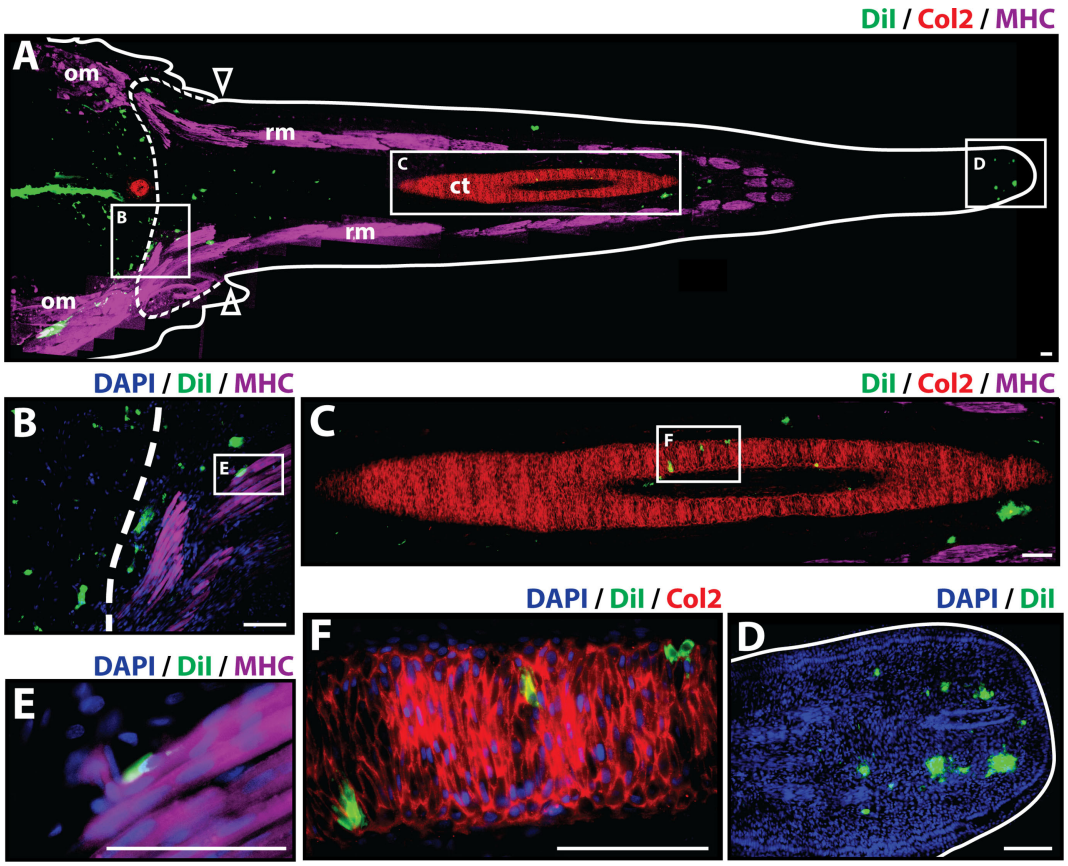

FIGURE 3 | Cartilage cells contribute to cartilage and muscle formation. DiI-labeled (green) cartilage cells were injected into original tails and visualized histologically 21 days post-amputation. **(A)** Longitudinal tissue section of regenerated tail. Tissue section includes original tissues (left of dotted line) and regenerated tissues (right of dotted line). Sections were immunolabeled with antibodies against Collagen type II (Col2—cartilage—red) and myosin heavy chain (MHC—muscle—purple). DiI-labeled cells (green) are visualized at the original injection site in the tail stump (left of dotted line), colocalized with MHC+ staining (inset B), colocalizing with Col2 staining in the cartilage tube (inset C), and in subapical space at the distal end (inset D). **(B)** Higher magnification of inset B in panel (A) showing colocalization of MHC+ staining (muscle) and DiI-labeled cartilage cells. **(C)** Higher magnification of inset C in panel (A) showing colocalization of Col2+ staining (cartilage) and DiI-labeled cartilage cells. **(D)** Higher magnification of inset D in panel (A) showing DiI-labeled cartilage cells in the subapical space. **(E)** Higher magnification of inset E in panel (B) showing colocalization of MHC+ staining (muscle) and DiI-labeled cartilage cells. **(F)** Higher magnification of inset F in panel (C) showing the colocalization of DiI-labeled cells and Col2+ staining (cartilage). Nuclei are stained with DAPI (blue). b, blastema; om, original muscle; ct, cartilage tube; rm, regenerated muscle. Bar = 75 μm.

tissue implanted into a diploid host (Namenwirth, 1974) and *via* implantation of labeled myotubes that subsequently formed multiple cell types after regeneration (Lo et al., 1993; Kumar et al., 2000). Other cell types such as Schwan cells have also been suggested to undergo dedifferentiation and metaplasia during regeneration (Wallace, 1972). However, as previously mentioned, dedifferentiation is not the only mechanism by which blastema can form in urodeles. A more recent study by Sandoval-Guzmán et al. (2014) showed that there seems to be heterogeneity with respect to the origin of blastemal cells even within closely related species. In this study, two salamander species were investigated: *Notophthalmus viridescens* (newts) and *Ambystoma mexicanum* (axolotl). This study found that myofiber dedifferentiation was an important part for limb regeneration in the newt but not in the axolotl. In the newt, myofiber fragmentation gives rise to proliferating, PAX7− mononuclear cells in the blastema that subsequently give rise to the muscle in the new limb, whereas in the axolotl, myofibers do not give rise to proliferating cells, nor do they contribute to newly regenerated muscle. Instead, resident PAX7+ cells appear to be responsible for the muscle regenerative activity in this species. The heterogeneity with respect to blastemal cell origin among closely related species may further explain the discrepancies between our findings in the mourning gecko and other regenerative organisms.

Besides heterogeneity with respect to blastemal cell origin, there are other important differences between epimorphic regeneration in amphibians and reptiles. While newts and salamanders have the ability to faithfully regenerate their limbs and tail as near perfect replicas of the original tissues (Stocum and Cameron, 2011)—and therefore are an appealing regenerative model, reptiles have a more restricted regenerative potential with only a limited number of lizard species being capable of regenerating an imperfect copy of the original tail (Bellairs and Bryant, 1985; Alibardi, 2010; Fisher et al., 2012). However,

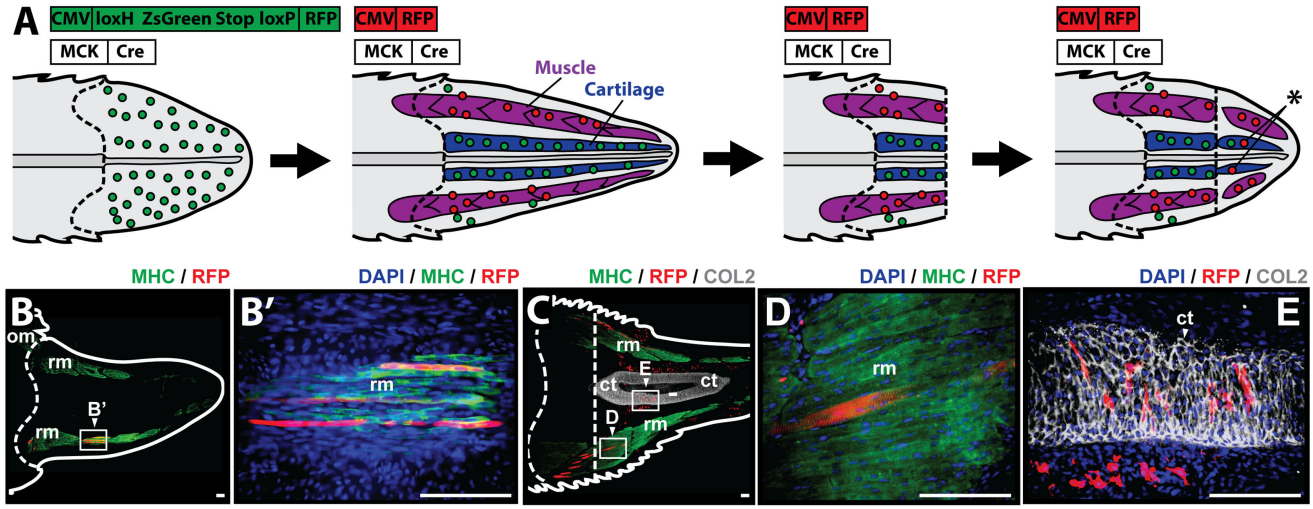

FIGURE 4 | Muscle cells contribute to cartilage and muscle formation. **(A)** Experimental scheme for tracing muscle cells during lizard tail regeneration. Tail blastemas are co-transfected with muscle creatine kinase (MCK) promoter-driven Cre expression reporters and CreStoplight constructs. Activation of MCK-Cre causes mature muscle cells to switch from green-to-red fluorescence. Regenerated tails are re-amputated and regenerate, and red fluorescent cells that have incorporated into non-muscle tissues indicate reporter cells that have switched lineages (asterisk). Muscle tissue is colored purple, and cartilage is colored blue. Dashed lines mark amputation planes. **(B)** Two weeks after injection and electrophoresis, red fluorescent protein (RFP) expression colocalizes with MHC+ staining confirming confinement to myocyte lineage. **(C)** Tails are re-amputated (dotted line), and allowed to regenerate for an additional 21 days. RFP containing cells colocalize with panels **(C,D)** MHC+ muscle cells and **(C,E)** Col2+ cartilage cells. Nuclei are stained with DAPI (blue). b, blastema; om, original muscle; ct, cartilage tube; rm, regenerated muscle. Bar = 75 μm.

newts and salamanders are anamniote organisms and therefore do not entirely replicate the developmental processes seen in mammals. As reptiles, on the other hand, lizards share many features with other amniote organisms including similar embryonic development, thyroid-hormone-dependent transition from a two-layered periderm to cornified epithelium, absence of metamorphosis, and the presence of amnion, chorion, and allantois membranes around the embryo. Hence, reptiles more closely recapitulate many of the developmental processes seen in mammals, and as such, are a valuable tool for the study of tissue regeneration and repair and the clinical translation of these findings.

The diverse origin of cell populations that contribute to the regenerated tissues may have important implications for the regenerative process. While the proximal region of the cartilage tube undergoes ossification, the distal region resists ossification and remains indefinitely as an intact cartilage-based structure (Lozito and Tuan, 2015, 2016). This difference may be explained by the heterogeneity of the cells that contribute to the cartilage tube. Both blastemal cells and progenitor cells within the perichondrium and periosteum have been shown to contribute to CT formation (Arai et al., 2002; Yoshimura et al., 2007; Lozito and Tuan, 2015), but fate mapping studies have shown that while the ossified portion of the CT is derived from periosteal progenitor cells in response to bone morphogenic property and Indian hedgehog signaling, the cartilaginous region that resists ossification is derived from blastemal cells responding to Shh signals from the spinal cord (Lozito and Tuan, 2015). Hence, cellular origin may play a key role in the determination of cell fate in lizard tail regeneration.

Most adult mammals have very limited regenerative potential, as the default healing response after significant injury typically leads to non-functional tissue deposition with scar tissue formation. In mammals, true regeneration is restricted to a few tissues including the bone marrow, the endometrium, and to a certain extent, the epidermis. As an avascular tissue, cartilage is particularly unsuitable for regeneration (Hunter, 1995), and skeletal muscle does not have the ability regenerate after volumetric muscle loss (Pollot and Corona, 2016). Interestingly, certain species such as the MRL (Clark et al., 1998) mouse and Spiny mouse (Seifert et al., 2012) have been observed to present features of blastema-based epimorphic regeneration, and hence, understanding the mechanisms or cartilage and muscle regeneration in other amniote animals such as the mourning gecko is particularly important.

The present study has a number of limitations. First, due to difficulty obtaining a significant yield, cartilage cells for Dil labeling and tracing after tail stump injection were isolated from regenerated cartilage tubes, not from original cartilage tissues *per se*, and therefore, these finding and conclusions may not apply to original cartilage cells. Second, the presence of Dil-labeled cells in the blastema was confirmed *via* localization of Dil-labeled cells to the blastema site, not by confirmed co-expression of progenitor cell markers due to lack of antibodies against these markers in this species. Likewise, the contribution of both cartilage and muscle cells to differentiated cartilage and muscle tissues was confirmed *via* colocalization of Dil and RFP with Col2+ staining in cartilage cells and MHC+ staining in muscle cells, respectively, and was not exhaustively investigated in other tissues. Finally, we were unable to use the

same experimental approach to investigate both chondrocyte and myocyte contributions. Specifically, all tested aggrecan promoter-driven constructs proved unsatisfactory for specifically labeling lizard cartilage tube cells. Thus, it was necessary to utilize Dil labeling of isolated chondrocytes, as opposed to electroporation with lineage-specific plasmids as it was done with myocytes, to trace cartilage contributions to regenerated tail tissues.

Maintenance of Col2+ staining by the embryonic growth plate-derived chondrocytes throughout the *in vitro* culture phase of the experiments confirmed the sustained differentiated state of these cells prior to injection—as differentiated chondrocytes from other species, including mammals, have been known to dedifferentiate in culture (Barbero et al., 2003; Tallheden et al., 2003), and even differentiate into myoblastic cells (de la Fuente et al., 2004). Hence, these results suggests that differentiated cartilage and muscle tissues may contribute to blastema formation and both regenerated lineages, but it does not address the question of whether this contribution occurs *via* dedifferentiation or *via* transdifferentiation nor does it examine the contribution of existing stem cell populations to regenerated tissues and therefore whether dedifferentiation/transdifferentiation is absolutely necessary for regeneration or merely contributes to this process remains to be addressed.

SUMMARY

In this study, we use the fluorescent tracer Dil and a creatine kinase promoter-driven Cre recombinase in conjunction with the Cre-responsive green-to-red fluorescence shift construct to trace the fate and differentiation potential of cartilage and muscles cells during tail regeneration in the mourning gecko. Our findings indicate that differentiated cartilage cells contribute to muscle tissues and reciprocally, differentiated muscle cells contribute to cartilage tissues during tail regeneration. These findings suggest that dedifferentiation and/or transdifferentiation are at least partially responsible for the regenerative outcome observed in this species.

ETHICS STATEMENT

All procedures were approved by and performed according to the guidelines of the Institutional Animal Care and Use Committee at the University of Pittsburgh (Protocol Number 15114947).

AUTHOR CONTRIBUTIONS

RL, WW, BW, and TL: experimental design, data gathering/interpretation, and writing.

ACKNOWLEDGMENTS

The authors thank members of the Tuan lab for helpful discussion and the two anonymous reviewers for the insightful comments on the manuscript. They apologize to the many authors whose work could not be sited owing to space constraints.

FUNDING

Funding for this research was provided by NIH National Research Service Award (NRSA) Grant Number GM115444.

SUPPLEMENTARY MATERIAL

The Supplementary Material for this article can be found online at http://www.frontiersin.org/article/10.3389/fbioe.2017.00070/full#supplementary-material.

REFERENCES

Alibardi, L. (2010). Morphological and cellular aspects of tail and limb regeneration in lizards: a model system with implications for tissue regeneration in mammals. *Adv. Anat. Embryol. Cell Biol.* 207, 1–122. doi:10.1007/978-3-642-03733-7_1

Alibardi, L. (2014). Immunolocalization of Nestin in the lizard *Podarcis muralis* indicates up-regulation during the process of tail regeneration and epidermal differentiation. *Ann. Anat.* 196, 135–143. doi:10.1016/j.aanat.2013.12.004

Arai, F., Ohneda, O., Miyamoto, T., Zhang, X. Q., and Suda, T. (2002). Mesenchymal stem cells in perichondrium express activated leukocyte cell adhesion molecule and participate in bone marrow formation. *J. Exp. Med.* 195, 1549–1563. doi:10.1084/jem.20011700

Aurich, M., Hofmann, G. O., Rolauffs, B., and Gras, F. (2014). Differences in injury pattern and prevalence of cartilage lesions in knee and ankle joints: a retrospective cohort study. *Orthop. Rev. (Pavia).* 6, 5611. doi:10.4081/or.2014.5611

Barbero, A., Ploegert, S., Heberer, M., and Martin, I. (2003). Plasticity of clonal populations of dedifferentiated adult human articular chondrocytes. *Arthritis Rheum.* 48, 1315–1325. doi:10.1002/art.10950

Bellairs, A., and Bryant, S. V. (1985). "Autotomy and regeneration in reptiles," in *Biology of the Reptilia, Vol. 15: Development B*. John Wiley & Sons, Inc., 301–410.

Bely, A. E., and Nyberg, K. G. (2010). Evolution of animal regeneration: re-emergence of a field. *Trends Ecol. Evol.* 25, 161–170. doi:10.1016/j.tree.2009.08.005

Bhatia, D., Bejarano, T., and Novo, M. (2013). Current interventions in the management of knee osteoarthritis. *J. Pharm. Bioallied Sci.* 5, 30–38. doi:10.4103/0975-7406.106561

Brittberg, M., Gomoll, A. H., Canseco, J. A., Far, J., Lind, M., and Hui, J. (2016). Cartilage repair in the degenerative ageing knee. *Acta Orthop.* 87, 26–38. doi:10.1080/17453674.2016.1265877

Bryant, S. V., French, V., and Bryant, P. J. (1981). Distal regeneration and symmetry. *Science* 212, 993–1002. doi:10.1126/science.212.4498.993

Burgess, A. M. C. (1967). The developmental potentialities of regeneration blastema cell nuclei as determined by nuclear transplantation. *J. Embryol. Exp. Morphol.* 18, 27–41.

Clark, L. D., Clark, R. K., and Heber-Katz, E. (1998). A new murine model for mammalian wound repair and regeneration. *Clin. Immunol. Immunopathol.* 88, 35–45. doi:10.1006/clin.1998.4519

Cox, P. G. (1969). Some aspects of tail regeneration in the lizard, *Anolis carolinensis*. I. A description based on histology and autoradiography. *J. Exp. Zool.* 171, 127–149. doi:10.1002/jez.1401710202

de la Fuente, R., Abad, J. L., García-Castro, J., Fernández-Miguel, G., Petriz, J., Rubio, D., et al. (2004). Dedifferentiated adult articular chondrocytes: a population of human multipotent primitive cells. *Exp. Cell Res.* 297, 313–328. doi:10.1016/j.yexcr.2004.02.026

Delorme, S. L., Lungu, I. M., and Vickaryous, M. K. (2012). Scar-free wound healing and regeneration following tail loss in the leopard gecko, *Eublepharis macularius*. *Anat. Rec. (Hoboken)* 295, 1575–1595. doi:10.1002/ar.22490

Echeverri, K., Clarke, J. D., and Tanaka, E. M. (2001). In vivo imaging indicates muscle fiber dedifferentiation is a major contributor to the regenerating tail blastema. *Dev. Biol.* 236, 151–164. doi:10.1006/dbio.2001.0312

Echeverri, K., and Tanaka, E. M. (2002). Ectoderm to mesoderm lineage switching during axolotl tail regeneration. *Science* 298, 1993–1996. doi:10.1126/science.1077804

Farr, J., and Yao, J. Q. (2011). Chondral defect repair with particulated juvenile cartilage allograft. *Cartilage* 2, 346–353. doi:10.1177/1947603511405838

Fisher, R. E., Geiger, L. A., Stroik, L. K., Hutchins, E. D., George, R. M., Denardo, D. F., et al. (2012). A histological comparison of the original and regenerated tail in the green anole, *Anolis carolinensis*. *Anat. Rec. (Hoboken)* 295, 1609–1619. doi:10.1002/ar.22537

French, V., Bryant, P. J., and Bryant, S. V. (1976). Pattern regulation in epimorphic fields. *Science* 193, 969–981. doi:10.1126/science.948762

Gilbert, E. A. B., Delorme, S. L., and Vickaryous, M. K. (2015). The regeneration blastema of lizards: an amniote model for the study of appendage replacement. *Regeneration* 2, 45–53. doi:10.1002/reg2.31

Griffith, C. M., Wiley, M. J., and Sanders, E. J. (1992). The vertebrate tail bud: three germ layers from one tissue. *Anat. Embryol.* 185, 101–113. doi:10.1007/BF00185911

Hay, E. D. (1959). Electron microscopic observations of muscle dedifferentiation in regenerating *Amblystoma* limbs. *Dev. Biol.* 1, 555–585. doi:10.1016/0012-1606(59)90018-1

Hunter, W. (1995). Of the structure and disease of articulating cartilages. 1743. *Clin. Orthop. Relat. Res.* 9, 3–6.

Kahn, E. B., and Simpson, S. B. (1974). Satellite cells in mature, uninjured skeletal muscle of the lizard tail. *Dev. Biol.* 37, 219–223. doi:10.1016/0012-1606(74)90181-X

Kamrin, R. P., and Singer, M. (1955). The influence of the spinal cord in regeneration of the tail of the lizard, *Anolis carolinensis*. *J. Exp. Zool.* 128, 611–627. doi:10.1002/jez.1401280314

Kragl, M., Knapp, D., Nacu, E., Khattak, S., Maden, M., Epperlein, H. H., et al. (2009). Cells keep a memory of their tissue origin during axolotl limb regeneration. *Nature* 460, 60–65. doi:10.1038/nature08152

Kumar, A., Velloso, C. P., Imokawa, Y., and Brockes, J. P. (2000). Plasticity of retrovirus-labelled myotubes in the newt limb regeneration blastema. *Dev. Biol.* 218, 125–136. doi:10.1006/dbio.1999.9569

Lewis, P. B., McCarty, L. P., Kang, R. W., and Cole, B. J. (2006). Basic science and treatment options for articular cartilage injuries. *J. Orthop. Sport. Phys. Ther.* 36, 717–727. doi:10.2519/jospt.2006.2175

Lo, D. C., Allen, F., and Brockes, J. P. (1993). Reversal of muscle differentiation during urodele limb regeneration. *Proc. Natl. Acad. Sci. U. S. A.* 90, 7230–7234. doi:10.1073/pnas.90.15.7230

Losina, E., Paltiel, A. D., Weinstein, A. M., Yelin, E., Hunter, D. J., Chen, S. P., et al. (2015). Lifetime medical costs of knee osteoarthritis management in the United States: impact of extending indications for total knee arthroplasty. *Arthritis Care Res. (Hoboken).* 67, 203–215. doi:10.1002/acr.22412

Lozito, T. P., and Tuan, R. S. (2015). Lizard tail regeneration: regulation of two distinct cartilage regions by Indian hedgehog. *Dev. Biol.* 399, 249–262. doi:10.1016/j.ydbio.2014.12.036

Lozito, T. P., and Tuan, R. S. (2016). Lizard tail skeletal regeneration combines aspects of fracture healing and blastema-based regeneration. *Development* 143, 2946–2957. doi:10.1242/dev.129585

McLean, K. E., and Vickaryous, M. K. (2011). A novel amniote model of epimorphic regeneration: the leopard gecko, *Eublepharis macularius*. *BMC Dev. Biol.* 11:50. doi:10.1186/1471-213X-11-50

Moffat, L. A., and Bellairs, A. D. (1964). The regenerative capacity of the tail in embryonic and post-natal lizards (*Lacerta vivipara* Jacquin). *J. Embryol. Exp. Morphol.* 12, 769–786.

Morgan, T. H. (1901). *Regeneration*. New York: Macmillan.

Namenwirth, M. (1974). The inheritance of cell differentiation during limb regeneration in the axolotl. *Dev. Biol.* 41, 42–56. doi:10.1016/0012-1606(74)90281-4

Naraghi, A. M., and White, L. M. (2016). Imaging of athletic injuries of knee ligaments and menisci: sports imaging series. *Radiology* 281, 23–40. doi:10.1148/radiol.2016152320

Needham, A. E. (1965). *Regeneration in Animals and Related Problems*, eds V. Kiortsis and H. A. L. Trampusch (Amsterdam: North-Holland Pub. Co.).

Pollot, B. E., and Corona, B. T. (2016). Volumetric muscle loss. *Methods Mol. Biol.* 1460, 19–31. doi:10.1007/978-1-4939-3810-0_2

Sandoval-Guzmán, T., Wang, H., Khattak, S., Schuez, M., Roensch, K., Nacu, E., et al. (2014). Fundamental differences in dedifferentiation and stem cell recruitment during skeletal muscle regeneration in two salamander species. *Cell Stem Cell* 14, 174–187. doi:10.1016/j.stem.2013.11.007

Saxby, D. J., and Lloyd, D. G. (2017). Osteoarthritis year in review 2016: mechanics. *Osteoarthr. Cartil.* 25, 190–198. doi:10.1016/j.joca.2016.09.023

Seifert, A. W., Kiama, S. G., Seifert, M. G., Goheen, J. R., Palmer, T. M., and Maden, M. (2012). Skin shedding and tissue regeneration in African spiny mice (Acomys). *Nature* 489, 561–565. doi:10.1038/nature11499

Simpson, S. B. (1964). Analysis of tail regeneration in the lizard *Lygosoma laterale*. I. Initiation of regeneration and cartilage differentiation: the role of ependyma. *J. Morphol.* 114, 425–435. doi:10.1002/jmor.1051140305

Slack, J. M. W. (2006). Amphibian muscle regeneration – dedifferentiation or satellite cells? *Trends Cell Biol.* 16, 273–275. doi:10.1016/j.tcb.2006.04.007

Stocum, D. L., and Cameron, J. A. (2011). Looking proximally and distally: 100 years of limb regeneration and beyond. *Dev. Dyn.* 240, 943–968. doi:10.1002/dvdy.22553

Tallheden, T., Dennis, J. E., Lennon, D. P., Sjögren-Jansson, E., Caplan, A. I., and Lindahl, A. (2003). Phenotypic plasticity of human articular chondrocytes. *J. Bone Joint Surg. Am.* 85–A(Suppl.),93–100. doi:10.2106/00004623-200300002-00012

Tetteh, E. S., Bajaj, S., Ghodadra, N. S., and Cole, B. J. (2012). The basic science and surgical treatment options for articular cartilage injuries of the knee. *J. Orthop. Sport. Phys. Ther.* 42, 243–253. doi:10.2519/jospt.2012.3673

Trifonov, V. A., Paoletti, A., Caputo Barucchi, V., Kalinina, T., O'Brien, P. C., Ferguson-Smith, M. A., et al. (2015). Comparative chromosome painting and NOR distribution suggest a complex hybrid origin of triploid *Lepidodactylus lugubris* (Gekkonidae). *PLoS ONE* 10:e0132380. doi:10.1371/journal.pone.0132380

Volobouev, V., and Pasteur, G. (1988). Presumptive sex chromosomes of a unisexual homomorphic species of lizards, *Lepidodactylus lugubris*. *Heredity (Edinb)* 60, 463–467. doi:10.1038/hdy.1988.65

Wallace, H. (1972). The components of regrowing nerves which support the regeneration of irradiated salamander limbs. *J. Embryol. Exp. Morphol.* 28, 419–435.

Wang, B., Li, J., Fu, F. H., Chen, C., Zhu, X., Zhou, L., et al. (2008). Construction and analysis of compact muscle-specific promoters for AAV vectors. *Gene Ther.* 15, 1489–1499. doi:10.1038/gt.2008.104

Werner, Y. L. (1967). Regeneration of the caudal axial skeleton in a gekkonid lizard (*Hemidactylus*) with particular reference to the 'latent' period. *Acta Zool.* 48, 103–125. doi:10.1111/j.1463-6395.1967.tb00134.x

Woodland, W. N. F. (1920). Memoirs: some observations on caudal autotomy and regeneration in the gecko (*Hemidactylus flaviviridis*, Rappel), with notes on the tails of *Sphenodon* and *Pygopus*. *Q. J. Microsc. Sci.* s2-65, 63–100.

Yoshimura, H., Muneta, T., Nimura, A., Yokoyama, A., Koga, H., and Sekiya, I. (2007). Comparison of rat mesenchymal stem cells derived from bone marrow, synovium, periosteum, adipose tissue, and muscle. *Cell Tissue Res.* 327, 449–462. doi:10.1007/s00441-006-0308-z

Zhou, Y., Xu, Q., Li, D., Zhao, L., Wang, Y., Liu, M., et al. (2013). Early neurogenesis during caudal spinal cord regeneration in adult Gekko japonicus. *J. Mol. Histol.* 44, 291–297. doi:10.1007/s10735-012-9466-3

Conflict of Interest Statement: This research was conducted in the absence of any commercial or financial relationships that could be construed as a potential conflict of interest.

frontiers in Bioengineering and Biotechnology

REVIEW
published: 15 May 2018
doi: 10.3389/fbioe.2018.00058

Microenvironmental Regulation of Chondrocyte Plasticity in Endochondral Repair—A New Frontier for Developmental Engineering

Sarah A. Wong[1,2], *Kevin O. Rivera*[1,2], *Theodore Miclau III*[1], *Eben Alsberg*[3], *Ralph S. Marcucio*[1,2] *and Chelsea S. Bahney*[1]*

[1] Department of Orthopaedic Surgery, Orthopaedic Trauma Institute, University of California, San Francisco, San Francisco, CA, United States, [2] School of Dentistry, University of California, San Francisco, San Francisco, CA, United States, [3] Department of Orthopaedic Surgery and Biomedical Engineering, Case Western Reserve University, Cleveland, OH, United States

OPEN ACCESS

Edited by:
Eric Farrell, Erasmus University Rotterdam, Netherlands

Reviewed by:
Natalina Quarto, University of Naples Federico II, Italy
Sourabh Ghosh, Indian Institute of Technology Delhi, India

***Correspondence:**
Chelsea S. Bahney
Chelsea.Bahney@ucsf.edu

Specialty section:
This article was submitted to Tissue Engineering and Regenerative Medicine, a section of the journal Frontiers in Bioengineering and Biotechnology

Received: *01 February 2018*
Accepted: *23 April 2018*
Published: *15 May 2018*

Citation:
Wong SA, Rivera KO, Miclau T III, Alsberg E, Marcucio RS and Bahney CS (2018) Microenvironmental Regulation of Chondrocyte Plasticity in Endochondral Repair—A New Frontier for Developmental Engineering. Front. Bioeng. Biotechnol. 6:58. doi: 10.3389/fbioe.2018.00058

The majority of fractures heal through the process of endochondral ossification, in which a cartilage intermediate forms between the fractured bone ends and is gradually replaced with bone. Recent studies have provided genetic evidence demonstrating that a significant portion of callus chondrocytes transform into osteoblasts that derive the new bone. This evidence has opened a new field of research aimed at identifying the regulatory mechanisms that govern chondrocyte transformation in the hope of developing improved fracture therapies. In this article, we review known and candidate molecular pathways that may stimulate chondrocyte-to-osteoblast transformation during endochondral fracture repair. We also examine additional extrinsic factors that may play a role in modulating chondrocyte and osteoblast fate during fracture healing such as angiogenesis and mineralization of the extracellular matrix. Taken together the mechanisms reviewed here demonstrate the promising potential of using developmental engineering to design therapeutic approaches that activate endogenous healing pathways to stimulate fracture repair.

Keywords: fracture, endochondral ossification, chondrocyte fate, developmental engineering, transdifferentiation

INTRODUCTION

Fractures heal through two pathways: endochondral ossification and intramembranous ossification (Thompson et al., 2002; Bahney et al., 2015). Both processes begin with the differentiation of local osteochondral progenitor cells found within the periosteum and endosteum (Colnot, 2009; Duchamp de Lageneste et al., 2018). During endochondral ossification, or indirect bone healing, progenitor cells primarily derived from the periosteum differentiate into chondrocytes to form a cartilage callus between the fractured bone ends (Duchamp de Lageneste et al., 2018). This cartilage is gradually replaced with bone in a process that resembles embryonic bone development and post-natal growth. Intramembranous ossification, or direct bone healing, occurs when periosteal and endosteal progenitor cells differentiate directly into osteoblasts. Fate of the osteochondral progenitor is determined by the relative stability of the fracture site, with motion stimulating

endochondral ossification and rigid microenvironments promoting intramembranous ossification (Thompson et al., 2002). In most cases, both healing pathways occur simultaneously such that a robust cartilage callus forms at the center of the fracture where the degree of motion is greatest, and intramembranous bone forms along the periosteal and endosteal surfaces (Thompson et al., 2002). Endochondral ossification is the predominant mechanism by which the majority of fractures heal and is the focus of this review (Silkstone et al., 2008; Bahney et al., 2015).

Formation of the cartilage callus functionally serves to stabilize the gap between the bone ends. To form the cartilage callus periosteal osteochondral progenitor cells migrate from the periosteum and undergo chondrogenic differentiation (Colnot, 2009). This occurs on top of the provisional fibrin matrix formed by the hematoma (Xing et al., 2010a). Growth factors produced by the hematoma promote cell migration and differentiation and also create a unique microenvironment with low pH and high lactate concentration (Wray, 1964). Formation of the hematoma and a strong pro-inflammatory response are essential to establishing a robust healing response (Park et al., 2002).

Following the initial hematoma, the subsequent steps of chondrogenesis and chondrocyte hypertrophy appear to parallel the molecular pathways involved in endochondral ossification in the growth plate during bone development (Kronenberg, 2003; Long and Ornitz, 2013). Chondrogenic programming is initiated by the expression of transcription factor Sox9, which is required for chondrogenesis (Bi et al., 1999; Akiyama et al., 2002). Sox9 regulates the expression of several chondrocyte-specific matrix components including collagen type II and aggrecan, the two predominant proteins within the cartilage matrix (Bell et al., 1997; Sekiya et al., 2000). This initial extracellular matrix is avascular and aneural until blood vessels and nerves penetrate the soft callus during later stages of healing (Gerber et al., 1999; Tatsuyama et al., 2000; Grässel, 2014; Hu et al., 2017). As chondrocytes mature, they produce collagen type X, mineralize their surrounding matrix, and undergo hypertrophy, increasing in volume and dry mass by ∼20-fold (Cooper et al., 2013).

There has been a centuries-long debate regarding the subsequent fate of hypertrophic chondrocytes during endochondral bone development and repair. In the early 1800's, cartilage was believed to turn into bone (Beresford, 1981; Hall, 2015). However, in the mid-1800's, Muller and Sharpy changed this paradigm by claiming that chondrocytes are terminally-differentiated and ultimately undergo cell death, resulting in the replacement of cartilage with bone derived from a separate population of cells (Beresford, 1981; Hall, 2015). The latter model of chondrocyte fate, for the most part, dominated in textbooks and became the *de facto* model of endochondral ossification. In recent years, modern murine genetics has enabled lineage tracing studies that can more accurately follow the fate of cells. Using a combination of over five different genetic models, evidence now demonstrates that a significant portion of chondrocytes survive, proliferate, and transform into osteoblasts that derive the new bone (Bahney et al., 2014; Yang et al., 2014; Zhou et al., 2014; Jing et al., 2015; Park et al., 2015; Houben et al., 2016; Hu et al., 2017).

Pathways that regulate chondrocyte to bone conversion have practical implications on fracture healing. Importantly, since conversion of cartilage to bone is necessary for bone regeneration, it is critical to understand the molecular mechanisms regulating this process. Not only will these mechanistic data improve our understanding of impaired healing, especially in the context of hypertrophic non-unions where cartilage fails to convert to bone, but they will also enable new opportunities for therapeutic intervention through modulation of cartilage to bone transformation. Here, known and candidate molecular regulators of chondrocyte-to-osteoblast transformation, along with potential sources for these biological signals, are reviewed. Finally, we propose how tissue engineering can be used to translate the evidence reviewed here into new and improved fracture therapies.

FRACTURE HEALING STANDARD OF CARE

Bone Grafting

Surgical intervention is currently the only effective treatment option for recalcitrant fractures (Bahney et al., 2015). Standard of care is to use bone autograft or allograft to stimulate healing (Hubble, 2002). Together this makes bone the second-most commonly transplanted tissue behind blood. While bone autografts stimulate strong bone repair, they come with the cost of significant donor site morbidity and limited supply. On the other hand, while bone allografts are readily available, they have significantly reduced bioactivity resulting in clinical failure associated with poor osteointegration and osteonecrosis of the graft (Brigman et al., 2004). Consequently, there is an unmet clinical need to develop pharmacologic agents, or "biologics," which can be used either as a non-invasive alternative or in conjunction with surgical treatment to stimulate endogenous healing mechanisms and improve fracture outcomes.

Bone Morphogenetic Proteins

Bone morphogenetic proteins (BMPs) are currently the most common clinically-used biologics. BMP signal transduction occurs through the binding of BMP ligands to type I and type II serine/threonine kinase receptors (BMPR-I, BMPR-II). This induces phosphorylation of BMP receptors and subsequent phosphorylation of receptor SMADS (R-SMADs) 1, 5, and 8. R-SMADS then form a complex with SMAD4, enabling it to enter the nucleus where it regulates gene expression (Lin and Hankenson, 2011; Long and Ornitz, 2013; Katagiri and Watabe, 2016; Salazar et al., 2016) (**Figure 1A**).

Pre-clinical studies indicated that the BMP pathway was an excellent target for therapeutic development due to its role in regulating osteoblastogenesis and the ability of several BMPs to strongly induce bone formation (Hoffmann and Gross, 2001; Karsenty and Wagner, 2002; Einhorn, 2010). This led to a series of clinical trials and FDA approval of two recombinant BMPs. Recombinant human BMP2 (INFUSE®) obtained pre-market approval for use in lumbar spinal fusion and for the treatment of compound tibial fractures (Einhorn, 2010; Chrastil et al., 2013). Recombinant human BMP7, also known as Osteogenic

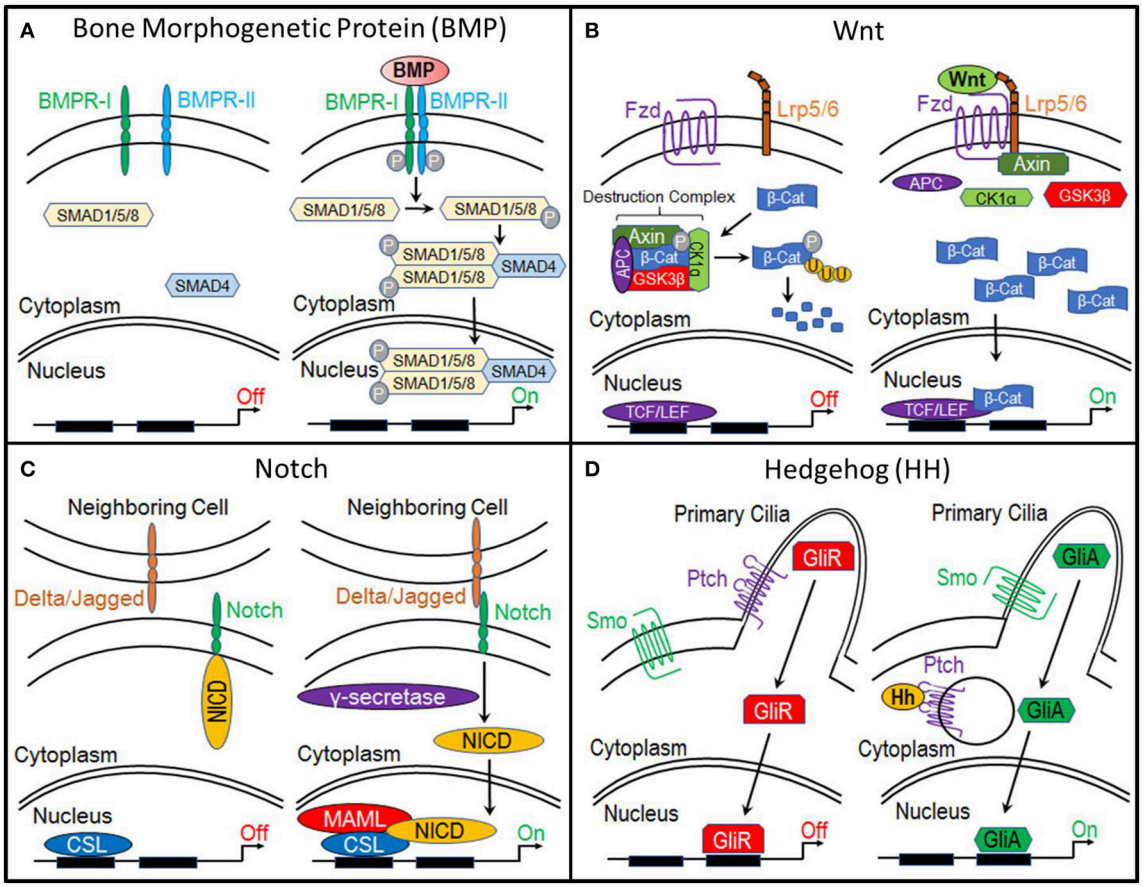

FIGURE 1 | Molecular pathways. **(A)** Bone Morphogenetic Protein (BMP), **(B)** Canonical Wnt, **(C)** Notch, and **(D)** Hedgehog.

Protein 1 (OP-1), received a Humanitarian Device Exemption for the treatment of recalcitrant long bone non-unions and for revisions of lumbar spinal fusions (Einhorn, 2010; Chrastil et al., 2013). However, although rhBMP2 has exhibited clinical success in spinal fusion, both rhBMP2 and rhOP-1 have shown less impressive results in the treatment of fracture non-unions (Einhorn, 2010). rhOP-1 has now been taken off the market and use of rhBMP2 has been significantly diminished as a result of reports of serious side effects, including heterotopic ossification and tumorigenesis, and by the expense of treatment ($5,000–$15,000 per treatment) (Einhorn, 2010; DeVine et al., 2012; Chrastil et al., 2013; Almubarak et al., 2016).

It has been postulated that the lack of clinical success with BMPs is due to limited understanding of the molecular signals responsible for regulating fracture repair and that a combination of biologics applied during the appropriate phases of the repair process will be required to effectively stimulate healing (Simmons et al., 2004; Sukul et al., 2015; Dang et al., 2016a). Furthermore, supraphysiological dosing, burse release kinetics, and rapid diffusion of BMPs are key factors contributing to heterotopic ossification (Krishnan et al., 2017). As reviewed recently, engineering scaffolds and drug delivery systems to promote sustained and local delivery of BMPs is a significant and active area of research that can translate into improved clinical outcomes (Bessa et al., 2008; Bhattacharjee et al., 2015; Agrawal and Sinha, 2017).

NOVEL MOLECULAR TARGETS FOR FRACTURE HEALING

To study the molecular signals regulating chondrocyte-to-osteoblast transformation, we have defined the chondro-osseous border in the fracture callus as the "Transition Zone" (Hu et al., 2017). Here, mature hypertrophic chondrocytes have been shown to express classic osteogenic markers (i.e., runx2, osterix, collagen type I, osteocalcin, osteopontin) indicating that these cells adopt an osteogenic fate (Hu et al., 2017). Interestingly, a recent publication by Hu et al. demonstrated that hypertrophic chondrocytes at the Transition Zone also express pluripotency transcription factors Sox2, Oct4, and Nanog, suggesting that chondrocytes acquire a stem cell-like state during transformation (Hu et al., 2017). Sox2 was shown to play an important role during chondrocyte transformation since its deletion resulted in significantly reduced bone formation and increased cartilage retention within the fracture callus (Hu et al., 2017).

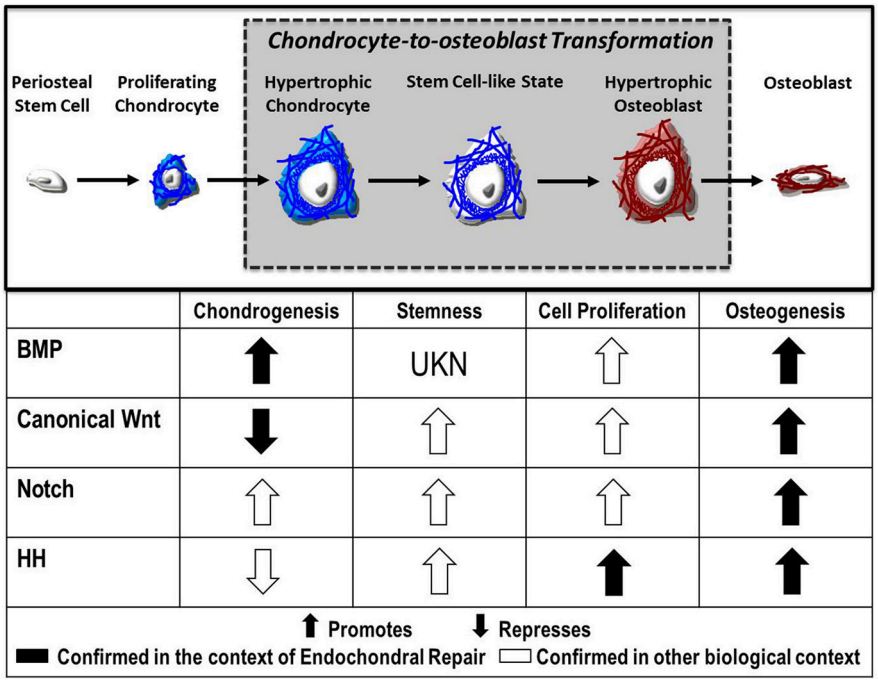

FIGURE 2 | Fate of the chondrocyte. During endochondral ossification, the formation of the cartilage callus begins with the differentiation of periosteal stem cells into chondrocytes, which proliferate and mature to a hypertrophic state. These hypertrophic chondrocytes then re-enter the cell cycle, express stem cell markers, and finally transform into osteoblasts that contribute to the formation of new bone. Published evidence suggests the Bone Morphogenetic Protein (BMP), Canonical Wnt, Notch, and Hedgehog (HH) pathways as candidate regulators of chondrocyte-to-osteoblast transformation due to their effects on chondrogenesis, stemness, cell proliferation, and osteogenesis in the context of endochondral repair (■) and in other biological contexts (▭).

Despite advances in our understanding of chondrocyte gene expression during transformation, the signaling mechanisms that direct this process remain largely unknown. Evidence suggests numerous molecular pathways as regulatory candidates, including canonical Wnt, Notch, FGF, and Hedgehog signaling, each of which will be explored here (**Figure 2**).

Canonical Wnt Signaling

Wnt signaling is traditionally categorized into the β-catenin-dependent canonical pathway and the β-catenin-independent non-canonical pathways (planar cell polarity and Ca^{2+}-mediated pathways), as recently reviewed (Gammons and Bienz, 2018). While some evidence suggests that the non-canonical pathways may play a role in regulating osteogenesis (Chen et al., 2007), the canonical Wnt/β-catenin pathway is the most studied and has been shown to play a dominant role in bone development and fracture repair. Thus, this review focuses on the canonical Wnt pathway.

The primary function of canonical Wnt signaling is to regulate the transcription of genes involved in cellular processes such as proliferation, differentiation, self-renewal, and survival. When this pathway is inactive, β-catenin, a transcriptional co-activator and the primary effector of this pathway, is bound by a multiprotein "destruction" complex, which consists of Axin, adenomatous polyposis coli (APC), and serine/threonine kinases glycogen synthase kinase 3β (GSK3β) and casein kinase 1α (CK1α). This destruction complex phosphorylates β-catenin, targeting it for ubiquitination and ultimately proteosomal degradation. However, when the pathway is activated by the binding of Wnt ligands to Frizzled and LRP5/6 receptors, the destruction complex is disrupted, enabling β-catenin to accumulate within the cytoplasm and translocate to the nucleus, where it interacts with members of the T-cell factor/lymphocyte elongation factor (TCF/LEF) family to activate transcription of target genes (Gammons and Bienz, 2018) (**Figure 1B**).

The canonical Wnt pathway has an established role in osteogenesis and skeletal formation by functioning as a molecular switch regulating lineage commitment between osteogenesis and chondrogenesis (Hill et al., 2005; Topol et al., 2009). During development, inhibition of canonical Wnt signaling through conditional deletion of β-catenin from limb and head mesenchyme using *Prx1*-CreERT, or conditional deletion from skeletogenic mesenchyme using *Dermo1*-Cre, inhibits bone formation and results in early osteoblast differentiation arrest (Day et al., 2005; Hill et al., 2005). Osteoblastogenesis halts at the osteochondral progenitor stage and cells differentiate into chondrocytes, resulting in the formation of ectopic cartilage (Day et al., 2005; Hill et al., 2005). Although cells express Runx2, an early marker of the osteoblast lineage, they fail to express osterix, indicating that these cells are incapable of committing to an osteogenic fate (Day et al., 2005; Hill et al., 2005). *In vitro* experiments inhibiting canonical Wnt signaling in mesenchymal progenitor cells provide similar findings (Hill et al., 2005).

Canonical Wnt signaling also plays a key role in directing osteogenesis during intramembranous repair (Kim et al., 2007). Using a transcortical defect model, which heals through intramembranous ossification, inhibition of Wnt signaling through adenoviral expression of Dkk1 prevented the differentiation of osteoprogenitor cells into osteoblasts and significantly reduced bone regeneration compared to controls (Kim et al., 2007). Conversely, activating the canonical Wnt pathway through deletion of pathway inhibitors (sclerostin or Axin2) significantly improved intramembranous bone formation (McGee-Lawrence et al., 2013). Furthermore, treatment of bone grafts with Wnt3a protein restored the osteogenic potential of aged bone grafts and promoted intramembranous healing of critical-sized defects in mouse calvaria and rabbit ulna (Leucht et al., 2013).

Less work has been done to determine the role of canonical Wnt signaling during endochondral bone formation and repair since traditionally the Wnt pathway is thought to promote direct osteogenesis. However, the mounting data demonstrating chondrocytes can directly form bone in development and repair (Bahney et al., 2014; Yang et al., 2014; Zhou et al., 2014; Jing et al., 2015; Park et al., 2015; Houben et al., 2016; Hu et al., 2017) suggests that canonical Wnt signaling may have a functional role in chondrocyte-to-osteoblast transdifferentiation. This was directly tested recently by Houben et al. who showed conditional deletion of β-catenin in *col10a1*-expressing hypertrophic chondrocytes resulted in significantly reduced bone, whereas stabilized β-catenin produced osteopetrotic tissue during endochondral development (Houben et al., 2016).

Since fracture repair in many ways recapitulates bone development, canonical Wnt signaling may play a similar role in regulating chondrocyte-to-osteoblast transformation during endochondral repair. Indeed, during endochondral healing, nuclear localization of β-catenin was seen in hypertrophic chondrocytes at the fracture callus Transition Zone, indicating that these cells undergo active canonical Wnt signaling (Hu et al., 2017). RT-qPCR analysis of fracture calli revealed that numerous Wnt ligands, receptors, and transduction machinery are expressed during fracture repair (Chen et al., 2007; Leucht et al., 2008). Huang et al. demonstrated that inhibition of Wnt/β-catenin signaling in chondrocytes, using an 82-amino-acid peptide called Inhibitor of β-catenin/TCF (ICAT) driven by *col2a1* expression, delayed cartilage formation and reduced bone formation (Huang et al., 2012b). Similarly, activation of canonical Wnt signaling through treatment with lithium chloride enhanced bone formation (Chen et al., 2007). Interestingly, enhanced bone regeneration was only observed when the Wnt pathway was activated at later time points, which corresponds biologically with chondrocyte-to-osteoblast transformation (Chen et al., 2007). Together, these data suggest that canonical Wnt signaling may play a role in regulating chondrocyte-to-osteoblast transformation during fracture healing.

The evidence outlined above are derived primarily from pre-clinical studies and *in vitro* systems. However, it is likely that the canonical Wnt pathway plays a similarly critical role in humans. Numerous human bone diseases are associated with mutations to components of the canonical Wnt pathway (Regard et al., 2012). Predisposition to osteoporosis has been associated with genomic polymorphisms in or close to Wnt/β-catenin signaling components (Regard et al., 2012). Loss-of-function mutations in the Wnt receptor LRP5 are associated with osteoporosis pseudoglioma (OPPG) syndrome and juvenile osteoporosis and gain-of-function mutations in the same receptor result in the opposite phenotype of high bone mass and enhanced bone strength (Einhorn, 2010; Regard et al., 2012). Sclerosteosis is a bone disease characterized by an overgrowth of bone and is caused by mutations in the gene and enhancer regions of the Wnt/β-catenin antagonist *sclerostin* (*SOST*) (Einhorn, 2010; Regard et al., 2012). Furthermore, the canonical Wnt pathway has been implicated in the context of human fracture repair since β-catenin and sclerostin levels have been shown to increase (Chen et al., 2007; Sarahrudi et al., 2012).

The canonical Wnt pathway is primed for translation. Numerous Wnt pathway regulators are being developed and several are already in clinical trials. The majority of these pathway modulators serve to activate the canonical Wnt pathway by neutralizing pathway inhibitors such as Dkk1 and sclerostin (Canalis, 2013). This indirect approach to pathway activation has been adopted primarily because direct pathway activation through treatment with Wnt ligands is clinically-irrelevant. Endogenous Wnts are hydrophobic due to palmitoylation, a form of lipidation required for the intracellular trafficking and full activation of Wnts (Willert et al., 2003; Takada et al., 2006; Janda et al., 2012). This makes Wnts challenging to extract and purify, requires that they be delivered using special liposome-based systems, and significantly increases the cost of treatment (Morrell et al., 2008). Fortunately, several of the Wnt pathway modulators acting to neutralize pathway inhibitors have shown promising osteogenic effects during clinical trials.

Of the Wnt pathway regulators currently in development, Romosozumab is closest to attaining FDA approval and is currently in Phase III clinical trials for treating osteoporosis (Regard et al., 2012; Canalis, 2013). It is a humanized monoclonal antibody that binds to and neutralizes the Wnt inhibitor sclerostin (Canalis, 2013). Studies show that treatment with Romosozumab significantly increases bone mineral density and reduces incidence of osteoporotic fractures (Canalis, 2013). Wnt pathway regulators, such as Romosozumab, could readily be repurposed for the context of fracture repair. However, the optimal dosage, timing, and the method of treatment still need to be determined.

Notch

Like, the canonical Wnt pathway, the functional roles of Notch signaling suggest it as a candidate regulator of chondrocyte-to-osteoblast transformation. Activation of this pathway begins when the Notch transmembrane receptor binds to membrane-bound ligands (Delta or Jagged) on the surface of neighboring cells. This triggers the proteolytic cleavage of the Notch intracellular domain (NICD) by γ-secretase. NICD then translocates to the nucleus where it forms a complex with and activates the transcription factor CSL, which recruits its co-activator Mastermind-like (MAML) and initiates transcription of target genes (Lin and Hankenson, 2011) (**Figure 1C**).

Notch signaling has been shown to promote osteoblastogenesis. *In vitro* inhibition of Notch signaling in mouse MSCs impaired osteoblast differentiation as assessed by alizarin red staining for matrix mineralization (Dishowitz et al., 2013). *In vivo*, gain-of-function Notch signaling in osteoblasts through the overexpression of NICD resulted in abnormally dense or osteosclerotic bone attributed to increased cell proliferation of immature osteoblasts (Engin et al., 2008). Similarly, loss-of-function Notch signaling in osteoblasts, through mutations to y-secretase, led to late-onset osteoporosis (Engin et al., 2008).

Notch signaling also appears to play a role in promoting hypertrophic maturation of chondrocytes. During development, inhibition of Notch signaling in chondrocytes impaired terminal stages of endochondral ossification in the limb cartilage, resulting in shorter limbs with an increased hypertrophic zone and reduced bone (Hosaka et al., 2013). In the context of disease, Notch signaling may promote osteoarthritis (OA), which resembles pathological activation of endochondral ossification (Hosaka et al., 2013). Nuclear localization of the intracellular domains of Notch-1 and -2 was observed in chondrocytes in mouse and human OA articular cartilage, indicating active Notch signaling in these cells (Hosaka et al., 2013). Functionally, inhibition of Notch signaling in chondrocytes conferred resistance to OA development in the knee joint (Hosaka et al., 2013).

Notch signaling has also been shown to play an important role during fracture repair. Notch signaling is upregulated during both intramembranous and endochondral ossification, but data suggest it is more highly activated during endochondral ossification (Dishowitz et al., 2012). During endochondral ossification, Notch signaling decreases as progenitors differentiate into chondrocytes and as chondrocytes mature to hypertrophy. However, mature hypertrophic chondrocytes at the Transition Zone re-expressed Jag1 and NICD2, indicating that these cells have re-activated the Notch pathway (Dishowitz et al., 2012). Whether the Notch pathway plays a functional role in regulating chondrocyte-to-osteoblast transformation is unknown. However, systemic inhibition of Notch signaling using the *Mx1*-Cre;*dnMAML*$^{fl/-}$ mouse impaired fracture healing primarily due to a prolonged inflammatory phase, decreased cartilage callus formation, and decreased osteoblast and osteoclast cell density (Dishowitz et al., 2013).

Hedgehog Signaling

The Hedgehog (Hh) pathway is essential to osteogenesis. When this pathway is inactive, cell surface receptor Patched (Ptch) prevents transmembrane protein Smoothened (Smo) from entering the primary cilia. This results in the proteolytic processing of Gli transcription factors into a repressor form (GliR). GliR then enters the nucleus and prevents Hedgehog target gene expression. Hedgehog signaling is activated by the binding of Hh ligands to Patched, thus relieving Patched-mediated suppression of Smoothened through Patched endocytosis. Smoothened enters the primary cilia where it prevents Gli transcription factors from being processed. Thus, Gli remains in its full-length, active form (GliA), which translocates to the nucleus and activates expression of Hedgehog target genes (Lin and Hankenson, 2011) (**Figure 1D**).

Of the three Hedgehog homologs, Sonic hedgehog (Shh) and Indian hedgehog (Ihh) have been implicated in osteoblastogenesis (Ehlen et al., 2006). Shh acts at early stages of development to direct patterning and growth (Zhu et al., 2008). Ihh is involved at later stages of endochondral ossification during limb development and consequently has been studied in greater depth in the context of bone formation and repair (Ehlen et al., 2006). Indian hedgehog is a central regulator of skeletogenesis and is required for osteoblastogenesis in endochondral, but not membranous bones (Kronenberg, 2003; Hill et al., 2005; Lin and Hankenson, 2011). Ihh is primarily expressed by pre- and early hypertrophic chondrocytes, where it controls proliferation and the onset of chondrocyte hypertrophy (St-Jacques et al., 1999; Long et al., 2001, 2004; Maeda et al., 2007). During development, chondrocyte expression of Ihh triggers Runx2 expression in the periosteum, thus coupling chondrocyte differentiation/maturation with osteoblastogenesis (Hill et al., 2005; Ehlen et al., 2006).

Like canonical Wnt signaling, evidence suggests that the Hedgehog pathway also serves as a molecular switch between osteogenesis and chondrogenesis. Chimeric embryos derived from Smoothened null and wild type embryonic cells exhibited abnormal bone collar formation (Long et al., 2004). Whereas, wild type cells underwent normal osteoblast differentiation, adjacent mutant cells failed to differentiate into osteoblasts and instead exhibited chondrocyte morphology, deposited cartilaginous matrix and expressed chondrocyte markers (collagen type II and X) (Long et al., 2004).

During development, Hedgehog signaling has also been shown to play an important role in trabecular bone formation. Inhibition of Hedgehog signaling through deletion of *Smoothened* in chondrocytes prevented formation of the primary spongiosa (Long et al., 2004). This loss in trabecular bone formation correlated with lost expression of the Hedgehog target gene, *Patched1*, at the chondro-osseous junction, suggesting that Hedgehog signaling promotes chondrocyte-to-osteoblast transformation (Long et al., 2004).

The Hedgehog pathway has also been implicated in regulating chondrocyte-to-osteoblast transformation during post-natal endochondral bone growth. Gli1-CreERT2 Hedgehog reporter mice demonstrated active Hedgehog signaling in hypertrophic chondrocytes and osteoprogenitors at the chondro-osseous junction of the growth plate (Haraguchi et al., 2018). Furthermore, deletion of Ihh from growth plate chondrocytes in post-natal mice resulted in continuous loss of trabecular bone with progression of age (Maeda et al., 2007).

Hedgehog signaling has been shown to promote osteogenesis during skeletal homeostasis. Systemic inhibition of Hedgehog signaling through treatment with cyclopamine decreased bone mass in adult mice (Ohba et al., 2008). In contrast, enhanced bone formation, was observed with forced activation of Hedgehog signaling in mature osteoblasts through global Patched1 haploinsufficiency or deletion (Ohba et al., 2008). Interestingly, enhanced Hedgehog activity also resulted in excessive bone resorption due to the role of Hedgehog

signaling in promoting osteoclastogenesis (Mak et al., 2008).

Evidence suggests that the hedgehog pathway promotes endochondral repair as signaling is upregulated during fracture healing (Liu et al., 2017). Furthermore, Gli1 reporter mice demonstrated that cells actively signaling through the hedgehog pathway contribute to both chondrocytes and osteoblasts during fracture healing (Shi et al., 2017). Inhibition of the Hedgehog pathway through treatment with a systemic Hedgehog inhibitor GDC-0449, delayed fracture healing (Liu et al., 2017). Chondrogenesis was unaffected, suggesting that the effects were due to Hedgehog regulation of chondrocyte transformation (Liu et al., 2017). In contrast, activation of Hedgehog signaling through local administration of a Hedgehog agonist known as Smoothened Agonist (SAG) accelerated endochondral repair due to increased chondrocyte proliferation, an enlarged cartilaginous callus, and an increased number of cells expressing osteoblast markers within the bony callus (Kashiwagi et al., 2016).

VASCULATURE REGULATION OF CHONDROCYTE-TO-OSTEOBLAST TRANSFORMATION

The vasculature plays a critical role during fracture repair. Whereas, the normal rate of impaired healing is 10–15%, this percentage increases to 46% when fractures occur in conjunction with severe vasculature injury (Bahney et al., 2015). The role of the vasculature begins at the outset of injury during hematoma formation where it helps to create the growth factor rich fibrin blood clot upon which periosteal stem cells differentiate to chondrocytes under a low pH, high lactate microenvironment (Wray, 1964; Xing et al., 2010a). After chondrogenic differentiation, the cartilage anlage is avascular and chondrogenic maturation happens in the absence of a regulatory role from the vasculature (Gerber et al., 1999; Tatsuyama et al., 2000; Hu et al., 2017).

In the later stages of repair, blood vessels are recruited into the cartilage fracture callus by hypertrophic chondrocytes expressing vascular endothelial growth factor (VEGF) (Gerber et al., 1999; Zelzer et al., 2002; Hu et al., 2017) and placental growth factor (PlGF) (Maes et al., 2006). Histologically, the cartilage to bone transition in the fracture callus occurs around this invading vasculature (Hu et al., 2017). Importantly, spatiotemporal expression of osteogenic genes and pluripotency transcription factors occurs in hypertrophic chondrocytes adjacent to the vasculature, suggesting that the vasculature plays a role in initiating chondrocyte-to-osteoblast transformation (Hu et al., 2017).

Growth Factor Secretion

Endothelial cells from the vasculature may functionally contribute to phenotypic modulation of the chondrocyte phenotype through secretion of pro-osteogenic growth factors. For example, it has been established that vascular tissues are a direct endogenous source of BMPs (Yu et al., 2010; Matsubara et al., 2012). Functionally it has been shown that secreted factors from vascular endothelial cell conditioned media were capable of inducing matrix mineralization and up-regulating the classic osteogenic gene *osteocalcin* (Bahney et al., 2014). It is likely that BMP expression contributed to this phenotype (Bahney et al., 2014). However, more recently it was also shown that the same vascular endothelial cell conditioned media induced expression of pluripotency transcription factors (Sox2, Oct4, Nanog) indicating that an additional factor may have a role in activating a stem-like state (Hu et al., 2017). While the complete secretome of vascular endothelial cells during fracture healing has not been detailed, it is known that this secretome is site specific (Nolan et al., 2013; Rafii et al., 2016). It is possible that fracture callus endothelial cells secrete factors other than BMP that may play a role in directing osteogenesis or chondrocyte plasticity.

Delivery of Macrophages

The vasculature is also responsible for delivering inflammatory cells to the fracture callus. These include circulatory macrophages, which are recruited by pro-inflammatory cytokines [Tumor necrosis factor (TNFα), Interleukin-1β (IL-1β), and IL-6] that activate a pro-inflammatory (M1) macrophage state (Wray, 1964). This pro-inflammatory phase has been shown to improve fracture repair by promoting cell proliferation and stem cell differentiation (Xing et al., 2010b; Wang et al., 2013).

While this inflammatory response is necessary for proper healing, it must be resolved in order for healing to progress (Wang et al., 2013). A prolonged pro-inflammatory state can delay fracture repair and is an underlying factor in impaired healing in elderly animals (Lu et al., 2008; Xing et al., 2010a,b; Abou-Khalil et al., 2014; Baht et al., 2015). Resolution of the pro-inflammatory state occurs when anti-inflammatory cytokines and growth factors [IL-10, arginase, TGFβ, EGF, PDGF, VEGF] push M1 macrophages toward the M2 phenotype (Laskin, 2009). Thus, it is possible that macrophages and their inflammatory resolution may help regulate chondrocyte-to-osteoblast transformation.

MATRIX MECHANOBIOLOGY

Recent studies have demonstrated that the extracellular matrix (ECM) plays an active role in regulating chondrogenic and osteogenic cell fate decisions. Changes in cell fate elicit changes to the surrounding matrix, thus producing a cycle of bi-directional interactions between cells and their surrounding matrix, a phenomenon known as "dynamic reciprocity" (Bissell et al., 1982). This cross-talk is modulated by the structural, mechanical, and biochemical cues provided by the ECM.

Remodeling of the ECM during endochondral ossification is a dynamic process that transforms the cartilaginous matrix into bone. This change in ECM contributes to the phenotypic adaptation that occurs during chondrocyte-to-osteoblast transformation. The major constituents of the cartilage ECM are collagens, hyaluronan, proteoglycans, and glycoproteins (Gentili and Cancedda, 2009). Collagens account for two-thirds of the tissue's dry weight, the most abundant of which is collagen type

II (Eyre et al., 2006). Collagen type II is a fibril-forming collagen that creates nonparallel crosslinks with collagens type IX and XI. These crosslinks create a robust meshwork that gives cartilage its tensile strength. Cartilage is further characterized by its high aggrecan content (Martel-Pelletier et al., 2008). Aggrecan is anchored to hyaluronan within the matrix and is a negatively charged proteoglycan that attracts water (Roughley and Mort, 2014). This attraction of water to aggrecan creates osmotic pressure within the tissue, making cartilage shock-absorbent and resistant to high-load compression (Maldonado and Nam, 2013). Together, the collagen II and aggrecan ultrastructure allows for limited but necessary deformation under compressive forces that contributes to distribution of nutrients across the avascular tissue (Muir, 1995).

During endochondral ossification, there is a change in the amount and type of collagens present in the ECM. Chondrocyte hypertrophy is marked by the deposition of collagen type X and the up-regulation of matrix metalloproteinase-13 (MMP-13), which leads to the degradation of collagen II and aggrecan (Ortega et al., 2004; Maldonado and Nam, 2013). The loss of collagen II and aggrecan leads to a temporary reduction in tensile strength and stiffness of the tissue, which changes the mechanical microenvironment of chondrocytes and exposes the cells to greater strains that may induce phenotypic changes **(Figure 3)** (Stockwell, 1981; Ashman and Jae Young Rho, 1988; Rho et al., 1993; Chintala et al., 1994; Mente and Lewis, 1994; Liu et al., 2016). Proteolysis of collagen II likely contributes to chondrocyte hypertrophy and increased hydration experienced by the cartilage matrix as a consequence of a weakened fibril network losing the ability to resist the influx of proteoglycan-attracted water (Dejica et al., 2012; Akkiraju and Nohe, 2015). These changes in hydrostatic pressure could enhance mineralization of cartilage through the diffusion of ions (Tanck et al., 1999).

Numerous studies have demonstrated that chondrogenic and osteogenic gene expression can be directly modulated by compressive loading and microenvironmental stiffness, as recently reviewed (Park et al., 2011; Lv et al., 2015; Carrion et al., 2016). For example, MSCs subjected to cyclic equibiaxial strain up-reguated expression of markers specific to osteoblast differentiation and mineralization of the ECM (Thomas and el Haj, 1996; Simmons et al., 2003; Liu et al., 2016). Remarkably, when MSCs were subjected to both axial compression and sheer stress, these led to an increase in chondrogenic gene expression and elicited production and accumulation of collagen II and proteoglycan (Schätti et al., 2011; Huang et al., 2012a). Hadden et al. used adipose-derived stem cells (ASCs) cultured on hydrogels with a defined stiffness gradient to demonstrate a stiffness-dependent variation in cellular morphology, migration, and differentiation (Hadden et al., 2017). Furthermore, Engler *et al* confirmed stem cell fate plasticity by culturing MSCs on matrices with varying tissue-level elasticity. After several weeks of culture, MSCs committed to the lineage dictated by matrix stiffness such that softer, stiffer, and rigid matrices proved to be neurogenic, myogenic, and osteogenic, respectively (Engler et al., 2006). However, findings by Jha et al. suggested that high affinity adhesive ligands can serve as a substitute for a rigid matrix likely by signal transduction following focal adhesion assembly (Jha et al., 2014).

In the midst of an altering microenvironment, hypertrophic chondrocytes begin to predominantly express collagen type X. In contrast to the fibril-forming properties of collagen II, collagen X is a network-forming collagen that creates "basket weave-like" structures (Tampieri and Sprio, 2016). This collagen X ultrastructure is proposed to functionally compartmentalize matrix vesicles containing mineral and newly expressed alkaline phosphatase within the hypertrophic cartilage ECM (Kwan et al., 1997). Interactions between collagen X and matrix vesicles activate the influx of Ca^{2+} into matrix vesicles thus promoting mineralization and increasing stiffness of the matrix (Shen, 2005).

Tissue architecture, or the manner in which matrix components are structured and organized at the micro- and nanoscale, has been shown to be a factor in naïve cell differentiation. Thus, structural changes could be a driving factor for chondrocyte-to-osteoblast transformation (Healy, 2004). There have been numerous observations of matrix architecture influencing stem cell fate by controlling cell engagement with surrounding matrix and neighboring cells (Guilak et al., 2009; Ahmed and ffrench-Constant, 2016). Moreover, matrix architecture can alter cell surface receptor and cytoskeletal spatial arrangement subsequently altering ligand signaling (Ekerdt et al., 2013). For example, Lu et al. have shown that collagen type II enhances chondrogenesis in ASCs by affecting cell shape and size through the β1 integrin-mediated Rho A/Rock signaling pathway (Lu et al., 2010).

Likewise, research groups have also shown that tissue topography has the ability to guide mesenchymal stem cell fate to either chondrogenic or osteoblastic phenotypes. Shong et al. demonstrated the synergistic effect of microtopography and biochemical supplements to direct MSC fate toward an osteogenic phenotype (Guilak et al., 2009; Song et al., 2015). Additionally, work by Uskoković and Desai suggests that topography may potentially be more of a dominant factor in cell/material surface interaction than the surface chemistry or stiffness (Uskoković and Desai, 2014).

Matrix as a Growth Factor Reservoir

The bioavailability, local concentration, and stabilization of growth factors (GFs) within the ECM of cartilage are primarily modulated via electrostatic interactions between the negatively charged sulfate groups of proteoglycans and the positively charged surfaces of signaling molecules (Tampieri and Sprio, 2016). Moreover, GFs are immobilized by binding to heparan sulfate glycosaminoglycans, for example; Chintala et al. demonstrated that fibroblast growth factor (FGF) has a high affinity to heparan sulfate in the matrix of growth plate cartilage (Chintala et al., 1994). Similarly, Martino et al. identified various GFs from the PDGF, VEGF, TGF-β, and neurotrophin families that possess heparin-binding domains (Martino et al., 2013).

As chondrocytes mature into hypertrophic chondrocytes, they secrete VEGF to stimulate angiogenesis, alkaline phosphatase to induce mineralization, and BMPs to promote osteogenesis (Bahney et al., 2014). These growth factors are retained

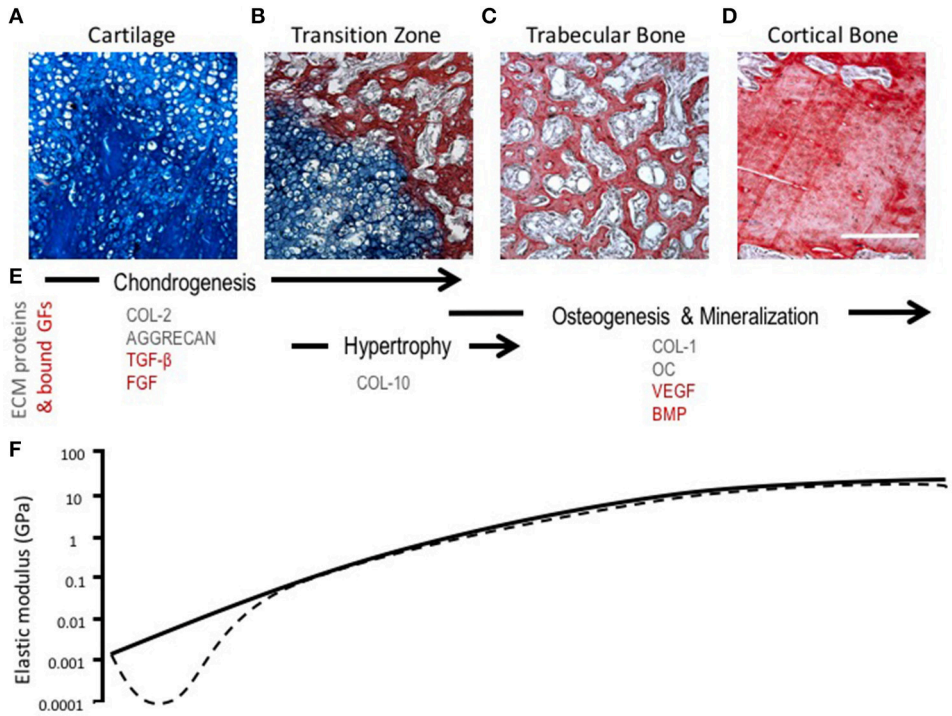

FIGURE 3 | Morphological, compositional, and mechanical changes during endochondral ossification (EO). **(A–D)** HBQ histology (blue = cartilage, red = bone) of representative tissues from a murine fracture callus throughout stages of healing: **(A)** cartilage, **(B)** transition zone, **(C)** trabecular bone, and **(D)** cortical bone. Scale bar = 200 μm. **(E)** Tissue matrix components and matrix-bound growth factors corresponding to the location and phases of EO (Chintala et al., 1994; Shen, 2005; Eyre et al., 2006; Martel-Pelletier et al., 2008; Maldonado and Nam, 2013; Martino et al., 2013; Tampieri and Sprio, 2016; Tomlinson et al., 2016). **(F)** Log scale difference in elastic modulus of human samples corresponding to each tissue matrix listed above. Solid line represents normal ossification, dotted line accounts for the initial decline in elastic modulus (osteoarthritis model) (Ashman and Jae Young Rho, 1988; Rho et al., 1993; Mente and Lewis, 1994; Silver et al., 2002; Pal, 2014).

within the matrix due to the combination of collagen X in compartmentalizing matrix components during endochondral ossification and through interaction with the heparin and/or sulfated proteoglycans (Shen, 2005). Thus, the dynamic promiscuity of the ECM in hypertrophic cartilage likely has a role in cellular signaling affecting physiological functions of endochondral ossification.

For these reasons tissue engineers in recent years have begun to fabricate scaffolds and microparticles that are believed to mimic the release kinetics of GFs found in the cartilage ECM during endochondral ossification. Jeon et al. harnessed the high affinity GFs have to heparin by incorporating heparin into photocrosslinkable alginate gels, recapitulating matrix-growth factor interactions allowing for controlled and sustained release of therapeutic proteins (Jeon et al., 2011). Exploiting the well-documented affinity of proteins to hydroxyapatite (HAp), Dang et al. have fabricated HAp-based microparticles that exhibit sustained delivery of BMP alone as well as controlled dual delivery of BMP with TGF-β to enhance bone tissue engineering via endochondral ossification (Bernardi et al., 1972; Dang et al., 2016a,b). Likewise, glucosamine has also been incorporated into engineered scaffolds because of its effects on chondrocyte proliferation, matrix synthesis, and gene expression via modulation of TGF-β expression levels (Varghese et al., 2007; Murab et al., 2015).

As permeability is typically very low in cartilage, this further accentuates the ECM's role in acting as a reservoir for latent growth factors (Pei et al., 2011). However, in the context of OA, a degenerative joint disease that exhibits endochondral ossification signaling, cartilage ECM degradation alters TGF-β signaling due to the displacement of TGF-β by fluid influx (Blaney Davidson et al., 2007). In native cartilaginous tissue, studies have shown that the loss of latent TGF-β induces chondrocyte hypertrophy and osteogenesis (Wu et al., 2016). Similarly, MSCs seeded onto tissue-engineered cartilage undergo hypertrophic differentiation in the presence of TGF-β, while in the absence of TGF-β MSCs undergo articular cartilage differentiation (Chawla et al., 2017). To that end, we can presume that changes in the properties of the matrix, whether directly or indirectly, have a significant role in the transformation of cartilage to bone during endochondral ossification.

DEVELOPMENTAL ENGINEERING TO RECAPITULATE ENDOCHONDRAL OSSIFICATION

Bone injuries are extremely common with ∼15 million fracture cases and over 2 million bone grafting procedures per year (Yelin et al., 2016). The current clinical gold

standard for stimulating bone regeneration is to promote intramembranous bone formation through application of bone grafts, increased biomechanical stability of the fracture with additional orthopedic hardware, or less commonly, through implantation of BMP2-soaked scaffolds (INFUSE®). Given the clinical downsides of each, there is an unmet clinical need for regenerative techniques that could improve vascularized bone regeneration.

While the established clinical approaches to bone regeneration promote intramembranous bone formation, bones both develop and heal through the process of endochondral ossification during which the cartilage callus creates an angiogenic and osteoconductive scaffold for bone formation. Recent pre-clinical studies have capitalized on this, proposing therapeutic strategies that parallel the natural healing process by utilizing engineered hypertrophic cartilage grafts to stimulate bone regeneration (Scotti et al., 2010, 2013; Farrell et al., 2011; Sheehy et al., 2013, 2014; Bahney et al., 2014; Bourgine et al., 2014; Bhattacharjee et al., 2015; Dang et al., 2017). Translating these pre-clinical studies may be one strategy to improve clinical outcomes (Nishitani and Schwarz, 2014).

Further, new mechanistic understanding of endochondral ossification could have a significant impact on the design of novel therapeutic approaches to fracture healing and bone regeneration. Since we now understand chondrocytes can be a direct precursor of osteoblasts (Yang et al., 2014; Zhou et al., 2014; Jing et al., 2015; Park et al., 2015; Hu et al., 2017) stimulating transformation of chondrocytes into osteoblasts becomes a clinically-relevant therapeutic approach. Very little work has been done to understand *how* chondrocytes become osteoblasts during endochondral ossification. If we understood the extrinsic mediators of chondrocyte to osteoblast transformation, we would not only be able to engineer an ideal treatment for hypertrophic nonunions, but we could also accelerate fracture healing under normal conditions.

AUTHOR CONTRIBUTIONS

SW, KR, and CB drafted the primary text. CB, TM, and RM financially supported this manuscript. All authors contributed to making the figures, editing the text, and approving the manuscript.

ACKNOWLEDGMENTS

This publication was supported financially by the National Institutes of Health (NIH) through the National Center for Advancing Translational Sciences Grant Numbers UCSF-UL1TR000004, the National Institute of Dental and Craniofacial Research F30 DE026359 (SW), National Institute of General Medical Sciences R25-GM056847, the AO Foundation Start-Up Grant (CB, #S-14-114B), the UCSF Core Center for Musculoskeletal Biology and Medicine Grant Number P30AR066262, and the Research Evaluation and Allocation Committee (REAC) UCSF School of Medicine. Its contents are solely the responsibility of the authors and do not necessarily represent the official views of the NIH or other funding agencies. The authors acknowledge institutional support from the UCSF/ZSFG Orthopedic Trauma Institute, editorial support by Tiffany Shao, and administrative support from Gina Baldoza and Anna Lissa Wi.

REFERENCES

Abou-Khalil, R., Yang, F., Mortreux, M., Lieu, S., Yu, Y. Y., Wurmser, M., et al. (2014). Delayed bone regeneration is linked to chronic inflammation in murine muscular dystrophy. *J. Bone Miner. Res. Off. J. Am. Soc. Bone Miner. Res.* 29, 304–315. doi: 10.1002/jbmr.2038

Agrawal, V., and Sinha, M. (2017). A review on carrier systems for bone morphogenetic protein-2. *J. Biomed. Mater. Res. B Appl. Biomater.* 105, 904–925. doi: 10.1002/jbm.b.33599

Ahmed, M., and ffrench-Constant, C. (2016). Extracellular matrix regulation of stem cell behavior. *Curr. Stem Cell Rep.* 2, 197–206. doi: 10.1007/s40778-016-0056-2

Akiyama, H., Chaboissier, M. -C., Martin, J. F., Schedl, A., and de Crombrugghe, B. (2002). The transcription factor Sox9 has essential roles in successive steps of the chondrocyte differentiation pathway and is required for expression of Sox5 and Sox6. *Genes Dev.* 16, 2813–2828. doi: 10.1101/gad.1017802

Akkiraju, H., and Nohe, A. (2015). Role of chondrocytes in cartilage formation, progression of osteoarthritis and cartilage regeneration. *J. Dev. Biol.* 3, 177–192. doi: 10.3390/jdb3040177

Almubarak, S., Nethercott, H., Freeberg, M., Beaudon, C., Jha, A., Jackson, W., et al. (2016). Tissue engineering strategies for promoting vascularized bone regeneration. *Bone* 83, 197–209. doi: 10.1016/j.bone.2015.11.011

Ashman, R. B., and Jae Young Rho (1988). Elastic modulus of trabecular bone material. *J. Biomech.* 21, 177–181. doi: 10.1016/0021-9290(88)90167-4

Bahney, C. S., Hu, D. P., Miclau, T., and Marcucio, R. S. (2015). The multifaceted role of the vasculature in endochondral fracture repair. *Front. Endocrinol. (Lausanne).* 6:4. doi: 10.3389/fendo.2015.00004

Bahney, C. S., Hu, D. P., Taylor, A. J., Ferro, F., Britz, H. M., Hallgrimsson, B., et al. (2014). Stem cell-derived endochondral cartilage stimulates bone healing by tissue transformation. *J. Bone Miner. Res. Off. J. Am. Soc. Bone Miner. Res.* 29, 1269–1282. doi: 10.1002/jbmr.2148

Baht, G. S., Silkstone, D., Vi, L., Nadesan, P., Amani, Y., Whetstone, H., et al. (2015). Exposure to a youthful circulation rejuvenates bone repair through modulation of β-catenin. *Nat. Commun.* 6:7131. doi: 10.1038/ncomms8131

Bell, D. M., Leung, K. K. H., Wheatley, S. C., Ng, L. J., Zhou, S., Ling, K. W., et al. (1997). SOX9 directly regulates the type-ll collagen gene. *Nat. Genet.* 16, 174–178. doi: 10.1038/ng0697-174

Beresford, W. A. (1981). Chondroid bone, secondary cartilage and metaplasia. *Q. Rev. Biol.* 56, 471–471. doi: 10.1086/412472

Bernardi, G., Giro, M. -G., and Gaillard, C. (1972). Chromatography of polypeptides and proteins on hydroxyapatite columns: some new developments. *Biochim. Biophys. Acta Protein Struct.* 278, 409–420. doi: 10.1016/0005-2795(72)90001-3

Bessa, P. C., Casal, M., and Reis, R. L. (2008). Bone morphogenetic proteins in tissue engineering: the road from the laboratory to the clinic, part I (basic concepts). *J. Tissue Eng. Regen. Med.* 2, 1–13. doi: 10.1002/term.63

Bhattacharjee, M., Coburn, J., Centola, M., Murab, S., Barbero, A., Kaplan, D. L., et al. (2015). Tissue engineering strategies to study cartilage development, degeneration and regeneration. *Adv. Drug Deliv. Rev.* 84, 107–122. doi: 10.1016/j.addr.2014.08.010

Bi, W., Deng, J. M., Zhang, Z., Behringer, R. R., and de Crombrugghe, B. (1999). *Sox9* is required for cartilage formation. *Nat. Genet.* 22, 85–89. doi: 10.1038/8792

Bissell, M. J., Hall, H. G., and Parry, G. (1982). How does the extracellular matrix direct gene expression? *J. Theor. Biol.* 99, 31–68. doi: 10.1016/0022-5193(82)90388-5

Blaney Davidson, E. N., van der Kraan, P. M., and van den Berg, W. B. (2007). TGF-beta and osteoarthritis. *Osteoarthr. Cartil.* 15, 597–604. doi: 10.1016/j.joca.2007.02.005

Bourgine, P. E., Scotti, C., Pigeot, S., Tchang, L. A., Todorov, A., and Martin, I. (2014). Osteoinductivity of engineered cartilaginous templates devitalized by inducible apoptosis. *Proc. Natl. Acad. Sci. U.S.A.* 111, 17426–17431. doi: 10.1073/pnas.1411975111

Brigman, B. E., Hornicek, F. J., Gebhardt, M. C., and Mankin, H. J. (2004). Allografts about the knee in young patients with high-grade sarcoma. *Clin. Orthop.* 232–239. doi: 10.1097/01.blo.0000127132.12576.05

Canalis, E. (2013). Wnt signalling in osteoporosis: mechanisms and novel therapeutic approaches. *Nat. Rev. Endocrinol.* 9, 575–583. doi: 10.1038/nrendo.2013.154

Carrion, B., Souzanchi, M. F., Wang, V. T., Tiruchinapally, G., Shikanov, A., Putnam, A. J., et al. (2016). The synergistic effects of matrix stiffness and composition on the response of chondroprogenitor cells in a 3D precondensation microenvironment. *Adv. Healthc. Mater.* 5, 1192–1202. doi: 10.1002/adhm.201501017

Chawla, S., Kumar, A., Admane, P., Bandyopadhyay, A., and Ghosh, S. (2017). Elucidating role of silk-gelatin bioink to recapitulate articular cartilage differentiation in 3D bioprinted constructs. *Bioprinting* 7, 1–13. doi: 10.1016/j.bprint.2017.05.001

Chen, Y., Whetstone, H. C., Lin, A. C., Nadesan, P., Wei, Q., Poon, R., et al. (2007). Beta-catenin signaling plays a disparate role in different phases of fracture repair: implications for therapy to improve bone healing. *PLoS Med.* 4:e249. doi: 10.1371/journal.pmed.0040249

Chintala, S. K., Miller, R. R., and McDevitt, C. A. (1994). Basic fibroblast growth factor binds to heparan sulfate in the extracellular matrix of rat growth plate chondrocytes. *Arch. Biochem. Biophys.* 310, 180–186. doi: 10.1006/abbi.1994.1155

Chrastil, J., Low, J. B., Whang, P. G., and Patel, A. A. (2013). Complications associated with the use of the recombinant human bone morphogenetic proteins for posterior interbody fusions of the lumbar spine. *Spine* 38, E1020–E1027. doi: 10.1097/BRS.0b013e3182982f8e

Colnot, C. (2009). Skeletal cell fate decisions within periosteum and bone marrow during bone regeneration. *J. Bone Miner. Res.* 24, 274–282. doi: 10.1359/jbmr.081003

Cooper, K. L., Oh, S., Sung, Y., Dasari, R. R., Kirschner, M. W., and Tabin, C. J. (2013). Multiple phases of chondrocyte enlargement underlie differences in skeletal proportions. *Nature* 495, 375–378. doi: 10.1038/nature11940

Dang, P. N., Dwivedi, N., Phillips, L. M., Yu, X., Herberg, S., Bowerman, C., et al. (2016a). Controlled dual growth factor delivery from microparticles incorporated within human bone marrow-derived mesenchymal stem cell aggregates for enhanced bone tissue engineering via endochondral ossification. *Stem Cells Transl. Med.* 5, 206–217. doi: 10.5966/sctm.2015-0115

Dang, P. N., Dwivedi, N., Yu, X., Phillips, L., Bowerman, C., Murphy, W. L., et al. (2016b). Guiding chondrogenesis and osteogenesis with mineral-coated hydroxyapatite and BMP-2 incorporated within high-density hMSC aggregates for bone regeneration. *ACS Biomater. Sci. Eng.* 2, 30–42. doi: 10.1021/acsbiomaterials.5b00277

Dang, P. N., Herberg, S., Varghai, D., Riazi, H., Varghai, D., McMillan, A., et al. (2017). Endochondral ossification in critical-sized bone defects via readily implantable scaffold-free stem cell constructs. *Stem Cells Transl. Med.* 6, 1644–1659. doi: 10.1002/sctm.16-0222

Day, T. F., Guo, X., Garrett-Beal, L., and Yang, Y. (2005). Wnt/β-catenin signaling in mesenchymal progenitors controls osteoblast and chondrocyte differentiation during vertebrate skeletogenesis. *Dev. Cell* 8, 739–750. doi: 10.1016/j.devcel.2005.03.016

Dejica, V. M., Mort, J. S., Laverty, S., Antoniou, J., Zukor, D. J., Tanzer, M., et al. (2012). Increased type II collagen cleavage by cathepsin K and collagenase activities with aging and osteoarthritis in human articular cartilage. *Arthritis Res. Ther.* 14:R113. doi: 10.1186/ar3839

DeVine, J. G., Dettori, J. R., France, J. C., Brodt, E., and McGuire, R. A. (2012). The use of rhBMP in spine surgery: is there a cancer risk? *Evid. Based Spine Care J.* 3, 35–41. doi: 10.1055/s-0031-1298616

Dishowitz, M. I., Mutyaba, P. L., Takacs, J. D., Barr, A. M., Engiles, J. B., Ahn, J., et al. (2013). Systemic inhibition of canonical notch signaling results in sustained callus inflammation and alters multiple phases of fracture healing. *PLoS ONE* 8:e68726. doi: 10.1371/journal.pone.0068726

Dishowitz, M. I., Terkhorn, S. P., Bostic, S. A., and Hankenson, K. D. (2012). Notch signaling components are upregulated during both endochondral and intramembranous bone regeneration. *J. Orthop. Res. Off. Publ. Orthop. Res. Soc.* 30, 296–303. doi: 10.1002/jor.21518

Duchamp de Lageneste, O., Julien, A., Abou-Khalil, R., Frangi, G., Carvalho, C., Cagnard, N., et al. (2018). Periosteum contains skeletal stem cells with high bone regenerative potential controlled by Periostin. *Nat. Commun.* 9:773. doi: 10.1038/s41467-018-03124-z

Ehlen, H. W. A., Buelens, L. A., and Vortkamp, A. (2006). Hedgehog signaling in skeletal development. *Birth Defects Res. C Embryo Today Rev.* 78, 267–279. doi: 10.1002/bdrc.20076

Einhorn, T. A. (2010). The Wnt signaling pathway as a potential target for therapies to enhance bone repair. *Sci. Transl. Med.* *2*:42ps36. doi: 10.1126/scitranslmed.3001149

Ekerdt, B. L., Segalman, R. A., and Schaffer, D. V. (2013). Spatial organization of cell-adhesive ligands for advanced cell culture. *Biotechnol. J.* 8, 1411–1423. doi: 10.1002/biot.201300302

Engin, F., Yao, Z., Yang, T., Zhou, G., Bertin, T., Jiang, M. M., et al. (2008). Dimorphic effects of Notch signaling in bone homeostasis. *Nat. Med.* 14, 299–305. doi: 10.1038/nm1712

Engler, A. J., Sen, S., Sweeney, H. L., and Discher, D. E. (2006). Matrix elasticity directs stem cell lineage specification. *Cell* 126, 677–689. doi: 10.1016/j.cell.2006.06.044

Eyre, D. R., Weis, M. A., and Wu, J. -J. (2006). Articular cartilage collagen: an irreplaceable framework? *Eur. Cell. Mater.* 12, 57–63. doi: 10.22203/eCM.v012a07

Farrell, E., Both, S. K., Odörfer, K. I., Koevoet, W., Kops, N., O'Brien, F. J., et al. (2011). *In-vivo* generation of bone via endochondral ossification by *in-vitro* chondrogenic priming of adult human and rat mesenchymal stem cells. *BMC Musculoskelet. Disord.* 12:31. doi: 10.1186/1471-2474-12-31

Gammons, M., and Bienz, M. (2018). Multiprotein complexes governing Wnt signal transduction. *Curr. Opin. Cell Biol.* 51, 42–49. doi: 10.1016/j.ceb.2017.10.008

Gentili, C., and Cancedda, R. (2009). Cartilage and bone extracellular matrix. *Curr. Pharm. Des.* 15, 1334–1348. doi: 10.2174/138161209787846739

Gerber, H. -P., Vu, T. H., Ryan, A. M., Kowalski, J., Werb, Z., and Ferrara, N. (1999). VEGF couples hypertrophic cartilage remodeling, ossification and angiogenesis during endochondral bone formation. *Nat. Med.* 5:623. doi: 10.1038/9467

Grässel, S. (2014). The role of peripheral nerve fibers and their neurotransmitters in cartilage and bone physiology and pathophysiology. *Arthritis Res. Ther.* 16:485. doi: 10.1186/s13075-014-0485-1

Guilak, F., Cohen, D. M., Estes, B. T., Gimble, J. M., Liedtke, W., and Chen, C. S. (2009). Control of stem cell fate by physical interactions with the extracellular matrix. *Cell Stem Cell* 5, 17–26. doi: 10.1016/j.stem.2009.06.016

Hadden, W. J., Young, J. L., Holle, A. W., McFetridge, M. L., Kim, D. Y., Wijesinghe, P., et al. (2017). Stem cell migration and mechanotransduction on linear stiffness gradient hydrogels. *Proc. Natl. Acad. Sci. U.S.A.* 114, 5647–5652. doi: 10.1073/pnas.1618239114

Hall, B. K. (2015). *Bones and Cartilage: Developmental and Evolutionary Skeletal Biology*. Academic Press. Available online at: https://www.sciencedirect.com/science/article/pii/B9780124166783000495

Haraguchi, R., Kitazawa, R., Imai, Y., and Kitazawa, S. (2018). Growth plate-derived hedgehog-signal-responsive cells provide skeletal tissue components in growing bone. *Histochem. Cell Biol.* 149, 365–373. doi: 10.1007/s00418-018-1641-5

Healy, K. E. (2004). Control of cell function with tunable hydrogel networks. *Conf. Proc. Annu. Int. Conf. IEEE Eng. Med. Biol. Soc.* 7:5035. doi: 10.1109/IEMBS.2004.1404391

Hill, T. P., Später, D., Taketo, M. M., Birchmeier, W., and Hartmann, C. (2005). Canonical Wnt/β-catenin signaling prevents osteoblasts from differentiating into chondrocytes. *Dev. Cell* 8, 727–738. doi: 10.1016/j.devcel.2005.02.013

Hoffmann, A., and Gross, G. (2001). BMP signaling pathways in cartilage and bone formation. *Crit. Rev. Eukaryot. Gene Expr.* 11, 23–45. doi: 10.1615/CritRevEukarGeneExpr.v11.i1-3.20

Hosaka, Y., Saito, T., Sugita, S., Hikata, T., Kobayashi, H., Fukai, A., et al. (2013). Notch signaling in chondrocytes modulates endochondral ossification and osteoarthritis development. *Proc. Natl. Acad. Sci. U.S.A.* 110, 1875–1880. doi: 10.1073/pnas.1207458110

Houben, A., Kostanova-Poliakova, D., Weissenböck, M., Graf, J., Teufel, S., Mark, K., et al. (2016). β-catenin activity in late hypertrophic chondrocytes locally orchestrates osteoblastogenesis and osteoclastogenesis. *Development* 143, 3826–3838. doi: 10.1242/dev.137489

Hu, D. P., Ferro, F., Yang, F., Taylor, A. J., Chang, W., Miclau, T., et al. (2017). Cartilage to bone transformation during fracture healing is coordinated by the invading vasculature and induction of the core pluripotency genes. *Development* 144, 221–234. doi: 10.1242/dev.130807

Huang, A. H., Baker, B. M., Ateshian, G. A., and Mauck, R. L. (2012a). Sliding contact loading enhances the tensile properties of mesenchymal stem cell-seeded hydrogels. *Eur. Cell. Mater.* 24, 29–45. doi: 10.22203/eCM.v024a03

Huang, Y., Zhang, X., Du, K., Yang, F., Shi, Y., Huang, J., et al. (2012b). Inhibition of β-catenin signaling in chondrocytes induces delayed fracture healing in mice. J. Orthop. *Res.* 30, 304–310. doi: 10.1002/jor.21505

Hubble, M. J. W. (2002). Bone grafts. *Surg. Technol. Int.* 10, 261–265.

Janda, C. Y., Waghray, D., Levin, A. M., Thomas, C., and Garcia, K. C. (2012). Structural basis of Wnt recognition by frizzled. *Science* 337, 59–64. doi: 10.1126/science.1222879

Jeon, O., Powell, C., Solorio, L. D., Krebs, M. D., and Alsberg, E. (2011). Affinity-based growth factor delivery using biodegradable, photocrosslinked heparin-alginate hydrogels. *J. Control. Release Off. J. Control. Release Soc.* 154, 258–266. doi: 10.1016/j.jconrel.2011.06.027

Jha, A. K., Jackson, W. M., and Healy, K. E. (2014). Controlling osteogenic stem cell differentiation via soft bioinspired hydrogels. *PLoS ONE* 9:e98640. doi: 10.1371/journal.pone.0098640

Jing, Y., Zhou, X., Han, X., Jing, J., von der Mark, K., Wang, J., et al. (2015). Chondrocytes directly transform into bone cells in mandibular condyle growth. *J. Dent. Res.* 94, 1668–1675. doi: 10.1177/0022034515598135

Karsenty, G., and Wagner, E. F. (2002). Reaching a genetic and molecular understanding of skeletal development. *Dev. Cell* 2, 389–406. doi: 10.1016/S1534-5807(02)00157-0

Kashiwagi, M., Hojo, H., Kitaura, Y., Maeda, Y., Aini, H., Takato, T., et al. (2016). Local administration of a hedgehog agonist accelerates fracture healing in a mouse model. *Biochem. Biophys. Res. Commun.* 479, 772–778. doi: 10.1016/j.bbrc.2016.09.134

Katagiri, T., and Watabe, T. (2016). Bone morphogenetic proteins. *Cold Spring Harb. Perspect. Biol.* 8: a021899. doi: 10.1101/cshperspect.a021899

Kim, J. -B., Leucht, P., Lam, K., Luppen, C., Ten Berge, D., Nusse, R., et al. (2007). Bone regeneration is regulated by Wnt signaling. *J. Bone Miner. Res.* 22, 1913–1923. doi: 10.1359/jbmr.070802

Krishnan, L., Priddy, L. B., Esancy, C., Klosterhoff, B. S., Stevens, H. Y., Tran, L., et al. (2017). Delivery vehicle effects on bone regeneration and heterotopic ossification induced by high dose BMP-2. *Acta Biomater.* 49, 101–112. doi: 10.1016/j.actbio.2016.12.012

Kronenberg, H. M. (2003). Developmental regulation of the growth plate. *Nature* 423, 332–336. doi: 10.1038/nature01657

Kwan, K. M., Pang, M. K. M., Zhou, S., Cowan, S. K., Kong, R. Y. C., Pfordte, T., et al. (1997). Abnormal compartmentalization of cartilage matrix components in mice lacking collagen X: implications for function. *J. Cell Biol.* 136, 459–471. doi: 10.1083/jcb.136.2.459

Laskin, D. L. (2009). Macrophages and inflammatory mediators in chemical toxicity: a battle of forces. *Chem. Res. Toxicol.* 22, 1376–1385. doi: 10.1021/tx900086v

Leucht, P., Jiang, J., Cheng, D., Liu, B., Dhamdhere, G., Fang, M. Y., et al. (2013). Wnt3a reestablishes osteogenic capacity to bone grafts from aged animals. *J. Bone Joint Surg. Am.* 95, 1278–1288. doi: 10.2106/JBJS.L.01502

Leucht, P., Minear, S., Ten Berge, D., Nusse, R., and Helms, J. A. (2008). Translating insights from development into regenerative medicine: the function of Wnts in bone biology. *Semin. Cell Dev. Biol.* 19, 434–443. doi: 10.1016/j.semcdb.2008.09.002

Lin, G. L., and Hankenson, K. D. (2011). Integration of BMP, Wnt, and notch signaling pathways in osteoblast differentiation. *J. Cell. Biochem.* 112, 3491–3501. doi: 10.1002/jcb.23287

Liu, Q., Hu, X., Zhang, X., Duan, X., Yang, P., Zhao, F., et al. (2016). Effects of mechanical stress on chondrocyte phenotype and chondrocyte extracellular matrix expression. *Sci. Rep.* 6:37268. doi: 10.1038/srep37268

Liu, X., McKenzie, J. A., Maschhoff, C. W., Gardner, M. J., and Silva, M. J. (2017). Exogenous hedgehog antagonist delays but does not prevent fracture healing in young mice. *Bone* 103, 241–251. doi: 10.1016/j.bone.2017.07.017

Long, F., Chung, U., Ohba, S., McMahon, J., Kronenberg, H. M., and McMahon, A. P. (2004). Ihh signaling is directly required for the osteoblast lineage in the endochondral skeleton. *Dev. Camb. Engl.* 131, 1309–1318. doi: 10.1242/dev.01006

Long, F., and Ornitz, D. M. (2013). Development of the endochondral skeleton. *Cold Spring Harb. Perspect. Biol.* 5:a008334. doi: 10.1101/cshperspect.a008334

Long, F., Zhang, X. M., Karp, S., Yang, Y., and McMahon, A. P. (2001). Genetic manipulation of hedgehog signaling in the endochondral skeleton reveals a direct role in the regulation of chondrocyte proliferation. *Development* 128, 5099–5108.

Lu, C., Hansen, E., Sapozhnikova, A., Hu, D., Miclau, T., and Marcucio, R. S. (2008). Effect of age on vascularization during fracture repair. *J. Orthop. Res. Off. Publ. Orthop. Res. Soc.* 26, 1384–1389. doi: 10.1002/jor.20667

Lu, Z., Doulabi, B. Z., Huang, C., Bank, R. A., and Helder, M. N. (2010). Collagen type II enhances chondrogenesis in adipose tissue-derived stem cells by affecting cell shape. *Tissue Eng. A* 16, 81–90. doi: 10.1089/ten.tea.2009.0222

Lv, H., Li, L., Sun, M., Zhang, Y., Chen, L., Rong, Y., et al. (2015). Mechanism of regulation of stem cell differentiation by matrix stiffness. *Stem Cell Res. Ther.* 6:103. doi: 10.1186/s13287-015-0083-4

Maeda, Y., Nakamura, E., Nguyen, M. -T., Suva, L. J., Swain, F. L., Razzaque, M. S., et al. (2007). Indian Hedgehog produced by postnatal chondrocytes is essential for maintaining a growth plate and trabecular bone. *Proc. Natl. Acad. Sci. U.S.A.* 104, 6382–6387. doi: 10.1073/pnas.0608449104

Maes, C., Coenegrachts, L., Stockmans, I., Daci, E., Luttun, A., Petryk, A., et al. (2006). Placental growth factor mediates mesenchymal cell development, cartilage turnover, and bone remodeling during fracture repair. *J. Clin. Invest.* 116, 1230–1242. doi: 10.1172/JCI26772

Mak, K. K., Bi, Y., Wan, C., Chuang, P. -T., Clemens, T., Young, M., et al. (2008). Hedgehog signaling in mature osteoblasts regulates bone formation and resorption by controlling PTHrP and RANKL expression. *Dev. Cell* 14, 674–688. doi: 10.1016/j.devcel.2008.02.003

Maldonado, M., and Nam, J. (2013). The role of changes in extracellular matrix of cartilage in the presence of inflammation on the pathology of osteoarthritis. *Biomed. Res. Int.* 2013:284873. doi: 10.1155/2013/284873

Martel-Pelletier, J., Boileau, C., Pelletier, J. -P., and Roughley, P. J. (2008). Cartilage in normal and osteoarthritis conditions. *Best Pract. Res. Clin. Rheumatol.* 22, 351–384. doi: 10.1016/j.berh.2008.02.001

Martino, M. M., Briquez, P. S., Ranga, A., Lutolf, M. P., and Hubbell, J. A. (2013). Heparin-binding domain of fibrin(ogen) binds growth factors and promotes tissue repair when incorporated within a synthetic matrix. *Proc. Natl. Acad. Sci. U.S.A.* 110, 4563–4568. doi: 10.1073/pnas.1221602110

Matsubara, H., Hogan, D. E., Morgan, E. F., Mortlock, D. P., Einhorn, T. A., and Gerstenfeld, L. C. (2012). Vascular tissues are a primary source of BMP2 expression during bone formation induced by distraction osteogenesis. *Bone* 51, 168–180. doi: 10.1016/j.bone.2012.02.017

McGee-Lawrence, M. E., Ryan, Z. C., Carpio, L. R., Kakar, S., Westendorf, J. J., and Kumar, R. (2013). Sclerostin deficient mice rapidly heal bone defects by activating β-catenin and increasing intramembranous ossification. *Biochem. Biophys. Res. Commun.* 441, 886–890. doi: 10.1016/j.bbrc.2013.10.155

Mente, P. L., and Lewis, J. L. (1994). Elastic modulus of calcified cartilage is an order of magnitude less than that of subchondral bone. *J. Orthop. Res. Off. Publ. Orthop. Res. Soc.* 12, 637–647. doi: 10.1002/jor.1100120506

Morrell, N. T., Leucht, P., Zhao, L., Kim, J. -B., ten Berge, D., Ponnusamy, K., et al. (2008). Liposomal packaging generates wnt protein with *in vivo* biological activity. *PLoS ONE* 3:e2930. doi: 10.1371/journal.pone.0002930

Muir, H. (1995). The chondrocyte, architect of cartilage. Biomechanics, structure, function and molecular biology of cartilage matrix macromolecules. *BioEssays News Rev. Mol. Cell. Dev. Biol.* 17, 1039–1048.

Murab, S., Samal, J., Shrivastava, A., Ray, A. R., Pandit, A., and Ghosh, S. (2015). Glucosamine loaded injectable silk-in-silk integrated system modulate mechanical properties in bovine *ex-vivo* degenerated intervertebral disc model. *Biomaterials* 55, 64–83. doi: 10.1016/j.biomaterials.2015.03.032

Nishitani, K., and Schwarz, E. M. (2014). Cartilage transplants hold promise for challenging bone defects. *Nat. Rev. Rheumatol.* 10, 129–130. doi: 10.1038/nrrheum.2013.216

Nolan, D. J., Ginsberg, M., Israely, E., Palikuqi, B., Poulos, M. G., James, D., et al. (2013). Molecular signatures of tissue-specific microvascular endothelial cell heterogeneity in organ maintenance and regeneration. *Dev. Cell* 26, 204–219. doi: 10.1016/j.devcel.2013.06.017

Ohba, S., Kawaguchi, H., Kugimiya, F., Ogasawara, T., Kawamura, N., Saito, T., et al. (2008). Patched1 haploinsufficiency increases adult bone mass and modulates Gli3 repressor activity. *Dev. Cell* 14, 689–699. doi: 10.1016/j.devcel.2008.03.007

Ortega, N., Behonick, D. J., and Werb, Z. (2004). Matrix remodeling during endochondral ossification. *Trends Cell Biol.* 14, 86–93. doi: 10.1016/j.tcb.2003.12.003

Pal, S. (2014). *Design of Artificial Human Joints & Organs.* New York, NY; Heidelberg; Dordrecht; London: Springer US.

Park, J., Gebhardt, M., Golovchenko, S., Perez-Branguli, F., Hattori, T., Hartmann, C., et al. (2015). Dual pathways to endochondral osteoblasts: a novel chondrocyte-derived osteoprogenitor cell identified in hypertrophic cartilage. *Biol. Open* 4, 608–621. doi: 10.1242/bio.201411031

Park, J. S., Chu, J. S., Tsou, A. D., Diop, R., Tang, Z., Wang, A., et al. (2011). The effect of matrix stiffness on the differentiation of mesenchymal stem cells in response to TGF-β. *Biomaterials* 32, 3921–3930. doi: 10.1016/j.biomaterials.2011.02.019

Park, S. -H., Silva, M., Bahk, W. -J., McKellop, H., and Lieberman, J. R. (2002). Effect of repeated irrigation and debridement on fracture healing in an animal model. *J. Orthop. Res.* 20, 1197–1204. doi: 10.1016/S0736-0266(02)00072-4

Pei, M., Li, J. T., Shoukry, M., and Zhang, Y. (2011). A review of decellularized stem cell matrix: a novel cell expansion system for cartilage tissue engineering. *Eur. Cell. Mater.* 22, 333–343; discussion 343. doi: 10.22203/eCM.v022a25

Rafii, S., Butler, J. M., and Ding, B. -S. (2016). Angiocrine functions of organ-specific endothelial cells. *Nature* 529, 316–325. doi: 10.1038/nature17040

Regard, J. B., Zhong, Z., Williams, B. O., and Yang, Y. (2012). Wnt signaling in bone development and disease: making stronger bone with Wnts. *Cold Spring Harb. Perspect. Biol.* 4:a007997. doi: 10.1101/cshperspect.a007997

Rho, J. Y., Ashman, R. B., and Turner, C. H. (1993). Young's modulus of trabecular and cortical bone material: ultrasonic and microtensile measurements. *J. Biomech.* 26, 111–119.

Roughley, P. J., and Mort, J. S. (2014). The role of aggrecan in normal and osteoarthritic cartilage. *J. Exp. Orthop.* 1:8. doi: 10.1186/s40634-014-0008-7

Salazar, V. S., Gamer, L. W., and Rosen, V. (2016). BMP signalling in skeletal development, disease and repair. *Nat. Rev. Endocrinol.* 12, 203–221. doi: 10.1038/nrendo.2016.12

Sarahrudi, K., Thomas, A., Albrecht, C., and Aharinejad, S. (2012). Strongly enhanced levels of sclerostin during human fracture healing. *J. Orthop. Res.* 30, 1549–1555. doi: 10.1002/jor.22129

Schätti, O., Grad, S., Goldhahn, J., Salzmann, G., Li, Z., Alini, M., et al. (2011). A combination of shear and dynamic compression leads to mechanically induced chondrogenesis of human mesenchymal stem cells. *Eur. Cell. Mater.* 22, 214–225. doi: 10.22203/eCM.v022a17

Scotti, C., Piccinini, E., Takizawa, H., Todorov, A., Bourgine, P., Papadimitropoulos, A., et al. (2013). Engineering of a functional bone organ through endochondral ossification. *Proc. Natl. Acad. Sci. U.S.A.* 110, 3997–4002. doi: 10.1073/pnas.1220108110

Scotti, C., Tonnarelli, B., Papadimitropoulos, A., Scherberich, A., Schaeren, S., Schauerte, A., et al. (2010). Recapitulation of endochondral bone formation using human adult mesenchymal stem cells as a paradigm for developmental engineering. *Proc. Natl. Acad. Sci. U.S.A.* 107, 7251–7256. doi: 10.1073/pnas.1000302107

Sekiya, I., Tsuji, K., Koopman, P., Watanabe, H., Yamada, Y., Shinomiya, K., et al. (2000). SOX9 enhances aggrecan gene promoter/enhancer activity and is up-regulated by retinoic acid in a cartilage-derived cell line, TC6. *J. Biol. Chem.* 275, 10738–10744. doi: 10.1074/jbc.275.15.10738

Sheehy, E. J., Vinardell, T., Buckley, C. T., and Kelly, D. J. (2013). Engineering osteochondral constructs through spatial regulation of endochondral ossification. *Acta Biomater.* 9, 5484–5492. doi: 10.1016/j.actbio.2012.11.008

Sheehy, E. J., Vinardell, T., Toner, M. E., Buckley, C. T., and Kelly, D. J. (2014). Altering the architecture of tissue engineered hypertrophic cartilaginous grafts facilitates vascularisation and accelerates mineralisation. *PLoS ONE* 9:e90716. doi: 10.1371/journal.pone.0090716

Shen, G. (2005). The role of type X collagen in facilitating and regulating endochondral ossification of articular cartilage. *Orthod. Craniofac. Res.* 8, 11–17. doi: 10.1111/j.1601-6343.2004.00308.x

Shi, Y., He, G., Lee, W. -C., McKenzie, J. A., Silva, M. J., and Long, F. (2017). Gli1 identifies osteogenic progenitors for bone formation and fracture repair. *Nat. Commun.* 8:2043. doi: 10.1038/s41467-017-02171-2

Silkstone, D., Hong, H., and Alman, B. A. (2008). Beta-catenin in the race to fracture repair: in it to Wnt. *Nat. Clin. Pract. Rheumatol.* 4, 413–419. doi: 10.1038/ncprheum0838

Silver, F. H., Bradica, G., and Tria, A. (2002). Elastic energy storage in human articular cartilage: estimation of the elastic modulus for type II collagen and changes associated with osteoarthritis. *Matrix Biol. J. Int. Soc. Matrix Biol.* 21, 129–137. doi: 10.1016/S0945-053X(01)00195-0

Simmons, C. A., Alsberg, E., Hsiong, S., Kim, W. J., and Mooney, D. J. (2004). Dual growth factor delivery and controlled scaffold degradation enhance *in vivo* bone formation by transplanted bone marrow stromal cells. *Bone* 35, 562–569. doi: 10.1016/j.bone.2004.02.027

Simmons, C. A., Matlis, S., Thornton, A. J., Chen, S., Wang, C. Y., and Mooney, D. J. (2003). Cyclic strain enhances matrix mineralization by adult human mesenchymal stem cells via the extracellular signal-regulated kinase (ERK1/2) signaling pathway. *J. Biomech.* 36, 1087–1096. doi: 10.1016/S0021-9290(03)00110-6

Song, S., Kim, E. J., Bahney, C. S., Miclau, T., Marcucio, R., and Roy, S. (2015). The synergistic effect of micro-topography and biochemical culture environment to promote angiogenesis and osteogenic differentiation of human mesenchymal stem cells. *Acta Biomater.* 18, 100–111. doi: 10.1016/j.actbio.2015.02.021

St-Jacques, B., Hammerschmidt, M., and McMahon, A. P. (1999). Indian hedgehog signaling regulates proliferation and differentiation of chondrocytes and is essential for bone formation. *Genes Dev.* 13, 2072–2086. doi: 10.1101/gad.13.16.2072

Stockwell, R. A. (1981). The mechanical properties of biological materials. *J. Anat.* 133, 99–100.

Sukul, M., Nguyen, T. B. L., Min, Y. -K., Lee, S. -Y., and Lee, B. -T. (2015). Effect of local sustainable release of BMP2-VEGF from nano-cellulose loaded in sponge biphasic calcium phosphate on bone regeneration. *Tissue Eng. A* 21, 1822–1836. doi: 10.1089/ten.tea.2014.0497

Takada, R., Satomi, Y., Kurata, T., Ueno, N., Norioka, S., Kondoh, H., et al. (2006). Monounsaturated fatty acid modification of Wnt protein: its role in Wnt secretion. *Dev. Cell* 11, 791–801. doi: 10.1016/j.devcel.2006.10.003

Tampieri, A., and Sprio, S. (2016). *Bio-Inspired Regenerative Medicine: Materials, Processes, and Clinical Applications*. Boca Raton, FL: CRC Press.

Tanck, E., van Driel, W. D., Hagen, J. W., Burger, E. H., Blankevoort, L., and Huiskes, R. (1999). Why does intermittent hydrostatic pressure enhance the mineralization process in fetal cartilage? *J. Biomech.* 32, 153–161. doi: 10.1016/S0021-9290(98)00165-1

Tatsuyama, K., Maezawa, Y., Baba, H., Imamura, Y., and Fukuda, M. (2000). Expression of various growth factors for cell proliferation and cytodifferentiation during fracture repair of bone. *Eur. J. Histochem.* 44, 269–278.

Thomas, G. P., and el Haj, A. J. (1996). Bone marrow stromal cells are load responsive *in vitro*. *Calcif. Tissue Int.* 58, 101–108. doi: 10.1007/BF02529731

Thompson, Z., Miclau, T., Hu, D., and Helms, J. A. (2002). A model for intramembranous ossification during fracture healing. *J. Orthop. Res.* 20, 1091–1098. doi: 10.1016/S0736-0266(02)00017-7

Tomlinson, R. E., Li, Z., Zhang, Q., Goh, B. C., Li, Z., Thorek, D. L. J., et al. (2016). NGF-TrkA signaling by sensory nerves coordinates the vascularization

and ossification of developing endochondral bone. *Cell Rep.* 16, 2723–2735. doi: 10.1016/j.celrep.2016.08.002

Topol, L., Chen, W., Song, H., Day, T. F., and Yang, Y. (2009). Sox9 inhibits Wnt signaling by promoting beta-catenin phosphorylation in the nucleus. *J. Biol. Chem.* 284, 3323–3333. doi: 10.1074/jbc.M808048200

Uskoković, V., and Desai, T. A. (2014). Does translational symmetry matter on the micro scale? Fibroblastic and osteoblastic interactions with the topographically distinct poly(ε-caprolactone)/hydroxyapatite thin films. *ACS Appl. Mater. Interfaces* 6, 13209–13220. doi: 10.1021/am503043t

Varghese, S., Theprungsirikul, P., Sahani, S., Hwang, N., Yarema, K. J., and Elisseeff, J. H. (2007). Glucosamine modulates chondrocyte proliferation, matrix synthesis, and gene expression. *Osteoarthr. Cartil.* 15, 59–68. doi: 10.1016/j.joca.2006.06.008

Wang, X., Yu, Y. Y., Lieu, S., Yang, F., Lang, J., Lu, C., et al. (2013). MMP9 regulates the cellular response to inflammation after skeletal injury. *Bone* 52, 111–119. doi: 10.1016/j.bone.2012.09.018

Willert, K., Brown, J. D., Danenberg, E., Duncan, A. W., Weissman, I. L., Reya, T., et al. (2003). Wnt proteins are lipid-modified and can act as stem cell growth factors. *Nature* 423, 448–452. doi: 10.1038/nature01611

Wray, J. B. (1964). Acute changes in femoral arterial blood flow after closed tibial fracture in dogs. *J. Bone Joint Surg. Am.* 46:1262. doi: 10.2106/00004623-196446060-00012

Wu, M., Chen, G., and Li, Y. -P. (2016). TGF-β and BMP signaling in osteoblast, skeletal development, and bone formation, homeostasis and disease. *Bone Res.* 4:16009. doi: 10.1038/boneres.2016.9

Xing, Z., Lu, C., Hu, D., Miclau, T., and Marcucio, R. S. (2010a). Rejuvenation of the inflammatory system stimulates fracture repair in aged mice. *J. Orthop. Res.* 28, 1000–1006. doi: 10.1002/jor.21087

Xing, Z., Lu, C., Hu, D., Yu, Y., Wang, X., Colnot, C., et al. (2010b). Multiple roles for CCR2 during fracture healing. *Dis. Model. Mech.* 3, 451–458. doi: 10.1242/dmm.003186

Yang, L., Tsang, K. Y., Tang, H. C., Chan, D., and Cheah, K. S. E. (2014). Hypertrophic chondrocytes can become osteoblasts and osteocytes in endochondral bone formation. *Proc. Natl. Acad. Sci. U.S.A.* 111, 12097–12102. doi: 10.1073/pnas.1302703111

Yelin, E., Weinstein, S., and King, T. (2016). The burden of musculoskeletal diseases in the United States. *Semin. Arthritis Rheum.* 46, 259–260. doi: 10.1016/j.semarthrit.2016.07.013

Yu, Y. Y., Lieu, S., Lu, C., Miclau, T., Marcucio, R. S., and Colnot, C. (2010). Immunolocalization of BMPs, BMP antagonists, receptors, and effectors during fracture repair. *Bone* 46, 841–851. doi: 10.1016/j.bone.2009.11.005

Zelzer, E., McLean, W., Ng, Y. -S., Fukai, N., Reginato, A. M., Lovejoy, S., et al. (2002). Skeletal defects in VEGF(120/120) mice reveal multiple roles for VEGF in skeletogenesis. *Development* 129, 1893–1904.

Zhou, X., von der Mark, K., Henry, S., Norton, W., Adams, H., and de Crombrugghe, B. (2014). Chondrocytes transdifferentiate into osteoblasts in endochondral bone during development, postnatal growth and fracture healing in mice. *PLoS Genet.* 10:e1004820. doi: 10.1371/journal.pgen.1004820

Zhu, J., Nakamura, E., Nguyen, M. -T., Bao, X., Akiyama, H., and Mackem, S. (2008). Uncoupling sonic hedgehog control of pattern and expansion of the developing limb bud. *Dev. Cell* 14, 624–632. doi: 10.1016/j.devcel.2008.01.008

Conflict of Interest Statement: The authors declare that the research was conducted in the absence of any commercial or financial relationships that could be construed as a potential conflict of interest.

frontiers in Bioengineering and Biotechnology

REVIEW
published: 13 November 2018
doi: 10.3389/fbioe.2018.00165

Computational Modeling and Reverse Engineering to Reveal Dominant Regulatory Interactions Controlling Osteochondral Differentiation: Potential for Regenerative Medicine

Raphaelle Lesage[1,2], *Johan Kerkhofs*[1,2†] *and Liesbet Geris*[1,2,3*]

[1] Prometheus, Division of Skeletal Tissue Engineering Leuven, KU Leuven, Leuven, Belgium, [2] Biomechanics Section, KU Leuven, Leuven, Belgium, [3] Biomechanics Research Unit, GIGA in silico Medicine, University of Liège, Liège, Belgium

OPEN ACCESS

Edited by:
Eric Farrell,
Erasmus University Rotterdam, Netherlands

Reviewed by:
Janine Nicole Post,
University of Twente, Netherlands
Andrew Anthony Pitsillides,
Royal Veterinary College (RVC), United Kingdom

***Correspondence:**
Liesbet Geris
liesbet.geris@uliege.be

†Present Address:
Johan Kerkhofs,
Red Cross Flanders, Mechelen, Belgium

Specialty section:
This article was submitted to Tissue Engineering and Regenerative Medicine, a section of the journal Frontiers in Bioengineering and Biotechnology

Received: 01 March 2018
Accepted: 22 October 2018
Published: 13 November 2018

Citation:
Lesage R, Kerkhofs J and Geris L (2018) Computational Modeling and Reverse Engineering to Reveal Dominant Regulatory Interactions Controlling Osteochondral Differentiation: Potential for Regenerative Medicine. Front. Bioeng. Biotechnol. 6:165. doi: 10.3389/fbioe.2018.00165

The specialization of cartilage cells, or chondrogenic differentiation, is an intricate and meticulously regulated process that plays a vital role in both bone formation and cartilage regeneration. Understanding the molecular regulation of this process might help to identify key regulatory factors that can serve as potential therapeutic targets, or that might improve the development of qualitative and robust skeletal tissue engineering approaches. However, each gene involved in this process is influenced by a myriad of feedback mechanisms that keep its expression in a desirable range, making the prediction of what will happen if one of these genes defaults or is targeted with drugs, challenging. Computer modeling provides a tool to simulate this intricate interplay from a network perspective. This paper aims to give an overview of the current methodologies employed to analyze cell differentiation in the context of skeletal tissue engineering in general and osteochondral differentiation in particular. In network modeling, a network can either be derived from mechanisms and pathways that have been reported in the literature (knowledge-based approach) or it can be inferred directly from the data (data-driven approach). Combinatory approaches allow further optimization of the network. Once a network is established, several modeling technologies are available to interpret dynamically the relationships that have been put forward in the network graph (implication of the activation or inhibition of certain pathways on the evolution of the system over time) and to simulate the possible outcomes of the established network such as a given cell state. This review provides for each of the aforementioned steps (building, optimizing, and modeling the network) a brief theoretical perspective, followed by a concise overview of published works, focusing solely on applications related to cell fate decisions, cartilage differentiation and growth plate biology. Particular attention is paid to an in-house developed example of gene regulatory network modeling of growth plate

chondrocyte differentiation as all the aforementioned steps can be illustrated. In summary, this paper discusses and explores a series of tools that form a first step toward a rigorous and systems-level modeling of osteochondral differentiation in the context of regenerative medicine.

Keywords: *in silico* modeling, gene regulatory network, network inference, chondrocyte, differentiation, regenerative medicine

INTRODUCTION

In the growing world of regenerative medicine, the ability to robustly control cell differentiation processes becomes increasingly important. This also applies to regeneration of osteochondral tissues since controlling cell fate decision and differentiation of chondrocytes might have great benefits for both bone defects and cartilage degenerative diseases.

Most of the mammalian skeleton is composed of bone that is formed through endochondral bone formation starting from a cartilaginous template. During development, recruited mesenchymal stem cells undergo condensation. Then, with the influence of a number of factors, the cells start to differentiate into chondrocytes and secrete cartilage matrix rich in type II, IX, and XI collagen. This stage in the chondrogenic differentiation cascade is marked by the expression of the transcription factor SOX9 (Lefrebvre and de Crombrugghe, 1998; Hata et al., 2017). The chondrogenic cells continue to proliferate in a columnar structure and at a certain stage they exit the cell cycle to undergo hypertrophy at the center of the condensation (primary ossification center). This event is associated with secretion of type X collagen (O'Keefe et al., 1994), mineralization of the extracellular matrix (ECM) and expression of molecular markers such as the transcription factor RUNX2, the matrix metalloproteinase MMP13 and the vascular endothelial growth factor VEGF. Although it is commonly accepted that hypertrophic cells tend to undergo apoptosis and be replaced by osteoblasts (bone forming cells), it is now confirmed that a certain percentage transdifferentiates into osteoblasts (Yang et al., 2014). The ensuing vascular invasion, degradation of the mineralized matrix and the production of bone matrix together achieve the bone formation. The same processes also occur at the articular end of the bone (the secondary ossification center), such that a zone of chondrocytes persists only between the primary and secondary ossification centers, called the growth plate. The growth plate has a columnar organization with zones of proliferating chondrocytes, hypertrophic chondrocytes, and bone formation (Long and Ornitz, 2013).

At the adult stage, the only hyaline (stable) cartilage found in long bones, in skeletal homeostasis, is at the joint surface. These chondrocytes do not undergo hypertrophy but remain in a stable phenotype characterized by a low rate of proliferation and the production of ECM rich in Col-II and Aggrecan. However, some degenerative diseases such as osteoarthritis have been associated with dysregulation of the stable cartilage where both the chondrocyte's rate of proliferation and its switch toward hypertrophy are modified leading to abnormal ossification of the joints.

A variety of possible treatment strategies are currently under investigation, both curative and restorative, with amongst them the use of drugs to inhibit the abnormal switch toward hypertrophy or the use of cartilage-engineered constructs to replace affected osteochondral tissues and promote regeneration. Indeed, tissue-engineered (TE) constructs are being developed to treat large tissue defects where spontaneous healing has failed.

Lenas et al. (2009a) presented the paradigm of "developmental engineering" arguing that a better understanding of the developmental skeletal tissue formation process and a better control of the developmentally-inspired *in vitro* process of chondrogenic differentiation will help to develop more qualitative and robust bone and cartilage TE constructs. In both aforementioned treatment strategies (drugs and TE), the ability to precisely control the cell differentiation and the switch from one genetic program (SOX9) to another (RUNX2) is implied.

Computer models provide a formal framework to study the dynamics of genetic programs within a cell. Computational biology is the field where informatics, engineering and biology meet to enhance the understanding of biological systems and, notably, their underlying regulatory networks (RN). Computer modeling can be used to interpret experimental findings, to help in the design of new experiments and to identify potential therapeutic targets. The importance of systems biology in the field of tissue engineering and regenerative medicine has increased over the last years (e.g., Sengers et al., 2008; Lenas et al., 2009b; Geris et al., 2010; Rajagopalan et al., 2013; Carlier et al., 2014; Geris, 2014; McNamara et al., 2015; Smeets, 2016). A variety of modeling technologies is being used, covering processes at different spatial and temporal scales (genes/protein, cell, tissue, organs, systems, . . .). One family of models, the (gene) regulatory network (G)RN models, may be of particular interest when it comes to deciphering signaling and the cell response implied in cell fate decision. Indeed, the human intuition is limited in its capacity to deal with the complex interplay present in signaling networks whereas a growing arsenal of *in silico* models shows how formal computer language can help to tackle these issues. The works of Aldridge et al. (2009), Saez-Rodriguez et al. (2009), Woolf et al. (2005), or Xia et al. (2006) are a non-exhaustive list of examples where *in silico* models were successfully used to unravel biological complexity and give new biological insights.

In this review we aim to provide an overview of the different methods that can be employed to generate such (G)RN models (see overview **Figure 1**). The first step is the generation of a network graph, which can be either derived from mechanisms and pathways that have been reported in the literature (knowledge-based approach) or it can be inferred directly from the data (data-driven approach). Combinatory approaches

allow further optimization of the network. This network graph provides a static (unchanging) picture of the biological process under study. Once a network is established, several modeling technologies are available to interpret dynamically the relationships that have been put forward in the network graph. A dynamic analysis amounts to simulating the evolution over time of the different network elements under specific conditions and to studying the possible outcomes (stable states) of the established network. We will start this review with the modeling part and subsequently discuss the network part. In each case, we will start by presenting the general principles and some of the computational methods currently available, followed by a non-exhaustive overview of the studies that already made use of those computational modeling approaches to study cell fate decision, mostly focusing on applications of chondrocyte differentiation and growth plate dynamics. Finally, we will discuss different strategies where knowledge-derived modeling approaches and data-based approaches can be used together to complement each other. This combination strategy will be illustrated by a case study focusing on a model of chondrocyte differentiation in the growth plate.

Here, we focus on regulatory networks at the intracellular level where e.g., the ECM and mechanical forces are represented by the intracellular signals they generate which activate the corresponding pathways in the regulatory network. Providing an overview of existing models at other spatio-temporal scales that can take these factors (ECM, mechanics etc.) into account in a more explicit manner, is beyond the scope of this paper. We refer the readers to review papers on the subject of multiscale modeling of skeletal tissue engineering and regeneration processes (Glimm et al., 2012; Julkunen et al., 2013; Geris, 2014; Yousefi et al., 2015). This review ultimately should provide biologists with the necessary vocabulary and information to understand the requirements and accomplishment of (G)RN models.

IN SILICO KNOWLEDGE-BASED MODELING OF REGULATORY NETWORKS TO STUDY CELL FATE DECISION

Mechanistic network-based models start from a static network and use knowledge and mechanisms gleaned from decades of biomedical experimental research to bring this static network toward a dynamic mathematical model. A mathematical model describes a system, for instance a biological system, using mathematical concepts. A model is composed of a set of variables and a set of equations. The variables are quantities with a value that can change according to the equations that establish rules between the variables. The equations are built using an ensemble of parameters with a given (fixed) value; they determine how variables evolve in simulations. It is not easy to determine the most appropriate *in silico* technology amongst all of the available *in silico* modeling methods; which is why several teams tackled this issue by proposing different kinds of classifications. Some of these classifications are based on the mathematical methodology, others are based on biological issues. Janes and Lauffenburger (2006) proposed a decision tree to classify and help to choose the methods best suited for answering a particular question according to various criteria. After a general introduction, the following sections will present some of these methods by classifying them into commonly accepted mathematical subgroups. This classification into subgroups is summarized in the lower part of **Figure 1**, adapted from Morris et al. (2010), showing the different mechanistic modeling approaches which are described in the text below starting with the distinction between quantitative and qualitative models.

General Principles and Formalism of Knowledge-Based Modeling

Quantitative Models (Differential Equations)

Usually biologists build regulatory pathway maps as a static representation of the knowledge they get from experiments while the goal of systems biology is to turn them into dynamic models. It means that the model should be "executable" through simulation instead of being a simple map. A common way to study a system's behavior in a quantitative way is by using differential equations (**Box 1**). In systems biology, the ordinary differential equations (ODE) describe changes over time whereas the partial differential equations (PDE) describe changes in space and time (Wolkenhauer et al., 2005). In order to capture the concentration changes of molecules over time and describe the interaction between variables, the differential equations rely on the law of mass action and its derivations such as the Hill equation. For RN, these mathematical formulations state that the expression level of a gene at time $t+1$ depends on the weighted expression levels of other genes at time t, making them perfectly suited to represent changes in levels of gene expression over time. The same formalism can be used to simulate changes in protein activity or protein concentration levels over time due to interactions with other proteins. The mathematical equations, describing these evolutions over time, contain parameters that are related to the network topology (i.e., the way the biological components are connected to each other) and to the strength of regulation (Liu et al., 2012). For instance when time-varying ODEs are used to represent biochemical reactions and a network of protein interactions, parameters typically are dissociation constants, kinetic rate constants, reaction order, etc. It is possible to add further terms/parameters that indicate the influence of additional substances (Schlitt and Brazma, 2007) if the purpose is, for instance, to simulate drug therapies. For a formal description of how to use ODEs in order to build a GRN model (see Klipp et al., 2005; Wolkenhauer et al., 2005).

A simple way to introduce a spatial component when time-varying ODE equations are used, is through compartmentalization. The same variables occurring at different locations within the cell are simulated as distinct variables. For instance, in kinetic models, the same proteins present in different cell compartments (organelles) are simulated as distinct variables and membrane diffusion or speed of translocation are the additional parameters associated with the compartmentalization (Janes and Lauffenburger, 2006).This is interesting, for instance, in the case of proteomic models where molecules can translocate from one organelle to another. When translocation occurs, there

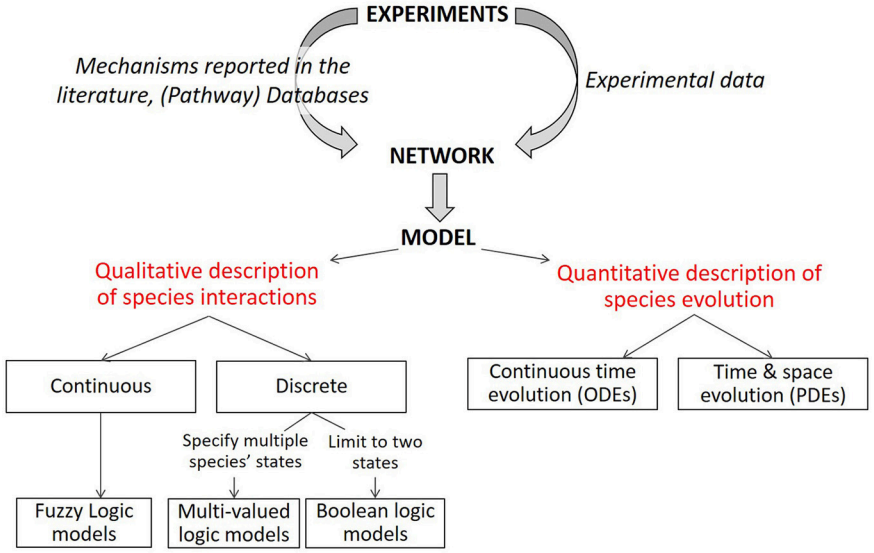

FIGURE 1 | Description of modeling formalisms. Starting from a static network graph obtained from experimental data, various modeling approaches can be used to simulate the evolution over time of the network components. Quantitative models describe the evolution of species over time with ordinary differential equations (ODE) and can introduce spatial resolution with partial differential equations. Qualitative models (limited here to logical models) describe the evolution of species in terms of logical statements. Discrete logic can specify two or more levels for each modeled species (only two for Boolean logic). Various methods of describing discrete or Boolean logical models with piece-wise continuous equations or logic-based ODEs have been successfully implemented to represent biochemical signaling networks. Modified from Morris et al. (2010).

Box 1 | Definitions of modeling types—in the context of systems biology applications.

Deterministic: A deterministic model is a model that will give the same output each time it is run with the same starting conditions.
Stochastic: By opposition to deterministic, in a stochastic model, one and the same initial state can lead to many different trajectories. This randomness is often used to represent biological uncertainty.
Differential equation: an equation relating a variable and its derivative(s).
Ordinary differential equation: In systems biology an ODE most commonly describes the evolution of a variable over time in function of other variables.
Partial differential equation: PDEs in systems biology typically describe the evolution of a variable with respect to time and space.
Multifactorial data: In GRN context, this is data obtained by slightly perturbing all genes simultaneously. It can typically be expression profiles coming from different patients or biological replicates. Multifactorial data are the most common data source as they are easier to obtain than knockout or time series-data.

could be an import/export mechanism generating a time delay that could have a significant influence on the behavior of the system, which can be captured by appropriate mathematical formulations (Wolkenhauer et al., 2005).

Important to remark is that ODE models depend on numerical parameters and initial conditions that are often difficult to measure (Wolkenhauer et al., 2005). That is why modelers usually perform sensitivity analyses. It means that one tries to assess how much a result can change when varying one or several of the parameters. For robust systems, the exact value of a particular parameter may not be essential. Robustness with respect to parameter values seems to be a typical property of most models capturing biological behavior, also termed "sloppiness" as explained in Gutenkunst et al. (2007). Studying the robustness of the system allows determining for which parameters an accurate value is necessary to obtain reliable model predictions and for which parameters that is not the case.

When there is a discrepancy between the experimental observations and the simulation results from models built on curated knowledge such as published protein interactions, the model can be used to suggest possible unknown interactions between the model variables that could help to better explain the experimental data. In that case, the hypothetic interactions proposed can be tested experimentally, which constitutes the iterative process that governs systems biology (McNamara et al., 2015). Following this approach, differential equation based models have been proven able to lead to new testable hypotheses. For instance, von Dassow et al. (2000) developed a differential equation system of developmental processes in Drosophila including 48 parameters (half-lives of messenger RNAs and proteins, binding ranges, etc.). The initial model described all known interactions, but the addition of at least two new hypothetical interactions was needed to ensure the results were fitting the experimental observations reported in the literature.

Qualitative Models

Qualitative models do not aim to provide exact values of concentrations of network components. They rather aim to capture the overall qualitative behavior of networks. In logical

models, variable values are the result of logical relationships (AND, OR, NOT gates) with other variables. Logical modeling was first applied to model GRNs by Stuart Kauffman (Kauffman, 1969, 1994; Glass and Kauffman, 1973). In Kauffman's approach, variables are evaluated using logical combinations of other variables and each variable can take only a discrete number of values (0 or 1 for Boolean models). René Thomas, another pioneer in logical models in systems biology, further refined the logical formalism by introducing multivalued variables and logical parameters equivalent to the kinetic parameters from differential equations (Thomas and Kaufman, 2001). This enabled him to introduce asynchronous updating of the system, which was later extended using temporal logic (Bernot et al., 2004). Indeed, logical systems can be updated in a synchronous way where all variables are updated at the same time during each transition, or in an asynchronous way where values of variables are updated one after the other. The ensemble of successive states through which a system passes during a simulation is called a trajectory and it can vary according to the initial state and the chosen updating strategy. Tracing all the trajectories across the ensemble of states allows to build a state-transition graph (Le Novère, 2015). With logical models, systems biologists usually study the stable states of the system, meaning that they try to identify in which stable state the system tends to settle. A stable state can be a fixed point or a discrete number of states in between which the system oscillates (e.g., for circadian rhythms the baseline behavior is a cyclic one). A system can settle in different stable states according to the initial condition from where it leaves. The ensemble of initial states leading the system to settle in the same stable state, is called the basin of attraction of the corresponding stable state (Mojtahedi et al., 2016). In regulatory networks theory, a system is characterized by its specific stable states. The study of the nature of the stable states and of their basin of attraction can give insight about cell states and cell state reachability, with application in cell fate decision and differentiation. Indeed, the size of a basin of attraction, meaning the number of initial states leading to a stable state, may give an estimate of how likely it is for a cell to reach this state (Abou-Jaoudé et al., 2016). For explicit cases of application see sections Current Computational Models as Predictive Tools for Cell Differentiation and Intracellular Regulatory Network Models of Growth Plate Cells.

Upstream regulators of one specific biological entity (gene/protein) and the ways they regulate it, may vary between different possibilities over time, depending on, for instance, external inputs and the concentrations of the regulators themselves. This behavior cannot be captured by the standard Boolean networks described in the previous paragraph. Probabilistic Boolean networks have been introduced in order to capture this uncertainty in the regulatory logic. In practice, the same initial state can lead to many different trajectories due to the stochastic nature of the model (**Box 1**). This is achieved by introducing several possible mathematical regulation functions (logical combinations of other biological entities) with different probabilities for each entity. At each time step, an entity is updated following one of its different regulation functions chosen randomly (Karlebach and Shamir, 2008). Another probabilistic approach is the Bayesian network but the dynamic aspects are not considered in these models since they often take the form of a directed acyclic graph (Liu et al., 2012). Karlebach and Shamir (2008) proposed dynamic Bayesian networks as a way to counter the lack of dynamic resolution of regular Bayesian networks.

Another good way to analyze model dynamics is through the use of Petri Nets since in that representation, nodes are not biological entities but places (= conditions) or transitions (= events) while directed arcs connect input places to transitions and transitions to output places. The number of transitions to reach a specific state can hence be assessed easily. This approach shows good results of prediction for some systems as illustrated in Steggles et al. (2007). It has the advantage of having an easy graphical representation, which makes this formalism a good common ground for biologists and mathematicians/modelers alike.

Whereas, differential equation based models of GRNs and signaling pathways suffer from the lack of kinetic information (Le Novère, 2015), qualitative models require a smaller amount of data (Karlebach and Shamir, 2008) and qualitative experimental observations might even be sufficient. Qualitative models constitute a good starting point when some interactions of the network remain unknown and it is easy to analyze variants of the same network (Ay and Arnosti, 2011). Indeed, despite the growing amount of biological knowledge about various biological phenomenon, it is not rare that the exact mechanisms remain not fully understood or even controversial. With missing detailed information it is often difficult to develop a mechanistic quantitative model. However, the missing information might not be detrimental to build a qualitative model which catches the wanted behavior, or, alternatively, allows to test different biological scenarios for their potential to capture the wanted behavior. Moreover, once a model explains an actual cell behavior, it becomes possible to study this system under various stress or perturbed conditions to give new predictions.

Fuzzy Logic and Alternative Classifications

Certain model approaches are situated between the previously discussed categories of quantitative and qualitative. Fuzzy logic is one of those model approaches that technically might be considered to be qualitative but allows to include more complexity, making it closer to semi-quantitative approaches. When the behavior that needs to be captured is too complex to capture with discrete logical models, fuzzy logic models allow to introduce continuous regulation as well as provide the capacity to handle a "graded truth." While Boolean logic takes into account only the values of 0 or 1 to describe the variables state (or additional discrete values in a multi-value discrete model), fuzzy logic accepts any value between 0 and 1. The main idea underlying fuzzy logic is that both subjective/abstract and objective knowledge can be integrated to solve a problem (Mendel, 1995). Indeed, the fuzzy logic can integrate intermediate values and even words, such as "low" and "high" concentrations (subjective knowledge) as suggested by Zadeh (1996). This is of particular relevance to the modeling of biological networks since in this field, the information is

sometimes subjective and imprecise, and it becomes difficult to use clear mathematical or logical values to express it. Additionally, it enables very naturally to model uncertainty in signaling networks. Aldridge et al. (2009) provide a good example of adaptation of fuzzy logic to cellular signaling network analysis. In that study the authors investigate the relationship between 2 signaling pathways that may account for the previously known influence of the protein MK2 in cancer cell survival whilst the exact mechanism was not yet fully deciphered. The fuzzy logic approach enabled them to incorporate qualitative (abstract) data drawn from literature such as "low," "medium," "high" state of variables and still produce quantitative predictions. They even used a time variable influencing the output state of some proteins with a "low" value for time referring to early signaling responses (0–2 h) and a "high" value referring to late signaling events (2–24 h).

Application to Cell Fate Decision and Osteochondral Differentiation

The various formalisms described above have been applied frequently for prediction of pluripotent and stem cell fate decision with application in regenerative medicine (Pir and Le Novère, 2016). This section gives an overview of different published models, focusing on (stem) cell fate decision in general and on chondrocyte differentiation and growth plate dynamics in particular.

Current Computational Models as Predictive Tools for Cell Differentiation

The model of Schittler et al. (2010) is a good example of a quantitative model predicting osteochondral cell fate decision. Indeed, they use a GRN, mathematically implemented with differential equations, for both single cell scenarios and cell population scenarios to investigate an osteochondral differentiation system. They modeled the switch mechanisms between three stable states, being the progenitor, osteogenic and chondrogenic states.

Since activation and loss of specific genetic programs governs cell fate decisions, logical GRN models may also be a tool of choice for studying and predicting cell differentiation. Indeed, in this formalism, nodes or variables represent genes or the activity of transcription factors (TF), and connections between the nodes represent regulatory interactions (activation or inhibition) between them. During simulation the model can reach some stable states (cf. section Qualitative Models), which can be considered to equate to a specific (mature) cell types (Glass and Kauffman, 1973). This corroboration between stable state of the network and cell phenotype is the major hypothesis at the basis of all possible cases of application of regulatory network studies.

Herberg and Roeder (2015) reviewed qualitative (Boolean) GRN modeling methods to study embryonic stem cells differentiation where the analysis of the landscape of states and transitions between states gave great insight into the dynamics governing cell fate decisions. The usefulness of random Boolean networks in representing cell type convergence was even extended by Bodaker et al. (2013) with a study showing tissue-like regeneration in multi-cellular organisms. Indeed, in that paper, each cell constituting the multi-cellular organism was represented by a random Boolean network at the intracellular level and the study was based on the fact that the function of cells, and so their differentiation, can be altered following the influence of external signals from a neighboring population of cells on their individual intracellular networks. This approach opens perspectives on how to integrate the influence of neighboring cells and extracellular signals in Boolean networks, which are typically used to study cells in isolation. Other examples of network models enabling predictive analysis of mesenchymal stem cell differentiation into chondrocytes and osteoblasts under various biochemical conditions can be found in Woolf et al. (2005), who used Bayesian networks as modeling technology.

Intracellular Regulatory Network Models of Growth Plate Cells

To date, very few *in silico* skeletal models have focused on the growth plate—especially at the intracellular level. Kerkhofs and coworkers implemented a series of models on the genetic switch between the chondrocyte's proliferative and hypertrophic state within the growth plate (Kerkhofs et al., 2012, 2016; Kerkhofs, 2015; Kerkhofs and Geris, 2015), The control of this switch was studied both in the context of regenerative medicine and tissue engineering, and in the context of degenerative cartilage diseases (Melas et al., 2014). The model that we originally developed (Kerkhofs et al., 2012) was an additive, multi-valued, Boolean model representing the genetic switch from a SOX9 positive stable state to a RUNX2 positive stable state, being the hallmark of the proliferative and the hypertrophic state of the chondrocyte, respectively (see section Qualitative Models for formal definition of stable states). Given that lack of human data, the network used in the Kerkhofs models was built mostly using mouse data (**Figure 2**). This network model gave a first *in silico* insight into the genetic regulation underlying chondrocyte phenotypes within the growth plate and was successful in capturing the effects of knockouts in the main regulatory pathways of the growth plate regulation described in the literature. In subsequent studies, the model was improved by adding (1) a quantitative resolution and (2) temporal priority classes that are absent in classic Boolean models. Adding quantitative resolution, meaning that each node can have any value ranging between 0 and 1, was handled through the implementation of an additive framework. In an additive approach, the value of each variable (= protein activity or gene expression level) is updated by a weighted sum of the values of upstream variables. The temporal resolution of the reactions was managed by incorporating priority classes to account for different reaction kinetics. All reactions related to slow processes such as mRNA or protein production, were referred to as slow reactions (lower priority) and those related to fast processes such as protein activity, were referred to as fast reactions (higher priority). For each node of the network, a fast ("protein activity") and slow ("gene expression") variable was defined with the total activity of any given node being the product of the fast and slow variable. When performing the model (asynchronous) updating, high priority interactions are taken into account first, before taking into account the lower priority interactions, reflecting the time difference between these categories of processes in

cellular systems. This approach enabled to capture dynamics and behaviors more complex than those found with classic Boolean models. For instance, in Kerkhofs and Geris (2015) we showed that the model was able to simulate dose response studies where different levels of stimuli in proliferative chondrocytes gave rise to qualitatively different responses. The framework was used furthermore to perform an analysis of the stable states and a stable state perturbation analysis, assessing the influence of specific factors of the network thanks to *in silico* over-activation or KO. We also investigated the relevance of the modeling results in osteoarthritis as abnormal chondrocyte hypertrophy plays a role in this disease (Kerkhofs et al., 2016). The perturbation study may point out potential key biological factors to be targeted experimentally to either promote the differentiation or to inhibit it.

The Kerkhofs models were implemented in a general computational software package called MATLAB (The Mathworks). In order to make the models easily accessible to the wider audience of non-modeling specialists, the interface is of great importance. Scholma et al. (2014) and Schivo et al. (2016) implemented the Kerkhofs models into a timed automata framework, called ANIMO. This modeling framework is available as a plug-in of Cytoscape and has been conceived particularly around its intuitive end user interface to facilitate use by a wider audience, including biologists.

DATA DRIVEN MODELING-NETWORK INFERENCE

The preceding section described methods used to generate model predictions, once a network has been established. This section will focus on establishing such networks. There are two main classes of approaches. In one approach (knowledge-based, literature-curated), networks are built using mechanisms described in the literature and aggregated in (pathway) databases such as the network used in the Kerkhofs models described above. In the other approach (data-driven), networks are inferred directly from experimental data. The difficulty with the latter approach is to find/perform experiments with a sufficiently high information-content, typically requiring a standard condition with sufficient and sufficiently strong perturbations of that standard condition. This section will focus on the inference process and its challenges.

General Principles of Network Inference

The Inverse Problem and Adaptation to Network Inference

In inverse problems, one aims to infer the parameters describing the system, given actual observations. In order to solve an inverse problem different methods can be used, depending on the exact nature of the question to be answered. Generally, inverse problems deal with an optimization problem since one needs to minimize a functional error between real values (data) and the simulated values (Tarantola, 2006; Liu et al., 2012).

Network inference can be considered as an inverse problem where the network parameters, being the absence, presence and direction of regulatory interactions, are derived directly from experimental data (Villaverde and Banga, 2013). With the huge progresses in the field of molecular biology these past few years, we currently dispose of large amounts of quantitative data such as mRNA levels, protein levels, phosphorylation states, etc. to use for model inference. However, it also raises the question of the identifiability of the network's parameters i.e., the ability to find an unambiguous set of parameters determined by the available data set, as, in many cases, several sets of parameters might fit the same data set.

Concise Overview of Methods for Network Inference

The development of a myriad of methods, formalisms and software tools helps to tackle the problem of inferring a network from microarray expression data as well as from RNA Sequencing data, protein-DNA binding data (ChIP-seq), CpG methylation, promoter sequence detection and proteomics data. Here we review a number of these methods following the categorization in four parts as found in Marbach et al. (2012) and Le Novère (2015). These categories are (1) the statistical methods, (2) probabilistic methods, (3) information theoretic methods, and (4) methods based on ODEs. Most of them propose, as an output, a ranked list of regulatory interactions from the one most likely to be a true interaction to the least likely one. Those interactions can represent protein interactions or associations, in the case of signaling network, but also interactions between transcription factors (TF) and genes in the case of gene networks. These interactions might be direct or indirect relationships. Details on the mathematics of the different methods for gene network inference can be found in **Supplemental Data 1**.

Most of these methods can work with multifactorial data (**Box 1**) and data of different types such as steady state and/or time series data. This is useful when considering the range of available data that often comes from experiments of one or multiple factor perturbations. Hence, combining different inference methods together (hybrid methods) might help to widen the scope of the type of data that can be taken into account. Moreover, the rationale behind GRN inference is to decipher the underlying existing regulatory network solely from perturbed gene expression data. Therefore, it is important to make sure that the biological material used to generate the data actually reliably reflects the biological system under investigation. This means that single-cell RNA-seq data is possibly the best way to ensure that the expression data does not capture the behavior of several heterogeneous systems but only that of the system of interest (Griffiths et al., 2018). For chondrocyte in the growth plate, the use of single-cell RNA-seq allowed the identification of regulatory molecular cascades important for the different stages of chondrocytes during development (Li et al., 2016). Nevertheless, single-cell data is not always available and inference from micro-array data or general RNA-seq data has been proven to perform well.

Strengths and Weaknesses of Inference Methods and the Ensemble Approach

The amount of inference methods has been increasing in recent years (Marbach et al., 2009). De Smet and Marchal

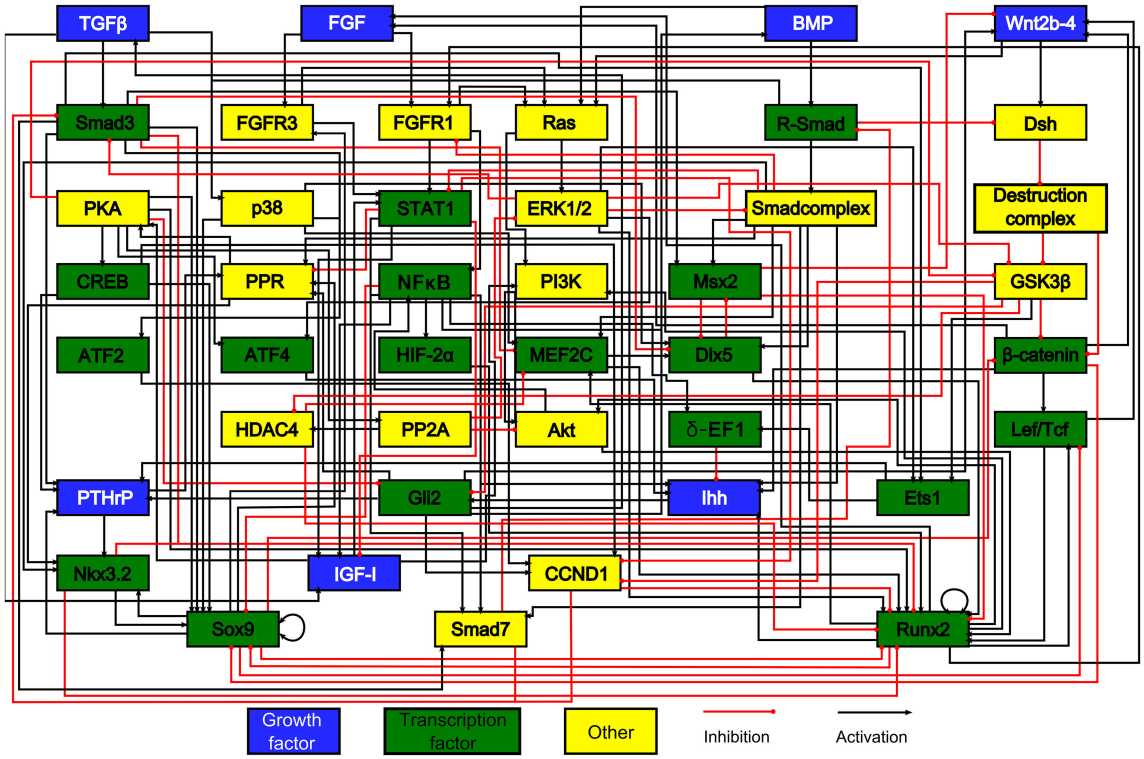

FIGURE 2 | The model's chondrocyte gene network. Every box represents a gene, its protein or in some cases a complex of them. The interactions are represented by red and black lines if they are inhibitory and stimulatory, respectively. Blue boxes denote growth factors, green boxes are transcription factors, yellow boxes do not belong to either category. Reproduced from Kerkhofs and Geris (2015).

(2010) argue that direct integration of inference tools in daily laboratory practice by biologists is still limited, because the choice of the inference is not always obvious. Hence, the authors propose a new classification of the inference tools based on their nature, i.e., supervised/unsupervised, integrative or not, direct inference or based or pre-module construction etc., which gives new insights in the strength and weakness of each methods. Several studies tend to highlight the advantages and weaknesses of various methods for specific applications, but some studies aim to compare multiple methods. Since 2006, a big consortium called "the Dialogue on Reverse-Engineering Assessment and Methods (DREAM) challenge" tries to develop an objective assessment of reverse engineering methods for biological networks (Stolovitzky et al., 2007; Saez-Rodriguez et al., 2016). During the yearly DREAM challenges, scientists of the field from all around the world are invited to use the inference method of their choice to a given data set following specific guidelines. In that way, the organizers can apply blinded cross-comparisons of the results with standard metrics and they are able to identify the specific strengths and weakness of each method. Such assessment will help systems biologists to choose the inference method best suited to the question they aim to answer, given the type of data they have at their disposal. Additionally, it provides teams trying to develop new inference methods with a more formal assessment process, a new way to test their own algorithm (Stolovitzky et al., 2007).

In later DREAM Challenges (Marbach et al., 2012), revealed that no single inference method performs optimally across diverse datasets but predictions from multiple inference methods combined do. Indeed, they have estimated the performance of a consensus network constructed as an average network of multiple inference methods and they showed it was performing better than other methods taken individually. The consensus network is then the result of a voting approach in which the top ranked interactions predicted by all methods, meaning the most likely to exist according to all methods, are maintained in a new network. In combining predictions made by disparate methods, the intersection of their predictions complements their strengths and their weaknesses. Voting was shown to be an effective strategy for network inference, but it should be said that rather than finding the "best" network, it serves to find the "least bad" one (Marbach et al., 2012; Kerkhofs, 2015).

Finally, inference algorithms offer a systematic way to infer regulatory networks directly from data without the need to curate literature manually, a process that inadvertently introduces curator-bias. Increasing performance of the published algorithms, improvement in the field of machine learning and consensus approaches gathering several methods, together enhance the reliability, and accuracy of such inferred regulatory

networks. This enables to produce a static map which can further be used as a starting point for computational simulations thanks to the modeling approaches described in section 2. Indeed, *in silico* simulations of such regulatory networks might give meaningful insight in the understanding of biological processes. Molinelli et al. (2013) provide a good example of a regulatory network inference process giving meaningful biological insight in the field of cancer. In their study, the authors first perform a large screening of experimental perturbations for high throughput measurement of proteomic changes (e.g., reverse phase protein arrays or mass spectrometry) and phenotypic changes (e.g., cell viability or apoptosis). They use this data as input to infer a network model of signaling in a RAF inhibitor resistant melanoma cell line (SKMEL-133). The constructed network enabled the authors to retrieve known pathways such as PI3K/Akt or MAPK pathways as well as new interactions that are consistent with known protein functions. Finally, from the network, they perform simulations of different *in silico* single or pairwise perturbations of nodes that were experimentally targeted or not in the input data. Their model is predictive of both the proteomic and phenotypic responses to drug combinations. Additionally, it successfully predicts the phenotypic response profiles of SKMEL-133 cells to novel drug targets, for instance, *in silico* simulations predicted that PLK1 inhibition was decreasing cell viability, which was validated *in vitro* with 99% of the cells eliminated with a 15 nM concentration of PLK1 inhibitor. Overall, this study uses the typical pipeline of *in vitro/in silico* integration to obtain new biological insights. Similar methodology could be of great interest to be applied to cell fate decision and osteochondral differentiation in order to identify the underlying regulatory networks involved and the key factors to target in order to modulate those processes. Therefore, some examples of network inference in this context are developed in the next sections.

Application to Cell Fate Decision and Osteochondral Differentiation

Inference of a Growth Plate Network Following a Consensus Approach

As a first illustration of inference methods and the consensus approach for osteochondral system, we return to the growth plate model described in section Intracellular Regulatory Network Models of Growth Plate Cells. We describe the inference process that we have followed, in a previous study, to build a data-driven network in order to validate the literature-curated one (Kerkhofs, 2015). The inference was executed using measurements from the mouse growth plate exclusively, as the topology of the literature-derived network from Kerkhofs et al. (2016) was derived mostly from studies performed in mice. An overview of the micro-array data can be found in **Table 1**. As can be seen, not all studies have divided the growth plate in the same zones, but the proposed network should be valid throughout the entirety of the growth plate. All the published experimental data were generated with Affymetrix Mouse 430.2 microarrays. All samples were normalized using the Guanine Cytosine Robust Multi-Array Analysis (Wu and Irizarry, 2004; Wu et al., 2004).

Only transcription factors were chosen as input nodes for inference because their mechanism of action is more directly measured, it is less influenced by post-translational modifications and TFs are typically represented by one measurement on the microarray. No proteomic data was exploited. Selecting only the TFs from the prior network to do the inference also helped to reduce the size of the optimization problem. As a result, the network was inferred between the following 13 genes: Gli2, Tcf7, Runx2, Sox9, MEF2C, STAT1, ATF2, NFκB, CCND1, Dlx5, Ets1, δ-EF1, HIF-α2. The subnetwork from the literature-derived model that includes the components used for the inference is shown in **Figure 3**.

The inference methods used in the consensus approach are recapitulated in **Table 2** and described in full in **Supplemental Data 1**. Each single method provided its own ranked list of inferred interactions. With the voting approach, a consensus network was inferred by providing a sorted list of inferred interactions according to their average rank over all the methods. To be noted also that the consensus network was built as undirected because most of the individual methods produce undirected networks. Undirected means that when a regulatory interaction is inferred, it only suggests that the interaction exists between two components but it does not presuppose which one of the components acts on the other.

TABLE 1 | Summary of literature sources for microarray data on the growth plate.

Origin	Samples	Study design	Reference
Primary growth plate chondrocytes	12	Cells treated with dexamethasone or control, 6 h or 24 h in culture, 3 replicates	James et al., 2007
Growth plate	8	Resting, proliferating, maturing and hypertrophic zone, 2 replicates each	Isshiki et al., 2011
Primary growth plate chondrocytes	15	Control and 4 individual inhibitors,24 h in culture, 3 replicates each	Ulici et al., 2010
Growth plate	12	Resting/proliferating, maturing/hypertrophic and mineralising zone, 4 replicates each	James et al., 2010
Explant culture	18	Treatment with CNP or control, 6 days in culture, Resting/proliferating, maturing/hypertrophic and mineralising zone, 3 replicates each	Agoston et al., 2007

The first column lists the origin of the sample. The second column indicates the amount of samples. The third column briefly summarizes the treatment and the amount of replicates. The final column indicates the reference for the samples.

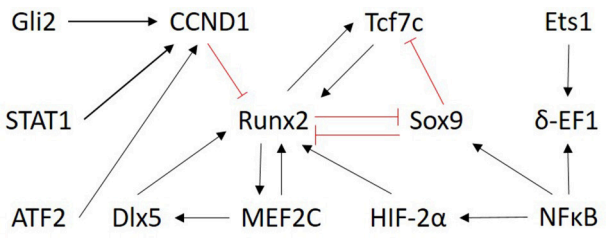

FIGURE 3 | Overview of the subnetwork of factors selected for inference. The regulatory interactions are those present in the literature derived model (Kerkhofs et al., 2016). Only the nodes are considered as input for the ensemble inference. Red and black arrows indicate inhibition and activation, respectively.

TABLE 2 | Summary of inference methods applied to microarray data.

Category	Methods
Statistical methods	Correlation (Pearson and Spearman), TIGRESS (Haury et al., 2012), GENIE3 (Huynh-Thu et al., 2010)
Information-theoretic methods	Mutual information, CLR (Faith et al., 2007), ARACNE (Margolin et al., 2006), MRNETB (Meyer et al., 2010)
Probabilistic methods	Bayesian (Friedman et al., 2000), GGM (Werhli et al., 2006)
Ode-based methods	Inferelator (Bonneau et al., 2006; Greenfield et al., 2013)

The methods are divided into four categories, though the match can be somewhat arbitrary and some methods are more hybrid-like.

Inference Methods Applied to Cell Fate Decisions

Rapid advances in high-throughput–omics techniques over the last decade have opened a myriad of possibilities for study of biological phenomena. Inferring regulatory networks is an essential part of the general omics analyses pipeline. In Griffiths et al. (2018) the authors reviewed RNA-seq data analysis pipelines to study the developmental process in general and cell fate decisions in particular and discussed the remaining challenges such as the issue in distinguishing small biologically meaningful variations from technical artifacts. Despite this difficulty, Li et al. (2017) were able to infer a network model for growth plate chondrocytes based on 5 human patient samples. Furthermore, Li et al. (2016) succeeded in deriving a regulatory network of mouse growth plate development based on single-cell RNA-seq data. The authors developed a systematic pipeline enabling the identification of genes and signaling pathways involved in this developmental process and suggest the pipeline could be used to investigate other developmental processes.

Other inference examples include Chen et al. (2015), who proposed a tool to infer a transcriptional regulatory network from single-cell transcriptional data in order to identify operational interactions corresponding to specific cell fate determination. Importantly, the authors intended to build a Boolean network model out of it, highlighting the importance of having an "executable" model for simulation and not a simple static map (see **Figure 1**). Finally, Weinreb et al. (2018) developed an inference algorithm and applied it to predict cell state decision from hematopoietic progenitor cells, illustrating the range of application possibilities for regenerative medicine.

If genomic and transcriptomic data can serve for GRN inference, proteomic data might be of interest to infer protein signaling networks. Melas et al. (2014) integrated phospho-proteomic and cytokine release data to build a mechanistic model of signal transduction in the adult chondrocyte. They inferred regulatory protein interactions directly from the data in order to identify previously reported as well as new key players involved in chondrocyte homeostasis. This could be very beneficial to find important biological factors with a potential for cartilage regeneration.

COMBINING KNOWLEDGE-DERIVED MODEL WITH NETWORK INFERENCE: CASE STUDY APPLIED TO CHONDROCYTE DIFFERENTIATION

General Principles

It should be kept in mind that both knowledge-driven and data-driven approaches can be relevant depending on the type of questions the model is supposed to answer and should be chosen wisely in a problem-centric approach (Janes and Lauffenburger, 2006). An alternative can be to mix both of them as was done for instance in Melas et al. (2011) where the authors developed a curated knowledge-derived topology linking external stimuli to signaling pathways, and subsequently used data-driven approaches to link signaling pathways to cellular responses. Following this approach, they produced an extended network that was shown to perform better in predicting qualitative cellular responses to specific cues than a purely data-derived model.

It is not only possible to link together literature-derived and data-based networks but one method can benefit from the insights gained with the other (**Figure 4**). There are two reciprocal benefits: (1) literature-derived models can gain from data-based optimization and (2) network inference algorithms can see their performance considerably increased by incorporating prior knowledge in the inference process.

With respect to the first benefit, one should bear in mind that molecular regulatory network models not only serve as a descriptor, but also as a predictor of the cell response. One of the limits of logical models is their lack of accuracy in yielding useful predictions and new insights, In Saez-Rodriguez et al. (2009), the authors explain how to turn network models into predictive logical models that are rigorously calibrated against experimental data. By training a general literature-derived network against cell specific data, they succeeded in identifying interactions that did not seem to be functional in the specific cell type under study. Additionally, they could propose new interactions not present in the initial generic model although being supported by other sources from literature.

As for the second benefit, there are indeed techniques that aim at inferring regulatory network from experimental data whilst incorporating curated knowledge as a prior within the algorithm in order to increase performance. For instance, for

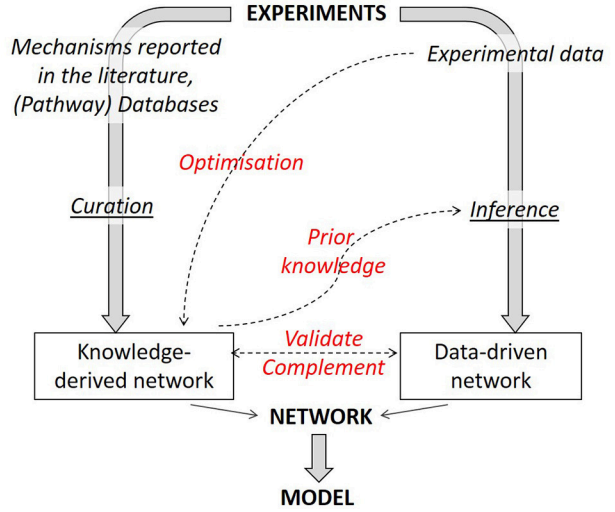

FIGURE 4 | Strategies to combine knowledge-derived and data-based modeling. When deriving a network graph from experimental results, different routes can be followed, either a mechanistic one (using available knowledge) or a data-driven one. Combining both strategies allows to obtain an optimized network graph. Knowledge-derived networks can be fitted against experimental data to optimize network parameters. Knowledge-derived networks can serve as prior knowledge within some inference algorithms in order to improve inference performance. Finally, data-driven networks can be used to validate or complement (add or remove interactions) a knowledge-derived one and vice versa.

the constructions of a predictive model of signal transduction in chondrocytes, Melas et al. (2014) combined the proteomic data with a priori knowledge of the proteins' connectivity. This is also the case in the "Inferelator" algorithm (Bonneau et al., 2006) which infers transcription factor—gene interactions.

Having the most reliable network possible is important since the dynamic of the resulting model will settle down into equilibrium states strictly complying with the topology of the regulatory interactions. Hence, the topology will define the outcome of the simulation. To illustrate the interactions as depicted in **Figure 4** (compare, validate, optimize, prior knowledge), we will return one more time to our growth plate example discussed in the previous sections.

Case Study: Chondrocyte Differentiation in the Growth Plate

Comparing Different Networks

In a direct approach, the interactions with the highest combined rank in the consensus-inferred network can be compared to the interactions present in the knowledge-derived network. By doing so, we found most of the interactions present in both networks (Kerkhofs, 2015), which can be interpreted as a corroboration of the knowledge-derived network. Additionally, we noticed that some interactions inferred with a high rank were not present in the literature-derived topology (for instance MEF2C-HIF-2a). This can be considered as a suggestion for complementing the knowledge-derived network.

Besides this direct comparison as mentioned in the previous paragraph, classical measures of performance can be used to assess rigorously the match between the micro-array data inferred network (discussed in section Data Driven Modeling—Network Inference) and the literature-derived network (discussed section *in silico* Knowledge-Based Modeling of Regulatory Networks to Study Cell Fate Decision). These measures include the receiver operating characteristic (ROC) curve, the Precision Recall (PR) curve and their respective area under the curve (AUROC and AUPR), see **Supplemental Data 1** for detailed definitions. They are based on the comparison between an inference algorithm and a gold standard and they are commonly used in the context of GRN inference (Marbach et al., 2012). In the chondrocyte network study (Kerkhofs, 2015), the main objective was to assess to what extent the topology inferred from micro-array data corresponds to the knowledge-based topology manually curated from the literature. Practically, the inferred network and the literature-derived network were compared while regarding the literature-derived network as a pseudo-gold standard.

In parallel, the inferred network was also compared to another network topology derived from an online database named STRING (Search Tool for the Retrieval of Interacting Genes/Proteins). The STRING network is not the result of a mathematical inference, instead, the STRING tool generates networks for which the connections represent functional associations (both direct and indirect) predicted from screening large databases containing protein-protein interactions gathered from genomic context predictions, text-mining from PubMed and co-expression data. The STRING network presented here was generated by querying the STRING tool, giving as an input the 13 proteins and the total number of interactions of the network depicted in **Figure 3**. Each interaction included in the obtained STRING network is annotated with a bibliographic or experimental reference to the study that enabled adding the interaction to the network. For a detailed description about the tool, we refer the readers to Szklarczyk et al. (2017). The aforementioned inferred network was tested against the STRING topology to assess whether the inferred network was better at fitting the literature-based model than at fitting the automatically produced STRING topology. In other words, it was tested to assess whether the manual literature curation and topology creation was superior to an automatic one in the cell specific context of a growth plate chondrocyte.

When comparing the ROC curves of the inferred network with respect to either the knowledge-based or the STRING derived model, it can be appreciated that the performance is better with the knowledge-based network (**Figures 5A,C**). Indeed, the concavity of the curve points toward a good correspondence between the inferred interactions and the ones in the knowledge-based network, whereas a line with a 45° slope through the origin, as is the case when comparing with the STRING topology, indicates a random performance. This is quantitatively confirmed by the higher AUROC value of the inferred vs. the knowledge-based network curve (0.69) compared to the inferred vs. STRING network curve (0.44). It means the literature-derived network depicted in **Figure 2** was able

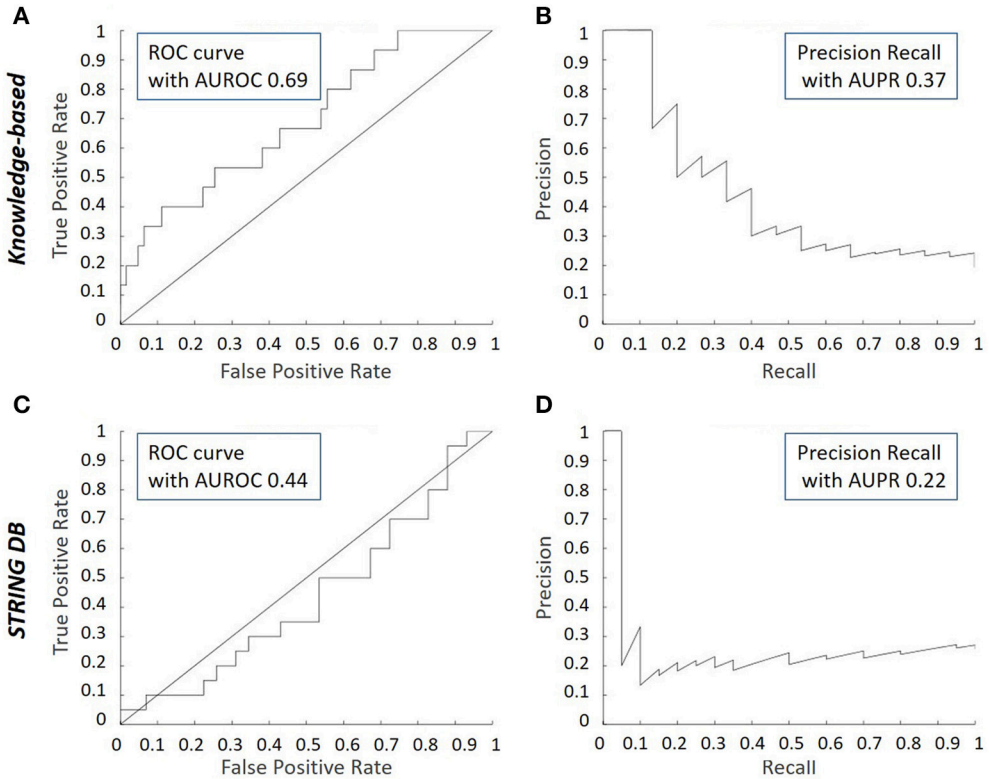

FIGURE 5 | Receiver Operating Characteristic (ROC) and Precision Recall (PR) curves for inferred consensus network with respect to knowledge-based network and STRING network. The ROC plots the True Prediction Rate (TPR) against the False Prediction Rate (FPR) for each (cumulative) interaction inferred. The PR curve plots the precision vs. the recall for each (cumulative) interaction inferred. **(A)** ROC curve for the inferred consensus network compared to the literature-derived topology. **(B)** PR curve for the inferred consensus network compared to literature-derived topology. **(C)** ROC curve for the inferred consensus topology compared to the STRING network. **(D)** PR curve for the inferred consensus topology compared to the STRING network.

to explain correctly an important part of the experimental behavior at the transcriptomic level. The superior behavior of the literature-derived network over the STRING network could be due to the latter including indirect interactions whereas the former mostly sticks to direct interactions. Another significant difference between the two networks was that most of the interactions included in the knowledge-derived network were derived from experiments on growth plate chondrocytes or a closely related cell type (Kerkhofs and Geris, 2015). In contrast, interactions from a wide variety of contexts, often from cancer cells, served to build the STRING database and the subsequent network. When comparing the precision-recall curves and the AUPR values (**Figures 5B,D**), it was clear that the knowledge-based network again outperformed the STRING network at least for the first few guesses (perfect PR being a straight line passing through the upper right corner with AUPR of 1). Overall, this section illustrates the fact that tools which automatically generate networks from public database curation may serve as a good starting point for regulatory network construction but also that this strategy is still missing the cell type and biological context specificity. This is particularly important for biological processes that are studied by smaller communities and for which less context-specific information is available in the public databases (which is the case for growth plate biology when compared with cancer biology). Indeed, automatic database curation with software tools may offer a systematic and more objective way to build networks from published information but it is very likely much improved by "manual" construction/adaptation of the network for specific biological questions.

Chondrocyte Network Inference With Integration of Prior Network

A number of inference algorithms permit the inclusion of known interactions as input to the inference process. The input knowledge usually takes the form of a matrix containing as many lines and columns as the number of factors, where the value at each location in the matrix indicates the presence/absence, direction and strength of the interaction between the factors depicted in that particular row and column. For a detailed explanation on the implementation of prior knowledge, see **Supplemental Data 1**. This use of prior knowledge will increase the probability of finding models that have a bigger similarity with the prior network. Of course, to keep the benefit of the data-inference from experimental data, a balance must be struck between forcing compliance with the prior network and fitting the data.

For the chondrocyte differentiation network the incorporation of prior knowledge was investigated through the sole use of the Inferelator algorithm as described in Greenfield et al. (2013). This method tunes influence of prior knowledge on the outcome through an adjustable parameter *g*. Since part of the literature-derived network was used as prior knowledge, the effect of the parameter *g* on the correspondence between the inferred and the literature-derived network (AUROC) was investigated, together with the error between experimental data and simulated values (SSR, see **Supplemental Data 2**). It was a way to identify which *g*-value was producing a model that matched the prior information without sacrificing compatibility with the microarray data.

In Kerkhofs (2015), we did a screening of different values for the parameter *g* in order to select a value so that the adherence to the prior network was not too strict. Therefore, the algorithm could infer new interactions explaining the experimental data while taking into account the prior knowledge about chondrocyte biology in the growth plate. **Table 3** reports the 11 regulatory interactions with the highest incidence in the inference process. Similarly to the consensus inference (section Inference of a Growth Plate Network Following a Consensus Approach), the integration of prior knowledge identified some high-ranking inferred interactions that were absent from the prior knowledge-based network such as the activation of Tcf by MEF2C (MEF2C→ Tcf7), Tcf7→ HIF-2α, and HIF-2α → δ-EF1. Some of these predicted interactions were in fact already described in literature such as MEF2C forming an enhanceosome with Tcf7 and other factors to upregulate the Runx2 activity in a synergistic way (Kawane et al., 2014). Therefore, the network may benefit from being supplemented with these interactions. However, for other predicted interactions, only weak evidence was present in the literature. Hence, the inference may provide an indication for subsequent experimental investigation into the veracity of those predicted interactions. Highlighting such interesting new interactions may make the model more accurate with respect to the data and possibly reinforces its predictability. Finally, the knowledge-based topology might also be improved through the exclusion of regulatory interactions that do not score well in the data-based analysis.

This illustration of network inference on the one hand shows how data-driven approaches may automatically, and relatively quickly, exploit experimental datasets to build interconnected network of gene and protein interactions. However, using these networks to propose further experiments is not straightforward since the output remains a static map. On the other hand, manual curation of networks created through a bottom-up approach is a very fastidious and time-consuming process, but these networks easily allow dynamic analyses and simulations that suggest new wet lab experiments. Hence, there is a necessity to develop methods that allow combining both approaches into a single framework having the best of both worlds as suggested by Poirel et al. (2013).

In the context of osteochondral regenerative medicine, the ultimate goal of reconstructing such network of regulation is to obtain a predictive model in order to gain understanding into the signaling or regulatory mechanism controlling cellular behavior and/or physiology of degenerative diseases. It might enable the identification of key factors for therapeutic targeting ensuring reliable cellular differentiation for tissue engineering applications or to propose potential disease-modifying therapies in the context of cartilage degenerative disease such as osteoarthritis (Hopkins, 2008). Application of such a methodology to the growth plate system already suggested new interactions and some factors as key regulators in the phenotypical transition of chondrocytes. For instance, in the inference previously presented (Kerkhofs, 2015), one of the highly ranked inferred interactions that was not present in the prior network, was NFkB-MEF2C with a negative correlation. MEF2C knockdown was shown to increase NFkB activity in endothelial cells (Xu et al., 2015) but no mRNA measurement was performed. This could constitute a suggestion of experimental design for validation of the *in silico* result. Finally, dynamic simulations associated with this growth plate network showed that *in silico* knock-out of NFkB was decreasing the reachability of the hypertrophic state in the optimized model, i.e., making it less likely for a cell to be in that state. The factors that were absolutely required to reach the hypertrophic state, as in their absence no Runx2+ stable state was found, were Ras, Ihh, Gli2, and FGF. The activation of Smad7 in the model was the most expedient way to remove the Sox9+ (proliferative) phenotype. Hence, according to the model, inhibiting Smad7 could be a strategy to decrease initiation of hypertrophic differentiation; or activation of Ras, Gli2, or FGF pathways might help to promote hypertrophy in order to produce sustainable bone TE constructs.

TABLE 3 | Inferred interactions with inferelator and prior knowledge ($g = 5$).

Source	Target	StoT	TtoS	Pearson	StoTorig	TtoSorig
MEF2C	Runx2	0.97	0.91	0.69	1	1
δ-EF1	Ets1	0.16	0.88	−0.38	0	1
CCND1	Atf2	0.02	0.91	0.61	0	1
Sox9	Runx2	0	0.90	−0.30	−1	−1
Dlx5	MEF2C	0.02	0.84	0.32	0	1
MEF2C	Tcf7	0.77	0	0.59	0	0
HIF-2α	Tcf7	0.14	0.51	0.62	0	0
HIF-2α	δ-EF1	0.56	0	0.39	0	0
NF-κB	Sox9	0.55	0	0.40	1	0
HIF-2α	NF-κB	0	0.53	0.04	0	1
HIF-2α	MEF2C	0	0.44	0.54	0	0

*Selection of the first ranked interactions. StoT is the fraction of times where a directed interaction from the source (1st column) to target (2nd column) is found in the bootstrap procedure. TtoS is the fraction of cases where a reverse directed interaction is found. The fifth column gives the Pearson correlation in the microarray dataset. StoTorig is the directed interaction from the source to target in the literature-derived network (**Figure 2**). TtoSorig is the reverse interaction. 0 indicates no interaction, 1 is an activation and −1 is an inhibition.*

CONCLUSION

As new computational tools become available, an increasing number of biological systems is investigated computationally with increasing effectiveness. Computational approaches have already shown their relevance in the field of regenerative

medicine with models of bioreactor studies and biomaterial design. However, this relevance also holds for the models focusing on the intracellular level, through the use of GRN models to understand the cellular decision-making processes, e.g., in the context of cell differentiation. Understanding and controlling these processes is a necessary step to increase quality and robustness of TE constructs. For the specific case of osteochondral tissue engineering, only few cell signaling or signal-response models have been reported in the literature up to date. We have reviewed our own published work on computer modeling of differentiation of growth plate chondrocytes to illustrate the potential of *in silico* approaches in designing proper culture strategies to control the transition of these chondrocytes from a proliferative to a hypertrophic phenotype and find those (potentially druggable) targets. Such targets would allow preventing a switch from the proliferative to the hypertrophic phenotype in the case of cartilage degenerative diseases such as osteoarthritis. Correcting aberrant cellular behavior with drugs requires knowledge about multiple interacting signaling proteins, which necessitates the use of computer tools (Kumar et al., 2006; Hopkins, 2008; Voit, 2012).

The last section of this paper illustrate the benefits that network inference from experimental data could bring to predictive computational models. The main obstacle currently preventing the expansion of *in silico* approaches is the lack of informative and quantitative experimental data. Indeed, modelers face the difficulty of obtaining data with a sufficiently high information content, such as perturbation data from human samples, to build and validate their models.

In silico modeling does not aim to replace traditional experimental methods but provides an additional tool to interpret the results obtained in those experiments and to suggest new informative experiments, as an integral part of the experimental research cycle. The objective of the models described in this review is to bring a higher level of understanding, increase time efficiency of experimentation and decrease costs in the process of therapy development.

AUTHOR CONTRIBUTIONS

JK and LG conceived and designed the models. RL and JK performed the simulations. RL, JK, and LG analyzed the results and wrote the paper.

FUNDING

RL and LG acknowledge funding from the European Research Council under the European Union's Seventh Framework Programme (FP/2007-2013)/ERC (Grant Agreement n. 279100) and from the European Union's Horizon 2020 research and innovation programme under Marie Sklodowska-Curie (Grant Agreement No 721432). JK acknowledges scholarship funding from the Research Foundation Flanders (FWO-Vlaanderen).

ACKNOWLEDGMENTS

This work is part of Prometheus, the KU Leuven R&D division for skeletal tissue engineering (http://www.kuleuven.be/prometheus).

SUPPLEMENTARY MATERIAL

The Supplementary Material for this article can be found online at: https://www.frontiersin.org/articles/10.3389/fbioe.2018.00165/full#supplementary-material

REFERENCES

Abou-Jaoudé, W., Traynard, P., Monteiro, P. T., Saez-Rodriguez, J., Helikar, T., Thieffry, D., et al. (2016). Logical modeling and dynamical analysis of cellular networks. *Front. Genet.* 7:94. doi: 10.3389/fgene.2016.00094

Agoston, H., Khan, S., James, C. G., Gillespie, J. R., Serra, R., Stanton, L. A., et al. (2007). C-type natriuretic peptide regulates endochondral bone growth through p38 MAP kinase-dependent and -independent pathways. *BMC Dev. Biol.* 7:18. doi: 10.1186/1471-213X-7-18

Aldridge, B. B., Saez-Rodriguez, J., Muhlich, J. L., Sorger, P. K., and Lauffenburger, D. A. (2009). Fuzzy logic analysis of kinase pathway crosstalk in TNF/EGF/insulin-induced signaling. *PLoS Comput. Biol.* 5:e1000340. doi: 10.1371/journal.pcbi.1000340

Ay, A., and Arnosti, D. N. (2011). Mathematical modeling of gene expression: a guide for the perplexed biologist. *Crit. Rev. Biochem. Mol. Biol.* 46, 137–151. doi: 10.3109/10409238.2011.556597

Bernot, G., Comet, J. P., Richard, A., and Guespin, J. (2004). Application of formal methods to biological regulatory networks: extending Thomas' asynchronous logical approach with temporal logic. *J. Theor. Biol.* 229, 339–347. doi: 10.1016/j.jtbi.2004.04.003

Bodaker, M., Louzoun, Y., and Mitrani, E. (2013). Mathematical conditions for induced cell differentiation and trans-differentiation in adult cells. *Bull. Math. Biol.* 75, 819–844. doi: 10.1007/s11538-013-9837-2

Bonneau, R., Reiss, D. J., Shannon, P., Facciotti, M., Hood, L., Baliga, N. S., et al. (2006). The Inferelator: an algorithm for learning parsimonious regulatory networks from systems-biology data sets *de novo*. *Genome Biol.* 7:R36. doi: 10.1186/gb-2006-7-5-r36

Carlier, A., van Gastel, N., Geris, L., Carmeliet, G., and Van Oosterwyck, H. (2014). Size does matter: an integrative *in vivo-in silico* approach for the treatment of critical size bone defects. *PLoS Comput. Biol.* 10:e1003888. doi: 10.1371/journal.pcbi.1003888

Chen, H., Guo, J., Mishra, S. K., Robson, P., Niranjan, M., and Zheng, J. (2015). Single-cell transcriptional analysis to uncover regulatory circuits driving cell fate decisions in early mouse development. *Bioinformatics* 31, 1060–1066. doi: 10.1093/bioinformatics/btu777

De Smet, R., and Marchal, K. (2010). Advantages and limitations of current network inference methods. *Nat. Rev. Microbiol.* 8, 717–729. doi: 10.1038/nrmicro2419

Faith, J. J., Hayete, B., Thaden, J. T., Mogno, I., Wierzbowski, J., Cottarel, G., et al. (2007). Large-scale mapping and validation of Escherichia coli transcriptional regulation from a compendium of expression profiles. *PLoS Biol.* 5:e8. doi: 10.1371/journal.pbio.0050008

Friedman, N., Linial, M., Nachman, I., and Pe'er, D. (2000). Using bayesian networks to analyze expression data. 7, 601–620. doi: 10.1089/106652700750050961

Geris, L. (2014). Regenerative orthopaedics: *in vitro*, *in vivo*. *in silico*. *Int. Orthop.* 38, 1771–1778. doi: 10.1007/s00264-014-2419-6

Geris, L., Schugart, R., and Van Oosterwyck, H. (2010). *In silico* design of treatment strategies in wound healing and bone fracture healing. *Philos. Trans. R. Soc. A Math. Phys. Eng. Sci.* 368, 2683–2706. doi: 10.1098/rsta.2010.0056

Glass, L., and Kauffman, S. A. (1973). The logical analysis of continuous, non-linear biochemical control networks. *J. Theor. Biol.* 39, 103–129. doi: 10.1016/0022-5193(73)90208-7

Glimm, T., Headon, D., and Kiskowski, M. A. (2012). Computational and mathematical models of chondrogenesis in vertebrate limbs. *Birth Defects Res. C Embryo Today Rev*. 96, 176–192. doi: 10.1002/bdrc.21014

Greenfield, A., Hafemeister, C., and Bonneau, R. (2013). Robust data-driven incorporation of prior knowledge into the inference of dynamic regulatory networks. *Bioinformatics* 29, 1060–1067. doi: 10.1093/bioinformatics/btt099

Griffiths, J. A., Scialdone, A., and Marioni, J. C. (2018). Using single-cell genomics to understand developmental processes and cell fate decisions. *Mol. Syst. Biol.* 14:e8046. doi: 10.15252/msb.20178046

Gutenkunst, R. N., Waterfall, J. J., Casey, F. P., Brown, K. S., Myers, C. R., and Sethna, J. P. (2007). Universally sloppy parameter sensitivities in systems biology models. *PLoS Comput. Biol.* 3, 1871–1878. doi: 10.1371/journal.pcbi.0030189

Hata, K., Takahata, Y., Murakami, T., and Nishimura, R. (2017). Transcriptional network controlling endochondral ossification. *J. Bone Metab.* 24, 75–82. doi: 10.11005/jbm.2017.24.2.75

Haury, A., Mordelet, F., Vera-licona, P., and Vert, J. (2012). TIGRESS: trustful inference of gene regulation using stability selection. *BMC Syst. Biol.* 6:145. doi: 10.1186/1752-0509-6-145

Herberg, M., and Roeder, I. (2015). Computational modelling of embryonic stem-cell fate control. *Development* 142, 2250–2260. doi: 10.1242/dev.116343

Hopkins, A. L. (2008). Network pharmacology: the next paradigm in drug discovery. *Nat. Chem. Biol.* 4, 682–690. doi: 10.1038/nchembio.118

Huynh-Thu, V. A., Irrthum, A., Wehenkel, L., and Geurts, P. (2010). Inferring regulatory networks from expression data using tree-based methods. *PLoS ONE* 5:e12776. doi: 10.1371/journal.pone.0012776

Isshiki, H., Sato, K., Horiuchi, K., Tsutsumi, S., Kano, M., Ikegami, H., et al. (2011). Gene expression profiling of mouse growth plate cartilage by laser microdissection and microarray analysis. *J. Orthop. Sci.* 16, 670–672. doi: 10.1007/s00776-011-0119-2

James, C. G., Stanton, L. A., Agoston, H., Ulici, V., Underhill, T. M., and Beier, F. (2010). Genome-wide analyses of gene expression during mouse endochondral ossification. *PLoS ONE* 5:e8693. doi: 10.1371/journal.pone.0008693

James, C. G., Ulici, V., Tuckermann, J., Michael, T. M., and Beier, F. (2007). Expression profiling of Dexamethasone-treated primary chondrocytes identifies targets of glucocorticoid signalling in endochondral bone development. *BMC Genomics* 8:205. doi: 10.1186/1471-2164-8-205

Janes, K. A., and Lauffenburger, D. A. (2006). A biological approach to computational models of proteomic networks. *Curr. Opin. Chem. Biol.* 10, 73–80. doi: 10.1016/j.cbpa.2005.12.016

Julkunen, P., Wilson, W., Isaksson, H., Jurvelin, J. S., Herzog, W., and Korhonen, R. K. (2013). A Review of the combination of experimental measurements and fibril-reinforced modeling for investigation of articular cartilage and chondrocyte response to loading. *Comput. Math. Methods Med.* 2013, 1–23. doi: 10.1155/2013/326150

Karlebach, G., and Shamir, R. (2008). Modelling and analysis of gene regulatory networks. *Nat. Rev. Mol. Cell Biol.* 9, 770–780. doi: 10.1038/nrm2503

Kauffman, S. A. (1969). Metabolic stability and epigenesis in randomly constructed genetic nets. *J. Theor. Biol.* 22, 437–67.

Kauffman, S. A. (1994). The origins of order; self organization and selection in evolution. *Int. J. Biochem.* 26:855. doi: 10.1016/0020-711X(94)90119-8

Kawane, T., Komori, H., Liu, W., Moriishi, T., Miyazaki, T., Mori, M., et al. (2014). Dlx5 and Mef2 regulate a novel Runx2 enhancer for osteoblast-specific expression. *J. Bone Miner. Res.* 29, 1960–1969. doi: 10.1002/jbmr.2240

Kerkhofs, J. (2015). *Chondrogenic Differentiation in the Growth Plate: A Computational Modelling Approach*. Doctoral Thesis, KU Leuven, University of Liege. Available online at: http://hdl.handle.net/2268/186583

Kerkhofs, J., and Geris, L. (2015). A Semiquantitative framework for gene regulatory networks: increasing the time and quantitative resolution of boolean networks. *PLoS ONE* 10:e0130033. doi: 10.1371/journal.pone.0130033

Kerkhofs, J., Leijten, J., Bolander, J., Luyten, F. P., Post, J. N., and Geris, L. (2016). A qualitative model of the differentiation network in chondrocyte maturation: a holistic view of chondrocyte hypertrophy. *PLoS ONE* 11:e0162052. doi: 10.1371/journal.pone.0162052

Kerkhofs, J., Roberts, S. J., Luyten, F. P., Van Oosterwyck, H., and Geris, L. (2012). Relating the chondrocyte gene network to growth plate morphology: from genes to phenotype. *PLoS ONE* 7:e34729. doi: 10.1371/journal.pone.0034729

Klipp, E., Herwig, R., Kowald, A., Wierling, C., and Lehrach, H. (2005). *Systems Biology in Practice: Concepts, Implementation and Application*. Weinheim: Wiley-VCH. doi: 10.1002/3527603603

Kumar, N., Hendriks, B. S., Janes, K. A., de Graaf, D., and Lauffenburger, D. A. (2006). Applying computational modeling to drug discovery and development. *Drug Discov. Today* 11, 806–811. doi: 10.1016/j.drudis.2006.07.010

Le Novère, N. (2015). Quantitative and logic modelling of molecular and gene networks. *Nat. Rev. Genet.* 16, 146–158. doi: 10.1038/nrg3885

Lefrebvre, V., and de Crombrugghe, B. (1998). Toward understanding S0X9 function in chondrocyte differentiation. *Matrix Biol.* 16, 529–540. doi: 10.1016/S0945-053X(98)90065-8

Lenas, P., Moos, M., and Luyten, F. P. (2009b). Developmental engineering: a new paradigm for the design and manufacturing of cell-based products. Part II: from genes to networks: tissue engineering from the viewpoint of systems biology and network science. *Tissue Eng. B Rev.* 15, 395–422. doi: 10.1089/ten.teb.2009.0461

Lenas, P., Moos, M. J., and Luyten, F. P. (2009a). Developmental engineering: a new paradigm for the design and manufacturing of cell based products. Part I: from three-dimensional cell growth to biomimetics of *in vivo* development. *Tissue Eng. B Rev.* 15, 381–394. doi: 10.1089/ten.teb.2008.0575

Li, B., Balasubramanian, K., Krakow, D., and Cohn, D. H. (2017). Genes uniquely expressed in human growth plate chondrocytes uncover a distinct regulatory network. *BMC Genomics* 18:983. doi: 10.1186/s12864-017-4378-y

Li, J., Luo, H., Wang, R., Lang, J., Zhu, S., Zhang, Z., et al. (2016). Systematic reconstruction of molecular cascades regulating GP development using single-cell RNA-seq. *Cell Rep.* 15, 1467–1480. doi: 10.1016/j.celrep.2016.04.043

Liu, L.-Z., Wu, F.-X., and Zhang, W.-J. (2012). Reverse engineering of gene regulatory networks from biological data. *Wiley Interdiscip. Rev. Data Min. Knowl. Discov.* 2, 365–385. doi: 10.1002/widm.1068

Long, F., and Ornitz, D. M. (2013). Development of the endochondral skeleton. *Cold Spring Harb. Perspect. Biol.* 5:a008334. doi: 10.1101/cshperspect.a008334

Marbach, D., Costello, J. C., Küffner, R., Vega, N. M., Prill, R. J., Camacho, D. M., et al. (2012). Wisdom of crowds for robust gene network inference. *Nat. Methods* 9, 796–804. doi: 10.1038/nmeth.2016

Marbach, D., Mattiussi, C., and Floreano, D. (2009). Replaying the evolutionary tape: biomimetic reverse engineering of gene networks. *Ann. N. Y. Acad. Sci.* 1158, 234–245. doi: 10.1111/j.1749-6632.2008.03944.x

Margolin, A. A., Nemenman, I., Basso, K., Wiggins, C., Stolovitzky, G., Favera, R., et al. (2006). ARACNE: an algorithm for the reconstruction of gene regulatory networks in a mammalian cellular context. *BMC Bioinform.* 7:S7. doi: 10.1186/1471-2105-7-S1-S7

McNamara, L. E., Turner, L. A., and Burgess, K., V (2015). Systems biology approaches applied to regenerative medicine. *Curr. Pathobiol. Rep.* 3, 37–45. doi: 10.1007/s40139-015-0072-4

Melas, I. N., Chairakaki, A. D., Chatzopoulou, E. I., Messinis, D. E., Katopodi, T., Pliaka, V., et al. (2014). Modeling of signaling pathways in chondrocytes based on phosphoproteomic and cytokine release data. *Osteoarthr. Cartil.* 22, 509–518. doi: 10.1016/j.joca.2014.01.001

Melas, I. N., Mitsos, A., Messinis, D. E., Weiss, T. S., and Alexopoulos, L. G. (2011). Combined logical and data-driven models for linking signalling pathways to cellular response. *BMC Syst. Biol.* 5:107. doi: 10.1186/1752-0509-5-107

Mendel, J. M. (1995). Fuzzy logic systems for engineering: a tutorial. *Proc. IEEE* 83, 345–377. doi: 10.1109/5.364485

Meyer, P., Marbach, D., Roy, S., and Kellis, M. (2010). "Information-theoretic inference of gene networks using backward elimination," in *Conference: International Conference on Bioinformatics & Computational Biology, BIOCOMP 2010* (Las Vegas, NV), 700–705. Available online at: http://compbio.mit.edu/marbach/papers/Meyer2010.pdf

Mojtahedi, M., Skupin, A., Zhou, J., Castaño, I. G., Leong-Quong, R. Y. Y., Chang, H., et al. (2016). Cell fate decision as high-dimensional critical state transition. *PLoS Biol.* 14:e2000640. doi: 10.1371/journal.pbio.2000640

Molinelli, E. J., Korkut, A., Wang, W., Miller, M. L., Gauthier, N. P., et al. (2013). Perturbation biology: inferring signaling networks in cellular systems. *PLoS Comput. Biol.* 9:e1003290. doi: 10.1371/journal.pcbi.1003290

Morris, M. K., Saez-Rodriguez, J., Sorger, P. K., and Lauffenburger, D. A. (2010). Logic-based models for the analysis of cell signaling networks. *Biochemistry* 49, 3216–3224. doi: 10.1021/bi902202q

O'Keefe, R. J., Puzas, J. E., Loveys, L., Hicks, D. G., and Rosier, R. N. (1994). Analysis of type II and type X collagen synthesis in cultured growth plate chondrocytes by *in situ* hybridization: rapid induction of type X collagen in culture. *J. Bone Miner. Res.* 9, 1713–1722.

Pir, P., and Le Novère, N. (2016). Mathematical models of pluripotent stem cells: at the dawn of predictive regenerative medicine. *Methods Mol. Biol.* 1386, 331–350. doi: 10.1007/978-1-4939-3283-2_15

Poirel, C. L., Rodrigues, R. R., Chen, K. C., Tyson, J. J., and Murali, T. M. (2013). Top-down network analysis to drive bottom-up modeling of physiological processes. *J. Comput. Biol.* 20, 409–418. doi: 10.1089/cmb.2012.0274

Rajagopalan, P., Kasif, S., and Murali, T. M. (2013). Systems biology characterization of engineered tissues. *Annu. Rev. Biomed. Eng.* 15, 55–70. doi: 10.1146/annurev-bioeng-071811-150120

Saez-Rodriguez, J., Alexopoulos, L. G., Epperlein, J., Samaga, R., Lauffenburger, D. A., Klamt, S., et al. (2009). Discrete logic modelling as a means to link protein signalling networks with functional analysis of mammalian signal transduction. *Mol. Syst. Biol.* 5:331. doi: 10.1038/msb.2009.87

Saez-Rodriguez, J., Costello, J. C., Friend, S. H., Kellen, M. R., Mangravite, L., Meyer, P., et al. (2016). Crowdsourcing biomedical research: leveraging communities as innovation engines. *Nat. Rev. Genet.* 17, 470–486. doi: 10.1038/nrg.2016.69

Schittler, D., Hasenauer, J., Allgower, F., and Waldherr, S. (2010). Cell differentiation modeled via a coupled two-switch regulatory network. *Chaos An Interdiscip. J. Nonlinear Sci.* 20:045121. doi: 10.1063/1.3505000

Schivo, S., Scholma, J., van der Vet, P. E., Karperien, M., Post, J. N., van de Pol, J., et al. (2016). Modelling with ANIMO: between fuzzy logic and differential equations. *BMC Syst. Biol.* 10:56. doi: 10.1186/s12918-016-0286-z

Schlitt, T., and Brazma, A. (2007). Current approaches to gene regulatory network modelling. *BMC Bioinform.* 8(Suppl. 6):S9. doi: 10.1186/1471-2105-8-S6-S9

Scholma, J., Schivo, S., Kerkhofs, J., Langerak, R., Karperien, H., Van de Pol, J., et al. (2014). "ECHO: the executable chondrocyte," in *Tissue Engineering and Regenerative Medicine International Society, European Chapter Meeting*, s1, Vol. 8 (Malden, MA: Wiley), 54. doi: 10.1002/term.1931

Sengers, B. G., van Donkelaar, C. C., Oomens, C. W. J., and Baaijens, F. P. T. (2008). Computational study of culture conditions and nutrient supply in cartilage tissue engineering. *Biotechnol. Prog.* 21, 1252–1261. doi: 10.1021/bp0500157

Smeets, B. (2016). *From Single Cell Mechanics and Intercellular Forces to Collective Aggregate Dynamics Individual Cell-Based Modeling of Cell Cultures for Tissue Engineering*. Available online at: https://lirias.kuleuven.be/handle/123456789/535633 (Accessed June 28, 2017).

Steggles, L. J., Banks, R., Shaw, O., and Wipat, A. (2007). Qualitatively modelling and analysing genetic regulatory networks: a Petri net approach. *Bioinformatics* 23, 336–343. doi: 10.1093/bioinformatics/btl596

Stolovitzky, G., Monroe, D., and Califano, A. (2007). Dialogue on reverse-engineering assessment and methods: the DREAM of high-throughput pathway inference. *Ann. N. Y. Acad. Sci.* 1115, 1–22. doi: 10.1196/annals.1407.021

Szklarczyk, D., Morris, J. H., Cook, H., Kuhn, M., Wyder, S., Simonovic, M., et al. (2017). The STRING database in 2017: quality-controlled protein–protein association networks, made broadly accessible. *Nucleic Acids Res.* 45, D362–D368. doi: 10.1093/nar/gkw937

Tarantola, A. (2006). *Inverse Problem Theory and Methods for Model Parameter Estimation*. Paris: Society for industrial and Applied Mathematics. doi: 10.1137/1.9780898717921

Thomas, R., and Kaufman, M. (2001). Multistationarity, the basis of cell differentiation and memory. II. Logical analysis of regulatory networks in terms of feedback circuits. *Chaos* 11, 180–195. doi: 10.1063/1.1349893

Ulici, V., James, C. G., Hoenselaar, K. D., and Beier, F. (2010). Regulation of gene expression by PI3K in mouse growth plate chondrocytes. *PLoS ONE* 5:e8866. doi: 10.1371/journal.pone.0008866

Villaverde, A. F., and Banga, J. R. (2013). Reverse engineering and identification in systems biology: strategies, perspectives and challenges. *J. R. Soc. Interface* 11, 20130505–20130505. doi: 10.1098/rsif.2013.0505

Voit, E. (2012). *A First Course in System Biology*. New York, NY: Garland Sciences.

von Dassow, G., Meir, E., Munro, E. M., and Odell, G. M. (2000). The segment polarity network is a robust developmental module. *Nature* 406, 188–192. doi: 10.1038/35018085

Weinreb, C., Wolock, S., Tusi, B. K., Socolovsky, M., and Klein, A. M. (2018). Fundamental limits on dynamic inference from single-cell snapshots. *Proc. Natl. Acad. Sci. U.S.A.* 115, E2467–E2476. doi: 10.1073/pnas.1714723115

Werhli, A. V., Grzegorczyk, M., and Husmeier, D. (2006). Comparative evaluation of reverse engineering gene regulatory networks with relevance networks, graphical gaussian models and bayesian networks. *Bioinformatics* 22, 2523–2531. doi: 10.1093/bioinformatics/btl391

Wolkenhauer, O., Ullah, M., Wellstead, P., and Cho, K. H. (2005). The dynamic systems approach to control and regulation of intracellular networks. *FEBS Lett.* 579, 1846–1853. doi: 10.1016/j.febslet.2005.02.008

Woolf, P. J., Prudhomme, W., Daheron, L., Daley, G. Q., and Lauffenburger, D. A. (2005). Bayesian analysis of signaling networks governing embryonic stem cell fate decisions. *Bioinformatics* 21, 741–753. doi: 10.1093/bioinformatics/bti056

Wu, Z., and Irizarry, R. (2004). Preprocessing of oligonucleotide array data. *Nat. Biotechnol.* 22, 656–657. doi: 10.1038/nbt0604-656b

Wu, Z., Irizarry, R. A., Gentleman, R., Martinez-Murillo, F., and Spencer, F. (2004). A model-based background adjustment for oligonucleotide expression arrays. *J. Am. Stat. Assoc.* 99, 909–917. doi: 10.1198/016214504000000683

Xia, K., Xue, H., Dong, D., Zhu, S., Wang, J., Zhang, Q., et al. (2006). Identification of the proliferation/differentiation switch in the cellular network of multicellular organisms. *PLoS Comput. Biol.* 2:e145. doi: 10.1371/journal.pcbi.0020145

Xu, Z., Yoshida, T., Wu, L., Maiti, D., Cebotaru, L., and Duh, E. J. (2015). Transcription factor MEF2C suppresses endothelial cell inflammation via regulation of NF-kB and KLF2. *J. Cell. Physiol.* 230, 1310–1320. doi: 10.1002/jcp.24870

Yang, L., Tsang, K. Y., Tang, H. C., Chan, D., and Cheah, K. S. (2014). Hypertrophic chondrocytes can become osteoblasts and osteocytes in endochondral bone formation. *Proc. Natl. Acad. Sci. U.S.A.* 111, 12097–12102. doi: 10.1073/pnas.1302703111

Yousefi, A. M., Hoque, M. E., Prasad, R. G. S. V., and Uth, N. (2015). Current strategies in multiphasic scaffold design for osteochondral tissue engineering: a review. *J. Biomed. Mater. Res. A* 103, 2460–2481. doi: 10.1002/jbm.a.35356

Zadeh, L. A. (1996). Fuzzy logic = computing with words. *IEEE Trans. Fuzzy Syst.* 4, 103–111. doi: 10.1109/91.493904

Conflict of Interest Statement: The authors declare that the research was conducted in the absence of any commercial or financial relationships that could be construed as a potential conflict of interest.

frontiers in Bioengineering and Biotechnology

MINI REVIEW
published: 21 March 2018
doi: 10.3389/fbioe.2018.00028

The Chondro-Osseous Continuum: Is It Possible to Unlock the Potential Assigned Within?

Behzad Javaheri[1], Soraia P. Caetano-Silva[1], Ioannis Kanakis[2], George Bou-Gharios[2] and Andrew A. Pitsillides[1]*

[1] *Skeletal Biology Group, Comparative Biomedical Sciences, The Royal Veterinary College, London, United Kingdom,*
[2] *Institute of Ageing and Chronic Disease, University of Liverpool, Liverpool, United Kingdom*

Endochondral ossification (EO), by which long bones of the axial skeleton form, is a tightly regulated process involving chondrocyte maturation with successive stages of proliferation, maturation, and hypertrophy, accompanied by cartilage matrix synthesis, calcification, and angiogenesis, followed by osteoblast-mediated ossification. This developmental sequence reappears during fracture repair and in osteoarthritic etiopathology. These similarities suggest that EO, and the cells involved, are of great clinical importance for bone regeneration as it could provide novel targeted approaches to increase specific signaling to promote fracture healing, and if regulated appropriately in the treatment of osteoarthritis. The long-held accepted dogma states that hypertrophic chondrocytes are terminally differentiated and will eventually undergo apoptosis. In this mini review, we will explore recent evidence from experiments that revisit the idea that hypertrophic chondrocytes have pluripotent capacity and may instead transdifferentiate into a specific sub-population of osteoblast cells. There are multiple lines of evidence, including our own, showing that local, selective alterations in cartilage extracellular matrix (ECM) remodeling also indelibly alter bone quality. This would be consistent with the hypothesis that osteoblast behavior in long bones is regulated by a combination of their lineage origins and the epigenetic effects of chondrocyte-derived ECM which they encounter during their recruitment. Further exploration of these processes could help to unlock potential novel targets for bone repair and regeneration and in the treatment of osteoarthritis.

Keywords: chondrocyte, transdifferentiation, cartilage, bone, extracellular matrix, osteoblast

OPEN ACCESS

Edited by:
Eric Farrell, Erasmus University Rotterdam, Netherlands

Reviewed by:
Roger Brooks, University of Cambridge, United Kingdom
Anne George, University of Illinois at Chicago, United States

****Correspondence:***
Behzad Javaheri
bjavaheri@rvc.ac.uk

Specialty section:
This article was submitted to Tissue Engineering and Regenerative Medicine, a section of the journal Frontiers in Bioengineering and Biotechnology

Received: *01 February 2018*
Accepted: *08 March 2018*
Published: *21 March 2018*

Citation:
Javaheri B, Caetano-Silva SP, Kanakis I, Bou-Gharios G and Pitsillides AA (2018) The Chondro-Osseous Continuum: Is It Possible to Unlock the Potential Assigned Within?. Front. Bioeng. Biotechnol. 6:28. doi: 10.3389/fbioe.2018.00028

INTRODUCTION

The mobility provided by a robust locomotor skeletal system is a major determinant of human health and quality of life. Loss of mobility is a leading cause of ill-health and ultimately death. Two common skeletal problems include defective bone healing and osteoarthritis (OA); despite increasing incidence their treatment remains unmodified for many years (Woolf and Pfleger, 2003; Hunter et al., 2014). Their scale is huge; some 1:25 people suffers a bone fracture each year and prevalence in the aged reaches 50%, yet as many as 20% do not heal (Johnell and Kanis, 2005). Large bone defects resulting from tumor resection add to this population. In these patients, sites from which bone is harvested often require follow-up surgery. The greatest mobility failure, however, arises from OA a painful, disabling syndrome affecting one third of those >65 years and many younger people. Despite

its extensive impact, OA treatment options remain palliative and conclude most often in joint replacement. These two problems are inextricably linked by cartilage and bone pathology, repair, and development.

Bone is not only essential for locomotion, support, and protection but crucial for many aspects of health. Specifically, bone is a calcium/phosphorous reservoir, is integral to glucose metabolism, houses the hematopoietic system and cross-talks with renal and reproductive systems. During development, ossification of the entire post-cranial, endochondral skeleton throughout ontogeny, growth and evolution relies entirely on chondrocytes and the specific extracellular matrix (ECM) they secrete. The continuous transition of cartilage to bone in this endochondral ossification (EO) process is the source of all longitudinal bone growth. A distinct osteoblast cell type is responsible for shaping and maintaining bone formation upon this cartilage ECM template. Of course, some bones arise intramembranously, wherein embryonic mesenchymal cell condensations differentiate directly into osteoprogenitor cells and later into osteoblasts (OB), which secrete an unmineralized osteoid bone matrix around blood vessels. The compact layer of mesenchymal cells surrounding the skeletal element becomes the periosteum; OB on its inner surface deposit osteoid to form layers of bone (Hall, 2005).

Endochondral ossification is initiated by migration of mesenchymal cells to form pre-cartilage condensations, which then undergo differentiation into chondrocytes that secrete ECM rich in aggrecan (Acan) and collagen type II. Calcification of this cartilaginous ECM in this primary ossification center is rapidly followed by its partial replacement and use as a template upon which bone is deposited by OB. This process involves the "propulsion" of the growth plate toward the epiphysis by a burst of proliferation, column formation followed by differentiation into pre-, early- and late, "terminally" differentiated, hypertrophic chondrocytes, associated with an increase in cell volume and deposition of their transient, calcified cartilage matrix (Ballock and O'keefe, 2003; Provot and Schipani, 2005; Mackie et al., 2008). The growing cartilage is invaded by blood vessels (Zelzer et al., 2002), leading to infiltration of bone-resorbing osteoclasts and OB, and ultimately cartilage matrix resorption and new bone formation ensue. Resorption at the chondro-osseous interface leaves calcified cartilage spicules on which OB deposit osteoid to form the primary trabecular bone spongiosa. EO spreads longitudinally from this primary center toward the bone ends and eventually a secondary ossification center forms, retaining the cartilaginous growth plate between each epiphysis and the primary ossification center (**Figure 1**) (Mackie et al., 2008).

In the context of bone healing, these EO processes are critically important in bridging the bone defect with a cartilage template that is later replaced by bone. Impaired bone healing is characterized by failure to undergo full EO in the cartilage tissue that is formed. In OA, in contrast, there is a failure to retain the stability of the articular cartilage at the joint's surface, which itself is required to sustain the mechanical environment required for healthy joint motion. Instead, it exhibits undesirable EO-like characteristics during which articular cartilage becomes vascularized, mineralized, and eventually replaced by bone (Kawaguchi, 2008). This EO is particularly evident at the joint margins where osteophytes—bony outgrowths—are formed (Pottenger et al., 1990; Boegård et al., 1998). It may also characterize the bone-marrow lesions now established as another OA hallmark (Felson et al., 2001; Kuttapitiya et al., 2017). Despite clear intimacy of this chondro-osseous interplay in growth, bone healing and OA, the mechanisms reinforcing the chondrocyte: osteoblast inter-relationship are incompletely defined.

An example, relates to the fate of the terminally differentiated chondrocytes. Historically, numerous studies have provided evidence that these hypertrophic chondrocytes undergo apoptosis as their final inevitable fate (Farnum and Wilsman, 1987, 1989; Gibson et al., 1995; Zenmyo et al., 1996; Aizawa et al., 1997; Gibson, 1998). The molecular mechanisms are not fully elucidated but molecular apoptotic signatures; activation of caspases and decreased expression of anti-apoptotic factor Bcl-2, have been reported in hypertrophic chondrocytes (Amling et al., 1997; Adams and Shapiro, 2002). Until recently, consensus was also that all OB originated from invading, periosteal-derived osteoprogenitor cells (Colnot et al., 2004; Maes et al., 2010). Remarkably, hypertrophic chondrocytes lack morphological characteristics of apoptosis; which challenges earlier reports (Emons et al., 2009; Carames et al., 2010) as it would be expected that cell chromatin condensation and nuclear fragmentation would readily be visible. Instead, the presence of autophagic vacuoles and expression of autophagy-regulating genes by growth plate chondrocytes suggest that they instead undergo processes resembling autophagy (Roach and Clarke, 2000; Shapiro et al., 2005).

It is clear nonetheless that these EO-related events are regulated by paracrine and endocrine signals (Day et al., 2005) including ECM constituents and ECM-modifying enzymes [matrix metalloproteinases (MMPs)] and their regulators (tissue inhibitors of MMPs; TIMPs) (Murphy and Nagase, 2008). Herein, we will (i) explore recent evidence that revisits the idea that hypertrophic chondrocytes may transdifferentiate into a specific sub-population of osteoblast cells and (ii) share data suggesting that osteoblast behavior in this sub-population relies partly upon a direct contribution from the cartilage ECM composition. There are multiple lines of evidence, including our own, showing that local, selective alterations in cartilage ECM remodeling indelibly alter bone quality. This would be consistent with the hypothesis that osteoblast behavior in long bones is regulated by a combination of their lineage origins and the epigenetic effects of chondrocyte-derived ECM which they encounter during their recruitment (**Figure 2**).

EMERGENCE OF A CHONDRO-OSSEOUS CELLULAR CONTINUUM

Endochondral ossification is predominantly understood through its function in long bone development, where mesenchymal-derived chondrocytes undergo a multistep process. These steps correspond to phases in which a precursor pool is maintained, an expansion in cell number, a halt upon division, entry into differentiation and matrix production and finally a dramatic increase

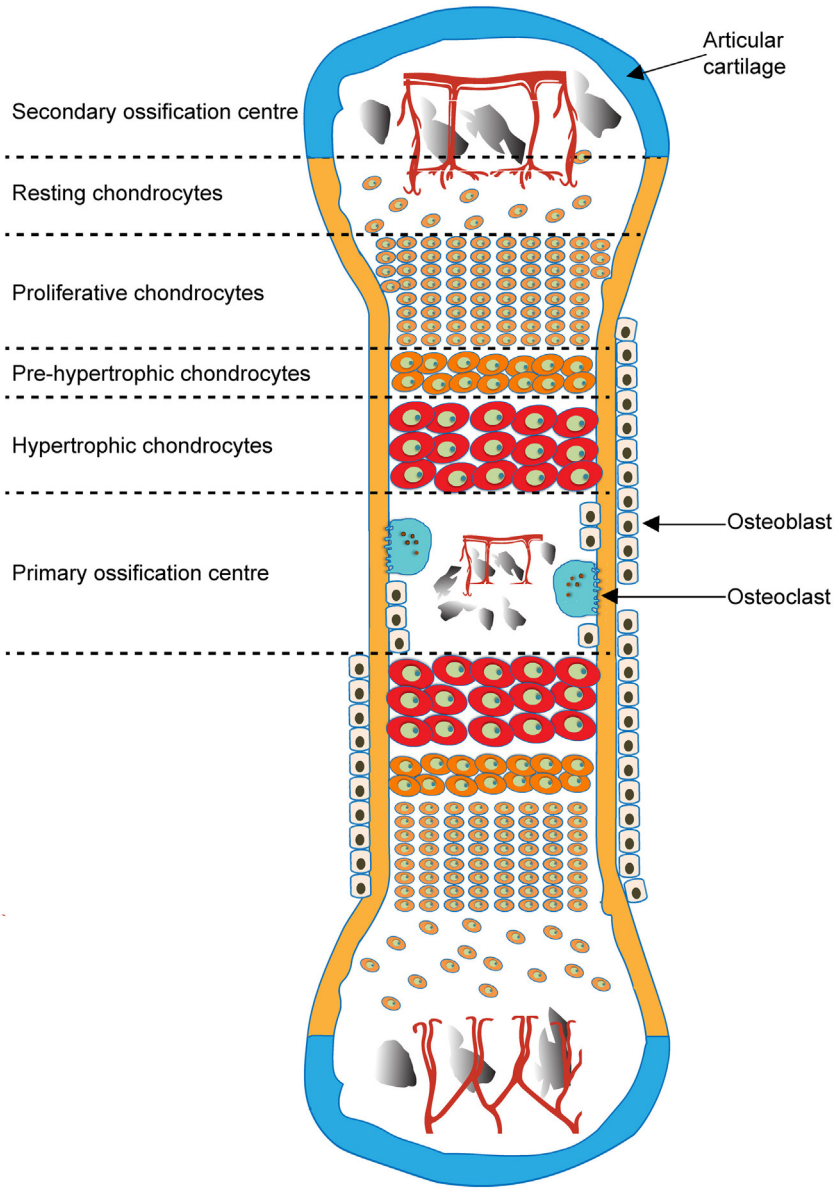

FIGURE 1 | Schematic of endochondral ossification and formation of primary and secondary ossification centers.

in size occur (Tsang et al., 2015). Hypertrophic chondrocytes are often characterized by expression of MMP-13, type X collagen and vascular endothelial growth factor (VEGF) that are hallmarks of their terminal maturation status. It has been assumed that these hallmarks precede their apoptotic death (Farnum and Wilsman, 1987, 1989; Gibson et al., 1995; Zenmyo et al., 1996; Aizawa et al., 1997; Amling et al., 1997; Gibson, 1998; Adams and Shapiro, 2002), which heralds the replacement of cartilage by bone that is initiated by OB and accompanied by vascular invasion of the ECM (Ortega et al., 2004).

An alternative fate and a question that was originally posed more than a century ago (Vander Stricht, 1890; Brachet, 1893) was: can hypertrophic chondrocytes "recycle," become OB and, therefore, contribute to the osteogenic lineage? This alternative theory has for a long time been a source of controversy. Initially, Dodds and Cameron used histological analysis in rats with rickets to suggest that cartilage cells undergo a form of differentiation that facilitates their eventual transition into osteocytes (Dodds and Cameron, 1939). Consistent with these suggestions, recent studies using a range of *in vivo* and *in vitro* strategies have demonstrated that hypertrophic chondrocytes can traverse this chondro-osseous interface to persist as OB and endorse their ultimate osteocytogenesis to assume a master bone-regulatory function. These studies indicate that newly transdifferentiated OB populate both trabecular and mature cortical bone.

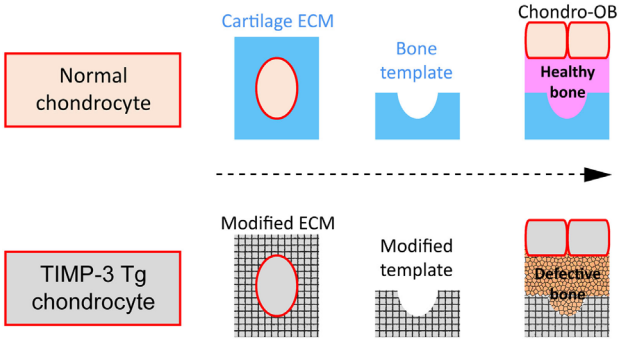

FIGURE 2 | Schematic of hypothesis. **(A)** Normal cartilage extracellular matrix (ECM) (blue) as template for successful (pink) bone formation by osteoblasts (OB) derived either from chondrocytes (Chondro-OB, beige, red outline) or from bone-marrow progeny (BM-OB, green); **(B)** Modified ECM (gray texturized) produced by TIMP3 Tg chondrocytes (gray, red outline) as template for defective bone formation by Chondro-OB (gray, red outline).

A number of studies explored this alternative fate further; Yoshioka and Yagi (1988) found hypertrophic chondrocytes within primary spongiosa of the rat mandibular condylar cartilage. In addition, Roach and others (Roach, 1992; Roach et al., 1995; Erenpreisa and Roach, 1996) reported asymmetric hypertrophic chondrocyte division in chick bones with one daughter cell transdifferentiating into an osteoblast and the other experiencing apoptosis. Several other studies reported, even in the absence of direct evidence for transdifferentiation, that hypertrophic chondrocytes and OB share many similarities including an osteogenic-specific gene expression profile; both express alkaline phosphatase, osteonectin, osteocalcin, osteopontin, and bone sialoprotein; suggesting common origins (Silbermann et al., 1983; Moskalewski and Malejczyk, 1989; Thesingh et al., 1991; Cancedda et al., 1992; Roach, 1992; Galotto et al., 1994; Roach et al., 1995; Gerstenfeld and Shapiro, 1996; Riminucci et al., 1998; Enishi et al., 2014).

Survival of hypertrophic chondrocytes during EO was found in pathology; chondrocytes in fracture repair calluses exhibited transdifferentiation to OB contributing to ossification. Convincing experimental evidence for a continuous chondrocyte-to-osteoblast lineage also came from use of a cell specific, tamoxifen inducible genetic recombination approach, where chondrocytes from the cartilage anlagen/growth plate were found as OB forming new bone, contributing to fracture repair (Zhou et al., 2014). This conclusion was supported by results from Yang et al., who used Col10a1 driven Cre/loxP to specifically target and tag hypertrophic chondrocytes *in vivo* to report that a hypertrophic chondrocyte sub-population expressing Col10a1 transform into Col1a1-expressing OB and mature osteocytes that express SCLEROSTIN, pre-/post-natally and during fracture repair (Yang et al., 2014). These OB, like those derived directly from osteoblast progenitors, potentially participate in other pathological states including OA. It is reasonable to postulate that any inherent chondrocytic defect could ultimately impact the behavior of their resulting bone cells and thus, that any gene expressed by chondrocytes influences this sub-population of OB ultimately affecting osteogenesis. Jing et al. reported that targeted cartilage-specific cell lineage-tracing leads not only to severe defects in chondrogenesis but complete cessation of EO, with absence of cartilage "remnants" in the subchondral bone (Jing et al., 2015). More importantly, bone phenotypes should now be scrutinized for mutations that also affect cartilage (Bahney et al., 2014).

This notion was further supported by an exploration of stem cell behaviors in endochondral bone healing, which revealed activation of the pluripotent transcription factor, Oct4A—a stem cell marker with proposed cell reprogramming roles—in vascularizing tissues and hypertrophic chondrocytes (Bahney et al., 2014). Despite poor clarity regarding Oct4A function, it appears that chondrocytes dedifferentiate by mechanisms resembling those described for induced pluripotent cells, to regain progenitor capabilities. This would be consistent with mechanism described by Song and Tuan (2004). Elucidation of the cellular reprogramming mechanism(s) that direct this transition from cartilage to bone is, therefore, an obvious target. However, the substantial overlap that exists between markers of hypertrophic chondrocytes and OB represent a significant hurdle in such elucidation (Lian et al., 1993; Stafford et al., 1994; Hughes et al., 1995; Gerstenfeld and Shapiro, 1996). These difficulties in discerning the reprogramming mechanisms are not altogether surprising, since chondrocytes and OB are known to share common osteochondral progenitor origins. More recently, Wang et al. found that SHP2, a cytoplasmic protein tyrosine phosphatase, modulates chondrocyte-to-osteoblast differentiation and that SHP2 deletion exerts a negative skeletal impact (Wang et al., 2017).

Ono et al. revealed that cells expressing Cre-recombinases driven by the collagen II (Col2) promoter/enhancer, and their descendants, contributed to osteoblast progenitors before Runx2 expression; using inducer Col2-creER, Sox9-creER, and Acan-creER approaches these authors reported that early postnatal cells progressively contribute to multiple mesenchymal lineages (Ono et al., 2014). Moreover, Enishi et al. reported that chondrocytes switch to osteoblast-like cells after vascular invasion (Enishi et al., 2014). More recently, Hu et al. described a spatially dependent phenotypic overlap between hypertrophic chondrocytes and OB at the chondro-osseous border in fracture callus, where the former activate expression of the pluripotency factors Sox2, Oct4 (Pou5f1), and Nanog (Hu et al., 2017). These studies also demonstrated that endothelial cell conditioned medium upregulates these genes in *ex vivo* fracture cultures, supporting histological evidence that transdifferentiation occurs adjacent to the vasculature. Moreover, Park et al. (2015) employed BAC-Col10-Cre deleter mice to activate ROSA26 LacZ and ROSA26 YFP reporter genes specifically in hypertrophic chondrocytes (Gebhard et al., 2008). They found that BAC-Col10-Cre;ROSA26 driven LacZ and YFP expression was restricted to hypertrophic chondrocytes before primary ossification center formation, but that substantial osteoblast numbers were positive for β-gal or YFP after onset of bone-marrow formation, leading to the proposal that these OB originated from Col10a1-expressing chondrocytes. This work further revealed the existence of a population of hypertrophic chondrocytes

close to the chondro-osseous junction that express stem cell and osteoblast markers (Park et al., 2015). In addition, Jing et al. (2015), using cartilage-specific cell lineage–tracing in mice containing ROSA 26tdTomato, 2.3 Col1GFP, and Acan CreERT2 or Col10-Cre reported that hypertrophic chondrocytes collectively expressed high levels of the anti-apoptotic protein, BCL2. In addition, alkaline phosphatase immunoreactivity was strong in hypertrophic chondrocytes, and BrdU data showed that some hypertrophic chondrocytes undergo cell division. Thus, hypertrophic chondrocytes resemble metabolically active OB rather than simply being inert, metabolically inactive cells, waiting to undergo apoptosis (Jing et al., 2015). These novel findings suggest that, at least, some OB originate from a source distinct from the periosteal-derived osteoprogenitors. Might OB with distinct origins vary in their behavior and activity?

We previously investigated whether OB with divergent origins from different bone types exhibit divergence in their behavior, by comparing growth, differentiation, and angiogenic potential of OB derived from structurally distinct subchondral, trabecular, and cortical bone from a singular skeletal vicinity (Clarkin and Olsen, 2010; Shah et al., 2015). We found that OB from trabecular bone showed slower proliferation, but higher RUNX2, SP7 and BSP-II mRNA levels, TNAP mRNA and protein activity, and lower TNFRSF11B:TNFSF11 mRNA ratios compared to subchondral and cortical bone. In contrast, subchondral OB showed higher VEGF-A mRNA and protein release, implying more intimate vascular relationships (Shah et al., 2015). These findings are consistent with data showing that the response of trabecular, cortical, and subchondral bone to *in vivo* challenges is not always identical (Lavigne et al., 2005; Wade-Gueye et al., 2012), with distinct transcriptional signatures in OB from long bone and calvaria (Akintoye et al., 2006; Rawlinson et al., 2009) and with OB displaying differing gene transcription depending on anatomical location (Candeliere et al., 2001). These data raise the possibility that osteoblast behaviors reflect progenitor origins related to the crossing of a chondro-osseous continuum.

The clearly strong relationships between cells of the growth plate, OB and the vasculature have been dealt with elegantly elsewhere (Maes, 2013). With particular relevance to the concepts shared herein, it is important that we highlight changes to ECM-modifying proteins have been shown to modify vascularization pre- and post-natally. Previous studies have shown that disruption of matrix remodeling *via* modification in MMPs leads to delayed vascularization, inefficient bone repair, and significant alteration in bone mass and architecture (Vu et al., 1998; Holmbeck et al., 1999; Zhou et al., 2000; Colnot et al., 2003; Stickens et al., 2004; Behonick et al., 2007; Lieu et al., 2011). Does this show that the behavior of OB derived from chondrocytes is determined by the cartilage ECM they encounter?

DO MODIFICATIONS IN THE CHONDRO-OSSEOUS ECM EPIGENETICALLY MODIFY OSTEOBLAST BEHAVIOR?

The ECM is a powerful driver of cell behavior. ECM–cell relationships are tightly conserved across evolution, highly dynamic and extend beyond mechanical control of cell fate. Defining how ECM "messages" guide cell performance provides translational impact for stem cell biologists, tissue engineers and biologists to transform approaches to regenerate, repair and remodel connective tissue across pathophysiological contexts. The ECM of the growth plate represents an alternative stimulus to regulate the behavior of cells crossing this chondro-osseous continuum, demonstrating the full intimacy of chondrocyte-osteoblast interplay.

Bone quality and functional integrity relies on interplay between resident cells and the cartilage ECM template. Evidence for this is strong; local control of cartilage ECM remodeling has down-stream effects on bone formation, with mice deficient in the MMPs and TIMP3 having severely disrupted growth plate ECM and bone defects (Vu et al., 1998; Holmbeck et al., 1999; Zhou et al., 2000; Stickens et al., 2004; Javaheri et al., 2016). Does this show that osteoblast behavior is determined by the cartilage ECM they encounter? It seems likely as expression of factors crucial to cartilage signaling (Indian hedgehog, patched and parathyroid hormone-related peptide) are not modified (Karaplis et al., 1994; Marigo et al., 1996; Vortkamp et al., 1996; Maeda et al., 2007). Furthermore, selective chondrocyte-specific Sox9-Cre mediated loss of disintegrin and metallopeptidase domain containing enzyme (ADAM17) leads to bone defects without modifying intrinsic proliferation of resident chondrocytes. Thus, chondrocyte ECM, not solely humoral factors or growth plate dynamics may guide bone mass, architecture, and function (Javaheri et al., 2016).

To test this hypothesis, we created mice with severely modified cartilage ECM remodeling by targeting TIMP3, a member of the metzincin family of MMP inhibitors that inhibits a wide spectrum of ECM-modifying enzymes. Our work in TIMP3-deficient mice and mice overexpressing TIMP3 specifically in chondrocytes, *via* a collagen type II promoter/enhancer (TIMP3 Tg) reveals (i) transient long bone shortening that is restored before adulthood; (ii) diminished bone mass with defective architecture and lower fracture resistance; (iii) restriction of TIMP3 Tg impact to only endochondral bones; and (iv) deficiencies in osteoblast proliferation and differentiation that persists *in vitro*. Our data show that bone formation relies partly upon the cartilage ECM encountered during osteoblast recruitment (Javaheri et al., 2016; Poulet et al., 2016). Our work also shows that aggrecanase inhibition increases and collagenase inhibition decreases bone mass, suggesting that balance in their activities is crucial; however, the identities of the growth plate ECM components that underpin these divergent phenotypes remains obscure.

While our findings confirm the existence of a cellular chondro-osseous continuum, they also crucially pinpoint how behavior of cells with divergent origins is controlled *in vivo* by the ECM they encounter. Since growth plate calcified cartilage serves as a template not only for bone formation but also osteoclast-mediated resorption, this implies that osteoclast behavior may also be modified in TIMP3 Tg mice to subsequently influence bone formation. However, our pilot studies suggest this is unlikely as we find no significant changes in osteoclast numbers in TIMP3 Tg mouse bone (Javaheri et al., 2016). In contrast, we find that

OB derived from these TIMP3 Tg mice have defective differentiation even upon *in vitro* isolation, supporting the likelihood that "imprinted" epigenetic modifications are contingent upon the ECM the OB encounter (Poulet et al., 2016). The precise nature of these epigenetic effects of chondrocyte-derived ECM remains unexplored. Nonetheless, multiple lines of evidence, including ours, show that local alterations in cartilage ECM remodeling indelibly alter bone quality, leading us to hypothesize that osteoblast behavior in long bones is regulated by a combination of their lineage origins and the epigenetic effects of chondrocyte-derived ECM they encounter during recruitment.

CONCLUSION

Recent evidence challenges a long-held paradigm regarding EO, indicating that chondrogenesis and osteogenesis are more closely linked than appreciated and, that cells derived originally from the cartilage niche, as opposed to solely osteoprogenitors, transform into bone-forming OB and ultimately osteocytes. We offer a fundamental extension to this paradigm proposing that these OB are epigenetically influenced by ECM encountered during this transition. We need to ascertain how hypertrophic chondrocyte transdifferentiation fate is controlled and which specific ECM factors regulate this transition to impact bone quality and integrity. This new concept challenges us to re-evaluate cartilage and bone stages in EO, such that we treat them as a continuum rather than entirely independent. It also prompts us to revisit EO as an "evolutionary" shift in which cartilage might provide new cells that can instead form bone rather than simply as a means of lengthening skeletal elements. As impaired bone healing and OA both involve EO it is conceivable that tissue engineering approaches might exploit these developmental principles, embracing the newly established cellular chondro-osseous continuum to better control cell fate decisions.

AUTHOR CONTRIBUTIONS

Conceived and designed the idea: BJ, GG, and AP. Wrote the mini review: BJ, SC-S, IK, GG, and AP. Revision and finalizing the mini review: BJ, GG, and AP.

FUNDING

This work was supported by funding from the BBSRC BB/I014608/1, Arthritis Research UK 20581 and 20039.

REFERENCES

Adams, C. S., and Shapiro, I. M. (2002). The fate of the terminally differentiated chondrocyte: evidence for microenvironmental regulation of chondrocyte apoptosis. *Crit. Rev. Oral Biol. Med.* 13, 465–473. doi:10.1177/154411130201300604

Aizawa, T., Kokubun, S., and Tanaka, Y. (1997). Apoptosis and proliferation of growth plate chondrocytes in rabbits. *J. Bone Joint Surg. Br.* 79, 483–486. doi:10.1302/0301-620X.79B3.7221

Akintoye, S. O., Lam, T., Shi, S., Brahim, J., Collins, M. T., and Robey, P. G. (2006). Skeletal site-specific characterization of orofacial and iliac crest human bone marrow stromal cells in same individuals. *Bone* 38, 758–768. doi:10.1016/j.bone.2005.10.027

Amling, M., Neff, L., Tanaka, S., Inoue, D., Kuida, K., Weir, E., et al. (1997). Bcl-2 lies downstream of parathyroid hormone-related peptide in a signaling pathway that regulates chondrocyte maturation during skeletal development. *J. Cell Biol.* 136, 205–213. doi:10.1083/jcb.136.1.205

Bahney, C. S., Hu, D. P., Taylor, A. J., Ferro, F., Britz, H. M., Hallgrimsson, B., et al. (2014). Stem cell-derived endochondral cartilage stimulates bone healing by tissue transformation. *J. Bone Miner. Res.* 29, 1269–1282. doi:10.1002/jbmr.2148

Ballock, R. T., and O'keefe, R. J. (2003). The biology of the growth plate. *JBJS* 85, 715–726. doi:10.2106/00004623-200304000-00021

Behonick, D. J., Xing, Z., Lieu, S., Buckley, J. M., Lotz, J. C., Marcucio, R. S., et al. (2007). Role of matrix metalloproteinase 13 in both endochondral and intramembranous ossification during skeletal regeneration. *PLoS ONE* 2:e1150. doi:10.1371/journal.pone.0001150

Boegård, T., Rudling, O., Petersson, I., and Jonsson, K. (1998). Correlation between radiographically diagnosed osteophytes and magnetic resonance detected cartilage defects in the patellofemoral joint. *Ann. Rheum. Dis.* 57, 395–400. doi:10.1136/ard.57.7.395

Brachet, A. (1893). Etude sur la resorption du cartilage et le developpement des os longs chez les oiseaux. *J. Anat. Physiol.* 10, 391–417.

Cancedda, F. D., Gentili, C., Manduca, P., and Cancedda, R. (1992). Hypertrophic chondrocytes undergo further differentiation in culture. *J. Cell Biol.* 117, 427–435. doi:10.1083/jcb.117.2.427

Candeliere, G. A., Liu, F., and Aubin, J. E. (2001). Individual osteoblasts in the developing calvaria express different gene repertoires. *Bone* 28, 351–361. doi:10.1016/S8756-3282(01)00410-0

Carames, B., Taniguchi, N., Otsuki, S., Blanco, F. J., and Lotz, M. (2010). Autophagy is a protective mechanism in normal cartilage, and its aging-related loss is linked with cell death and osteoarthritis. *Arthritis Rheum.* 62, 791–801. doi:10.1002/art.27305

Clarkin, C., and Olsen, B. R. (2010). On bone-forming cells and blood vessels in bone development. *Cell Metab.* 12, 314–316. doi:10.1016/j.cmet.2010.09.009

Colnot, C., Lu, C., Hu, D., and Helms, J. A. (2004). Distinguishing the contributions of the perichondrium, cartilage, and vascular endothelium to skeletal development. *Dev. Biol.* 269, 55–69. doi:10.1016/j.ydbio.2004.01.011

Colnot, C., Thompson, Z., Miclau, T., Werb, Z., and Helms, J. A. (2003). Altered fracture repair in the absence of MMP9. *Development* 130, 4123–4133. doi:10.1242/dev.00559

Day, T. F., Guo, X., Garrett-Beal, L., and Yang, Y. (2005). Wnt/beta-catenin signaling in mesenchymal progenitors controls osteoblast and chondrocyte differentiation during vertebrate skeletogenesis. *Dev. Cell* 8, 739–750. doi:10.1016/j.devcel.2005.03.016

Dodds, G. S., and Cameron, H. C. (1939). The behaviour and fate of the cartilage remnants in the rachitic metaphysis. *Am. J. Pathol.* XV, 723–743.

Emons, J., Chagin, A. S., Hultenby, K., Zhivotovsky, B., Wit, J. M., Karperien, M., et al. (2009). Epiphyseal fusion in the human growth plate does not involve classical apoptosis. *Pediatr. Res.* 66, 654–659. doi:10.1203/PDR.0b013e3181beaa8c

Enishi, T., Yukata, K., Takahashi, M., Sato, R., Sairyo, K., and Yasui, N. (2014). Hypertrophic chondrocytes in the rabbit growth plate can proliferate and differentiate into osteogenic cells when capillary invasion is interposed by a membrane filter. *PLoS ONE* 9:e104638. doi:10.1371/journal.pone.0104638

Erenpreisa, J., and Roach, H. I. (1996). Epigenetic selection as a possible component of transdifferentiation. Further study of the commitment of hypertrophic chondrocytes to become osteocytes. *Mech. Ageing Dev.* 87, 165–182. doi:10.1016/0047-6374(96)01703-4

Farnum, C. E., and Wilsman, N. J. (1987). Morphologic stages of the terminal hypertrophic chondrocyte of growth plate cartilage. *Anat. Rec.* 219, 221–232. doi:10.1002/ar.1092190303

Farnum, C. E., and Wilsman, N. J. (1989). Condensation of hypertrophic chondrocytes at the chondro-osseous junction of growth plate cartilage in Yucatan swine: relationship to long bone growth. *Am. J. Anat.* 186, 346–358.

Felson, D. T., Chaisson, C. E., Hill, C. L., Totterman, S. M., Gale, M. E., Skinner, K. M., et al. (2001). The association of bone marrow lesions with pain in knee osteoarthritis. *Ann. Intern. Med.* 134, 541–549. doi:10.7326/0003-4819-134-7-200104030-00007

Galotto, M., Campanile, G., Robino, G., Cancedda, F. D., Bianco, P., and Cancedda, R. (1994). Hypertrophic chondrocytes undergo further differentiation to osteoblast-like cells and participate in the initial bone formation in developing chick embryo. *J. Bone Miner. Res.* 9, 1239–1249. doi:10.1002/jbmr.5650090814

Gebhard, S., Hattori, T., Bauer, E., Schlund, B., Bösl, M. R., de Crombrugghe, B., et al. (2008). Specific expression of Cre recombinase in hypertrophic cartilage under the control of a BAC-Col10a1 promoter. *Matrix Biol.* 27, 693–699. doi:10.1016/j.matbio.2008.07.001

Gerstenfeld, L., and Shapiro, F. (1996). Expression of bone-specific genes by hypertrophic chondrocytes: implications of the complex functions of the hypertrophic chondrocyte during endochondral bone development. *J. Cell. Biochem.* 62, 1–9. doi:10.1002/(SICI)1097-4644(199607)62:1<1::AID-JCB1>3.0.CO;2-X

Gibson, G. (1998). Active role of chondrocyte apoptosis in endochondral ossification. *Microsc. Res. Tech.* 43, 191–204. doi:10.1002/(SICI)1097-0029(19981015)43:2<191::AID-JEMT10>3.0.CO;2-T

Gibson, G. J., Kohler, W. J., and Schaffler, M. B. (1995). Chondrocyte apoptosis in endochondral ossification of chick sterna. *Dev. Dyn.* 203, 468–476. doi:10.1002/aja.1002030409

Hall, B. K. (2005). *Bones and Cartilage: Developmental and Evolutionary Skeletal Biology*. Amsterdam, London: Elsevier Academic.

Holmbeck, K., Bianco, P., Caterina, J., Yamada, S., Kromer, M., Kuznetsov, S. A., et al. (1999). MT1-MMP-deficient mice develop dwarfism, osteopenia, arthritis, and connective tissue disease due to inadequate collagen turnover. *Cell* 99, 81–92. doi:10.1016/S0092-8674(00)80064-1

Hu, D. P., Ferro, F., Yang, F., Taylor, A. J., Chang, W., Miclau, T., et al. (2017). Cartilage to bone transformation during fracture healing is coordinated by the invading vasculature and induction of the core pluripotency genes. *Development* 144, 221–234. doi:10.1242/dev.130807

Hughes, S. S., Hicks, D. G., O'Keefe, R. J., Hurwitz, S. R., Crabb, I. D., Krasinskas, A. M., et al. (1995). Shared phenotypic expression of osteoblasts and chondrocytes in fracture callus. *J. Bone Miner. Res.* 10, 533–544. doi:10.1002/jbmr.5650100405

Hunter, D. J., Schofield, D., and Callander, E. (2014). The individual and socioeconomic impact of osteoarthritis. *Nat. Rev. Rheumatol.* 10, 437–441. doi:10.1038/nrrheum.2014.44

Javaheri, B., Hopkinson, M., Poulet, B., Pollard, A. S., Shefelbine, S. J., Chang, Y. M., et al. (2016). Deficiency and also transgenic overexpression of Timp-3 both lead to compromised bone mass and architecture in vivo. *PLoS ONE* 11:e0159657. doi:10.1371/journal.pone.0159657

Jing, Y., Zhou, X., Han, X., Jing, J., von der Mark, K., Wang, J., et al. (2015). Chondrocytes directly transform into bone cells in mandibular condyle growth. *J. Dent. Res.* 94, 1668–1675. doi:10.1177/0022034515598135

Johnell, O., and Kanis, J. (2005). Epidemiology of osteoporotic fractures. *Osteoporosis Int.* 16, S3–S7. doi:10.1007/s00198-004-1702-6

Karaplis, A. C., Luz, A., Glowacki, J., Bronson, R. T., Tybulewicz, V. L., Kronenberg, H. M., et al. (1994). Lethal skeletal dysplasia from targeted disruption of the parathyroid hormone-related peptide gene. *Genes Dev.* 8, 277–289. doi:10.1101/gad.8.3.277

Kawaguchi, H. (2008). Endochondral ossification signals in cartilage degradation during osteoarthritis progression in experimental mouse models. *Mol. Cells* 25, 1–6.

Kuttapitiya, A., Assi, L., Laing, K., Hing, C., Mitchell, P., Whitley, G., et al. (2017). Microarray analysis of bone marrow lesions in osteoarthritis demonstrates upregulation of genes implicated in osteochondral turnover, neurogenesis and inflammation. *Ann. Rheum. Dis.* 76, 1764–1773. doi:10.1136/annrheumdis-2017-211396

Lavigne, P., Benderdour, M., Lajeunesse, D., Reboul, P., Shi, Q., Pelletier, J. P., et al. (2005). Subchondral and trabecular bone metabolism regulation in canine experimental knee osteoarthritis. *Osteoarthr. Cartil.* 13, 310–317. doi:10.1016/j.joca.2004.12.015

Lian, J., McKee, M., Todd, A., and Gerstenfeld, L. C. (1993). Induction of bone-related proteins, osteocalcin and osteopontin, and their matrix ultrastructural localization with development of chondrocyte hypertrophy in vitro. *J. Cell. Biochem.* 52, 206–219. doi:10.1002/jcb.240520212

Lieu, S., Hansen, E., Dedini, R., Behonick, D., Werb, Z., Miclau, T., et al. (2011). Impaired remodeling phase of fracture repair in the absence of matrix metalloproteinase-2. *Dis. Model Mech.* 4, 203–211. doi:10.1242/dmm.006304

Mackie, E. J., Ahmed, Y. A., Tatarczuch, L., Chen, K. S., and Mirams, M. (2008). Endochondral ossification: how cartilage is converted into bone in the developing skeleton. *Int. J. Biochem. Cell Biol.* 40, 46–62. doi:10.1016/j.biocel.2007.06.009

Maeda, Y., Nakamura, E., Nguyen, M. T., Suva, L. J., Swain, F. L., Razzaque, M. S., et al. (2007). Indian Hedgehog produced by postnatal chondrocytes is essential for maintaining a growth plate and trabecular bone. *Proc. Natl. Acad. Sci. U.S.A.* 104, 6382–6387. doi:10.1073/pnas.0608449104

Maes, C. (2013). Role and regulation of vascularization processes in endochondral bones. *Calcif. Tissue Int.* 92, 307–323. doi:10.1007/s00223-012-9689-z

Maes, C., Kobayashi, T., Selig, M. K., Torrekens, S., Roth, S. I., Mackem, S., et al. (2010). Osteoblast precursors, but not mature osteoblasts, move into developing and fractured bones along with invading blood vessels. *Dev. Cell* 19, 329–344. doi:10.1016/j.devcel.2010.07.010

Marigo, V., Johnson, R. L., Vortkamp, A., and Tabin, C. J. (1996). Sonic hedgehog differentially regulates expression of GLI and GLI3 during limb development. *Dev. Biol.* 180, 273–283. doi:10.1006/dbio.1996.0300

Moskalewski, S., and Malejczyk, J. (1989). Bone formation following intrarenal transplantation of isolated murine chondrocytes: chondrocyte-bone cell transdifferentiation? *Development* 107, 473–480.

Murphy, G., and Nagase, H. (2008). Progress in matrix metalloproteinase research. *Mol. Aspects Med.* 29, 290–308. doi:10.1016/j.mam.2008.05.002

Ono, N., Ono, W., Nagasawa, T., and Kronenberg, H. M. (2014). A subset of chondrogenic cells provides early mesenchymal progenitors in growing bones. *Nat. Cell Biol.* 16, 1157–1167. doi:10.1038/ncb3067

Ortega, N., Behonick, D. J., and Werb, Z. (2004). Matrix remodeling during endochondral ossification. *Trends Cell Biol.* 14, 86–93. doi:10.1016/j.tcb.2003.12.003

Park, J., Gebhardt, M., Golovchenko, S., Perez-Branguli, F., Hattori, T., Hartmann, C., et al. (2015). Dual pathways to endochondral osteoblasts: a novel chondrocyte-derived osteoprogenitor cell identified in hypertrophic cartilage. *Biol Open* 4, 608–621. doi:10.1242/bio.201411031

Pottenger, L. A., Phillips, F. M., and Draganich, L. F. (1990). The effect of marginal osteophytes on reduction of varus-valgus instability in osteoarthritic knees. *Arthritis Rheum.* 33, 853–858. doi:10.1002/art.1780330612

Poulet, B., Liu, K., Plumb, D., Vo, P., Shah, M., Staines, K., et al. (2016). Overexpression of TIMP-3 in chondrocytes produces transient reduction in growth plate length but permanently reduces adult bone quality and quantity. *PLoS ONE* 11:e0167971. doi:10.1371/journal.pone.0167971

Provot, S., and Schipani, E. (2005). Molecular mechanisms of endochondral bone development. *Biochem. Biophys. Res. Commun.* 328, 658–665. doi:10.1016/j.bbrc.2004.11.068

Rawlinson, S. C., McKay, I. J., Ghuman, M., Wellmann, C., Ryan, P., Prajaneh, S., et al. (2009). Adult rat bones maintain distinct regionalized expression of markers associated with their development. *PLoS ONE* 4:e8358. doi:10.1371/journal.pone.0008358

Riminucci, M., Bradbeer, J. N., Corsi, A., Gentili, C., Descalzi, F., Cancedda, R., et al. (1998). Vis-a-vis cells and the priming of bone formation. *J. Bone Miner. Res.* 13, 1852–1861. doi:10.1359/jbmr.1998.13.12.1852

Roach, H. (1992). Trans-differentiation of hypertrophic chondrocytes into cells capable of producing a mineralized bone matrix. *Bone Miner.* 19, 1–20. doi:10.1016/0169-6009(92)90840-A

Roach, H. I., and Clarke, N. M. (2000). Physiological cell death of chondrocytes in vivo is not confined to apoptosis. New observations on the mammalian growth plate. *J. Bone Joint Surg. Br.* 82, 601–613. doi:10.1302/0301-620X.82B4.9846

Roach, H. I., Erenpreisa, J., and Aigner, T. (1995). Osteogenic differentiation of hypertrophic chondrocytes involves asymmetric cell divisions and apoptosis. *J. Cell Biol.* 131, 483–494. doi:10.1083/jcb.131.2.483

Shah, M., Gburcik, V., Reilly, P., Sankey, R. A., Emery, R. J., Clarkin, C. E., et al. (2015). Local origins impart conserved bone type-related differences in human osteoblast behaviour. *Eur. Cell. Mater.* 29, 155–75;discussion75–6. doi:10.22203/eCM.v029a12

Shapiro, I. M., Adams, C. S., Freeman, T., and Srinivas, V. (2005). Fate of the hypertrophic chondrocyte: microenvironmental perspectives on apoptosis and survival in the epiphyseal growth plate. *Birth Defects Res. C Embryo Today* 75, 330–339. doi:10.1002/bdrc.20057

Silbermann, M., Lewinson, D., Gonen, H., Lizarbe, M. A., and von der Mark, K. (1983). In vitro transformation of chondroprogenitor cells into osteoblasts and

the formation of new membrane bone. *Anat. Rec.* 206, 373–383. doi:10.1002/ar.1092060404

Song, L., and Tuan, R. S. (2004). Transdifferentiation potential of human mesenchymal stem cells derived from bone marrow. *FASEB J.* 18, 980–982. doi:10.1096/fj.03-1100fje

Stafford, H., Roberts, M., Oni, O., Hay, J., and Gregg, P. (1994). Localisation of bone-forming cells during fracture healing by osteocalcin immunocytochemistry: an experimental study of the rabbit tibia. *J. Orthop. Res.* 12, 29–39. doi:10.1002/jor.1100120105

Stickens, D., Behonick, D. J., Ortega, N., Heyer, B., Hartenstein, B., Yu, Y., et al. (2004). Altered endochondral bone development in matrix metalloproteinase 13-deficient mice. *Development* 131, 5883–5895. doi:10.1242/dev.01461

Thesingh, C. W., Groot, C. G., and Wassenaar, A. M. (1991). Transdifferentiation of hypertrophic chondrocytes into osteoblasts in murine fetal metatarsal bones, induced by co-cultured cerebrum. *Bone Miner.* 12, 25–40. doi:10.1016/0169-6009(91)90119-K

Tsang, K. Y., Chan, D., and Cheah, K. S. (2015). Fate of growth plate hypertrophic chondrocytes: death or lineage extension? *Dev. Growth Differ.* 57, 179–192. doi:10.1111/dgd.12203

Van der Stricht, O. (1890). Recherches sur le cartilage articulaire des oiseaux. *Arch. Biol.* 10, 1–41.

Vortkamp, A., Lee, K., Lanske, B., Segre, G. V., Kronenberg, H. M., and Tabin, C. J. (1996). Regulation of rate of cartilage differentiation by Indian hedgehog and PTH-related protein. *Science* 273, 613–622. doi:10.1126/science.273.5275.613

Vu, T. H., Shipley, J. M., Bergers, G., Berger, J. E., Helms, J. A., Hanahan, D., et al. (1998). MMP-9/gelatinase B is a key regulator of growth plate angiogenesis and apoptosis of hypertrophic chondrocytes. *Cell* 93, 411–422. doi:10.1016/S0092-8674(00)81169-1

Wade-Gueye, N. M., Boudiffa, M., Vanden-Bossche, A., Laroche, N., Aubin, J. E., Vico, L., et al. (2012). Absence of bone sialoprotein (BSP) impairs primary bone formation and resorption: the marrow ablation model under PTH challenge. *Bone* 50, 1064–1073. doi:10.1016/j.bone.2012.02.014

Wang, L., Huang, J., Moore, D. C., Zuo, C., Wu, Q., Xie, L., et al. (2017). SHP2 Regulates the osteogenic fate of growth plate hypertrophic chondrocytes. *Sci. Rep.* 7, 12699. doi:10.1038/s41598-017-12767-9

Woolf, A. D., and Pfleger, B. (2003). Burden of major musculoskeletal conditions. *Bull. World Health Organ.* 81, 646–656.

Yang, L., Tsang, K. Y., Tang, H. C., Chan, D., and Cheah, K. S. (2014). Hypertrophic chondrocytes can become osteoblasts and osteocytes in endochondral bone formation. *Proc. Natl. Acad. Sci. U.S.A.* 111, 12097–12102. doi:10.1073/pnas.1302703111

Yoshioka, C., and Yagi, T. (1988). Electron microscopic observations on the fate of hypertrophic chondrocytes in condylar cartilage of rat mandible. *J. Craniofac. Genet. Dev. Biol.* 8, 253–264.

Zelzer, E., McLean, W., Ng, Y. S., Fukai, N., Reginato, A. M., Lovejoy, S., et al. (2002). Skeletal defects in VEGF(120/120) mice reveal multiple roles for VEGF in skeletogenesis. *Development* 129, 1893–1904.

Zenmyo, M., Komya, S., Kawabata, R., Sasaguri, Y., Inoue, A., and Morimatsu, M. (1996). Morphological and biochemical evidence for apoptosis in the terminal hypertrophicchondrocytesofthegrowthplate.*J. Pathol.*180,430–433.doi:10.1002/(SICI)1096-9896(199612)180:4<430::AID-PATH691>3.0.CO;2-H

Zhou, X., von der Mark, K., Henry, S., Norton, W., Adams, H., and de Crombrugghe, B. (2014). Chondrocytes transdifferentiate into osteoblasts in endochondral bone during development, postnatal growth and fracture healing in mice. *PLoS Genet.* 10:e1004820. doi:10.1371/journal.pgen.1004820

Zhou, Z., Apte, S. S., Soininen, R., Cao, R., Baaklini, G. Y., Rauser, R. W., et al. (2000). Impaired endochondral ossification and angiogenesis in mice deficient in membrane-type matrix metalloproteinase I. *Proc. Natl. Acad. Sci. U.S.A.* 97, 4052–4057. doi:10.1073/pnas.060037197

Conflict of Interest Statement: The authors declare that all financial, commercial or other relationships that might be perceived by the academic community as representing a potential conflict of interest are disclosed.

frontiers in Bioengineering and Biotechnology

REVIEW
published: 31 July 2018
doi: 10.3389/fbioe.2018.00105

Tissue Engineering and Cell-Based Therapies for Fractures and Bone Defects

*Jose R. Perez[1], Dimitrios Kouroupis[1,2], Deborah J. Li[1], Thomas M. Best[1], Lee Kaplan[1] and Diego Correa[1,2]**

[1] Department of Orthopedics, UHealth Sports Medicine Institute, Miller School of Medicine, University of Miami, Miami, FL, United States, [2] Diabetes Research Institute & Cell Transplant Center, Miller School of Medicine, University of Miami, Miami, FL, United States

OPEN ACCESS

Edited by:
Roberto Narcisi,
Erasmus Medical Center, Erasmus University Rotterdam, Netherlands

Reviewed by:
Arnaud Scherberich,
University Hospital Basel, Switzerland
Hugo Fernandes,
University of Coimbra, Portugal
Federico Ferro,
National University of Ireland Galway, Ireland

***Correspondence:**
Diego Correa
dxc821@med.miami.edu

Specialty section:
This article was submitted to Tissue Engineering and Regenerative Medicine, a section of the journal Frontiers in Bioengineering and Biotechnology

Received: 13 December 2017
Accepted: 09 July 2018
Published: 31 July 2018

Citation:
Perez JR, Kouroupis D, Li DJ, Best TM, Kaplan L and Correa D (2018) Tissue Engineering and Cell-Based Therapies for Fractures and Bone Defects. Front. Bioeng. Biotechnol. 6:105. doi: 10.3389/fbioe.2018.00105

Bone fractures and segmental bone defects are a significant source of patient morbidity and place a staggering economic burden on the healthcare system. The annual cost of treating bone defects in the US has been estimated to be $5 billion, while enormous costs are spent on bone grafts for bone injuries, tumors, and other pathologies associated with defective fracture healing. Autologous bone grafts represent the gold standard for the treatment of bone defects. However, they are associated with variable clinical outcomes, postsurgical morbidity, especially at the donor site, and increased surgical costs. In an effort to circumvent these limitations, tissue engineering and cell-based therapies have been proposed as alternatives to induce and promote bone repair. This review focuses on the recent advances in bone tissue engineering (BTE), specifically looking at its role in treating delayed fracture healing (non-unions) and the resulting segmental bone defects. Herein we discuss: (1) the processes of endochondral and intramembranous bone formation; (2) the role of stem cells, looking specifically at mesenchymal (MSC), embryonic (ESC), and induced pluripotent (iPSC) stem cells as viable building blocks to engineer bone implants; (3) the biomaterials used to direct tissue growth, with a focus on ceramic, biodegradable polymers, and composite materials; (4) the growth factors and molecular signals used to induce differentiation of stem cells into the osteoblastic lineage, which ultimately leads to active bone formation; and (5) the mechanical stimulation protocols used to maintain the integrity of the bone repair and their role in successful cell engraftment. Finally, a couple clinical scenarios are presented (non-unions and avascular necrosis—AVN), to illustrate how novel cell-based therapy approaches can be used. A thorough understanding of tissue engineering and cell-based therapies may allow for better incorporation of these potential therapeutic approaches in bone defects allowing for proper bone repair and regeneration.

Keywords: tissue engineering, stem cells, bone defects, fracture repair, biomaterials, mechanical stimulation, avascular necrosis, non-union

INTRODUCTION

Fracture healing typically occurs uninterrupted during the first 6–8 weeks following an injury, although this process can be delayed by structural parameters such as the presence of thick cortices, which require more time to heal, as well as unfavorable mechanical and biological environments generated from excessive fracture site movement and/or gaps to general factors including aging, alcohol, tobacco, and steroid abuse and medical conditions such as infection, type 1 diabetes, anemia, and deficient nutrition (Kostenuik and Mirza, 2017). Occasionally, a combination of these unfavorable environments results in impaired fracture healing as damaged vascular supply and periosteum coincides with polytrauma or soft tissue damage (Gómez-Barrena et al., 2015). As a result, delayed union or even nonunion can occur following failed fracture healing after 4 or 6 months, respectively, ranging from 1.7% up to 18.5%. These fracture healing disruptions remain major orthopedic complications as they are not only a health care burden but also present significant challenges to the surgeon given the underlying biological difficulties re-routing bone structures toward adequate healing (Fong et al., 2013; Gómez-Barrena et al., 2015). This also raises the potential for increased rates of critical sized bone defects, which are more than 2 cm in length involving over half the circumference of the affected bone, resulting from failed spontaneous healing despite surgical intervention (Watanabe et al., 2016).

In an effort to treat these defects, different types of bone grafts have been used including autografts, allografts, and synthetic grafts. Allografts have several drawbacks including graft rejection and disease transmission, while some synthetic grafts show an increased susceptibility to wear and tear (Salgado et al., 2004). Autologous bone grafts, on the other hand, are considered the gold standard to treat bone defects due to their established osteoinductive and osteoconductive properties, obviating the histocompatibility issue. When compared to allografts, autografts result in shorter time to union (Flierl et al., 2013). Even though autografts constitute a popular graft option, they also have drawbacks such as donor site morbidity, muscle weakness, and surgical complications such as pain, hemorrhage, infection, and nerve injury at the donor site (Younger and Chapman, 1989). In addition to these complications, these grafts have a staggering impact on healthcare costs. An estimated 1.6 million bone grafts are used annually in the U.S. for degenerative diseases, injuries, tumors, and infections, accounting for approximately $244 billion, with trauma and fracture management representing almost 40% of those costs (O'Keefe and Mao, 2011).

Furthermore, after 10 years of incorporation, as high as 60% of grafts may fail to integrate leading to nonunions and late graft fractures (Soucacos et al., 2006). In an effort to find alternative therapies to treat bony defects and the complications associated with them, bone tissue engineering (BTE) has grown in popularity and is now being studied as a possible alternative in fracture management. This review discusses the process by which bone formation occurs and the role BTE may play by examining its different components including: (1) stem cells, (2) biomaterials, (3) growth factors, and (4) mechanical stimulation. Finally, we review the role of stem cell therapies in bone formation to treat non-unions and avascular necrosis of the femoral head, with and without core decompression.

BONE FORMATION AND FRACTURE HEALING

Physiological Bone Formation

During development, skeletal and craniofacial structures form following two distinct processes, endochondral and intramembranous ossification, respectively, yet with some exceptions. Endochondral ossification is a process which leads to the formation of the axial and appendicular skeleton including the medial half of the clavicle and fragments of the scapula, through the formation of primary and secondary ossification centers. The cascade of endochondral bone formation begins with the differentiation of mesenchymal precursors into chondroblasts at the center of long bone condensations. The resulting chondrocytes in this avascular environment form the framework for subsequent bone growth by secreting a matrix consisting primarily of collagen II and proteoglycans. Chondrocytes stop to proliferate and differentiate into various intermediate phenotypes culminating in hypertrophic cells. These hypertrophic chondrocytes participate in the capillary invasion into the cartilage (White and Wallis, 2001), where osterix-expressing osteoblast precursors are brought as perivascular cells, following further differentiation into osteoblasts and ultimately to bone matrix-embedded osteocytes (Maes et al., 2010). Intramembranous ossification, on the other hand, is responsible for the development of flat bones, as well as the lateral half of the clavicle, without the necessity of forming a cartilaginous intermediate template. In this process, mesenchymal progenitors directly differentiate into osteogenic cells (Kanczler and Oreffo, 2008).

Physiological Fracture Healing Cascade

The process by which bones heal following fracture differs from natural bone formation; however, following fracture fixation, ossification may occur via endochondral and/or intramembranous pathways depending on the vascular supply and stability of the fracture fixation (Dimitriou et al., 2005). The initial stages of bone repair after fracture include the formation of a hematoma secondary to vascular damage to the injury site. Simultaneously, injury to soft tissues is coupled with recruitment of neutrophils to phagocytize microorganisms and tissue debris within the site of injury. This process is initiated via release of multiple cytokines which causes vasodilation and hyperemia at the site of injury and continues for several days during the inflammatory phase until fibrous tissue, and later bone and cartilage formation is initiated during the repair phase (Claes et al., 2012). Following the influx of neutrophils, macrophages entering the injury site continue phagocytizing debris and initiate the repair cascade by promoting an angiogenic response (Wu et al., 2013). Days following the initial injury, granulation tissue begins to replace the hematoma and necrotic tissue is removed via osteoclasts. Revascularization of the injured site not only re-establishes normoxic conditions and help removing

debris, but is also necessary for the recruitment of mesenchymal osteochondroprogenitor cells (Marsell and Einhorn, 2011). After 2–3 weeks post-injury, hematoma is replaced with extracellular matrix formed by fibroblasts and chondroblasts derived from the recruited progenitor cells, developing the soft callus that is characterized by decreased motion of soft tissues, pain, and swelling. During this process, intramembranous bone growth begins as progenitor cells are stimulated to directly form osteoblasts at the periosteum and endosteum, ultimately fueling the woven bone formed peripherally. The soft callus is slowly converted into hard callus over the course of 3–4 months as endochondral ossification is initiated within the fracture gap to allow for woven bone formation. This process begins peripherally and progresses centrally as woven bone fills the fracture gap and unites the two ends of the fracture. Following completion of the hard callus, the woven bone is then remodeled into lamellar bone over the course of months to years, which allows for restoration of the canal and its bony properties.

As mentioned before fracture healing is a complex biological process involving a number of phases namely the acute inflammatory response, the recruitment of Mesenchymal Stem cells (MSCs), the generation of cartilaginous/periosteal bony callus, revascularization, mineralization, and resorption of cartilaginous callus, and finally bone remodeling. Within this cascade the homing of resident or systemically mobilized MSCs to the fracture site is of outmost importance and mainly mediated by signaling cascades such as stromal cell-derived factor (SDF)1/CXC chemokine receptor (CXCR) 4 signaling axis (Shirley et al., 2005; Kitaori et al., 2009). Moreover, during bone resorption active TGF-β1 release from bone matrices induces the recruitment of MSCs to the fracture site through SMAD signaling pathway (Tang et al., 2009) whereas MSCs stimulate neo-vessel formation enhancing further the fracture healing cascade (Todeschi et al., 2015). In a delicate review, Herrmann et al. present strategies to enhance MSC homing to the fracture site including local delivery of homing factors, delivery of genes and genetic manipulation of transplanted cells (Herrmann et al., 2015). Overall, MSCs are coupling bone resorption and bone formation processes and their homing augments fracture healing by regulating bone remodeling and neo-angiogenesis phases.

BONE TISSUE ENGINEERING

The concept of BTE involves the integration of various concerting components: stem cells held together by a tri-dimensional biomaterial framework which provides the shape and initial mechanical strength, and molecular signals that induce differentiation of progenitor cells into the osteoblastic phenotype. The resulting construct can then be mechanically pre-conditioned *in vitro* to acclimate the growing structure to *in vivo* conditions, thus improving the functional coupling to the host bone (Petite et al., 2000). Here, we review the four fundamental components that take part in BTE, specifically: stem cells, biomaterials, growth factors/morphogens, and mechanical stimulation (**Figure 1**).

Stem Cells

Tissue-specific cells (e.g., osteoblasts) can be used as the cellular component of engineered bone implants. However, technical difficulties associated with their harvesting, expansion into meaningful numbers and phenotypic maintenance undermine the benefits of using primary cells. Consequently, various types of stem cells have been largely proposed as a viable and easy source of osteoblast progenitors during the creation of engineered bone implants.

Mesenchymal Stem Cells

Mesenchymal stem cells (MSCs) are multipotent adult stem cells that exhibit great differentiation potential into many different types of tissue lineages, including bone (osteoblasts), cartilage (chondrocytes), muscle (myocytes), and fat (adipocytes). Adult MSCs act as an inducible reserve force for tissue regeneration after injury (Caplan and Correa, 2011a,b), and therefore have been studied extensively for their therapeutic potential in fracture healing and bone regeneration. MSCs can be isolated from many different tissues including bone marrow, skeletal muscle, synovial membrane, and adipose tissue. There has consequently been substantial research regarding the osteogenic potential of MSCs obtained from different tissue sites.

Bone marrow-derived stem cells (BMSCs) are currently the most commonly utilized and researched source of adult mesenchymal stem cells due to their relatively easy harvesting, high proliferative capacity, and established regenerative potential (Baksh et al., 2007). Various animal models of clinically significant bone defects have shown that a cell-based therapy with allogenic BMSCs grafts is effective in regenerating bone, providing evidence for a viable alternative to autologous bone transplants (Jones et al., 2016). Studies have found BMSCs to be more efficient at differentiating into osteoblasts compared to adipose-derived MSCs (ADSCs) (Han et al., 2014). Cultured-expanded BMSCs have also been used in large cohort clinical trials showing no complications in long-term follow-up. In early clinical trials, autologous cultured BMSCs were seeded on ceramic biomaterials to treat large bone segmental defects. Local implantation at the defect site of 2.0×10^7 MSCs per ml resulted in complete fusion at 5–7 months post-surgery. Most importantly, 6–7 years follow-up showed that good integration was maintained with no further fractures (Marcacci et al., 2007). In a large clinical trial consisting of 64 patients, various long bone fractures have been treated by local injection of 3.0×10^7 osteogenically differentiated autologous BMSCs per ml mixed with fibrin. Two months follow-up, osteoblast injection showed no complications and significant fracture healing acceleration (Kim et al., 2009). Interestingly, Zhao et al. showed that early stage osteonecrosis of femoral head can be treated by local injection of 2.0×10^6 autologous BMSCs (Zhao et al., 2012). No complications were observed whereas 5 years follow-up only 2 of 53 BMSC-treated femoral heads progressed and underwent vascularized bone grafting. Upper limb non-unions have been also treated in 8 patients using $0.25–1.0 \times 10^6$ osteogenically differentiated autologous BMSCs per ml in fibrin clot constructs. Up to 6 years follow-up no complications were observed whereas all patients recovered limb function (Giannotti et al., 2013).

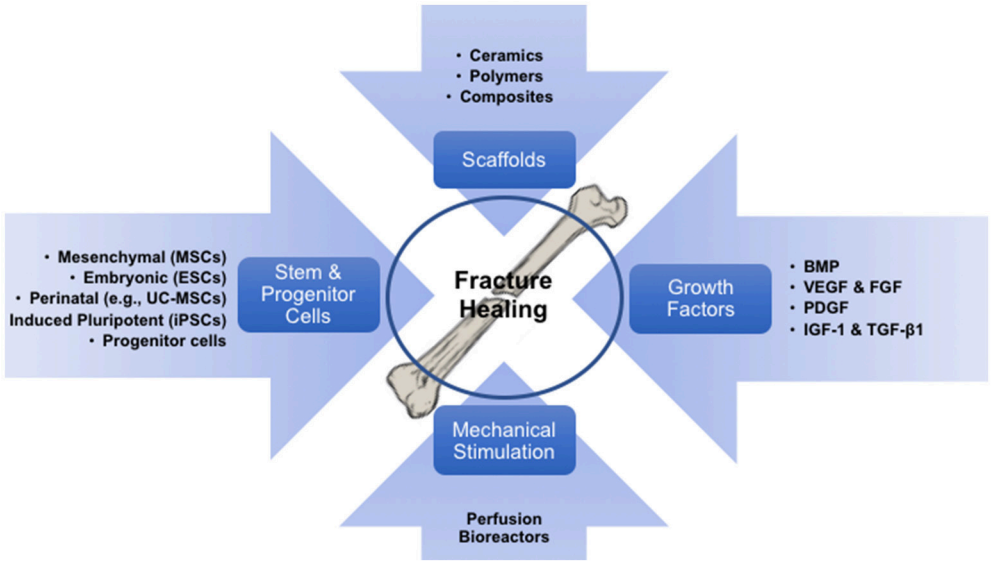

FIGURE 1 | Diagram illustrating the processes which fuels bone tissue engineering, involving its components (cells, biomaterials/scaffolds and growth factors), and the required exposure to mechanical environments to pre-conditioning the engineered implants.

Overall, the current body of literature provides support for the viability and utility of BMSCs in the clinical setting of bone defects. However, limitations regarding BMSCs cell yields during harvest, especially in older patients (Mareschi et al., 2006), the requirement of expansion when used alone (not as part of BMAC), the proven reduced regenerative ability with extended expansions (Both et al., 2011) and an increased patient morbidity and risk related to the increased number of surgical procedures all necessitate the need for further research into alternative MSCs harvest sites.

Minimal manipulation of BM is an alternative way to treat various bone defects by using non-cultured, heterogeneous, point-of-care BM aspirate concentrate (BMAC) or "viable allografts." Bone marrow concentrates are originating from density gradient centrifugation and their MSC content is usually evaluated based on *in vitro* CFU-F capacity (Woodell-May et al., 2015). In contrast, viable allografts are extracted from cadaveric cancellous bone after the selective removal of the immune cell component from the graft, while preserving the MSC fraction (Baboolal et al., 2014). On this basis, Hernigou et al. have used BMAC to treat various orthopedic complications including avascular necrosis, fracture nonunion and rotator cuff repair (reviewed in Jones et al., 2016). Interestingly, they looked at diabetic patients with ankle nonunion, comparing autologous BMSC-containing BMAC with standard bone iliac crest autograft. They found that 82.1% of BMAC-treated patients showed nonunion healing with minimal complications, while only 62.3% in autograft-treated patients showed nonunion healing with major complications observed (Hernigou et al., 2015).

Another readily available source of MSCs under investigation is adipose tissue as it can be easily isolated from plastic surgery or biopsies. The stromal vascular fraction (SVF) derived from adipose tissue is composed of heterogenous cell populations including adipose-derived stem cells (ADSCs), vascular endothelial cells, vascular smooth muscle cells, preadipocytes, and haematopoietic origin cells (Zuk et al., 2001, 2002; Daher S. R. et al., 2009). Although direct grafting of ADSCs has not demonstrated much success in healing critical sized bone defects (Peterson et al., 2005), there is increasing interest in applying osteoinductive factors to ADSCs in the hopes of enhancing osteogenesis. A study by Di Bella et al. demonstrated bone regeneration in rabbit critical-sized skull defects treated with autologous, osteogenically-induced ADSCs grafted onto fibronectin-coated polylactic acid biomaterials (Di Bella et al., 2008). Another study demonstrated repair of a cranial bone defect in canine models using osteogenically-induced ADSCs grafted onto a coral biomaterial (Cui et al., 2007). A recent paper by Fan et al. showed enhancing osteogenic differentiation of ADSCs through treatment with phenamil, a positive regulator of BMP signaling, along with suppression of the BMP antagonist noggin through gene manipulation (Fan et al., 2016). Interestingly, two clinical studies combining ADSCs with specialized biomaterials (Mesimäki et al., 2009) or autologous bone grafting (Lendeckel et al., 2004) indicated bone reconstruction *in vivo*. In a case study, Mesimaki et al. performed maxillary reconstruction using a microvascular flap construct generated by combining autologous ADSCs, β-tricalcium phosphate and bone morphogenetic protein-2. At 36 months follow-up the implants were osteo-integrated without any adverse effects and the defect was fully reconstructed (Mesimäki et al., 2009). In another case study, Lendeckel et al. treated severe calvarial defects using autologous ADSCs in fibrin glue combined with autologous cancellous bone graft. At 3 months follow-up, new bone formation and near complete calvarial continuity were observed (Lendeckel et al., 2004). Collectively,

these studies demonstrate novel methods of enhancing bone formation using ADSCs, providing promising evidence for the potential therapeutic role ADSCs could play in BTE. However, further studies are required to assess and verify the safe outcome of the clinical procedures using *in vitro* cultured ADSCs.

Several other tissues contain MSCs, including synovial membrane and skeletal muscle, all of them sharing a perivascular phenotype as pericytes (Caplan, 2008; Crisan et al., 2008). Synovial membrane-derived MSCs (SMSCs) are multipotential stromal cells that provide a good therapeutic alternative to tissue engineering protocols for focal cartilage injuries (Ogata et al., 2015; Kubosch et al., 2018). However, previous studies showed that MSCs derived from normal or OA synovium have the potential to differentiate toward osteogenesis *in vitro* (De Bari et al., 2001; Sakaguchi et al., 2005). Interestingly in a recent study, Hatakeyama et al. showed that SMSCs derived from knee joints have superior osteogenic and adipogenic capacity than SMSCs derived from hip joints (Hatakeyama et al., 2017). However, another study showed that SMSCs have inferior osteogenic capacity from periosteum-derived MSCs (De Bari et al., 2008). Therefore, further preclinical studies have to be performed to evaluate SMSCs' applicability in bone regeneration. On the other hand, current literature suggests that skeletal muscle-derived MSCs (SMDCs) are able to differentiate into several different types of mesenchymal lineages and show potential for *in vivo* bone regeneration when combined with osteoinductive biomaterials (Owston et al., 2016). Many previous studies have successfully demonstrated SMDCs' osteogenic potential *in vitro* (Jackson et al., 2011; Gao et al., 2013, 2014; Downey et al., 2015). However, Sakaguchi et al. indicated lower osteogenic potency for SMDCs compared to matched BM, synovium and periosteum MSCs (Sakaguchi et al., 2005). Similar results were obtained from Jackson et al. showing lower amounts and significantly lower ALP upregulation in SMDCs compared to BMSCs (Jackson et al., 2011). Recently, Miao et al. were able to induce a 24-fold increase in alkaline phosphatase activity (an early marker for early osteogenesis) in skeletal muscle discs cultured in osteogenic medium, with demonstrable calcified mineral deposits appearing on the superficial layers of the muscle discs after 8 weeks of osteoinduction. This study demonstrated the potential role of skeletal muscle in expedited BTE and provides support for further investigation of this tissue site for MSCs extraction (Miao et al., 2017).

One tissue site just recently being explored for musculoskeletal bone regeneration is dental pulp-derived stem cells (DPSCs). DPSCs were first isolated and characterized by Gronthos et al. within the dental pulp core and found to have similarities to BMSCs (Gronthos et al., 2000). DPSCs have the advantage of being relatively easy to harvest with very low rates of morbidity compared to BMSCs (Graziano et al., 2008). In addition, they can be safely cryopreserved and possess extensive differentiation ability into adipogenic, chondrogenic, and osteogenic lines (Graziano et al., 2008). Specifically, DPSCs have been successfully differentiated toward osteogenesis in both *in vitro* and *in vivo* settings indicating increased expression of bone-related markers and newly bone formation (Lindroos et al., 2008). In a pioneering study, d'Aquino et al. showed that DPSCs synergistically differentiate into osteoblasts and endotheliocytes *in vitro* whereas their transplantation in immunocompromised rat model result in the formation of bone tissue structure with an integral blood supply similar to adult human bone structure (d'Aquino et al., 2007). Kanafi et al. indicated the increased DPSC osteogenic capacity in alginate microsphere platform by observing enhanced mineralization and upregulated levels of osteo-related genes. Interestingly, the same group showed that DSPCs immobilization in alginate microspheres initiate their osteogenic differentiation without any medium induction (Kanafi et al., 2013). Recently, Akkouch et al. demonstrated successful extracellular mineralization of osteoblast-like cells derived from DPSCs seeded onto collagen-hydroxyapatite-poly(l-lactide-co-ϵ-caprolactone) matrix (Akkouch et al., 2014). In a rat calvarial critical-sized defect model, Maraldi et al. showed that DPSCs embedded in collagen sponges result in newly bone formation at 4 week and in almost complete bringing of the defect at 8 week of cranial implantation (Maraldi et al., 2013). Despite the potential of DPSCs in BTE, very few clinical trials have been reported so far and further research is needed to assess their applicability for clinical application. According to the previous studies, DPSCs' combination with specialized biomaterials can harness their increased osteogenic capacity for effective bone reconstruction clinical applications.

Finally, perinatal tissues such as umbilical cord blood (UCB), umbilical cord tissue (UC) and placenta have been considered as alternative sources of MSCs. Moreover, UC and UCB are readily available sources of allogeneic MSCs for therapeutic applications due to the worldwide existence of both public and private cord blood (CB) stem cell banks. In various preclinical models, CB-derived MSCs have successfully enhanced bone regeneration in conditions of non-systemic and systemic bone loss (Guillot et al., 2008; Jäger et al., 2009; Liu et al., 2009). Although, CB-derived MSCs are considered to circulate in preterm fetus blood, their isolation is not consistent (Secco et al., 2009). In contrast, MSCs can be easily isolated from various compartments of UC tissue including Wharton's Jelly, umbilical vein and umbilical artery areas (Kouroupis et al., 2013). Unlike ESCs, there are no reports of UC MSC teratoma formation capacity whereas studies showed that compared with BM MSCs and ESCs, UC MSCs show a gene expression profile similar to that of ESCs and faster self-renewal capacity from BM MSCs (Hsieh et al., 2010; Fong et al., 2011). In a previous study, Mennan et al. compared MSCs from all different UC tissue regions and indicated that Wharton's Jelly MSCs show the best osteogenic differentiation capacity (Mennan et al., 2013). *In vivo*, UC MSCs have been successfully used to treat critical-sized craniofacial defects in rat model (Chen et al., 2013). Chen et al. compared the regenerative capacity of UC MSCs and BM MSCs combined with RGD-modified macroporous calcium phosphate cements (CPC) in a critical-sized athymic rat pariental bone defect model. Moreover, 24 weeks post-implantation UC MSC-CPC and BM MSC-CPC groups showed similar high bone mineral density, new bone amount and vessel density (Chen et al., 2013). Importantly, in a clinical study allogeneic UC MSCs have been successfully used to treat infected nonunion of large bone segmental defect (Dilogo et al., 2017).

Overall, compared to ESCs, perinatal stem cells show crucial benefits for effective therapeutic applications. Perinatal cells are isolated from a formerly discarded tissue that has unlimited availability whereas their collection, preparation and application is not raising any ethical issues (Watson et al., 2015). Additionally, perinatal cells share stemness markers with both ESCs and MSCs, they are not tumorigenic and they are hypoimmunogenic (Kim et al., 2013).

Embryonic Stem Cells

First derived in 1998 from human blastocysts, pluripotent human embryonic stem cells (hESCs) maintain the developmental potential for all three embryonic germ layers even after months of *in vitro* proliferation (Thomson et al., 1998), thus demonstrating a potential source for tissue engineering-based therapies. Successful differentiation of hESCs into the osteogenic lineage has been demonstrated in numerous studies both *in vitro* and *in vivo* (Tang et al., 2012; Taiani et al., 2014). A number of researchers have developed ways to derive hMSCs from hESCs that are morphologically and phenotypically similar to BMSCs without the use of a feeder layer (Olivier et al., 2006), providing an alternative and plentiful source of reproducible and more embryonic-like hMSCs. There have also been multiple studies demonstrating that hESCs treated with osteogenic factors will undergo differentiation toward an osteogenic lineage. In fact, after osteogenic induction, hESCs have been shown to possess molecular and structural features resembling bone tissue by the formation of mineralized bone nodules *in vitro* (Woll et al., 2006; Arpornmaeklong et al., 2010). Although several advantages have been discovered concerning the use of hESCs, potential limitations exist regarding the use of pluripotent cells secondary to their unexpected differentiation, especially their link to teratoma formation (Cunningham et al., 2012).

Related to tissue engineering, one *in vitro* study was able to induce attachment, proliferation, and bone mineral synthesis of hESC-derived MSCs on a novel calcium phosphate cement-chitosan-RGD biomaterial (Chen et al., 2013). Kim et al. demonstrated significant *in vivo* bone formation in immunodeficient mice by subcutaneously seeding osteogenic cells derived from ESCs onto a three-dimensional porous poly (d,l-lactic-co-glycolic acid)/hydroxyapatite composite biomaterial (Kim et al., 2008). Both of these studies provide evidence in favor for the proliferative and osteogenic compatibility of ESCs with various engineered biomaterials and a secondary functional secretion of bone matrix. Interestingly, though osteogenic cultures of ESCs are generally derived from embryoid bodies, one study found that culturing hESCs without going through that stage led to a seven-fold increase in the number of osteogenic cells produced, as well as spontaneous bone nodule formation much sooner than cells differentiated from embryoid bodies directly (Karp et al., 2006).

Despite the excitement generated by their enormous potential for proliferation and differentiation, hESCs have several limitations that must be further investigated. Challenges concerning the complicated conditions required to culture hESCs, including the feasibility and viability of using feeder layers, the danger of teratoma formation and immune reactions, as well as the surrounding ethical, religious and moral debate, all pose challenges to the role of hESCs as active participants of regenerative medicine-based clinical protocols (Richards et al., 2003; de Miguel-Beriain, 2015).

Induced Pluripotent Stem Cells

Induced pluripotent stem cells (iPSCs), which are derived and reprogrammed directly from adult somatic cells (e.g., skin fibroblast), have the ability to give rise to every type of cell in the body and to propagate indefinitely. They were first developed by Takahashi and Yamanaka in 2006, through the lentiviral-based introduction of a defined set of reprogramming transcription factors (c-Myc, Oct3/4, Sox2, and Klf4), which induced a pluripotent state comparable to ESC. Consequently, iPSCs hold enormous potential for the entire field of regenerative medicine, as they possess a comparable pluripotency and differentiation potential as hESCs (Takahashi and Yamanaka, 2006), yet avoid immune rejection since they are derived from the patient's own cells (Im, 2015). In addition, given that the generation of iPSCs bypasses the use of human embryos, that provides a potential answer to the ethical dilemma surrounding ESCs.

iPSCs generated through embryoid bodies have been shown to generate MSC-like cells *in vitro* that have the potential of further differentiating into osteoblasts (Li et al., 2010), while also demonstrating osteogenic potential comparable to that of BMSCs *in vivo* (Ko et al., 2014). Additionally, animal studies have demonstrated that MSC-like cells cultured from iPSCs have the capacity to form mature mineralized material that is histologically similar to bone (Hynes et al., 2013). In addition to a low efficiency during the generation of iPSCs, the potential formation of teratomas is of clinical concern. Levi et al. demonstrated the *in vivo* differentiation and *de novo* bone formation of iPSCs without the formation of a teratoma when grafted onto a hydroxyapatite-coated, BMP-2-releasing poly-L-lactic acid biomaterial (Levi et al., 2012). Similarly, Kang et al. demonstrated the first direct differentiation of human iPSCs (hiPSCs) into functional osteoblasts that subsequently went on to deposit calcified bone matrix. By using adenosine to induce osteogenesis of hiPSCs, they were able to demonstrate that the hiPSC-derived osteoblasts participated in the healing of critical sized bone defects without the formation of a teratoma (Kang et al., 2016). In a recent pioneering study, Kouroupis et al. generated a bioartificial ACL graft *ex vivo* by simultaneously differentiating MSC-like cells cultured from iPSCs toward bone and ligament at the ends and central part of a biomaterial using either BMP-2/FGF-2 or TGF-β/FGF-2 growth factor combinations, respectively. ACL graft *in vivo* implantation in a swine ACL injury model resulted in superior morphological and biochemical ACL tissue formation for both the bony and ligamentous parts of the reconstructed tissue (Kouroupis et al., 2016). Though the area of iPSC research is still new, taken together, these findings indicate the exciting promise iPSCs hold for the future of osteogenic tissue engineering. Nevertheless, further clinical investigation focusing not only on efficacy (e.g., osteogenic potential) but also safety (e.g., teratoma formation) becomes paramount before accepting iPSCs as a viable therapeutic option.

Finally, iPSC-based therapy brings additional challenges such as the technical and logistical issues related with their generation. Tissue sourcing, manufacturing protocols, required expansion, systematic testing and quality control, validation, and storage constitute technical aspects that impact the costs associated the generation of these "off the shelf" products, delaying their translation into potential clinical therapies. In order to advance the field toward standardization, as product reproducibility need to meet specific standards, a number of consortiums and forums (e.g., CCRM, CIRM, HiPSCi, STemBANCC, ISCF, and ISCBI) have been established to support with best practices to generate and supply hiPSCs lines for basic and potential clinical research. Consequently, manufacturers have initiated projects aiming at generating iPSC products based on strict cGMP-compliant conditions to overcome some of these challenges, involving best practices for cell culture, documentation and quality control (Stacey et al., 2013).

Progenitor Cells

Endochondral BTE using chondrocytes and chondroprogenitors has been recently reported by various groups. Two independent studies showed that both human (Narcisi et al., 2011) and porcine (Jeong Claire et al., 2012) articular chondrocytes can be induced toward endochondral ossification and produce a hypertrophic phenotype upon induction with TGFβ-1 and BMP-2, respectively. Although, *in vitro* TGFβ-1-expanded cells showed strong mineralisation and impaired p38 kinase activity which is related to chondrocyte differentiation, their *in vivo* ectopic implantation with ceramic biomaterial failed to reach overt ossification (Narcisi et al., 2011). Also, Jeong et al. showed that seeded chondrocytes on BMP-2-loaded polycaprolactone biomaterials when subcutaneously implanted *in vivo* can result in bone formation but only at the periphery of the biomaterial (Jeong Claire et al., 2012). Therefore, the use of mature chondrocytes for BTE may be limited due to their mature phenotype, reduced *in vitro* expansion and the risk of arthritic development. In contrast, others showed that chondrocyte-like progenitors possessing a transient phenotype *in vitro*, can be effectively induced toward endochondral bone formation in *in vivo* settings (Oliveira et al., 2008; Weiss et al., 2012). On this basis, studies showed that MSCs induced for 21 days toward chondrogenesis *in vitro*, with the common TGF-β based chondrogenic cocktail, are gradually obtaining a transient hypertrophic phenotype that can result in subsequent bone formation upon implantation *in vivo* (Vinardell et al., 2012; Giavaresi et al., 2013). Interestingly, extended induction for 7 additional days with β-glycerol-phosphate (Wang et al., 2011) or for 14 additional days with β-glycerol-phosphate and thyroxine (Scotti et al., 2013) result in increased bone formation *in vivo*. Further, examples of tissue-engineered cartilage constructs that can result through endochondral progression to bone formation *in vivo* are reviewed in Thompson Emmet et al. (2014). However, using mature metabolically active hypertrophic cells may not be advantageous as they show limited bioactive lifespan compare to the high molecular plasticity of MSCs in activating pathways related to endochondral bone formation process.

Biomaterials

It is now nearly 50 years since Professor Hench in 1969 introduced the term "bioactivity" in biomaterials field, which is the characteristic chemical bonding between biomaterials and cells (Hench, 2006). Specifically, the function of the biomaterial in BTE is to serve as a tri-dimensional framework for the stem cells to attach, grow and differentiate. There are several components of the biomaterial required for successful incorporation and functionality, including: (1) biocompatibility: incorporation into host tissues without eliciting an immune response; (2) biodegradability: as bone replaces the biomaterial, it provides supportive mechanical properties to withstand loading forces and uniformly distribute stresses; (3) proper surface properties and porosity: to influence cellular proliferation and differentiation; and (4) osteoinductive and osteoconductive properties: to recruit osteoprogenitors to the defect region and provide a controlled release of differentiation cues (Liu et al., 2013). Here we focus on three categories of biomaterials commonly used: ceramics, biodegradable polymers, and composite biomaterials. The applicability of various biomaterials combined with MSCs for bone segmental defects treatment in preclinical settings is presented in **Table 1**.

Ceramics

Known for their effective biocompatibility, ceramic biomaterials are used more commonly in compressive loading conditions as they have very low wear rates due to their high hardness values. However, ceramics are also highly brittle. Because of their properties, ceramic-based biomaterials are commonly used on articulating surfaces, with calcium phosphate (CaP) and tricalcium phosphate being the most common.

In one study, dense calcium sulfate (D-CaS), ultraporous tricalcium phosphate (beta-TCP) and porous silicated calcium phosphate (Si-CaP) biomaterials were used in rabbits. They observed rapid resorption of D-CaS, which left the defect site empty prior to new bone formation. High rates of dissolution have been found to cause biological reactions by inducing inflammation (Lu et al., 2004), as was noted in the D-CaS group. Although both the Si-CaP and beta-TCP biomaterials support early bone apposition, beta-TCP produced an inflammatory response which impaired and reversed bone apposition. Ultimately, Si-CaP biomaterials were found to allow for stable bone apposition with new bone and resorption of the biomaterial with local loads, facilitating production of functional bone at the defect site (Hing et al., 2007). Although beta-TCP impaired bone apposition, other studies have shown it to be an effective biomaterial. Kondo et al. demonstrated purified beta-tricalcium phosphate has the potential for good biocompatibility as bone formation and resorption starts at an early stage after implantation in rat femoral condyles. They noted new bone formation after day 7 and bone marrow within the implanted region by day 28 (Kondo et al., 2005).

Although CaP-based biomaterials have been demonstrated to contain important properties required for BTE such as bioactivity and biocompatibility, their use is limited by their stiffness and low osteoinductivity. Studies have shown this can be resolved with addition of recombinant human bone

TABLE 1 | Preclinical studies using MSCs and biomaterials for the treatment of bone segmental defects.

References	Cells	Biomaterials	Animal Model	Outcome
Bruder et al. (1998)	Canine BMSCs (7.5×10^6/ml)	Three groups used: 1) HA-TCP-BMSCs, 2) HA-TCP, 3) Untreated	Segmental femoral bone defect (2.1 cm) in canine model	- At 16 weeks, radiographic union was established rapidly at the interface between the host bone and the HA-TCP-BMSCs implants only - Both woven and lamellar bone had filled the pores of the HA-TCP-BMSCs implants
Kon et al. (2000)	Ovine BMSCs (2.5×10^5/ml)	Two groups used: 1) HA-BMSCs 2) HA	Segmental tibial bone defect (3.5 cm) in ovine model	- At 2 months, extensive bone formation in HA-BMSCs implants within the macropore space and around the implant - Stiffness higher in HA-BMSCs implant/bone complex compared to HA control group
Arinzeh et al. (2003)	Canine BMSCs (7.5×10^6/ml)	Three groups used: 1) HA-TCP-allogeneic BMSCs 2) HA-TCP 3) Untreated	Segmental femoral bone defect (2.1 cm) in canine model	- No lymphocytic infiltration occurred and no antibodies against allogeneic cells were detected - At 16 weeks, new bone had formed throughout the HA-TCP-allogeneic BMSCs implant
Bensaïd et al. (2005)	Ovine BMSCs (1×10^7/ml)	Four groups used: 1) Coral HA-BMSCs 2) Coral HA 3) Autologous bone graft 4) Untreated	Segmental metatarsus bone defect (2.5 cm) in ovine model	- At 4 months, coral HA-BMSCs implants show the same amount of newly formed bone - with autologous bone and at 14 months are completely replaced by newly formed, structurally competent bone
Viateau et al. (2007)	Ovine BMSCs ($8.28 \pm 1.32 \times 10^6$/implant)	Three groups used: 1) Coral-BMSCs 2) Coral 3) Untreated	Segmental metatarsus bone defect (2.5 cm) in ovine model	- At 6 months, radiographic, histological, and computed tomographic tests performed showed that the osteogenic abilities of the coral-BMSCs implants were significantly greater than those of coral scaffold alone
Zhu et al. (2006)	Caprine BMSCs (20×10^6/ml)	Two groups used: 1) Coral-BMSCs 2) Coral	Segmental femoral bone defect (2.5 cm) in caprine model	- At 4 months bony union was observed in coral-BMSCs implant and engineered bone was further remodeled into newly formed cortexed bone at 8 months
Mastrogiacomo et al. (2007)	Ovine BMSCs ($0.5–1.0 \times 10^8$/ml)	Two groups used: 1) Si-TCP-BMSCs 2) Si-TCP	Segmental tibial bone defect (4 cm) in ovine model	- At 4 months, 4 out of 5 animals implanted with Si-TCP-BMSCs implants, a progressive new bone formation, from the osteotomy defect edge toward the implant mid zone, was observed - Neither bone formation nor scaffold resorption was observed in Si-TCP group
Liu et al. (2008)	Caprine BMSCs (2×10^7/ml)	Three groups used: 1) β-TCP-BMSCs 2) β-TCP 3) Untreated	Segmental tibial bone defect (2.6 cm) in caprine model	- At 32 weeks, bony union can be observed at β-TCP-BMSCs group by gross view, X-ray and micro-computed tomography detection, and histological observation - In β-TCP-BMSCs group the implants are almost completely replaced by tissue-engineered bone whereas bone mineral density is significantly higher than in β-TCP group
Giannoni et al. (2008)	Ovine BMSCs ($70–100 \times 10^6$)	Three groups used: 1) HA-Si-TCP-BMSCs 2) HA-Si-TCP 3) Autologous bone graft	Segmental tibial bone defect (4.5 cm) in ovine model	- At 20–24 weeks, autologous bone graft group performed best - as assessed radiologically - In other groups very limited healing was detected whereas a partial bone deposition occurred at the periphery of the bony stumps only in HA-Si-TCP-BMSCs group

(Continued)

TABLE 1 | Continued

References	Cells	Biomaterials	Animal Model	Outcome
Nair et al. (2008)	Caprine BMSCs (1×10^5/cm2)	Two groups used: 1) HASi + BMSCs 2) HASi	Segmental femoral bone defect (2 cm) in caprine model	- At 4 months, both HASi + BMSCs and HASi implants showed good osteointegration and osteoconduction - The superior performance of HASi + BMSCs implant was evident by the lamellar bone organization of newly formed bone throughout the defect together with the degradation of the material
Niemeyer et al. (2010)	Human and Ovine BMSCs (2×10^7/ml)	Three groups used: 1) HA-COL-human BMSCs 2) HA-COL-ovine BMSCs (allogeneic) 3) Untreated	Segmental tibial bone defect (3 cm) in ovine model	- At 26 weeks, radiology and histology demonstrated significantly better bone formation in HA-COL-ovine BMSCs group compared to HA-COL-human BMSCs and untreated groups
Nair et al. (2009)	Caprine BMSCs (1×10^5 cm2)	Three groups used: 1) HASi + BMSCs 2) HASi + BMSCs + PRP 3) HASi	Segmental femoral bone defect (2 cm) in caprine model	- At 2 months, in HASi + BMSCs and HASi + BMSCs + PRP groups 60–70% of the mid region of the defect was occupied by woven bone, in line with material degradation
Zhu et al. (2010)	Caprine BMSCs (5×10^7/ml)	Two groups used: 1) Coral-BMSCs 2) Coral-AdBMP-7-BMSCs	Segmental femoral bone defect (2.5 cm) in caprine model	- Much callus was found in the coral-AdBMP-7- BMSCs group, and nails were taken off after 3 months of implantation, indicating that regenerated bone in the defect can be remodeled by load-bearing, whereas this happened after 6 months in the coral-BMSCs group
Cai et al. (2011)	Canine BMSCs (20×10^6/ml)	Four groups used: 1) Coral HA-BMSCs 2) Coral HA-BMSCs (vascularized) 3) Coral HA (vascularized) 4) Coral HA	Segmental fibula bone defect (1 cm) in canine model	- At 3 months, vascularization improved 2-fold bone formation compared to non-vascular group
Reichert et al. (2012)	Ovine BMSCs (35×10^6 cells/250 μl) BMP-7 (3.5 mg/implant)	Five groups used: 1) mPCL-TCP-BMSCs + PRP 2) mPCL-TCP-BMP-7 3) mPCL-TCP 4) Autologous bone graft 5) Untreated	Segmental tibial bone defect (3 cm) in ovine model	- At 12 months, biomechanical analysis and microcomputed tomography imaging showed significantly greater bone formation and superior strength for the biomaterial loaded with rhBMP-7 compared to the autograft
Manassero et al. (2013)	Ovine BMSCs ($7.5 \pm 1.2 \times 10^6$/implant)	Two groups used: 1) Coral-BMSCs 2) Coral	Segmental metatarsus bone defect (2.5 cm) in ovine model	- At 6 months, coral-BMSCs implants showed 2-fold increase in bone formation compared to coral alone
Berner et al. (2013)	Ovine BMSCs (35×10^6/500 μl)	Four groups used: 1) mPCL-TCP-BMSCs (autologous) 2) mPCL-TCP-BMSCs (allogeneic) 3) mPCL-TCP 4) Autologous bone graft	Segmental tibial bone defect (3 cm) in ovine model	- At 12 weeks radiology, biomechanical testing and histology revealed no significant differences in bone formation between the autologous and allogenic mPCL-TCP-BMSCs groups - Both cell groups showed more bone formation than the biomaterial alone
Fan et al. (2014)	Non-human primate BMSCs (5×10^6/implant)	Five groups used: 1) TCP-β-BMSCs 2) TCP-β-BMSCs-fascia flap 3) TCP-β-BMSCs-saphenous vascular bundle 4) TCP-β 5) Untreated	Segmental tibial bone defect (2 cm) in non-human primate model	- At 4, 8, and 12 weeks, the TCP-β-BMSCs-saphenous vascular bundle group could augment new bone formation and capillary vessel in-growth. It had significantly higher values of vascularization and radiographic grading score compared with other groups.

(Continued)

TABLE 1 | Continued

References	Cells	Biomaterials	Animal Model	Outcome
Yoon et al. (2015)	Canine ADMSCs (1×10^6/50 μl)	Five groups used: 1) ASA-ADMSCs 2) ASA-β-TCP-ADMSCs 3) ASA-β-TCP 4) ASA 5) Untreated	Segmental ulna bone defect (1.5 cm) in canine model	- At 16 weeks, histomorphometric analysis showed that ASA biomaterials with ADMSCs had significantly greater new bone formation than other groups
Berner et al. (2015)	Ovine BMSCs (100×10^6)	Three groups used: 1) PCL-HA-allogeneic BMSCs 2) PCL-HA 3) Autologous bone graft	Segmental tibial bone defect (3 cm) in ovine model	- Minimally invasive percutaneous injection of allogeneic BMSCs into biodegradable composite biomaterials 4 weeks after the defect surgery led to significantly improved bone regeneration compared with preseeded biomaterial/cell and biomaterial-only groups
Masaoka et al. (2016)	Non-human primate BMSCs ($1.3–4.1 \times 10^6$/ml)	Two groups used: 1) β-TCP-BMSCs 2) β-TCP	Segmental femoral bone defect (5 cm) in non-human primate model	- At 8–15 months, five of the seven animals treated with β-TCP-BMSCs implant showed successful bone regeneration
Smith et al. (2017)	Ovine BMSCs (1×10^7/implant)	Three groups used: 1) PLLA-PCL-BMSCs 2) PLLA-PCL 3) Untreated	Segmental tibial bone defect (3.5 cm) in ovine model	- At 12 weeks, both PLLA-PCL-BMSCs and PLLA-PCL groups showed enhanced quantitative bone regeneration - Significant bone regeneration was evident only in the PLLA-PCL-BMSCs group whereas complete defect bridging was not achieved in any group
Berner et al. (2017)	Ovine MPCs, mOB, tOB (35×10^6 cells)	Four groups used: 1) mPCL-TCP-PRP 2) mPCL-TCP-allogenic-MPC 3) mPCL-TCP-allogenic-mOB 4) mPCL-TCP-allogenic-tOB	Segmental tibial bone defect (3 cm) in ovine model	- At 6 months, mPCL-TCP-allogenic-MPC group showed a trend toward a better outcome in biomechanical testing and the mean values of newly formed bone

BMSCs, bone marrow tissue-derived MSCs; ADMSCs, adipose tissue-derived MSCs; MPCs, mesenchymal progenitor cells; tOBs, axial skeleton osteoblasts; mOBs, orofacial skeleton osteoblasts; PRP, platelet rich plasma; HA, hydroxyapatite; HA-TCP, hydroxyapatite-tricalcium phosphate; HA-COL, hydroxyapatite-collagen; Coral HA, coral hydroxyapatite; HASi, triphasic ceramic-coated hydroxyapatite; Si-TCP, silicon stabilized tricalcium phosphate; mPCL-TCP, medical grade polycaprolactone-tricalcium phosphate; ASA, autologous serum-derived albumin; PCL-HA, polycaprolactone-hydroxyapatite; PLLA-PCL, poly(L-lactic acid)-poly(ε-caprolactone) ; AdBMP-7, adenovirus mediated bone morphogenetic protein 7.

morphogenetic proteins (rhBMPs) which allow for the potential of bone formation similar to that of autografts, as well as excellent stiffness (Sun and Yang, 2015). CaP-based biomaterials have proven to be an effective ceramic biomaterial –however, porous hydroxyapatite (HA) scaffolds have also shown promising results in improving critical sized long bone defects. In a study by Maracci et al. four patients with large diaphyseal defects were treated with porous HA biomaterials seeded with bone marrow stroma. They reported complete fusion between the implant and host bone between 5 and 7 months post-surgery and good integration of implants after long-term follow-up (Marcacci et al., 2007). As extensively reviewed by Habraken et al. (2016) osteoinduction has been demonstrated in preclinical settings for various CaP phases including HA, TCP, biphasic calcium phosphate (BCP), dicalcium phosphate dehydrate (DCPD), dicalcium phosphate (DCPA), carbonated apatite (CA), and osteocalcium phosphate (OCP), and in various formats including cements, coatings, sintered ceramics, and coral-derived ceramics. Material properties essential for rendering a ceramic osteoinductive are its chemical composition, its macrostructure and its surface micro- and nanostructural properties. It is well accepted that enhanced CaP osteoinduction can be achieved by simultaneously increasing *in vivo* material's degradability while keeping relatively stable material's surface for effective ceramic-induced *de novo* bone formation. An important method to enhance the CaP osteoinductivity is through the incorporation of bioinorganic compounds such as strontium ranelate and fluoride, which are usually found in trace amounts in human body but result in accelerated bone formation and improve bone bonding in orthopedic, craniomaxillofacial, and dental applications (Habibovic and Barralet, 2011).

Overall, ceramic biomaterials show good biocompatibility and bioactivity but they demonstrate low toughness and insufficient strength. This is a major disadvantage and as a result, ceramic biomaterials can be used in non- or low-loading orthopedic applications. Nowadays, biomaterial engineering efforts are focused on improving their properties by the use of nanoscale second phase reinforcing (including nanoparticles, nanotubes,

and nanosheets), the formation of surface coatings (such as polymers and glasses) (Hee Ay et al., 2014), and the use of self-toughening methods (via microstructure design) (Li et al., 2012).

Polymers

Biodegradable polymer biomaterials, including polylactides (PLLA, PDLA), collagen, polyglycolide (PGA), and poly(ε-caprolactone) (PCL), are best known for their capacity to support tissue growth and remodeling prior to being resorbed. These biomaterials are hydrolytically stable as they contain ester bonds in their backbone, specifically short aliphatic chains, which allows them to be used as degradable biomedical constructs (Valappil et al., 2006). Polymers may be natural or synthetic, with each type providing unique properties regarding their biodegradable rates, consistency, predictability, and their ability to interact with host tissues.

Poly (lactic acid) (PLA) has been proven to be an effective polymer as studies have shown it can induce mature osteogenic phenotypes after 4 weeks of cell seeding. PLA-based biomaterials have shown adhesion and growth of human osteoprogenitors cells ultimately leading to bone healing (Yang et al., 2001). In contrast to PLA, PGA polymers have a longer chain synthesis and are not soluble in most organic solvents—however, they are also vulnerable in load bearing areas as they also contain poor mechanical properties and unfavorable surfaces for cell attachment and proliferation product (Kinoshita et al., 2008), limiting its use as a biomaterial. Further research should be done as some studies have shown the potential to improve stem cell adherence by adding bioactive materials. PLGA is another polymer that has been used to generate biomaterials given the weakening integrity of the polymer as bone healing progresses, which allows a flexible adaptation to bone growth (Habal and Pietrzak, 1999). Its use in BTE has been supported when combined with BMSCs, an osteoinductive medium, and specific bioreactor conditions (Koc et al., 2008).

Given its high permeability and thermal stability secondary to its aliphatic, semi-crystalline properties, PCL is the most heavily researched polymer (Woodruff and Hutmacher, 2010). PCL is a favorable biomaterial for BTE, especially in long-term implantable systems as it is known to maintain its mechanical properties for up to 6 months and then gradually degrade over a 2 year period (Calvert et al., 2000). In addition, PCL is FDA approved, easy to manufacture and manipulate for different anatomical locations, and is highly biocompatible, making it a favorable source for biomaterial design. Overall, biodegradable polymer biomaterials are widely used but they show some limitations in orthopedic applications which include being prone to deformation, weak mechanical properties, and failure to integrate strongly with bone as they exhibit different elastic properties to that of both cancellous and cortical bone (Asti and Gioglio, 2014). Specifically, natural polymers show poor thermal stability, processability and degradation control whereas synthetic polymers show poor cell adhesion as they lack bioactivity (Gautam et al., 2013; Asti and Gioglio, 2014). Most importantly, the degradation products of synthetic polymers are mildly acidic causing local reduction of cell growth and non-specific inflammation (Kim et al., 2007; Song et al., 2011). To address these issues, researchers have focused on improving polymer degradation rates, bioactivity and mechanical properties. Similar to ceramic biomaterials, polymers can be reinforced by nanoscale second phase method (Guo et al., 2009). Studies showed that polymer properties can be improved by the formation of composites with bioactive ceramics and/or other polymers (see Composites section) (Choi et al., 2010; Meseguer Olmo et al., 2012). Therefore, degradation rates can be controlled by adjusting the ratios of biomaterials used to generate composites (Wu et al., 2012) whereas biomaterials' acidic degradation products can be neutralized by adding alkaline materials to polymers (Westhauser et al., 2016).

Composites

Composite biomaterials consist of polymers combined with ceramics, merging the benefits of both classes while limiting their short-comings. They possess suitable properties for BTE such as mechanical toughness, improved biocompatibility, decreased creep-induced failure, load-bearing capabilities, host-implant interactions, and bioactivity (Niemeyer et al., 2004). By adding metals to these composites, additional benefits can be seen in bone interactions, strength, and osteogenesis. Resorbable polymer composites have been successfully used in oral and maxillofacial surgery (Schimming, 2004) however resorbable polymers degrade when expose to body fluid and therefore show poor mechanical properties for load-bearing orthopedic applications. Non-resorbable additives such as polyamide fibers can significantly enhance polymer properties (Mehboob and Chang, 2014) but the need for a second surgery to remove them lead to the use of completely resorbable and/or bioceramics as reinforcement for the composites. Resorbable polymeric composites can be generated by combining HA/PLA, TCP/PLGA, and phosphate glass fiber/PLA whereas their degradation rates can be controlled by the addition of fibers, coatings and various coupling agents (Parsons et al., 2009; Haque et al., 2010; Ahmed et al., 2011; Harper et al., 2012). Moreover, Fielding et al. found increased average density, faster cell proliferation, and a 2.5 fold increase in compressive strength of tricalcium phosphate by incorporating silica (SiO(2)) (0.5 wt%) and zinc oxide (ZnO) (0.25 wt%) dopants into the biomaterial (Fielding et al., 2012). Other study have also found increased compressive strength of almost 2 MPa in a zirconia (ZrO2)/β-tricalcium phosphate (β-TCP) composites. Interestingly, they noted a suitable environment for osteoblast survival and bone regeneration *in vitro* when the composite was used (Alizadeh et al., 2016).

Other studies using CaP biomaterials modified with PEGylated poly (glycerol sebacate) (PEGS) polymers also demonstrate optimization of their mechanical characteristics and bioactivity in BTE applications (Ma et al., 2016). Repair of bone defects can be effective when implementing chitosan-β-tricalcium phosphate composite, as a study by Yang et al. demonstrated effective osteogenesis and vascularization after MSCs injection (Yang et al., 2015). The ratio of composite biomaterials also plays a role in its effectiveness as was demonstrated in a study comparing porous composite

biomaterials of PGA/beta-TCP, in a 1:1 and 1:3 weight ratio, for repair of critical defects in rat femoral medial-epicondyles. They noted that by 90 days, bone replacement was almost complete and appeared healthy. Bone mineral density and biodegradation of the repair was highest amongst the PGA/beta-TCP groups, with the 1:3 biomaterial ratio showcasing the highest results (Cao and Kuboyama, 2010).

While different ratios and combinations of composites have been investigated, other studies have examined techniques to improve functional performance of poly(ε-caprolactone)/tri-calcium phosphate (PCL/TCP) biomaterials by coating them with carbonated hydroxyapatite (CHA)-gelatin composite via biomimetic co-precipitation. They found an increased proliferation rate of cultured porcine BMSCs of about 2.3 times that of non-coated CHA-coated composites. In addition, the CHA-gelatin composite coated PCL/TCP biomaterials stimulated BMSCs osteogenic differentiation the most (Arafat et al., 2011). Overall, results of composite biomaterials show promising results as frameworks for BTE.

Growth Factors

Physiologically growth factors are usually stored in bone ECM, actively released after injury and play crucial role in bone repair with bone morphogenetic proteins (BMPs), vascular endothelial growth factor (VEGF), fibroblast growth factor (FGF), platelet derived growth factor (PDGF), transforming growth factor-β1 (TGF-β1), and insulin-like growth factor 1 (IGF-1) being the major regulators of bone remodeling cascade. The therapeutic use of recombinant growth factors is based on the hypothesis that through appropriate signaling they induce and/or accelerate the bone healing process. However, only a number of recombinant growth factors (such as BMP-2 and BMP-7) have achieved commercial success due to limitations related to their safety, cost-effectiveness, low stability, short half-life and rapid deactivation of their actions in *in vivo* settings. To optimize recombinant growth factor delivery *in vivo* three different strategies can be used physical immobilization, non-selective covalent immobilization through growth factor's functional residues, and bioaffinity immobilization. Lately, biocompatible nanoparticles combined with protein immobilization strategies have been shown to augment the delivery and effectiveness of growth factors, and to mimic the physiological bone healing cascade (Wang et al., 2017).

BMP

Discovered more than 50 years ago as an inducting agent for *de novo* bone formation (Urist, 1965), bone morphogenetic proteins (BMPs) are today recognized as the most efficient growth factor family in aiding the healing of large bone defects. Two of its members constitute the only osteoinductive growth factors approved by the FDA for clinical use, commercialized as INFUSE (rhBMP-2, Medtronic) and OP-1 Putty (rhBMP-7/OP-1, Stryker) (Cahill et al., 2015). To date, over 20 BMPs have been identified, and several have been shown to play important roles in the induction of osteogenesis, including BMP-2, 4, 5, 6, and 7 (Ferreira et al., 2013; Fischerauer et al., 2013). Clinically, BMPs have been utilized to heal open tibial fractures and nonunions (Kanakaris et al., 2008), form new bone in the disc spaces for spinal fusion procedures (Brandoff et al., 2008), and induce the formation of new bone in dental procedures (Lan et al., 2007). However, only BMP-2 has been shown to be absolutely essential to the osteogenic process, while BMP-2 and BMP-7 are approved for clinical use in the healing of major bone defects (Chen et al., 2012).

BMP-7, also termed osteogenic protein-1 (OP-1), has been identified as an osteogenic factor in the repair of critical sized long bone defects and craniofacial bones (White et al., 2007). Early studies have shown that treatment with BMP-7-infused collagen sponges are equally efficacious in healing fracture nonunions as autografts and demineralized bone matrix (Geesink et al., 1999). A randomized controlled trial of 120 patients with long bone nonunions treated with BMP-7/collagen constructs demonstrated a significant increase in union rate (86.7%) compared with an alternative therapy (i.e., PRP−68.3%) (Calori et al., 2008). In parallel, there have been numerous long-term observational studies demonstrating the safety and efficacy of rhBMP-7 in the treatment of long bone nonunions (Kanakaris et al., 2008).

Murine models have shown that BMP-2 is not an essential part of prenatal limb formation, however, it is absolutely necessary during postnatal fracture healing. Successful bone engraftment depends upon BMP-2 as a stimulus for the repair process, and a loss in BMP-2 in the host or donor periosteal cells results in a failure of callus formation or subsequent bone healing (Wang et al., 2011). A 2002 randomized control study looking at 450 patients with open tibial fracture demonstrated that patients treated with collagen sponges loaded with rhBMP-2 had significantly better fracture healing post-operatively compared to control patients (Govender et al., 2002). A large body of literature exists documenting the successful use of BMP-2 in osteoinduction and bone healing, but there still remains concern regarding the large dose of BMP required for treatment, modes of delivery, heterotopic ossification, and the possibility of an increased risk of cancer (Cahill et al., 2015). In addition to these concerns, major complications have been related to the "off-labeled" use of INFUSE (BMP-2) in spine surgery, most notably being marked dysphagia, seromas and hematomas, swelling, and/or the need for intubation/tracheostomy (Epstein, 2013).

VEGF and FGF

Bone is a highly vascularized tissue that requires oxygen, minerals, growth factors, and other signaling factors to survive. When a fracture disrupts the blood supply, growth factors are required to re-vascularize the damaged area to bring osteoprogenitor pericytes and promote the formation of new bone (Di Bella et al., 2008). Vascular endothelial growth factor (VEGF) is a fundamental mediator of angiogenesis in fracture healing. The growth of the new blood vessels allows for the delivery of mesenchymal progenitors which differentiate into osteoblasts (Maes et al., 2010; Chen et al., 2012), a process that is further stimulated by the chemotactic effect of VEGF on MSCs (Mishima and Lotz, 2008). VEGF has also been found to induce differentiation of progenitor cells into osteoblasts through the secretion of osteotropic growth factors from endothelial cells

directly induced by VEGF (Wang et al., 1997). Early studies have demonstrated that blockade of VEGF in mice and primates by monoclonal antibodies suppresses nearly all blood vessel invasion in the area, consequently impairing trabecular bone formation (Ryan et al., 1999), while stopping anti-VEGF treatment results in the return of normal bone growth (Ferrara et al., 2003). Street *et al.* found that mice with neutralized VEGF receptors had decreased angiogenesis and bone formation in femoral fractures (impaired endochondral ossification), as well as significantly inhibited healing of tibial cortical bone defects (compromised intramembranous ossification), demonstrating how VEGF is essential to bone healing through chondrocyte intermediate and direct repair mechanisms (Street et al., 2002). Additionally, administration of VEGF through PLGA biomaterial has been shown to significantly increase neovascularization and bone regeneration in irradiated osseous defects in rats. Taken together, these studies further demonstrate the necessary role VEGF plays in the fracture healing cascade.

Fibroblast growth factor, specifically FGF-2, is another signaling peptide implicated in angiogenesis and bone regeneration. FGF-2 administered via collagen sponge to rat calvarial critical-size bone defects has been shown to promote greater osteoblast differentiation as well as higher blood vessel and bone volume generation in a concentration-dependent manner (Kigami et al., 2013). Additionally, there has been some suggestion that FGF could play a role in up regulating VEGF, helping to augment the bone healing process through cross-talk with other growth factors (Rabie and Lu, 2004).

PDGF

Platelet derived growth factor (PDGF) is a signaling molecule that plays a critical role in angiogenesis and the migration and proliferation of MSCs. Though there are multiple isoforms, PDGF-BB is considered the universal growth factor in this family due to its ability to bind to all isoforms of the PDGF receptor (Hollinger et al., 2008). PDGF is a chemoattractant for pericytes, facilitating their recruitment and attachment to vascular endothelial cells to aid in the structural stability of newly forming vasculature (Caplan and Correa, 2011a). It has been suggested that PDGF, secreted by endothelial cells, facilitates the release of pericytes from the vessel wall. These free pericytes then give rise to MSCs, which can be stimulated by PDGF to differentiate into osteoblastic progenitors, facilitating fracture repair. It should be noted that the release of the pericytes/MSCs from the vasculature only happens during active angiogenesis, such as what occurs during new bone formation (Caplan and Correa, 2011a). When a fracture occurs, an inflammatory response releases large numbers of bioactive factors in the site of injury, including a high concentration of PDGF-BB from aggregating platelets potentially facilitating the release of pericytes in the fracture site, providing progenitors for the formation of osteoblasts that will lay down new bone.

Due to its mechanism of action, exogenously applied PDGF only remains at the fracture site for a few days taking several weeks to show effects of increased bone growth and volume. Animal studies examining the effects of PDGF-BB on tibial fractures have found that PDGF-BB delivered with a collagen matrix significantly enhances fracture repair compared to controls (Nash et al., 1994). A large, prospective, randomized controlled study involving 11 clinical centers compared the effectiveness of rhPDGF-BB to beta-tricalcium phosphate (beta-TCP) and found PDGF-BB to be safe and more effective in treating periodontal osseous defects compared to beta-TCP (Nevins et al., 2005). Given the important role PDGF plays in the induction of osteoblastic activity, vascular growth, and subsequent fracture healing, there is enormous potential in utilizing PDGF in clinical orthopedic settings.

IGF-1 and TGF-β1

The skeleton undergoes constant remodeling, a process that involves close coupling of bone resorption and formation through osteoclasts and osteoblasts, respectively (Raggatt and Partridge, 2010). During osteoclastic activity, signaling factors are released from the bone matrix through the resorption process which helps recruit osteoblastic BMSCs to the site, inducing bone formation. It has been largely demonstrated that transforming growth factor-β1 (TGF-β1) and insulin-like growth factor 1 (IGF-1) each play critical roles in the coupled pathway of skeletal remodeling.

TGF-β1 is one of the most abundant cytokines present in the bone matrix, residing in its inactive form by remaining non-covalently bound to a latency-associated protein (LAP) until cleaved and activated by osteoclasts. Once active, TGF-β1 functions as a chemotactic agent to recruit local MSCs for osteogenic differentiation through the SMAD intracellular signaling transduction pathway. A study by Tang et al. used mice to demonstrate that TGF- β1 is necessary and responsible for inducing migration of BMSCs to skeletal remodeling sites in response to osteoclastic bone resorption. This study also showed that an induced mutation in the *TGF-β1* gene leading to overexpression of the active form of TGF-β1 resulted in defective bone remodeling due to formation of osteoblastic cell clusters and impaired migration of BMSCs to bone resorption sites (Tang et al., 2009). These results are consistent with human skeletal disorders that result from mutations causing premature activation of the TGF-β1 gene (Janssens et al., 2000). Tang et al. was able to partially rescue the uncoupled bone resorption in TGF-β1 mutant mice through a receptor inhibitor, demonstrating a possible mode of therapy in treating bone remodeling diseases (Tang et al., 2009).

Even though TGF-β1 is responsible for recruiting BMSCs to the site of bone resorption, they do not provide the signal for active osteoblastic differentiation. Instead, IGF-1, which is also one of the most abundant growth factors present in the bone matrix (Seck et al., 1998), is responsible for creating the osteogenic microenvironment required for differentiating recruited BMSCs into osteoblasts (Xian et al., 2012). In a study by Xian et al., IGF-1 knockout mice ($Igf1r^{-/-}$) showed a reduction in mature osteoblasts at the site of bone remodeling as well as a reduction in bone formation, demonstrating how IGF-1 signaling is necessary for bone remodeling. They were able to determine that when IGF-1 is released from the bone matrix during osteoclast activity, it is able to activate mTOR signaling to stimulate osteoblastic differentiation of BMSCs recruited

by TGF- β1. Additionally, IGF-1 levels in the bone matrix were found to be low in rats with age-related reduction of bone mass (Xian et al., 2012). This is consistent with previous knowledge that diseases involving low IGF-1 serum and matrix concentrations have high incidence of low bone mass and high risk of osteoporosis and fracture (Langlois et al., 1998). Delivery of exogenous IGF-1 to aged rats was enough to stimulate some new bone formation (Xian et al., 2012). Since IGF-1 is necessary for the maintenance of healthy bone mass, it is worth further investigating its therapeutic potential in preventing disease states that put patients at high risk for fracture.

Mechanical Stimulation

As clinical demand for bone grafts to treat congenital and trauma related skeletal defects continues to increase, the method of seeding hMSCs onto biological and synthetic biomaterials along with osteoinductive growth factors has been a significant advancement in the field of tissue engineering. However, the size of the tissue constructs that can be created under static conditions is greatly limited due to diffusional constraints of nutrients reaching bone cells which have very high metabolic requirements (Grayson et al., 2011). A solution to this problem is the utilization of perfusion bioreactors which can effectively disseminate nutrients and oxygen throughout graft constructs with a core larger than 200 μm (generally thought to be the upper limit for oxygen diffusion and a bone graft in static culture). In addition to convective transport of nutrients and waste, the dynamic flow of perfusion bioreactors creates a mechanical stimulus that enhances osteogenesis and mineral deposition of cells in the graft (Gomes et al., 2003). It has been shown in various studies that use of a bioreactor allows for the cultivation of functional, clinically-sized bone grafts that can be used for transplantation (Grayson et al., 2011).

In vitro studies have shown that marrow stromal osteoblasts significantly increase mineralization on 3D biomaterials with increasing flow rate in a perfusion bioreactor (Bancroft et al., 2002). Moreover, medium perfusion rates from 0.01 to 0.2 mL/min appear to be optimal for increasing the number of viable cells, as perfusion rates approaching 1 mL/min results in substantial cell death (Cartmell et al., 2003). The mechanical shear stress stimulation from the perfusion of the bone cells is a strong stimulant for osteogenic growth. In fact, there are several studies providing evidence that the shear stress from fluid flow could be a stronger stimulus for osteoblastic activity compared to hydrostatic compression or deformation of the extracellular matrix (Bancroft et al., 2002). Despite these advantages, one problem regarding bone grafts constructed in perfusion bioreactors is their inherent lack of vasculature, which can lead to a necrotic core once implanted. Ball et al. investigated the use of 3D printed vascular structures applied in conjunction with a perfusion bioreactor and found that cell viability increased by 50% within the core graft constructs (Ball et al., 2016). Though it remains to be seen if tissue-engineered bone grafts can replace the current gold standard autograft in fracture repair, perfusion bioreactors and the advances in spatial resolution provided by 3D printing, as well as growing understanding of stem cell differentiation into osteochondral structures (Stephenson et al., 2017) provide tools that can be used to increase the viability and osteogenic potential of bone grafts for therapeutic use. In addition, as noted by Forrestal et al. culturing and integrating unique geometry in patient-specific grafts by coupling bioreactors and biomaterial s of vary shapes, complexities, and sizes, remains an area of investigation that could yield positive results in tissue engineering (Forrestal et al., 2017).

CELL-BASED THERAPY APPLICATIONS IN BONE DEFECTS

Several factors determine the success of cell-based therapies for bone defects, including (1) the type of cells and vehicle used to transport them, (2) final cell concentration, (3) immature or progenitor cell status, (4) time of therapy, (5) mode of administration and (6) availability of osteoblastic progenitors at the fracture site. We have discussed some of these factors above in relation with cells, biomaterials or growth factors employed. However, the availability of osteoblastic cells at the fracture site constitutes another critical factor, which in fact can be manipulated. Overall, recruitment (i.e., homing) of endogenous MSCs to bone defect sites presents benefits and limitations when compared to exogenously administered autologous or allogeneic MSCs. Different strategies to induce homing of endogenous MSCs to bone defects are reviewed in Herrmann et al. (2015). On the one hand, and as mentioned before, homing of endogenous MSCs to bone defects can be triggered by locally injected growth factors combined with various biomaterials. In such cases, endogenous MSC recruitment does not involve *ex vivo* MSC manipulation that putatively affect their phenotypic and molecular profiles, thus having easier regulatory pathways. On the other hand, in some cases the recruitment of endogenous MSCs might not be adequate as the MSC functionality has been shown to be affected by intrinsic factors such as patient's pathological conditions (for example type 1 diabetes and autoimmune conditions) and age. In addition, bone segmental defects where bone loss cannot be compensated even by autologous bone grafting there is need to combine all different aspects of BTE including stem cells, growth factors, scaffolds and mechanical stimulation for effective bone regeneration (**Figure 1**). For these reasons, and not to discriminate against such approaches, we will only present a couple clinical scenarios using exogenously-administered cells, complemented by a list of available clinical studies using expanded MSC to treat bone defects (**Table 2**).

Delayed Fracture Healing

Nonunions are complications that may occur 6 months following incomplete healing of a bone fracture. Studies have compared the function and pools of BMSCs and circulating endothelial progenitor cells (EPCs) in atrophic nonunion patients to healthy subjects in an effort to better understand the molecular and cellular mechanisms which lead to nonunions. Patients with nonunions were shown to exhibit a decreased pool of BMSCs and changes in the serum levels of chemokines and growth factors required for their recruitment and proliferation (Mathieu

TABLE 2 | Clinical studies using cultured MSCs for the treatment of bone defects.

References	Cell type	Biomaterials/grafts	Delivery method	Patient's group	Average follow up	Outcome
Kawate et al. (2006)	BM MSCs	β-TCP ceramics and free vascularized fibula	Local implantation of BM MSC/ β-TCP composites with free vascularized fibula	Steroid-induced osteonecrosis $N = 3$	27–48 months	Osteonecrosis did not progress any further and early bone regeneration was observed
Quarto et al. (2001); Marcacci et al. (2007)	BM MSCs	Porous HA ceramic	Local implantation, 2.0×10^7 MSCs per ml mixed with biomaterial	Large long bone defects $N = 3$, 4–7 cm segment from tibia, ulna, humerus	6–7 years	No complications observed. Complete fusion between implant and host bone 5–7 months post surgery. At 6–7 years post surgery good integration was maintained and no late fractures observed
Kim et al. (2009)	Osteogenically differentiated BM MSCs	–	Local injection, 1.2×10^7 MSCs per 0.4 ml mixed with fibrin at 1:1 ratio	Various long bone fractures $N = 64$	2 months	No complications observed. Autologous osteoblast injection resulted in significant fracture healing acceleration
Zhao et al. (2012)	BM MSCs	–	Local injection, 2.0×10^6 MSCs in 2 ml of saline	AVN of femoral head $N = 53$	5 years	No complications observed. At 5 years post surgery only 2 of the 53 BM MSC-treated femoral heads progressed and underwent vascularized bone grafting. Improved measures of femoral head function and decreased volume of the necrotic lesion
Giannotti et al. (2013)	Osteogenically differentiated BM MSCs	–	Local implantation, $0.5–2.0 \times 10^6$ MSCs in 2 ml of fibrin clot	Upper limb non-unions N= 8	6 years and 3 months	No complications observed. All patients recovered limb function with no evidence of tissue overgrowth or tumor formation
Aoyama et al. (2014)	BM MSCs	β-TCP ceramics combined with vascularized bone grafts	Local implantation, $0.5–1.0 \times 10^8$ MSCs mixed with β-TCP and vascularized bone grafts	AVN of femoral head $N = 10$	24 months	No complications observed. All procedures were successfully performed and some young patients with extensive necrotic lesions with pain demonstrated good bone regeneration with amelioration of symptoms.
Cai et al. (2014)	BMMNCs and UC MSCs	-	Infusion in femoral artery of 60–80 mL of BMMNCs and 30–50 mL of UC MSCs	AVN of femoral head $N = 30$	12 months	No complications observed. After the treatment, 28/30, 26/30, and 26/30 of patients showed relief of hip pain, improvement of joint function, and extended walking distances, respectively.

et al., 2013). Although the literature regarding stem cell use in the treatment of nonunions is limited to pre-clinical animal models, there have been reports of successful use of autologous BMSCs combined with calcium sulfate (CaSO4) to clinically and radiologically heal nonunions 2 months after implantation (Bajada et al., 2007). Another example involves the successful implantation of engineered osteogenic bone discs around the osteosynthesis material (i.e., intra-medullary nail in this case), in a patient with a critical bone defect of 72 mm in the distal tibia. The engineered bone discs were made with decellularized bovine bone matrix (DBM) seeded with autologous bone marrow aspirate and cultured *in vitro* before implantation. In this typical tissue engineering approach, the engineered implant demonstrated good integration with host tissue and functional clinical outcomes as early as 6 weeks post-surgery (Hesse et al., 2010).

Pre-clinical studies have used rat models to evaluate the efficacy of local injections and cell sheets of BMSCs to treat nonunions. BMSCs have shown the ability to complete bone bridging with woven bone within rat femoral osteotomies when compared to their controls (Shimizu et al., 2015). Using cell sheet transplantation of BMSCs cultured using dexamethasone and ascorbic acid phosphate has also been shown to aid in the repair of nonunions. Researchers demonstrated that transplanted cells without the use of biomaterials has the ability to differentiate into an osteogenic lineage and could contribute to hard tissue reconstructions in cases involving nonunions (Nakamura et al., 2010). Studies have also proven that BMSCs injected into bone defects have the potential to not only remodel bone, but to provide a greater degree of biomechanical stiffness when compared to contralateral uninjured limbs. For instance, in a study by Kallai et al.,

the biomechanical and microarchitecture properties of repaired murine radius bones following implantation of MSCs was found to have an axial stiffness 2 times higher compared to contralateral limbs when repaired with MSCs (Kallai et al., 2010).

Bone marrow aspirate concentrate (BMAC) has been explored as a viable source of BMSCs for the treatment of bone nonunions. BMAC is a heterogeneous cell mixture containing various cell types including hematopoietic and mesenchymal progenitors (i.e., BMSCs) along with EPC, monocytes, granulocytes and other cell types. Several studies have been reported using BMAC for nonunions, bone defects, distraction osteogenesis and others for potential complications of the therapy. The overall consensus of those studies is the clinical efficacy of BMAC inducing bone healing, its superiority to bone grafts, and reduced complications (Fayaz et al., 2011; Imam et al., 2017).

Avascular Necrosis of the Femoral Head

Avascular necrosis of the femoral head (AVN) is a disease which affects the younger population resulting in several complications. AVN can be idiopathic or secondary to chemotherapy, steroid therapy, trauma, chronic alcohol use, or sickle cell disease. Old reports have shown that more than 80% of patients with AVN develop end-stage osteoarthritis necessitating joint replacement (Mont et al., 1996). As a result, other modalities have been investigated in an effort to mitigate the progression of joint disease, specifically therapies using core decompression, cell-based therapies, or a combination of the two.

Core decompression (CD) provides relief by decreasing the intra-medullary pressure, which alleviates the symptoms but does not impact progression of the disease (Radke et al., 2003). It is typically reserved for patients in the early stages of osteonecrosis, prior to mechanical failure/collapse. Compared to conservative-treatment, CD can effectively relieve hip pain from AVN, however, there is no difference when compared to conservative treatment in preventing collapse of the femoral head from osteonecrosis as early established (Koo et al., 1995). Incomplete reconstruction of the femoral head secondary to deficiency of osteoprogenitor cells in the proximal femur may contribute to the failure of CD in preventing collapse of the femoral head.

In an effort to prevent the progression of AVN, studies have investigated the use of cells-based therapy in treating hip osteonecrosis. One highly explored method involves implanting BMAC into the osteonecrotic zone on the femoral head to create an environment of osteoblast differentiation and vascular proliferation to promote repair (Zhao et al., 2012; Hernigou et al., 2015). Studies have also investigated the efficacy of culture-expanded BMSCs compared to CD, revealing that the presence of BMSCs significantly increased Harris Hip Scores and decreased the volume of necrotic lesions when compared to CD (Hernigou et al., 2016). They concluded that autologous BMSCs, obtained from the iliac crest, can reliably provide a greater number of cells for efficient expansion and further femoral head implantation and could effectively delay or avoid its collapse. Finally, a meta-analysis comparing the clinical efficacy of core decompression with BMSC revealed that the cells-based group progressed to a significantly fewer number of grafting events as well as a significantly better clinical outcome compared to CD (Li et al., 2014).

Studies have also investigated how CD in conjunction with cell-based therapy can be beneficial for patients with AVN. Villa et al. revealed patients treated with a combination of BMSCs with CD, compared to controls and CD alone, had a lower risk of femoral head collapse (Villa et al., 2016). Other studies have replicated these results as Gangji et al. compared patients with AVN treated with CD or CD with bone marrow cells in the form of BMAC. They found that the group with cells had less pain and joint symptoms, as well as reduced incidence of fractural stages. These results were maintained after 60 months as there was a significant difference in failure rates between the two groups (Gangji et al., 2011). These results are supported by additional studies showing cells injected in conjunction with CD to provide a significant difference in the time to collapse when compared to patients treated with just CD (Gangji et al., 2004).

CONCLUSIONS

A major challenge for the upcoming decade in the bone regeneration field is to elucidate the underlying cellular and molecular mechanisms of stem cell actions in bone defect therapeutics. In previous years, both pre-clinical and some clinical studies have shown beneficial effects, mainly with MSCs and osteoblastic progenitors in bone healing but the exact mechanisms of actions remain unclear. Although encouraging clinical results have been obtained by transplanting either uncultured MSCs or expanded MSCs, the exact dosage and route of application remain to be optimized and the fate of transplanted cells and their mechanisms of action need to be better monitored in larger clinical trials. On this basis, clinical applications of stem cell-based bone therapies are still limited due to various hurdles such as (a) ethical concerns related to ESCs and iPSCs therapeutic application, (b) proper phenotypic and molecular qualitative evaluation of stem cell products (c) laborious and expensive *ex vivo* expansion of adequate stem cell populations for effective *in vivo* applications c) putative immunological rejection of allogeneic stem cell infusion *in vivo* and donor-related differences and (d) other translational difficulties. Specifically, for the treatment of delayed fracture healing and avascular necrosis bone defects, local administration of stem cell therapies in combination with specialized osteo-conductive biomaterials, osteo-inductive growth factors and adequate mechanical stimulation may further resolve more effectively and more rapidly these complicated orthopedic conditions. Collectively, a better understanding of the functional roles of stem cells in health, aging and disease will provide the foundations for the design of novel and advanced therapeutic strategies for skeletal disorders.

AUTHOR CONTRIBUTIONS

All authors contributed substantially to the conception or design of the work, the drafting of the work or revising it, reviewing for

final approval, and agreement to be accountable for all aspects of the work in ensuring that questions related to the accuracy or integrity of any part of the work are appropriately investigated and resolved.

FUNDING

The authors are grateful to the Soffer Family Foundation for their generous support.

REFERENCES

Ahmed, I., Bernard, J., Farmer, J., Scotchford, C. A., Walker, G. S., and Rudd, C. D. (2011). Composites for bone repair: phosphate glass fibre reinforced PLA with varying fibre architecture. *J. Mater. Sci. Mater. Med.* 22, 1825–1834. doi: 10.1007/s10856-011-4361-0

Akkouch, A., Zhang, Z., and Rouabhia, M. (2014). Engineering bone tissue using human dental pulp stem cells and an osteogenic collagen-hydroxyapatite-poly (L-lactide-co-epsilon-caprolactone) scaffold. *J. Biomater. Appl.* 28, 922–936. doi: 10.1177/0885328213486705

Alizadeh, A., Moztarzadeh, F., Ostad, S. N., Azami, M., Geramizadeh, B., Hatam, G., et al. (2016). Synthesis of calcium phosphate-zirconia scaffold and human endometrial adult stem cells for bone tissue engineering. *Artif. Cells Nanomed. Biotechnol.* 44, 66–73. doi: 10.3109/21691401.2014.909825

Aoyama, T., Goto, K., Kakinoki, R., Ikeguchi, R., Ueda, M., Kasai, Y., et al. (2014). An exploratory clinical trial for idiopathic osteonecrosis of femoral head by cultured autologous multipotent mesenchymal stromal cells augmented with vascularized bone grafts. *Tissue Eng. Part B Rev.* 20, 233–242. doi: 10.1089/ten.TEB.2014.0090

Arafat, M. T., Lam, C. X. F., Ekaputra, A. K., Wong, S. Y., Li, X., and Gibson, I. (2011). Biomimetic composite coating on rapid prototyped scaffolds for bone tissue engineering. *Acta Biomater.* 7, 809–820. doi: 10.1016/j.actbio.2010.09.010

Arinzeh, T. L., Peter, S. J., Archambault, M. P., van den Bos, C., Gordon, S., Kraus, K., et al. (2003). Allogeneic mesenchymal stem cells regenerate bone in a critical-sized canine segmental defect. *J. Bone Joint Surg. Am.* 85-A, 1927–1935. doi: 10.2106/00004623-200310000-00010

Arpornmaeklong, P., Wang, Z., Pressler, M. J., Brown, S. E., and Krebsbach, P. H. (2010). Expansion and characterization of human embryonic stem cell-derived osteoblast-like cells. *Cell. Reprogram.* 12, 377–389. doi: 10.1089/cell.2009.0079

Asti, A., and Gioglio, L. (2014). Natural and synthetic biodegradable polymers: different scaffolds for cell expansion and tissue formation. *Int. J. Artif. Organs* 37, 187–205. doi: 10.5301/ijao.5000307

Baboolal, T. G., Boxall, S. A., El-Sherbiny, Y. M., Moseley, T. A., Cuthbert, R. J., Giannoudis, P. V., et al. (2014). Multipotential stromal cell abundance in cellular bone allograft: comparison with fresh age-matched iliac crest bone and bone marrow aspirate. *Regen. Med.* 9, 593–607. doi: 10.2217/rme.14.17

Bajada, S., Harrison, P. E., Ashton, B. A., Cassar-Pullicino, V. N., Ashammakhi, N., and Richardson, J. B. (2007). Successful treatment of refractory tibial nonunion using calcium sulphate and bone marrow stromal cell implantation. *J Bone Joint Surg. Br.* 89-B, 1382–1386. doi: 10.1302/0301-620x.89b10.19103

Baksh, D., Boland, G. M., and Tuan, R. S. (2007). Cross-talk between Wnt signaling pathways in human mesenchymal stem cells leads to functional antagonism during osteogenic differentiation. *J. Cell Biochem.* 101, 1109–1124. doi: 10.1002/jcb.21097

Ball, O., Nguyen, B.-N. B., Placone, J. K., and Fisher, J. P. (2016). 3D printed vascular networks enhance viability in high-volume perfusion bioreactor. *Ann. Biomed. Eng.* 44, 3435–3445. doi: 10.1007/s10439-016-1662-y

Bancroft, G. N., Sikavitsas, V. I., van den Dolder, J., Sheffield, T. L., Ambrose, C. G., Jansen, J. A., et al. (2002). Fluid flow increases mineralized matrix deposition in 3D perfusion culture of marrow stromal osteoblasts in a dose-dependent manner. *Proc. Natl. Acad. Sci. U.S.A.* 99, 12600–12605. doi: 10.1073/pnas.202296599

Bensaïd, W., Oudina, K., Viateau, V., Potier, E., Bousson, V., Blanchat, C., et al. (2005). *De novo* reconstruction of functional bone by tissue engineering in the metatarsal sheep model. *Tissue Eng.* 11, 814–824. doi: 10.1089/ten.2005.11.814

Berner, A., Henkel, J., Woodruff, M. A., Saifzadeh, S., Kirby, G., Zaiss, S., et al. (2017). Scaffold-cell bone engineering in a validated preclinical animal model: precursors vs differentiated cell source. *J. Tissue Eng. Regen. Med.* 11, 2081–2089. doi: 10.1002/term.2104

Berner, A., Henkel, J., Woodruff, M. A., Steck, R., Nerlich, M., Schuetz, M. A., et al. (2015). Delayed minimally invasive injectionof allogenic bone marrow stromal cell sheets regenerates large bone defects in an ovine preclinical animal model. *Stem Cells Transl. Med.* 4, 503–512. doi: 10.5966/sctm.2014-0244

Berner, A., Reichert, J. C., Woodruff, M. A., Saifzadeh, S., Morris, A. J., Epari, D. R., et al. (2013). Autologous vs. allogenic mesenchymal progenitor cells for the reconstruction of critical sized segmental tibial bone defects in aged sheep. *Acta Biomater.* 9, 7874–7884. doi: 10.1016/j.actbio.2013.04.035

Both, S. K., van Apeldoorn, A. A., Jukes, J. M., Englund, M. C. O., Hyllner, J., van Blitterswijk, C. A., et al. (2011). Differential bone-forming capacity of osteogenic cells from either embryonic stem cells or bone marrow-derived mesenchymal stem cells. *J. Tissue Eng. Regen. Med.* 5, 180–190. doi: 10.1002/term.303

Brandoff, J. F., Silber, J. S., and Vaccaro, A. R. (2008). Contemporary alternatives to synthetic bone grafts for spine surgery. *Am. J. Orthoped.* 37, 410–414.

Bruder, S. P., Kraus, K. H., Goldberg, V. M., and Kadiyala, S. (1998). The effect of implants loaded with autologous mesenchymal stem cells on the healing of canine segmental bone defects. *J. Bone Joint Surg.* 80, 985–996.

Cahill, K. S., McCormick, P. C., and Levi, A. D. (2015). A comprehensive assessment of the risk of bone morphogenetic protein use in spinal fusion surgery and postoperative cancer diagnosis. *J. Neurosurg. Spine* 23, 86–93. doi: 10.3171/2014.10.SPINE14338

Cai, J., Wu, Z., Huang, L., Chen, J., Wu, C., Wang, S., et al. (2014). Cotransplantation of bone marrow mononuclear cells and umbilical cord mesenchymal stem cells in avascular necrosis of the femoral head. *Transplant. Proc.* 46, 151–155. doi: 10.1016/j.transproceed.2013.06.021

Cai, L., Wang, Q., Gu, C., Wu, J., Wang, J., Kang, N., et al. (2011). Vascular and micro-environmental influences on MSC-coral hydroxyapatite construct-based bone tissue engineering. *Biomaterials* 32, 8497–8505. doi: 10.1016/j.biomaterials.2011.07.087

Calori, G. M., d'Imporzano, M., and Albisetti, W. (2008). Application of rhBMP-7 and platelet-rich plasma in the treatment of long bone non-unions: a prospective randomised clinical study on 120 patients. *Injury* 39, 1391–1402. doi: 10.1016/j.injury.2008.08.011

Calvert, J. W., Marra, K. G., Cook, L., Kumta, P. N., DiMilla, P. A., and Weiss, L. E. (2000). Characterization of osteoblast-like behavior of cultured bone marrow stromal cells on various polymer surfaces. *J. Biomed. Mater. Res.* 52, 279–284. doi: 10.1002/1097-4636(200011)52:2<279::aid-jbm6>3.0.co;2-8

Cao, H., and Kuboyama, N. (2010). A biodegradable porous composite scaffold of PGA/beta-TCP for bone tissue engineering. *Bone* 46, 386–395. doi: 10.1016/j.bone.2009.09.031

Caplan, A. I. (2008). All MSCs are pericytes? *Cell Stem Cell* 3, 229–230. doi: 10.1016/j.stem.2008.08.008

Caplan, A. I., and Correa, D. (2011a). PDGF in bone formation and regeneration: new insights into a novel mechanism involving MSCs. *J. Orthop. Res.* 29, 1795–1803. doi: 10.1002/jor.21462

Caplan, A. I., and Correa, D. (2011b). The MSC: an injury drugstore. *Cell Stem Cell* 9, 11–15. doi: 10.1016/j.stem.2011.06.008

Cartmell, S. H., Porter, B. D., García AJ., and Guldberg, R. E. (2003). Effects of medium perfusion rate on cell-seeded three-dimensional bone constructs *in vitro*. *Tissue Eng.* 9, 1197–1203. doi: 10.1089/10763270360728107

Chen, G., Deng, C., and Li, Y. P. (2012). TGF-beta and BMP signaling in osteoblast differentiation and bone formation. *Int. J. Biol. Sci.* 8, 272–288. doi: 10.7150/ijbs.2929

Chen, W., Liu, J., Manuchehrabadi, N., Weir, M. D., Zhu, Z., and Xu, H. H. K. (2013). Umbilical cord and bone marrow mesenchymal stem cell seeding on macroporous calcium phosphate for bone regeneration in rat cranial defects. *Biomaterials* 34, 9917–9925. doi: 10.1016/j.biomaterials.2013.09.002

Choi, W.-Y., Kim, H.-E., Kim, M.-J., Kim, U.-C., Kim, J.-H., and Koh, Y.-H. (2010). Production and characterization of calcium phosphate

(CaP) whisker-reinforced poly(ε-caprolactone) composites as bone regenerative. *Mater. Sci. Eng.* 30, 1280–1284. doi: 10.1016/j.msec.2010.07.018

Claes, L., Recknagel, S., and Ignatius, A. (2012). Fracture healing under healthy and inflammatory conditions. *Nat. Rev. Rheumatol.* 8, 133–143. doi: 10.1038/nrrheum.2012.1

Crisan, M., Yap, S., Casteilla, L., Chen, C. W., Corselli, M., Park, T. S., et al. (2008). A perivascular origin for mesenchymal stem cells in multiple human organs. *Cell Stem Cell* 3, 301–313. doi: 10.1016/j.stem.2008.07.003

Cui, L., Liu, B., Liu, G., Zhang, W., Cen, L., Sun, J., et al. (2007). Repair of cranial bone defects with adipose derived stem cells and coral scaffold in a canine model. *Biomaterials* 28, 5477–5486. doi: 10.1016/j.biomaterials.2007.08.042

Cunningham, J. J., Ulbright, T. M., Pera, M. F., and Looijenga, L. H. (2012). Lessons from human teratomas to guide development of safe stem cell therapies. *Nat. Biotechnol.* 30, 849–857. doi: 10.1038/nbt.2329

Daher S. R., Johnstone, B. H., Phinney, D. G., and March, K. L. (2009). adipose stromal/stem cells: basic and translational advances: the IFATS collection. *Stem Cells* 26, 2664–2665. doi: 10.1634/stemcells.2008-0927

d'Aquino, R., Graziano, A., Sampaolesi, M., Laino, G., Pirozzi, G., De Rosa, A., et al. (2007). Human postnatal dental pulp cells co-differentiate into osteoblasts and endotheliocytes: a pivotal synergy leading to adult bone tissue formation. *Cell Death Differ.* 14, 1162–1171. doi: 10.1038/sj.cdd.4402121

De Bari, C., Dell'Accio, F., Karystinou, A., Guillot, P. V., Fisk, N. M., Jones, E. A., et al. (2008). A biomarker-based mathematical model to predict bone-forming potency of human synovial and periosteal mesenchymal stem cells. *Arthritis Rheum* 58, 240–250. doi: 10.1002/art.23143

De Bari, C., Dell'Accio, F., Tylzanowski, P., and Luyten, F. P. (2001). Multipotent mesenchymal stem cells from adult human synovial membrane. *Arthritis Rheum* 44, 1928–1942. doi: 10.1002/1529-0131(200108)44:8

de Miguel-Beriain, I. (2015). The ethics of stem cells revisited. *Adv. Drug Deliv. Rev.* 82–83, 176–180. doi: 10.1016/j.addr.2014.11.011

Di Bella, C., Farlie, P., and Penington, A. J. (2008). Bone regeneration in a rabbit critical-sized skull defect using autologous adipose-derived cells. *Tissue Eng. Part A* 14, 483–490. doi: 10.1089/tea.2007.0137

Dilogo, I. H., Primaputra, M. R. A., Pawitan, J. A., and Liem, I. K. (2017). Modified Masquelet technique using allogeneic umbilical cord-derived mesenchymal stem cells for infected non-union femoral shaft fracture with a 12 cm bone defect: a case report. *Int. J. Surg. Case Rep.* 34, 11–16. doi: 10.1016/j.ijscr.2017.03.002

Dimitriou, R., Tsiridis, E., and Giannoudis, P. V. (2005). Current concepts of molecular aspects of bone healing. *Injury* 36, 1392–1404. doi: 10.1016/j.injury.2005.07.019

Downey, J., Lauzier, D., Kloen, P., Klarskov, K., Richter, M., Hamdy, R., et al. (2015). Prospective heterotopic ossification progenitors in adult human skeletal muscle. *Bone* 71, 164–170. doi: 10.1016/j.bone.2014.10.020

Epstein, N. E. (2013). Complications due to the use of BMP/INFUSE in spine surgery: the evidence continues to mount. *Surg. Neurol. Int.* 4, S343–S352. doi: 10.4103/2152-7806.114813

Fan, H., Zeng, X., Wang, X., Zhu, R., and Pei, G. (2014). Efficacy of prevascularization for segmental bone defect repair using β-tricalcium phosphate scaffold in rhesus monkey. *Biomaterials* 35, 7407–7415. doi: 10.1016/j.biomaterials.2014.05.035

Fan, J., Im, C. S., Guo, M., Cui, Z. K., Fartash, A., Kim, S., et al. (2016). Enhanced osteogenesis of adipose-derived stem cells by regulating bone morphogenetic protein signaling antagonists and agonists. *Stem Cells Transl. Med.* 5, 539–551. doi: 10.5966/sctm.2015-0249

Fayaz, H. C., Giannoudis, P. V., Vrahas, M. S., Smith, R. M., Moran, C., Pape, H. C., et al. (2011). The role of stem cells in fracture healing and nonunion. *Int. Orthop.* 35, 1587–1597. doi: 10.1007/s00264-011-1338-z

Ferrara, N., Gerber, H. P., and LeCouter, J. (2003). The biology of VEGF and its receptors. *Nat. Med.* 9, 669–676. doi: 10.1038/nm0603-669

Ferreira, C. L., Abreu, F. A., Silva, G. A., Silveira, F. F., Barreto, L. B., Paulino, Tde P., et al. (2013). TGF-β1 and BMP-4 carried by liposomes enhance the healing process in alveolar bone. *Arch. Oral Biol.* 58, 646–656. doi: 10.1016/j.archoralbio.2012.11.013

Fielding, G. A., Bandyopadhyay, A., and Bose, S. (2012). Effects of silica and zinc oxide doping on mechanical and biological properties of 3D printed tricalcium phosphate tissue engineering scaffolds. *Dent. Mater.* 28, 113–122. doi: 10.1016/j.dental.2011.09.010

Fischerauer, E. E., Janezic, G., Pichler, K., Ebner, B., and Weinberg, A. M. (2013). BMP-6 and BMPR-1a are up-regulated in the growth plate of the fractured tibia. *J. Orthop. Res.* 31, 357–363. doi: 10.1002/jor.22238

Flierl, M. A., Smith, W. R., Mauffrey, C., Irgit, K., Williams, A. E., Ross, E., et al. (2013). Outcomes and complication rates of different bone grafting modalities in long bone fracture nonunions: a retrospective cohort study in 182 patients. *J. Orthopaed. Surg. Res.* 8:33. doi: 10.1186/1749-799X-8-33

Fong, C.-Y., Chak, L.-L., Biswas, A., Tan, J.-H., Gauthaman, K., Chan, W.-K., et al. (2011). Human Wharton's jelly stem cells have unique transcriptome profiles compared to human embryonic stem cells and other mesenchymal stem cells. *Stem Cell Rev* 7, 1–16. doi: 10.1007/s12015-010-9166-x

Fong, K., Truong, V., Foote, C. J., Petrisor, B., Williams, D., Ristevski, B., et al. (2013). Predictors of nonunion and reoperation in patients with fractures of the tibia: an observational study. *BMC Musculoskelet. Disord.* 14:103. doi: 10.1186/1471-2474-14-103

Forrestal, D. P., Klein, T. J., and Woodruff, M. A. (2017). Challenges in engineering large customized bone constructs. *Biotechnol. Bioeng.* 114, 1129–1139. doi: 10.1002/bit.26222

Gangji, V., De Maertelaer, V., and Hauzeur, J.-P. (2011). Autologous bone marrow cell implantation in the treatment of non-traumatic osteonecrosis of the femoral head: five year follow-up of a prospective controlled study. *Bone* 49, 1005–1009. doi: 10.1016/j.bone.2011.07.032

Gangji, V., Hauzeur, J.-P., Matos, C., De Maertelaer, V., Toungouz, M., and Lambermont, M. (2004). Treatment of osteonecrosis of the femoral head with implantation of autologous bone-marrow cells. A pilot study. *J. Bone Joint Surg. Am.* 86-A, 1153–1160. doi: 10.2106/00004623-200406000-00006

Gao, X., Usas, A., Lu, A., Tang, Y., Wang, B., Chen, C.-W., et al. (2013). BMP2 is superior to BMP4 for promoting human muscle-derived stem cell-mediated bone regeneration in a critical-sized calvarial defect model. *Cell Transplant* 22, 2393–2408. doi: 10.3727/096368912X658854

Gao, X., Usas, A., Tang, Y., Lu, A., Tan, J., Schneppendahl, J., et al. (2014). A comparison of bone regeneration with human mesenchymal stem cells and muscle derived stem cells and the critical role of BMP. *Biomaterials* 35, 6859–6870. doi: 10.1016/j.biomaterials.2014.04.113

Gautam, S., Dinda, A. K., and Mishra, N. C. (2013). Fabrication and characterization of PCL/gelatin composite nanofibrous scaffold for tissue engineering applications by electrospinning method. *Mater. Sci. Eng. C* 33, 1228–1235. doi: 10.1016/j.msec.2012.12.015

Geesink, R. G., Hoefnagels, N. H., and Bulstra, S. K. (1999). Osteogenic activity of OP-1 bone morphogenetic protein (BMP-7) in a human fibular defect. *J. Bone Joint Surg. Br.* 81, 710–718.

Giannoni, P., Mastrogiacomo, M., Alini, M., Pearce, S. G., Corsi, A., Santolini, F., et al. (2008). Regeneration of large bone defects in sheep using bone marrow stromal cells. *J. Tissue Eng. Regen. Med.* 2, 253–262. doi: 10.1002/term.90

Giannotti, S., Trombi, L., Bottai, V., Ghilardi, M., D'Alessandro, D., Danti, S., et al. (2013). Use of autologous human mesenchymal stromal cell/fibrin clot constructs in upper limb non-unions: long-term assessment. *PLoS ONE* 8:e73893. doi: 10.1371/journal.pone.0073893

Giavaresi, G., Bondioli, E., Melandri, D., Giardino, R., Tschon, M., Torricelli, P., et al. (2013). Response of human chondrocytes and mesenchymal stromal cells to a decellularized human dermis. *BMC Musculoskelet. Disord.* 14:12. doi: 10.1186/1471-2474-14-12

Gomes, M. E., Sikavitsas, V. I., Behravesh, E., Reis, R. L., and Mikos, A. G. (2003). Effect of flow perfusion on the osteogenic differentiation of bone marrow stromal cells cultured on starch-based three-dimensional scaffolds. *J. Biomed. Mater. Res. A* 67, 87–95. doi: 10.1002/jbm.a.10075

Gómez-Barrena E., Rosset, P., Lozano, D., Stanovici, J., Ermthaller, C., and Gerbhard, F. (2015). Bone fracture healing: cell therapy in delayed unions and nonunions. *Bone* 70, 93–101. doi: 10.1016/j.bone.2014.07.033

Govender, S., Csimma, C., Genant, H. K., and Valentin-Opran, A. (2002). Recombinant human bone morphogenetic protein-2 for treatment of open tibial fractures: a prospective, controlled, randomized study of four hundred and fifty patients. *J. Bone Joint Surg. Am.* 84, 2123–2134. doi: 10.2106/00004623-200212000-00001

Grayson, W. L., Bhumiratana, S., Cannizzaro, C., and Vunjak-Novakovic, G. (2011). Bioreactor cultivation of functional bone grafts. *Methods Mol. Biol.* 698, 231–241. doi: 10.1007/978-1-60761-999-4_18

Graziano, A., d'Aquino, R., Laino, G., and Papaccio, G. (2008). Dental pulp stem cells: a promising tool for bone regeneration. *Stem Cell Rev. Rep.* 4, 21–26. doi: 10.1007/s12015-008-9013-5

Gronthos, S., Mankani, M., Brahim, J., Robey, P. G., and Shi, S. (2000). Postnatal human dental pulp stem cells (DPSCs) *in vitro* and *in vivo*. *Proc. Natl. Acad. Sci. U.S.A.* 97, 13625–13630. doi: 10.1073/pnas.240309797

Guillot, P. V., Abass, O., Bassett, J. H. D., Shefelbine, S. J., Bou-Gharios, G., Chan, J., et al. (2008). Intrauterine transplantation of human fetal mesenchymal stem cells from first-trimester blood repairs bone and reduces fractures in osteogenesis imperfecta mice. *Blood* 111, 1717–1725. doi: 10.1182/blood-2007-08-105809

Guo, Z., Lee, S. E., Kim, H., Park, S., Hahn, H. T., Karki, A. B., et al. (2009). Fabrication, characterization and microwave properties of polyurethane nanocomposites reinforced with iron oxide and barium titanate nanoparticles. *Acta Mater.* 57, 267–277. doi: 10.1016/j.actamat.2008.09.024

Habal, M. B., and Pietrzak, W. S. (1999). Key points in the fixation of the craniofacial skeleton with absorbable biomaterial. *J. Craniofac. Surg.* 10, 491–499.

Habibovic, P., and Barralet, J. E. (2011). Bioinorganics and biomaterials: bone repair. *Acta Biomater.* 7, 3013–3026. doi: 10.1016/j.actbio.2011.03.027

Habraken, W., Habibovic, P., Epple, M., and Bohner, M. (2016). Calcium phosphates in biomedical applications: materials for the future? *Biochem. Pharmacol.* 19, 69–87. doi: 10.1016/j.mattod.2015.10.008

Han, D. S., Chang, H. K., Kim, K. R., and Woo, S. M. (2014). Consideration of bone regeneration effect of stem cells: comparison of bone regeneration between bone marrow stem cells and adipose-derived stem cells. *J. Craniofac. Surg.* 25, 196–201. doi: 10.1097/SCS.0000000000000378

Haque, P., Parsons, A. J., Barker, I. A., Ahmed, I., Irvine, D. J., Walker, G. S., et al. (2010). Interfacial properties of phosphate glass fibres/PLA composites: effect of the end functionalities of oligomeric PLA coupling agents. *Comp. Sci. Technol.* 70, 1854–1860. doi: 10.1016/j.compscitech.2010.06.012

Harper, L. T., Ahmed, I., Felfel, R. M., and Qian, C. (2012). Finite element modelling of the flexural performance of resorbable phosphate glass fibre reinforced PLA composite bone plates. *J. Mech. Behav. Biomed. Mater.* 15, 13–23. doi: 10.1016/j.jmbbm.2012.07.002

Hatakeyama, A., Uchida, S., Utsunomiya, H., Tsukamoto, M., Nakashima, H., Nakamura, E., et al. (2017). Isolation and characterization of synovial mesenchymal stem cell derived from hip joints: a comparative analysis with a matched control knee group. *Stem Cells Int.* 2017, 9312329–9312313. doi: 10.1155/2017/9312329

Ching, H. A., Dipankar, C., Md Julker, N., and Noor Azuan Abu, O. (2014). Effects of surface coating on reducing friction and wear of orthopaedic implants. *Sci. Technol. Adv. Mat.* 15:014402. doi: 10.1088/1468-6996/15/1/014402

Hench, L. L. (2006). The story of Bioglass®. *J. Mater. Sci. Mater. Med.* 17, 967–978. doi: 10.1007/s10856-006-0432-z

Hernigou, P., Flouzat-Lachaniette, C. H., Delambre, J., Poignard, A., Allain, J., Chevallier, N., et al. (2015). Osteonecrosis repair with bone marrow cell therapies: state of the clinical art. *Bone* 70, 102–109. doi: 10.1016/j.bone.2014.04.034

Hernigou, P., Trousselier, M., Roubineau, F., Bouthors, C., Chevallier, N., Rouard, H., et al. (2016). Stem cell therapy for the treatment of hip osteonecrosis: a 30-year review of progress. *Clin. Orthop. Surg.* 8, 1–8. doi: 10.4055/cios.2016.8.1.1

Herrmann, M., Verrier, S., and Alini, M. (2015). Strategies to stimulate mobilization and homing of endogenous stem and progenitor cells for bone tissue repair. *Front. Bioeng. Biotechnol.* 3, 3300–3311. doi: 10.3389/fbioe.2015.00079

Hesse, E., Kluge, G., Atfi, A., Correa, D., Haasper, C., Berding, G., et al. (2010). Repair of a segmental long bone defect in human by implantation of a novel multiple disc graft. *Bone* 46, 1457–1463. doi: 10.1016/j.bone.2010.02.011

Hing, K. A., Wilson, L. F., and Buckland, T. (2007). Comparative performance of three ceramic bone graft substitutes. *Spine J.* 7, 475–490. doi: 10.1016/j.spinee.2006.07.017

Hollinger, J. O., Hart, C. E., Hirsch, S. N., Lynch, S., and Friedlaender, G. E. (2008). Recombinant human platelet-derived growth factor: biology and clinical applications. *J. Bone Joint Surg. Am.* 90(Suppl. 1), 48–54. doi: 10.2106/JBJS.G.01231

Hsieh, J.-Y., Fu, Y.-S., Chang, S.-J., Tsuang, Y.-H., and Wang, H.-W. (2010). Functional module analysis reveals differential osteogenic and stemness potentials in human mesenchymal stem cells from bone marrow and wharton's jelly of umbilical cord. *Stem Cells Dev.* 19, 1895–1910. doi: 10.1089/scd.2009.0485

Hynes, K., Menicanin, D., Mrozik, K., Gronthos, S., and Bartold, P. M. (2013). Generation of functional mesenchymal stem cells from different induced pluripotent stem cell lines. *Stem Cells Dev.* 23, 1084–1096. doi: 10.1089/scd.2013.0111

Im, G.-I. (2015). Stem cells for reutilization in bone regeneration. *J. Cell Biochem.* 116, 487–493. doi: 10.1002/jcb.25027

Imam, M. A., Holton, J., Ernstbrunner, L., Pepke, W., Grubhofer, F., Narvani, A., et al. (2017). A systematic review of the clinical applications and complications of bone marrow aspirate concentrate in management of bone defects and nonunions. *Int. Orthop.* 41, 2213–2220. doi: 10.1007/s00264-017-3597-9

Jackson, W. M., Lozito, T. P., Djouad, F., Kuhn, N. Z., Nesti, L. J., and Tuan, R. S. (2011). Differentiation and regeneration potential of mesenchymal progenitor cells derived from traumatized muscle tissue. *J. Cell Mol. Med.* 15, 2377–2388. doi: 10.1111/j.1582-4934.2010.01225.x

Jäger, M., Degistirici, Ö., Knipper, A., Fischer, J., Sager, M., and Krauspe, R. (2009). Bone healing and migration of cord blood—derived stem cells into a critical size femoral defect after xenotransplantation. *J. Bone Miner. Res.* 22, 1224–1233. doi: 10.1359/jbmr.070414

Janssens, K., Gershoni-Baruch, R., Guanabens, N., Migone, N., Ralston, S., Bonduelle, M., et al. (2000). Mutations in the gene encoding the latency-associated peptide of TGF-beta 1 cause Camurati-Engelmann disease. *Nat. Genet.* 26, 273–275. doi: 10.1038/81563

Jeong, C. G., Zhang, H., and Hollister Scott, J. (2012). Three-dimensional polycaprolactone scaffold-conjugated bone morphogenetic protein-2 promotes cartilage regeneration from primary chondrocytes *in vitro* and *in vivo* without accelerated endochondral ossification. *J. Biomed. Mater. Res. A* 100A, 2088–2096. doi: 10.1002/jbm.a.33249

Jones, E. A., Giannoudis, P. V., and Kouroupis, D. (2016). Bone repair with skeletal stem cells: rationale, progress to date and clinical application. *Ther. Adv. Musculoskelet. Dis.* 8, 57–71. doi: 10.1177/1759720X16642372

Kallai, I., van Lenthe, G. H., Ruffoni, D., Zilberman, Y., Muller, R., Pelled, G., et al. (2010). Quantitative, structural, and image-based mechanical analysis of nonunion fracture repaired by genetically engineered mesenchymal stem cells. *J. Biomech.* 43, 2315–2320. doi: 10.1016/j.jbiomech.2010.04.031

Kanafi, M. M., Ramesh, A., Gupta, P. K., and Bhonde, R. R. (2013). Dental pulp stem cells immobilized in alginate microspheres for applications in bone tissue engineering. *Int. Endodont. J.* 47, 687–697. doi: 10.1111/iej.12205

Kanakaris, N. K., Calori, G. M., Verdonk, R., Burssens, P., De Biase, P., Capanna, R., et al. (2008). Application of BMP-7 to tibial non-unions: a 3-year multicenter experience. *Injury* 39(Suppl. 2), S83–S90. doi: 10.1016/S0020-1383(08)70019-6

Kanczler, J. M., and Oreffo, R. O. C. (2008). Osteogenesis and angiogenesis: the potential for engineering bone. *Eur. Cell Mater.* 15, 100–114. doi: 10.22203/ecm.v015a08

Kang, H., Shih, Y.-R. V., Nakasaki, M., Kabra, H., and Varghese, S. (2016). Small molecule-driven direct conversion of human pluripotent stem cells into functional osteoblasts. *Sci. Adv.* 2:e1600691. doi: 10.1126/sciadv.1600691

Karp, J. M., Ferreira, L. S., Khademhosseini, A., Kwon, A. H., Yeh, J., and Langer, R. S. (2006). Cultivation of human embryonic stem cells without the embryoid body step enhances osteogenesis *in vitro*. *Stem Cells* 24, 835–843. doi: 10.1634/stemcells.2005-0383

Kawate, K., Yajima, H., Ohgushi, H., Kotobuki, N., Sugimoto, K., Ohmura, T., et al. (2006). Tissue-engineered approach for the treatment of steroid-induced osteonecrosis of the femoral head: transplantation of autologous mesenchymal stem cells cultured with beta-tricalcium phosphate ceramics and free vascularized fibula. *Artif. Organs* 30, 960–962. doi: 10.1111/j.1525-1594.2006.00333.x

Kigami, R., Sato, S., Tsuchiya, N., Yoshimakai, T., Arai, Y., and Ito, K. (2013). FGF-2 angiogenesis in bone regeneration within critical-sized bone defects in rat calvaria. *Implant Dent.* 22, 422–427. doi: 10.1097/ID.0b013e31829d19f0

Kim, D.-W., Staples, M., Shinozuka, K., Pantcheva, P., Kang, S.-D., and Borlongan, C. V. (2013). Wharton's jelly-derived mesenchymal stem cells:

phenotypic characterization and optimizing their therapeutic potential for clinical applications. *IJMS* 14, 11692–11712. doi: 10.3390/ijms140611692

Kim, M. S., Ahn, H. H., Shin, Y. N., Cho, M. H., Khang, G., and Lee, H. B. (2007). An *in vivo* study of the host tissue response to subcutaneous implantation of PLGA- and/or porcine small intestinal submucosa-based scaffolds. *Biomaterials* 28, 5137–5143. doi: 10.1016/j.biomaterials.2007.08.014

Kim, S., Kim, S. S., Lee, S. H., Eun Ahn, S., Gwak, S. J., Song, J. H., et al. (2008). *In vivo* bone formation from human embryonic stem cell-derived osteogenic cells in poly(d,l-lactic-co-glycolic acid)/hydroxyapatite composite scaffolds. *Biomaterials* 29, 1043–1053. doi: 10.1016/j.biomaterials.2007.11.005

Kim, S.-J., Shin, Y.-W., Yang, K.-H., Kim, S.-B., Yoo, M.-J., Han, S.-K., et al. (2009). A multi-center, randomized, clinical study to compare the effect and safety of autologous cultured osteoblast(OssronTM) injection to treat fractures. *BMC Musculoskelet. Disord.* 10:20. doi: 10.1186/1471-2474-10-20

Kinoshita, Y., Matsuo, M., Todoki, K., Ozono, S., Fukuoka, S., Tsuzuki, H., et al. (2008). Alveolar bone regeneration using absorbable poly(L-lactide-co-epsilon-caprolactone)/beta-tricalcium phosphate membrane and gelatin sponge incorporating basic fibroblast growth factor. *Int. J. Oral Maxillofac. Surg.* 37, 275–281. doi: 10.1016/j.ijom.2007.11.010

Kitaori, T., Ito, H., Schwarz, E. M., Tsutsumi, R., Yoshitomi, H., Oishi, S., et al. (2009). Stromal cell–derived factor 1/CXCR4 signaling is critical for the recruitment of mesenchymal stem cells to the fracture site during skeletal repair in a mouse model. *Arthritis Rheum* 60, 813–823. doi: 10.1002/art.24330

Ko, J.-Y., Park, S., and Im, G.-I. (2014). Osteogenesis from human induced pluripotent stem cells: an *in vitro* and *in vivo* comparison with mesenchymal stem cells. *Stem Cells Dev.* 23, 1788–1797. doi: 10.1089/scd.2014.0043

Koc, A., Emin, N., Elcin, A. E., and Elcin, Y. M. (2008). *In vitro* osteogenic differentiation of rat mesenchymal stem cells in a microgravity bioreactor. *J. Bioactive Comp. Polymers* 23, 244–261. doi: 10.1177/0883911508091828

Kon, E., Muraglia, A., Corsi, A., Bianco, P., Marcacci, M., Martin, I., et al. (2000). Autologous bone marrow stromal cells loaded onto porous hydroxyapatite ceramic accelerate bone repair in critical-size defects of sheep long bones. *J. Biomed. Mater. Res.* 49, 328–337. doi: 10.1002/(SICI)1097-4636(20000305)49:3<328::AID-JBM5>3.0.CO;2-Q

Kondo, N., Ogose, A., Tokunaga, K., Ito, T., Arai, K., Kudo, N., et al. (2005). Bone formation and resorption of highly purified beta-tricalcium phosphate in the rat femoral condyle. *Biomaterials* 26, 5600–5608. doi: 10.1016/j.biomaterials.2005.02.026

Koo, K. H., Kim, R., Ko, G. H., Song, H. R., Jeong, S. T., and Cho, S. H. (1995). Preventing collapse in early osteonecrosis of the femoral head. A randomised clinical trial of core decompression. *J. Bone Joint Surg. Br.* 77, 870–874

Kostenuik, P., and Mirza, F. M. (2017). Fracture healing physiology and the quest for therapies for delayed healing and nonunion. *J. Orthop. Res.* 35, 213–223. doi: 10.1002/jor.23460

Kouroupis, D., Churchman, S. M., English, A., Emery, P., Giannoudis, P. V., McGonagle, D., et al. (2013). Assessment of umbilical cord tissue as a source of mesenchymal stem cell/endothelial cell mixtures for bone regeneration. *Regen. Med.* 8, 569–581. doi: 10.2217/rme.13.47

Kouroupis, D., Kyrkou, A., Triantafyllidi, E., Katsimpoulas, M., Chalepakis, G., Goussia, A., et al. (2016). Generation of stem cell-based bioartificial anterior cruciate ligament (ACL) grafts for effective ACL rupture repair. *Stem Cell Res.* 17, 448–457. doi: 10.1016/j.scr.2016.04.016

Kubosch, E. J., Gernot, L., David, F., David, K., Kaywan, I., Bernd, R., et al. (2018). The potential for synovium-derived stem cells in cartilage repair. *Curr. Stem Cell Res. Ther.* 13, 174–184. doi: 10.2174/1574888X12666171002111026

Lan, J., Wang, Z. F., Shi, B., Xia, H. B., and Cheng, X. R. (2007). The influence of recombinant human BMP-2 on bone-implant osseointegration: biomechanical testing and histomorphometric analysis. *Int. J. Oral Maxillofac. Surg.* 36, 345–349. doi: 10.1016/j.ijom.2006.10.019

Langlois, J. A., Rosen, C. J., Visser, M., Hannan, M. T., Harris, T., Wilson, P. W., et al. (1998). Association between insulin-like growth factor I and bone mineral density in older women and men: the Framingham Heart Study. *J. Clin. Endocrinol. Metab.* 83, 4257–4262. doi: 10.1210/jcem.83.12.5308

Lendeckel, S., Jödicke, A., Christophis, P., Heidinger, K., Wolff, J., Fraser, J. K., et al. (2004). Autologous stem cells (adipose) and fibrin glue used to treat widespread traumatic calvarial defects: case report. *J. Craniomaxillofac. Surg.* 32, 370–373. doi: 10.1016/j.jcms.2004.06.002

Levi, B., Hyun, J. S., Montoro, D. T., Lo, D. D., Chan, C. K., Hu, S., et al. (2012). *In vivo* directed differentiation of pluripotent stem cells for skeletal regeneration. *Proc. Natl. Acad. Sci. U.S.A.* 109, 20379–20384. doi: 10.1073/pnas.1218052109

Li, F., Bronson, S., and Niyibizi, C. (2010). Derivation of murine induced pluripotent stem cells (iPS) and assessment of their differentiation toward osteogenic lineage. *J. Cell Biochem.* 109, 643–652. doi: 10.1002/jcb.22440

Li, X., Xu, X., and Wu, W. (2014). Comparison of bone marrow mesenchymal stem cells and core decompression in treatment of osteonecrosis of the femoral head: a meta-analysis. *Int. J. Clin. Exp. Pathol.* 7, 5024–5030.

Li, Z., Munroe, P., Jiang, Z.-T., Zhao, X., Xu, J., Zhou, Z.-F., et al. (2012). Designing superhard, self-toughening CrAlN coatings through grain boundary engineering. *Acta Mater.* 60, 5735–5744. doi: 10.1016/j.actamat.2012.06.049

Lindroos, B., Mäenpää, K., Ylikomi, T., Oja, H., Suuronen, R., and Miettinen, S. (2008). Characterisation of human dental stem cells and buccal mucosa fibroblasts. *Biochem. Biophys. Res. Commun.* 368, 329–335. doi: 10.1016/j.bbrc.2008.01.081

Liu, G., Li, Y., Sun, J., Zhou, H., Zhang, W., Cui, L., et al. (2009). *In vitro* and *in vivo* evaluation of osteogenesis of human umbilical cord blood-derived mesenchymal stem cells on partially demineralized bone matrix. *Tissue Eng. Part A* 16, 971–982. doi: 10.1089/ten.tea.2009.0516

Liu, G., Zhao, L., Zhang, W., Cui, L., Liu, W., and Cao, Y. (2008). Repair of goat tibial defects with bone marrow stromal cells and beta-tricalcium phosphate. *J. Mater. Sci. Mater. Med.* 19, 2367–2376. doi: 10.1007/s10856-007-3348-3

Liu, Y., Lim, J., and Teoh, S. H. (2013). Review: development of clinically relevant scaffolds for vascularised bone tissue engineering. *Biotechnol. Adv.* 31, 688–705. doi: 10.1016/j.biotechadv.2012.10.003

Lu, J., Blary, M. C., Vavasseur, S., Descamps, M., Anselme, K., and Hardouin, P. (2004). Relationship between bioceramics sintering and micro-particles-induced cellular damages. *J. Mater. Sci. Mater. Med.* 15, 361–365. doi: 10.1023/B:Jmsm.0000021102.68509.65

Ma, Y., Zhang, W., Wang, Z., Wang, Z., Xie, Q., Niu, H., et al. (2016). PEGylated poly(glycerol sebacate)-modified calcium phosphate scaffolds with desirable mechanical behavior and enhanced osteogenic capacity. *Acta Biomater.* 44, 110–124. doi: 10.1016/j.actbio.2016.08.023

Maes, C., Kobayashi, T., Selig, M. K., Torrekens, S., Roth, S. I., Mackem, S., et al. (2010). Osteoblast precursors, but not mature osteoblasts, move into developing and fractured bones along with invading blood vessels. *Dev. Cell* 19, 329–344. doi: 10.1016/j.devcel.2010.07.010

Manassero, M., Viateau, V., Deschepper, M., Oudina, K., Logeart-Avramoglou, D., Petite, H., et al. (2013). Bone regeneration in sheep using acropora coral, a natural resorbable scaffold, and autologous mesenchymal stem cells. *Tissue Eng. Part A* 19, 1554–1563. doi: 10.1089/ten.TEA.2012.0008

Maraldi, T., Riccio, M., Pisciotta, A., Zavatti, M., Carnevale, G., Beretti, F., et al. (2013). Human amniotic fluid-derived and dental pulp-derived stem cells seeded into collagen scaffold repair critical-size bone defects promoting vascularization. *Stem Cell Res. Ther.* 4, 53–53. doi: 10.1186/scrt203

Marcacci, M., Kon, E., Moukhachev, V., Lavroukov, A., Kutepov, S., Quarto, R., et al. (2007). Stem cells associated with macroporous bioceramics for long bone repair: 6-to 7-year outcome of a pilot clinical study. *Tissue Eng.* 13, 947–955. doi: 10.1089/ten.2006.0271

Mareschi, K., Ferrero, I., Rustichelli, D., Aschero, S., Gammaitoni, L., Aglietta, M., et al. (2006). Expansion of mesenchymal stem cells isolated from pediatric and adult donor bone marrow. *J. Cell Biochem.* 97, 744–754. doi: 10.1002/jcb.20681

Marsell, R., and Einhorn, T. A. (2011). The biology of fracture healing. *Injury* 42, 551–555. doi: 10.1016/j.injury.2011.03.031

Masaoka, T., Yoshii, T., Yuasa, M., Yamada, T., Taniyama, T., Torigoe, I., et al. (2016). Bone defect regeneration by a combination of a β-tricalcium phosphate scaffold and bone marrow stromal cells in a non-human primate model. *Open Biomed. Eng. J.* 10, 2–11. doi: 10.2174/1874120701610010002

Mastrogiacomo, M., Papadimitropoulos, A., Cedola, A., Peyrin, F., Giannoni, P., Pearce, S. G., et al. (2007). Engineering of bone using bone marrow stromal cells and a silicon-stabilized tricalcium phosphate bioceramic: evidence for a coupling between bone formation and scaffold resorption. *Biomaterials* 28, 1376–1384. doi: 10.1016/j.biomaterials.2006.10.001

Mathieu, M., Rigutto, S., Ingels, A., Spruyt, D., Stricwant, N., Kharroubi, I., et al. (2013). Decreased pool of mesenchymal stem cells is associated with altered chemokines serum levels in atrophic nonunion fractures. *Bone* 53, 391–398. doi: 10.1016/j.bone.2013.01.005

Mehboob, H., and Chang, S.-H. (2014). Application of composites to orthopedic prostheses for effective bone healing: a review. *Comp. Struct.* 118, 328–341. doi: 10.1016/j.compstruct.2014.07.052

Mennan, C., Wright, K., Bhattacharjee, A., Balain, B., Richardson, J., and Roberts, S. (2013). Isolation and characterisation of mesenchymal stem cells from different regions of the human umbilical cord. *Biomed. Res. Int.* 2013, 916136–916138. doi: 10.1155/2013/916136

Meseguer Olmo, L., Vicente Ortega, V., Alcaraz Baños, M., Calvo Guirado José, L., Vallet Reg,í, M., Arcos, D., et al. (2012). *In-vivo* behavior of Si-hydroxyapatite/polycaprolactone/DMB scaffolds fabricated by 3D printing. *J. Biomed. Mater. Res. A* 101A, 2038–2048. doi: 10.1002/jbm.a.34511

Mesimäki K, Lindroos, B., Tornwall, J., Mauno, J., Lindqvist, C., Kontio, R., et al. (2009). Novel maxillary reconstruction with ectopic bone formation by GMP adipose stem cells. *Int. J. Oral Maxillofac. Surg.* 38, 201–209. doi: 10.1016/j.ijom.2009.01.001

Miao, C., Zhou, L., Tian, L., Zhang, Y., Zhang, W., Yang, F., et al. (2017). Osteogenic differentiation capacity of *in vitro* cultured human skeletal muscle for expedited bone tissue engineering. *Biomed. Res. Int.* 2017, 8619385–8619387. doi: 10.1155/2017/8619385

Mishima, Y., and Lotz, M. (2008). Chemotaxis of human articular chondrocytes and mesenchymal stem cells. *J. Orthop. Res.* 26, 1407–1412. doi: 10.1002/jor.20668

Mont, M. A., Carbone, J. J., and Fairbank, A. C. (1996). Core decompression versus nonoperative management for osteonecrosis of the hip. *Clin. Orthop. Relat. Res.* 169–178

Nair, M. B., Varma, H. K., Menon, K. V., Shenoy, S. J., and John, A. (2008). Tissue regeneration and repair of goat segmental femur defect with bioactive triphasic ceramic-coated hydroxyapatite scaffold. *J. Biomed. Mater. Res.* 91A, 855–865. doi: 10.1002/jbm.a.32239

Nair, M. B., Varma, H. K., Menon, K. V., Shenoy, S. J., and John, A. (2009). Reconstruction of goat femur segmental defects using triphasic ceramic-coated hydroxyapatite in combination with autologous cells and platelet-rich plasma. *Acta Biomater.* 5, 1742–1755. doi: 10.1016/j.actbio.2009.01.009

Nakamura, A., Akahane, M., Shigematsu, H., Tadokoro, M., Morita, Y., Ohgushi, H., et al. (2010). Cell sheet transplantation of cultured mesenchymal stem cells enhances bone formation in a rat nonunion model. *Bone* 46, 418–424. doi: 10.1016/j.bone.2009.08.048

Narcisi, R., Quarto, R., Ulivi, V., Muraglia, A., Molfetta, L., and Giannoni, P. (2011). TGF β-1 administration during *ex vivo* expansion of human articular chondrocytes in a serum-free medium redirects the cell phenotype toward hypertrophy. *J. Cell Physiol.* 227, 3282–3290. doi: 10.1002/jcp.24024

Nash, T. J., Howlett, C. R., Martin, C., Steele, J., Johnson, K. A., and Hicklin, D. J. (1994). Effect of platelet-derived growth factor on tibial osteotomies in rabbits. *Bone* 15, 203–208.

Nevins, M., Giannobile, W. V., McGuire, M. K., Kao, R. T., Mellonig, J. T., Hinrichs, J. E., et al. (2005). Platelet-derived growth factor stimulates bone fill and rate of attachment level gain: results of a large multicenter randomized controlled trial. *J. Periodontol.* 76, 2205–2215. doi: 10.1902/jop.2005.76.12.2205

Niemeyer, P., Krause, U., Fellenberg, J., Kasten, P., Seckinger, A., Ho, A. D., et al. (2004). Evaluation of mineralized collagen and alpha-tricalcium phosphate as scaffolds for tissue engineering of bone using human mesenchymal stem cells. *Cells Tissues Organs* 177, 68–78. doi: 10.1159/000079182

Niemeyer, P., Schönberger, T. S., Hahn, J., Kasten, P., Fellenberg, J., Suedkamp, N., et al. (2010). Xenogenic transplantation of human mesenchymal stem cells in a critical size defect of the sheep tibia for bone regeneration. *Tissue Eng.* 16, 33–43. doi: 10.1089/ten.TEA.2009.0190

Ogata, Y., Mabuchi, Y., Yoshida, M., Suto, E. G., Suzuki, N., Muneta, T., et al. (2015). purified human synovium mesenchymal stem cells as a good resource for cartilage regeneration. *PLoS ONE* 10:e0129096. doi: 10.1371/journal.pone.0129096

O'Keefe, R. J., and Mao, J. (2011). Bone tissue engineering and regeneration: from discovery to the clinic—an overview. *Tissue Eng. Part B Rev.* 17, 389–392. doi: 10.1089/ten.teb.2011.0475

Oliveira, S. M., Mijares, D. Q., Turner, G., Amaral, I. F., Barbosa, M. A., and Teixeira, C. C. (2008). Engineering endochondral bone: *in vivo* studies. *Tissue Eng. Part A* 15, 635–643. doi: 10.1089/ten.tea.2008.0052

Olivier, E. N., Rybicki, A. C., and Bouhassira, E. E. (2006). Differentiation of human embryonic stem cells into bipotent mesenchymal stem cells. *Stem Cells* 24, 1914–1922. doi: 10.1634/stemcells.2005-0648

Owston, H., Giannoudis, P. V., and Jones, E. (2016). Do skeletal muscle MSCs in humans contribute to bone repair? A systematic review. *Injury* 47(Suppl. 6), S3–S15. doi: 10.1016/S0020-1383(16)30834-8

Parsons, A. J., Ahmed, I., Haque, P., Fitzpatrick, B., Niazi, M. I. K., Walker, G. S., et al. (2009). Phosphate glass fibre composites for bone repair. *J. Bionic Eng.* 6, 318–323. doi: 10.1016/S1672-6529(08)60132-8

Peterson, B., Zhang, J., Iglesias, R., Kabo, M., Hedrick, M., Benhaim, P., et al. (2005). Healing of critically sized femoral defects, using genetically modified mesenchymal stem cells from human adipose tissue. *Tissue Eng.* 11, 120–129. doi: 10.1089/ten.2005.11.120

Petite, H., Viateau, V., Bensaid, W., Meunier, A., de Pollak, C., Bourguignon, M., et al. (2000). Tissue-engineered bone regeneration. *Nat. Biotechnol.* 18, 959–963. doi: 10.1038/79449

Quarto, R., Mastrogiacomo, M., Cancedda, R., Kutepov, S. M., Mukhachev, V., Lavroukov, A., et al. (2001). Repair of large bone defects with the use of autologous bone marrow stromal cells. *N. Engl. J. Med.* 344, 385–386. doi: 10.1056/NEJM200102013440516

Rabie, A. B., and Lu, M. (2004). Basic fibroblast growth factor up-regulates the expression of vascular endothelial growth factor during healing of allogeneic bone graft. *Arch. Oral Biol.* 49, 1025–1033. doi: 10.1016/j.archoralbio.2004.05.012

Radke, S., Rader, C., Kenn, W., Kirschner, S., Walther, M., and Eulert, J. (2003). Transient marrow edema syndrome of the hip: results after core decompression. a prospective MRI-controlled study in 22 patients. *Arch. Orthop. Trauma Surg.* 123, 223–227. doi: 10.1007/s00402-003-0506-z

Raggatt, L. J., and Partridge, N. C. (2010). Cellular and molecular mechanisms of bone remodeling. *J. Biol. Chem* 285, 25103–25108. doi: 10.1074/jbc.R109.041087

Reichert, J. C., Cipitria, A., Epari, D. R., Saifzadeh, S., Krishnakanth, P., Berner, A., et al. (2012). A tissue engineering solution for segmental defect regeneration in load-bearing long bones. *Sci. Transl. Med.* 4:141ra93. doi: 10.1126/scitranslmed.3003720

Richards, M., Richards, M., Tan, S., Fong, C.-Y., Biswas, A., Chan, W.-K., et al. (2003). Comparative evaluation of various human feeders for prolonged undifferentiated growth of human embryonic stem cells. *Stem Cells* 21, 546–556. doi: 10.1634/stemcells.21-5-546

Ryan, A. M., Eppler, D. B., Hagler, K. E., Bruner, R. H., Thomford, P. J., Hall, R. L., et al. (1999). Preclinical safety evaluation of rhuMAbVEGF, an antiangiogenic humanized monoclonal antibody. *Toxicol. Pathol.* 27, 78–86. doi: 10.1177/019262339902700115

Sakaguchi, Y., Sekiya, I., Yagishita, K., and Muneta, T. (2005). Comparison of human stem cells derived from various mesenchymal tissues - Superiority of synovium as a cell source. *Arthritis Rheum* 52, 2521–2529. doi: 10.1002/art.21212

Salgado, A. J., Coutinho, O. P., and Reis, R. L. (2004). Bone tissue engineering: state of the art and future trends. *Macromol. Biosci.* 4, 743–765. doi: 10.1002/mabi.200400026

Schimming, R. (2004). Tissue-engineered bone for maxillary sinus augmentation. *J. Oral Maxillofac. Surg.* 62, 724–729. doi: 10.1016/j.joms.2004.01.009

Scotti, C., Piccinini, E., Takizawa, H., Todorov, A., Bourgine, P., Papadimitropoulos, A., et al. (2013). Engineering of a functional bone organ through endochondral ossification. *Proc. Natl. Acad. Sci. U.S.A.* 110:3997. doi: 10.1073/pnas.1220108110

Secco, M., Zucconi, E., Vieira Natassia, M., Fogaça Luciana, L. Q., Cerqueira, A., Carvalho Maria Denise, F., et al. (2009). Multipotent stem cells from umbilical cord: cord is richer than blood! *Stem Cells* 26, 146–150. doi: 10.1634/stemcells.2007-0381

Seck, T., Scheppach, B., Scharla, S., Diel, I., Blum, W. F., Bismar, H., et al. (1998). Concentration of insulin-like growth factor (IGF)-I and -II in iliac crest bone matrix from pre- and postmenopausal women: relationship to age, menopause, bone turnover, bone volume, and circulating

IGFs. *J. Clin. Endocrinol. Metab.* 83, 2331–2337. doi: 10.1210/jcem.83.7.4967

Shimizu, T., Akahane, M., Morita, Y., Omokawa, S., Nakano, K., Kira, T., et al. (2015). The regeneration and augmentation of bone with injectable osteogenic cell sheet in a rat critical fracture healing model. *Injury* 46, 1457–1464. doi: 10.1016/j.injury.2015.04.031

Shirley, D., Marsh, D., Jordan, G., McQuaid, S., and Li, G. (2005). Systemic recruitment of osteoblastic cells in fracture healing. *J. Orthop. Res.* 23, 1013–1021. doi: 10.1016/j.orthres.2005.01.013

Smith, J. O., Tayton, E. R., Khan, F., Aarvold, A., Cook, R. B., Goodship, A., et al. (2017). Large animal *in vivo* evaluation of a binary blend polymer scaffold for skeletal tissue-engineering strategies; translational issues. *J. Tissue Eng. Regen. Med.* 11, 1065–1076. doi: 10.1002/term.2007

Song, Y., Kwon, J., Kim, B., Jeon, Y., Khang, G., and Lee, D. (2011). Physicobiological properties and biocompatibility of biodegradable poly(oxalate-co-oxamide). *J. Biomed. Mater. Res. A* 98A, 517–526. doi: 10.1002/jbm.a.33135

Soucacos, P. N., Dailiana, Z., Beris, A. E., and Johnson, E. O. (2006). Vascularised bone grafts for the management of non-union. *Injury* 37(Suppl. 1), S41–S50. doi: 10.1016/j.injury.2006.02.040

Stacey, G. N., Crook, J. M., Hei, D., and Ludwig, T. (2013). Banking human induced pluripotent stem cells: lessons learned from embryonic stem cells? *Cell Stem Cell* 13, 385–388. doi: 10.1016/j.stem.2013.09.007

Stephenson, M. K., Farris, A. L., and Grayson, W. L. (2017). Recent advances in tissue engineering strategies for the treatment of joint damage. *Curr. Rheumatol. Rep.* 19:44. doi: 10.1007/s11926-017-0671-7

Street, J., Bao, M., deGuzman, L., Bunting, S., Peale, F. V. J., Ferrara, N., et al. (2002). Vascular endothelial growth factor stimulates bone repair by promoting angiogenesis and bone turnover. *Proc. Natl. Acad. Sci. U.S.A.* 99, 9656–9661. doi: 10.1073/pnas.152324099

Sun, H., and Yang, H. L. (2015). Calcium phosphate scaffolds combined with bone morphogenetic proteins or mesenchymal stem cells in bone tissue engineering. *Chin. Med. J.* 128, 1121–1127. doi: 10.4103/0366-6999.155121

Taiani, J. T., Buie, H. R., Campbell, G. M., Manske, S. L., Krawetz, R. J., Rancourt, D. E., et al. (2014). Embryonic stem cell therapy improves bone quality in a model of impaired fracture healing in the mouse; tracked temporally using *in vivo* micro-CT. *Bone* 64, 263–272. doi: 10.1016/j.bone.2014.04.019

Takahashi, K., and Yamanaka, S. (2006). Induction of pluripotent stem cells from mouse embryonic and adult fibroblast cultures by defined factors. *Cell* 126, 663–676. doi: 10.1016/j.cell.2006.07.024

Tang, M., Chen, W., Weir, M. D., Thein-Han, W., and Xu, H. H. (2012). Human embryonic stem cell encapsulation in alginate microbeads in macroporous calcium phosphate cement for bone tissue engineering. *Acta Biomater.* 8, 3436–3445. doi: 10.1016/j.actbio.2012.05.016

Tang, Y., Wu, X., Lei, W., Pang, L., Wan, C., Shi, Z., et al. (2009). TGF-beta1-induced migration of bone mesenchymal stem cells couples bone resorption with formation. *Nat. Med.* 15, 757–765. doi: 10.1038/nm.1979

Thompson E, M., Matsiko, A., Farrell, E., Kelly, D. J., and O'Brien, F. J. (2014). Recapitulating endochondral ossification: a promising route to *in vivo* bone regeneration. *J. Tissue Eng. Regen. Med.* 9, 889–902. doi: 10.1002/term.1918

Thomson, J. A., Itskovitz-Eldor, J., Shapiro, S. S., Waknitz, M. A., Swiergiel, J. J., Marshall, V. S., et al. (1998). Embryonic stem cell lines derived from human blastocysts. *Science* 282, 1145–1147.

Todeschi, M. R., El Backly, R., Capelli, C., Daga, A., Patrone, E., Introna, M., et al. (2015). Transplanted umbilical cord mesenchymal stem cells modify the *in vivo* microenvironment enhancing angiogenesis and leading to bone regeneration. *Stem Cells Dev* 24, 1570–1581. doi: 10.1089/scd.2014.0490

Urist, M. R. (1965). Bone: formation by autoinduction. *Science* 150, 893–899.

Valappil, S. P., Misra, S. K., Boccaccini, A. R., and Roy, I. (2006). Biomedical applications of polyhydroxyalkanoates: an overview of animal testing and *in vivo* responses. *Expert Rev. Med. Dev.* 3, 853–868. doi: 10.1586/17434440.3.6.853

Viateau, V., Guillemin, G., Bousson, V., Oudina, K., Hannouche, D., Sedel, L., et al. (2007). Long-bone critical-size defects treated with tissue-engineered grafts: a study on sheep. *J. Orthop. Res.* 25, 741–749. doi: 10.1002/jor.20352

Villa, J. C., Husain, S., van der List, J. P., Gianakos, A., and Lane, J. M. (2016). Treatment of pre-collapse stages of osteonecrosis of the femoral head: a systematic review of randomized control trials. *HSS J* 12, 261–271. doi: 10.1007/s11420-016-9505-9

Vinardell, T., Sheehy, E. J., Buckley, C. T., and Kelly, D. J. (2012). A comparison of the functionality and *in vivo* phenotypic stability of cartilaginous tissues engineered from different stem cell sources. *Tissue Eng. Part A* 18, 1161–1170. doi: 10.1089/ten.TEA.2011.0544

Wang, D. S., Miura, M., Demura, H., and Sato, K. (1997). Anabolic effects of 1,25-dihydroxyvitamin D3 on osteoblasts are enhanced by vascular endothelial growth factor produced by osteoblasts and by growth factors produced by endothelial cells. *Endocrinology* 138, 2953–2962. doi: 10.1210/endo.138.7.5275

Wang, Q., Huang, C., Xue, M., and Zhang, X. (2011). Expression of endogenous BMP-2 in periosteal progenitor cells is essential for bone healing. *Bone* 48, 524–532. doi: 10.1016/j.bone.2010.10.178

Wang, Z., Wang, Z., Lu, W. W., Zhen, W., Yang, D., and Peng, S. (2017). Novel biomaterial strategies for controlled growth factor delivery for biomedical applications. *NPG Asia Materials* 9:e435. doi: 10.1038/am.2017.171

Watanabe, Y., Harada, N., Sato, K., Abe, S., Yamanaka, K., and Matushita, T. (2016). Stem cell therapy: is there a future for reconstruction of large bone defects? *Injury* 47(Suppl. 1), S47–S51. doi: 10.1016/S0020-1383(16)30012-2

Watson, N., Divers, R., Kedar, R., Mehindru, A., Mehindru, A., Borlongan, M. C., et al. (2015). Discarded Wharton's jelly of the human umbilical cord: a viable source for mesenchymal stem cells. *Cytotherapy* 17, 18–24. doi: 10.1016/j.jcyt.2014.08.009

Weiss, H. E., Roberts, S. J., Schrooten, J., and Luyten, F. P. (2012). A semi-autonomous model of endochondral ossification for developmental tissue engineering. *Tissue Eng. Part A* 18, 1334–1343. doi: 10.1089/ten.tea.2011.0602

Westhauser, F., Weis, C., Prokscha, M., Bittrich, L. A., Li, W., Xiao, K., et al. (2016). Three-dimensional polymer coated 45S5-type bioactive glass scaffolds seeded with human mesenchymal stem cells show bone formation *in vivo*. *J. Mater. Sci. Mater. Med.* 27:119. doi: 10.1007/s10856-016-5732-3

White, A. P., Vaccaro, A. R., Hall, J. A., Whang, P. G., Friel, B. C., and McKee, M. D. (2007). Clinical applications of BMP-7/OP-1 in fractures, nonunions and spinal fusion. *Int. Orthop.* 31, 735–741. doi: 10.1007/s00264-007-0422-x

White, A., and Wallis, G. (2001). Endochondral ossification: a delicate balance between growth and mineralisation. *Curr. Biol.* 11, R589–R591. doi: 10.1016/S0960-9822(01)00359-1

Woll, N. L., Heaney, J. D., and Bronson, S. K. (2006). Osteogenic nodule formation from single embryonic stem cell-derived progenitors. *Stem Cells Dev.* 15, 865–879. doi: 10.1089/scd.2006.15.865

Woodell-May, J. E., Tan, M. L., King, W. J., Swift, M. J., Welch, Z. R., Murphy, M. P., et al. (2015). Characterization of the cellular output of a point-of-care device and the implications for addressing critical limb ischemia. *Biores. Open Access* 4, 417–424. doi: 10.1089/biores.2015.0006

Woodruff, M. A., and Hutmacher, D. W. (2010). The return of a forgotten polymer-Polycaprolactone in the 21st century. *Prog. Polym. Sci.* 35, 1217–1256. doi: 10.1016/j.progpolymsci.2010.04.002

Wu, A. C., Wu, A. C., Raggatt, L. J., Raggatt, L. J., Alexander, K. A., Alexander, K. A., et al. (2013). Unraveling macrophage contributions to bone repair. *Bonekey Rep.* 2:373. doi: 10.1038/bonekey.2013.107

Wu, F., Wei, J., Liu, C., O'Neill, B., and Ngothai, Y. (2012). Fabrication and properties of porous scaffold of zein/PCL biocomposite for bone tissue engineering. *Comp. Part B Eng.* 43, 2192–2197. doi: 10.1016/j.compositesb.2012.02.040

Xian, L., Wu, X., Pang, L., Lou, M., Rosen, C. J., Qiu, T., et al. (2012). Matrix IGF-1 maintains bone mass by activation of mTOR in mesenchymal stem cells. *Nat. Med.* 18, 1095–1101. doi: 10.1038/nm.2793

Yang, L., Wang, Q., Peng, L., Yue, H., and Zhang, Z. (2015). Vascularization of repaired limb bone defects using chitosan-β-tricalcium phosphate composite as a tissue engineering bone scaffold. *Mol. Med. Rep.* 12, 2343–2347. doi: 10.3892/mmr.2015.3653

Yang, X. B., Roach, H. I., Clarke, N. M., Howdle, S. M., Quirk, R., Shakesheff, K. M., et al. (2001). Human osteoprogenitor growth and differentiation on synthetic biodegradable structures after surface modification. *Bone* 29, 523–531. doi: 10.1016/s8756-3282(01)00617-2

Yoon, D., Kang, B. J., Kim, Y., Lee, S. H., Rhew, D., Kim, W. H., et al. (2015). Effect of serum-derived albumin scaffold and canine adipose tissue-derived mesenchymal stem cells on osteogenesis in canine segmental bone defect model. *J. Vet. Sci.* 16, 397–404. doi: 10.4142/jvs.2015.16.4.397

Younger, E. M., and Chapman, M. W. (1989). Morbidity at bone graft donor sites. *J. Orthop. Trauma* 3, 192–195.

Zhao, D., Cui, D., Wang, B., Tian, F., Guo, L., Yang, L., et al. (2012). Treatment of early stage osteonecrosis of the femoral head with autologous implantation of bone marrow-derived and cultured mesenchymal stem cells. *Bone* 50, 325–330. doi: 10.1016/j.bone.2011.11.002

Zhu, L., Chuanchang, D., Wei, L., Yilin, C., and Jiasheng, D. (2010). Enhanced healing of goat femur-defect using BMP7 gene-modified BMSCs and load-bearing tissue-engineered bone. *J. Orthop. Res.* 28, 412–418. doi: 10.1002/jor.20973

Zhu, L., Liu, W., Cui, L., and Cao, Y. (2006). Tissue-engineered bone repair of goat-femur defects with osteogenically induced bone marrow stromal cells. *Tissue Eng.* 12, 423–433. doi: 10.1089/ten.2006.12.423

Zuk, P. A., Zhu, M., Ashjian, P., De Ugarte, D. A., Huang, J. I., Mizuno, H., et al. (2002). Human adipose tissue is a source of multipotent stem cells. *Mol. Biol. Cell* 13, 4279–4295. doi: 10.1091/mbc.E02-02-0105

Zuk, P. A., Zhu, M., Mizuno, H., Huang, J., Futrell, J. W., Katz, A. J., et al. (2001). Multilineage cells from human adipose tissue: implications for cell-based therapies. *Tissue Eng.* 7, 211–228. doi: 10.1089/107632701300062859

Conflict of Interest Statement: The authors declare that the research was conducted in the absence of any commercial or financial relationships that could be construed as a potential conflict of interest.

frontiers in Bioengineering and Biotechnology

MINI REVIEW
published: 14 March 2018
doi: 10.3389/fbioe.2018.00022

Interplay of Inflammatory Mediators with Epigenetics and Cartilage Modifications in Osteoarthritis

*Swarna Raman[1], Una FitzGerald[2] and J. Mary Murphy[1]**

[1] Orthobiology, Regenerative Medicine Institute, National University of Ireland Galway, Galway, Ireland, [2] School of Natural Sciences, National University of Ireland Galway, Galway, Ireland

Osteoarthritis (OA), a degenerative disease of diarthrodial joints, is influenced by mechanical and inflammatory factors with aging, obesity, chronic injuries, and secondary diseases thought to be major factors driving the process of articular cartilage degeneration. Chondrocytes, the cellular component of cartilage, reside in an avascular environment and normally have limited potential to replicate. However, extrinsic factors such as injury to the joint or intrinsic alterations to the chondrocytes themselves can lead to an altered phenotype and development of OA. Synovial inflammation is also a pivotal element of the osteoarthritic, degenerative process: influx of pro-inflammatory cytokines and production of matrix metalloproteinases accelerate advanced cellular processes such as synovitis and cartilage damage. As well as a genetic input, recent data have highlighted epigenetic factors as contributing to disease. Studies conducted over the last decade have focused on three key aspects in OA; inflammation and the immune response, genome-wide association studies that have identified important genes undergoing epigenetic modifications, and finally how chondrocytes transform in their function during development and disease. Data highlighted here have identified critical inflammatory genes involved in OA and how these factors impact chondrocyte hypertrophy in the disease. This review also addresses key inflammatory factors in synovial inflammation, epigenetics, and chondrocyte fate, and how agents that inhibit epigenetic mechanisms like DNA methylation and histone modifications could aid in development of long-term treatment strategies for the disease.

Keywords: inflammation, chondrocytes, osteoarthritis, epigenetics, cartilage, methylation, microRNA, hypertrophy

OPEN ACCESS

Edited by:
Roberto Narcisi, Erasmus Medical Center, Erasmus University Rotterdam, Netherlands

Reviewed by:
Wan-ju Li, University of Wisconsin-Madison, United States
Andrea Barbero, University Hospital of Basel, Switzerland

****Correspondence:***
J. Mary Murphy
mary.murphy@nuigalway.ie

Specialty section:
This article was submitted to Tissue Engineering and Regenerative Medicine, a section of the journal Frontiers in Bioengineering and Biotechnology

Received: *17 December 2017*
Accepted: *22 February 2018*
Published: *14 March 2018*

Citation:
Raman S, FitzGerald U and Murphy JM (2018) Interplay of Inflammatory Mediators with Epigenetics and Cartilage Modifications in Osteoarthritis. Front. Bioeng. Biotechnol. 6:22. doi: 10.3389/fbioe.2018.00022

INTRODUCTION

Osteoarthritis (OA) is the most common musculoskeletal disorder impacting life quality of patients with about 35–40 million Europeans and ~355 million affected worldwide (Barry and Murphy, 2013; Mobasheri, 2013). With the disease predominantly affecting the aging population, the impact of OA is set to increase exponentially in coming decades (Kim et al., 2015). Understanding of OA has progressed from what was regarded as a condition affecting articular cartilage to the concept that the disease process has broader consequences affecting all joint tissues, including the synovium and ligaments as well as the underlying subchondral bone (Gupta et al., 2012; Barry and Murphy, 2013) and is characterized as a whole-joint disease. OA is also a multifaceted disease based on recent findings that, apart from cellular and molecular mechanisms, inflammation, metabolic processes, and epigenetic modifications (Shen et al., 2017) are involved in the pathogenesis and progression of

the disease (Blanco and Rego-Perez, 2014; Ishijima et al., 2014; Courties et al., 2015).

CARTILAGE AND ASSOCIATED COMPONENTS

Articular cartilage is a highly specialized connective tissue that ensures normal function and optimal load-bearing capacity (Sophia Fox et al., 2009). It coordinates with the synovial membrane and associated synovial fluid to bring about frictionless movement. The components of articular cartilage are the extracellular matrix (ECM) with sparsely distributed specialized cells called chondrocytes, collagen fibers (mainly type II and IX), proteoglycans, water, and a small volume of non-collagenous proteins and glycoproteins such as fibronectin (Sophia Fox et al., 2009). Chondrocytes are indispensable for the development, maintenance, and repair of the cartilaginous ECM. They are highly specialized, non-proliferating cells with adult articular cartilage being an avascular tissue in nature (Goldring et al., 2011; den Hollander et al., 2015). Under normal conditions, permanent hyaline cartilage found in articulating joints does not undergo terminal differentiation (van der Kraan and van den Berg, 2012). However, based on *in vitro* and *in vivo* evidence, re-programming of articular chondrocytes toward a hypertrophic, degradative phenotype frequently occurs as OA develops (van der Kraan and van den Berg, 2007, 2012). OA chondrocytes behave like terminally differentiated chondrocytes in the growth plate with processes such as aging, biomechanical stress, inflammation, and altered methylation status triggering abnormal phenotypic changes with active production of metalloproteinases, particularly matrix metalloproteinases (MMP)-13 for example (van der Kraan and van den Berg, 2012).

With respect to the collagen network, the complex triple helical structure of the collagen type II α-polypeptide chains along with associated collagenous and non-collagenous matrix proteins provides vital sheer and tensile properties to stabilize the matrix (Goldring, 2000a,b). Aggrecan (ACAN) is the most abundant proteoglycan, followed by decorin, biglycan, and fibromodulin. The interaction of ACAN with hyaluronan through link protein to form proteoglycan aggregates is optimal for resisting compressive loads (Sophia Fox et al., 2009). Other associated matrix components playing a vital role in cartilage structure and function in association with the collagen network include, small leucine-rich proteoglycans, like decorin, biglycan, fibromodulin, and lumican (Heinegard et al., 2006). Therefore, in OA, local loss of proteoglycan and cleavage of type II collagen at the cartilage surface results in an influx of water content and loss of tensile strength in the cartilage ECM matrix as lesions progress (Goldring, 2000a,b). Cartilage matrix disruption in OA is usually associated with altered chondrocyte behavior and clustering, which in turn changes the composition of matrix components (Goldring, 2000a,b, Goldring and Otero, 2011). Several studies conducted both *in vitro* and *in vivo* have proved the involvement of pro-inflammatory cytokines and metalloproteinases in matrix disruption. These factors mainly target chondrocytes, causing aberrant expression of catabolic and anabolic genes. Of the matrix-degrading enzymes produced by hypertrophic chondrocytes, MMP-13 is critical in its ability to cleave type II collagen with cleavage products shown to produce OA-like effects in the mouse knee joint (Neuhold et al., 2001; Goldring et al., 2011).

SYNOVIAL INFLAMMATION AND OA

The synovial membrane is vital for maintenance of articular cartilage and the health of the joint as a whole. It functions to (1) secrete synovial fluid for joint lubrication with hyaluronic acid the principal component that provides the required viscosity; (2) supplement nutrition to chondrocytes and draining waste metabolites, and (3) act as the source of synoviocytes, macrophages, and fibroblasts that express a wide range of cellular markers required for specialized functions relating to innate and adaptive immunity (Hettinga, 1979; Scanzello and Goldring, 2012). Inflammation of the synovium, or synovitis, is associated with OA and is seen in both early and late OA (Benito et al., 2005; Sohn et al., 2012). It is believed that inflammation is one of the major causes for acceleration of cartilage destruction and ultimately disease progression (Egloff et al., 2012). Synovitis has also been documented with meniscal injury leading to OA and is associated with pain and dysfunction (Berenbaum, 2013). Synovitis is known to directly influence many clinical symptoms including knee effusion, redness, heat, and swelling (Ayral et al., 1999; Sellam and Berenbaum, 2010). Ultrasonography and MRI have also depicted synovitis in OA and the aforementioned symptoms and synovitis have been associated with the radiographic progression of OA (Ledingham et al., 1995; Iagnocco and Coari, 2000; Benito et al., 2005; Loeuille et al., 2005). Microarray and gene pattern analysis of synovial tissues from patients without radiographic evidence of OA undergoing arthroscopic meniscectomy showed that 43% of patients had synovial inflammation that correlated with traumatic meniscal injury and pain. Synovial biopsy specimens that showed high inflammation scores, recorded a strong chemokine signature, involving significant levels of chemokine ligand-5 (CCL5), CCL7, CCL19, and interleukin-8 (IL-8) (Scanzello et al., 2011).

Synovial inflammation is classically characterized by influx of macrophages and T cells, increased neovascularization, and subsequent secretion of pro-inflammatory cytokines (Sellam and Berenbaum, 2010). The impact of synovitis throughout disease progression was demonstrated by Benito et al. who compared key immunohistological features of inflammation during early and late OA. Immunohistochemical staining of synovial tissue samples with gross synovial hypertrophy showed high expression of markers of inflammatory cell infiltration ($CD4^+$ and $CD68^+$) angiogenesis with increased levels of vascular endothelial growth factor (VEGF), blood vessel formation (factor VIII), and intercellular adhesion molecule-1 and the pro-inflammatory cytokines, tumor necrosis factor-α (TNF-α), and IL1ß in both early and late OA, with significantly higher expression in early OA (Benito et al., 2005). Analysis of proteins in the synovial fluid collected from patients with knee OA showed the presence of 108 different proteins that included plasma proteins, serine protease inhibitors, proteins pertaining to cartilage turnover, and proteins involved in inflammation and immunity (Sohn

et al., 2012). In addition to this, Sohn et al., demonstrated higher levels of pro-inflammatory cytokines like TNF-α, interleukin-6 (IL-6), and VEGF in OA synovial fluid compared to healthy individuals. Analysis of stimulated macrophages derived from TLR-4 deficient and wild-type mice proved that plasma proteins and inflammatory cytokines present in synovial fluid indeed function as damage-associated molecular patterns signaling through TLRs to mediate an early response to injury and damage to the joint (Scanzello et al., 2008; Midwood et al., 2009; Sohn et al., 2012).

EPIGENETIC MECHANISMS AND OA

The term "epigenetics" can be explained as heritable modifications to gene expression/transcription, without altering the underlying DNA sequence (Blanco and Rego-Perez, 2014; Zhang et al., 2015). Mechanisms of epigenetic regulation documented in OA pathogenesis include DNA methylation, histone modification, and non-coding RNAs (Simon and Jeffries, 2017) (Zhang et al., 2015). DNA methylation has been documented in OA as both hypo and hypermethylation that generally occurs in promoter CpG sites of target genes (Im and Choi, 2013). Methylation, ubiquitination, acetylation, sumoylation, and phosphorylation are some of the histone modifications, with methylation and acetylation documented as the most recurrent histone changes in OA (Blanco and Rego-Perez, 2014; Kim et al., 2015). Short ncRNAs such as microRNAs (miRNAs) act as catalytic or regulatory RNAs by binding to specific sites in the 3′-untranslated region of target mRNAs, resulting in mRNA degradation and/or inhibition of translation (Zhang and Wang, 2015; Ramos and Meulenbelt, 2017).

Therefore, like all somatic cells, normal functional adult articular chondrocytes are subjected to epigenetic mechanisms that aid in stabilizing their phenotype. However, certain innate environmental interactions can cause epigenetic changes in chondrocyte gene expression, which are passed on to daughter cells in subsequent divisions (Goldring and Otero, 2011). This generates "modified/altered chondrocytes," with respect to their phenotype and function that is associated with overexpression of cartilage-degrading proteases and inflammatory mediators (Blanco and Rego-Perez, 2014). This process culminates in disruption of cellular homeostasis, causing cartilage ECM degradation and a constant pathological loop involving inflammation and epigenetic modifications resulting in expedited disease progression (**Figure 1**). There is no doubt that OA has a strong genetic component (Valdes and Spector, 2011; Barter et al., 2012; Blanco and Rego-Perez, 2014). However, "low penetrance polymorphisms" in the population, partly due to inheritance of epigenetic modifications, is a reason for limited data generation to aid in the identification of genes responsible for the genetic susceptibility to OA (Valdes and Spector, 2011; Barter et al., 2012). In the last decade or so, candidate gene studies and genome-wide approaches have shown how inflammatory genes are modulated by epigenetic modifications [reviewed in Rogers et al. (2015)]. These data link specific inflammatory mediators, including transcription factors, proteinases, cytokines, chemokines, growth factors, and ECM proteins with a well-defined role of

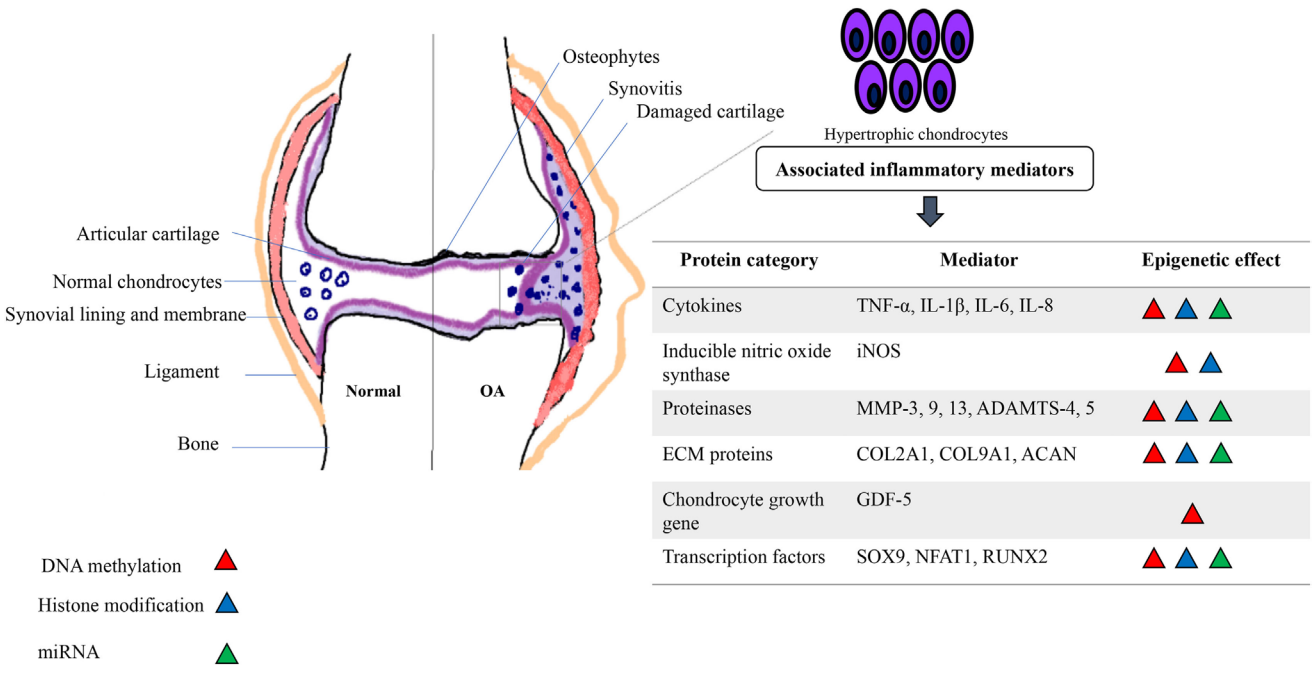

Protein category	Mediator	Epigenetic effect
Cytokines	TNF-α, IL-1β, IL-6, IL-8	▲▲▲
Inducible nitric oxide synthase	iNOS	▲▲
Proteinases	MMP-3, 9, 13, ADAMTS-4, 5	▲▲▲
ECM proteins	COL2A1, COL9A1, ACAN	▲▲▲
Chondrocyte growth gene	GDF-5	▲
Transcription factors	SOX9, NFAT1, RUNX2	▲▲▲

FIGURE 1 | Schematic depicting the association of inflammatory mediators and epigenetic modifications in an osteoarthritic joint. A pathological loop is created due to constant release of cartilage degrading proteins and cytokines and aberrant epigenetic modifications further alter the phenotype and function of normal adult chondrocytes, pushing toward a "hypertrophic state" causing further damage to the joint.

epigenetic changes in OA and induction of synovial inflammation. Interleukin-1 beta (IL-1β) is a classic example of a pro-inflammatory cytokine involved in the immune-pathogenesis of OA that is epigenetically regulated (Goldring et al., 2011; Reynard and Loughlin, 2012) and promotes inflammation of the synovium (Scanzello and Goldring, 2012). It is seen to be elevated in the synovial fluid of OA patients (Sandy et al., 2015) and micro-array analysis of IL-1 gene expression showed that *IL1R,* encoding the IL-1 receptor, is also upregulated in OA (Rogers et al., 2015). In addition to effects on synovial inflammation, epigenetic control of these mediators is also associated with chondrocyte fate toward cartilage destruction and hypertrophic chondrocyte formation.

INFLAMMATORY MEDIATORS AND EPIGENETIC MECHANISMS

Cytokines

Cytokines secreted by immune cells have been known to have pleotropic effects in models of rheumatoid arthritis (RA) for many years (Feldmann et al., 1996). Inflammation is also a driving factor in disease progression in OA with aberrant expression of cytokines a major cause in both animal and human models of the disease (Goldring and Otero, 2011). Among the cytokines studied in OA, tumor necrosis factor-alpha (TNF-α) and interleukin-1 beta (IL-1β) are two of the most extensively researched pro-inflammatory cytokines with respect to their gene activation, methylation status, and their indirect effects on proteinases like MMP-13 (**Table 1**) (Goldring, 2000a,b; Hashimoto et al., 2009, 2013; Kapoor et al., 2011).

Hashimoto et al. studied the epigenetic regulation of IL-1β expression in OA cartilage by analyzing CpG sites in the IL-1β promoter and identified that methylation of CpG site-299 modulated promoter activity by suppression of transcriptional function (Hashimoto et al., 2013). In another study conducted by the same authors, demethylation of the same CpG site in the IL-1β promoter of human articular chondrocytes resulted in elevated transcription of other inflammatory cytokines in response to treatment by IL-1β itself (Hashimoto et al., 2009). In addition to being epigenetically regulated, IL-1β also impacts miRNA production by chondrocytes (Akhtar et al., 2010). Among the miRNAs studied in association with pro-inflammatory cytokines, miRs 140, 149, and 146a have shown a prominent association with human articular cartilage homeostasis, OA pathogenesis, and chondrocyte alteration (Yamasaki et al., 2009; Li et al., 2011; Zhang and Wang, 2015). miR146a was shown to be expressed in low-grade OA with significantly increased expression seen after stimulation with IL-1β (Yamasaki et al., 2009). Downregulation of miR149 in OA chondrocytes revealed its modulatory effect in the actual production of TNF-α, IL-1β, and IL-6 (Santini et al., 2014). IL-1β signaling also modulated the expression of 909 out of 3,459 genes in primary human articular chondrocytes in addition to induction of IL11 and CCL-5 (Saas et al., 2006; Rogers et al., 2015).

The impact of IL-1β expression *via* its promoter activity and the capacity of this cytokine in stimulating other cartilage degrading proteases can be interrogated through the use of histone modification and histone deacetylase inhibitors (HDACi). The process of acetylation is orchestrated by histone acetyltransferases, located on specific lysine residues on the histone N-terminal tails, resulting in the unraveling of the histone and providing access to the DNA structure and transcriptional machinery (Clayton et al., 2006; Barter et al., 2012). HDAC activity is critical for the maintenance of chondrocyte phenotype (Huh et al., 2007) and based on previous reports, HDAC 1 and 2 are upregulated in OA chondrocytes (Hong et al., 2009). Depletion of HDAC7 was also found to be directly proportional to MMP-13 expression (Higashiyama et al., 2010). HDACi have been used in models of RA (Chung et al., 2003) and OA (Chen et al., 2010) to investigate the catabolic activity of HDAC in chondrocytes, and the use of HDACi has elicited beneficial effects by suppressing synovitis, reducing secretion of inflammatory cytokines (particularly IL-1) and preventing the redifferentiation of dedifferentiated chondrocytes (Huh et al., 2007).

Elevation of IL-1β can cause an influx of nitric oxide (NO) (de Andrés et al., 2013), a short-lived, multi-functional inflammatory molecule, expressed in the form of the inducible isoform of NO synthase (iNOS) (**Table 1**) (Charles et al., 1993). However, addition of HDACi, trichostatin, and butyric acid to IL-β-stimulated human chondrocytes suppressed the expression of iNOS and prostaglandin E2 and prevented IL-1-induced proteoglycan release from cartilage explants (Chabane et al., 2008). This clearly depicts the effect of HDACs on IL-1 and in turn on chondrocyte function in OA; further research into HDACi inhibitors could provide directions toward treatment of OA by targeting aberrant epigenetic modifications. Expression of iNOS can also be altered by DNA methylation. When human chondrocytes were co-transfected with nuclear factor kappa-light-chain-enhancer of activated B cells (NF-κB) subunit p65 and an enhancer element carrying the NO gene with or without p50, demethylation of 6 out of 7 CpG sites in the iNOS promoter element was documented, confirming the effect of methylation in iNOS induction (de Andrés et al., 2013).

Interleukin-8, also called CXCL-8, is a more recent inflammatory chemokine to be studied in the context of OA. Alongside IL-1β and leukemia inhibitory factor, IL-8 induces chondrocyte hypertrophy and differentiation (Borzì et al., 1999; Borzi et al., 2002; Merz et al., 2003; Takahashi et al., 2015). In a study conducted by Pierzchala et al. (2011), synovial fluid from OA patients showed significantly increased levels of IL-8 compared to controls (Takahashi et al., 2015). Demethylation of CpG sites in the IL-8 promoter resulted in a 37-fold higher gene expression in cultured chondrocytes from OA patients. On the other hand, *in vitro* DNA methylation reduced basal activity of the IL-8 promoter (**Table 1**) (Takahashi et al., 2015). IL-6 is a macrophage-derived pro-inflammatory cytokine seen in high levels in synovial fibroblasts (SF), with DNA hypo-methylation and histone hyper-acetylation influencing its overexpression in OA. Yang et al. showed that SF from OA patients had significant DNA hypo-methylation at three specific CpG sites in the IL-6 promoter. Similarly, these cells showed increased H3K9/K14 and H4K12 acetylation in the IL-6 promoter region compared to SF from non-arthritic donors. Furthermore, treatment of OA SF

TABLE 1 | Critical genes associated with chondrocyte fate and synovial inflammation.

Critical genes	Protein category	Association	Epigenetic mechanism	Reference
IL-1β	Cytokine	Synovium and chondrocyte alteration	DNA methylation, microRNA (miRNA) (34a, 140a, 146a) histone modification	Hashimoto et al. (2009, 2013); Yamasaki et al. (2009)
Tumor necrosis factor-α	Cytokine	Synovium and chondrocyte alteration	miRNA (149)	Zhang and Wang (2015)
Interleukin-8	Cytokine	Synovium and chondrocyte hypertrophy	DNA methylation	Takahashi et al. (2015)
Interleukin-6	Cytokine	Synovium	DNA methylation and histone modification	Yang et al. (2017)
Nitric oxide (NO)	Isoform of NO synthase release-NF-κB pathway	Synovium and chondrocyte hypertrophy	DNA methylation, histone modification	de Andrés et al. (2013)
Matrix metalloproteinases (MMP)-3	Proteinase	Chondrocyte alteration	DNA methylation	Roach et al. (2005)
MMP-9	Proteinase	Chondrocyte alteration	DNA methylation	Roach et al. (2005)
MMP-13	Proteinase	Synovium and chondrocyte alteration	DNA methylation, miRNA (22, 27a, 27b, 146a) histone modification	Roach et al. (2005); Higashiyama et al. (2010)
ADAMTS-4	Proteinase	Chondrocyte alteration	DNA methylation	Roach et al. (2005); Hashimoto et al. (2009)
ADAMTS-5	Proteinase	Synovium	miRNA (140a, 27a, 27b, 146a)	Goldring and Marcu (2012); Ukai et al. (2012)
COL2A1	Extracellular matrix (ECM) protein	Chondrocyte alteration	Histone modification, miRNA (34a, 675)	Tsuda et al. (2003); Goldring and Marcu (2012); Ukai et al. (2012)
COL9A1	ECM protein	Chondrocyte alteration	DNA methylation	Imagawa et al. (2014)
ACAN	ECM protein	Chondrocyte alteration	Histone modification, miRNA (337)	Pöschl et al. (2005); Huh et al. (2007); Hong et al. (2009); Ukai et al. (2012); Zhong et al. (2012); Im and Choi (2013)
GDF-5	Growth and differentiation factor	Synovium and chondrocyte alteration	DNA methylation(hypo)	Miyamoto et al. (2007); Southam et al. (2007); Egli et al. (2009)
RUNX-2	Transcription factor	Chondrocyte alteration	DNA methylation	Wang et al. (2004); Kamekura et al. (2006); Hecht et al. (2007); Higashikawa et al. (2009)
NFAT1	Transcription factor	Chondrocyte alteration	Histone modification	Rodova et al. (2011); Zhang and Wang (2015)
SOX-9	Transcription factor	Chondrocyte alteration	DNA methylation, miRNA (574-3p), histone modification	Martinez-Sanchez et al. (2012); Kim et al. (2013)

with DNA methyltransferase 3 alpha or anacardic acid, a histone acetyltransferase inhibitor, resulted in increased DNA methylation and decreased histone acetylation, leading to a suppression in IL-6 overexpression (Yang et al., 2017). These studies clearly show the effect of epigenetic mechanisms of cytokines and their subsequent expression during OA and determination of chondrocyte fate.

Transcription Factors

Transcription factors, also known to regulate chondrocyte differentiation, act by controlling the transcriptional rate of target genes and aberrant expression is known to influence OA pathogenesis as a consequence of chondrocyte hypertrophy (van der Kraan and van den Berg, 2012; Zhang and Wang, 2015). Some of the key factors involved in altering chondrocyte fate include Runt-related transcription factor 2 (Runx2), nuclear factor of activated T cells 1 (Nfat1), sex determining region Y-Box 9 (SOX9) (**Table 1**), and hypoxia-inducible factor-2alpha (HIF-2alpha) (van der Kraan and van den Berg, 2012). Recent genome-wide analysis showed that demethylation of 5mC to 5hmC was associated with dynamic expression changes in expression of Runx2 and SOX9 during mouse embryonic skeletal development and early and late chondrogenic differentiation (Taylor et al., 2016). Runx2 controls chondrogenic differentiation, specifically, chondrocyte hypertrophic differentiation, with evidence of elevated expression seen in human OA cartilage and many experimental models (Wang

et al., 2004; Kamekura et al., 2006; Hecht et al., 2007; Higashikawa et al., 2009).

NFAT1 is a well-known regulator of expression of cytokine genes during the immune response, and interestingly, exhibits an age-dependent expression in mouse articular cartilage (Zhang and Wang, 2015). Rodova et al. conducted a study assessing the effect of histone methylation in Nfat1 expression in wild-type and Nfat1-deficient mice. Nfat1 expression in wild-type articular chondrocytes was seen to be low during embryonic stages and increased in adult mice. As a consequence of histone methylation, embryonic articular chondrocytes showed increased Nfat1 expression with a simultaneous increase in H3K4me2, a histone associated with transcriptional activation. However, decreased expression of Nfat1 in 6-month-old articular chondrocytes, correlated with increased H3K9me2 and transcriptional repression, suggestive of the crucial role played by histone methylation in age-related Nfat1 expression (**Table 1**) (Rodova et al., 2011; Zhang and Wang, 2015). This indeed provides the rationale for further study to identify how Nfat1 expression is influenced by epigenetics modifications in human OA.

A key transcription factor for chondrogenesis during the development of skeletal system, SOX9 is one of the earliest markers expressed by mesenchymal stem/stromal cells and is essential for expression of cartilage-specific matrix proteins (Han and Lefebvre, 2008; Zhang and Wang, 2015). Kim et al. (2013) reported the downregulation of SOX9 expression in late stage hip OA chondrocytes due to DNA and histone methylation and histone acetylation. Elevated miR145 in human chondrocytes is also associated with direct repression of SOX9 expression (Martinez-Sanchez et al., 2012).

KEY OA RISK GENE-GROWTH AND DIFFERENTIATION FACTOR 5 (GDF5)

Among many genes subjected to candidate gene association analysis (Ryder et al., 2008) for OA, GDF5 has shown consistent association with OA in the form of a single nucleotide polymorphism rs143383, located in the 5' untranslated region of the gene (**Table 1**) (Chapman et al., 2008). GDF5, an important member of TGF-β superfamily and an extracellular signaling molecule, influences the development, maintenance, and repair of the synovial joint and tissue structures (Khan et al., 2007). Allelic transition from C to T methylation of the associated CpG dinucleotide results in a differential allelic expression (DAE) imbalance, thereby affecting joint tissue. In OA patient joint tissues examined, reduction in GDF5 transcription was found to be a result of a functional rs143383, with the T allele mediating this effect. Additionally, this effect was seen in both older and younger cartilage samples, indicative of a chronic and deeper involvement of DAE imbalance in OA (Miyamoto et al., 2007; Southam et al., 2007; Egli et al., 2009). A similar effect of rs143383 was seen in a mouse model, where a reduction in GDF5 mRNA and protein, recapitulated an OA-like phenotype (Daans et al., 2011). Hence, maintenance of GDF5 protein has been found to be critical for normal joint function (Reynard and Loughlin, 2012).

ECM Proteins

Maintaining optimal amounts of ECM components, such as collagen and proteoglycan, is also crucial for preserving normal articular cartilage architecture and function. Gene mutations of collagen proteins are typically associated with early-onset of OA (Chan et al., 1995). For example, collagen type IX (COL9A1)-deficient mice portray OA-like cartilage degradation (**Table 1**) (Fässler et al., 1994; Saamanen et al., 2000). Histone modifications are also known to affect type-II collagen (COL2A1) gene expression in OA. Histone acetylation at the COL2A1 promoter enhanced its transcription activity due to complex formation of SOX9 with the HAT p300/CBP in chondrocytes (Tsuda et al., 2003; Ramos and Meulenbelt, 2017).

Interactions of HDACi with chondrocytes have conflicting effects on COL2A1, COL9A1, and ACAN gene expression. Short-term HDACi treatment of chondrocytes enhances the expression of these genes, whereas long-term treatment represses their expression. This switch in effects could be attributed to overexpression of HDAC1 and 2 (**Table 1**) (Huh et al., 2007; Hong et al., 2009; Im and Choi, 2013). Hypermethylation at CpG sites in the COL9A1 promoter attenuated SOX9 binding to COL9A1, leading to downregulation of the collagen in OA cartilage (Imagawa et al., 2014). DNA methylation does not influence the CpG sites in the ACAN promoter, unlike HDACs that control ACAN in both normal aged and OA chondrocytes (Pöschl et al., 2005) and miR199a-3p and 193b in human OA chondrocytes (Ukai et al., 2012).

Proteinases

Normal human articular cartilage expresses very low levels of matrix proteinases such as aggrecanases, collagenases, and MMPs with elevated levels in OA associated with ECM degradation and altered chondrocyte phenotype (Burrage et al., 2006; Huang and Wu, 2008). Aggrecanases, ADAMTS (a disintegrin and metalloproteinase with thrombospondin motifs) -4 and -5, and MMPs-3, 9, and 13 are the most prominent proteinases involved in chondrocyte hypertrophy and inflammation with DNA methylation and histone modifications involved in their control (**Table 1**) (Roach et al., 2005; Hashimoto et al., 2009; Ramos and Meulenbelt, 2017). Alteration in chondrocyte phenotype due to changed gene expression is not seen in all OA chondrocytes, but specifically in those proximal to weight-bearing regions and in the surface zone (Roach and Tilley, 2007; Hashimoto et al., 2009). Previous studies have documented elevated expression of MMP-3, 9, 13, and ADAMTS-4 in late-stage OA chondrocytes as a result of hypomethylation of promoter CpG sites (Roach et al., 2005; Cheung et al., 2009; da Silva et al., 2009).

MicroRNAs have a strong role to play in the regulation of MMPs and aggrecanases. ADAMTS-5 expression is highly regulated by miRNA in human OA (Ukai et al., 2012). In a study conducted by Young et al., comparing cultured SW1353 chondrosarcoma cells and primary human chondrocytes, addition of HDACi downregulated the expression of MMP-13, a critical marker of chondrocyte hypertrophy (Higashiyama et al., 2010). In fact, many studies have demonstrated how miR-140, 27a, and 29a directly target MMP-13 (Tardif et al., 2009; Li et al., 2016).

These data expand the possibilities for targeted OA therapy by focusing on miRNA regulation in chondrocyte fate and function.

CONCLUSION

Osteoarthritis is indeed a multifactorial disease underpinned by a complex interplay of inflammation and epigenetic modifications. Genome-wide analyses and studies focused on the identification of candidate OA-risk associated genes conducted in the last decade have thrown light on the mechanism of how chondrocytes undergo hypertrophy and cause progression of the disease. Future studies targeting markers involved in both chondrocyte and synovial hypertrophy could perhaps provide further insight into the use of epigenetic knockdown models and inhibitors to attenuate chondrocyte terminal differentiation and in turn restore cartilage homeostasis.

AUTHOR CONTRIBUTIONS

SR contributed to the development of the concept underpinning the review, researched the relevant literature, and wrote the body of the review. UF also contributed to the concept of the submission and provided guidance on the scientific writing. MM participated in conception and review design, manuscript preparation, on-going and final review of the submission.

FUNDING

SR is funded by a NUI Galway Hardiman scholarship. MM has received funding from the European Union's Horizon 2020 research and innovation program under grant agreements no 667932 (AUTOSTEM) and 643809 (ADIPOA2), and from Science Foundation Ireland/Abbvie (Grant no.13/RC/2073).

REFERENCES

Akhtar, N., Rasheed, Z., Ramamurthy, S., Anbazhagan, A. N., Voss, F. R., and Haqqi, T. M. (2010). MicroRNA-27b regulates the expression of matrix metalloproteinase 13 in human osteoarthritis chondrocytes. *Arthritis Rheum.* 62, 1361–1371. doi:10.1002/art.27329

Ayral, X., Ravaud, P., Bonvarlet, J. P., Simonnet, J., Lecurieux, R., Nguyen, M., et al. (1999). Arthroscopic evaluation of post-traumatic patellofemoral chondropathy. *J. Rheumatol.* 26, 1140–1147.

Barry, F., and Murphy, M. (2013). Mesenchymal stem cells in joint disease and repair. *Nat. Rev. Rheumatol.* 9, 584–594. doi:10.1038/nrrheum.2013.109

Barter, M. J., Bui, C., and Young, D. A. (2012). Epigenetic mechanisms in cartilage and osteoarthritis: DNA methylation, histone modifications and microRNAs. *Osteoarthr. Cartil.* 20, 339–349. doi:10.1016/j.joca.2011.12.012

Benito, M. J., Veale, D. J., FitzGerald, O., van den Berg, W. B., and Bresnihan, B. (2005). Synovial tissue inflammation in early and late osteoarthritis. *Ann. Rheum. Dis.* 64, 1263–1267. doi:10.1136/ard.2004.025270

Berenbaum, F. (2013). Osteoarthritis as an inflammatory disease (osteoarthritis is not osteoarthrosis!). *Osteoarthr. Cartil.* 21, 16–21. doi:10.1016/j.joca.2012.11.012

Blanco, F. J., and Rego-Perez, I. (2014). Editorial: is it time for epigenetics in osteoarthritis? *Arthritis Rheumatol.* 66, 2324–2327. doi:10.1002/art.38710

Borzì, R. M., Mazzetti, I., Macor, S., Silvestri, T., Bassi, A., Cattini, L., et al. (1999). Flow cytometric analysis of intracellular chemokines in chondrocytes in vivo: constitutive expression and enhancement in osteoarthritis and rheumatoid arthritis. *FEBS Lett.* 455, 238–242. doi:10.1016/S0014-5793(99)00886-8

Borzi, R. M., Mazzetti, I., Magagnoli, G., Paoletti, S., Uguccioni, M., Gatti, R., et al. (2002). Growth-related oncogene α induction of apoptosis in osteoarthritis chondrocytes. *Arthritis Rheumatol.* 46, 3201–3211. doi:10.1002/art.10650

Burrage, P. S., Mix, K. S., and Brinckerhoff, C. E. (2006). Matrix metalloproteinases: role in arthritis. *Front. Biosci.* 11:529–543. doi:10.2741/1817

Chabane, N., Zayed, N., Afif, H., Mfuna-Endam, L., Benderdour, M., Boileau, C., et al. (2008). Histone deacetylase inhibitors suppress interleukin-1beta-induced nitric oxide and prostaglandin E2 production in human chondrocytes. *Osteoarthr. Cartil.* 16, 1267–1274. doi:10.1016/j.joca.2008.03.009

Chan, D., Cole, W. G., Chow, C. W., Mundlos, S., and Bateman, J. F. (1995). A COL2A1 mutation in achondrogenesis type II results in the replacement of type II collagen by type I and III collagens in cartilage. *J. Biol. Chem.* 270, 1747–1753. doi:10.1074/jbc.270.4.1747

Chapman, K., Takahashi, A., Meulenbelt, I., Watson, C., Rodriguez-Lopez, J., Egli, R., et al. (2008). A meta-analysis of European and Asian cohorts reveals a global role of a functional SNP in the 5' UTR of GDF5 with osteoarthritis susceptibility. *Hum. Mol. Genet.* 17, 1497–1504. doi:10.1093/hmg/ddn038

Charles, I. G., Palmer, R. M., Hickery, M. S., Bayliss, M. T., Chubb, A. P., Hall, V. S., et al. (1993). Cloning, characterization, and expression of a cDNA encoding an inducible nitric oxide synthase from the human chondrocyte. *Proc. Natl. Acad. Sci. U.S.A* 90, 11419–11423. doi:10.1073/pnas.90.23.11419

Chen, W. P., Bao, J. P., Hu, P. F., Feng, J., and Wu, L. D. (2010). Alleviation of osteoarthritis by Trichostatin A, a histone deacetylase inhibitor, in experimental osteoarthritis. *Mol. Biol. Rep.* 37, 3967–3972. doi:10.1007/s11033-010-0055-9

Cheung, K. S., Hashimoto, K., Yamada, N., and Roach, H. I. (2009). Expression of ADAMTS-4 by chondrocytes in the surface zone of human osteoarthritic cartilage is regulated by epigenetic DNA de-methylation. *Rheumatol. Int.* 29, 525–534. doi:10.1007/s00296-008-0744-z

Chung, Y. L., Lee, M. Y., Wang, A. J., and Yao, L. F. (2003). A therapeutic strategy uses histone deacetylase inhibitors to modulate the expression of genes involved in the pathogenesis of rheumatoid arthritis. *Mol. Ther.* 8, 707–717. doi:10.1016/S1525-0016(03)00235-1

Clayton, A. L., Hazzalin, C. A., and Mahadevan, L. C. (2006). Enhanced histone acetylation and transcription: a dynamic perspective. *Mol. Cell* 23, 289–296. doi:10.1016/j.molcel.2006.06.017

Courties, A., Gualillo, O., Berenbaum, F., and Sellam, J. (2015). Metabolic stress-induced joint inflammation and osteoarthritis. *Osteoarthr. Cartil.* 23, 1955–1965. doi:10.1016/j.joca.2015.05.016

da Silva, M. A., Yamada, N., Clarke, N. M., and Roach, H. I. (2009). Cellular and epigenetic features of a young healthy and a young osteoarthritic cartilage compared with aged control and OA cartilage. *J. Orthop. Res.* 27, 593–601. doi:10.1002/jor.20799

Daans, M., Luyten, F. P., and Lories, R. J. (2011). GDF5 deficiency in mice is associated with instability-driven joint damage, gait and subchondral bone changes. *Ann. Rheum. Dis.* 70, 208–213. doi:10.1136/ard.2010.134619

de Andrés, M. C., Imagawa, K., Hashimoto, K., Gonzalez, A., Roach, H. I., Goldring, M. B., et al. (2013). Loss of methylation in CpG sites in the NF-κB enhancer elements of inducible nitric oxide synthase is responsible for gene induction in human articular chondrocytes. *Arthritis Rheum.* 65, 732–742. doi:10.1002/art.37806

den Hollander, W., Ramos, Y. F., Bomer, N., Elzinga, S., van der Breggen, R., Lakenberg, N., et al. (2015). Transcriptional associations of osteoarthritis-mediated loss of epigenetic control in articular cartilage. *Arthritis Rheumatol.* 67, 2108–2116. doi:10.1002/art.39162

Egli, R. J., Southam, L., Wilkins, J. M., Lorenzen, I., Pombo-Suarez, M., Gonzalez, A., et al. (2009). Functional analysis of the osteoarthritis susceptibility-associated GDF5 regulatory polymorphism. *Arthritis Rheum.* 60, 2055–2064. doi:10.1002/art.24616

Egloff, C., Hugle, T., and Valderrabano, V. (2012). Biomechanics and pathomechanisms of osteoarthritis. *Swiss Med. Wkly.* 142, w13583. doi:10.4414/smw.2012.13583

Fässler, R., Schnegelsberg, P. N., Dausman, J., Shinya, T., Muragaki, Y., McCarthy, M. T., et al. (1994). Mice lacking alpha 1 (IX) collagen develop noninflammatory degenerative joint disease. *Proc. Natl. Acad. Sci. U.S.A* 91, 5070–5074. doi:10.1073/pnas.91.11.5070

Feldmann, M., Brennan, F. M., and Maini, R. N. (1996). Role of cytokines in rheumatoid arthritis. *Annu. Rev. Immunol.* 14, 397–440. doi:10.1146/annurev.immunol.14.1.397

Goldring, M. B. (2000a). Osteoarthritis and cartilage: the role of cytokines. *Curr. Rheumatol. Rep.* 2, 459–465. doi:10.1007/s11926-000-0021-y

Goldring, M. B. (2000b). The role of the chondrocyte in osteoarthritis. *Arthritis Rheum.* 43, 1916–1926. doi:10.1002/1529-0131(200009)43:9<1916::AID-ANR2>3.0.CO;2-I

Goldring, M. B., and Marcu, K. B. (2012). Epigenomic and microRNA-mediated regulation in cartilage development, homeostasis, and osteoarthritis. *Trends Mol. Med.* 18, 109–118. doi:10.1016/j.molmed.2011.11.005

Goldring, M. B., and Otero, M. (2011). Inflammation in osteoarthritis. *Curr. Opin. Rheumatol.* 23, 471–478. doi:10.1097/BOR.0b013e328349c2b1

Goldring, M. B., Otero, M., Plumb, D. A., Dragomir, C., Favero, M., El Hachem, K., et al. (2011). Roles of inflammatory and anabolic cytokines in cartilage metabolism: signals and multiple effectors converge upon MMP-13 regulation in osteoarthritis. *Eur. Cell. Mater.* 21, 202–220. doi:10.22203/eCM.v021a16

Gupta, P. K., Das, A. K., Chullikana, A., and Majumdar, A. S. (2012). Mesenchymal stem cells for cartilage repair in osteoarthritis. *Stem Cell Res Ther.* 3, 25. doi:10.1186/scrt116

Han, Y., and Lefebvre, V. (2008). L-Sox5 and Sox6 drive expression of the aggrecan gene in cartilage by securing binding of Sox9 to a far-upstream enhancer. *Mol. Cell. Biol.* 28, 4999–5013. doi:10.1128/MCB.00695-08

Hashimoto, K., Oreffo, R. O., Gibson, M. B., Goldring, M. B., and Roach, H. I. (2009). DNA demethylation at specific CpG sites in the IL1B promoter in response to inflammatory cytokines in human articular chondrocytes. *Arthritis Rheum.* 60, 3303–3313. doi:10.1002/art.24882

Hashimoto, K., Otero, M., Imagawa, K., de Andres, M. C., Coico, J. M., Roach, H. I., et al. (2013). Regulated transcription of human matrix metalloproteinase 13 (MMP13) and interleukin-1beta (IL1B) genes in chondrocytes depends on methylation of specific proximal promoter CpG sites. *J. Biol. Chem.* 288, 10061–10072. doi:10.1074/jbc.M112.421156

Hecht, J., Seitz, V., Urban, M., Wagner, F., Robinson, P. N., Stiege, A., et al. (2007). Detection of novel skeletogenesis target genes by comprehensive analysis of a Runx2(-/-) mouse model. *Gene Expr. Patterns* 7, 102–112. doi:10.1016/j.modgep.2006.05.014

Heinegard, D., Lorenzo, P., and Saxne, T. (2006). "Non-collagenous proteins; glycoproteins and related proteins," in *Dynamics of Bone and Cartilage Metabolism*, 2nd Edn, eds M. J., Seibel, S. P., Robins, and J. P., Bilezikian (Burlington: Academic Press), 71–84.

Hettinga, D. L. (1979). I. Normal joint structures and their reaction to injury*. *J. Orthop. Sports Phys. Ther.* 1, 16–22. doi:10.2519/jospt.1979.1.1.16

Higashikawa, A., Saito, T., Ikeda, T., Kamekura, S., Kawamura, N., Kan, A., et al. (2009). Identification of the core element responsive to runt-related transcription factor 2 in the promoter of human type X collagen gene. *Arthritis Rheum.* 60, 166–178. doi:10.1002/art.24243

Higashiyama, R., Miyaki, S., Yamashita, S., Yoshitaka, T., Lindman, G., Ito, Y., et al. (2010). Correlation between MMP-13 and HDAC7 expression in human knee osteoarthritis. *Mod. Rheumatol.* 20, 11–17. doi:10.1007/s10165-009-0224-7

Hong, S., Derfoul, A., Pereira-Mouries, L., and Hall, D. J. (2009). A novel domain in histone deacetylase 1 and 2 mediates repression of cartilage-specific genes in human chondrocytes. *FASEB J.* 23, 3539–3552. doi:10.1096/fj.09-133215

Huang, K., and Wu, L. D. (2008). Aggrecanase and aggrecan degradation in osteoarthritis: a review. *J. Int. Med. Res.* 36, 1149–1160. doi:10.1177/147323000803600601

Huh, Y. H., Ryu, J. H., and Chun, J. S. (2007). Regulation of type II collagen expression by histone deacetylase in articular chondrocytes. *J. Biol. Chem.* 282, 17123–17131. doi:10.1074/jbc.M700599200

Iagnocco, A., and Coari, G. (2000). Usefulness of high resolution US in the evaluation of effusion in osteoarthritic first carpometacarpal joint. *Scand. J. Rheumatol.* 29, 170–173. doi:10.1080/030097400750002049

Im, G. I., and Choi, Y. J. (2013). Epigenetics in osteoarthritis and its implication for future therapeutics. *Expert Opin. Biol. Ther.* 13, 713–721. doi:10.1517/14712598.2013.764410

Imagawa, K., de Andrés, M. C., Hashimoto, K., Itoi, E., Otero, M., Roach, H. I., et al. (2014). Association of reduced type IX collagen gene expression in human osteoarthritic chondrocytes with epigenetic silencing by DNA hypermethylation. *Arthritis Rheumatol.* 66, 3040–3051. doi:10.1002/art.38774

Ishijima, M., Kaneko, H., and Kaneko, K. (2014). The evolving role of biomarkers for osteoarthritis. *Ther. Adv. Musculoskelet. Dis.* 6, 144–153. doi:10.1177/1759720X14541175

Kamekura, S., Kawasaki, Y., Hoshi, K., Shimoaka, T., Chikuda, H., Maruyama, Z., et al. (2006). Contribution of runt-related transcription factor 2 to the pathogenesis of osteoarthritis in mice after induction of knee joint instability. *Arthritis Rheum.* 54, 2462–2470. doi:10.1002/art.22041

Kapoor, M., Martel-Pelletier, J., Lajeunesse, D., Pelletier, J.-P., and Fahmi, H. (2011). Role of proinflammatory cytokines in the pathophysiology of osteoarthritis. *Nat. Rev. Rheumatol.* 7, 33–42. doi:10.1038/nrrheum.2010.196

Khan, I. M., Redman, S. N., Williams, R., Dowthwaite, G. P., Oldfield, S. F., and Archer, C. W. (2007). The development of synovial joints. *Curr. Top. Dev. Biol.* 79, 1–36. doi:10.1016/S0070-2153(06)79001-9

Kim, H., Kang, D., Cho, Y., and Kim, J. H. (2015). Epigenetic regulation of chondrocyte catabolism and anabolism in osteoarthritis. *Mol. Cells* 38, 677–684. doi:10.14348/molcells.2015.0200

Kim, K.-I., Park, Y.-S., and Im, G.-I. (2013). Changes in the epigenetic status of the SOX-9 promoter in human osteoarthritic cartilage. *J. Bone Miner. Res.* 28, 1050–1060. doi:10.1002/jbmr.1843

Ledingham, J., Regan, M., Jones, A., and Doherty, M. (1995). Factors affecting radiographic progression of knee osteoarthritis. *Ann. Rheum. Dis.* 54, 53–58. doi:10.1136/ard.54.1.53

Li, X., Gibson, G., Kim, J. S., Kroin, J., Xu, S., van Wijnen, A. J., et al. (2011). MicroRNA-146a is linked to pain-related pathophysiology of osteoarthritis. *Gene* 480, 34–41. doi:10.1016/j.gene.2011.03.003

Li, X., Zhen, Z., Tang, G., Zheng, C., and Yang, G. (2016). MiR-29a and MiR-140 protect chondrocytes against the anti-proliferation and cell matrix signaling changes by IL-1beta. *Mol. Cells* 39, 103–110. doi:10.14348/molcells.2016.2179

Loeuille, D., Chary-Valckenaere, I., Champigneulle, J., Rat, A. C., Toussaint, F., Pinzano-Watrin, A., et al. (2005). Macroscopic and microscopic features of synovial membrane inflammation in the osteoarthritic knee: correlating magnetic resonance imaging findings with disease severity. *Arthritis Rheum.* 52, 3492–3501. doi:10.1002/art.21373

Martinez-Sanchez, A., Dudek, K. A., and Murphy, C. L. (2012). Regulation of human chondrocyte function through direct inhibition of cartilage master regulator SOX9 by microRNA-145 (miRNA-145). *J. Biol. Chem.* 287, 916–924. doi:10.1074/jbc.M111.302430

Merz, D., Liu, R., Johnson, K., and Terkeltaub, R. (2003). IL-8/CXCL8 and growth-related oncogene α/CXCL1 induce chondrocyte hypertrophic differentiation. *J. Immunol.* 171, 4406. doi:10.4049/jimmunol.171.8.4406

Midwood, K., Sacre, S., Piccinini, A. M., Inglis, J., Trebaul, A., Chan, E., et al. (2009). Tenascin-C is an endogenous activator of toll-like receptor 4 that is essential for maintaining inflammation in arthritic joint disease. *Nat. Med.* 15, 774–780. doi:10.1038/nm.1987

Miyamoto, Y., Mabuchi, A., Shi, D., Kubo, T., Takatori, Y., Saito, S., et al. (2007). A functional polymorphism in the 5' UTR of GDF5 is associated with susceptibility to osteoarthritis. *Nat. Genet.* 39, 529–533. doi:10.1038/2005

Mobasheri, A. (2013). The future of osteoarthritis therapeutics: targeted pharmacological therapy. *Curr. Rheumatol. Rep.* 15, 364. doi:10.1007/s11926-013-0364-9

Neuhold, L. A., Killar, L., Zhao, W., Sung, M. L., Warner, L., Kulik, J., et al. (2001). Postnatal expression in hyaline cartilage of constitutively active human collagenase-3 (MMP-13) induces osteoarthritis in mice. *J. Clin. Invest.* 107, 35–44. doi:10.1172/JCI10564

Pierzchala, A. W., Kusz, D. J., and Hajduk, G. (2011). CXCL8 and CCL5 expression in synovial fluid and blood serum in patients with osteoarthritis of the knee. *Arch. Immunol. Ther. Exp.* 59, 151–155. doi:10.1007/s00005-011-0115-4

Pöschl, E., Fidler, A., Schmidt, B., Kallipolitou, A., Schmid, E., and Aigner, T. (2005). DNA methylation is not likely to be responsible for aggrecan down regulation in aged or osteoarthritic cartilage. *Ann. Rheum. Dis.* 64, 477. doi:10.1136/ard.2004.022509

Ramos, Y. F., and Meulenbelt, I. (2017). The role of epigenetics in osteoarthritis: current perspective. *Curr. Opin. Rheumatol.* 29, 119–129. doi:10.1097/BOR.0000000000000355

Reynard, L. N., and Loughlin, J. (2012). Genetics and epigenetics of osteoarthritis. *Maturitas* 71, 200–204. doi:10.1016/j.maturitas.2011.12.001

Roach, H. I., and Tilley, S. (2007). "The pathogenesis of osteoarthritis," in *Bone and Osteoarthritis*, eds F. Bronner and M. C. Farach-Carson (London: Springer London), 1–18.

Roach, H. I., Yamada, N., Cheung, K. S., Tilley, S., Clarke, N. M., Oreffo, R. O., et al. (2005). Association between the abnormal expression of matrix-degrading enzymes by human osteoarthritic chondrocytes and demethylation of specific CpG sites in the promoter regions. *Arthritis Rheum.* 52, 3110–3124. doi:10.1002/art.21300

Rodova, M., Lu, Q., Li, Y., Woodbury, B. G., Crist, J. D., Gardner, B. M., et al. (2011). Nfat1 regulates adult articular chondrocyte function through its age-dependent expression mediated by epigenetic histone methylation. *J. Bone Miner. Res.* 26, 1974–1986. doi:10.1002/jbmr.397

Rogers, E. L., Reynard, L. N., and Loughlin, J. (2015). The role of inflammation-related genes in osteoarthritis. *Osteoarthr. Cartil.* 23, 1933–1938. doi:10.1016/j.joca.2015.01.003

Ryder, J. J., Garrison, K., Song, F., Hooper, L., Skinner, J., Loke, Y., et al. (2008). Genetic associations in peripheral joint osteoarthritis and spinal degenerative disease: a systematic review. *Ann. Rheum. Dis.* 67, 584–591. doi:10.1136/ard.2007.073874

Saamanen, A. K., Salminen, H. J., Dean, P. B., De Crombrugghe, B., Vuorio, E. I., and Metsaranta, M. P. (2000). Osteoarthritis-like lesions in transgenic mice harboring a small deletion mutation in type II collagen gene. *Osteoarthr. Cartil.* 8, 248–257. doi:10.1053/joca.2000.0298

Saas, J., Haag, J., Rueger, D., Chubinskaya, S., Sohler, F., Zimmer, R., et al. (2006). IL-1beta, but not BMP-7 leads to a dramatic change in the gene expression pattern of human adult articular chondrocytes – portraying the gene expression pattern in two donors. *Cytokine* 36, 90–99. doi:10.1016/j.cyto.2006.10.005

Sandy, J. D., Chan, D. D., Trevino, R. L., Wimmer, M. A., and Plaas, A. (2015). Human genome-wide expression analysis reorients the study of inflammatory mediators and biomechanics in osteoarthritis. *Osteoarthr. Cartil.* 23, 1939–1945. doi:10.1016/j.joca.2015.03.027

Santini, P., Politi, L., Vedova, P. D., Scandurra, R., and Scotto d'Abusco, A. (2014). The inflammatory circuitry of miR-149 as a pathological mechanism in osteoarthritis. *Rheumatol. Int.* 34, 711–716. doi:10.1007/s00296-013-2754-8

Scanzello, C. R., and Goldring, S. R. (2012). The role of synovitis in osteoarthritis pathogenesis. *Bone* 51, 249–257. doi:10.1016/j.bone.2012.02.012

Scanzello, C. R., McKeon, B., Swaim, B. H., DiCarlo, E., Asomugha, E. U., Kanda, V., et al. (2011). Synovial inflammation in patients undergoing arthroscopic meniscectomy: molecular characterization and relationship to symptoms. *Arthritis Rheum.* 63, 391–400. doi:10.1002/art.30137

Scanzello, C. R., Plaas, A., and Crow, M. K. (2008). Innate immune system activation in osteoarthritis: is osteoarthritis a chronic wound? *Curr. Opin. Rheumatol.* 20, 565–572. doi:10.1097/BOR.0b013e32830aba34

Sellam, J., and Berenbaum, F. (2010). The role of synovitis in pathophysiology and clinical symptoms of osteoarthritis. *Nat. Rev. Rheumatol.* 6, 625–635. doi:10.1038/nrrheum.2010.159

Shen, J., Abu-Amer, Y., O'Keefe, R. J., and McAlinden, A. (2017). Inflammation and epigenetic regulation in osteoarthritis. *Connect. Tissue Res.* 58, 49–63. doi:10.1080/03008207.2016.1208655

Simon, T. C., and Jeffries, M. A. (2017). The Epigenomic Landscape in Osteoarthritis. *Curr. Rheumatol. Rep.* 19, 30. doi:10.1007/s11926-017-0661-9

Sohn, D. H., Sokolove, J., Sharpe, O., Erhart, J. C., Chandra, P. E., Lahey, L. J., et al. (2012). Plasma proteins present in osteoarthritic synovial fluid can stimulate cytokine production via toll-like receptor 4. *Arthritis Res. Ther.* 14, R7. doi:10.1186/ar3555

Sophia Fox, A. J., Bedi, A., and Rodeo, S. A. (2009). The basic science of articular cartilage: structure, composition, and function. *Sports Health* 1, 461–468. doi:10.1177/1941738109350438

Southam, L., Rodriguez-Lopez, J., Wilkins, J. M., Pombo-Suarez, M., Snelling, S., Gomez-Reino, J. J., et al. (2007). An SNP in the 5'-UTR of GDF5 is associated with osteoarthritis susceptibility in Europeans and with in vivo differences in allelic expression in articular cartilage. *Hum. Mol. Genet.* 16, 2226–2232. doi:10.1093/hmg/ddm174

Takahashi, A., de Andres, M. C., Hashimoto, K., Itoi, E., and Oreffo, R. O. (2015). Epigenetic regulation of interleukin-8, an inflammatory chemokine, in osteoarthritis. *Osteoarthr. Cartil.* 23, 1946–1954. doi:10.1016/j.joca.2015.02.168

Tardif, G., Hum, D., Pelletier, J. P., Duval, N., and Martel-Pelletier, J. (2009). Regulation of the IGFBP-5 and MMP-13 genes by the microRNAs miR-140 and miR-27a in human osteoarthritic chondrocytes. *BMC Musculoskelet. Disord.* 10:148. doi:10.1186/1471-2474-10-148

Taylor, S. E., Li, Y. H., Smeriglio, P., Rath, M., Wong, W. H., and Bhutani, N. (2016). Stable 5-hydroxymethylcytosine (5hmC) acquisition marks gene activation during chondrogenic differentiation. *J. Bone Miner. Res.* 31, 524–534. doi:10.1002/jbmr.2711

Tsuda, M., Takahashi, S., Takahashi, Y., and Asahara, H. (2003). Transcriptional co-activators CREB-binding protein and p300 regulate chondrocyte-specific gene expression via association with Sox9. *J. Biol. Chem.* 278, 27224–27229. doi:10.1074/jbc.M303471200

Ukai, T., Sato, M., Akutsu, H., Umezawa, A., and Mochida, J. (2012). MicroRNA-199a-3p, microRNA-193b, and microRNA-320c are correlated to aging and regulate human cartilage metabolism. *J. Orthop. Res.* 30, 1915–1922. doi:10.1002/jor.22157

Valdes, A. M., and Spector, T. D. (2011). Genetic epidemiology of hip and knee osteoarthritis. *Nat. Rev. Rheumatol.* 7, 23–32. doi:10.1038/nrrheum.2010.191

van der Kraan, P. M., and van den Berg, W. B. (2007). Osteophytes: relevance and biology. *Osteoarthritis Cartilage* 15, 237–244. doi:10.1016/j.joca.2006.11.006

van der Kraan, P. M., and van den Berg, W. B. (2012). Chondrocyte hypertrophy and osteoarthritis: role in initiation and progression of cartilage degeneration? *Osteoarthr. Cartil.* 20, 223–232. doi:10.1016/j.joca.2011.12.003

Wang, X., Manner, P. A., Horner, A., Shum, L., Tuan, R. S., and Nuckolls, G. H. (2004). Regulation of MMP-13 expression by RUNX2 and FGF2 in osteoarthritic cartilage. *Osteoarthr. Cartil.* 12, 963–973. doi:10.1016/j.joca.2004.08.008

Yamasaki, K., Nakasa, T., Miyaki, S., Ishikawa, M., Deie, M., Adachi, N., et al. (2009). Expression of microRNA-146a in osteoarthritis cartilage. *Arthritis Rheum.* 60, 1035–1041. doi:10.1002/art.24404

Yang, F., Zhou, S., Wang, C., Huang, Y., Li, H., Wang, Y., et al. (2017). Epigenetic modifications of interleukin-6 in synovial fibroblasts from osteoarthritis patients. *Sci. Rep.* 7, 43592. doi:10.1038/srep43592

Zhang, M., Egan, B., and Wang, J. (2015). Epigenetic mechanisms underlying the aberrant catabolic and anabolic activities of osteoarthritic chondrocytes. *Int. J. Biochem. Cell Biol.* 67, 101–109. doi:10.1016/j.biocel.2015.04.019

Zhang, M., and Wang, J. (2015). Epigenetic regulation of gene expression in osteoarthritis. *Genes Dis.* 2, 69–75. doi:10.1016/j.gendis.2014.12.005

Zhong, N., Sun, J., Min, Z., Zhao, W., Zhang, R., Wang, W., et al. (2012). MicroRNA-337 is associated with chondrogenesis through regulating TGFBR2 expression. *Osteoarthr. Cartil.* 20, 593–602. doi:10.1016/j.joca.2012.03.002

Conflict of Interest Statement: The authors declare that the research was conducted in the absence of any commercial or financial relationships that could be construed as a potential conflict of interest.

frontiers in Bioengineering and Biotechnology

REVIEW
published: 19 March 2018
doi: 10.3389/fbioe.2018.00018

Recent Insights into the Contribution of the Changing Hypertrophic Chondrocyte Phenotype in the Development and Progression of Osteoarthritis

Ellen G. J. Ripmeester†, Ufuk Tan Timur†, Marjolein M. J. Caron‡ and Tim J. M. Welting‡*

Laboratory for Experimental Orthopedics, Department of Orthopedic Surgery, Maastricht University Medical Center, Maastricht, Netherlands

OPEN ACCESS

Edited by:
Eric Farrell, Erasmus University Rotterdam, Netherlands

Reviewed by:
Katherine A. Staines, Edinburgh Napier University, United Kingdom
Andrea Lolli, Erasmus Medical Center, Erasmus University Rotterdam, Netherlands

***Correspondence:**
Tim J. M. Welting
t.welting@maastrichtuniversity.nl

†Co-first authors.

‡Co-last authors.

Specialty section:
This article was submitted to Tissue Engineering and Regenerative Medicine, a section of the journal Frontiers in Bioengineering and Biotechnology

Received: *18 December 2017*
Accepted: *08 February 2018*
Published: *19 March 2018*

Citation:
Ripmeester EGJ, Timur UT, Caron MMJ and Welting TJM (2018) Recent Insights into the Contribution of the Changing Hypertrophic Chondrocyte Phenotype in the Development and Progression of Osteoarthritis. Front. Bioeng. Biotechnol. 6:18. doi: 10.3389/fbioe.2018.00018

Osteoarthritis (OA) is an extremely prevalent age-related condition. The economic and societal burden due to the cost of symptomatic treatment, inability to work, joint replacement, and rehabilitation is huge and increasing. Currently, there are no effective medical therapies that delay or reverse the pathological manifestations of OA. Current treatment options are, without exception, focused on slowing down progression of the disease to postpone total joint replacement surgery for as long as possible and keeping the associated pain and joint immobility manageable. Alterations in the articular cartilage chondrocyte phenotype might be fundamental in the pathological mechanisms of OA development. In many ways, the changing chondrocyte phenotype in osteoarthritic cartilage resembles the process of endochondral ossification as seen, for instance, in developing growth plates. However, the relative contribution of endochondral ossification to the changing chondrocyte phenotype in the development and progression of OA remains poorly described. In this review, we will discuss the current knowledge regarding the cartilage endochondral phenotypic changes occurring during OA development and progression, as well as the molecular and environmental effectors driving these changes. Understanding how these molecular mechanisms determine the chondrocyte cell fate in OA will be essential in enabling cartilage regenerative approaches in future treatments of OA.

Keywords: chondrocytes, osteoarthritis, hypertrophy, cartilage, phenotype, endochondral ossification

INTRODUCTION

Osteoarthritis (OA) is the most common degenerative joint disorder worldwide and its incidence rises with age (Loeser et al., 2012). The economic and societal burden due to costs of symptomatic treatment, inability to work, joint replacement surgery (and coinciding implant infections), rehabilitation, and social isolation is huge (Bijlsma et al., 2011; Le et al., 2012). Identifying the main molecular mechanisms by which OA is initiated and progresses is still one of the biggest challenges in this field. However, our current knowledge teaches us that the initial trigger for developing OA is multifactorial with risk factors, including obesity, diabetes, genetics, and trauma (Felson et al., 2000). Despite the diversity of initial triggers OA disease progression follows a predictable cell

biological progression. While pain experience, joint immobility, and speed of disease progression are some of the few patient-variable parameters. Depending on the OA-stage, interventions are mainly based on alleviating chronic pain and preserving joint mobility by visco-supplementation, and physiotherapy to postpone joint replacement surgery (Lo et al., 2003; Zhang et al., 2010; Page et al., 2011). While there is a lack of treatment options that are disease-modifying and improve joint-tissue homeostasis. Substantial effort is required to identify targetable pathways or individual factors that alter the diseased cartilage phenotype in OA.

A prominent feature of OA is cartilage degradation. Other joint structures, such as the synovium, Hoffa's fat pad (HFP), meniscus, and subchondral bone have been demonstrated to experience OA-specific pathologic changes. Changes in these joint structures include not only infiltration of active immune cells in the synovium and HFP, but also fibrillation of the meniscus and sclerosis of the subchondral bone. Together, these changes lead to a loss of joint mobility and function, accompanied by chronic pain (Loeser et al., 2012).

From a biochemical perspective, the cartilage degradation observed in OA has been attributed to an elevated production of proteolytic enzymes, such as matrix metalloprotease 13 (MMP13) and aggrecanases, such as a disintegrin and metalloproteinase with thrombospondin motifs (ADAMTS) 4 and 5. These degrade important cartilage matrix components, such as type II collagen (COL2A1) and aggrecan (Hunter, 2011). In addition to elevated production of proteolytic enzymes in OA cartilage, other observed features in OA cartilage include the expression of chondrocyte hypertrophic markers [such as type 10 collagen (COL10A1)] (Little et al., 2009), vascularization, and focal calcification. Since, these features resemble the endochondral ossification process that occurs in the hypertrophic zone of the growth plate, it has been hypothesized that OA is a disease characterized by ectopic recapitulation of the endochondral ossification process (Dreier, 2010; Pitsillides and Beier, 2011; van der Kraan and van den Berg, 2012).

Post-developmental healthy articular cartilage homeostasis is thought to be "protected" against hypertrophic or catabolic changes by several pathways employing soluble mediators, including BMP-, TGF-β-, and hedgehog signaling (Dreier, 2010; Pitsillides and Beier, 2011). These pathways transcriptionally control the chondrocyte phenotype by tuning the activity and levels of major chondrocyte phenotype-determining downstream transcription factors, such as SOX9, RUNX2, and SMADs (van der Kraan and van den Berg, 2012). Many risk factors for developing OA are thought to (in)directly influence the activity of these pathways, and thus ultimately resulting in a changing chondrocyte phenotype that becomes disposed to entering endochondral ossification. This may place, besides the local inflammatory condition (among others caused by synovitis), the chondrocyte/cartilage differentiation status central to the progression, or cause of OA.

The relation between the chondrocyte/cartilage differentiation status and OA development and -progression has been well-described and was acknowledged in the past by a number of excellent reviews (Dreier, 2010; Pitsillides and Beier, 2011; van der Kraan and van den Berg, 2012). In this review, we present an overview of the literature from the past 10 years, describing recent insights in the contribution of endochondral ossification-related processes in OA disease development and -progression. We conducted a PubMed literature search including papers from the past 10 years discussing endochondral ossification and its accompanying processes also occurring in OA disease progression. Molecular insight in the role of chondrocyte hypertrophic processes involved in OA initiation and progression is expected to provide valuable information for drug development targeting these processes for OA disease modification.

REVIEW PROCEDURE

To provide a current status on the role of hypertrophic changes in OA we searched for English manuscripts from the past 10 years on PubMed using the following search strategy (**Figure 1**): (OA OR osteoarthrosis OR osteoarthritis OR non-inflammatory arthritis OR degenerative arthritis OR osteoarthritic) AND (hypertrophic OR hypertrophy OR terminal differentiation OR hypertrophic differentiation OR end stage differentiation, OR endochondral ossification OR chondrocyte hypertrophy OR transdifferentiation OR mineralization OR mineralisation OR mineralized OR mineralised OR calcification) and chondrocyte. At May 3rd, 2017 a total of 461 papers were found and screened *via* title and abstract by two separate observers (ER and UT) using the following inclusion criteria: papers describing osteoarthritis, biomolecular data, and literature describing an OA process that resembles endochondral ossification in the title and abstract. Articles referring to apoptosis and autophagy were excluded as we wanted to focus on processes occurring during OA initiation and progression and we considered apoptosis and autophagy as end-stage processes. Besides apoptosis and autophagy, reviews were also excluded. When there was a discrepancy in paper selection, consensus was reached with all authors. This resulted in a short-list of 147 articles whose full-text was manually screened by four observers (ER, UT, MC, and TW) using the same inclusion criteria. Papers with missing full-texts were excluded. This resulted in a total of 76 papers being included in this review (**Figure 1**).

RESULTS

Our search yielded a diverse range of publications from the past 10 years confirming earlier reports describing endochondral cellular phenotypic changes in OA cartilage and describing associations of these endochondral cellular phenotypic changes with the development and progression of OA. During our search, we noticed that the majority of the papers could be classified into signaling pathways known to be involved in endochondral ossification, such as *Wnt-, Ihh/PTHrP-, TGF-β-, MAP-kinases, FGF-, Notch signaling*, *inflammatory signaling, and hypoxia-associated signaling pathways.* Besides these pathways also papers describing processes, such as angiogenesis and matrix mineralization were found. These pathways and processes involved in endochondral ossification will be described now separately and new insights from the selected literature will be discussed with respect to these pathways.

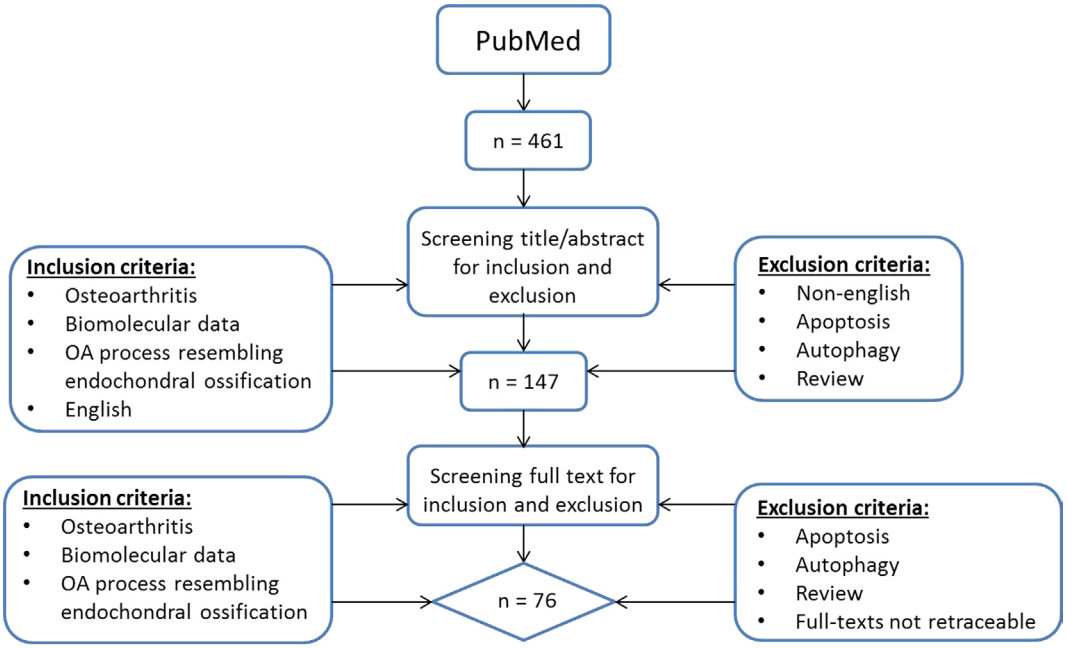

FIGURE 1 | Literature search flowchart.

Wnt Signaling

A thoroughly studied pathway involved in chondrocyte differentiation and hypertrophy is Wnt signaling. The canonical Wnt/β-catenin pathway (Wu et al., 2009; Borzi et al., 2010; Pitsillides and Beier, 2011; Castano Betancourt et al., 2012; Facchini et al., 2012; Papathanasiou et al., 2012; Leijten et al., 2013; van den Bosch et al., 2014; Guidotti et al., 2015; Chen et al., 2016; Staines et al., 2016) is activated by binding one of the canonical Wnt ligands to a Frizzled family receptor and an LRP5/6 co-receptor, which passes the signal *via* GSK-3β to inhibit the β-catenin destruction complex, causing an accumulation of β-catenin in the cytoplasm and eventual its translocation into the nucleus (MacDonald et al., 2009). This enables transcriptional coactivation with TCF/LEF transcription factors which are active in the transcription of Wnt-target genes, such as RUNX2 (MacDonald et al., 2009). In our review procedure, we did not find literature regarding non-canonical Wnt signaling that matched the search criteria. An overview of newly acquired insights into this pathway and its involvement in development of OA chondrocyte hypertrophy is provided in **Table 1**a and **Figure 2**.

It is well established that β-catenin signaling is associated with chondrocyte hypertrophy (Wu et al., 2009; Borzi et al., 2010; Castano Betancourt et al., 2012; Facchini et al., 2012; Papathanasiou et al., 2012; Leijten et al., 2013; van den Bosch et al., 2014; Guidotti et al., 2015; Chen et al., 2016; Staines et al., 2016). Next to its role in chondrocyte hypertrophy, recent advancements in knowledge regarding OA and the involvement of Wnt signaling now demonstrate that expression levels of Wnt signaling- and β-catenin-inducing factors, as well as downstream Wnt effectors, such as LEF1 and AXIN2, are directly or indirectly associated with OA (Wu et al., 2009; Borzi et al., 2010; Castano Betancourt et al., 2012; Facchini et al., 2012; Papathanasiou et al., 2012; Leijten et al., 2013; van den Bosch et al., 2014; Guidotti et al., 2015; Chen et al., 2016; Staines et al., 2016).

A causative relationship between canonical Wnt signaling and OA initiation/progression has been suggested by two recent studies. Cartilage-specific SMURF2-mediated ubiquitination and proteasomal degradation of GSK-3β resulted in increased β-catenin signaling (Wu et al., 2009). Tibial and femoral articular cartilage in this *Col2a1-Smurf2* mouse model demonstrated that 2.5-week-old mice displayed an increased basal layer of the deep articular cartilage with higher *Col10a1* expression. These early hypertrophic changes in the articular cartilage of these mice were subsequently followed by cartilage degeneration and osteophyte formation when the mice became older (Wu et al., 2009), suggesting a direct relationship between early hypertrophic changes followed by OA development. Another study by Chen et al. provided evidence for the activation of Wnt/β-catenin signaling in OA development. This study investigated the effects of EZH2 inhibition on OA development in a surgically induced OA mouse model (Chen et al., 2016). EZH2 is the catalytic unit of the polycomb repressive complex 2 (PRC2), responsible for transcriptional silencing of a multitude of genes involved in differentiation (Morey and Helin, 2010). EZH2 expression was higher in OA chondrocytes compared to healthy chondrocytes and overexpression of EZH2 in normal chondrocytes resulted in activation of β-catenin signaling, including higher mRNA expression of its downstream effectors, *AXIN2* and *LEF1*. Confirming the association between increased β-catenin signaling and OA development, intra-articular injection with a pharmacological EZH2 inhibitor in a surgically induced mouse OA model resulted in reduced cartilage degradation compared

TABLE 1 | (A–K) Hypertrophy associated-factors.

Abbreviation	Name	Reference
A: Wnt/β-catenin		
AXIN2	Axis inhibition protein 2	Chen et al. (2016)
S-oxo-dG	8-Oxo-2'-deoxyguanosine	Guidotti et al. (2015)
DKK1	Dickkopf 1 homolog	Leijten et al. (2013)
DMP1	Dentin matrix acidic phosphoprotein 1	Staines et al. (2016)
DOT1L	Disruptor of teiomeric silencing 1-like	Castano Betancourt et al. (2012)
EZH2	Enhancer of zeste homolog 2	Chen et al. (2016)
FR1ZB	Frizzled-related protein	Leijten et al. (2013)
GADD45b	Growth arrest and DNA damage inducible beta	Ijiri et al. (2008) and Guidotti et al. (2015)
GSK-3β	Glycogen synthase kinase 3 beta	Guidotti et al. (2015)
LEF1	Lymphoid enhancer-binding factor 1	Papathanasiou et al. (2012) and Chen et al. (2016)
LRP5	Low-density lipoprotein receptor-related protein 5	Papathanasiou et al. (2012)
LRP6	Low-density lipoprotein receptor-related protein 6	Papathanasiou et al. (2012)
MEPE1	Matrix extracellular phosphoglycoprotein p21	Staines et al. (2016)
PAS	Periodic acid-Schiff staining	Guidotti et al. (2015)
PHEX	Phosphate-regulating neutral endopeptidase, X-linked	Staines et al. (2016)
SAβ Galactosidase	Senescence-associated beta-gal actosidase	Guidotti et al. (2015)
SFRP1	Secreted frizzled-related protein 1	Chen et al. (2016)
SMURF2	SMAD-specific E3 ubiquitin protein ligase 2	Wu et al. (2009)
SOST	Sclerostin	Papathanasiou et al. (2015)
TCF1	Transcription factor 1	Castano Betancourt et al. (2012)
TCF4	Transcription factor 4	Castano Betancourt et al. (2012) and Papathanasiou et al. (2012)
WISP	WNT1-inducible-signalhg pathway protein 1	van den Bosch et al. (2014)
WNT3α	Wingless-related integrationsite 3a	Leijten et al. (2013) and van den Bosch et al. (2014)
WNT8	Wingless-related integrated site 8	van den Bosch et al. (2014)
H2AX	Gamma-H2A histone family, member X	Guidotti et al. (2015)
	β-catenin	Borzi et al. (2010), Facchini et al. (2012), Papathanasiou et al. (2012), Chen et al. (2016)
B: Ihh/PTHrP		
EZH2	Enhancer of zeste homolog 2	Chen et al. (2016)
HES1	Hairy and enhancerof split-1	Hosaka et al. (2013) and Lin et al. (2016)
IHH	Indian hedgehog homolog	Chang et al. (2009), Saito et al. (2010), Wei et al. (2012), Zhou et al. (2014), Garciadiego-Cazares et al. (2015), Thompson et al. (2015), Chen et al. (2016), Yahara et al. (2016), Zhou et al. (2016), and Zhang et al. (2017)
Mef2c	Myocyte-specific enhancer factor 2C	Yahara et al. (2016)
mTOR	Mechanistic target of rapamycin	Zhang et al. (2017)
OC	Osteocalcin	Castano Betancourt et al. (2012), Cavaco et al. (2016), and Lin et al. (2016)
PAI1	Plasminogen-activator inhibitor-1	Ailixiding et al. (2015)
PPR/PTHR1	PTH-related protein receptor/parathyroid hormone 1 receptor	Zhang et al. (2017)
p-S6	Phospho-S6	Zhang et al. (2017)
PTCH1	Protein patched homolog 1	Thompson et al. (2015), and Lin et al. (2016)
PTCH2	Protein patched homolog 2	Zhou et al. (2014) and Lin et al. (2016)
PTHrP	Parathyroid hormone-related protein	Brew et al. (2010), Eswaramoorthy et al. (2012), Pesesse et al. (2014), and Zhang et al. (2017)
SIK3	Salt-Inducible kinase 3	Yahara et al. (2016)
C: TGF-β superfamily		
SOST	Sclerostin	Papathanasiou et al. (2015)
ALK1	Activin receptor-like kinase 1	Blaney Davidson et al. (2009) and van den Bosch et al. (2014)
ALK5	Activin receptor-like kinase 5	Blaney Davidson et al. (2009) and van den Bosch et al. (2014)
ATF2	Activating transcription factor 2	Li et al. (2010)
BAPX1/NKX3.2	Bagpipe homeobox homologl/NK3 homeobox 2	Chang et al. (2009) and Caron et al. (2015)
BMP-2	Bone morphogenetic protein 2	Papathanasiou et al. (2012)
BMP-4	Bone morphogenetic protein 4	Papathanasiou et al. (2012)
BMP-7	Bone morphogenetic protein 7	Papathanasiou et al. (2012) and Garciadiego-Cazares et al. (2015)
BMPR1A	Bone morphogenetic protein receptor, type 1A	Papathanasiou et al. (2012)
CAGA12 promotor activity		Gao et al. (2012)

(*Continued*)

TABLE 1 | Continued

Abbreviation	Name	Reference
FN	Fibronectin	Garciadiego-Cazares et al. (2015)
GDF-5	Growth/differentiation factor 5	Garciadiego-Cazares et al. (2015)
GREM1	Gremlin 1	Leijten et al. (2013)
	Integrin a1	Johnson et al. (2008) and Garciadiego-Cazares et al. (2015)
	Integrin a5	Garciadiego-Cazares et al. (2015)
	Integrin aV	Garciadiego-Cazares et al. (2015)
	Integrin b1	Garciadiego-Cazares et al. (2015)
MATN3	Matrilin 3	Yang et al. (2014)
SMAD1	Mothers against decapentaplegic homolog 1	Gao et al. (2012), Yang et al. (2014), and Papathanasiou et al. (2015)
SMAD2	Mothers against decapentaplegic homolog 2	Gao et al. (2012)
SMAD3	Mothers against decapentaplegic homolog 3	Li et al. (2010) and Gao et al. (2012)
SMAD5	Mothers against decapentaplegic homolog 5	Gao et al. (2012) and Papathanasiou et al. (2015)
SMAD8	Mothers against decapentaplegic homolog 8	Gao et al. (2012) and Papathanasiou et al. (2015)
TGF-β	Transforming growth factor beta	van den Bosch et al. (2014)
D: MAPK/ERK		
(p)ERK	(phosphorylated) extra-cellular-regulated kinases	Prasadam et al. (2010), Prasadam et al. (2013), Bianchi et al. (2016), Xu et al. (2016), and Zhang et al. (2017)
(p)JNK	(phosphorylated) c-Jun N-terminal kinase	Xu et al. (2016)
(p-)P38	(phosphorylated) P38	Johnson et al. (2008), Prasadam et al. (2013), Philipot et al. (2014), Bianchi et al. (2016), and Xu et al. (2016)
FXIIIA, F13A	Factor XIII	Johnson et al. (2008)
	Integrin α1β1	Garciadiego-Cazares et al. (2015)
(p)FAK	(phosphorylated) focal adhesion kinase	Johnson et al. (2008)
TG2, TGM2	Transglutaminase 2	Johnson et al. (2008) and Huebner et al. (2009)
E: Inflammatory signaling		
AP-2 ε	Activating enhancer binding protein 2 epsilon	Wenke et al. (2009) and Wenke et al. (2011)
CD36	Cluster of differentiation 36	Cecil et al. (2009)
CD45	Cluster of differentiation 45	Cavaco et al. (2016)
COX2	Cyclo-oxygenase 2	Caron et al. (2015) and Cavaco et al. (2016)
CXCL1	Chemokine (C-X-C motif) ligand 1	Wenke et al. (2011)
CXCL6	Chemokine (C-X-C motif) ligand 6	Sherwood et al. (2015)
CXCR2	C-X-C motif chemokine receptor 2	Sherwood et al. (2015)
HDAC2	Histone deacetylase 2	Queirolo et al. (2016)
HDAC4	Histone deacetylase 4	Lu et al. (2014a) and Queirolo et al. (2016)
IKKα	Inhibitor of nuclear factor kappa-B kinase subunit alpha	Olivotto et al. (2008) and Guidotti et al. (2015)
IKKβ	Inhibitor of nuclear factor kappa-B kinase subunit beta	Olivotto et al. (2008) and Guidotti et al. (2015)
IL-1β	Interleukin-1β	Thompson et al. (2015), Cavaco et al. (2016) and Nasi et al. (2016)
IL-6	Interleukin-6	Philipot et al. (2014), Ailixiding et al. (2015), Caron et al. (2015), and Nasi et al. (2016)
IL-8	Interleukin-8	Pesesse et al. (2014) and Philipot et al. (2014)
iNOS	Nitric oxide synthase	Aini et al., 2012
LOX-1	Lectin-like oxidized low-density lipoprotein receptor-1	Hashimoto et al. (2016)
MiR24	MicroRNA24	Philipot et al. (2014)
MiR320	MicroRNA320	Meng et al. (2016)
NF-κB	Nuclear factor kappa-light-chain-enhancer of activated Bcells	Ijiri et al. (2008)
NITEGE	Aggrecan neoepitopes	Cecil et al. (2009)
ODC	Ornithine decarboxylase	Facchini et al. (2012)
PGE2	Prostaglandin E2	Caron et al. (2015) and Cavaco et al. (2016)
PKCε	Protein kinase C epsilon type	Queirolo et al. (2016)
	$P16^{INK4a}$	Philipot et al. (2014)
RAGE	Receptor for advanced glycation end products	Cecil et al. (2009)
S100A11	S100 calcium-binding protein A11	Cecil et al. (2009)
TNFα	Tumor necrosis factor alpha	Lai et al. (2014) and Ailixiding et al. (2015)
SIRT-1	Sirtuin-1	Fujita et al. (2011)
SIRT-6	Sirtuin-6	Ailixiding et al. (2015)
F: Hypoxic and angiogenic factors		
BSP/OPN	Bone sialoprotein/osteopontin	Fukai et al. (2010), Pesesse et al. (2013), Pesesse et al. (2014), Cavaco et al. (2016), and Staines et al. (2016)
C/EBPβ	CCAAT-enhancer-binding proteins	Hirata et al. (2012)

(*Continued*)

TABLE 1 | Continued

Abbreviation	Name	Reference
CHM-1	Chondromodulin-1	Wang et al. (2012) and Zhang et al. (2016a,b)
CTGF	Connective tissue growth factor	Wang et al. (2012)
DDR2	Discoid in domain receptor 2	Zhang et al. (2014a,b)
DIO2	Type II iodothyronine deiodinase	Bomer et al. (2015)
HAS2	Hyaluronan synthase 2	Markway et al. (2013)
HIF-1α	Hypoxia-inducible factor 1α	Markway et al. (2013) and Zhang et al. (2016b)
HIF-2α/EPAS1	Hypoxia-inducible factor 2α/ endothelial PAS domain-containing protein 1	Saito et al. (2010), Markway et al. (2013), Bomer et al. (2015), and Zhang et al. (2016b)
HIF-3α	Hypoxia-inducible factor 3α	Markway et al. (2015)
	Hypoxia	Markway et al. (2013, 2015)
TSP	Thrombospondin-1	Pesesse et al. (2014)
VEGF	Vascular endothelial growth factor	Johnson et al. (2008), Ray and Ray (2008), Borzi et al. (2010), Brew et al. (2010), Fukai et al. (2010), Saito et al. (2010), Hirata et al. (2012), Wang et al. (2012), Hosaka et al. (2013), Bianchi et al. (2016), and Zhang et al. (2016a,b)
G: FGF		
FGF23	Fibroblast growth factor 23	Orfanidou et al. (2009) and Bianchi et al. (2016)
FGFR1	Fibroblast growth factor receptor 1	Bianchi et al. (2016)
FGFR2	Fibroblast growth factor receptor 2	Bianchi et al. (2016)
FGFR3	Fibroblast growth factor receptor 3	Bianchi et al. (2016), Zhou et al. (2016), and Zhang et al. (2017)
FGFR4	Fibroblast growth factor receptor 4	Bianchi et al. (2016)
	Klotho	Bianchi et al. (2016)
mTOR	Mechanistic target of rapamycin	Zhang et al. (2017)
	P73	Zhang et al. (2017)
p-36	Phospho-36	Zhang et al. (2017)
H: Notch		
GLI1	GLI family zinc finger 1	Thompson et al. (2015) and Lin et al. (2016)
GLI2	GLI family zinc finger 2	Thompson et al. (2015) and Lin et al. (2016)
Hes1	Hairy and enhancer of split-1	Hosaka et al. (2013) and Lin et al. (2016)
JAG1	Jagged 1	Lin et al. (2016)
NICD1	Notch intracellular domain 1	Hosaka et al. (2013) and Lin et al. (2016)
NICD2	Notch intracellular domain 2	Hosaka et al. (2013)
NOTCH		Hosaka et al. (2013) and Lin et al. (2016)
RBPjκ	Recombination signal binding protein for immunoglobulin kappa J	Hosaka et al. (2013)
I: Mineralization		
ANK	Progressive ankylosis protein	Nguyen et al. (2013) and Nasi et al. (2016)
AKT1	RAC-alphaserine/threonine-protein kinase	Sherwood et al. (2015) and Bianchi et al. (2016)
Anx5	Annexin 5	Nasi et al. (2016)
BCP	Basic calcium phosphate	Fuerst et al. (2009) and Nasi et al. (2016)
CA	Carbonated-apatite	Nasi et al. (2016)
Ca^{2+}	Calcium	Olivotto et al. (2008), Fuerst et al. (2009), Facchini et al. (2012), Nguyen et al. (2013), Olivotto et al. (2013), Cavaco et al. (2016), Nasi et al. (2016), Queirolo et al. (2016), and Yahara et al. (2016)
cOMP	Cartilage oligomeric matrix protein	Lai et al. (2014) and Cavaco et al. (2016)
CPPD	Calcium pyrophosphate dehydrates	Nasi et al. (2016)
	Fetuin	Wallin et al. (2010)
GGCX	Vitamin K-dependent gamma-carboxylase	Cavaco et al. (2016)
[(un)carboxylated] GRP	Gla-rich protein	Cavaco et al. (2016)
HA	Hydroxyapatite	Nasi et al. (2016)
IL-6	interleukin-6	Nasi et al. (2016)
[(un)carboxylated] MGP	Matrix Gla protein	Wallin et al. (2010) and Cavaco et al. (2016)
NTPPPH	Nucleoside triphosphate pyrophosphohydrolase	Pesesse et al. (2013)
OCP	Octacalcium phosphate	Nasi et al. (2016)
OCRL1	Lowe oculocerebrorenal syndrome protein	Zhu et al. (2015)
OSX	Osterix	Cavaco et al. (2016)
PC-1/ENPP1, NPP1	Plasma-cell membrane glycoprotein 1/ ectonucleotide pyrophosphatase/ phosphodiesterase 1	Nguyen et al. (2013) and Nasi et al. (2016)
Pi	inorganic phosphate	Fukai et al. (2010)
PIT1	Inorganic phosphate transporter 1	Nguyen et al. (2013) and Nasi et al. (2016)

(*Continued*)

TABLE 1 | Continued

Abbreviation	Name	Reference
PIT2	Inorganic phosphate transporter 2	Nasi et al. (2016)
PKCε	Protein kinase C epsilon type	Queirolo et al. (2016)
Ppi	Inorganic pyrophosphate	Fukai et al. (2010)
RAC1	Ras-related C3 botulinum toxin substrate 1	Wang and Beier (2005)
TNAP	Transporter and tissue-nonspecific alkaline phosphatases	Nguyen et al. (2013) and Nasi et al. (2016)
VKOR	Vitamin K epoxide reductase y-Carboxylase activity	Cavaco et al. (2016) Wallin et al. (2010)
J: Hypertrophic differentiation markers		
AGC, ACAN	Aggrecan	Chang et al. (2009), Aini et al., 2012, Castano Betancourt et al. (2012), Papathanasiou et al. (2012), Markway et al. (2013), Lai et al. (2014), Lu et al. (2014a), Philipot et al. (2014), Ailixiding et al. (2015), Bomer et al. (2015), Caron et al. (2015), Garciadiego-Cazares et al. (2015), Sherwood et al. (2015), Filip et al. (2016), Xu et al. (2016), and Zhang et al. (2016a,b)
ADAMTS1	A disintegrin and metalloproteinase with thrombospondin motifs 1	Lai et al. (2014)
ADAMTS4	A disintegrin and metalloproteinase with thrombospondin motifs 4	Little et al. (2009), Lai et al. (2014), Lu et al. (2014a), and Chen et al. (2016)
ADAMTS5	A disintegrin and metalloproteinase with thrombospondin motifs 5	Huebner et al. (2009), Hirata et al. (2012), Prasadam et al. (2013), Lai et al. (2014), Lu et al. (2014a), Bomer et al. (2015), Caron et al. (2015), Thompson et al. (2015), Zhu et al. (2015), Chen et al. (2016), Lin et al. (2016), Nasi et al. (2016), Xu et al. (2016), and Zhou et al. (2016)
ADAMTS7	A disintegrin and metalloproteinase with thrombospondin motifs 7	Lai et al. (2014)
ALPL	Alkaline phosphatase	Chang et al. (2009), Prasadam et al. (2010), Hirata et al. (2012), Pesesse et al. (2013), Zhang et al. (2014a,b), Bomer et al. (2015), Caron et al. (2015), Zhu et al. (2015), Filip et al. (2016), Yahara et al. (2016), and Zhang et al. (2016a)
CASP3	Caspase3	Xu et al. (2016)
COL1	Type 1 collagen	Castano Betancourt et al. (2012), Gao et al. (2012), Markway et al. (2013), Nagase et al. (2013), Bomer et al. (2015), Bianchi et al. (2016), and Yahara et al. (2016)
COL10A1	Type X collagen	Johnson et al. (2008), Cecil et al. (2009), Chang et al. (2009), Huebner et al. (2009), Wu et al. (2009), Borzi et al. (2010), Brew et al. (2010), Fukai et al. (2010), Li et al. (2010), Prasadam et al. (2010), Saito et al. (2010), Fujita et al. (2011), Aini et al., 2012, Castano Betancourt et al. (2012), Eswaramoorthy et al. (2012), Facchini et al. (2012), Gao et al. (2012), Hirata et al. (2012), Papathanasiou et al. (2012), Wei et al. (2012), Hosaka et al. (2013), Markway et al. (2013), Olivotto et al. (2013), Pesesse et al. (2013), Prasadam et al. (2013), Lai et al. (2014), Lu et al. (2014b), Pesesse et al. (2014), Yang et al. (2014), Zhang et al. (2014b), Zhou et al. (2014), Ailixiding et al. (2015), Bomer et al. (2015), Caron et al. (2015), Markway et al. (2015), Sherwood et al. (2015), Zhu et al. (2015), Bianchi et al. (2016), Cavaco et al. (2016), Chen et al. (2016), Filip et al. (2016), Hashimoto et al. (2016), Lin et al. (2016), Nasi et al. (2016), Queirolo et al. (2016), Staines et al. (2016), Yahara et al. (2016), Zhang et al. (2016a), Zhang et al. (2016b), Zhou et al. (2016), and Zhang et al. (2017)
COL2A1	Type II collagen	Johnson et al. (2008), Chang et al. (2009), Huebner et al. (2009), Wu et al. (2009), Aini et al., 2012, Castano Betancourt et al. (2012), Eswaramoorthy et al. (2012), Facchini et al. (2012), Gao et al. (2012), Papathanasiou et al. (2012), Markway et al. (2013), Nagase et al. (2013), Olivotto et al. (2013), Prasadam et al. (2013), Lu et al. (2014a), Zhang et al. (2014b), Zhou et al. (2014), Bomer et al. (2015), Caron et al. (2015), Garciadiego-Cazares et al. (2015), Markway et al. (2015), Sherwood et al. (2015), Bianchi et al. (2016), Cavaco et al. (2016), Filip et al. (2016), Nasi et al. (2016), Queirolo et al. (2016), Xu et al. (2016), Yahara et al. (2016), and Zhang et al. (2016a)
COL3	Type III Collagen	Gao et al. (2012) and Bianchi et al. (2016)
CTS	Cathepsin	Appleton et al. (2007) and Zhu et al. (2015)
GAG	Glycosaminoglycans	Chang et al. (2009), Markway et al. (2013), Bomer et al. (2015), Garciadiego-Cazares et al. (2015), and Sherwood et al. (2015)
MMP1	Matrix metalloproteinase 1	Ray and Ray (2008), Wei et al. (2012), Markway et al. (2013), Lai et al. (2014), Lu et al. (2014a), Philipot et al. (2014)

(*Continued*)

TABLE 1 | Continued

Abbreviation	Name	Reference
MMP10	Matrix metalloproteinase 10	Olivotto et al. (2013) and Guidotti et al. (2015)
	Matrix metalloproteinase 13	Appleton et al. (2007), Johnson et al. (2008), Blaney Davidson et al. (2009), Huebner et al. (2009), Orfanidou et al. (2009), Borzi et al. (2010), Brew et al. (2010), Saito et al. (2010), Facchini et al. (2012), Hirata et al. (2012), Papathanasiou et al. (2012), Wei et al. (2012), Hosaka et al. (2013), Markway et al. (2013), Nagase et al. (2013), Olivotto et al. (2013), Pesesse et al. (2013), Lai et al. (2014), Lu et al. (2014a), Philipot et al. (2014), Zhang et al. (2014b), Zhou et al. (2014), Ailixiding et al. (2015), Bomer et al. (2015), Caron et al. (2015), Markway et al. (2015), Thompson et al. (2015), Bianchi et al. (2016), Cavaco et al. (2016), Chen et al. (2016), Filip et al. (2016), Meng et al. (2016), Nasi et al. (2016), Queirolo et al. (2016), Staines et al. (2016), Xu et al. (2016), Zhang et al. (2016a), Zhang et al. (2016b), and Zhou et al. (2016)
MMP14	Matrix metalloproteinase 14	Markway et al. (2013) and Lai et al. (2014)
MMP2	Matrix metalloproteinase 2	Markway et al. (2013) and Prasadam et al. (2013)
MMP3	Matrix metalloproteinase 3	Hirata et al. (2012), Wei et al. (2012), Markway et al. (2013), Lai et al. (2014), Lu et al. (2014a), Chen et al. (2016), and Nasi et al. (2016)
MMP9	Matrix metalloproteinase 9	Ray and Ray (2008), Hirata et al. (2012), Wang et al. (2012), Nagase et al. (2013), and Lai et al. (2014)
	Osteophyte	Ray and Ray (2008), Fukai et al. (2010), and Lin et al. (2016)
PCNA	Proliferating cell nuclear antigen	Zhou et al. (2016)
PRG4	Proteoglycan 4/lubricin	Yahara et al. (2016), Zhou et al. (2016)
	Proteoglycans	Hirata et al. (2012), Wei et al. (2012), Hosaka et al. (2013), Prasadam et al. (2013), Lin et al. (2016), Queirolo et al. (2016), Yahara et al. (2016), Aini et al., 2012, Eswaramoorthy et al. (2012), Ailixiding et al. (2015), Caron et al. (2015), Markway et al. (2015), Bianchi et al. (2016), Filip et al. (2016), Hashimoto et al. (2016), Lin et al. (2016), Nasi et al. (2016), Xu et al. (2016), Yahara et al. (2016), and Zhang et al. (2016a,b)
RUNX2/CBFα1	Runt-related transcription factor 2/ Core-binding factor subunit alpha-1	Olivotto et al. (2008), Orfanidou et al. (2009), Borzi et al. (2010), Prasadam et al. (2010), Saito et al. (2010), Facchini et al. (2012), Hirata et al. (2012), Olivotto et al. (2013), Pesesse et al. (2013), Lu et al. (2014b), Zhou et al. (2014), Bomer et al. (2015), Caron et al. (2015), Zhu et al. (2015), Bianchi et al. (2016), Hashimoto et al. (2016), Nasi et al. (2016), Queirolo et al. (2016), Yahara et al. (2016), Zhang et al. (2016a,b), Zhou et al. (2016), and Zhang et al. (2017)
SOX9		Olivotto et al. (2008), Chang et al. (2009), Orfanidou et al. (2009), Wenke et al. (2009), Borzi et al. (2010), Facchini et al. (2012), Lu et al. (2014b), Caron et al. (2015), Sherwood et al. (2015), Bianchi et al. (2016), Chen et al. (2016), Filip et al. (2016), Nasi et al. (2016), Queirolo et al. (2016), Yahara et al. (2016), and Zhang et al. (2016a)
K: Not pathway associated		
	Bone bridges	Staines et al. (2016)
	Bone volume/density	Lu et al. (2014b)
	Cell adhesion	Pesesse et al. (2013)
	Cell number	Olivotto et al. (2008)
	Cell size	Olivotto et al. (2008)
	Cortical bone	Lu et al. (2014b)
	Femur length	Lu et al. (2014b)
	Hypertrophic cells	Pesesse et al. (2013)
	Proliferation	Guidotti et al. (2015), Staines et al. (2016)
	Thickness	Prasadam et al. (2013), Zhou et al. (2016)
	Total cartilage area	Zhang et al. (2017)
	Wound healing	Pesesse et al. (2013)
ACTA1	Actin, Alpha 1	Appleton et al. (2007)
AQP1	Aquaporin 1	Nagase et al. (2013)
ASPN	Asporin	Nagase et al. (2013)
BST1	Bone marrow stromal cell antigen-1	Appleton et al. (2007)
CIS	Complement C1s	Appleton et al. (2007)
CASQ2	Calsequestrin-2	Appleton et al. (2007)
CD14	Cluster of differentiation 14	Appleton et al. (2007)
CD53	Cluster of differentiation 53	Appleton et al. (2007)
CHI3L1	Chitinase-3 like 1	Appleton et al. (2007)
CHN2	Chimerin 2	Appleton et al. (2007)
CXCR4	C-X-C motif chemokine receptor 4	Appleton et al. (2007)

(*Continued*)

TABLE 1 | Continued

Abbreviation	Name	Reference
CYBB/Nox2	Cytochrome b-245 heavy chain/NADPH oxidase 2	Appleton et al. (2007)
CYP4B1	Cytochrome P450 4B1	Nagase et al. (2013)
DBP	D site of albumin promoter binding protein	Appleton et al. (2007)
DCAMKL1	Doublecortin-like kinase 1	Appleton et al. (2007)
ECM1	Extracellular Matrix Protein 1	Appleton et al. (2007)
F3	Coagulation Factor III	Appleton et al. (2007)
FCGR3	Low affinity immunoglobulin gamma Fc region receptor III-A	Appleton et al. (2007)
GADD5A	Growth arrest and DNA-damage-inducible 45 alpha protein	Appleton et al. (2007)
GAP43	Growth-associated protein 43	Appleton et al. (2007)
GAS-6	Growth arrest-specific 6	Appleton et al. (2007)
GBP2	Guanylate binding protein 2	Appleton et al. (2007)
GPM6b	Glycoprotein M6B	Appleton et al. (2007)
HFE	Human hemochromatosis protein	Appleton et al. (2007)
IGFbp6	Insulin like growth factor binding protein 6	Appleton et al. (2007)
IGSF6	Immunoglobulin superfamily member 6	Appleton et al. (2007)
IL2RG	Interteukin-2 receptor subunit gamma	Appleton et al. (2007)
LBP	Lipopolysaccharide binding protein	Appleton et al. (2007)
LTBP2	Latent transforming growth factor beta binding protein 2	Appleton et al. (2007)
MCAM	Melanoma cell adhesion molecule	Appleton et al. (2007)
MGL	Monoacylglycerol lipase	Appleton et al. (2007)
MPEG1	Macrophage expressed 1	Appleton et al. (2007)
MT1A	Metallothionein 1A,	Appleton et al. (2007)
NR1D1	Nuclear receptor subfamily 1 Group D Member 1	Appleton et al. (2007)
PER3	Period circadian protein homolog 3	Appleton et al. (2007)
PTPRC	Protein tyrosine phosphatase, receptor type C	Appleton et al. (2007)
PTPRO	Protein tyrosine phosphatase, receptor type O	Appleton et al. (2007)
RELN	Reelin	Appleton et al. (2007)
RGS5	Regulator of G protein signaling 5	Appleton et al. (2007)
SCNN1A	Sodium channel epithelial 1 alpha subunit	Nagase et al. (2013)
SERPIN1	Serine protease inhibitor 1	Appleton et al. (2007)
SPON1	Spondin 1	Nagase et al. (2013)
THBD	Thrombomodulin	Appleton et al. (2007)
THBS4	Thrombospondin-4	Appleton et al. (2007)
TLR2	Toll-like receptor 2	Appleton et al. (2007)

After our literature search, the remaining 76 papers reporting on chondrocyte hypertrophy in osteoarthritis (OA) were screened for markers which were reported by the authors to be associated with the phenotypic change in OA. Markers are ordered by their associated signaling pathway or other groups.

to mice injected with a saline control. In the cartilage this was accompanied by reduced mRNA expression of *Col10a1, Adamts5, Mmp13, Mmp3,* and increased mRNA expression of the Wnt inhibitor *Sfrp1* as well as lower mRNA expression of β-catenin.

Other studies provide additional links between the Wnt/β-catenin pathway and OA (Borzi et al., 2010; Castano Betancourt et al., 2012; Papathanasiou et al., 2012; Leijten et al., 2013; van den Bosch et al., 2014). The expression of Wnt and BMP antagonists dickkopf 1 homolog (*DKK1*), frizzled-related protein (*FRZB*), and Gremlin 1 (*GREM1*) were reduced in OA cartilage compared to post-mortem healthy controls (Leijten et al., 2013). These Wnt and BMP antagonists were able to inhibit hypertrophic chondrocyte differentiation when added to chondrogenically differentiated mesenchymal stem cells (MSCs). This study also described crosstalk between the Wnt pathway and BMP signaling pathway (Leijten et al., 2013). This was functionally revealed through the decreased expression of the Wnt target gene *AXIN2* (axis inhibition protein 2) and the BMP target gene *ID1* (DNA-binding inhibitor protein 1), following treatment with BMP-2 or WNT3A, respectively (Leijten et al., 2013). This feedback loop allows tight control and balance between BMP and Wnt signaling (Leijten et al., 2013). New insight into this crosstalk between Wnt and BMP signaling pathways was obtained through the observation that BMP-2-induced Wnt signaling through influencing the SMAD1/5/8-depending LRP5 promoter activity in human OA articular chondrocytes (Papathanasiou et al., 2012). LRP5 is a co-receptor of the Wnt/β-catenin signaling pathway and its expression is increased in OA chondrocytes (Papathanasiou et al., 2012). It was indicated that the increase in mRNA levels of genes, such as *Col10a1, Mmp13,* and *Adamts5* after BMP stimulation could be abrogated by LRP5 siRNA-mediated knockdown, indicating that the hypertrophic effects of BMP signaling may promote cartilage destruction *via* increased Wnt/β-catenin signaling (Papathanasiou et al., 2012). Other intriguing crosstalk was identified between Wnt and TGF-β signaling through the finding

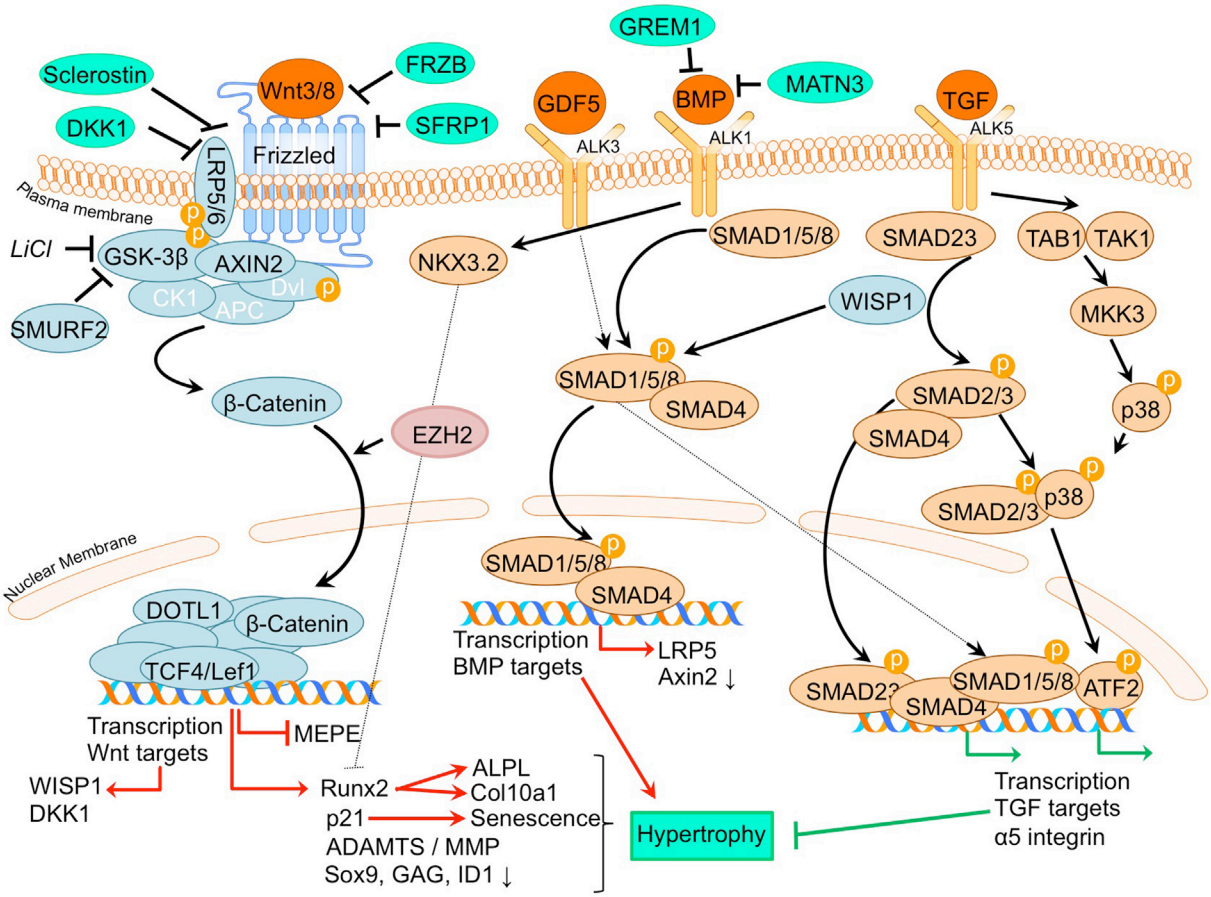

FIGURE 2 | Overview of the canonical Wnt- and TGFβ superfamily signaling pathways and newly acquired insights into their relation to the development of the osteoarthritic (OA) chondrocyte hypertrophic phenotype. The canonical pathway was updated with recent insights in the role of Wnt- and TGFβ superfamily signaling in the hypertrophic switch occuring during OA development. In green pro-chondrogenic relations are shown, while pro-hypertrophic relations are depicted in red.

that downstream TGF-β activity is altered after chondrocytes were exposed to WNT3A and the downstream canonical Wnt signaling protein WISP1 (van den Bosch et al., 2014). *In vitro* stimulation of chondrocytes or *in vivo* viral expression of WNT3, WNT8, and or WISP1 skews TGF-β signaling from ALK5 (resulting in SMAD 2/3 signaling), toward signaling *via* ALK1 (resulting in SMAD 1/5/8 phosphorylation), inducing a hypertrophic chondrocyte phenotype (van den Bosch et al., 2014).

Further support associating Wnt signaling to OA development comes from a study in which a single nucleotide polymorphism in the *DOT1L* gene results in a reduced risk for hip OA. The underlying mechanism was identified as decreased Wnt signaling activity, which was confirmed *via* reduced expression levels of the Wnt target genes, *AXIN2* and *TCF1*. DOT1L was found to be involved in chondrogenic differentiation and is thought to co-transcriptionally regulate transcription of Wnt-target genes *via* direct interaction with TCF4 (Castano Betancourt et al., 2012). Activation of Wnt signaling *via* LiCl-mediated GSK3-β inactivation led to chondrocyte cellular senescence, as indicated by increased *p21* expression, production of reactive oxygen species, SAβ galactosidase activity, and activation of the DNA damage response (Guidotti et al., 2015). Moreover it was concluded that the inhibition of GSK3-β activity promotes a chondrocyte hypertrophic phenotype, thereby supporting that Wnt signaling activity has an important balancing influence on major cell biological parameters with consequences for the chondrocyte phenotype (Guidotti et al., 2015). ShRNA-mediated MMP13 knockdown in primary human chondrocytes resulted in reduced expression of β-catenin. This was accompanied by reduced expression of RUNX2, and an increased nuclear presence of SOX9 as well as a higher glycosaminoglycan (GAG) content. This indicates that a loss of MMP13 may ameliorate chondrocyte homeostasis in a feedback loop *via* reduction of β-catenin levels (Borzi et al., 2010).

In another study, it was suggested that increased Wnt signaling may be associated with OA progression (Staines et al., 2016). STR/Ort mice develop OA spontaneously, and expression of the Wnt signaling inhibitor sclerostin (*Sost*) decreased during OA progression in these mice. Furthermore, sclerostin expression was reduced in regions with more cartilage degradation, again linking increased Wnt signaling to cartilage degradation. Intriguingly, this study also provided links between endochondral growth defects and OA progression. STR/Ort mice

display an abnormal growth plate development, with greater expression levels of COL10A1 and MMP13. This supports an association between endochondral defects and cartilage degradation (Staines et al., 2016). In contrast to the study by Staines *et al.* Papathanasiou et al. found an increased expression of the Wnt inhibitor sclerostin in human OA chondrocytes compared to normal (Papathanasiou et al., 2015). This was accompanied with a decreased methylation of the *SOST* promotor, enhancing the binding affinity of SMAD1/5/8 to the CpG region of the *SOST* promotor. Whether upregulation of *SOST* expression in articular chondrocytes is a causal factor or a result in OA has to be further determined (Papathanasiou et al., 2015).

Overall these studies together confirm the involvement of canonical Wnt signaling in chondrocyte hypertrophy and revealed novel mechanisms that appear to tune canonical Wnt signaling responses and which relate to the development of OA.

Ihh/PTHrP Signaling

PTHrP- and Indian hedgehog signaling pathways generate a feedback loop which is involved in controlling the chondrocyte phenotype in the growth plate in skeletal development, as well as in determining the homeostasis that keeps articular cartilage healthy (Kronenberg, 2003). When IHH reaches its target cell, it binds to the Patched-1 (PTCH1) receptor. In the absence of ligand, PTCH1 inhibits Smoothened (SMO), the binding of IHH relieves SMO inhibition, leading to activation of the GLI transcription factors: the activators GLI1 and GLI2 and the repressor GLI3. Activated GLI accumulates in the nucleus and controls the transcription of hedgehog target genes (Yang et al., 2015). Insight into the mechanism of action of PTH and PTHrP has been provided by the discovery of the type I PTH/PTHrP receptor (PTHR). This G protein-coupled receptor (GPCR) is associated with, among others, the adenylyl cyclase/protein kinase A (PKA) pathway (Mannstadt et al., 1999). The PTHrP/Ihh feedback loop is a major determinant of the chondrocyte hypertrophic phenotype, and thus postulated to be pivotal in OA development. It is thought that part of the contra-hypertrophic action of PTHrP originates from inducing the expression of BAPX1/NKX3.2 (Provot et al., 2006), a potent hypertrophic switch (Caron et al., 2015). Some of the pertinent evidence that chondrocyte hypertrophy is an intrinsic part of OA development comes from papers regarding PTHrP/Ihh signaling. An overview of the newly acquired insights into this pathway and its involvement in development of OA chondrocyte hypertrophy is provided in **Table 1**b and **Figure 3**.

Given that PTHrP maintains the function of proliferating chondrocytes in the growth plate and inhibits chondrocyte differentiation toward hypertrophy, it has been suggested that PTHrP may be protective against OA (Kronenberg, 2003). Several studies demonstrate direct evidence that inhibiting hypertrophic processes results in protection against OA. Confirming an

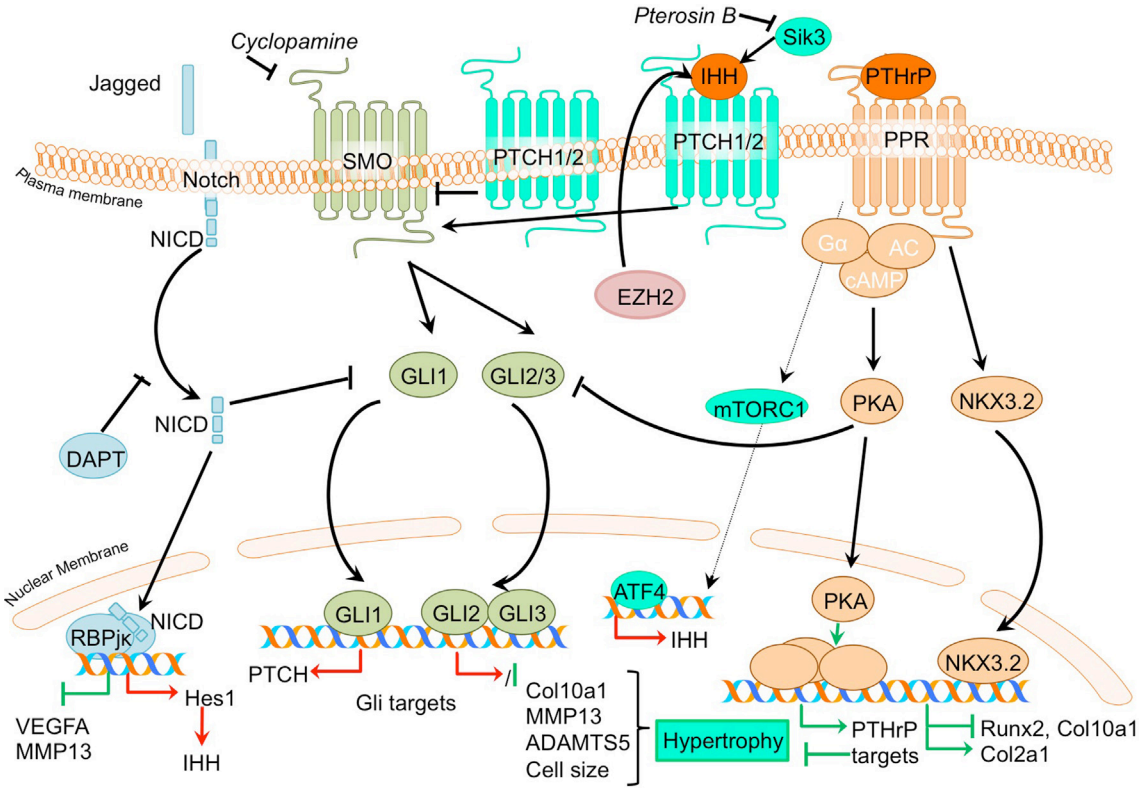

FIGURE 3 | Overview of the canonical Ihh/PTHrP and Notch signaling pathways and newly acquired insights into their relation to the development of the osteoarthritic (OA) chondrocyte hypertrophic phenotype. The canonical pathway was updated with recent insights in the role of Ihh/PTHrP and Notch signaling in the hypertrophic switch occuring during OA development. In green pro-chondrogenic relations are shown, while pro-hypertrophic relations are depicted in red.

anti-hypertrophic and OA protective effect of PTHrP, it was shown that PTHrP can inhibit terminal differentiation of normal human articular chondrocytes and that intra-articular PTHrP administration in a chemically induced rat OA model reduces OA, as evidenced by reduced GAG loss (Chang et al., 2009). Along with reduced matrix loss, PTHrP treatment of chemically OA-induced knees also resulted in increased *Col2a1* levels and reduced *Col10a1* levels in the cartilage compared to OA-induced knees without PTHrP injection (Chang et al., 2009). Another study confirmed the chondroprotective and anti-hypertrophic role of PTHrP signaling in cartilage by revealing that incorporating PTHrP into a drug delivery system reduced OA severity in a chemically induced mouse OA model. This was evidenced through reduced GAG loss accompanied by decreased COL10A1 staining (Eswaramoorthy et al., 2012). The anti-hypertrophic role of PTHrP signaling was further confirmed in a study in which OA chondrocytes incorporated in alginate beads were treated with PTHrP, leading to reduced *COL10A1* expression (Pesesse et al., 2014).

While PTHrP has been associated with anti-hypertrophic actions in the growth plate and in OA, Ihh expression is considered as a marker gene for hypertrophic chondrocytes in growth plates (Weisser et al., 2002). In concert with an important role for Ihh in chondrocyte hypertrophy, inhibition of the Ihh pathway protected against OA development (Zhou et al., 2014). In this study, a cartilage-specific *Ihh* knockout mouse was used to genetically confirm that Ihh drives the development of OA (Zhou et al., 2014). Cartilage-specific deletion of *Ihh* largely protected against the development of post-traumatic OA. Next to the decreased OA severity [as determined by the OOCHAS score (Osteoarthritis Cartilage Histopathology Assessment System)], *Ihh*-deleted mice revealed decreased expression of COL10A1 and MMP13, as well as decreased activity of cartilage proteolytic enzymes. A study by Yahara et al. illustrated a reduction of hypertrophic changes in *Sik3* deficient mice including reduced *Ihh* levels (Yahara et al., 2016). The precise mechanism behind the anti-hypertrophic actions of Pterosin B *via* SIK3 is unknown, but KEGG (Kyoto Encyclopedia of Genes and Genomes) pathway analysis indicated an inhibition of *Ihh* by Pterosin B, which is a SIK3 inhibitor.

It was demonstrated that the expression of *IHH* is increased in OA cartilage compared to cartilage obtained from non-OA patients (Wei et al., 2012). Furthermore, *IHH* levels were also higher in OA synovial fluid compared to non-OA synovial fluid (Wei et al., 2012). Since, expression of *IHH* was higher in more severely degenerated cartilage areas, as determined by the modified Mankin score, this also indicated an association of cartilage hypertrophic changes with OA progression (Wei et al., 2012). The authors in this study provided important evidence that chondrocyte hypertrophy is involved in the association between *IHH* and OA, showing that OA chondrocytes treated with Ihh displayed increased mRNA expression levels of markers of chondrocyte hypertrophy *COL10A1* and *MMP13*. Furthermore, both *IHH* expression and chondrocyte size (the phenotypic hallmark of hypertrophy) were associated with OA severity. Modulation of Ihh signaling activity by the inhibitor cyclopamine caused a reduction of *COL10A1* and *MMP13* expression, suggesting that dampening the activity of the Ihh pathway may provide a target for OA treatment (Wei et al., 2012). Additional support connecting Ihh signaling to OA comes from an earlier mentioned study that described that the inhibition of EZH2 reduces cartilage degradation *in vivo*. It was found that *IHH* expression was increased after overexpression of *EZH2* in chondrocytes, and was associated with an overall increased hypertrophic phenotype (Chen et al., 2016).

To isolate the effects of hedgehog pathway activation, the consequences of its activation for cartilage degradation have been investigated (Thompson et al., 2015). In contrast to the large body of evidence for an OA promoting role of Ihh, studies in bovine and human cartilage explants revealed that activation of hedgehog signaling by exposure to IHH did not increase *ADAMTS5* or *MMP13* expression. Chondrocyte hypertrophic phenotype development was not extensively addressed in this study, but it appears that the catabolic effects of hedgehog signaling in OA may be context dependent.

Recent advancements in research regarding crosstalk with other signaling pathways shows that hedgehog signaling crosstalks with the Notch signaling pathway (Lin et al., 2016) and with the Wnt signaling, BMP signaling, FGF (Zhou et al., 2016), and mTOR signaling pathways (Leijten et al., 2013). Inhibition of Notch1 resulted in an increased, HES1 dependent, hedgehog signaling activity (Lin et al., 2016). This increased activity led to an exacerbation of experimental OA, characterized by increased levels hedgehog target genes, *osteocalcin*, *COL10A1*, *ADAMTS5*, osteophyte formation, and reduced OARSI scores (Lin et al., 2016). It is still not completely understood as to how Notch signaling controls hedgehog signaling. It has, however, been suggested that Notch signaling activity may limit hypertrophy-provoking hedgehog signaling in articular chondrocytes (Lin et al., 2016). Interestingly, mTORC1 activation in mouse articular cartilage from 2-month-old mice resulted in upregulation of Ihh expression, along with other hypertrophic markers, such as RUNX2 and COL10A1, suggesting interplay between mTOR and Ihh signaling (Zhang et al., 2017). Along with an early increase in hypertrophic markers, mice in which mTORC1 was activated developed progressive OA, together with an increasing ratio of calcified cartilage relative to hyaline cartilage through time. In this study, it was also suggested that mTORC1 activation inhibits PTHrP signaling *via* downregulating the PPR receptor which ultimately results in impaired prevention of the initiation of chondrocyte hypertrophic differentiation (Zhang et al., 2017). Ihh signaling was also shown to crosstalk with the fibroblast growth factor (FGF) pathway, since the OA-like changes in the temporomandibular joints of FGFR3 knockout mice could be ameliorated using an Ihh signaling inhibitor (Zhou et al., 2016).

Together these studies underline the involvement of the PTHrP/Ihh feedback loop in determining the chondrocyte phenotype, and recent developments reveal that a disruption of this well-balanced system can initiate a hypertrophic switch, ultimately leading toward OA disease initiation and progression.

TGF-β Superfamily Signaling

The TGF-β superfamily is a group of multifunctional cytokines that play critical roles in cartilage homeostasis and have well established roles in endochondral ossification (Dangelo et al.,

2001). In the classical TGF-β superfamily signaling pathway, superfamily ligands, such as TGF-β and BMP isoforms, bind to their respective cell surface receptors and, upon type I and -II receptor dimerization, activate a signaling cascade which includes the recruitment, phosphorylation, and interaction of different SMAD proteins. Upon activation, SMAD complexes translocate to the nucleus to drive transcription of genes regulating a variety of biological responses (van der Kraan et al., 2009). TGF-β has been strongly implicated in OA pathogenesis, since it has been well established that deregulation of TGF-β signaling is associated with OA (van der Kraan et al., 2009; van der Kraan, 2017). An overview of newly acquired insights into this pathway and its involvement in development of OA chondrocyte hypertrophy is provided in **Table 1**c and **Figure 2**.

Several studies have demonstrated an increased expression of TGF-β superfamily members or their receptors and down-stream signaling molecules in human OA chondrocytes compared to non-OA chondrocytes (Papathanasiou et al., 2012, 2015). TGF-β superfamily ligands can signal in chondrocytes *via* SMAD2/3 and also *via* SMAD1/5/8 (van der Kraan, 2017). The type I receptor ALK1 is associated with SMAD1/5/8 activity and hypertrophy and mineralization (Blaney Davidson et al., 2009). Additionally, a high correlation was found between ALK1 and the hypertrophic marker MMP13 (Blaney Davidson et al., 2009). In contrast, the type I receptor ALK5 is associated with SMAD2/3 activity and has anti-hypertrophic chondroprotective effects (van der Kraan et al., 2009). Together with the association of ALK1 with the hypertrophic marker MMP13, the study by Blaney Davidson et al. revealed that the ALK1/ALK5 ratio is increased in a post-traumatic model of OA using the destabilization of the medial meniscus (DMM) mouse OA model, and also increased with OA progression (Blaney Davidson et al., 2009), again highlighting the involvement of chondrocyte hypertrophic processes in OA development. The association of SMAD1/5/8 signaling with chondrocyte hypertrophy and OA is further confirmed in another study by Yang et al. Here, an association between the noncollagenous extracellular matrix protein Matrilin-3 (MATN3), and the SMAD1 pathway was confirmed (Yang et al., 2014). Authors of this study had earlier shown that *Matn3* KO mice displayed premature articular cartilage hypertrophy and accelerated OA-like joint pathology (van der Weyden et al., 2006) and sought to determine molecular explanations for increased chondrocyte hypertrophy after *Matn3* knockout. It was demonstrated that BMP-2 expression in embryonic chicken chondrocytes and a murine chondrocyte cell line lead to increased SMAD1 phosphorylation, resulting in increased *Col10a1* promotor activity (Yang et al., 2014). MATN3 was able to directly interact with BMP-2 and acts as a BMP-2 antagonist inhibiting BMP-2-induced SMAD1 phosphorylation and reducing *Col10a1* expression levels and chondrocyte hypertrophy.

TGF-β superfamily members can tune the activity and levels of chondrocyte phenotype-determining downstream transcriptional regulators. Examples of these downstream transcriptional regulators controlling the chondrocyte phenotype are BAPX1/NKX3.2 and ATF2. It was demonstrated that the anti-hypertrophic effect of BMP-7 on OA chondrocytes, evidenced by a reduction in mRNA expression levels of *COL10A1*, *MMP13,* and *RUNX2,* could be blocked with BAPX1/NKX3.2 knockdown, indicating that BMP-7 suppresses the hypertrophic phenotype in OA chondrocytes *via* BAPX1/NKX3.2 (Caron et al., 2015). ATF2 has been demonstrated to be expressed in the resting and proliferating zones of the growth plate, but not the hypertrophic zone (Reimold et al., 1996). It was established that ATF2 phosphorylation via TAK1 and p38 (which activates ATF2) was decreased as a consequence of SMAD3 ablation in DMM-induced OA in mice (Li et al., 2010). This study also revealed that ATF2 was able to reduce the increase in *Col10a1* mRNA expression levels induced by BMP-2 stimulation, hinting at ATF2 as a protective factor to dampen chondrocyte hypertrophy.

TGF-β superfamily members have also been revealed to modulate the expression of integrins, which are ECM receptors involved in chondrocyte differentiation (Garciadiego-Cazares et al., 2015). Treatment of differentiating mesenchymal stem cells with TGF-β superfamily member GDF-5 induced α5 integrin expression and prevented chondrocyte hypertrophy (Garciadiego-Cazares et al., 2015). It was demonstrated that in articular cartilage of rats with surgically induced OA α5 integrin expression was reduced and associated with chondrocyte hypertrophy. It was concluded that α5 integrin expression is protective against hypertrophic changes.

In conclusion, these studies further establish that different TGF-β superfamily members are involved in regulating the chondrocyte phenotype *via* tuning of different downstream factors involved in gene transcription, which ultimately leads to either chondroprotective or pro-hypertrophic responses.

MAP Kinases

The MAP kinase (MAPK) pathway consists of a sequence of intracellular signaling proteins which transduce a signal from various cell receptors to the nucleus (Schaeffer and Weber, 1999). Activity of MAPKs is regulated in response to environmental stress and to cytokines and growth factors, such as members of the Wnt family (Bikkavilli and Malbon, 2009) or the TGF-β superfamily (Derynck and Zhang, 2003). After activation, a cascade of phosphorylating events takes place intracellularly, finally resulting in phosphorylation of the MAPKs themselves. The three major MAPK pathways, include p38, c-Jun N-terminal (JNK) kinase, and extra-cellular-regulated kinases (ERK) (Johnson and Lapadat, 2002). The currently held doctrine considers MAPKs as signaling mediators involved in the endochondral ossification process (Stanton et al., 2003), but they are also able to regulate the activity of multiple mediators of cartilage destruction (Loeser et al., 2008). Studies suggest that the ERK pathway is involved in destructive OA responses (Prasadam et al., 2013), while the p38 pathway is OA protective (Li et al., 2010; Prasadam et al., 2010). An overview of the newly acquired insights into this pathway and its involvement in development of OA chondrocyte hypertrophy is provided in **Table 1**d and **Figure 4**.

It was demonstrated that phosphorylation of ERK1/2 was increased in OA tibial cartilage together with an increased hypertrophic phenotype, characterized by increased COL10A1 and RUNX2 expression levels in a surgically induced rat OA model (Prasadam et al., 2013). On the other hand, expression levels of phosphorylated p38 were decreased in OA compared

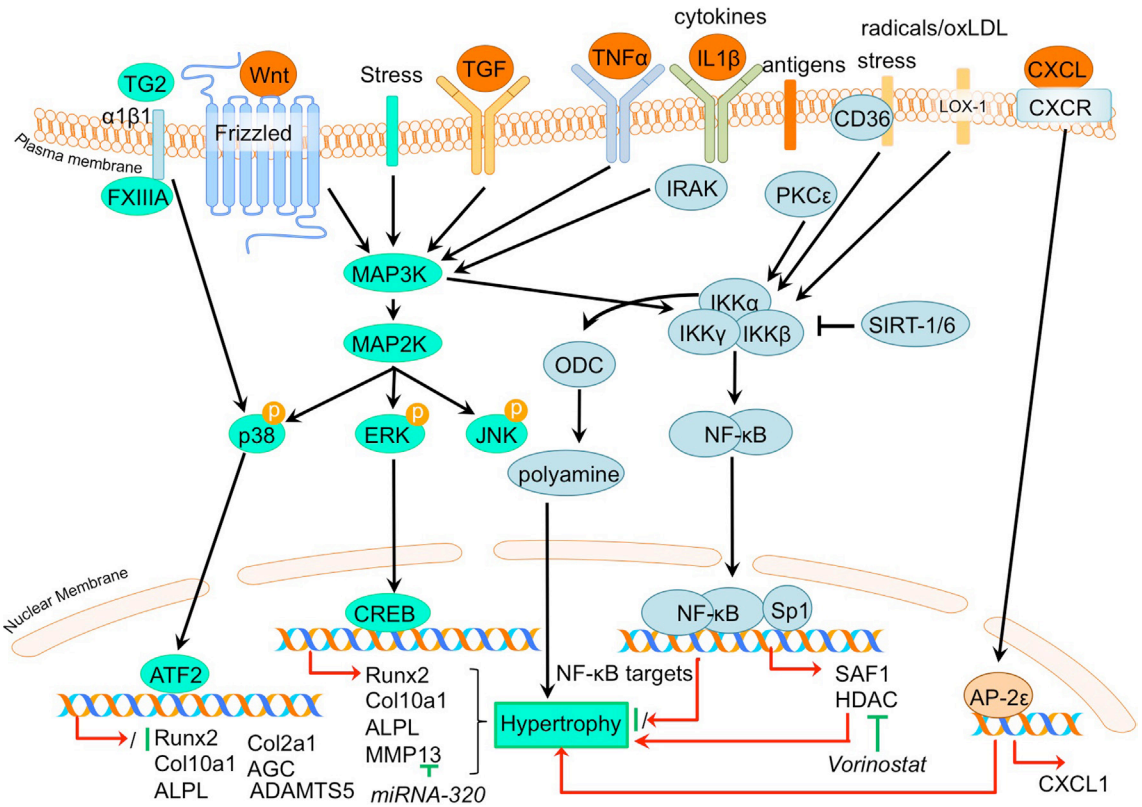

FIGURE 4 | Overview of the canonical MAP kinase (MAPK) and inflammatory signaling pathways and newly acquired insights into their relation to the development of the osteoarthritic (OA) chondrocyte hypertrophic phenotype. The canonical pathway was updated with recent insights in the role of MAPK and inflammatory signaling in the hypertrophic switch occuring during OA development. In green pro-chondrogenic relations are shown, while pro-hypertrophic relations are depicted in red.

to non-OA cartilage (Prasadam et al., 2013). This study also revealed that pharmacological ERK inhibition together with hyaluronic acid treatment resulted in a synergistic chondroprotective effect compared to hyaluronic acid treatment only. This was characterized by significantly reduced Mankin scores, accompanied by reduced COL10A1 expression levels (Prasadam et al., 2013). Higher pERK levels, along with increased expression levels of hypertrophic markers, such as *ALPL* and *RUNX2* were also found in OA articular chondrocytes compared to healthy articular chondrocytes (Prasadam et al., 2010). Furthermore, VEGF-induced hypertrophy of chondrocytes was accompanied by pERK activation (Zhang et al., 2016a,b).

In contrast to pERK, p38 has been negatively associated with OA. P38 expression levels were higher in wild-type murine articular cartilage compared to *Smad3* knockout mice displaying cartilage damage (Li et al., 2010). P38 levels were also lower in human OA articular chondrocytes compared to healthy human articular chondrocytes (Prasadam et al., 2010).

The pro-hypertrophic effects of pERK and contra-hypertrophic effects of p38 were further substantiated in a co-culture system using subchondral osteoblasts (Prasadam et al., 2010). Co-culturing human articular chondrocytes with subchondral osteoblasts induced hypertrophic changes in the articular chondrocytes, evidenced by increased *RUNX2*, *ALPL*, and *COL10A1* expression and decreased *COL2A1* and *AGC* expression. Hypertrophic induction in these articular chondrocytes was accompanied by increased pERK phosphorylation and phosphorylation of p38 was decreased. Inhibition of pERK in cultures was able to reduce the hypertrophic induction of articular chondrocytes, in contrast to inhibition of p38 that resulted in hypertrophic induction (Prasadam et al., 2010). Furthermore, confirming a role for pERK in hypertrophic processes in OA chondrocytes, ERK1/2 inhibition abolished FGF23-induced *MMP13* expression (Bianchi et al., 2016).

Although p38 is generally considered to act in a chondroprotective manner, it has been evidenced that under certain conditions the p38 activation may result in hypertrophic differentiation in cultured chondrocytes (Merz et al., 2003; Wang and Beier, 2005). In a study by Johnson et al. (2008) it was found that the transglutaminases (TG) TG2 and factor XIIIA (FXIIIA) were increased in hypertrophic chondrocytes from the growth plate and in OA articular chondrocytes (Johnson et al., 2008). Externalization of TG2 is mediated by FXIIIA *via* its interaction with α1β1 integrins and results in activation of the p38 MAPK signaling pathway, which ultimately led to increased COL10A1 expression in this study (Johnson et al., 2008). Additionally, TG2 expression was found to be associated with enhanced articular chondrocyte hypertrophy in a Hartley Guinea Pig Model of OA

as determined by increased MMP13 and ADAMTS5 and an enhanced *Col10a1:Col2a1* ratio (Huebner et al., 2009).

Taken together, specific MAP kinases have been demonstrated to regulate both hypertrophic and chondrogenic responses in the chondrocyte and inhibition of specific MAP kinases could potentially be a strategy to block OA progression *via* modulating the hypertrophic chondrocyte phenotype.

Inflammatory Signaling

Not surprisingly, regarding the inflammatory nature of OA, the involvement of the NF-κB (nuclear factor kappa-light-chain-enhancer of activated B cells) pathway has been described as involved in the regulation of hypertrophic differentiation in OA (Marcu et al., 2010). Many stimuli (such as stress, cytokines, free radicals, heavy metals, ultraviolet irradiation, oxidized LDL, and bacterial or viral antigens), activate NF-κB, mostly through IκB kinase-dependent (IKK-dependent) phosphorylation and subsequent degradation of NF-κB inhibitory IκB proteins. The liberated NF-κB dimer enters the nucleus, where it regulates transcription of diverse target genes (Marcu et al., 2010). An overview of newly acquired insights into this pathway and its involvement in development of OA chondrocyte hypertrophy is provided in **Table 1**e and **Figure 4**.

Providing evidence for a role of NF-κB signaling in chondrocyte hypertrophy, it was demonstrated that IKKα and IKKβ knockdown in OA chondrocyte micromass cultures results in an increased GAG content, COL2A1 expression, and reduced calcium deposits. IKKα and IKKβ also appeared to have differential activities, since IKKα knockdown, but not IKKβ knockdown, resulted in smaller OA hypertrophic chondrocytes (Olivotto et al., 2008). Furthermore, only IKKα knockdown resulted in reduced RUNX2 levels, while IKKβ knockdown resulted in increased SOX9 levels. The pro-hypertrophic role of IKKα was later confirmed by the same group (Olivotto et al., 2013), as well as another group (Facchini et al., 2012). Facchini et al. revealed that expression of IKKα is related to chondrocyte hypertrophy and knockdown of IKKα results in reduced synthesis and activity of ornithine decarboxylase (ODC). ODC mediates the increase of polyamine levels that in turn increases *RUNX2* expression, as well as RUNX2 nuclear translocation, leading to hypertrophic chondrocytes (Facchini et al., 2012). Additionally, a study by Meng et al. also revealed a role for NF-kB signaling in chondrocyte hypertrophy (Meng et al., 2016). In this study it was found that microRNA- (MiRNA)320 negatively regulates *MMP13* expression by binding to the 3'UTR (3' untranslated region) of the *MMP13* mRNA. In turn, miRNA320 expression is reduced by IL-1β-induced NF-κB and MAPK signaling activity (Meng et al., 2016). This study thus revealed a link between a hypertrophy-dependent decrease of miRNA-320 and an increase of *MMP13 via* the NF-κB and MAPK signaling pathway. Oxidized low-density lipoprotein (ox-LDL) binding to lectin-like ox-LDL receptor-1 (LOX-1) in cultured bovine articular chondrocytes increased production of intracellular reactive oxygen species (ROS), resulting in the activation of the inflammatory signaling pathway *via* NF-κB (Nishimura et al., 2004). Hashimoto et al. demonstrated a role for LOX-1 in chondrocyte hypertrophy, as COL10A1 expression in a DMM mice OA model was induced by expression of the LOX-1. This resulted in decreased articular cartilage GAG content (Hashimoto et al., 2016). *LOX-1*$^{-/-}$ mice on the other hand, revealed a reduced OA score and a reduction in osteophyte formation. LOX-1 co-localized with RUNX2 and COL10A1 expression in articular chondrocytes as well as in osteophyte forming-cells, indicating a role in the pathogenesis of DMM-induced OA through endochondral ossification (Hashimoto et al., 2016).

In a study by Zhong et al. it was found that in IL-1β-treated OA chondrocytes, expression of the NF-κB subunit p65 was reduced in response to the HDAC-inhibitor vorinostat. Besides this inflammatory pathway, HDAC inhibition by vorinostat also resulted in decreased p38 and ERK1/2 activation in IL-1β-exposed human OA chondrocytes (Zhong et al., 2013). During OA progression in human articular chondrocytes, PKCε (protein kinase C epsilon) levels were reduced, which lead to an upregulation of *HDAC2* and reduction of *HDAC4* (Queirolo et al., 2016). This resulted in an increase of the *HDAC2:HDAC4* ratio, which then induced RUNX2 and ultimately resulted in increased expression of MMP13, ADAMTS4, and ADAMTS5 (Queirolo et al., 2016). Interestingly, the decreased expression of HDAC4, related to the loss of PKCε in OA chondrocytes (Queirolo et al., 2016), was confirmed in another study by Lu et al. (2014a). However, in contradiction to the previous study, Lu et al. found that silencing of *HDAC4* resulted in a decrease of chondrocyte hypertrophic marker expression, while additionally HDAC4 was decreased with increasing severity of OA, suggesting a role for HDAC4 in the onset of OA.

Besides NF-κB, ELR + CXC chemokines, which are characterized by their glutamic acid-leucine-arginine (ELR+) motif, provide new links connecting OA to hypertrophic changes (Wenke et al., 2011). AP-2ε is a transcription factor which acts in hypertrophic cartilage differentiation and its expression is increased in OA chondrocytes compared to primary chondrocytes (Wenke et al., 2009). This study described that *CXCL1* expression accompanied the increase in *AP-2ε* expression levels during hypertrophic differentiation of MSCs (Wenke et al., 2011). Expression of *CXCL1* appeared to be under transcriptional control of AP-2ε, since AP-2ε was demonstrated to bind and transactivate the *CXCL1* promotor, indicating that the observed increase in AP-2ε in OA chondrocytes may lead to hypertrophic changes *via* regulating CXCL1 activity (Wenke et al., 2011). Another chemokine that was revealed to be involved in OA pathogenesis is CXCL6 (Sherwood et al., 2015). It was shown that the expression of this chemokine is reduced in human OA cartilage (Sherwood et al., 2015) and also in a mouse DMM OA model (Sherwood et al., 2015). Knockout of the CXCL6 receptor, *CXCR2*, resulted in more severe OA development after DMM surgery, as evidenced by higher OARSI scores (Sherwood et al., 2015). This was also accompanied by a more hypertrophic phenotype verified by increased COL10A1 protein expression. These data suggest a chondroprotective action of the CXCL6-CXCR2 axis.

In addition to chemokines, different inflammatory cytokines have been implicated in OA pathophysiology, one of them being TNFα (Lai et al., 2014). It was recently confirmed that TNFα induces *Adamts7* expression in murine cartilage, and ADAMTS7

was able to induce the expression of *Tnfα,* creating a positive feedback loop (Lai et al., 2014). TNFα-mediated transactivation of an *Adamts7* promotor reporter construct was dose-dependently inhibited by Bay 11-7082, a NF-κB-specific inhibitor, indicating NF-κB-mediated activation of *Adamts7* after TNFα stimulation. Interestingly, mice overexpressing ADAMTS7 displayed OA-like phenotypes characterized by reduced cartilage GAG content, osteophyte formation, thinner cartilage, and an upregulation of hypertrophic marker expression such as Col10a1 and MMP13. Furthermore, ADAMTS7 overexpression resulted in an acceleration of OA development in a mouse DMM experiment which was also accompanied by increased expression of chondrocyte hypertrophic markers *Col10a1* and *Mmp13* (Lai et al., 2014). The ADAMTS7 overexpressing mice also displayed several skeletal developmental abnormalities, including a reduced hypertrophic zone and reduced COL10A1 levels in the growth plate and lower bone mineral density.

The inflammatory S100A11, a ligand for the receptor for advanced glycation end products (RAGE), is associated with chondrocyte hypertrophy (Cecil et al., 2009). However, the deletion of RAGE was not chondroprotective in an instability induced knee OA mouse model (Cecil et al., 2009). Cecil et al. (2009) demonstrated that the alternative patterning receptor CD36, a marker for growth plate chondrocyte hypertrophy, promotes OA *via* mediation of inflammatory and differentiation responses. Indeed, CD36 co-localized with COL10A1 expression in all zones of knee articular cartilage, as well as the aggrecan NITEGE aggrecanase neoepitope in the articular cartilage superficial zone. Surprisingly, overexpression of CD36 in CH-8 cells led to an inhibition of chondrocyte hypertrophic markers (Cecil et al., 2009), while S100A11 gained the capacity to induce proteoglycan synthesis in CH-8 chondrocytes (Cecil et al., 2009). These results indicate that CD36 is a hypertrophic chondrocyte-expressed patterning receptor that induces cartilage repair when exposed to inflammatory stimuli (Cecil et al., 2009). This demonstrates that besides pro-hypertrophic processes, inflammatory responses in articular chondrocytes can also result in a chondroprotective effect.

The semicarbazide-sensitive amine oxidase (SSAO) found in the hypertrophic chondrocytes of the growth plate is known to be involved in leukocyte extravasation from the blood to the inflammation site. Additionally, it may be associated with the differentiation of chondrocytes toward a hypertrophic phenotype (Filip et al., 2016). In line with this, inhibition of SSAO reduced *Mmp13, Alpl,* and *Opn* expression, potentially by modulation of glucose transport in rat hypertrophic articular chondrocytes (Filip et al., 2016). In humans, similar expression patterns were seen for SSAO in healthy and OA articular cartilage, supporting the idea that SSAO plays a role in the process of hypertrophic differentiation of the articular chondrocyte (Filip et al., 2016). OA is a disease associated with aging, which could be a result of tissue accumulation of $p16^{INK4a}$ positive cells. $p16^{INK4a}$ is suggested to support chronic inflammation, as $p16^{INK4a}$ positive cells exhibit a specific secretome called SASP (senescence-associated secretory phenotype) including pro-inflammatory cytokines. OA chondrocytes are characterized by an accumulation of $p16^{INK4a}$ as a result of reduced *miRNA24* levels, which acts as a negative regulator for $p16^{INK4a}$ (Philipot et al., 2014). $p16^{INK4a}$ is also upregulated during chondrogenesis, indicating a recapitulation of a developmental process in OA.

Since inflammation and angiogenesis are closely correlated in the pathogenesis of OA, Ray et al. hypothesized the presence of common regulators controlling both processes simultaneously (Ray and Ray, 2008). In their study they found that overexpression of the inflammation responsive transcription factor SAF-1 in transgenic mice leads to the development of severe cartilage degradation and OA. SAF-1-overexpressing mice also showed neo-vasculature in the perichondrium and synovium, suggesting a link between angiogenesis and inflammation. Indeed, the *VEGF* promotor contains two tandem binding sites for SAF-1 (Ray and Ray, 2008), providing evidence for the link between inflammation and OA development and pathogenesis. Furthermore, SAF-1 has binding sites in the *MMP1* and *MMP9* promotor sequences (Ray and Ray, 2008), controlling their expression. In human OA articular chondrocytes, SAF-1 expression is increased and together with NF-κB and SP1 acts synergistically to induce MMP activation in OA chondrocytes.

Another factor involved in inflammatory signaling and OA disease progression is SIRT-1. SIRT-1 inhibits NF-κB by deacetylating the p65 NF-κB subunit, priming p65 for proteasome degradation, thus modulating the inflammatory signaling pathway (Liu-Bryan, 2015). The association of SIRT-1 with chondrocyte hypertrophy was demonstrated after inhibition of SIRT-1 by RNAi, which induced *COL10A1* expression. Since OA chondrocytes display decreased SIRT-1 expression compared to healthy controls, this may provide a route for chondrocytes to acquire an endochondral cellular phenotype (Fujita et al., 2011). Besides SIRT-1, SIRT-6 also modulates inflammation. *SIRT-6* haploinsufficiency enhanced OA progression in high fat diet-induced obese mice by stimulating the inflammatory response as shown by increased expression of *Tnfα* and *IL-6* in the HFP (Ailixiding et al., 2015). Additionally, *SIRT-6* haplo-insufficient mice on a high fat diet revealed an increase in osteophytes and synovial tissue with increased infiltration of inflammatory cells, as well as increased MMP13 expression in the cartilage. These results indicate a higher inflammation status of the HFP and synovium in obese mice with *SIRT-6* haplo-insufficiency accompanied with increased osteophyte formation, leading to OA.

To conclude cytokines and chemokines and their downstream intracellular pathways have been revealed to lead to hypertrophic as well as anti-hypertrophic changes in the chondrocyte. While inflammation-induced hypertrophic changes have been established as associated with processes involved in cartilage matrix degradation, inflammation-induced anti-hypertrophic changes have been described to lead to chondroprotective responses.

HYPOXIC AND ANGIOGENIC FACTORS

The proliferative zone of the growth plate is an avascular hypoxic mesenchymal tissue (Maes et al., 2012). Intriguingly, chondrocytes are competent at surviving and differentiating in this challenging environment. It has been suggested that this survival and capability of differentiation is, at least in part, by virtue of the actions of hypoxia-inducible factors (HIFs),

such as HIF1-α (Maes et al., 2012). Furthermore, the process of endochondral ossification in the growth plate is driven by vascularization and hypertrophic chondrocytes in the growth plate that secrete angiogenic stimuli which actively support vascularization (Maes et al., 2012). This hypertrophy associated angiogenic switch is a major driver of active growth plate cartilage remodeling toward bony tissue (Maes et al., 2012). The analogy between endochondral ossification processes and molecular processes observed in OA also led to the theory that OA pathophysiology may involve hypoxic/angiogenic mediators, such as HIFs and VEGF. An overview of the newly acquired insights into this pathway and its involvement in development of OA chondrocyte hypertrophy is provided in **Table 1**f and **Figure 5**.

A direct link between HIF-2α and OA development became evident by a study reported by Saito et al (Saito et al., 2010). It revealed that HIF-2α is localized predominantly in the hypertrophic zone of mouse growth plates, and *Hif-2α*$^{+/-}$ mice display reduced proliferative and hypertrophic zone lengths, together with impaired bone length, indicating impaired endochondral ossification during limb development. Confirming its role in OA pathophysiology, HIF-2α expression was increased in articular chondrocytes of a surgically induced OA mouse model, while *Hif-2α*$^{+/-}$ caused significant resistance to cartilage degradation, osteophyte formation, and subchondral bone sclerosis in this model (Saito et al., 2010). Furthermore, in the same study HIF-2α expression was revealed to be higher in more severely OA-affected human cartilage samples than in mild OA affected regions. The crucial role of HIF-2α in OA pathophysiology was confirmed in another study, which described that *Hif-2α*$^{+/-}$ mice display less cartilage degradation in a surgically induced mouse OA model (Hirata et al., 2012). Furthermore, it was evident that in chondrocytes, HIF-2α is a potent inducer of C/EBPβ (Hirata et al., 2012). Confirming a role for C/EBPβ in OA pathophysiology, *C/Ebpβ*$^{+/-}$ mice developed less severe OA cartilage damage in a surgically induced mouse OA model (Hirata et al., 2012). Furthermore, C/EBPβ together with RUNX2 is higher expressed in human OA cartilage with higher Mankin scores compared to human OA cartilage with lower Mankin scores, and can activate *MMP13* expression in chondrocytes (Hirata et al., 2012).

Dio2 is upregulated in OA cartilage (Nagase et al., 2013) and is responsible for active thyroid hormone (T3) production. T3 in turn induces terminal chondrocyte differentiation with increased HIF-2α expression, as well as *COL10A1, ALPL, osteocalcin, RUNX2, MMP13,* and *ADAMTS5* expression (Nagase et al., 2013; Bomer et al., 2015). The upregulation of *HIF-2α* expression after T3 treatment suggests a link between DIO2 levels and OA development *via* HIF-2α signaling and activating mutations in the *DIO2* allele result in a predisposition for OA development in human patients (Bomer et al., 2015). Additionally, it was demonstrated in an experimental *Dio2* transgenic rat OA model that overexpression of DIO2 results in increased OA-associated

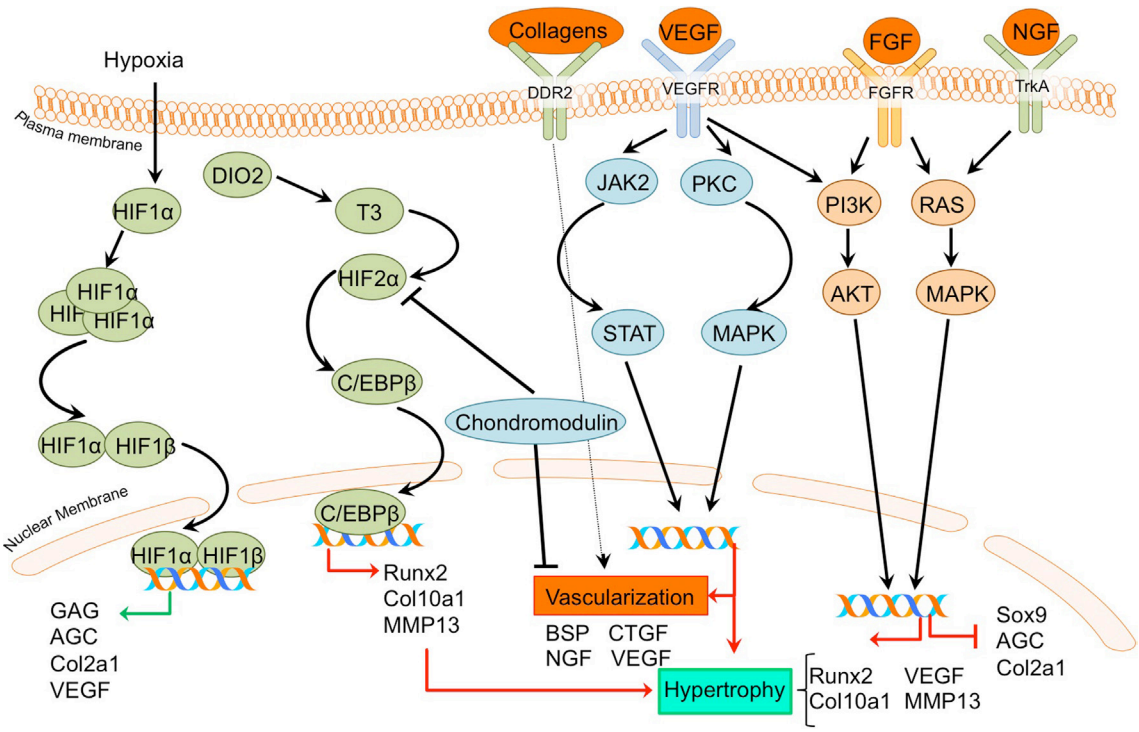

FIGURE 5 | Overview of the processes of hypoxia and angiogenesis and the canonical fibroblast growth factor (FGF) signaling pathway and newly acquired insights into their relation to the development of the osteoarthritic (OA) chondrocyte hypertrophic phenotype. The processes and canonical FGF signaling pathway was updated with recent insights in the role of the processes of hypoxia and angiogenesis and the FGF signaling pathway in the hypertrohic switch occuring during OA development. In green pro-chondrogenic relations are shown, while pro-hypertrophic relations are depicted in red.

cartilage degradation with higher COL10A1 expression levels (Nagase et al., 2013). Confirming parallels between chondrocyte signaling events that take place in the growth plate and those of hypertrophic chondrocytes in OA-affected articular cartilage, DIO2 activity was also increased during chondrogenesis of BMSCs (Bomer et al., 2015).

Despite the general recognition that HIF expression in cartilage is associated with OA disease progression, a study by Markway et al. could not detect a differential expression of HIF-1α and HIF-2α in OA versus healthy chondrocytes under hypoxic conditions (Markway et al., 2013). In this study, hypoxia-induced HIF expression resulted in increased COL2A1, ACAN, and GAG levels (Markway et al., 2013). While HIF-2α is normally described as associated with hypertrophy, HIF-3α is not. HIF-3α expression is higher in the resting and proliferative zones of the growth plate compared to the hypertrophic zone (Markway et al., 2015). Furthermore, chondrogenically differentiated BMSCs showed *MMP13* and *COL10A1* induction, while *HIF-3*α expression was low.

In addition to HIF-2α, VEGF was demonstrated to be involved in OA development. In a surgically induced rat OA model, inhibition of *Vegf* with a shRNA resulted in less cartilage degradation compared to rats without *Vegf* inhibition at 5–9 weeks after OA induction. This chondroprotective effect was accompanied by reduced *Col10a1* levels (Zhang et al., 2016a).

Another protein essential in vascularization during endochondral ossification is chondromodulin. Proliferative chondrocytes in the growth plate are resistant to vascular invasion because of the presence of angiogenic inhibitors, such as chondromodulin (ChM-1) (Hiraki and Shukunami, 2005). Chondromodulin overexpression protected against OA development in a surgically induced rat OA model, evidenced by lower Mankin scores, less COL10A1 expression and higher COL2A1 and AGC levels (Zhang et al., 2016a,b). Likewise, *Chm-1* levels in OA cartilage were lower in a surgically induced rat OA model compared to cartilage from control joints (Zhang et al., 2016b). Furthermore, Chm-1 expression was decreased in more severely damaged human OA cartilage in comparison to mild OA cartilage (Zhang et al., 2016b). Chondromodulin also protected against TNFα-induced chondrocyte hypertrophy (Zhang et al., 2016b). Additional experiments in the C28/I2 chondrocyte cell line revealed that chondromodulin delays HIF-2α nuclear translocation, indicating that the anti-hypertrophic and chondroprotective effects of chondromodulin are caused by the repression of pro-hypertrophic HIF-2α activity (Zhang et al., 2016b).

Vascularization is essential for the endochondral ossification process and it has also been associated with OA. Indeed, OA cartilage is invaded by blood vessels into the non-calcified articular cartilage, likely due to an increased production of pro-angiogenic factors (Mapp and Walsh, 2012; Wang et al., 2012). This has been attributed to the increase in subchondral bone porosity (Botter et al., 2011), which has been hypothesized to result in disruption of the osteochondral junction. A disruption of the osteochondral junction with a subsequent invasion of blood vessels may lead to further structural damage, leading to progression of OA.

A role for chondrocyte hypertrophic processes in OA progression was further described by a study in which conditioned medium of hypertrophic OA chondrocytes induced wound healing in human umbilical vascular endothelial cells and increased endothelial cell adhesion and migration (Pesesse et al., 2013). Furthermore, the gene expression of pro-angiogenic factors, such as *BSP* and *NGF* was increased (Pesesse et al., 2013). Osteochondral angiogenesis was also assessed in a study by Wang et al. in which OA was evoked by disordered occlusion in rat mandibular joints (Wang et al., 2012). Experimental groups demonstrated OA-like changes, with a loss of cartilage surface integrity and osteophyte formation. Additionally, hypertrophic chondrocytes adjacent to the osteochondral interface showed increased expression of VEGF, CTGF, and MMP9 at 20 or 24 weeks post OA-induction surgery. Thus, hypertrophic chondrocytes may exacerbate the disruption of the osteochondral junction by stimulating angiogenesis, which can lead to progression of OA. Another study described the association between pro-angiogenic factors, hypertrophy, and OA severity. Discoidin domain receptor 2 (DDR2) was higher expressed in more severely damaged human OA cartilage compared to cartilage with lower Mankin scores (Zhang et al., 2014a). DDR2 is a receptor tyrosine kinase that can be activated by various collagens. Since DDR2 activity can induce COL10A1 expression in chicken chondrocytes (Zhang et al., 2014b), and given the fact that DDR2 has been associated with a pro-angiogenic function (Zhang et al., 2014a), this supports a link between chondrocyte hypertrophic pro-angiogenic factors and OA progression.

In conclusion, these results reveal the importance of angiogenesis in enabling OA disease progression. The differential activation of hypoxic and angiogenic pathways observed in OA appear to be key factors in OA development.

FGF Signaling

Fibroblast growth factors comprise a group of morphogens involved in wound healing, angiogenesis, and are involved in processes such as proliferation and differentiation in different cell types (Turner and Grose, 2010). They also have been described as being involved in endochondral ossification, since FGF23 and FGF receptor 1 are produced by growth plate hypertrophic chondrocytes (Raimann et al., 2013). Given that OA chondrocytes also produce FGF family members (Orfanidou et al., 2009), studies have investigated the involvement of FGF signaling in the chondrocyte phenotypic alterations observed in OA cartilage. An overview of newly acquired insights into this pathway and its involvement in development of OA chondrocyte hypertrophy is provided in **Table 1**g and **Figure 5**.

It has been demonstrated that the expression of FGFR1, FGF23, and its co-receptor KLOTHO is higher in OA chondrocytes compared to non-OA chondrocytes. Expression of these factors was also increased in cartilage samples with more severe macroscopic OA compared to less severe macroscopic OA within the same patient (Bianchi et al., 2016). Exogenous addition of FGF23 to human OA primary chondrocytes resulted in hypertrophic changes, as evidenced by *COL10A1* and *VEGFA* induction *via* FGFR1 (Bianchi et al., 2016). Another study confirmed the increase in FGF23 expression levels in OA compared to non-OA chondrocytes (Orfanidou et al., 2009). This study confirmed the hypertrophic phenotype in OA chondrocytes

with higher RUNX2 and lower SOX9 levels compared to non-OA chondrocytes, and also revealed that exogenous addition of FGF23 to non-OA chondrocytes induced a hypertrophic phenotype characterized by increased RUNX2 expression levels (Orfanidou et al., 2009). Involvement of FGF signaling as an OA-inducing pathway was demonstrated in a study in which G141, a pharmacological FGFR1 inhibitor was used. In a surgically induced mouse OA model, G141 delayed the progression of cartilage degradation, accompanied by a decrease of MMP13 and COL10A1 chondrocyte hypertrophic marker expression, suggesting that OA articular cartilage damage could be reduced *via* inhibition of hypertrophic processes (Xu et al., 2016).

On the other hand, FGFR3 seems to be crucial for cartilage homeostasis and inhibition of a hypertrophic phenotype, since FGFR3 knockout mice displayed OA-like defects in the temporomandibular joint together with an increased expression of hypertrophic markers COL10A1 and MMP13 (Zhou et al., 2016). Further support indicative of an association between chondrocyte hypertrophy and FGFR3 comes from a study in which it was revealed that FGFR3 levels were reduced in *mtorc1* knockout mice which display cartilage degradation and chondrocyte hypertrophy (Zhang et al., 2017).

Taken together, recent studies have demonstrated that the FGF signaling pathway is active in OA and also provided new insights in the contribution of this signaling pathway to OA disease initiation or progression.

Notch Signaling

The Notch signaling pathway consists of five identified ligands (Jagged 1, Jagged 2, Dll1, Dll3, and Dll4) that can interact with four receptors (Notch 1–4) (Bray, 2016). Upon binding of Notch ligands, the Notch receptor cleavage site becomes accessible for cleavage by ADAM10. The residual transmembrane Notch fragment in turn is cleaved *via* proteolysis by the γ-secretase complex, releasing NICD. This intracellular domain of the receptor translocates to the nucleus, where it binds to the transcription factor recombination signal binding protein for immunoglobulin kappa J (RBPjκ), to participate in gene transcription of Notch target genes, such as *Hes1*. These target genes are involved in cellular processes, such as cell proliferation and differentiation (Nye and Kopan, 1995). Notch signaling is involved in endochondral ossification (Hosaka et al., 2013), and, therefore, studies have investigated its involvement in OA development as well. An overview of newly acquired insights into this pathway and its involvement in development of OA chondrocyte hypertrophy is provided in **Table 1**h and **Figure 3**.

Providing evidence for a role of Notch signaling in endochondral processes and OA development, it has been reported that RBPjκ is involved in endochondral ossification. Knockout of *Rbpj*κ resulted in reduced cartilage damage in a surgically induced OA model, together with reduced expression of MMP13, VEGFA, and HES1 in articular chondrocytes (Hosaka et al., 2013). Furthermore, in this study it was revealed that during OA development, the expression of Notch ligand Jagged1 is increased in OA cartilage, indicating that this ligand may regulate Notch signaling during OA progression (Hosaka et al., 2013). Confirming again a role for Notch signaling in OA development, it was demonstrated that the pharmacological Notch signaling inhibitor *N*-[*N*-(3,5-difluorophenylacetate)-L-alanyl]-(*S*)-phenylglycine t-butyl ester (DAPT), resulted in the same chondroprotective effect in a surgically induced mouse OA model (Hosaka et al., 2013), as observed with the *Rbpj*κ knockout mouse.

In concert with a role in chondrocyte hypertrophy, the intracellular domains of Notch ligands, NOTCH1 and NOTCH2 was shown to be located at the chondrocyte plasma membrane in resting and proliferative zone chondrocytes, while these intracellular domains were translocated (and thus potentially active) to the nucleus in hypertrophic zone chondrocytes (Hosaka et al., 2013). Similar as in the growth plate's hypertrophic zone, the intracellular domains of NOTCH1 and NOTCH2 were also located to the chondrocyte's nucleus in surgically induced mouse OA cartilage (Hosaka et al., 2013). An increase in Notch signaling activity was also observed in a further study. In this study, an increase in mRNA levels of Notch ligand *Jagged 1* and its receptor *Notch 1* in OA areas of human articular cartilage, together with induced mRNA levels of the Notch target gene *HES1* was reported (Lin et al., 2016). Interestingly, inhibition of NOTCH1 resulted in an increased, HES1 dependent, hedgehog signaling activity, leading to an exacerbation of OA (Lin et al., 2016). These results are in contrast with the general theory that inhibition of Notch attenuates OA development. The increase in hypertrophy may be a result of a crosstalk between the Notch and hedgehog signaling pathway, previously described in the Ihh/PTHrP signaling paragraph.

In conclusion, these results provide evidence that the Notch signaling pathway is positively associated with hypertrophic changes in the chondrocyte. Inhibition of the Notch signaling pathway may be used as a therapeutic tool to block OA disease progression, based on reducing hypertrophic changes in the chondrocyte.

Mineralization

Mineralization is also an important consequence of chondrocyte hypertrophy in OA (Fuerst et al., 2009; Fukai et al., 2010; Wallin et al., 2010; Nguyen et al., 2013; Zhu et al., 2015; Cavaco et al., 2016; Nasi et al., 2016; Queirolo et al., 2016). The mineralization process is analogous to the last phase of endochondral ossification as it is observed in the growth plate (Kronenberg, 2003). Here, hypertrophic chondrocytes secrete matrix vesicles containing high concentrations of phosphatases, such as alkaline phosphatase (ALPL) and PHOSPHO1 (Anderson, 2003; Houston et al., 2004; Stewart et al., 2006; McKee et al., 2013). During matrix vesicle biogenesis, vesicles are formed by polarized budding and pinching-off of vesicles from the plasma membranes. Within these matrix vesicles, the first mineral crystals are formed by phosphatases hydrolyzing inorganic pyrophosphate (PPi) to create inorganic phosphate (Pi). Pi ions in turn crystallize with calcium, resulting in crystals which are released through the vesicles membranes. When these pre-formed hydroxyapatite crystals come in contact with the extracellular fluid containing Ca^{2+} and PO_4^{3-} ions a process of continuous crystal formation takes place in the matrix (Anderson, 2003; Orimo, 2010). This mineralized matrix is then vascularized, further supporting

mineralization and enabling the infiltration of osteoblasts and osteoclasts. Osteoblasts secrete osteoid, which forms the bone trabecula, while osteoclasts, formed from macrophages, breakdown spongy bone to form the medullary (bone marrow) cavity (Kronenberg, 2003). An overview of newly acquired insights into this process and its involvement in development of OA chondrocyte hypertrophy is provided in **Table 1**I and **Figure 6**.

During endochondral ossification, AKT1 induces mineralization without affecting the hypertrophic and proliferative zone in the growth plate (Fukai et al., 2010). Surgically DMM OA-induced *Akt1*$^{-/-}$ mice specifically revealed a reduction of calcified osteophyte formation, while cartilage degradation was unaltered, supporting results observed in the growth plate. This may be the result of an increase of inorganic pyrophosphate (PPi) due to *Akt1* inhibition, which antagonizes the ability of inorganic phosphate (Pi) ions to crystallize with calcium. Indeed, levels of PPi-regulators *Ank* and *Npp1* were increased after *Akt1* inhibition (Fukai et al., 2010).

A further relationship was found between RAC1 and hypertrophy (Zhu et al., 2015). Lenti-viral expression of the RAC1 inhibitor OCRL1 resulted in protection against cartilage degradation in a mouse OA model. Additionally, OCRL1 resulted in decreased ALPL activity in human primary chondrocytes. Pretreatment of chondrocytes with IL-1β, resulted in an upregulation of ADAMTS5, Col10a1, RUNX2, MMP13, and ALPL activity, but overexpression of OCRL1 blocked these hypertrophic reactions, and reduced mineralization. Besides the mineralization modulators AKT1 and OCRL1, calcium deposition is also regulated by protein kinase C epsilon. In OA chondrocyte micromasses PKCε expression was reduced, resulting in an increase of calcium deposition and calcium crystals and thus increase in the matrix mineralization (Queirolo et al., 2016).

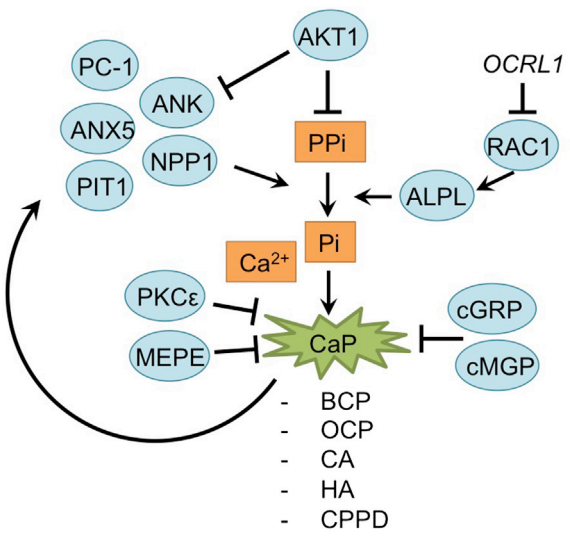

FIGURE 6 | Overview of the mineralization process and newly acquired insights into its relation to the development of the osteoarthritic (OA) chondrocyte hypertrophic phenotype. The mineralization process was updated with recent insights in the role of mineralization in the hypertrophic switch occuring during OA development.

Mineralization is also modulated by MEPE, a matrix mineralization inhibitor (Staines et al., 2016). MEPE was detectable at the lateral OA-unaffected side of STR/Ort mice, while its expression was decreased in the medial affected OA-side of the knee joints. Interestingly, this endochondral phenotype in STR/Ort mice cartilage exists before OA-like changes appear, which suggest that these endochondral changes initiate later development of OA (Staines et al., 2016).

Articular cartilage of many OA patients hosts calcium-containing crystals, which are present in the superficial and deep layers of the cartilage, as well as in synovial fluid and the meniscus (Fuerst et al., 2009; Nguyen et al., 2013). The calcium deposits mainly consist of basic calcium phosphate (BCP), including octacalcium phosphate (OCP), carbonated-apatite (CA), and hydroxyapatite (HA) crystals or calcium pyrophosphate dihydrate (CPPD). Treatment of murine chondrocytes with BCP results in an increase of IL-6 secretion, which in turn induces the expression of pro-mineralizing genes, such as *Ank*, *Anx5*, *Pc-1* [plasma-cell membrane glycoprotein 1/*Enpp1* (ectonucleotide pyrophosphatase/ phosphodiesterase 1)] and *Pit1* (Nasi et al., 2016). PC-1, ANK, and TNAPs control extracellular Pi and PPi levels, which are critical determinants of mineralization. Expression of these regulatory proteins is increased in chondrocytes with calcium-containing crystals, forming a positive feedback loop (Nguyen et al., 2013; Nasi et al., 2016).

Another factor involved in OA pathophysiology is Gla-rich protein (GRP). GRP was revealed to inhibit calcification and exerted anti-inflammatory effects in both chondrocytes and synoviocytes (Cavaco et al., 2016). Its expression was increased in OA chondrocytes and synoviocytes compared to non-OA controls. Furthermore, expression of *GRP* was also increased overtime when chondrocyte or synoviocyte mineralization was induced *via* addition of $CaCl_2$, evidencing its association with mineralization. Interestingly, GRP was only able to inhibit calcification in its carboxylated form, and since OA chondrocytes and synoviocytes displayed reduced *y*-carboxylation capacity, it was hypothesized that the GRP increase in OA-derived cells is not able to inhibit calcification processes (Cavaco et al., 2016). Besides GRP, MGP, another mineralization inhibitor, has been described as becoming less carboxylated in OA chondrocytes. Lower levels of cMGP lead to a reduction of the fetuin-MGP complex in OA chondrocytes and in released vesicles. This reduction of fetuin-MGP containing vesicles, results in reduced extracellular transport of cMGP, lowering its extracellular concentration. Ultimately, the reduced extracellular cMGP levels lead to an impaired inhibition of matrix mineralization (Wallin et al., 2010).

Taken together, mineralization appears to be an important hallmark of osteoarthritic cartilage and is associated with OA chondrocyte hypertrophy.

DISCUSSION

The analogs events which are observed during development of OA and endochondral ossification have been described in previous reviews (Dreier, 2010; Pitsillides and Beier, 2011; van der Kraan and van den Berg, 2012). On the contrary, Brew et al. found

no evidence of a generalized chondrocyte hypertrophic change in OA (Brew et al., 2010). Despite the lack of evidence found by Brew *et al*., all other papers found in our literature search do describe the endochondral cellular phenotypic changes occurring in OA cartilage. Various signaling pathways and processes involved in endochondral processes, such as Wnt-, Ihh/PTHrP-, TGF-β-, MAP-kinases, FGF-, Notch signaling, inflammatory signaling, and hypoxia-associated signaling pathways, but also processes, such as angiogenesis and matrix mineralization have been described in OA disease progression. Interestingly, from some studies it became evident that crosstalk exists between the different signaling pathways involved in OA disease progression (Ray and Ray, 2008; Papathanasiou et al., 2012; Leijten et al., 2013; van den Bosch et al., 2014; Lin et al., 2016; Zhou et al., 2016). Next to cartilage degradation, which is the main hallmark of OA, it is well established that OA includes changes in several joint structures. Hence, OA should be considered as a total joint disease. Alterations in subchondral bone, meniscal degradation and inflammatory changes in intra-articular tissues, such as the synovium and Hoffa's fat pad have been widely described. Unraveling mechanisms of feedback and crosstalk among these different joint tissues and their influence on cartilage hypertrophy will further provide important insights in OA pathophysiology.

In this review, we aimed to provide a recent overview of new insights into the contribution of the changing hypertrophic chondrocyte phenotype in the development and progression of OA. In order to include all papers from the past 10 years discussing the endochondral cellular phenotypic changes occurring during OA, we specifically used a search in PubMed which included the term "endochondral ossification," but also includes terms such as "hypertrophic differentiation," "hypertrophy," "mineralization," and "calcification," which are all processes occurring during endochondral ossification. Interestingly, different studies use different molecular markers to evaluate the hypertrophic phenotype in the chondrocyte and an unambiguous definition of "hypertrophy" seems lacking (**Table 1**). This is most likely related to the complexity of the endochondral ossification process with various molecular pathways being involved. In future research, it will be important to reach a consensus and implement a standardized definition to describe "chondrocyte hypertrophy in OA." We expect that this will support better data comparison between different studies.

A striking realization from our literature search is that it seems that in OA animal models the hypertrophic changes in OA cartilage pathology can be initiated or prevented by a single alteration in many different signaling pathways. While late OA disease progression follows a predictable cell biological progression, little is known about causal relations between the herein described pathways/processes and early OA disease initiation in man. Together this raises the question if OA can even be considered as a generalized single disease (Luyten et al., 2017). Indeed, it is becoming increasingly apparent that different OA phenotypes exist (van der Esch et al., 2015; Deveza et al., 2017; Dell'Isola and Steultjens, 2018). Different early OA phenotypes/disease initiation may result from alterations in molecular pathways that are specifically connected with clinical risk factors for developing OA, like obesity, aging, metabolic syndrome, joint shape/malalignment, or earlier cartilage trauma. We speculate that a phenotyping of early OA, in which dominant deregulation of a specific molecular pathway is taken into account, may provide additional resolution to the already described OA phenotypes. This will not only be important for diagnostic purposes, but equally important for developing new OA disease-modifying compounds and selecting the right patient populations for clinical studies testing novel OA disease-modifying drugs and -approaches.

It can be concluded that articular cartilage/chondrocyte homeostasis is fragile and disruption of chondrocyte homeostasis can be initiated by multiple factors leading to a cascade of intracellular changes in one or multiple pathways. This ultimately results in a chondrocyte hypertrophic/endochondral phenotype that is observed in OA. Understanding the relevance, mechanism-of-action, and crosstalk of processes and signaling pathways involved in OA initiation and progression is expected to further fuel the development of OA disease-modifying drugs and -approaches.

AUTHOR CONTRIBUTIONS

All four authors ER, UT, MC, and TW have contributed to literature searches, reading, selecting, and interpretation of papers, and writing of the manuscript. ER and UT have contributed to layout of the tables and MC has contributed to the layout of the figures. The manuscript was approved by all four co-authors prior to submission. ER and UT have contributed equally as first author and MC and TW have contributed equally as last author.

FUNDING

The work of the four authors is supported by grants from the Dutch Arthritis Foundation (grants LLP14, 15-3-403), the Annadal Foundation and Stichting de Weijerhorst.

REFERENCES

Ailixiding, M., Aibibula, Z., Iwata, M., Piao, J., Hara, Y., Koga, D., et al. (2015). Pivotal role of Sirt6 in the crosstalk among ageing, metabolic syndrome and osteoarthritis. *Biochem. Biophys. Res. Commun.* 466, 319–326. doi:10.1016/j.bbrc.2015.09.019

Aini, H., Ochi, H., Iwata, M., Okawa, A., Koga, D., Okazaki, M., et al. (2012). Procyanidin B3 prevents articular cartilage degeneration and heterotopic cartilage formation in a mouse surgical osteoarthritis model. *PLoS One* 7:e37728. doi:10.1371/journal.pone.0037728

Anderson, H. C. (2003). Matrix vesicles and calcification. *Curr. Rheumatol. Rep.* 5, 222–226. doi:10.1007/s11926-003-0071-z

Appleton, C. T., Pitelka, V., Henry, J., and Beier, F. (2007). Global analyses of gene expression in early experimental osteoarthritis. *Arthritis Rheum* 56, 1854–1868.

Bianchi, A., Guibert, M., Cailotto, F., Gasser, A., Presle, N., Mainard, D., et al. (2016). Fibroblast growth factor 23 drives MMP13 expression in human osteoarthritic chondrocytes in a Klotho-independent manner. *Osteoarthr. Cartil.* 24, 1961–1969. doi:10.1016/j.joca.2016.06.003

Bijlsma, J. W., Berenbaum, F., and Lafeber, F. P. (2011). Osteoarthritis: an update with relevance for clinical practice. *Lancet* 377, 2115–2126. doi:10.1016/s0140-6736(11)60243-2

Bikkavilli, R. K., and Malbon, C. C. (2009). Mitogen-activated protein kinases and Wnt/beta-catenin signaling: molecular conversations among signaling pathways. *Commun. Integr. Biol.* 2, 46–49. doi:10.4161/cib.2.1.7503

Blaney Davidson, E. N., Remst, D. F., Vitters, E. L., van Beuningen, H. M., Blom, A. B., Goumans, M. J., et al. (2009). Increase in ALK1/ALK5 ratio as a cause for elevated MMP-13 expression in osteoarthritis in humans and mice. *J. Immunol.* 182, 7937–7945. doi:10.4049/jimmunol.0803991

Bomer, N., den Hollander, W., Ramos, Y. F., Bos, S. D., van der Breggen, R., Lakenberg, N., et al. (2015). Underlying molecular mechanisms of DIO2 susceptibility in symptomatic osteoarthritis. *Ann. Rheum. Dis.* 74, 1571–1579. doi:10.1136/annrheumdis-2013-204739

Borzi, R. M., Olivotto, E., Pagani, S., Vitellozzi, R., Neri, S., Battistelli, M., et al. (2010). Matrix metalloproteinase 13 loss associated with impaired extracellular matrix remodeling disrupts chondrocyte differentiation by concerted effects on multiple regulatory factors. *Arthritis Rheum.* 62, 2370–2381. doi:10.1002/art.27512

Botter, S. M., van Osch, G. J., Clockaerts, S., Waarsing, J. H., Weinans, H., and van Leeuwen, J. P. (2011). Osteoarthritis induction leads to early and temporal subchondral plate porosity in the tibial plateau of mice: an in vivo microfocal computed tomography study. *Arthritis Rheum.* 63, 2690–2699. doi:10.1002/art.30307

Bray, S. J. (2016). Notch signalling in context. *Nat. Rev. Mol. Cell Biol.* 17, 722. doi:10.1038/nrm.2016.94

Brew, C. J., Clegg, P. D., Boot-Handford, R. P., Andrew, J. G., and Hardingham, T. (2010). Gene expression in human chondrocytes in late osteoarthritis is changed in both fibrillated and intact cartilage without evidence of generalised chondrocyte hypertrophy. *Ann. Rheum. Dis.* 69, 234–240. doi:10.1136/ard.2008.097139

Caron, M. M., Emans, P. J., Surtel, D. A., van der Kraan, P. M., van Rhijn, L. W., and Welting, T. J. (2015). BAPX-1/NKX-3.2 acts as a chondrocyte hypertrophy molecular switch in osteoarthritis. *Arthritis Rheumatol.* 67, 2944–2956. doi:10.1002/art.39293

Castano Betancourt, M. C., Cailotto, F., Kerkhof, H. J., Cornelis, F. M., Doherty, S. A., Hart, D. J., et al. (2012). Genome-wide association and functional studies identify the DOT1L gene to be involved in cartilage thickness and hip osteoarthritis. *Proc. Natl. Acad. Sci. U.S.A.* 109, 8218–8223. doi:10.1073/pnas.1119899109

Cavaco, S., Viegas, C. S., Rafael, M. S., Ramos, A., Magalhaes, J., Blanco, F. J., et al. (2016). Gla-rich protein is involved in the cross-talk between calcification and inflammation in osteoarthritis. *Cell. Mol. Life Sci.* 73, 1051–1065. doi:10.1007/s00018-015-2033-9

Cecil, D. L., Appleton, C. T., Polewski, M. D., Mort, J. S., Schmidt, A. M., Bendele, A., et al. (2009). The pattern recognition receptor CD36 is a chondrocyte hypertrophy marker associated with suppression of catabolic responses and promotion of repair responses to inflammatory stimuli. *J. Immunol.* 182, 5024–5031. doi:10.4049/jimmunol.0803603

Chang, J. K., Chang, L. H., Hung, S. H., Wu, S. C., Lee, H. Y., Lin, Y. S., et al. (2009). Parathyroid hormone 1-34 inhibits terminal differentiation of human articular chondrocytes and osteoarthritis progression in rats. *Arthritis Rheum.* 60, 3049–3060. doi:10.1002/art.24843

Chen, L., Wu, Y., Wu, Y., Wang, Y., Sun, L., and Li, F. (2016). The inhibition of EZH2 ameliorates osteoarthritis development through the Wnt/beta-catenin pathway. *Sci. Rep.* 6, 29176. doi:10.1038/srep29176

Dangelo, M., Sarment, D. P., Billings, P. C., and Pacifici, M. (2001). Activation of transforming growth factor beta in chondrocytes undergoing endochondral ossification. *J. Bone Miner. Res.* 16, 2339–2347. doi:10.1359/jbmr.2001.16.12.2339

Dell'Isola, A., and Steultjens, M. (2018). Classification of patients with knee osteoarthritis in clinical phenotypes: data from the osteoarthritis initiative. *PLoS ONE* 13:e0191045. doi:10.1371/journal.pone.0191045

Derynck, R., and Zhang, Y. E. (2003). Smad-dependent and Smad-independent pathways in TGF-beta family signalling. *Nature* 425, 577–584. doi:10.1038/nature02006

Deveza, L. A., Melo, L., Yamato, T. P., Mills, K., Ravi, V., and Hunter, D. J. (2017). Knee osteoarthritis phenotypes and their relevance for outcomes: a systematic review. *Osteoarthr. Cartil.* 25, 1926–1941. doi:10.1016/j.joca.2017.08.009

Dreier, R. (2010). Hypertrophic differentiation of chondrocytes in osteoarthritis: the developmental aspect of degenerative joint disorders. *Arthritis Res. Ther.* 12, 216. doi:10.1186/ar3117

Eswaramoorthy, R., Chang, C. C., Wu, S. C., Wang, G. J., Chang, J. K., and Ho, M. L. (2012). Sustained release of PTH(1-34) from PLGA microspheres suppresses osteoarthritis progression in rats. *Acta Biomater.* 8, 2254–2262. doi:10.1016/j.actbio.2012.03.015

Facchini, A., Borzi, R. M., Olivotto, E., Platano, D., Pagani, S., Cetrullo, S., et al. (2012). Role of polyamines in hypertrophy and terminal differentiation of osteoarthritic chondrocytes. *Amino Acids* 42, 667–678. doi:10.1007/s00726-011-1041-9

Felson, D. T., Lawrence, R. C., Dieppe, P. A., Hirsch, R., Helmick, C. G., Jordan, J. M., et al. (2000). Osteoarthritis: new insights. Part 1: the disease and its risk factors. *Ann. Intern. Med.* 133, 635–646. doi:10.7326/0003-4819-133-8-200010170-00016

Filip, A., Pinzano, A., Bianchi, A., Feve, B., Jalkanen, S., Gillet, P., et al. (2016). Expression of the semicarbazide-sensitive amine oxidase in articular cartilage: its role in terminal differentiation of chondrocytes in rat and human. *Osteoarthr. Cartil.* 24, 1223–1234. doi:10.1016/j.joca.2016.01.340

Fuerst, M., Bertrand, J., Lammers, L., Dreier, R., Echtermeyer, F., Nitschke, Y., et al. (2009). Calcification of articular cartilage in human osteoarthritis. *Arthritis Rheum.* 60, 2694–2703. doi:10.1002/art.24774

Fujita, N., Matsushita, T., Ishida, K., Kubo, S., Matsumoto, T., Takayama, K., et al. (2011). Potential involvement of SIRT1 in the pathogenesis of osteoarthritis through the modulation of chondrocyte gene expressions. *J. Orthop. Res.* 29, 511–515. doi:10.1002/jor.21284

Fukai, A., Kawamura, N., Saito, T., Oshima, Y., Ikeda, T., Kugimiya, F., et al. (2010). Akt1 in murine chondrocytes controls cartilage calcification during endochondral ossification under physiologic and pathologic conditions. *Arthritis Rheum.* 62, 826–836. doi:10.1002/art.27296

Gao, Z. Q., Guo, X., Duan, C., Ma, W., Xu, P., Wang, W., et al. (2012). Altered aggrecan synthesis and collagen expression profiles in chondrocytes from patients with Kashin-Beck disease and osteoarthritis. *J. Int. Med. Res.* 40, 1325–1334. doi:10.1177/147323001204000411

Garciadiego-Cazares, D., Aguirre-Sanchez, H. I., Abarca-Buis, R. F., Kouri, J. B., Velasquillo, C., and Ibarra, C. (2015). Regulation of alpha5 and alphaV integrin expression by GDF-5 and BMP-7 in chondrocyte differentiation and osteoarthritis. *PLoS ONE* 10:e0127166. doi:10.1371/journal.pone.0127166

Guidotti, S., Minguzzi, M., Platano, D., Cattini, L., Trisolino, G., Mariani, E., et al. (2015). Lithium chloride dependent glycogen synthase kinase 3 inactivation links oxidative DNA damage, hypertrophy and senescence in human articular chondrocytes and reproduces chondrocyte phenotype of obese osteoarthritis patients. *PLoS ONE* 10:e0143865. doi:10.1371/journal.pone.0143865

Hashimoto, K., Mori, S., Oda, Y., Nakano, A., Sawamura, T., and Akagi, M. (2016). Lectin-like oxidized low density lipoprotein receptor 1-deficient mice show resistance to instability-induced osteoarthritis. *Scand. J. Rheumatol.* 45, 412–422. doi:10.3109/03009742.2015.1135979

Hiraki, Y., and Shukunami, C. (2005). Angiogenesis inhibitors localized in hypovascular mesenchymal tissues: chondromodulin-I and tenomodulin. *Connect. Tissue Res.* 46, 3–11. doi:10.1080/03008200590935547

Hirata, M., Kugimiya, F., Fukai, A., Saito, T., Yano, F., Ikeda, T., et al. (2012). C/EBPbeta and RUNX2 cooperate to degrade cartilage with MMP-13 as the target and HIF-2alpha as the inducer in chondrocytes. *Hum. Mol. Genet.* 21, 1111–1123. doi:10.1093/hmg/ddr540

Hosaka, Y., Saito, T., Sugita, S., Hikata, T., Kobayashi, H., Fukai, A., et al. (2013). Notch signaling in chondrocytes modulates endochondral ossification and osteoarthritis development. *Proc. Natl. Acad. Sci. U.S.A.* 110, 1875–1880. doi:10.1073/pnas.1207458110

Houston, B., Stewart, A. J., and Farquharson, C. (2004). PHOSPHO1 – a novel phosphatase specifically expressed at sites of mineralisation in bone and cartilage. *Bone* 34, 629–637. doi:10.1016/j.bone.2003.12.023

Huebner, J. L., Johnson, K. A., Kraus, V. B., and Terkeltaub, R. A. (2009). Transglutaminase 2 is a marker of chondrocyte hypertrophy and osteoarthritis severity in the Hartley guinea pig model of knee OA. *Osteoarthr. Cartil.* 17, 1056–1064. doi:10.1016/j.joca.2009.02.015

Hunter, D. J. (2011). Pharmacologic therapy for osteoarthritis – the era of disease modification. *Nat. Rev. Rheumatol.* 7, 13–22. doi:10.1038/nrrheum.2010.178

Ijiri, K., Zerbini, L. F., Peng, H., Otu, H. H., Tsuchimochi, K., Otero, M., et al. (2008). Differential expression of GADD45beta in normal and osteoarthritic cartilage: potential role in homeostasis of articular chondrocytes. *Arthritis. Rheum.* 58, 2075–2087. doi:10.1002/art.23504

Johnson, G. L., and Lapadat, R. (2002). Mitogen-activated protein kinase pathways mediated by ERK, JNK, and p38 protein kinases. *Science* 298, 1911–1912. doi:10.1126/science.1072682

Johnson, K. A., Rose, D. M., and Terkeltaub, R. A. (2008). Factor XIIIA mobilizes transglutaminase 2 to induce chondrocyte hypertrophic differentiation. *J. Cell. Sci.* 121(Pt 13), 2256–2264. doi:10.1242/jcs.011262

Kronenberg, H. M. (2003). Developmental regulation of the growth plate. *Nature* 423, 332–336. doi:10.1038/nature01657

Lai, Y., Bai, X., Zhao, Y., Tian, Q., Liu, B., Lin, E. A., et al. (2014). ADAMTS-7 forms a positive feedback loop with TNF-alpha in the pathogenesis of osteoarthritis. *Ann. Rheum. Dis.* 73, 1575–1584. doi:10.1136/annrheumdis-2013-203561

Le, T. K., Montejano, L. B., Cao, Z., Zhao, Y., and Ang, D. (2012). Health care costs in US patients with and without a diagnosis of osteoarthritis. *J. Pain Res.* 5, 23–30. doi:10.2147/jpr.s27275

Leijten, J. C., Bos, S. D., Landman, E. B., Georgi, N., Jahr, H., Meulenbelt, I., et al. (2013). GREM1, FRZB and DKK1 mRNA levels correlate with osteoarthritis and are regulated by osteoarthritis-associated factors. *Arthritis Res. Ther.* 15, R126. doi:10.1186/ar4306

Li, T. F., Gao, L., Sheu, T. J., Sampson, E. R., Flick, L. M., Konttinen, Y. T., et al. (2010). Aberrant hypertrophy in Smad3-deficient murine chondrocytes is rescued by restoring transforming growth factor beta-activated kinase 1/activating transcription factor 2 signaling: a potential clinical implication for osteoarthritis. *Arthritis Rheum.* 62, 2359–2369. doi:10.1002/art.27537

Lin, N. Y., Distler, A., Beyer, C., Philipi-Schobinger, A., Breda, S., Dees, C., et al. (2016). Inhibition of Notch1 promotes hedgehog signalling in a HES1-dependent manner in chondrocytes and exacerbates experimental osteoarthritis. *Ann. Rheum. Dis.* 75, 2037–2044. doi:10.1136/annrheumdis-2015-208420

Little, C. B., Barai, A., Burkhardt, D., Smith, S. M., Fosang, A. J., Werb, Z., et al. (2009). Matrix metalloproteinase 13-deficient mice are resistant to osteoarthritic cartilage erosion but not chondrocyte hypertrophy or osteophyte development. *Arthritis Rheum.* 60, 3723–3733. doi:10.1002/art.25002

Liu-Bryan, R. (2015). Inflammation and intracellular metabolism: new targets in OA. *Osteoarthr. Cartil.* 23, 1835–1842. doi:10.1016/j.joca.2014.12.016

Lo, G. H., LaValley, M., McAlindon, T., and Felson, D. T. (2003). Intra-articular hyaluronic acid in treatment of knee osteoarthritis: a meta-analysis. *JAMA* 290, 3115–3121. doi:10.1001/jama.290.23.3115

Loeser, R. F., Erickson, E. A., and Long, D. L. (2008). Mitogen-activated protein kinases as therapeutic targets in osteoarthritis. *Curr. Opin. Rheumatol.* 20, 581–586. doi:10.1097/BOR.0b013e3283090463

Loeser, R. F., Goldring, S. R., Scanzello, C. R., and Goldring, M. B. (2012). Osteoarthritis: a disease of the joint as an organ. *Arthritis Rheum.* 64, 1697–1707. doi:10.1002/art.34453

Lu, J., Sun, Y., Ge, Q., Teng, H., and Jiang, Q. (2014a). Histone deacetylase 4 alters cartilage homeostasis in human osteoarthritis. *BMC Musculoskelet. Disord.* 15:438. doi:10.1186/1471-2474-15-438

Lu, Y., Ding, M., Li, N., Wang, Q., Li, J., Li, X., et al. (2014b). Col10a1-Runx2 transgenic mice with delayed chondrocyte maturation are less susceptible to developing osteoarthritis. *Am. J. Transl. Res*. 6, 736–745.

Luyten, F. P., Bierma-Zeinstra, S., Dell'Accio, F., Kraus, V. B., Nakata, K., Sekiya, I., et al. (2017). Toward classification criteria for early osteoarthritis of the knee. *Semin. Arthritis Rheum.* 4, 457–463. doi:10.1016/j.semarthrit.2017.08.006

MacDonald, B. T., Tamai, K., and He, X. (2009). Wnt/β-catenin signaling: components, mechanisms, and diseases. *Dev. Cell* 17, 9–26. doi:10.1016/j.devcel.2009.06.016

Maes, C., Carmeliet, G., and Schipani, E. (2012). Hypoxia-driven pathways in bone development, regeneration and disease. *Nat. Rev. Rheumatol.* 8, 358–366. doi:10.1038/nrrheum.2012.36

Mannstadt, M., Juppner, H., and Gardella, T. J. (1999). Receptors for PTH and PTHrP: their biological importance and functional properties. *Am. J. Physiol.* 277(5 Pt 2), F665–F675.

Mapp, P. I., and Walsh, D. A. (2012). Mechanisms and targets of angiogenesis and nerve growth in osteoarthritis. *Nat. Rev. Rheumatol.* 8, 390–398. doi:10.1038/nrrheum.2012.80

Marcu, K. B., Otero, M., Olivotto, E., Borzi, R. M., and Goldring, M. B. (2010). NF-κB signaling: multiple angles to target OA. *Curr. Drug Targets* 11, 599–613. doi:10.2174/138945010791011938

Markway, B. D., Cho, H., and Johnstone, B. (2013). Hypoxia promotes redifferentiation and suppresses markers of hypertrophy and degeneration in both healthy and osteoarthritic chondrocytes. *Arthritis Res. Ther.* 15, R92. doi:10.1186/ar4272

Markway, B. D., Cho, H., Zilberman-Rudenko, J., Holden, P., McAlinden, A., and Johnstone, B. (2015). Hypoxia-inducible factor 3-alpha expression is associated with the stable chondrocyte phenotype. *J. Orthop. Res.* 33, 1561–1570. doi:10.1002/jor.22930

McKee, M. D., Yadav, M. C., Foster, B. L., Somerman, M. J., Farquharson, C., and Millan, J. L. (2013). Compounded PHOSPHO1/ALPL deficiencies reduce dentin mineralization. *J. Dent. Res.* 92, 721–727. doi:10.1177/0022034513490958

Meng, F., Zhang, Z., Chen, W., Huang, G., He, A., Hou, C., et al. (2016). MicroRNA-320 regulates matrix metalloproteinase-13 expression in chondrogenesis and interleukin-1beta-induced chondrocyte responses. *Osteoarthr. Cartil.* 24, 932–941. doi:10.1016/j.joca.2015.12.012

Merz, D., Liu, R., Johnson, K., and Terkeltaub, R. (2003). IL-8/CXCL8 and growth-related oncogene α/CXCL1 induce chondrocyte hypertrophic differentiation. *J. Immunol.* 171, 4406–4415. doi:10.4049/jimmunol.171.8.4406

Morey, L., and Helin, K. (2010). Polycomb group protein-mediated repression of transcription. *Trends Biochem. Sci.* 35, 323–332. doi:10.1016/j.tibs.2010.02.009

Nagase, H., Nagasawa, Y., Tachida, Y., Sakakibara, S., Okutsu, J., Suematsu, N., et al. (2013). Deiodinase 2 upregulation demonstrated in osteoarthritis patients cartilage causes cartilage destruction in tissue-specific transgenic rats. *Osteoarthr. Cartil.* 21, 514–523. doi:10.1016/j.joca.2012.12.013

Nasi, S., So, A., Combes, C., Daudon, M., and Busso, N. (2016). Interleukin-6 and chondrocyte mineralisation act in tandem to promote experimental osteoarthritis. *Ann. Rheum. Dis.* 75, 1372–1379. doi:10.1136/annrheumdis-2015-207487

Nguyen, C., Bazin, D., Daudon, M., Chatron-Colliet, A., Hannouche, D., Bianchi, A., et al. (2013). Revisiting spatial distribution and biochemical composition of calcium-containing crystals in human osteoarthritic articular cartilage. *Arthritis Res. Ther.* 15, R103. doi:10.1186/ar4283

Nishimura, S., Akagi, M., Yoshida, K., Hayakawa, S., Sawamura, T., Munakata, H., et al. (2004). Oxidized low-density lipoprotein (ox-LDL) binding to lectin-like ox-LDL receptor-1 (LOX-1) in cultured bovine articular chondrocytes increases production of intracellular reactive oxygen species (ROS) resulting in the activation of NF-κB. *Osteoarthr. Cartil.* 12, 568–576. doi:10.1016/j.joca.2004.04.005

Nye, J. S., and Kopan, R. (1995). Developmental signaling. Vertebrate ligands for Notch. *Curr. Biol.* 5, 966–969. doi:10.1016/S0960-9822(95)00189-8

Olivotto, E., Borzi, R. M., Vitellozzi, R., Pagani, S., Facchini, A., Battistelli, M., et al. (2008). Differential requirements for IKKalpha and IKKbeta in the differentiation of primary human osteoarthritic chondrocytes. *Arthritis Rheum.* 58, 227–239. doi:10.1002/art.23211

Olivotto, E., Otero, M., Astolfi, A., Platano, D., Facchini, A., Pagani, S., et al. (2013). IKKalpha/CHUK regulates extracellular matrix remodeling independent of its kinase activity to facilitate articular chondrocyte differentiation. *PLoS ONE* 8:e73024. doi:10.1371/journal.pone.0073024

Orfanidou, T., Iliopoulos, D., Malizos, K. N., and Tsezou, A. (2009). Involvement of SOX-9 and FGF-23 in RUNX-2 regulation in osteoarthritic chondrocytes. *J. Cell. Mol. Med.* 13, 3186–3194. doi:10.1111/j.1582-4934.2009.00678.x

Orimo, H. (2010). The mechanism of mineralization and the role of alkaline phosphatase in health and disease. *J. Nippon Med. Sch.* 77, 4–12. doi:10.1272/jnms.77.4

Page, C. J., Hinman, R. S., and Bennell, K. L. (2011). Physiotherapy management of knee osteoarthritis. *Int. J. Rheum. Dis.* 14, 145–151. doi:10.1111/j.1756-185X.2011.01612.x

Papathanasiou, I., Kostopoulou, F., Malizos, K. N., and Tsezou, A. (2015). DNA methylation regulates sclerostin (SOST) expression in osteoarthritic chondrocytes by bone morphogenetic protein 2 (BMP-2) induced changes in Smads binding affinity to the CpG region of SOST promoter. *Arthritis Res. Ther.* 17, 160. doi:10.1186/s13075-015-0674-6

Papathanasiou, I., Malizos, K. N., and Tsezou, A. (2012). Bone morphogenetic protein-2-induced Wnt/beta-catenin signaling pathway activation through enhanced low-density-lipoprotein receptor-related protein 5 catabolic activity contributes to hypertrophy in osteoarthritic chondrocytes. *Arthritis Res. Ther.* 14, R82. doi:10.1186/ar3805

Pesesse, L., Sanchez, C., Delcour, J. P., Bellahcene, A., Baudouin, C., Msika, P., et al. (2013). Consequences of chondrocyte hypertrophy on osteoarthritic cartilage: potential effect on angiogenesis. *Osteoarthr. Cartil.* 21, 1913–1923. doi:10.1016/j.joca.2013.08.018

Pesesse, L., Sanchez, C., Walsh, D. A., Delcour, J. P., Baudouin, C., Msika, P., et al. (2014). Bone sialoprotein as a potential key factor implicated in the pathophysiology of osteoarthritis. *Osteoarthr. Cartil.* 22, 547–556. doi:10.1016/j.joca.2014.01.010

Philipot, D., Guerit, D., Platano, D., Chuchana, P., Olivotto, E., Espinoza, F., et al. (2014). p16INK4a and its regulator miR-24 link senescence and chondrocyte

terminal differentiation-associated matrix remodeling in osteoarthritis. *Arthritis Res. Ther.* 16, R58. doi:10.1186/ar4494

Pitsillides, A. A., and Beier, F. (2011). Cartilage biology in osteoarthritis – lessons from developmental biology. *Nat. Rev. Rheumatol.* 7, 654–663. doi:10.1038/nrrheum.2011.129

Prasadam, I., Mao, X., Shi, W., Crawford, R., and Xiao, Y. (2013). Combination of MEK-ERK inhibitor and hyaluronic acid has a synergistic effect on anti-hypertrophic and pro-chondrogenic activities in osteoarthritis treatment. *J. Mol. Med. (Berl)* 91, 369–380. doi:10.1007/s00109-012-0953-5

Prasadam, I., van Gennip, S., Friis, T., Shi, W., Crawford, R., and Xiao, Y. (2010). ERK-1/2 and p38 in the regulation of hypertrophic changes of normal articular cartilage chondrocytes induced by osteoarthritic subchondral osteoblasts. *Arthritis Rheum.* 62, 1349–1360. doi:10.1002/art.27397

Provot, S., Kempf, H., Murtaugh, L. C., Chung, U. I., Kim, D. W., Chyung, J., et al. (2006). Nkx3.2/Bapx1 acts as a negative regulator of chondrocyte maturation. *Development* 133, 651–662. doi:10.1242/dev.02258

Queirolo, V., Galli, D., Masselli, E., Borzi, R. M., Martini, S., Vitale, F., et al. (2016). PKCepsilon is a regulator of hypertrophic differentiation of chondrocytes in osteoarthritis. *Osteoarthr. Cartil.* 24, 1451–1460. doi:10.1016/j.joca.2016.04.003

Raimann, A., Ertl, D. A., Helmreich, M., Sagmeister, S., Egerbacher, M., and Haeusler, G. (2013). Fibroblast growth factor 23 and Klotho are present in the growth plate. *Connect. Tissue Res.* 54, 108–117. doi:10.3109/03008207.2012.753879

Ray, A., and Ray, B. K. (2008). An inflammation-responsive transcription factor in the pathophysiology of osteoarthritis. *Biorheology* 45, 399–409. doi:10.3233/BIR-2008-0500

Reimold, A. M., Grusby, M. J., Kosaras, B., Fries, J. W., Mori, R., Maniwa, S., et al. (1996). Chondrodysplasia and neurological abnormalities in ATF-2-deficient mice. *Nature* 379, 262–265. doi:10.1038/379262a0

Saito, T., Fukai, A., Mabuchi, A., Ikeda, T., Yano, F., Ohba, S., et al. (2010). Transcriptional regulation of endochondral ossification by HIF-2alpha during skeletal growth and osteoarthritis development. *Nat. Med.* 16, 678–686. doi:10.1038/nm.2146

Schaeffer, H. J., and Weber, M. J. (1999). Mitogen-activated protein kinases: specific messages from ubiquitous messengers. *Mol. Cell. Biol.* 19, 2435–2444. doi:10.1128/MCB.19.4.2435

Sherwood, J., Bertrand, J., Nalesso, G., Poulet, B., Pitsillides, A., Brandolini, L., et al. (2015). A homeostatic function of CXCR2 signalling in articular cartilage. *Ann. Rheum. Dis.* 74, 2207–2215. doi:10.1136/annrheumdis-2014-205546

Staines, K. A., Madi, K., Mirczuk, S. M., Parker, S., Burleigh, A., Poulet, B., et al. (2016). Endochondral growth defect and deployment of transient chondrocyte behaviors underlie osteoarthritis onset in a natural murine model. *Arthritis Rheumatol.* 68, 880–891. doi:10.1002/art.39508

Stanton, L. A., Underhill, T. M., and Beier, F. (2003). MAP kinases in chondrocyte differentiation. *Dev. Biol.* 263, 165–175. doi:10.1016/S0012-1606(03)00321-X

Stewart, A. J., Roberts, S. J., Seawright, E., Davey, M. G., Fleming, R. H., and Farquharson, C. (2006). The presence of PHOSPHO1 in matrix vesicles and its developmental expression prior to skeletal mineralization. *Bone* 39, 1000–1007. doi:10.1016/j.bone.2006.05.014

Thompson, C. L., Patel, R., Kelly, T. A., Wann, A. K., Hung, C. T., Chapple, J. P., et al. (2015). Hedgehog signalling does not stimulate cartilage catabolism and is inhibited by Interleukin-1beta. *Arthritis Res. Ther.* 17, 373. doi:10.1186/s13075-015-0891-z

Turner, N., and Grose, R. (2010). Fibroblast growth factor signalling: from development to cancer. *Nat. Rev. Cancer* 10, 116–129. doi:10.1038/nrc2780

van den Bosch, M. H., Blom, A. B., van Lent, P. L., van Beuningen, H. M., Blaney Davidson, E. N., van der Kraan, P. M., et al. (2014). Canonical Wnt signaling skews TGF-beta signaling in chondrocytes towards signaling via ALK1 and Smad 1/5/8. *Cell. Signal.* 26, 951–958. doi:10.1016/j.cellsig.2014.01.021

van der Esch, M., Knoop, J., van der Leeden, M., Roorda, L. D., Lems, W. F., Knol, D. L., et al. (2015). Clinical phenotypes in patients with knee osteoarthritis: a study in the Amsterdam osteoarthritis cohort. *Osteoarthr. Cartil.* 23, 544–549. doi:10.1016/j.joca.2015.01.006

van der Kraan, P. M. (2017). The changing role of TGFβ in healthy, ageing and osteoarthritic joints. *Nat. Rev. Rheumatol.* 13, 155. doi:10.1038/nrrheum.2016.219

van der Kraan, P. M., Blaney Davidson, E. N., Blom, A., and van den Berg, W. B. (2009). TGF-beta signaling in chondrocyte terminal differentiation and osteoarthritis: modulation and integration of signaling pathways through receptor-Smads. *Osteoarthr. Cartil.* 17, 1539–1545. doi:10.1016/j.joca.2009.06.008

van der Kraan, P. M., and van den Berg, W. B. (2012). Chondrocyte hypertrophy and osteoarthritis: role in initiation and progression of cartilage degeneration? *Osteoarthr. Cartil.* 20, 223–232. doi:10.1016/j.joca.2011.12.003

van der Weyden, L., Wei, L., Luo, J., Yang, X., Birk, D. E., Adams, D. J., et al. (2006). Functional knockout of the matrilin-3 gene causes premature chondrocyte maturation to hypertrophy and increases bone mineral density and osteoarthritis. *Am. J. Pathol.* 169, 515–527. doi:10.2353/ajpath.2006.050981

Wallin, R., Schurgers, L. J., and Loeser, R. F. (2010). Biosynthesis of the vitamin K-dependent matrix Gla protein (MGP) in chondrocytes: a fetuin-MGP protein complex is assembled in vesicles shed from normal but not from osteoarthritic chondrocytes. *Osteoarthr. Cartil.* 18, 1096–1103. doi:10.1016/j.joca.2010.05.013

Wang, G., and Beier, F. (2005). Rac1/Cdc42 and RhoA GTPases antagonistically regulate chondrocyte proliferation, hypertrophy, and apoptosis. *J. Bone Miner. Res.* 20, 1022–1031. doi:10.1359/jbmr.050113

Wang, Q. Y., Dai, J., Kuang, B., Zhang, J., Yu, S. B., Duan, Y. Z., et al. (2012). Osteochondral angiogenesis in rat mandibular condyles with osteoarthritis-like changes. *Arch. Oral Biol.* 57, 620–629. doi:10.1016/j.archoralbio.2011.12.006

Wei, F., Zhou, J., Wei, X., Zhang, J., Fleming, B. C., Terek, R., et al. (2012). Activation of Indian hedgehog promotes chondrocyte hypertrophy and upregulation of MMP-13 in human osteoarthritic cartilage. *Osteoarthr. Cartil.* 20, 755–763. doi:10.1016/j.joca.2012.03.010

Weisser, J., Riemer, S., Schmidl, M., Suva, L. J., Poschl, E., Brauer, R., et al. (2002). Four distinct chondrocyte populations in the fetal bovine growth plate: highest expression levels of PTH/PTHrP receptor, Indian hedgehog, and MMP-13 in hypertrophic chondrocytes and their suppression by PTH (1-34) and PTHrP (1-40). *Exp. Cell Res.* 279, 1–13. doi:10.1006/excr.2002.5580

Wenke, A. K., Grassel, S., Moser, M., and Bosserhoff, A. K. (2009). The cartilage-specific transcription factor Sox9 regulates AP-2epsilon expression in chondrocytes. *FEBS J.* 276, 2494–2504. doi:10.1111/j.1742-4658.2009.06973.x

Wenke, A. K., Niebler, S., Grassel, S., and Bosserhoff, A. K. (2011). The transcription factor AP-2 epsilon regulates CXCL1 during cartilage development and in osteoarthritis. *Osteoarthr. Cartil.* 19, 206–212. doi:10.1016/j.joca.2010.11.011

Wu, Q., Huang, J. H., Sampson, E. R., Kim, K. O., Zuscik, M. J., O'Keefe, R. J., et al. (2009). Smurf2 induces degradation of GSK-3beta and upregulates beta-catenin in chondrocytes: a potential mechanism for Smurf2-induced degeneration of articular cartilage. *Exp. Cell Res.* 315, 2386–2398. doi:10.1016/j.yexcr.2009.05.019

Xu, W., Xie, Y., Wang, Q., Wang, X., Luo, F., Zhou, S., et al. (2016). A novel fibroblast growth factor receptor 1 inhibitor protects against cartilage degradation in a murine model of osteoarthritis. *Sci. Rep.* 6, 24042. doi:10.1038/srep24042

Yahara, Y., Takemori, H., Okada, M., Kosai, A., Yamashita, A., Kobayashi, T., et al. (2016). Corrigendum: pterosin B prevents chondrocyte hypertrophy and osteoarthritis in mice by inhibiting Sik3. *Nat. Commun.* 7, 12117. doi:10.1038/ncomms12117

Yang, J., Andre, P., Ye, L., and Yang, Y.-Z. (2015). The Hedgehog signalling pathway in bone formation. *Int. J. Oral Sci.* 7, 73. doi:10.1038/ijos.2015.14

Yang, X., Trehan, S. K., Guan, Y., Sun, C., Moore, D. C., Jayasuriya, C. T., et al. (2014). Matrilin-3 inhibits chondrocyte hypertrophy as a bone morphogenetic protein-2 antagonist. *J. Biol. Chem.* 289, 34768–34779. doi:10.1074/jbc.M114.583104

Zhang, H., Wang, H., Zeng, C., Yan, B., Ouyang, J., Liu, X., et al. (2017). mTORC1 activation downregulates FGFR3 and PTH/PTHrP receptor in articular chondrocytes to initiate osteoarthritis. *Osteoarthr. Cartil.* 25, 952–963. doi:10.1016/j.joca.2016.12.024

Zhang, S., Bu, X., Zhao, H., Yu, J., Wang, Y., Li, D., et al. (2014a). A host deficiency of discoidin domain receptor 2 (DDR2) inhibits both tumour angiogenesis and metastasis. *J. Pathol.* 232, 436–448. doi:10.1002/path.4311

Zhang, S., Zhong, Y., Li, R., Wang, W., Zeng, L., Wang, Z., et al. (2014b). Experimental chondrocyte hypertrophy is promoted by the activation of discoidin domain receptor 2. *Mol. Med. Rep.* 10, 1543–1548. doi:10.3892/mmr.2014.2340

Zhang, W., Nuki, G., Moskowitz, R. W., Abramson, S., Altman, R. D., Arden, N. K., et al. (2010). OARSI recommendations for the management of hip and knee osteoarthritis: part III: changes in evidence following systematic cumulative

update of research published through January 2009. *Osteoarthr. Cartil.* 18, 476–499. doi:10.1016/j.joca.2010.01.013

Zhang, X., Crawford, R., and Xiao, Y. (2016a). Inhibition of vascular endothelial growth factor with shRNA in chondrocytes ameliorates osteoarthritis. *J. Mol. Med. (Berl)* 94, 787–798. doi:10.1007/s00109-016-1425-0

Zhang, X., Prasadam, I., Fang, W., Crawford, R., and Xiao, Y. (2016b). Chondromodulin-1 ameliorates osteoarthritis progression by inhibiting HIF-2alpha activity. *Osteoarthr. Cartil.* 24, 1970–1980. doi:10.1016/j.joca.2016.06.005

Zhong, H.-M., Ding, Q.-H., Chen, W.-P., and Luo, R.-B. (2013). Vorinostat, a HDAC inhibitor, showed anti-osteoarthritic activities through inhibition of iNOS and MMP expression, p38 and ERK phosphorylation and blocking NF-κB nuclear translocation. *Int. Immunopharmacol.* 17, 329–335. doi:10.1016/j.intimp.2013.06.027

Zhou, J., Chen, Q., Lanske, B., Fleming, B. C., Terek, R., Wei, X., et al. (2014). Disrupting the Indian hedgehog signaling pathway in vivo attenuates surgically induced osteoarthritis progression in Col2a1-CreERT2; Ihhfl/fl mice. *Arthritis Res. Ther.* 16, R11. doi:10.1186/ar4437

Zhou, S., Xie, Y., Li, W., Huang, J., Wang, Z., Tang, J., et al. (2016). Conditional deletion of Fgfr3 in chondrocytes leads to osteoarthritis-like defects in temporomandibular joint of adult mice. *Sci. Rep.* 6, 24039. doi:10.1038/srep24039

Zhu, S., Dai, J., Liu, H., Cong, X., Chen, Y., Wu, Y., et al. (2015). Down-regulation of Rac GTPase-activating protein OCRL1 causes aberrant activation of Rac1 in osteoarthritis development. *Arthritis Rheumatol.* 67, 2154–2163. doi:10.1002/art.39174

Conflict of Interest Statement: MC and TW are listed as inventor on filed patents: WO2017178251 and WO2017178253. TW has shares in Chondropeptix BV.

The reviewer AL and handling editor declared their shared affiliation.

frontiers in Bioengineering and Biotechnology

MINI REVIEW
published: 09 February 2018
doi: 10.3389/fbioe.2018.00010

Vascular Calcification: Is it rather a Stem/Progenitor Cells Driven Phenomenon?

Aleksandra Leszczynska[1] and J. Mary Murphy[2]*

[1] Regenerative Medicine Institute, Cedars-Sinai Medical Center, Los Angeles, CA, United States, [2] Regenerative Medicine Institute, National University of Ireland Galway, Galway, Ireland

Vascular calcification (VC) has witnessed a surge of interest. Vasculature is virtually an omnipresent organ and has a notably high capacity for repair throughout embryonic and adult life. Of the vascular diseases, atherosclerosis is a leading cause of morbidity and mortality on account of ectopic cartilage and bone formation. Despite the identification of a number of risk factors, all the current theories explaining pathogenesis of VC in atherosclerosis are far from complete. The most widely accepted response to injury theory and smooth muscle transdifferentiation to explain the VC observed in atherosclerosis is being challenged. Recent focus on circulating and resident progenitor cells in the vasculature and their role in atherogenesis and VC has been the driving force behind this review. This review discusses intrinsic cellular players contributing to fate determination of cells and tissues to form ectopic cartilage and bone formation.

Keywords: vascular calcification, stem cells, atherosclerosis, pericytes, progenitor cells

OPEN ACCESS

Edited by:
Roberto Narcisi, Erasmus University Rotterdam, Netherlands

Reviewed by:
Roberta Tasso, Ospedale San Martino (IRCCS), Italy
Anna Lange-Consiglio, University of Milan, Italy

****Correspondence:***
Aleksandra Leszczynska
aleksandra.leszczynska@gmail.com

Specialty section:
This article was submitted to Tissue Engineering and Regenerative Medicine, a section of the journal Frontiers in Bioengineering and Biotechnology

Received: *31 October 2017*
Accepted: *22 January 2018*
Published: *09 February 2018*

Citation:
Leszczynska A and Murphy JM (2018) Vascular Calcification: Is it rather a Stem/Progenitor Cells Driven Phenomenon? Front. Bioeng. Biotechnol. 6:10. doi: 10.3389/fbioe.2018.00010

INTRODUCTION

Vascular calcification (VC) is an important complication of atherosclerosis contributing to cardiovascular morbidity and mortality (Alexopoulos and Raggi, 2009), given the increased risk of heart attack with calcified coronaries and the growing incidence of calcified aortic stenosis (Rajamannan et al., 2007). It is increasingly being accepted that VC is far from a passive degenerative process as thought for the last few decades. Rather, the most recent concept is that VC is an active, organized, complex, and highly regulated process reflecting the plasticity of vasculature (Bostrom, 2016). In particular, calcification of atherosclerotic plaque recapitulates virtually the same biologic reactions inherent to normal physiologic bone formation (Neven and D'Haese, 2011). This recapitulation is evidenced by the presence of bone-like structures in the atherosclerotic arteries and valves, which in many cases is structurally complete trabecular bone (Hunt et al., 2002). This resemblance is not just at the macroscopic level but even at microscopic level shows features such as completely formed marrow cavities with hematopoietic and marrow stromal cells (Bunting, 1906; Soor et al., 2008). Energy dispersive X-ray analysis has shown that the mineral in vascular lesions is hydroxyapatite (Ewence et al., 2008) the same mineral as in bone, not just amorphous calcium phosphate.

Inflammation has been shown to be a contributing factor (Bessueille and Magne, 2015). The expression of growth factors, matrix proteins, and other bone-related proteins that are involved in both the initiation and inhibition of mineralization supports the dogma of VC being a cell controlled event (Dallas and Bonewald, 2010). Calcifying vascular cells (CVCs), a subpopulation of vascular smooth muscle cells (VSMCs), that form bone-like calcifying nodules, have been found (Watson et al., 1994; Ting et al., 2011). In fact, the likelihood for the presence of a number of stem progenitor niches

and/or lineages in vasculature has been described (Martinez-Agosto et al., 2007; Bautch, 2011). Therefore, despite the fact that the understanding of these resident stem progenitor populations is currently at an early stage, tantalizing prospects for their biological and pathological role are being envisaged. This review focuses on different resident and circulating cells that play a role in ectopic cartilage and bone formation in the vessel wall.

PROGENITOR STEM CELLS IN VC

A number of cell types have been implicated in VC (**Table 1**). The cells in all three layers of the vessel wall (Media, Intima, and Adventitia) respond to cues in local microenvironment and undergo chondrogenic/osteogenic differentiation. Along with these resident cells, circulating cells have been shown to migrate into the vessel wall and contribute to VC.

Smooth Muscle Progenitor Cells (SMPCs) and Smooth Muscle Cells (SMCs)

Smooth muscle cell proliferation and matrix protein synthesis, including collagen, elastin, and/or proteoglycans, lead to plaque accretion (Bentzon et al., 2006, 2007) making fibrous tissue a major component of plaque (Cappendijk et al., 2005) and may contribute significantly to coronary artery stenosis (Kataoka et al., 2009). The risk of plaque rupture and a subsequent thrombotic event increases substantially with scarcity of SMCs in the fibrous cap (Schwartz et al., 2000). They also play a role in healing the ruptured plaque by secretion of ECM (Mann and Davies, 1999; Bentzon et al., 2007). However, this healing may result in increased plaque size causing further stenosis (Mann and Davies, 1999; Burke et al., 2001). SMCs found in plaque may be sourced from locally available preexisting SMCs which migrate to the outer layer of plaque (Hu et al., 2004). The SMCs, present in media and intima of the vessel wall, but more importantly cells from the media (Zoll et al., 2008), may form the fibrous component of the plaque while acquiring a synthetic and migrating phenotype through a process called phenotypic modulation (Hao et al., 2006).

TABLE 1 | Potential cell types in vascular calcification.

Cell types	Source/location	Ref.
SMCs	Resident	Speer et al. (2009), Tintut et al. (1998), and Speer et al. (2009)
SMC progenitors	Resident	Kramann et al. (2016) and Bardeesi et al. (2017)
Endothelial progenitors	Resident	Wirrig and Yutzey (2014) and Yao et al. (2015)
Circulating stem cells progenitors	Circulating	Cho et al. (2013) and Hu et al. (2003)
HSCs	Circulating	Cianciolo et al. (2016), Nakahara et al. (2017), and Sata et al. (2002)
MSCs	Circulating	Liao et al. (2012)
Pericytes	Resident	Canfield et al. (2000), Davaine et al. (2014), Bardeesi et al. (2017), and Kirton et al. (2006)
Adventitial cells	Resident	Tigges et al. (2013), Kramann et al. (2016), and Bussolati et al. (2017)

This hypothesis that SMC recruitment and phenotypic modulation is being challenged with suggestions that differentiation of progenitor cells such as hematopoietic stem cells (HSCs) contributes to pathogenesis of atherosclerosis (Sata et al., 2002). Also, another possibility suggests that migration of progenitor cells from adventitia contributes to atherosclerotic plaque. Bone marrow-derived circulating progenitor cells have also been claimed as the source of a sizeable proportion of SMCs found in the atherosclerotic lesion (Tanaka et al., 2008). According to some researchers, the phenotypical differences between contractile SMCs with an abundance of myofilaments and synthetic SMCs with plenty of rough ER and golgi complexes do not suggest phenotypic modulation but rather hint toward different sources, such as a subpopulation in the arterial media with a synthetic phenotype (Frid et al., 1994), stem cells in adventitia (Hu et al., 2004; Torsney et al., 2007) or circulating SMPCs (Saiura et al., 2001). In the case of plaque rupture, local SMCs have been reported to have short telomeres and other markers of senescence (Matthews et al., 2006; Minamino and Komuro, 2008), thus suggesting that rupture healing SMCs are not locally proliferating SMCs and may very well be derived from circulating progenitor cells. This is also suggested by the fact that circulating cells can be induced to express SMC proteins like α-smooth muscle actin (α-SMA) or smooth muscle myosin heavy chain. Furthermore, studies have showed that mesenchymal stem cells (MSCs) express α-SMA protein and so also do stem cells derived from the arterial wall (da Silva Meirelles et al., 2006; Klein et al., 2011). The role of SMPCs in atherosclerosis is more complicated. The severity of luminal stenosis has been related to SMPCs, whereas a decrease in SMPC number may be involved in causing a thinner neointima and unstable plaque.

Thus, over the years, research investigating the origin of SMCs in atherosclerotic lesions has swung from an underlying medial origin to circulating progenitor cells of bone marrow origin. However, there are reports with detailed studies showing that the contribution of circulating bone marrow-derived cells to intimal tissue is less likely (Hu et al., 2002; Hillebrands et al., 2003; Daniel et al., 2010). In one study, the authors investigated the origin of SMCs at the healed plaque rupture sites and showed that SMCs healing the plaque ruptures originate from the local vascular wall (Bentzon et al., 2007).

Endothelial Progenitor Stem Cells and Circulating Progenitor Stem Cells

The functional integrity of the endothelial layer to prevent atherogenic processes is crucial. The known risk factors of coronary artery disease have been shown to induce apoptosis in endothelial cells (ECs), leading to disruption of monolayer integrity (Rossig et al., 2001; Urbich and Dimmeler, 2004b). In atherosclerosis, activation of the damaged ECs triggers the development of the lesions (Zampetaki et al., 2008). Increasingly, it is being understood that endothelial progenitor cells (EPCs) have a strong role in vascular repair by contributing to regeneration of the injured endothelial layer. A negative correlation between severity of atherosclerosis and number of EPCs in patients has been established and an increased number of EPCs has been reported to decrease risk

of stroke. EPCs have been described to express CD34, CD133, or vascular endothelial growth factor receptor 2. Of the multiple precursors, hemangioblasts, bone marrow-derived monocytic cells, or tissue resident stem cells are prominent (Zampetaki et al., 2008).

Studies in mice demonstrated that circulating EPCs are directly incorporated in the vessel wall and are involved in re-endothelialization (Zampetaki et al., 2008). A study has shown that the newly regenerated ECs in a model of transplant atherosclerosis were derived from circulating blood from the recipient and not from donor vessels (Hu et al., 2003). In fact, disease development can be prevented by treatment with bone marrow-derived progenitor cells from young non-atherosclerotic ApoE$^{-/-}$ mice in aged ApoE$^{-/-}$ mice (Rauscher et al., 2003). A number of studies have established a direct link between number of EPCs and endothelial repair and reduction in neointima formation (Griese et al., 2003; Wassmann et al., 2006).

However, the new vessel formation supported by these progenitor cells may prove to be detrimental as shown by a study using a hind limb ischemia model in ApoE$^{-/-}$ mice which demonstrated increased plaque size along with improved blood supply to the ischemic areas (Silvestre et al., 2003). Another study observed that EPC treatment led to increased instability of the plaque which can be attributed to their pro-inflammatory effects with a finding of reduced local IL-10 levels. Thus, it seems that EPCs can have opposite effects; impaired mobilization of EPCs may hamper re-endothelialization while excessive mobilization may cause stenosis (Inoue et al., 2007). However, while evaluating the effects of EPCs, their heterogenicity must be considered as different isolation protocols have been shown to affect the functionality of the cells (Seeger et al., 2007). The role of microvessels in the vessel wall in atherogenesis has been emphasized (Kahlon et al., 1992; Moulton et al., 1999; Ross et al., 2001); however, it has also been demonstrated that ECs in these microvessels are derived from progenitor cells (Hu et al., 2003). Thus, considering their role in endothelial repair and plaque angiogenesis, it is clear that EPCs play both beneficial and detrimental roles, at least in transplant atherosclerosis.

Hematopoietic Stem Cells

Hematopoietic stem cells reside in the arterial tissue and are believed to be involved in maintaining the vascular system on account of their capacity for self-renewal and differentiation to multiple lineages (Feng et al., 2012). Recruitment of circulating blood leukocytes in the vessel wall has been implicated in the development of atherosclerotic plaque (Lusis, 2000; Binder et al., 2002). The role of HSCs in atherosclerosis was investigated recently by inactivating p27 which resulted in enhanced HSC proliferation in arterial macrophages an inflammatory response and accelerated atherosclerosis (Diez-Juan et al., 2004).

Mesenchymal Stem Cells

Plasticity of MSCs shows their ability to differentiate into several cell types (Narcisi et al., 2015) and is influenced by milieu they are presented with. It has been shown that when primed with chondrogenic factors mimicking the cellular niche present in endochondral ossification, mineralization, and vascularization by MSCs is promoted (Freeman et al., 2016). Processes similar to endochondral or intramembranous ossification also occur in the vascular wall (Neven et al., 2011). In addition, MSCs from bone marrow and resident in the vessel wall, have been demonstrated to differentiate into ECs and SMCs, respectively (Urbich and Dimmeler, 2004a; Torsney et al., 2005).

Circulating MSCs can migrate through the blood stream and reach the site of injury in the vessel wall (Abedin et al., 2004). It is now believed that previously described CVCs in the arterial wall are a type of MSCs, one generation below in mesenchymal hierarchy as suggested by their self-renewal and pluripotent plasticity with lack of adipogenic lineage (Tintut et al., 2003). Regarding the differentiation of MSCs to SMCs, the controversy still remains although, through studies investigating the pathogenesis of transplant arteriosclerosis, the role of MSCs or EPCs in repair of ECs is quite clear along with the apparent role of vascular stem cells in replenishing dead cells (Xu, 2008).

In a study with balloon injury in hyperlipidemic rats, bone marrow-derived MSCs (BM-MSCs) were found to clearly increase the size of atherosclerotic lesions (Liao et al., 2012). In this study, transferring BM-MSCs resulted in VC in medial layers detected at 6 weeks after balloon angioplasty (Liao et al., 2012). Although the exact mechanism of calcification following BM-MSCs transfer is not clear, there was a possible association with upregulation of BMP-2 (Nakagawa et al., 2010; Liao et al., 2012). Evidence suggests that the regulation of this calcification involves locally expressed bone calcification regulatory factors (Hruska et al., 2005; Johnson et al., 2006; Ketteler et al., 2006). Another study has demonstrated that transfer of bone marrow and EPCs not only stimulate disease progression in atherosclerosis but also impacted stability of the plaque (George et al., 2005). Studies have provided enough evidence to suggest a link between MSC transfer and pathogenesis of atherosclerosis (Saiura et al., 2001; Sata et al., 2002).

Vascular Stem Cells

There is evidence that stem or progenitor cells reside in different organs and differentiate to repair the injury. However, it might be that these resident stem/progenitor cells are not only contributing to the repair but play an important role to the pathogenesis of atherosclerosis (Kawabe and Hasebe, 2014; Yu et al., 2017). A number of cell types present in vessel wall have been shown to potentially be the vascular stem cells (Tilki et al., 2009; Bautch, 2011; Psaltis et al., 2011; Torsney and Xu, 2011; Bostrom et al., 2012). By far, pericytes are the most important VSCs and will be discussed further.

Pericytes

Pericytes are elongated cells, around 70 μm long, embedded within the basement membrane adjacent to the EC junctions (Voisin et al., 2010; Proebstl et al., 2012). Being closely associated with endothelium, they play a crucial function in maintaining vessel wall integrity and contributing to the generation of the venular basement membrane (Armulik et al., 2005; Edelman et al., 2006). Pericytes have been identified in the inner intimal layer and also the outer layer of the media in vasa vasora in adventitia of large, medium, or small arteries and veins.

It has been suggested that pericytes are MSCs associated with the blood vessel walls where they serve as a support to these vessels (Caplan, 2008, 2017; Crisan et al., 2009). These cells can differentiate not only into fibroblasts, SMC but also into different lineages, especially to osteoblasts (Canfield et al., 1996; Collett and Canfield, 2005; Klein et al., 2011), chondrocytes (Schor et al., 1990; Farrington-Rock et al., 2004; Klein et al., 2011), or adipocytes (Farrington-Rock et al., 2004; Klein et al., 2011) under appropriate cell culture conditions. Pericytes can also act as macrophage precursors and express macrophage markers such as CD4 class I and class II MHC molecules and perform macrophage-like activities (Bergers and Song, 2005; Hall, 2006).

The heterogeneity of pericytes is reflected in their function (Schor et al., 1990). In large arteries, pericytes are embedded within the endothelial basement membrane. They facilitate and integrate cell communication (Armulik et al., 2005). Usually, pericytes overlap several ECs and regulate certain functions by secretion of factors (Armulik et al., 2005; Thanabalasundaram et al., 2011). Pericytes extend long processes exhibiting contractile microfilament bundles which wrap around the blood vessel (Dore-Duffy and Cleary, 2011). They can also form more confined finger like projections and retract them when migrating (Dore-Duffy and Cleary, 2011).

Pericyte coverage varies considerably in different organs, implying their varied functions in different tissues (Proebstl et al., 2012). Similar to VSMCs, pericytes are thought to have multiple origins. In the axial and lateral plate mesenchyme, the vessel wall cells around the developing trunk vessels have been attributed to a mesodermal origin (Hungerford and Little, 1999). In the central nervous system, they might also be derived from neurocrest (Etchevers et al., 2002; Bergers and Song, 2005), at least partly (Etchevers et al., 2001), or mesodermal precursors called angioblasts (Carmeliet, 2004). On the other hand, coronary vessel wall cells have been thought to develop from epicardial cells which have a splanchnic mesodermal origin (Gittenberger-de Groot et al., 1999; Vrancken Peeters et al., 1999). Nevertheless, in general, pericytes are considered to be of mesenchymal origin. They are thought to be associated with MSCs (Creazzo et al., 1998; Armulik et al., 2005; Lamagna and Bergers, 2006) since they can differentiate into different cell types. A study investigating adult angiogenesis confirmed the bone marrow origin of mural cells (Rajantie et al., 2004). Though not a major pathway of pericyte formation in normal physiological development, there has been some evidence of transdifferentiation from ECs (DeRuiter et al., 1997; Rajantie et al., 2004; Armulik et al., 2005), where TGF-β3 can initiate the differentiation.

Pericytes are distinguished from other cell types by their marker expression. They express different markers during the different stages of their growth and also depending on their origin. Pericytes are clearly distinguished from other stromal cells such as SMCs and ECs; however, they share many similarities with other cells like myofibroblasts (Alexander et al., 2005). There are several markers which are used to characterize pericytes like α-SMA (Morikawa et al., 2002; Song et al., 2005), NG2 (Ozerdem et al., 2002; Song et al., 2005; Klein et al., 2011) (nerve/glial antigen 2), PDGFR-β (Winkler et al., 2010; Klein et al., 2011), aminopeptidase A (Ozerdem and Stallcup, 2003), and RGS5 (Gerhardt and Betsholtz, 2003) (regulator of G-protein signaling 5). It is believed that none of the markers absolutely characterize the pericytes on account of their different origins and stage of development. Some of the markers might be expressed dynamically and vary between different organs. 3G5,

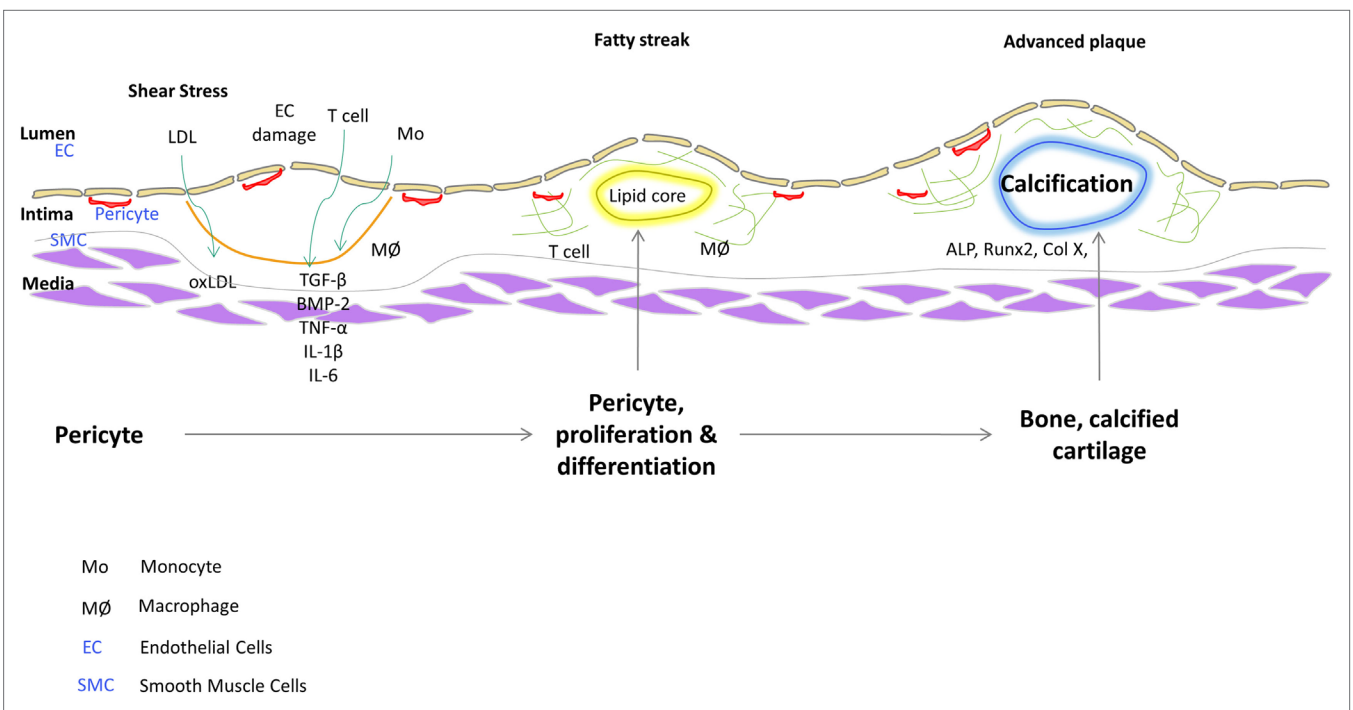

FIGURE 1 | Plausible role of vascular stem cells/pericytes in progression of atherosclerotic plaque.

considered to be a pericyte-specific marker is found on the surface of the pericytes (Nayak et al., 1988; Juchem et al., 2010). 3G5 is expressed in pericytes of human and bovine aorta (Bostrom et al., 1993; Juchem et al., 2010). The role of pericytes as cellular models of atherogenesis has recently been reviewed (Ivanova and Orekhov, 2016). **Figure 1** shows a schematic that illustrates a role of vascular stem cells or pericytes in atherosclerotic plaque progression based on our findings. In fact, we have described a population of pericyte-like progenitor cells isolated from aortae of ApoE$^{-/-}$ mice and control C57BL/6 mice and shown their possible role in aberrant tissue formation in the atheromatous plaque (Leszczynska et al., 2016).

As we continue to unravel the mysteries underlying disease progression in atherosclerosis and decipher the role of the contributing stem/progenitors in VC, the importance of understanding the cell–cell and cell–tissue communication, especially through the microvesicular/exosomal pathway, cannot be overemphasized. In fact, many studies in recent years have shown important role played by exosomes in communication protocol in atherosclerosis (Huber and Holvoet, 2015; Gao et al., 2016; Perrotta and Aquila, 2016; Lu, 2017).

CONCLUSION

A number of stem progenitor cells are involved in VC, in fact they are emerging as the most important players. On account of their plasticity and involvement in VC and inflammation, pericytes are arguably the most interesting ones among the different contributors. Going forward, it will be increasingly important to understand how exosomes execute the bio-message delivery among different key players and exploit therapeutic potential thereof.

AUTHOR CONTRIBUTIONS

AL and JMM conceived the idea of this article. AL wrote this mini review and JMM revised and finalized it.

FUNDING

This work was supported by the Irish Research Council for Science, Engineering and Technology, and Science Foundation Ireland under grant no. 09/SRC/B1794.

REFERENCES

Abedin, M., Tintut, Y., and Demer, L. L. (2004). Mesenchymal stem cells and the artery wall. *Circ. Res.* 95, 671–676. doi:10.1161/01.RES.0000143421.27684.12

Alexander, M. Y., Wilkinson, F. L., Kirton, J. P., Rock, C. F., Collett, G. D., Jeziorska, M., et al. (2005). Identification and characterization of vascular calcification-associated factor, a novel gene upregulated during vascular calcification in vitro and in vivo. *Arterioscler. Thromb. Vasc. Biol.* 25, 1851–1857. doi:10.1161/01.ATV.0000175750.94742.46

Alexopoulos, N., and Raggi, P. (2009). Calcification in atherosclerosis. *Nat. Rev. Cardiol.* 6, 681–688. doi:10.1038/nrcardio.2009.165

Armulik, A., Abramsson, A., and Betsholtz, C. (2005). Endothelial/pericyte interactions. *Circ. Res.* 97, 512–523. doi:10.1161/01.RES.0000182903.16652.d7

Bardeesi, A. S. A., Gao, J., Zhang, K., Yu, S., Wei, M., Liu, P., et al. (2017). A novel role of cellular interactions in vascular calcification. *J. Transl. Med.* 15, 95. doi:10.1186/s12967-017-1190-z

Bautch, V. L. (2011). Stem cells and the vasculature. *Nat. Med.* 17, 1437–1443. doi:10.1038/nm.2539

Bentzon, J. F., Sondergaard, C. S., Kassem, M., and Falk, E. (2007). Smooth muscle cells healing atherosclerotic plaque disruptions are of local, not blood, origin in apolipoprotein E knockout mice. *Circulation* 116, 2053–2061. doi:10.1161/CIRCULATIONAHA.107.722355

Bentzon, J. F., Weile, C., Sondergaard, C. S., Hindkjaer, J., Kassem, M., and Falk, E. (2006). Smooth muscle cells in atherosclerosis originate from the local vessel wall and not circulating progenitor cells in ApoE knockout mice. *Arterioscler. Thromb. Vasc. Biol.* 26, 2696–2702. doi:10.1161/01.ATV.0000247243.48542.9d

Bergers, G., and Song, S. (2005). The role of pericytes in blood-vessel formation and maintenance. *Neuro Oncol.* 7, 452–464. doi:10.1215/S1152851705000232

Bessueille, L., and Magne, D. (2015). Inflammation: a culprit for vascular calcification in atherosclerosis and diabetes. *Cell. Mol. Life Sci.* 72, 2475–2489. doi:10.1007/s00018-015-1876-4

Binder, C. J., Chang, M. K., Shaw, P. X., Miller, Y. I., Hartvigsen, K., Dewan, A., et al. (2002). Innate and acquired immunity in atherogenesis. *Nat. Med.* 8, 1218–1226. doi:10.1038/nm1102-1218

Bostrom, K., Watson, K. E., Horn, S., Wortham, C., Herman, I. M., and Demer, L. L. (1993). Bone morphogenetic protein expression in human atherosclerotic lesions. *J. Clin. Invest.* 91, 1800–1809. doi:10.1172/JCI116391

Bostrom, K. I. (2016). Where do we stand on vascular calcification? *Vascul. Pharmacol.* 84, 8–14. doi:10.1016/j.vph.2016.05.014

Bostrom, K. I., Garfinkel, A., Yao, Y., and Jumabay, M. (2012). Concise review: applying stem cell biology to vascular structures. *Stem Cells* 30, 386–391. doi:10.1002/stem.1027

Bunting, C. H. (1906). The formation of true bone with cellular (red) marrow in a sclerotic aorta. *J. Exp. Med.* 8, 365–376. doi:10.1084/jem.8.3.365

Burke, A. P., Kolodgie, F. D., Farb, A., Weber, D. K., Malcom, G. T., Smialek, J., et al. (2001). Healed plaque ruptures and sudden coronary death: evidence that subclinical rupture has a role in plaque progression. *Circulation* 103, 934–940. doi:10.1161/01.CIR.103.7.934

Bussolati, B., Deregibus, M. C., and Camussi, G. (2017). Role of adventitial MSC-like cells in chronic kidney disease. *Stem Cell Investig.* 4, 2. doi:10.21037/sci.2016.12.03

Canfield, A. E., Doherty, M. J., Wood, A. C., Farrington, C., Ashton, B., Begum, N., et al. (2000). Role of pericytes in vascular calcification: a review. *Z. Kardiol.* 89(Suppl. 2), 20–27. doi:10.1007/s003920070096

Canfield, A. E., Sutton, A. B., Hoyland, J. A., and Schor, A. M. (1996). Association of thrombospondin-1 with osteogenic differentiation of retinal pericytes in vitro. *J. Cell. Sci.* 109(Pt 2), 343–353.

Caplan, A. I. (2008). All MSCs are pericytes? *Cell Stem Cell* 3, 229–230. doi:10.1016/j.stem.2008.08.008

Caplan, A. I. (2017). New MSC: MSCs as pericytes are sentinels and gatekeepers. *J. Orthop. Res.* 35, 1151–1159. doi:10.1002/jor.23560

Cappendijk, V. C., Cleutjens, K. B., Kessels, A. G., Heeneman, S., Schurink, G. W., Welten, R. J., et al. (2005). Assessment of human atherosclerotic carotid plaque components with multisequence MR imaging: initial experience. *Radiology* 234, 487–492. doi:10.1148/radiol.2342032101

Carmeliet, P. (2004). Manipulating angiogenesis in medicine. *J. Intern. Med.* 255, 538–561. doi:10.1111/j.1365-2796.2003.01297.x

Cho, H. J., Cho, H. J., Lee, H. J., Song, M. K., Seo, J. Y., Bae, Y. H., et al. (2013). Vascular calcifying progenitor cells possess bidirectional differentiation potentials. *PLoS Biol.* 11:e1001534. doi:10.1371/journal.pbio.1001534

Cianciolo, G., Capelli, I., Cappuccilli, M., Schillaci, R., Cozzolino, M., and La Manna, G. (2016). Calcifying circulating cells: an uncharted area in the setting of vascular calcification in CKD patients. *Clin. Kidney J.* 9, 280–286. doi:10.1093/ckj/sfv145

Collett, G. D., and Canfield, A. E. (2005). Angiogenesis and pericytes in the initiation of ectopic calcification. *Circ. Res.* 96, 930–938. doi:10.1161/01.RES.0000163634.51301.0d

Creazzo, T. L., Godt, R. E., Leatherbury, L., Conway, S. J., and Kirby, M. L. (1998). Role of cardiac neural crest cells in cardiovascular development. *Annu. Rev. Physiol.* 60, 267–286. doi:10.1146/annurev.physiol.60.1.267

Crisan, M., Chen, C. W., Corselli, M., Andriolo, G., Lazzari, L., and Peault, B. (2009). Perivascular multipotent progenitor cells in human organs. *Ann. N. Y. Acad. Sci.* 1176, 118–123. doi:10.1111/j.1749-6632.2009.04967.x

da Silva Meirelles, L., Chagastelles, P. C., and Nardi, N. B. (2006). Mesenchymal stem cells reside in virtually all post-natal organs and tissues. *J. Cell. Sci.* 119(Pt 11), 2204–2213. doi:10.1242/jcs.02932

Dallas, S. L., and Bonewald, L. F. (2010). Dynamics of the transition from osteoblast to osteocyte. *Ann. N. Y. Acad. Sci.* 1192, 437–443. doi:10.1111/j.1749-6632.2009.05246.x

Daniel, J. M., Bielenberg, W., Stieger, P., Weinert, S., Tillmanns, H., and Sedding, D. G. (2010). Time-course analysis on the differentiation of bone marrow-derived progenitor cells into smooth muscle cells during neointima formation. *Arterioscler. Thromb. Vasc. Biol.* 30, 1890–1896. doi:10.1161/ATVBAHA.110.209692

Davaine, J. M., Quillard, T., Brion, R., Laperine, O., Guyomarch, B., Merlini, T., et al. (2014). Osteoprotegerin, pericytes and bone-like vascular calcification are associated with carotid plaque stability. *PLoS ONE* 9:e107642. doi:10.1371/journal.pone.0107642

DeRuiter, M. C., Poelmann, R. E., VanMunsteren, J. C., Mironov, V., Markwald, R. R., and Gittenberger-de Groot, A. C. (1997). Embryonic endothelial cells transdifferentiate into mesenchymal cells expressing smooth muscle actins in vivo and in vitro. *Circ. Res.* 80, 444–451. doi:10.1161/01.RES.80.4.444

Diez-Juan, A., Perez, P., Aracil, M., Sancho, D., Bernad, A., Sanchez-Madrid, F., et al. (2004). Selective inactivation of p27(Kip1) in hematopoietic progenitor cells increases neointimal macrophage proliferation and accelerates atherosclerosis. *Blood* 103, 158–161. doi:10.1182/blood-2003-07-2319

Dore-Duffy, P., and Cleary, K. (2011). Morphology and properties of pericytes. *Methods Mol. Biol.* 686, 49–68. doi:10.1007/978-1-60761-938-3_2

Edelman, D. A., Jiang, Y., Tyburski, J., Wilson, R. F., and Steffes, C. (2006). Pericytes and their role in microvasculature homeostasis. *J. Surg. Res.* 135, 305–311. doi:10.1016/j.jss.2006.06.010

Etchevers, H. C., Couly, G., and Le Douarin, N. M. (2002). Morphogenesis of the branchial vascular sector. *Trends Cardiovasc. Med.* 12, 299–304. doi:10.1016/S1050-1738(02)00178-0

Etchevers, H. C., Vincent, C., Le Douarin, N. M., and Couly, G. F. (2001). The cephalic neural crest provides pericytes and smooth muscle cells to all blood vessels of the face and forebrain. *Development* 128, 1059–1068.

Ewence, A. E., Bootman, M., Roderick, H. L., Skepper, J. N., McCarthy, G., Epple, M., et al. (2008). Calcium phosphate crystals induce cell death in human vascular smooth muscle cells: a potential mechanism in atherosclerotic plaque destabilization. *Circ. Res.* 103, e28–e34. doi:10.1161/CIRCRESAHA.108.181305

Farrington-Rock, C., Crofts, N. J., Doherty, M. J., Ashton, B. A., Griffin-Jones, C., and Canfield, A. E. (2004). Chondrogenic and adipogenic potential of microvascular pericytes. *Circulation* 110, 2226–2232. doi:10.1161/01.CIR.0000144457.55518.E5

Feng, Y., Schouteden, S., Geenens, R., Van Duppen, V., Herijgers, P., Holvoet, P., et al. (2012). Hematopoietic stem/progenitor cell proliferation and differentiation is differentially regulated by high-density and low-density lipoproteins in mice. *PLoS ONE* 7:e47286. doi:10.1371/journal.pone.0047286

Freeman, F. E., Stevens, H. Y., Owens, P., Guldberg, R. E., and McNamara, L. M. (2016). Osteogenic differentiation of mesenchymal stem cells by mimicking the cellular niche of the endochondral template. *Tissue Eng. Part A* 22, 1176–1190. doi:10.1089/ten.TEA.2015.0339

Frid, M. G., Moiseeva, E. P., and Stenmark, K. R. (1994). Multiple phenotypically distinct smooth muscle cell populations exist in the adult and developing bovine pulmonary arterial media in vivo. *Circ. Res.* 75, 669–681. doi:10.1161/01.RES.75.4.669

Gao, W., Liu, H., Yuan, J., Wu, C., Huang, D., Ma, Y., et al. (2016). Exosomes derived from mature dendritic cells increase endothelial inflammation and atherosclerosis via membrane TNF-alpha mediated NF-kappaB pathway. *J. Cell. Mol. Med.* 20, 2318–2327. doi:10.1111/jcmm.12923

George, J., Afek, A., Abashidze, A., Shmilovich, H., Deutsch, V., Kopolovich, J., et al. (2005). Transfer of endothelial progenitor and bone marrow cells influences atherosclerotic plaque size and composition in apolipoprotein E knockout mice. *Arterioscler. Thromb. Vasc. Biol.* 25, 2636–2641. doi:10.1161/01.ATV.0000188554.49745.9e

Gerhardt, H., and Betsholtz, C. (2003). Endothelial-pericyte interactions in angiogenesis. *Cell Tissue Res.* 314, 15–23. doi:10.1007/s00441-003-0745-x

Gittenberger-de Groot, A. C., DeRuiter, M. C., Bergwerff, M., and Poelmann, R. E. (1999). Smooth muscle cell origin and its relation to heterogeneity in development and disease. *Arterioscler. Thromb. Vasc. Biol.* 19, 1589–1594. doi:10.1161/01.ATV.19.7.1589

Griese, D. P., Ehsan, A., Melo, L. G., Kong, D., Zhang, L., Mann, M. J., et al. (2003). Isolation and transplantation of autologous circulating endothelial cells into denuded vessels and prosthetic grafts: implications for cell-based vascular therapy. *Circulation* 108, 2710–2715. doi:10.1161/01.CIR.0000096490.16596.A6

Hall, A. P. (2006). Review of the pericyte during angiogenesis and its role in cancer and diabetic retinopathy. *Toxicol. Pathol.* 34, 763–775. doi:10.1080/01926230600936290

Hao, H., Gabbiani, G., Camenzind, E., Bacchetta, M., Virmani, R., and Bochaton-Piallat, M. L. (2006). Phenotypic modulation of intima and media smooth muscle cells in fatal cases of coronary artery lesion. *Arterioscler. Thromb. Vasc. Biol.* 26, 326–332. doi:10.1161/01.ATV.0000199393.74656.4c

Hillebrands, J. L., Klatter, F. A., and Rozing, J. (2003). Origin of vascular smooth muscle cells and the role of circulating stem cells in transplant arteriosclerosis. *Arterioscler. Thromb. Vasc. Biol.* 23, 380–387. doi:10.1161/01.ATV.0000059337.60393.64

Hruska, K. A., Mathew, S., and Saab, G. (2005). Bone morphogenetic proteins in vascular calcification. *Circ. Res.* 97, 105–114. doi:10.1161/01.RES.00000175571.53833.6c

Hu, Y., Davison, F., Ludewig, B., Erdel, M., Mayr, M., Url, M., et al. (2002). Smooth muscle cells in transplant atherosclerotic lesions are originated from recipients, but not bone marrow progenitor cells. *Circulation* 106, 1834–1839. doi:10.1161/01.CIR.0000031333.86845.DD

Hu, Y., Davison, F., Zhang, Z., and Xu, Q. (2003). Endothelial replacement and angiogenesis in arteriosclerotic lesions of allografts are contributed by circulating progenitor cells. *Circulation* 108, 3122–3127. doi:10.1161/01.CIR.0000105722.96112.67

Hu, Y., Zhang, Z., Torsney, E., Afzal, A. R., Davison, F., Metzler, B., et al. (2004). Abundant progenitor cells in the adventitia contribute to atherosclerosis of vein grafts in ApoE-deficient mice. *J. Clin. Invest.* 113, 1258–1265. doi:10.1172/JCI19628

Huber, H. J., and Holvoet, P. (2015). Exosomes: emerging roles in communication between blood cells and vascular tissues during atherosclerosis. *Curr. Opin. Lipidol.* 26, 412–419. doi:10.1097/MOL.0000000000000214

Hungerford, J. E., and Little, C. D. (1999). Developmental biology of the vascular smooth muscle cell: building a multilayered vessel wall. *J. Vasc. Res.* 36, 2–27. doi:10.1159/000025622

Hunt, J. L., Fairman, R., Mitchell, M. E., Carpenter, J. P., Golden, M., Khalapyan, T., et al. (2002). Bone formation in carotid plaques: a clinicopathological study. *Stroke* 33, 1214–1219. doi:10.1161/01.STR.0000013741.41309.67

Inoue, T., Sata, M., Hikichi, Y., Sohma, R., Fukuda, D., Uchida, T., et al. (2007). Mobilization of CD34-positive bone marrow-derived cells after coronary stent implantation: impact on restenosis. *Circulation* 115, 553–561. doi:10.1161/CIRCULATIONAHA.106.621714

Ivanova, E. A., and Orekhov, A. N. (2016). Cellular model of atherogenesis based on pluripotent vascular wall pericytes. *Stem Cells Int.* 2016, 7321404. doi:10.1155/2016/7321404

Johnson, R. C., Leopold, J. A., and Loscalzo, J. (2006). Vascular calcification: pathobiological mechanisms and clinical implications. *Circ. Res.* 99, 1044–1059. doi:10.1161/01.RES.0000249379.55535.21

Juchem, G., Weiss, D. R., Gansera, B., Kemkes, B. M., Mueller-Hoecker, J., and Nees, S. (2010). Pericytes in the macrovascular intima: possible physiological and pathogenetic impact. *Am. J. Physiol. Heart Circ. Physiol.* 298, H754–H770. doi:10.1152/ajpheart.00343.2009

Kahlon, R., Shapero, J., and Gotlieb, A. I. (1992). Angiogenesis in atherosclerosis. *Can. J. Cardiol.* 8, 60–64.

Kataoka, T., Mathew, V., Rubinshtein, R., Rihal, C. S., Lennon, R., Lerman, L. O., et al. (2009). Association of plaque composition and vessel remodeling in atherosclerotic renal artery stenosis: a comparison with coronary artery disease. *JACC Cardiovasc. Imaging* 2, 327–338. doi:10.1016/j.jcmg.2008.08.008

Kawabe, J., and Hasebe, N. (2014). Role of the vasa vasorum and vascular resident stem cells in atherosclerosis. *Biomed Res. Int.* 2014, 701571. doi:10.1155/2014/701571

Ketteler, M., Schlieper, G., and Floege, J. (2006). Calcification and cardiovascular health: new insights into an old phenomenon. *Hypertension* 47, 1027–1034. doi:10.1161/01.HYP.0000219635.51844.da

Kirton, J. P., Wilkinson, F. L., Canfield, A. E., and Alexander, M. Y. (2006). Dexamethasone downregulates calcification-inhibitor molecules and accelerates osteogenic differentiation of vascular pericytes: implications for vascular calcification. *Circ. Res.* 98, 1264–1272. doi:10.1161/01.RES.0000223056.68892.8b

Klein, D., Weisshardt, P., Kleff, V., Jastrow, H., Jakob, H. G., and Ergun, S. (2011). Vascular wall-resident CD44+ multipotent stem cells give rise to pericytes and smooth muscle cells and contribute to new vessel maturation. *PLoS ONE* 6:e20540. doi:10.1371/journal.pone.0020540

Kramann, R., Goettsch, C., Wongboonsin, J., Iwata, H., Schneider, R. K., Kuppe, C., et al. (2016). Adventitial MSC-like cells are progenitors of vascular smooth muscle cells and drive vascular calcification in chronic kidney disease. *Cell Stem Cell* 19, 628–642. doi:10.1016/j.stem.2016.08.001

Lamagna, C., and Bergers, G. (2006). The bone marrow constitutes a reservoir of pericyte progenitors. *J. Leukoc. Biol.* 80, 677–681. doi:10.1189/jlb.0506309

Leszczynska, A., O'Doherty, A., Farrell, E., Pindjakova, J., O'Brien, F. J., O'Brien, T., et al. (2016). Differentiation of vascular stem cells contributes to ectopic calcification of atherosclerotic plaque. *Stem Cells* 34, 913–923. doi:10.1002/stem.2315

Liao, J., Chen, X., Li, Y., Ge, Z., Duan, H., Zou, Y., et al. (2012). Transfer of bone-marrow-derived mesenchymal stem cells influences vascular remodeling and calcification after balloon injury in hyperlipidemic rats. *J. Biomed. Biotechnol.* 2012, 165296. doi:10.1155/2012/165296

Lu, X. (2017). The role of exosomes and exosome-derived microRNAs in atherosclerosis. *Curr. Pharm. Des.* doi:10.2174/1381612823666170413125507

Lusis, A. J. (2000). Atherosclerosis. *Nature* 407, 233–241. doi:10.1038/35025203

Mann, J., and Davies, M. J. (1999). Mechanisms of progression in native coronary artery disease: role of healed plaque disruption. *Heart* 82, 265–268. doi:10.1136/hrt.82.3.265

Martinez-Agosto, J. A., Mikkola, H. K., Hartenstein, V., and Banerjee, U. (2007). The hematopoietic stem cell and its niche: a comparative view. *Genes Dev.* 21, 3044–3060. doi:10.1101/gad.1602607

Matthews, C., Gorenne, I., Scott, S., Figg, N., Kirkpatrick, P., Ritchie, A., et al. (2006). Vascular smooth muscle cells undergo telomere-based senescence in human atherosclerosis: effects of telomerase and oxidative stress. *Circ. Res.* 99, 156–164. doi:10.1161/01.RES.0000233315.38086.bc

Minamino, T., and Komuro, I. (2008). Vascular aging: insights from studies on cellular senescence, stem cell aging, and progeroid syndromes. *Nat. Clin. Pract. Cardiovasc. Med.* 5, 637–648. doi:10.1038/ncpcardio1324

Morikawa, S., Baluk, P., Kaidoh, T., Haskell, A., Jain, R. K., and McDonald, D. M. (2002). Abnormalities in pericytes on blood vessels and endothelial sprouts in tumors. *Am. J. Pathol.* 160, 985–1000. doi:10.1016/S0002-9440(10)64920-6

Moulton, K. S., Heller, E., Konerding, M. A., Flynn, E., Palinski, W., and Folkman, J. (1999). Angiogenesis inhibitors endostatin or TNP-470 reduce intimal neovascularization and plaque growth in apolipoprotein E-deficient mice. *Circulation* 99, 1726–1732. doi:10.1161/01.CIR.99.13.1726

Nakagawa, Y., Ikeda, K., Akakabe, Y., Koide, M., Uraoka, M., Yutaka, K. T., et al. (2010). Paracrine osteogenic signals via bone morphogenetic protein-2 accelerate the atherosclerotic intimal calcification in vivo. *Arterioscler. Thromb. Vasc. Biol.* 30, 1908–1915. doi:10.1161/ATVBAHA.110.206185

Nakahara, T., Dweck, M. R., Narula, N., Pisapia, D., Narula, J., and Strauss, H. W. (2017). Coronary artery calcification: from mechanism to molecular imaging. *JACC Cardiovasc. Imaging* 10, 582–593. doi:10.1016/j.jcmg.2017.03.005

Narcisi, R., Cleary, M. A., Brama, P. A., Hoogduijn, M. J., Tuysuz, N., ten Berge, D., et al. (2015). Long-term expansion, enhanced chondrogenic potential, and suppression of endochondral ossification of adult human MSCs via WNT signaling modulation. *Stem Cell Reports* 4, 459–472. doi:10.1016/j.stemcr.2015.01.017

Nayak, R. C., Berman, A. B., George, K. L., Eisenbarth, G. S., and King, G. L. (1988). A monoclonal antibody (3G5)-defined ganglioside antigen is expressed on the cell surface of microvascular pericytes. *J. Exp. Med.* 167, 1003–1015. doi:10.1084/jem.167.3.1003

Neven, E., De Schutter, T. M., De Broe, M. E., and D'Haese, P. C. (2011). Cell biological and physicochemical aspects of arterial calcification. *Kidney Int.* 79, 1166–1177. doi:10.1038/ki.2011.59

Neven, E., and D'Haese, P. C. (2011). Vascular calcification in chronic renal failure: what have we learned from animal studies? *Circ. Res.* 108, 249–264. doi:10.1161/CIRCRESAHA.110.225904

Ozerdem, U., Monosov, E., and Stallcup, W. B. (2002). NG2 proteoglycan expression by pericytes in pathological microvasculature. *Microvasc. Res.* 63, 129–134. doi:10.1006/mvre.2001.2376

Ozerdem, U., and Stallcup, W. B. (2003). Early contribution of pericytes to angiogenic sprouting and tube formation. *Angiogenesis* 6, 241–249. doi:10.1023/B:AGEN.0000021401.58039.a9

Perrotta, I., and Aquila, S. (2016). Exosomes in human atherosclerosis: an ultrastructural analysis study. *Ultrastruct. Pathol.* 40, 101–106. doi:10.3109/01913123.2016.1154912

Proebstl, D., Voisin, M. B., Woodfin, A., Whiteford, J., D'Acquisto, F., Jones, G. E., et al. (2012). Pericytes support neutrophil subendothelial cell crawling and breaching of venular walls in vivo. *J. Exp. Med.* 209, 1219–1234. doi:10.1084/jem.20111622

Psaltis, P. J., Harbuzariu, A., Delacroix, S., Holroyd, E. W., and Simari, R. D. (2011). Resident vascular progenitor cells—diverse origins, phenotype, and function. *J. Cardiovasc. Transl. Res.* 4, 161–176. doi:10.1007/s12265-010-9248-9

Rajamannan, N. M., Bonow, R. O., and Rahimtoola, S. H. (2007). Calcific aortic stenosis: an update. *Nat. Clin. Pract. Cardiovasc. Med.* 4, 254–262. doi:10.1038/ncpcardio0827

Rajantie, I., Ilmonen, M., Alminaite, A., Ozerdem, U., Alitalo, K., and Salven, P. (2004). Adult bone marrow-derived cells recruited during angiogenesis comprise precursors for periendothelial vascular mural cells. *Blood* 104, 2084–2086. doi:10.1182/blood-2004-01-0336

Rauscher, F. M., Goldschmidt-Clermont, P. J., Davis, B. H., Wang, T., Gregg, D., Ramaswami, P., et al. (2003). Aging, progenitor cell exhaustion, and atherosclerosis. *Circulation* 108, 457–463. doi:10.1161/01.CIR.0000082924.75945.48

Ross, J. S., Stagliano, N. E., Donovan, M. J., Breitbart, R. E., and Ginsburg, G. S. (2001). Atherosclerosis and cancer: common molecular pathways of disease development and progression. *Ann. N. Y. Acad. Sci.* 947, 271–92; discussion 292–73. doi:10.1111/j.1749-6632.2001.tb03949.x

Rossig, L., Dimmeler, S., and Zeiher, A. M. (2001). Apoptosis in the vascular wall and atherosclerosis. *Basic Res. Cardiol.* 96, 11–22. doi:10.1007/s003950170073

Saiura, A., Sata, M., Hirata, Y., Nagai, R., and Makuuchi, M. (2001). Circulating smooth muscle progenitor cells contribute to atherosclerosis. *Nat. Med.* 7, 382–383. doi:10.1038/86394

Sata, M., Saiura, A., Kunisato, A., Tojo, A., Okada, S., Tokuhisa, T., et al. (2002). Hematopoietic stem cells differentiate into vascular cells that participate in the pathogenesis of atherosclerosis. *Nat. Med.* 8, 403–409. doi:10.1038/nm0402-403

Schor, A. M., Allen, T. D., Canfield, A. E., Sloan, P., and Schor, S. L. (1990). Pericytes derived from the retinal microvasculature undergo calcification in vitro. *J. Cell. Sci.* 97(Pt 3), 449–461.

Schwartz, S. M., Virmani, R., and Rosenfeld, M. E. (2000). The good smooth muscle cells in atherosclerosis. *Curr. Atheroscler. Rep.* 2, 422–429. doi:10.1007/s11883-000-0081-5

Seeger, F. H., Tonn, T., Krzossok, N., Zeiher, A. M., and Dimmeler, S. (2007). Cell isolation procedures matter: a comparison of different isolation protocols of bone marrow mononuclear cells used for cell therapy in patients with acute myocardial infarction. *Eur. Heart J.* 28, 766–772. doi:10.1093/eurheartj/ehl509

Silvestre, J. S., Gojova, A., Brun, V., Potteaux, S., Esposito, B., Duriez, M., et al. (2003). Transplantation of bone marrow-derived mononuclear cells in ischemic apolipoprotein E-knockout mice accelerates atherosclerosis without altering plaque composition. *Circulation* 108, 2839–2842. doi:10.1161/01.CIR.0000106161.43954.DF

Song, S., Ewald, A. J., Stallcup, W., Werb, Z., and Bergers, G. (2005). PDGFRbeta+ perivascular progenitor cells in tumours regulate pericyte differentiation and vascular survival. *Nat. Cell Biol.* 7, 870–879. doi:10.1038/ncb1288

Soor, G. S., Vukin, I., Leong, S. W., Oreopoulos, G., and Butany, J. (2008). Peripheral vascular disease: who gets it and why? A histomorphological analysis of 261 arterial segments from 58 cases. *Pathology* 40, 385–391. doi:10.1080/00313020802036764

Speer, M. Y., Yang, H. Y., Brabb, T., Leaf, E., Look, A., Lin, W. L., et al. (2009). Smooth muscle cells give rise to osteochondrogenic precursors and chondrocytes in calcifying arteries. *Circ. Res.* 104, 733–741. doi:10.1161/CIRCRESAHA.108.183053

Tanaka, K., Sata, M., Natori, T., Kim-Kaneyama, J. R., Nose, K., Shibanuma, M., et al. (2008). Circulating progenitor cells contribute to neointimal formation in nonirradiated chimeric mice. *FASEB J.* 22, 428–436. doi:10.1096/fj.06-6884com

Thanabalasundaram, G., El-Gindi, J., Lischper, M., and Galla, H. J. (2011). Methods to assess pericyte-endothelial cell interactions in a coculture model. *Methods Mol. Biol.* 686, 379–399. doi:10.1007/978-1-60761-938-3_19

Tigges, U., Komatsu, M., and Stallcup, W. B. (2013). Adventitial pericyte progenitor/mesenchymal stem cells participate in the restenotic response to arterial injury. *J. Vasc. Res.* 50, 134–144. doi:10.1159/000345524

Tilki, D., Hohn, H. P., Ergun, B., Rafii, S., and Ergun, S. (2009). Emerging biology of vascular wall progenitor cells in health and disease. *Trends Mol. Med.* 15, 501–509. doi:10.1016/j.molmed.2009.09.004

Ting, T. C., Miyazaki-Anzai, S., Masuda, M., Levi, M., Demer, L. L., Tintut, Y., et al. (2011). Increased lipogenesis and stearate accelerate vascular calcification in calcifying vascular cells. *J. Biol. Chem.* 286, 23938–23949. doi:10.1074/jbc.M111.237065

Tintut, Y., Alfonso, Z., Saini, T., Radcliff, K., Watson, K., Bostrom, K., et al. (2003). Multilineage potential of cells from the artery wall. *Circulation* 108, 2505–2510. doi:10.1161/01.CIR.0000096485.64373.C5

Tintut, Y., Parhami, F., Bostrom, K., Jackson, S. M., and Demer, L. L. (1998). cAMP stimulates osteoblast-like differentiation of calcifying vascular cells. Potential signaling pathway for vascular calcification. *J. Biol. Chem.* 273, 7547–7553. doi:10.1074/jbc.273.13.7547

Torsney, E., Hu, Y., and Xu, Q. (2005). Adventitial progenitor cells contribute to arteriosclerosis. *Trends Cardiovasc. Med.* 15, 64–68. doi:10.1016/j.tcm.2005.02.003

Torsney, E., Mandal, K., Halliday, A., Jahangiri, M., and Xu, Q. (2007). Characterisation of progenitor cells in human atherosclerotic vessels. *Atherosclerosis* 191, 259–264. doi:10.1016/j.atherosclerosis.2006.05.033

Torsney, E., and Xu, Q. (2011). Resident vascular progenitor cells. *J. Mol. Cell. Cardiol.* 50, 304–311. doi:10.1016/j.yjmcc.2010.09.006

Urbich, C., and Dimmeler, S. (2004a). Endothelial progenitor cells functional characterization. *Trends Cardiovasc. Med.* 14, 318–322. doi:10.1016/j.tcm.2004.10.001

Urbich, C., and Dimmeler, S. (2004b). Endothelial progenitor cells: characterization and role in vascular biology. *Circ. Res.* 95, 343–353. doi:10.1161/01.RES.0000137877.89448.78

Voisin, M. B., Probstl, D., and Nourshargh, S. (2010). Venular basement membranes ubiquitously express matrix protein low-expression regions: characterization in multiple tissues and remodeling during inflammation. *Am. J. Pathol.* 176, 482–495. doi:10.2353/ajpath.2010.090510

Vrancken Peeters, M. P., Gittenberger-de Groot, A. C., Mentink, M. M., and Poelmann, R. E. (1999). Smooth muscle cells and fibroblasts of the coronary arteries derive from epithelial-mesenchymal transformation of the epicardium. *Anat. Embryol. (Berl)* 199, 367–378. doi:10.1007/s004290050235

Wassmann, S., Werner, N., Czech, T., and Nickenig, G. (2006). Improvement of endothelial function by systemic transfusion of vascular progenitor cells. *Circ. Res.* 99, e74–e83. doi:10.1161/01.RES.0000246095.90247.d4

Watson, K. E., Bostrom, K., Ravindranath, R., Lam, T., Norton, B., and Demer, L. L. (1994). TGF-beta 1 and 25-hydroxycholesterol stimulate osteoblast-like vascular cells to calcify. *J. Clin. Invest.* 93, 2106–2113. doi:10.1172/JCI117205

Winkler, E. A., Bell, R. D., and Zlokovic, B. V. (2010). Pericyte-specific expression of PDGF beta receptor in mouse models with normal and deficient PDGF beta receptor signaling. *Mol. Neurodegener.* 5, 32. doi:10.1186/1750-1326-5-32

Wirrig, E. E., and Yutzey, K. E. (2014). Conserved transcriptional regulatory mechanisms in aortic valve development and disease. *Arterioscler. Thromb. Vasc. Biol.* 34, 737–741. doi:10.1161/ATVBAHA.113.302071

Xu, Q. (2008). Stem cells and transplant arteriosclerosis. *Circ. Res.* 102, 1011–1024. doi:10.1161/CIRCRESAHA.108.171488

Yao, J., Guihard, P. J., Blazquez-Medela, A. M., Guo, Y., Moon, J. H., Jumabay, M., et al. (2015). Serine protease activation essential for endothelial-mesenchymal transition in vascular calcification. *Circ. Res.* 117, 758–769. doi:10.1161/CIRCRESAHA.115.306751

Yu, B., Chen, Q., Le Bras, A., Zhang, L., and Xu, Q. (2017). Vascular stem/progenitor cell migration and differentiation in atherosclerosis. *Antioxid. Redox Signal.* doi:10.1089/ars.2017.7171

Zampetaki, A., Kirton, J. P., and Xu, Q. (2008). Vascular repair by endothelial progenitor cells. *Cardiovasc. Res.* 78, 413–421. doi:10.1093/cvr/cvn081

Zoll, J., Fontaine, V., Gourdy, P., Barateau, V., Vilar, J., Leroyer, A., et al. (2008). Role of human smooth muscle cell progenitors in atherosclerotic plaque development and composition. *Cardiovasc. Res.* 77, 471–480. doi:10.1093/cvr/cvm034

Conflict of Interest Statement: The authors declare that the research was conducted in the absence of any commercial or financial relationships that could be construed as a potential conflict of interest.

Advantages of publishing in Frontiers

OPEN ACCESS
Articles are free to read for greatest visibility and readership

FAST PUBLICATION
Around 90 days from submission to decision

HIGH QUALITY PEER-REVIEW
Rigorous, collaborative, and constructive peer-review

TRANSPARENT PEER-REVIEW
Editors and reviewers acknowledged by name on published articles

Frontiers
Avenue du Tribunal-Fédéral 34
1005 Lausanne | Switzerland

Visit us: www.frontiersin.org
Contact us: info@frontiersin.org | +41 21 510 17 00

REPRODUCIBILITY OF RESEARCH
Support open data and methods to enhance research reproducibility

DIGITAL PUBLISHING
Articles designed for optimal readership across devices

FOLLOW US
@frontiersin

IMPACT METRICS
Advanced article metrics track visibility across digital media

EXTENSIVE PROMOTION
Marketing and promotion of impactful research

LOOP RESEARCH NETWORK
Our network increases your article's readership